GEOLOGICAL SURVEY OF CANADA
COMMISSION GÉOLOGIQUE DU CANADA

CURRENT RESEARCH 1996-C
CANADIAN SHIELD

RECHERCHES EN COURS 1996-C
BOUCLIER CANADIEN

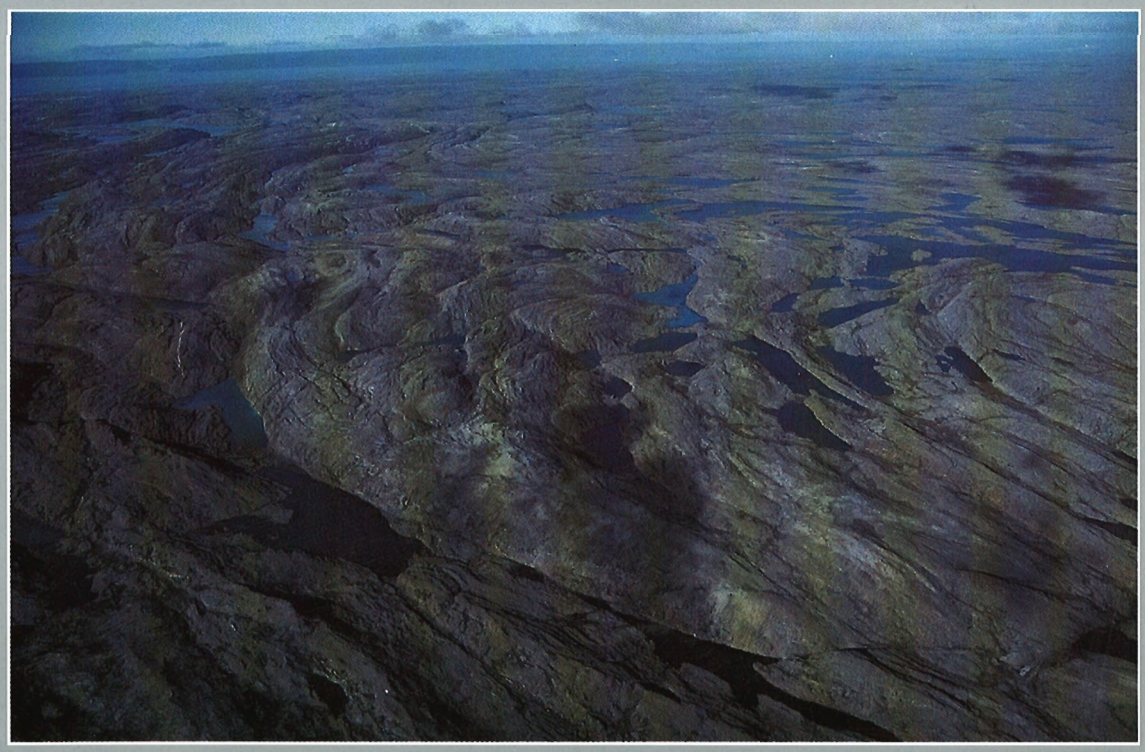

1996

Natural Resources Canada
Ressources naturelles Canada

Canada

NOTICE TO LIBRARIANS AND INDEXERS

The Geological Survey's Current Research series contains many reports comparable in scope and subject matter to those appearing in scientific journals and other serials. Most contributions to Current Research include an abstract and bibliographic citation. It is hoped that these will assist you in cataloguing and indexing these reports and that this will result in a still wider dissemination of the results of the Geological Survey's research activities.

AVIS AUX BIBLIOTHÉCAIRES ET PRÉPARATEURS D'INDEX

La série Recherches en cours de la Commission géologique contient plusieurs rapports dont la portée et la nature sont comparables à ceux qui paraissent dans les revues scientifiques et autres périodiques. La plupart des articles publiés dans Recherches en cours sont accompagnés d'un résumé et d'une bibliographie, ce qui vous permettra, on l'espère, de cataloguer et d'indexer ces rapports, d'où une meilleure diffusion des résultats de recherche de la Commission géologique.

GEOLOGICAL SURVEY OF CANADA
COMMISSION GÉOLOGIQUE DU CANADA

CURRENT RESEARCH 1996-C

CANADIAN SHIELD

RECHERCHES EN COURS 1996-C

BOUCLIER CANADIEN

1996

Available in Canada from

Geological Survey of Canada offices:

601 Booth Street
Ottawa, Canada K1A 0E8

3303-33rd Street N.W.
Calgary, Alberta T2L 2A7

100 West Pender Street
Vancouver, B.C. V6B 1R8

or from

Canada Communication Group – Publishing
Ottawa, Canada K1A 0S9

and through authorized bookstore agents
and other bookstores

A deposit copy of this publication is also available for reference
in public libraries across Canada

Cat. No. M44-1996/3E
ISBN 0-660-16285-7

Price subject to change without notice

Cover description

Oblique aerial photograph of folded siliciclastic units in the hinge zone of the northwest-plunging Lake Harbour Group synclinorium, southern Baffin Island, Northwest Territories. View is towards southwest. Width of the middle field of view is 2 km. See reports by St-Onge et al. and by Hanmer et al. in this volume. GSC 1995-360

Photo aérienne oblique de séquences silicoclastiques plissées, observées dans la zone axiale du synclinorium du Groupe de Lake Harbour (à plongement vers le nord-ouest), île de Baffin, Territoires du Nord-Ouest. La photo est prise en regardant vers le sud-ouest. La distance horizontale du champ de vue est de 2 km. Voir les articles de St-Onge et al. ainsi que de Hanmer et al. du présent volume de «Recherches en cours». (GSC 1995-360)

Separates

A limited number of separates of the papers that appear in this volume are available by direct request to the individual authors. The addresses of the Geological Survey of Canada offices follow:

Geological Survey of Canada
601 Booth Street
OTTAWA, Ontario
K1A 0E8
(FAX: 613-996-9990)

Geological Survey of Canada (Calgary)
3303-33rd Street N.W.
CALGARY, Alberta
T2L 2A7
(FAX: 403-292-5377)

Geological Survey of Canada (Victoria)
100 West Pender Street
VANCOUVER, B.C.
V6B 1R8
(FAX: 604-666-1124)

Geological Survey of Canada (Victoria)
P.O. Box 6000
9860 Saanich Road
SIDNEY, B.C.
V8L 4B2
(Fax: 604-363-6565)

Geological Survey of Canada (Atlantic)
Bedford Institute of Oceanography
P.O. Box 1006
DARTMOUTH, N.S.
B2Y 4A2
(FAX: 902-426-2256)

Quebec Geoscience Centre/INRS
2535, boulevard Laurier
C.P. 7500
Sainte-Foy (Québec)
G1V 4C7
(FAX: 418-654-2615)

Tirés à part

On peut obtenir un nombre limité de «tirés à part» des articles qui paraissent dans cette publication en s'adressant directement à chaque auteur. Les adresses des différents bureaux de la Commission géologique du Canada sont les suivantes :

Commission géologique du Canada
601, rue Booth
OTTAWA, Ontario
K1A 0E8
(facsimilé : 613-996-9990)

Commission géologique du Canada (Calgary)
3303-33rd St. N.W.,
CALGARY, Alberta
T2L 2A7
(facsimilé : 403-292-5377)

Commission géologique du Canada (Victoria)
100 West Pender Street
VANCOUVER, British Columbia
V6B 1R8
(facsimilé : 604-666-1124)

Commission géologique du Canada (Victoria)
P.O. Box 6000
9860 Saanich Road
SIDNEY, British Columbia
V8L 4B2
(facsimilé : 604-363-6565)

Commission géologique du Canada (Atlantique)
Institut océanographique Bedford
P.O. Box 1006
DARTMOUTH, Nova Scotia
B2Y 4A2
(facsimilé : 418-654-2615)

Centre géoscientifique de Québec/INRS
2535, boulevard Laurier
C.P. 7500
Sainte-Foy (Québec)
G1V 4C7

CONTENTS

Precambrian geology of northern Wellington Inlier, Victoria Island, Northwest Territories
A.N. LeCheminant, R.H. Rainbird, and M.E. Villeneuve 1

Lamprophyre dykes in the Awry plutonic suite, North Arm, Great Slave Lake, Northwest Territories
A.N. LeCheminant 11

Stratigraphy of the southern portion of an Archean stratovolcano in the Back River volcanic complex, Slave Province, Northwest Territories
M.B. Lambert 19

Regional gravity survey of western Great Slave Lake, Northwest Territories: a GSC contribution to the SNORCLE transect
C. Lowe and D.A. Seemann 29

Thematic structural studies in the Slave Province, Northwest Territories: the Sleepy Dragon Complex
W. Bleeker 37

Stratabound and stratiform sediment-hosted uranium-copper prospects in the Paleoproterozoic Amer Group, Churchill Structural Province, Northwest Territories
A.R. Miller 49

Geology of the Meta Incognita Peninsula, south Baffin Island, Northwest Territories: tectonostratigraphic units and regional correlations
M.R. St-Onge, S. Hanmer, and D.J. Scott 63

Structural geology of the Meta Incognita thrust belt, south Baffin Island, Northwest Territories
S. Hanmer, M.R. St-Onge, and D.J. Scott 73

Geology of the Hall Peninsula east of Iqaluit, southern Baffin Island, Northwest Territories
D.J. Scott 83

Structural geology of the Flin Flon area, Manitoba and Saskatchewan
D. Gale, S.B. Lucas, and J.M. Dixon 93

The structural anatomy of the central Flin Flon Belt, northern Manitoba
J.J. Ryan and P.F. Williams 105

The application of digital geophysical data to the restoration of crustal deformation in the Canadian Shield, Ontario
R.T. Bird, W.R. Roest, M. Pilkington, R.E. Ernst, and K.L. Buchan 117

Geological investigations in the Swayze greenstone belt, southern Superior Province, Ontario: a final field update
K.B. Heather, G.T. Shore, and O. van Breemen 125

Arsenic in surface waters, Cobalt, Ontario
J.B. Percival, C.G. Dumaresq, Y.T.J. Kwong, K.B. Hendry, and F.A. Michel 137

Geometric aspects of a large extensional vein, Donalda deposit, Rouyn-Noranda, Quebec
F. Robert, A.-M. Boullier, and K. Firdaous 147

Granite-greenstone terranes of the northern Minto block, northeastern Superior Province, Quebec
J.A. Percival, T. Skulski, and L. Nadeau 157

Ground penetrating radar survey to define fractures in bedrock, Little French River, Ontario
J. Pilon, J. Scaife, P. Gerabek, E. Timoshenko, and P. Kurfurst 169

Un kame sur la batture aux Alouettes, près de l'embouchure du Saguenay, Québec
J.-C. Dionne 177

Troctolitic rocks of the Reid Brook intrusion, Nain Plutonic Suite, Voisey Bay area, Labrador
R.F. Emslie 183

Surficial sediments, permafrost, and geomorphic processes, Kikerk Lake and Coppermine map areas, west Kitikmeot, District of Mackenzie, Northwest Territories
D.E. Kerr, S.A. Wolfe, B.C. Ward, and L.A. Dredge 197

Author Index 205

Precambrian geology of northern Wellington Inlier, Victoria Island, Northwest Territories[1]

A.N. LeCheminant, R.H. Rainbird, and M.E. Villeneuve
Continental Geoscience Division, Ottawa

LeCheminant, A.N., Rainbird, R.H., and Villeneuve, M.E. 1996: Precambrian geology of northern Wellington Inlier, Victoria Island, Northwest Territories; in Current Research 1996-C; Geological Survey of Canada, p. 1-10.

Abstract: In Wellington Inlier, two unconformity-bounded Paleoproterozoic sedimentary successions overlie foliated syenogranite to granodiorite basement. The north-northeast- to northeast-striking plutonic rocks are cut by two generations of pegmatites and contain minor enclaves of supracrustal rocks. A U-Pb zircon age of 2601 ± 3 Ma suggests the basement is a northern extension of the Slave Province.

The sedimentary successions are correlated with the 1.9 Ga Burnside and 1.7 Ga Ellice formations in Bathurst Inlet. They were deposited by braided rivers flowing westward away from the exposed craton. East-southeast- to southeast-striking diabase dykes intruded the folded Burnside Formation and are overlain by the Ellice Formation. An unusual mafic dyke, rich in granite xenoliths, was emplaced into the Ellice Formation. Younger gabbro sills, containing minor base and precious metals, intruded both sedimentary successions and the basement during 1.27 Ga Mackenzie and/or 0.72 Ga Franklin magmatism.

Résumé : Dans la fenêtre de Wellington, deux successions sédimentaires du Paléoprotérozoïque limitées par une discordance reposent sur un socle folié variant en composition du syénogranite à la granodiorite. Les roches plutoniques d'orientation nord-nord-est à nord-est sont recoupées par deux générations de pegmatites et contiennent des enclaves moins importantes de roches supracrustales. Selon une datation U-Pb sur zircon de 2 601 ± 3 Ma, le socle serait un prolongement septentrional de la Province des Esclaves.

Les successions sédimentaires sont corrélées aux formations de Burnside (1,9 Ga) et d'Ellice (1,7 Ga) dans l'inlet Bathurst. Elles ont été déposées par des cours d'eau anastomosés s'écoulant vers l'ouest en provenance du craton affleurant. Les dykes de diabase d'orientation est-sud-est à sud-est recoupent la Formation de Burnside, qui est plissée, et sont sous-jacents à la Formation d'Ellice. Un dyke mafique inhabituel, riche en xénolites de granite, a fait intrusion dans la Formation d'Ellice. Des filons-couches de gabbro plus récents, contenant un peu de métaux communs et précieux, ont injecté les deux successions sédimentaires et le socle durant l'épisode magmatique de Mackenzie (1,27 Ga) ou celui de Franklin (0,72 Ga).

[1] Industrial Partners Project 94-031, involving the Geological Survey of Canada and Ascot Resources Ltd.

INTRODUCTION

Bedrock mapping of northern Wellington Inlier (WI) in 1994 was completed as part of an agreement between Ascot Resources Ltd. and the Geological Survey of Canada. The area was mapped at 1: 50 000 scale from helicopter-supported fly camps.

Knowledge of Precambrian basement structure and crustal evolution beneath Victoria Island is minimal. In this report, we establish the age of a granite within the only exposed basement in central Victoria Island. Details of the extent and timing of Proterozoic sedimentation and mafic magmatism are inferred from field relationships of two successions of sedimentary rocks that overlie the basement and are intruded by numerous mafic dykes and sills.

PREVIOUS WORK

Geological reconnaissance of Victoria Island was undertaken by Washburn (1947), who mapped along the south coast and summarized previous geological observations. Thorsteinsson and Tozer (1962) completed the reconnaissance mapping and assigned the north-northwest-trending belt of Proterozoic sedimentary rocks between Wellington Bay and Washburn Lake (Fig. 1) to the Glenelg Formation of the Shaler Group. Proterozoic rocks are exposed in topographic highs on the sub-Paleozoic surface (Thorsteinsson and Tozer, 1962), and the exhumed belt extending inland from Wellington Bay has been variously named the Wellington Arch, the Wellington topographic high (Christie et al., 1972), the Wellington high (Young, 1974) and the Wellington Inlier (Dixon, 1979). Christie (1964) emphasized the abundance of diabase-gabbro intruding Proterozoic successions on Victoria Island and mapped sills and dykes in Wellington Inlier as far north as Washburn Lake (Fig. 3, in Christie, 1964).

Granite is exposed in a small region north of Washburn Lake (Chernoff, unpublished report, 1974; Bond, 1977; Dixon 1979). Two attempts to date the plutons yielded K-Ar muscovite ages of 1673 ± 42 Ma for a syenite (Wanless, et al., 1979) and 1735 ± 41 Ma for a granite (Stevens et al., 1982).

Young (1974) described red fluvial sandstone and conglomerate in southern Wellington Inlier. Christie et al. (1972) and Young and Jefferson (1975) suggested the successions may be pre-Shaler Group and equivalent to rocks in Bathurst Inlet, a correlation supported by Campbell and Cecile (1979) and Dixon (1979). Campbell and Cecile (1979) correlated southern Wellington Inlier sediments with the Burnside Formation and further suggested that underlying dolomitic rocks may be equivalent to the Western River Formation. Dixon (1979) also concluded that the sandstone and conglomerate correlate with the Burnside Formation. Near the outlet of Ferguson Lake, white quartzarenite and conglomerate unconformably overlie red Burnside Formation rocks (Campbell and Cecile, 1979). They correlated the upper succession with either the Ellice Formation or the Glenelg Formation (now the Nelson Head Formation of the Shaler Supergroup, Rainbird et al., 1994). Bond (1977) also reported that quartzarenite and conglomerate unconformably overlie folded Burnside quartzite along the west side of Wellington Inlier and correlated the succession with the Glenelg Formation.

Southwest of Ferguson Lake (Fig. 1), large gabbro sills intruded quartzite and conglomerate. A whole rock K-Ar age of 1150 ± 92 Ma (Stevens et al., 1982) for one sill suggests that gabbros in southern Wellington Inlier were emplaced during 1.27 Ga Mackenzie magmatism (LeCheminant and Heaman, 1989) and confirms that the quartzite and conglomerate intruded by the gabbro predate the Shaler Supergroup.

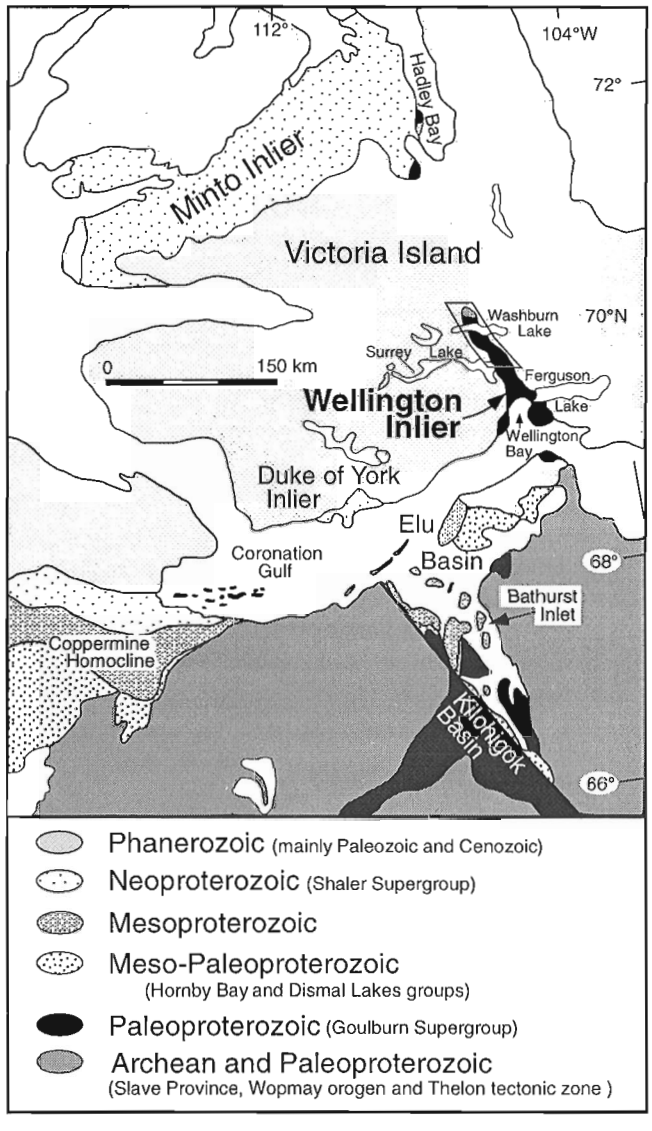

Figure 1. *Geological map of the northwestern Canadian Shield and adjacent regions. The geology of the region outlined in northern Wellington Inlier is shown in Figures 2a and 2b.*

GRANITIC BASEMENT

Exploration programs in the 1970s outlined an area of granitic basement exposed in topographic highs north of Washburn Lake (Chernoff, unpublished report, 1974; Bond, 1977; Dixon, 1979). Isolated knolls of granite are surrounded by nearly flat-lying Cambrian-Ordovician dolostone, partly filling depressions between granite hills with a paleotopography of ca 100 m (Fig. 2a). In addition, the region is variably draped by glacial deposits, so that exposed granite comprises about 40 km^2 within a 100 km^2 region. Low-lying outcrops of Ellice Formation quartzarenite and conglomerate border the basement rocks to the west and, in two areas, the granites are separated from the sedimentary rocks by gabbro intrusions.

The granitic terrane is dominated by medium- to coarse-grained foliated plutonic rocks ranging in composition from leucocratic biotite-muscovite syenogranite to biotite-hornblende monzogranite and minor granodiorite. Porphyritic varieties contain microcline phenocrysts up to 2 cm long. The granites are regionally deformed and have a variably developed foliation with a consistent north-northeast to northeast strike and moderate southeasterly dips. Locally, a muscovite lineation plunges shallowly to the south-southwest. Several granite hills have a prominent northeast ribbing that is caused by resistant pegmatite dykes and more eroded muscovite-rich zones.

No large enclaves of supracrustal rocks were noted, although local zones within the granite have high muscovite content and there are lenses of quartz-muscovite schist of possible metasedimentary origin, and one small band of amphibolite. The schist is strongly deformed and contains plagioclase porphyroclasts and polycrystalline quartz ribbons aligned parallel to muscovite grains that define the schistosity. Apatite is abundant in muscovite-rich layers; other accessory minerals are microcline and biotite, with rare tourmaline and zircon.

Medium- to coarse-grained porphyritic syenogranite is the dominant plutonic rock throughout the basement. Deformation is highly variable and the granite typically contains rotated and broken microcline phenocrysts, broken plagioclase laths with polycrystalline margins, fine myrmekite and polycrystalline quartz. Accessory minerals are muscovite and biotite, partly altered to chlorite, and minor apatite, carbonate, titanomagnetite, and rutile. The more mafic-rich monzogranite and granodiorite also are variably deformed; they are interpreted to form a single plutonic suite with the syenogranite. Their mineralogy is similar to syenogranite, with the addition of hornblende and allanite. Zoned allanite crystals, now largely metamict, are rimmed by epidote. Accessory minerals are apatite, opaques, carbonate, and zircon. Epidote, titanite, and chlorite are common alteration phases, with only minor muscovite.

The plutonic rocks are cut by pink, muscovite-rich pegmatite pods and dykes, and minor aplite dykes and quartz veins. Pegmatite, composed of large microcline and quartz crystals and books of muscovite to 10 cm, contains central pods of massive white quartz. Most pegmatite units are <1 m wide, although some are up to 10 m across. They are oriented parallel or subparallel to regional foliation and, in strongly deformed zones, at least two ages of pegmatites can be recognized by dismembered dykes within the foliation and later partly cross-cutting dykes.

Geochronology

One granite from the plutonic suite has been dated. U-Pb analyses (Table 1) and data reduction followed methods described in Parrish et al. (1987) and Roddick (1987). The porphyritic syenogranite contains large zircons that record a complex magmatic growth history with multiple growth stages. A small yield of poor quality zircon was recovered and split into three fractions for analysis. The zircons were multicoloured, euhedral to subhedral crystals and fragments, many with noticeable fractures and clear, elongate inclusions. Plots of two of the three analyses overlap (see Fig. 3); they are about 2% discordant and the third is 11% discordant (Table 1). A three point regression defines an upper intercept of 2601 ± 3 Ma and a lower intercept of 665 ± 44 Ma. Because of the coincidence of fractions A and C, the slope of the regression line is strongly influenced by the 11% discordant fraction D. As such, the calculated error represents analytical

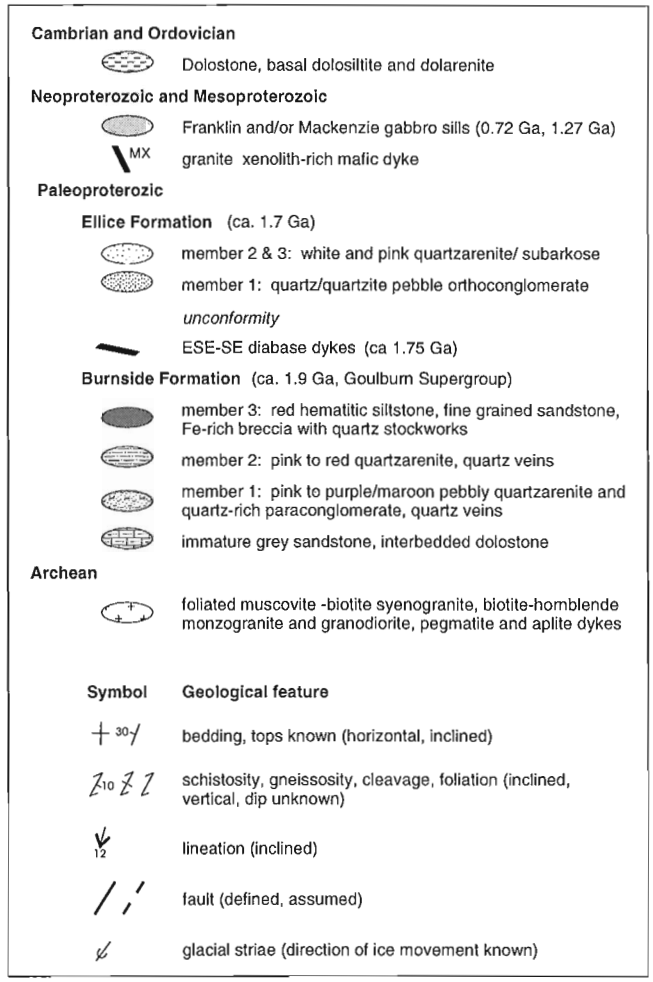

Figure 2. *Legend*

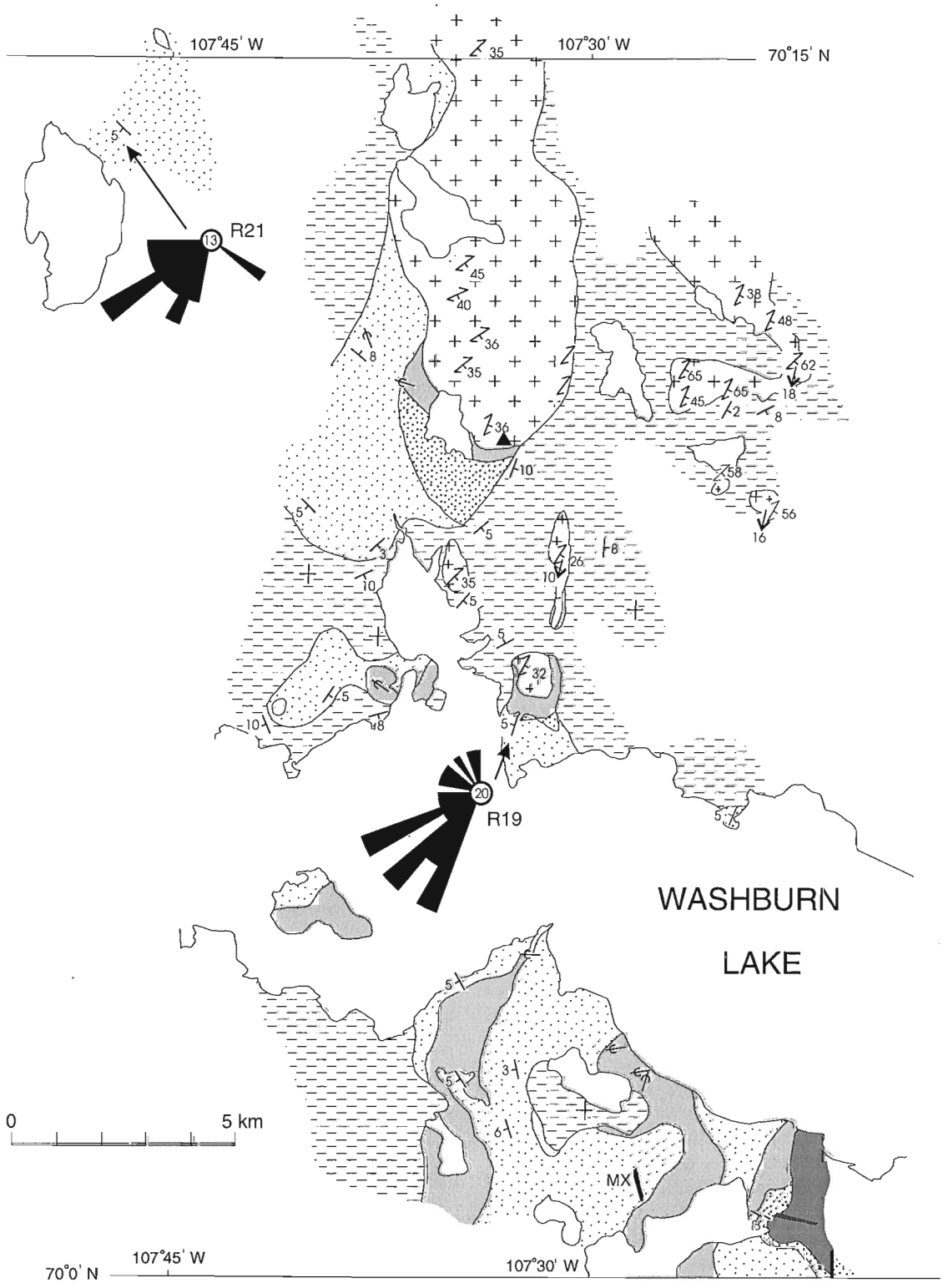

Figure 2. *Geological maps showing the Precambrian geology of northern Wellington Inlier and adjacent Paleozoic rocks.* ***a)*** *NTS area 77E/4. Paleocurrent rose diagrams (equal area) from foreset dip azimuths of crossbeds from the Ellice and Burnside formations – arrows indicate station locations. Additional paleocurrent data for correlative rocks are reported by Campbell and Cecile (1979).*

uncertainty only, and there is an additional uncertainty in the intercept ages that cannot be determined by statistical regression techniques. Nevertheless, because the two coincident fractions are only 2% discordant, 2601 Ma represents a minimum, and probably realistic estimate of the crystallization age.

PROTEROZOIC SUCCESSIONS

We recognize two Proterozoic sedimentary successions in northern Wellington Inlier (Fig. 2a, b) and correlate them with the ca 1.9 Ga Burnside Formation (Bear Creek Group, Goulburn Supergroup; McCormick and Grotzinger, 1993)

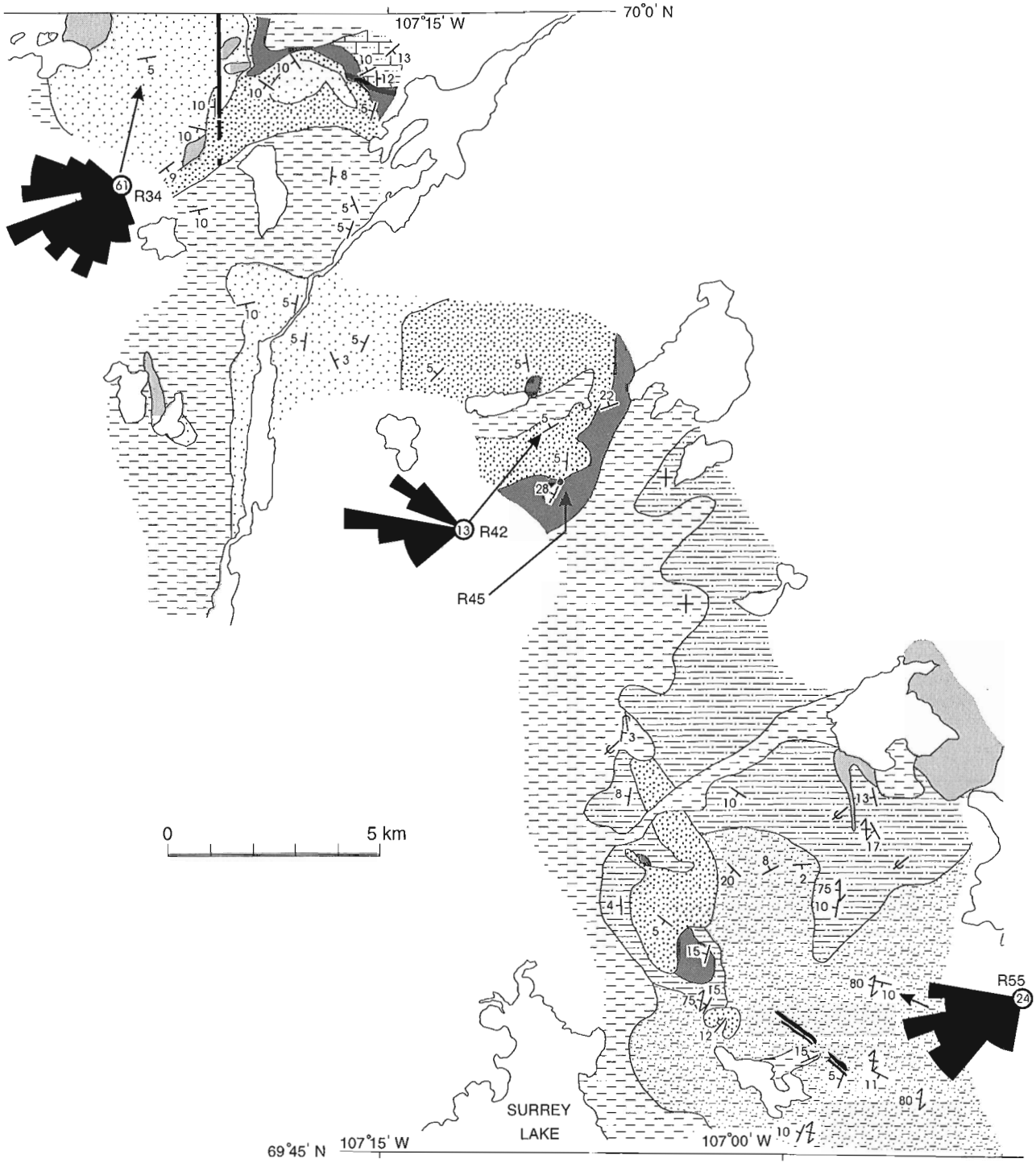

Figure 2. b) *NTS areas 77D/13 and 77D/14.*

and the ca 1.7 Ga Ellice Formation (Campbell and Cecile, 1979; Gall, 1992). The two Wellington Inlier successions are comparable with successions exposed at Hadley Bay (Campbell, 1981), and in the Elu and Kilohigok basins of the Bathurst Inlet region (Campbell and Cecile, 1979).

Burnside Formation

The basal Proterozoic succession in northern Wellington Inlier comprises three members of the Burnside Formation and an older, sandstone-carbonate unit. All are folded into broad open folds about north-northeast-striking axes. Bedding dips at <30° and a steep to vertical east-dipping north-south fracture cleavage is developed locally. Many outcrops contain resistant zones of pervasive silicification and hematitization up to 15 m wide, that are characterized by closely spaced, en échelon, quartz-filled, tension fractures.

Member 1, the lowermost, thickest and most extensive unit, comprises pink to purple-maroon, medium- to coarse-grained pebbly subarkose to quartzarenite. The rocks are strongly indurated with characteristic blocky weathering, conchoidal fracture, and quartz veining that distinguishes them from similar rocks in the overlying succession. The sandstone units include horizons of paraconglomerate containing clasts of sub-angular to sub-rounded white quartz and well-rounded quartzite. Small- to medium-scale trough cross-bedding, the dominant sedimentary structure, indicates paleotransport between northwest and southwest (Fig. 2b). Framework grains are dominantly single quartz grains (>90%), various types of polycrystalline quartz, and rare jasper, with smaller opaques and zircon. Some rocks have an opaque-dusted, polycrystalline "chert" pseudo-matrix and most quartz grains display clear syntaxial overgrowths.

Member 2 is a fine- to medium-grained, red to pink-grey and white, well-sorted and well indurated quartzarenite with conchoidal fracture, blocky weathering and poorly defined

Table 1. U-Pb zircon data.

Fraction[a]	Wt.[b] µg	U ppm	Pb[c] ppm	$^{206}Pb/^{204}Pb$[d]	Pb[e] pg	$^{208}Pb/^{206}Pb$[f]	Radiogenic ratios (±1σ, %)[f] $^{207}Pb/^{235}U$	$^{206}Pb/^{238}U$	$^{207}Pb/^{206}Pb$	$^{207}Pb/^{206}Pb$ Age (Ma)[g]	Discord.[h] %
WELLINGTON INLIER GRANITE (94-LAA-T65, Z3608; 70.1751°N 107.5580°E)											
A (Z)	6	56	28	1690	2	0.040	11.633±0.14	0.4857±0.12	0.17370±0.07	2594±2	1.94
D (Z)	5	179	90	1259	20	0.190	10.120±0.12	0.4325±0.11	0.16973±0.06	2555±2	11.08
C (Z)	2	64	36	1097	4	0.200	11.622±0.26	0.4852±0.32	0.17372±0.19	2594±6	2.06

[a] All zircon fractions are abraded; (Z)=Zircon
[b] Error on weight = ±0.001 mg
[c] Radiogenic Pb
[d] Measured ratio corrected for spike and Pb fractionation of 0.09±0.03%/AMU
[e] Total common Pb on analysis corrected for fractionation and spike, of blank model Pb composition
[f] Corrected for blank and spike Pb and U and common Pb (Stacey-Kramers model Pb composition equivalent to the $^{207}Pb/^{206}Pb$ age)
[g] Age error is ±2SE in Ma
[h] Discordance along a discordia to origin.

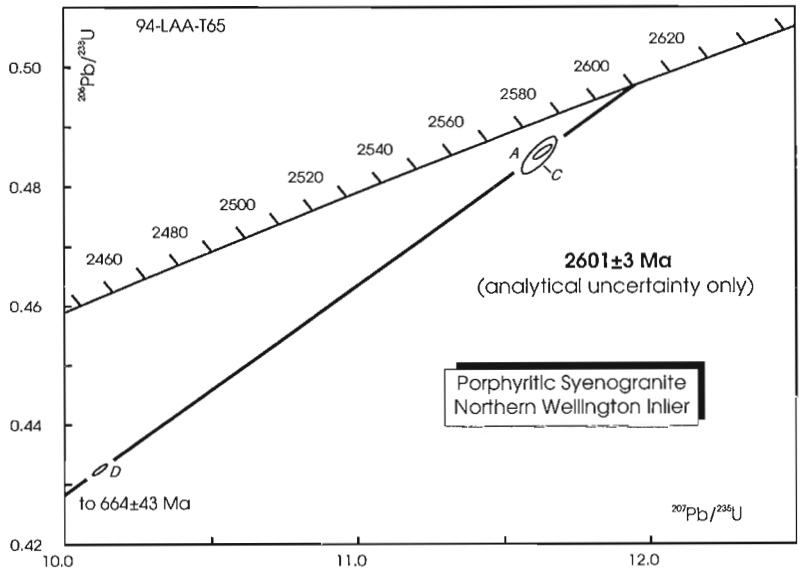

Figure 3.

U-Pb concordia diagram for zircon from porphyritic syenogranite. Error ellipses show 2 sigma uncertainty. Refer to text for discussion of uncertainties. Sample location is indicated by a black triangle in Figure 2a.

bedding. Sedimentary structures are difficult to recognize, although vague parallel bedding is visible in some outcrops. Member 2 is reddest near its top where it gradationally underlies member 3. The white quartzarenite appears to underlie the red, but its relationship with member 1 is unclear.

Member 3 is a thin-laminated to thin-bedded red, hematitic siltstone and very fine-grained sandstone. Siltstone exhibits thin parallel lamination and thicker, coarser layers have well-defined wave and current ripples along with desiccation cracks and rare raindrop impressions. At R45 (Fig. 2b), interbedded red siltstone and fine grained sandstone are invaded by a quartz stockwork, associated with a 10 m wide zone of extensive hematite mineralization. Petrography reveals multiple stages of brecciation, iron mineralization and quartz cementation. The iron-rich altered zone is overlain with angular unconformity by Ellice Formation conglomerate.

The dirty sandstone/carbonate unit is a fine grained, pink-weathering, mica-rich, grey sandstone, with well developed bedding and rare ripple marks, interbedded with brown weathering, thinly bedded, dolostone. The rocks have a spaced cleavage that is axial planar to gently north-plunging open folds. The unit underlies red siltstone (member 3) of the Burnside Formation south of Washburn Lake (Fig. 2b), and may correlate with member B of the Hadley Formation west of Hadley Bay (Campbell, 1981).

Ellice Formation

Clastic rocks, similar to those described by Campbell and Cecile (1979), and correlated with the Ellice Formation of Elu Basin, unconformably overlie the folded Burnside Formation in northern Wellington Inlier. This upper succession has been divided in three members.

Member 1 is an orthoconglomerate containing well rounded pebble- to cobble-size clasts, with boulder-size clasts near the base. Clasts comprise mainly milky white and clear vein quartz and Burnside Formation quartzarenite. Near the basal unconformity, other Burnside Formation clasts, including conglomerate, red siltstone, and ironstone are common The matrix is composed of medium- to coarse-grained sand, similar to overlying member 2 sandstone and, in general, the matrix component increases upsection. Member 1 varies from a few metres thick at Washburn Lake to 40-50 m thick at the south edge of the map area (Fig 2a, b). Basal conglomerate is massive to parallel stratified; crossbedding is apparent up-section. Low to moderate induration and weathered-out framework are characteristic and reflect a clay-rich matrix.

Member 2 is a medium- to coarse-grained pink to red pebbly subarkose with subordinate conglomeratic interlayers. The moderately well-sorted rocks contain a high percentage of angular, locally derived rock fragments and degraded feldspar, presumably derived from paleo-regolith developed on underlying basement rocks. In most exposures, moderate- to large-scale tabular trough-crossbedding is well developed and yields consistent, unimodal, southwest paleocurrent data (Fig. 2a, b). As with member 1, induration is moderate owing to abundant clay cement.

Member 3 is a texturally mature, fine- to medium-grained, pink to white quartzarenite that is exposed in the northwest part of the map area. Small- to medium-scale, broad tabular trough-crossbedding is abundant and shows transport to the southwest. The crossbeds differ from those in member 2 in that they have superposed ripples and interbedded ripple crosslamination indicating paleocurrents roughly perpendicular to the crossbeds.

The basal unconformity with the Burnside Formation is exposed in two places. At one locality, conglomerate overlies member 3 hematitic siltstone with profound angular unconformity exposing paleotopographic relief of about 15 m. The red basal conglomerate includes many angular siltstone clasts. At the second locality, conglomerate overlies member 1 Burnside Formation rocks, with local paleotopographic relief of up to 40 m. Additional regional paleotopographic relief is implied by the absence of both member 2 and 3 of the Burnside Formation at this locality.

GABBRO/DIABASE

East-southeast- to southeast-striking diabase dykes

East-southeast- to southeast-striking diabase dykes form linear ridges flanked by red Burnside Formation rocks (Fig. 2a, b). South of Washburn Lake, a north-south fault separates two dyke segments. The 1 km long, >20 m wide western segment is a medium- to coarse-grained, red-brown gabbro that is variably altered and deeply weathered, although primary ophitic textures are preserved. The dyke is exposed only at, or below, the level of basal Ellice Formation rocks. Gabbro close to the unconformity is characterized by intense hematitic alteration and thin quartz-specularite-dolomite-chlorite veins. These observations indicate the dykes are older than the Ellice Formation. Although fresh plagioclase and clinopyroxene are preserved locally, the gabbro contains extensive secondary amphibole, chlorite, and hematite. Minor, primary chalcopyrite is rimmed by hematite, and secondary copper minerals occur with barite. The second dyke segment, 4 km to the east, is identical mineralogically, but is >40 m wide and strikes more southeasterly. The northern contact of the dyke with folded sandstone is well exposed, adjacent sedimentary rocks are hornfelsed and there is a zone of intense vertical jointing parallel to the contact.

East of Surrey Lake, two 130°-striking dykes outcrop intermittently for about 2 km and form parallel ridges of red-brown, spheroidal weathering gabbro, about 25 m and 55 m wide (Fig. 2b). Contacts with adjacent Burnside Formation rocks are not exposed. Texturally and mineralogically the gabbro resembles the dyke segments near Washburn Lake; primary plagioclase and pyroxene are strongly altered with some pyroxenes completely replaced by amphibole, chlorite, serpentine, oxides and carbonate. Primary titanomagnetite-ilmenite grains are partly replaced by titanite and chalcopyrite is rimmed by feathery intergrowths of specularite. Other accessory minerals are baddeleyite, zirconolite, zircon, a REE silicate and a Th,Y-rich mineral.

Granite xenolith-rich mafic dyke

A mafic dyke, rich in granitic xenoliths, is exposed discontinuously for about 0.6 km south of Washburn Lake (Fig 2a). The 18-20 m wide vertical dyke forms a 170°-striking linear within Ellice Formation quartzarenite; contact zones are rusty-weathering and contain minor quartz-barite veins. The dyke is interpreted to be older than nearby gabbro sills (see below) because it is more altered, contains no gabbro xenoliths and cannot be traced into the sills.

Pink granitic xenoliths, similar to basement rocks exposed to the north, are abundant and randomly distributed throughout the dyke. They have sharp, embayed contacts with the dyke rock, range in size up to 1.1 m, and make up 20-50% of the intrusion. The partly melted and recrystallized xenoliths contain polycrystalline quartz and albitized feldspars that are recrystallized along xenolith margins. Some quartz grains project into the host rock and these, along with isolated quartz xenoliths, have a thin rim of biotite/chlorite and amphibole, indicative of quartz dissolution by the host magma. Most xenoliths in the dyke are derived from disaggregation of granite, although some polycrystalline quartz xenoliths resemble Ellice Formation quartzarenite.

The fine grained, pink to black host rock has an equigranular texture. It contains 20-30% quartz intergrown with altered feldspar laths, probably originally plagioclase, but now replaced by albite and sericite. Intergrowths of chlorite, sericite, biotite and pale amphibole replace primary mafic minerals. The rock contains ca. 10% Fe-Ti oxides; some euhedral titanomagnetite grains contain minor Al and Cr and may be primary oxides. Accessory minerals are apatite, monazite and baddeleyite. Compositionally, the dyke is a hybrid, produced by partial assimilation of granitic inclusions by mafic magma.

0.72 Ga Franklin and/or 1.27 Ga Mackenzie sills and dykes

Gabbro sills within the Ellice Formation are exposed on hills north and south of Washburn Lake and on an island in the lake (Fig. 2a). North of the lake, gabbro units extend as flat-lying sheets up to 3 km into the basement and, in two areas, intrusions separate basement from Ellice Formation rocks to the west. The gabbro sheets range up to 70 m thick and have sharp chilled contacts with foliated granite. Upper contacts are approximately flat except along the interface between basement and the Ellice Formation, where the intrusions are domed upwards. Here, both the upper contact with granite and the lower contact with quartzarenite and conglomerate are exposed. Contact effects of gabbro intrusion on the granite and quartz-rich sedimentary rocks are minimal. The chilled margin contains fresh clinopyroxene and plagioclase microphenocrysts set in a matrix of the same minerals, plus abundant fine opaques. Locally, the margin is spotted with amphibole and contains a network of thin amphibole-rich cooling veins.

In addition to the large gabbro sheets, a single diabase dyke cuts foliated granite in the eastern granite hills. The 3 m wide, 115°-striking, vertical dyke has unaltered chilled margins and a uniform, fine-grained centre. This fresh diabase differs from the larger and more altered dykes cutting the Burnside Formation. Mineralogically, it is similar to the gabbro sills and is likely the same age.

South of Washburn Lake, major gabbro sills intrude Ellice Formation quartzarenite. Contacts are flat or gently west dipping; nearby quartzarenites are well indurated and contain prominent joint sets and local quartz veins. Sheeting and columnar jointing are well developed within the sills near upper and lower contacts. Overall, the map pattern indicates there are at least three major sills, up to 90 m thick, separated by thin sedimentary units. The lowermost (eastern) sill intruded at about the level of the unconformity between the Ellice and Burnside formations. The sills form irregular north-south-striking bodies with a gentle west dip, consistent with the enclosing sedimentary rocks.

Coarse grained gabbros from the interior of sills have ophitic to subophitic textures, and contain zoned plagioclase laths enclosed by subequant to elongate pyroxene grains. Clinopyroxene dominates, but orthopyroxene and clinopyroxene can occur together, and some gabbros carry up to 3% equant olivine grains. Accessory minerals include euhedral and skeletal titanomagnetite-ilmenite intergrowths and interstitial hornblende, biotite, allanite, quartz-alkali feldspar granophyre, apatite, monazite, baddeleyite, zirconolite, and zircon. Minor alteration minerals are chlorite, zoisite, tourmaline, and carbonate. The sills contain trace disseminated sulphides, but no zones of sulphide concentration were encountered. Chalcopyrite is the most abundant sulphide, and locally pyrite, sphalerite, and galena and rare 2-5 μm platinum-group minerals occur with chalcopyrite. Platinum group minerals identified include a Pd-Bi arsenide, a Pt-Fe arsenide and a Pt-Fe alloy, with minor Cu. Other minerals are a Co-rich mineral (Co, S, As, Fe, Ni), a (Ag, Pb) selenide, and a (Pb, Fe, Ni, Co) Se, S phase.

A plagioclase-phyric gabbro in contact with the Burnside Formation underlies 10 km^2 in the southwestern part of the map area (Fig. 2b). Only the upper 20-30 m of the flat-sheeted intrusion is exposed. The gabbro contains up to 30% plagioclase phenocrysts to 1 cm, with rare megacrysts to 3 cm; phenocrysts are randomly oriented and are concentrated near chilled margins. Coarse grained gabbro within the intrusion is only sparsely porphyritic and has a black spotted appearance on weathered surfaces. Mineralogically, the gabbro is fresh and contains zoned plagioclase laths, partly enclosed by elongate feathery pyroxenes rimmed by amphiboles, plus euhedral and skeletal ilmenite-titanomagnetite intergrowths. Quartz and alkali feldspar form a well-developed granophyre associated with apatite, biotite, baddeleyite, zirconolite, zircon, and minor carbonate. Other minerals identified include pyrite and minor chalcopyrite, sphalerite, and a Co-Ni sulphide, along with one 20 μm grain of Ag. Stratigraphically, this porphyritic intrusion is the lowest sill mapped in northern Wellington Inlier, and it is more fractionated than sills near Washburn Lake.

PALEOZOIC ROCKS

Descriptions of the Paleozoic stratigraphy of Victoria Island are limited to the work of Washburn (1947) and Thorsteinsson and Tozer (1962), who subdivided the successions into three

units. Only the lowermost unit is exposed in southern Victoria Island, where it was divided into a lower clastic member of possible Cambrian age and an upper carbonate member of possible Ordovician or Silurian age. The carbonate member borders northern Wellington Inlier and includes thin, wavy bedded dolosiltite and dolarenite with minor interbeds of sandy dolarenite. The rocks generally are flat lying to gently dipping and are exposed in <10 m sections on the sides of low, rounded hills. Sandy beds are normally graded with bases that contain angular grains of quartz, microcline and muscovite derived from adjacent granites. The sandy dolostone passes up into pure, massive to wavy bedded dolostone, locally containing well developed, laterally linked, domal, columnar stromatolites.

DISCUSSION AND CONCLUSIONS

Granitic basement in northern Wellington Inlier is dominated by foliated plutonic rocks, ranging in composition from syenogranite to granodiorite. Felsic rocks in the plutonic suite resemble 2600-2585 Ma muscovite-bearing granite of the Slave Province (van Breemen et al., 1992; Davis et al., 1994) and the one dated syenogranite has a similar U-Pb zircon age (2601 ± 3 Ma, Fig. 3). This suggests the basement is a northern extension of the Slave Province. Northern Wellington Inlier basement rocks have a consistent north-northeast- to northeast-striking foliation and north-northeast-striking anomalies characterize magnetic and gravity maps of central and eastern Victoria Island. We suggest the anomalies reflect buried Archean basement rocks consisting of linear supracrustal belts (highs) separated by granite-rich domains (lows). The main deformation in northern Wellington Inlier is Archean; limited pre-1.7 Ga deformation is indicated by the open folding and weak metamorphism of 1.9 Ga Burnside Formation rocks. Basement K-Ar muscovite ages of 1673 ± 42 and 1735 ± 41 Ma (Wanless et al., 1979; Stevens et al., 1982) are interpreted to date this younger event.

The two Paleoproterozoic sedimentary successions in northern Wellington Inlier are comparable with two unconformity-bounded successions exposed in northeast Minto Inlier (Hadley Bay) to the north, and in the Elu and Kilohigok basins of the Bathurst Inlet region to the south (Fig. 1). The Burnside Formation was deposited by a northwesterly prograding alluvial braidplain that originated in the foreland of Thelon orogen (McCormick and Grotzinger, 1993). Members 1-3 in Wellington Inlier, herein assigned to the Burnside Formation, are interpreted to be part of the same fluvial system. At Hadley Bay, the lower succession comprises three members similar to those we assign to the Burnside Formation in Wellington Inlier. Campbell (1981) correlated the Hadley Bay rocks with the Western River Formation, although his descriptions indicated that the upper and lower members are similar to rocks described by the same author as Burnside Formation in southern Wellington Inlier (Campbell and Cecile, 1979). If the Burnside Formation correlation can be extended to Hadley Bay, then the fluvial system may have been very extensive. The dirty sandstone/carbonate unit at the base of the Burnside Formation in northern Wellington Inlier probably was deposited in a marine setting and its stratigraphic position below the other units suggests that it may be part of an older succession, such as the Kimerot Group (lower Goulburn Supergroup; McCormick and Grotzinger, 1993).

The lower succession at Hadley Bay is overlain with angular unconformity by conglomerate and quartzarenite (Campbell, 1981). A similar succession in southern Wellington Inlier is correlated with the Ellice Formation of the Elu Basin (Campbell and Cecile, 1979). In northern Wellington Inlier, conglomerate and quartzarenite, which we correlate with the Ellice Formation, unconformably overlie gently folded Burnside Formation sedimentary rocks. These rocks are strikingly similar to successions of the Hornby Bay, Elu, Thelon and Athabasca basins, thought to be erosional remnants of an extensive cratonic cover that developed over most of the northwestern Canadian Shield at about 1.7 Ga (Gall, 1992). The Ellice Formation in northern Wellington Inlier was deposited by braided rivers with strong southwesterly paleocurrents suggesting a significant, unexposed basement source to the northeast. Member 3 rocks may have been deposited by eolian systems, which reworked the underlying member 1 and 2 fluvial deposits. Evidence for eolian deposition includes high textural and compositional maturity and paleocurrent data, especially from ripples, which are oriented perpendicular to crossbed foreset dip directions. Possible correlative strata of the Hornby Bay Group exhibit similar eolian indicators (Kerans et al., 1981).

Altered east-southeast- to southeast-striking dykes cut the Burnside Formation in northern Wellington Inlier, but are unconformably overlain by Ellice Formation rocks. The dykes resemble 085-090°-striking dykes exposed west of Hadley Bay. There, the dykes cut west-dipping quartzarenite, which Campbell (1981) correlated with the Ellice Formation in southern Wellington Inlier. Mineralogically, the northern Wellington Inlier and Hadley Bay dykes are identical. Both contain altered plagioclase and clinopyroxene with secondary amphibole and chlorite, and there are numerous quartz-carbonate-hematite veins. One baddeleyite fraction separated from a Hadley Bay dyke yielded a ^{207}Pb-^{206}Pb age of 1747 Ma (L.M. Heaman, pers. comm., 1995), which raises a problem, because the dyke cuts rocks correlated with the 1.7 Ga Ellice Formation. Significantly, in northern Wellington Inlier, the east-southeast- to southeast-striking dykes are truncated by the pre-Ellice unconformity suggesting they are pre-1.7 Ga. Since, the Wellington Inlier dykes are suitable for geochronology they may provide a key age to clarify correlations between northern Wellington Inlier and Hadley Bay.

The unusual xenolith-rich mafic dyke emplaced into the Ellice Formation is interpreted to predate nearby gabbro sills. Large granitic xenoliths are abundant throughout the dyke and have reacted extensively with the carrier magma to produce a hybrid rock. Incorporation of the xenoliths caused the magma to cool quickly, resulting in a uniform fine grained texture. The ability of this magma to transport and partly assimilate xenoliths suggests that it had a higher volatile content than magmas that fed other dykes and sills in northern Wellington Inlier. Based on field relationships, the age of intrusion is <1.7 Ga and >1.27 Ga; the regional significance of this magmatic event is unknown.

There are at least three major gabbro sills near Washburn Lake that are separated by Ellice Formation rocks and, to the southeast, a plagioclase-phyric gabbro intruded the Burnside Formation. A gabbro sill at Ferguson Lake in southern Wellington Inlier has a K-Ar age of 1150 ± 92 Ma (Stevens et al., 1982), consistent with emplacement during the 1.27 Ga Mackenzie events. Provisionally, gabbro mapped in northern Wellington Inlier is also considered to be of Mackenzie age, as it intruded the same sedimentary successions as the Ferguson Lake sill and differs slightly in texture and mineralogy from 0.72 Ga Franklin sills emplaced into Shaler Supergroup successions to the west (Heaman et al., 1992; Jefferson et al., 1994). Olivine-bearing sills near Washburn Lake are most similar to Franklin gabbro; the southern plagioclase-phyric intrusion is not typical of either Mackenzie or Franklin gabbro. Because of the wide range of differentiation possible in thick gabbro sills emplaced during large-scale mafic magmatism, unequivocal assignment of northern Wellington Inlier gabbro to either 1.27 or 0.72 Ga magmatism awaits U-Pb geochronology. All gabbro units contain trace amounts of disseminated sulphides. Chalcopyrite is the most abundant, and there is a wide range of associated base and precious metal-bearing minerals including Zn, Pb, Ni, Co, Ag and platinum group sulphides, selenides and native metals.

ACKNOWLEDGMENTS

The 1994 field work was carried out with logistic support from Ascot Resources Ltd. We thank Tim Sandberg, Nick Szabo, Frank Ferguson, the Ascot field crew, and Ken Morley of Discovery Mining Services, for sharing camp facilities and for co-operation and assistance with all aspects of our mapping. Great Slave Helicopters provided reliable helicopter support. We are grateful to Deborah Lemkow for assistance with figure production; to Dave Sharpe and Doug Hodgson for information on glacial geology; to Armand Tsai for expert assistance on the SEM; and to Charlie Jefferson and Bill Davis for discussions and review.

REFERENCES

Bond, K.
1977: Victoria Island - 1976 Final Report; Uranerz Exploration and Mining Ltd; Project 71-22, 14 p. + appendix and maps.

Campbell, F.H.A.
1981: Stratigraphy and tectono-depositional relationships of the Proterozoic rocks of the Hadley Bay area, northern Victoria Island, District of Franklin; in Current Research, Part A; Geological Survey of Canada, Paper 81-1A, p. 15-22.

Campbell, F.H.A. and Cecile, M.P.
1979: The northeastern margin of the Aphebian Kilohigok Basin, Melville Sound, Victoria Island, District of Franklin; in Current Research, Part A; Geological Survey of Canada, Paper 79-1A, p. 91-94.

Christie, R.L.
1964: Diabase-gabbro sills and related rocks of Banks and Victoria Islands, Arctic Archipelago; Geological Survey of Canada, Bulletin 105, 13 p.

Christie, R.L., Cook, D.G., Nassichuk, W.W., Trettin, H.P., and Yorath, C.J.
1972: The Canadian Arctic Islands and the Mackenzie region; 24th International Geological Congress, Montreal, Guidebook, Field excursion A66, 146 p.

Davis, W.J., Fryer, B.J., and King, J.E.
1994: Geochemistry and evolution of Late Archean plutonism and its significance to the tectonic development of the Slave craton; Precambrian Research, v. 67, p. 207-241.

Dixon, J.
1979: Comments on the Proterozoic stratigraphy of Victoria Island and the Coppermine area, Northwest Territories; in Current Research, Part B; Geological Survey of Canada, Paper 79-1B, p. 263-267.

Gall, Q.
1992: Precambrian paleosols in Canada; Canadian Journal of Earth Sciences, v. 29, p. 2530-2536.

Heaman, L.M., LeCheminant, A.N., and Rainbird, R.H.
1992: Nature and timing of Franklin igneous events, Canada: implications for a late Proterozoic mantle plume and the break-up of Laurentia; Earth and Planetary Science Letters, v. 109, p. 117-131.

Kerans, C., Ross, G.M., Donaldson, J.A., and Geldsetzer, H.J.
1981: Tectonism and depositional history of the Helikian Hornby Bay and Dismal Lakes groups, Distrcit of Mackenzie; in Proterozoic Basins of Canada, (ed.) F.H.A. Campbell; Geological Survey of Canada, Paper 81-10, p. 157-182.

Jefferson, C.W., Hulbert, L.J., Rainbird, R.H., Hall, G.E.M., Grégoire, D.C., and Grinenko, L.
1994: Mineral resource assessment of the Neoproterozoic Franklin igneous events of Arctic Canada: comparison with the Permo-Triassic Noril'sk-Talnakh Ni-Cu-PGE deposits of Russia; Geological Survey of Canada, Open File 2789, 48 p.

LeCheminant, A.N. and Heaman, L.M.
1989: Mackenzie igneous events, Canada: Middle Proterozoic hotspot magmatism associated with ocean opening; Earth and Planetary Science Letters, v. 96, p. 38-48.

McCormick, D.S. and Grotzinger, J.P.
1993: Distinction of marine from alluvial facies in the Paleoproterozoic (1.9 Ga) Burnside Formation, Kilohigok basin, N.W.T., Canada; Journal of Sedimentary Petrology, v. 63, p. 398-419.

Parrish, R.R., Roddick, J.C., Loveridge, W.D., and Sullivan, R.W.
1987: Uranium-lead analytical techniques at the geochronology laboratory, Geological Survey of Canada; in Radiogenic Age and Isotope Studies: Report 1; Geological Survey of Canada, Paper 87-2, p. 3-7.

Rainbird, R.H., Jefferson, C.W., Hildebrand, R.S., and Worth, J.K.
1994: The Shaler Supergroup and revision of Neoproterozoic stratigraphic nomenclature in the Amundsen Basin, Districts of Franklin and Mackenzie; in Current Research 1994-A, Geological Survey of Canada, p. 61-70.

Roddick, J.C.
1987: Generalized numerical error analysis with applications to geochronology and thermodynamics; Geochimica and Cosmochimica Acta, v. 51, p. 2129-2135.

Stevens, R.D., Delabio, R.N., and Lachance, G.R.
1982: Age determinations and geological studies, K-Ar Isotopic Ages, Report 16; Geological Survey of Canada, Paper 82-2, p. 33.

Thorsteinsson, R. and Tozer, E.T.
1962: Banks, Victoria, and Steffanson Islands, Arctic Archipelago; Geological Survey of Canada, Memoir 330, 83 p.

van Breemen, O., Davis, W.J., and King, J.E.
1992: Temporal distribution of granitoid plutonic rocks in the Archean Slave Province, northwest Canadian Shield; Canadian Journal of Earth Sciences, v. 29, p. 2186-2199.

Wanless, R.K., Stevens, R.D., Lachance, G.R., and Delabio, R.N.
1979: Age determinations and geological studies, K-Ar Isotopic Ages, Report 14; Geological Survey of Canada, Paper 79-2, p. 31.

Washburn, A.L.
1947: Reconnaissance geology of portions of Victoria Island and adjacent regions, Arctic Canada; Geological Society of America, Memoir 22, 142 p.

Young, G.M.
1974: Stratigraphy paleocurrents and stromatolites of the Hadrynian (Upper Precambrian) rocks of Victoria Island, Arctic Archipelago, Canada; Precambrian Research, v. 1, p. 13-41.

Young, G.M. and Jefferson, C.J.
1975: Late Precambrian shallow water deposits, Banks and Victoria Islands, Arctic Archipelago; Canadian Journal of Earth Sciences, v. 12, p. 1734-1748.

Geological Survey of Canada Project 890011

Lamprophyre dykes in the Awry plutonic suite, North Arm, Great Slave Lake, Northwest Territories

A.N. LeCheminant
Continental Geoscience Division, Ottawa

LeCheminant, A.N., 1996: Lamprophyre dykes in the Awry plutonic suite, North Arm, Great Slave Lake, Northwest Territories; in Current Research 1996-C; Geological Survey of Canada, p. 11-18.

Abstract: Northerly- to northeasterly-striking lamprophyre dykes intrude Paleoproterozoic diabase dykes and the Archean Awry plutonic suite 80 km west of Yellowknife. The lamprophyres, classified as clinopyroxene or hornblende spessartites, contain chromite xenocrysts of upper mantle origin, olivine pseudomorphs, and abundant clinopyroxene and hornblende phenocrysts and xenocrysts set in a groundmass rich in amphibole and sodic plagioclase. Well-defined internal zoning and strong preferred orientation of crystals within the narrow dykes result from flow differentiation. Disaggregated granitoid xenoliths and resorbed quartz and feldspar xenocrysts in the lamprophyres indicate significant crustal contamination. The lamprophyric magmas originated as mantle-derived partial melts produced under volatile-rich melting conditions. They underwent fractional crystallization and crustal contamination during ascent. The magmas tapped metasomatized lithospheric mantle beneath the Slave Province, perhaps originally altered in the Archean and possibly modified by fluids released during east-dipping subduction beneath the Slave craton during formation of Wopmay orogen.

Résumé : À 80 km à l'ouest de Yellowknife, des dykes de lamprophyre d'orientation nord à nord-est recoupent des dykes de diabase du Paléoprotérozoïque et la suite plutonique d'Awry de l'Archéen. Les lamprophyres, classifiés dans les spessartites à clinopyroxène ou à hornblende, contiennent des xénocristaux de chromite provenant du manteau supérieur, des cristaux pseudomorphes d'olivine et d'abondants phénocristaux et xénocristaux de clinopyroxène et de hornblende dans une matrice riche en amphiboles et en plagioclases sodiques. La zonalité interne bien définie et l'orientation fortement préférentielle des cristaux dans les dykes étroits sont dues à la différenciation d'écoulement. La désagrégation des xénolites de granitoïde et la résorption des xénocristaux de quartz et de feldspath dans les lamprophyres indiquent une contamination crustale significative. Les magmas lamprophyriques proviennent de roches partiellement fondues issues du manteau dans des conditions de fusion riches en matières volatiles. Ils ont subi une cristallisation fractionnée et une contamination par la croûte durant leur ascension. Les magmas ont transpercé le manteau lithosphérique métasomatisé sous la Province des Esclaves, peut-être initialement altéré au cours de l'Archéen et probablement modifié par les fluides libérés durant la subduction à pendage est sous le craton des Esclaves tout au long de l'orogenèse de Wopmay.

INTRODUCTION

Recent discoveries of diamond-rich Eocene kimberlites in the central Slave Province (Schiller, 1994; Pell, 1995) and on-going diamond exploration throughout the province have increased interest in the structure and history of the lithospheric mantle beneath the craton. The distribution, age, and composition of mantle-derived rocks, such as kimberlites and lamprophyres, provide important evidence about the deep crustal and mantle processes that formed and modified the craton. Lamprophyre dykes are a widespread but often ignored feature of Precambrian cratons worldwide (Rock, 1991); however, surprisingly few lamprophyres have been reported from the Slave Province. An Archean ultramafic lamprophyre, rich in crustal xenoliths, intrudes the Yellowknife greenstone belt at the Con Gold mine (Webb and Kerrich, 1988). North-striking clinopyroxene-rich lamprophyres containing abundant groundmass biotite cut the Awry plutonic suite east of the Stagg River fault in the Yellowknife map area (J.B. Henderson, pers. comm., 1995). Field notes from the Lac de Gras area (Folinsbee, 1949) report several small lamprophyre dykes; most are foliated porphyritic hornblende- and clinopyroxene-bearing rocks of Archean age (B.A. Kjarsgaard, pers. comm., 1995). A carbonated minette breccia pipe, carrying subrounded gneiss clasts, is associated with calcitic magmatic activity during late stages of emplacement of the 2188 Ma Big Spruce Lake alkaline intrusion (Cavell and Baadsgaard, 1986). Other alkaline intrusions of similar age within the Slave Province, such as the 2176 Ma Blatchford Lake intrusive suite (Bowring et al., 1984; Sinclair et al., 1994), have no reported association with lamprophyres.

In 1993 and 1994, during sampling of Paleoproterozoic Indin diabase dykes near Yellowknife, several crosscutting amphibole-rich lamprophyre dykes were noted. Traverses in 1995, in a small area 80 km west of Yellowknife (Fig. 1), indicated the lamprophyres form a discontinuous array of northerly- to northeasterly-striking dykes that intrude both the Indin dykes and an Archean granite of the Awry plutonic suite. This report presents field descriptions of the lamprophyres, plus initial results of petrographic and microprobe studies. The lamprophyres contain chromite xenocrysts, olivine pseudomorphs, abundant clinopyroxene and amphibole phenocrysts and xenocrysts, and minor phlogopite/biotite. Disaggregated granitoid xenoliths, and resorbed quartz and feldspar xenocrysts attest to significant crustal contamination.

GEOLOGICAL SETTING

Archean granite of the post-Yellowknife Supergroup Awry plutonic suite (Henderson, 1985) is well-exposed in lichen-free outcrops throughout the area mapped (Fig. 1). The massive, medium grained, pink leucocratic syenogranite contains minor pegmatitic patches, but otherwise the syenogranite is uniform in composition and inclusion-free.

Numerous northerly- to northeasterly-striking diabase dykes transect the granite and are responsible for many of the wooded, linear structures throughout the area. A few dykes are exposed across widths of up to 50 m, but many are recessive and only chilled margins against granite can be seen. Locally, small diabase dykes are abundant and they have a wide range of primary orientations controlled, in part, by pre-existing joint sets in the granite. The small dykes are characterized by irregular branching segments and zigzag contacts; continuity of chilled margins indicates that even right-angle branches are primary features formed during one emplacement event. There are no exposed crosscutting relationships to indicate more than one age of diabase emplacement, however, the diabase dyke distribution in the northeastern part of the area suggests there could be covered intersections. The dykes are part of the Indin swarm (McGlynn and Irving, 1975), a major set of northeast- and northwest-striking dykes throughout the southwestern Slave Province. K-Ar and Rb-Sr whole rock age determinations suggest the Indin dykes are a conjugate set, emplaced at about 2.1-2.0 Ga (Leech, 1966; Gates and Hurley, 1973). These ages are consistent with paleomagnetic data for the swarm (McGlynn and Irving, 1975), which show a remanence similar to that of the 2.03 Ga Lac de Gras swarm (LeCheminant, 1994; LeCheminant et al., 1995).

A northwest-striking fault is interpreted to underlie a chain of lakes across the map area (Fig. 1), defining two domains with different diabase dyke patterns. Regional air photo interpretation indicates this fault is one of numerous left-lateral faults that offset Indin diabase dykes and the Awry plutonic suite. They are part of a major array of left-lateral faults throughout the southwestern Slave Province (Henderson, 1985) that offset Indin dykes and partly controlled Paleoproterozoic uplift of Archean high grade rocks 100 km north of the lamprophyre locality (Henderson and Chacko, 1995; Fig. 1). The faults offset the Blatchford Lake intrusive suite, emplaced at 2176 Ma, but are older than the Great Slave Lake Supergroup, deposited before 1865 Ma (Bowring et al., 1984; Henderson, 1985; Sinclair et al., 1994).

LAMPROPHYRE DYKE SWARM

Thin, northerly- to north-northeasterly-striking lamprophyre dykes occur throughout the map area (Fig. 1). Dyke continuity is not sufficient to determine their age relative to the northwest fault, and the regional extent of the swarm outside the area mapped in detail is not known. The lamprophyres crosscut Indin diabase dykes at a low-angle, and occur in clusters of two or three sub-parallel dykes. The average strike of the swarm is 007°; many dyke contacts are steep to vertical, however, several segments have dips as low as 50°. All lamprophyre dykes are <1.5 m thick, and they typically range in width from 10 cm to 1.0 m. Individual dykes are widest and most continuous in segments oriented approximately perpendicular to the regional strike of the swarm. Abrupt changes in direction and thickness of some dykes are influenced locally by joint sets in the host granite. Some lamprophyres are parallel to small diabase dykes (Fig. 2a) that intruded beside larger continuous dykes of the Indin swarm. Sharp jogs in the lamprophyres exploit pre-existing joints to form thin, locally discontinuous dyke segments. Irregular horns project a short distance from many of these offsets; most horns are parallel to the main dyke segment and tips point in both directions,

with no consistent pattern. Some dykes are offset into overlapping en-echelon segments with both left- and right-lateral offsets and, locally, single dykes branch into two or three smaller dykes, several metres apart. One dyke tapers into a narrow breccia zone containing a discontinuous central lamprophyre with parallel joints on both sides. The narrow lamprophyre is locally altered and cut by thin dolomite-barite veins.

Primary textures and mineralogy are well-preserved in the lamprophyres. The amphibole-rich rocks are brown-weathering and the dykes have well-defined internal zones parallel to their margins resulting from alignment and concentration of mafic phenocrysts and xenocrysts (Fig. 2b). Exposed surfaces are pitted due to weathering of altered olivine xenocrysts; most dykes also contain fresh clinopyroxene and/or amphibole phenocrysts to 1 cm. Narrow dykes,

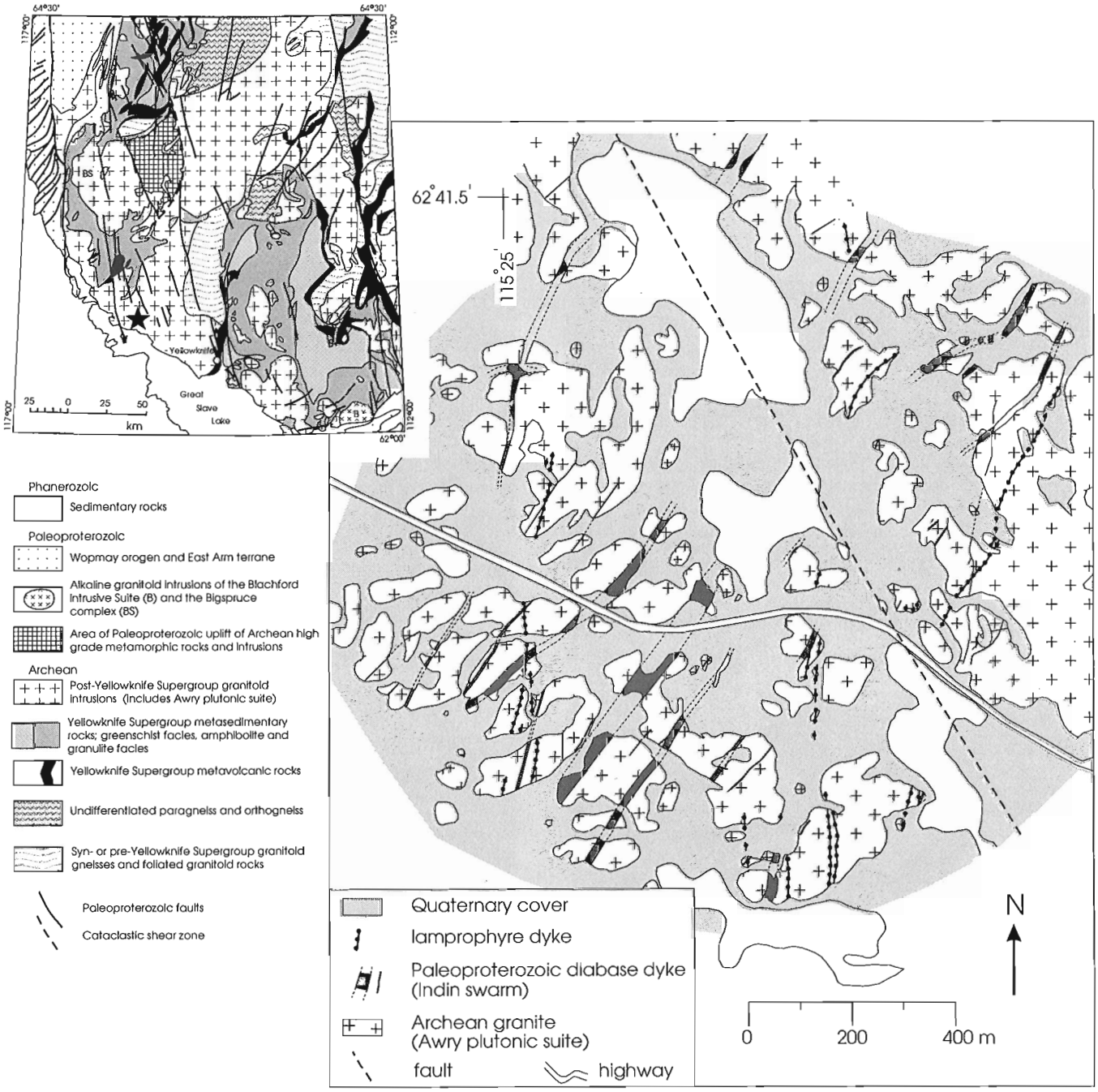

Figure 1. *Detailed geological map showing outcrop distribution of lamprophyre and Indin diabase dykes cutting granite of the Awry plutonic suite 80 km west of Yellowknife. The location of the map area is indicated by a black star on the inset map of the southwestern Slave Province (modified from Henderson and Chacko, 1995).*

particularly those <30 cm wide, have a well-defined central zone containing up to 50% phenocrysts and xenocrysts, primarily altered olivine plus euhedral clinopyroxene or acicular amphibole, with minor phlogopite/biotite and oxides. In dykes >1 m wide, the central zone is more diffuse and contains irregular, late-crystallizing feldspar-rich patches, and blue quartz and pink feldspar xenocrysts. Rounded xenoliths of granite, similar to the country rock, are sparsely distributed. Amphiboles are strongly aligned near chilled margins, and several dykes contain carbonate-rich ocelli and elongate carbonate-rich amygdules aligned at a shallow angle to dyke walls.

PETROGRAPHY

The fine grained lamprophyres contain abundant mafic phenocrysts and xenocrysts set in a groundmass rich in amphibole and sodic plagioclase (Fig. 3a-c). They are classified as clinopyroxene or hornblende spessartites (Streckeisen, 1979; Rock, 1984;), however, the dykes are highly variable mineralogically and texturally and the two rock types are gradational into each other. Dykes contain 5-20% mineral aggregates interpreted as pseudomorphs after olivine (Fig 3a). The aggregates, made up of talc+calcite±quartz or chlorite+calcite±epidote±colourless amphibole, contain small euhedral chromite inclusions and some are surrounded by a thin amphibole rim. Chromites also occur as larger, isolated xenocrysts in the groundmass.

Clinopyroxene spessartites contain up to 30% clinopyroxene phenocrysts, both as zoned euhedral crystals and as partly disaggregated crystal clusters (Fig. 3b). Some euhedral crystals have partly resorbed, pale green, Na-bearing cores, with more Mg-rich colourless rims that contain minor Cr. Typically, the clinopyroxene crystals are not altered, although some rocks contain crystals with altered carbonate-replaced cores, or pseudomorphs completely altered to carbonate with

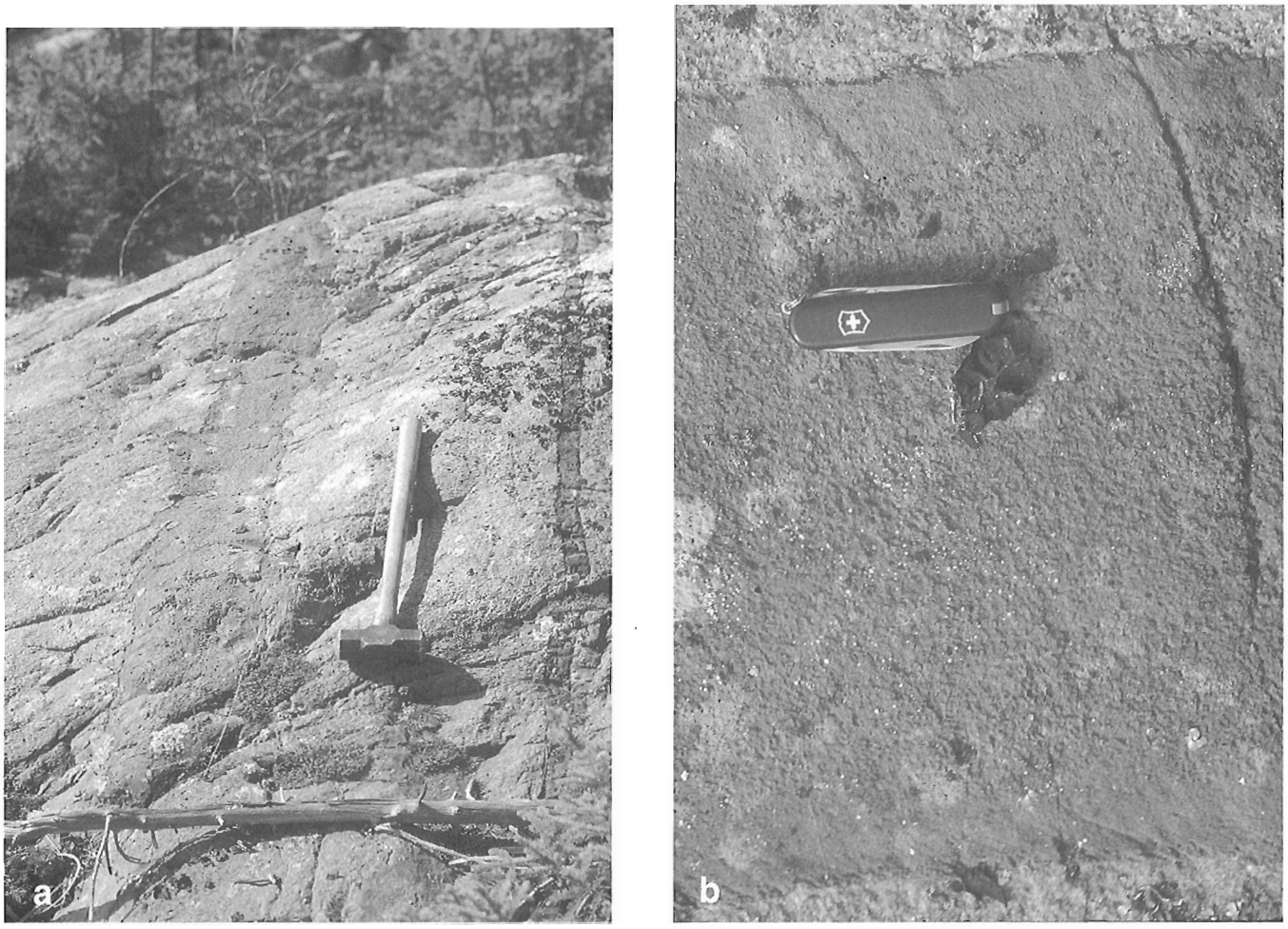

Figure 2. a) *Parallel lamprophyre and diabase dykes cutting granite of the Awry plutonic suite. The younger lamprophyre, left of the hammer, has irregular joint-controlled contacts in contrast to the straight contacts of the small diabase to the right. Note: variations in surface texture and lichen cover help distinguish the crystal rich central zone of the lamprophyre from the chilled margins. Hammer head is 15 cm long.* ***b)*** *Closeup view of another lamprophyre dyke. Variation in the texture of the weathered surface distinguishes the crystal-rich centre of the dyke from the chilled margins in contact with granite on each side. Penknife is 6 cm long.*

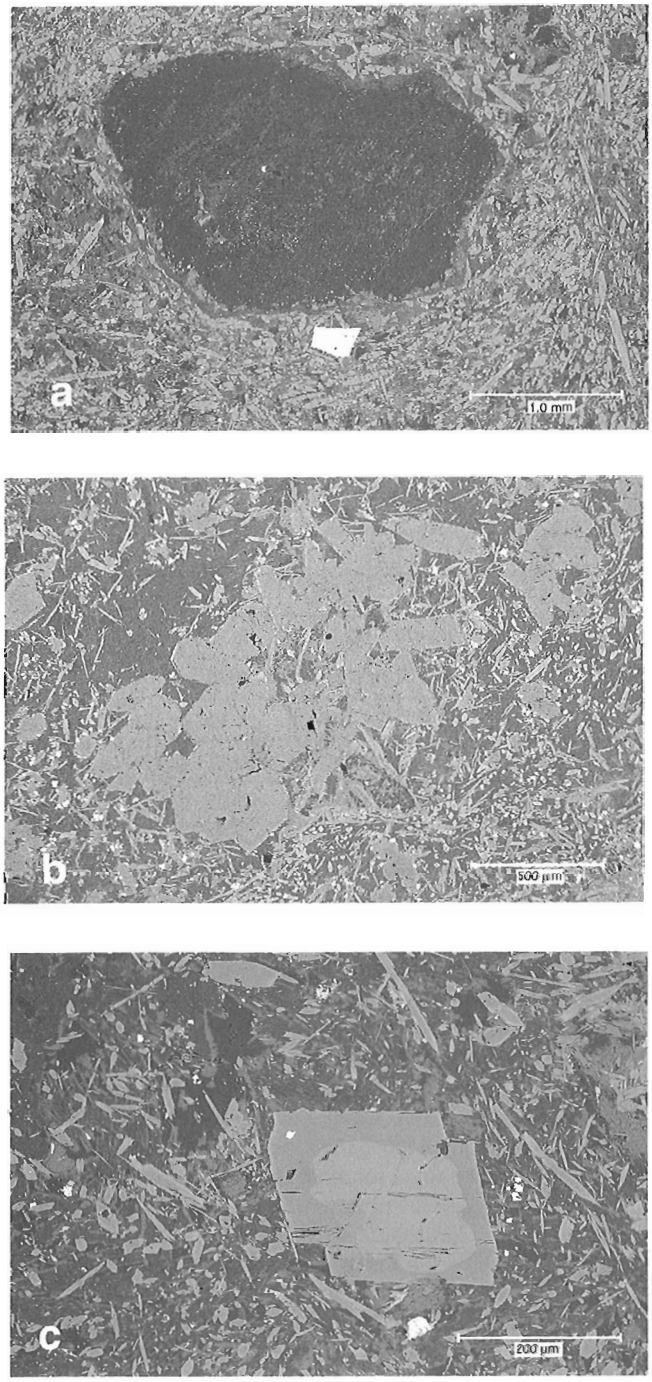

Figure 3. *Backscattered electron images of lamprophyres.* ***a)*** *Two altered mafic xenocrysts (black) are enclosed in a groundmass rich in acicular amphibole (light grey) and feldspar. Single chromite grains (white) occur in each of the altered xenocrysts; a larger angular chromite grain is isolated in the groundmass – refer to Table 1 for analyses (hornblende spessartite 94 LAA T153-1).* ***b)*** *Partly disaggregated clinopyroxene cluster (light grey) set in a feldspar-rich matrix, with variable proportions of acicular hornblende (clinopyroxene spessartite 95 LAA T141-3).* ***c)*** *Hornblende microphenocryst with a xenocrystic Fe-rich core, and a zoned, more Mg-rich rim (hornblende spessartite 94 LAA T153-4).*

disseminated opaques. Hornblende is abundant in the groundmass of clinopyroxene spessartites (Fig. 3b), but only rarely occurs as phenocrysts. Hornblende spessartites, on the other hand, contain both abundant groundmass amphibole and up to 20% brown hornblende phenocrysts and microphenocrysts (Fig. 3c). Olivine pseudomorphs containing chromite inclusions are common, but hornblende-phyric dykes contain little or no fresh clinopyroxene. Many of the zoned hornblende phenocrysts have a darker Fe-rich core, with a sharp break to a zoned, lighter coloured rim. Cores are pleochroic from medium brown to pale yellow brown; rims are the same colour but lighter in intensity. A few phenocrysts have multiply-zoned cores and contain rare oxide and red-brown biotite inclusions. Both core and rim amphiboles contain K and Na, and the lighter coloured rims have higher Mg and lower Fe. Strongly pleochroic, zoned biotite/phlogopite microphenocrysts comprise up to 4% of the rocks. They are aligned parallel to nearby amphiboles, and can be partly altered to chlorite and opaques.

The groundmass contains up to 30% elongate, zoned amphibole needles that are strongly aligned around phenocrysts and parallel to chilled margins. Plagioclase is the other abundant primary groundmass mineral. Irregular-shaped interstitial grains make up 30-50% of the rock. The sodic plagioclase is zoned and contains variable sericite, chlorite and carbonate replacement and alteration. Dusty brown K-feldspar and clear interstitial quartz are less common groundmass minerals, along with accessory biotite, Fe-Ti oxides and apatite. Alteration minerals include locally abundant carbonate and pale green chlorite, and minor rutile, titanite, pyrite, chalcopyrite, and sphalerite. Barite and a few grains of strontianite occur in late seams associated with altered xenocrysts.

Many rocks in thin section, and to a lesser extent macroscopically, have a distinctive feldspathic globular structure, common in other lamprophyres worldwide (Rock, 1991). In these lamprophyres, irregular, coarser segregations rich in feldspar are separated by zones of abundant flow-oriented amphibole needles. Also, amphibole needles are concentrated and strongly aligned around hornblende and clinopyroxene phenocrysts, and they rim olivine pseudomorphs and chlorite-quartz-carbonate amygdules/ocelli. Quartz and quartz-microcline xenocrysts are embayed and can be surrounded by a thin quartz and K-feldspar rich zone.

CHROMITE XENOCRYSTS

Chromite occurs as small inclusions within altered mafic xenocrysts and, rarely, as isolated xenocrysts in the groundmass (Fig. 3a). Microprobe analyses of one isolated xenocryst (Table 1) indicates the chromite has up to 54% Cr_2O_3 and uniform high Mg and Al contents. The grain contains inclusions of phlogopite and apatite and has a thin outer rim with low Mg, higher Fe and Ti, and variable high Mn and Zn. Small euhedral chromite grains within altered xenocrysts have a similar range of compositions, many with high Mn, Zn, and Ti rims. Chromite-bearing spessartite dykes have been reported from Japan (Suzuki and Shiraki, 1980) and Béziat et al. (1993) noted the presence of Zn-rich chromite in

Table 1. Microprobe analyses of chromites in lamprophyres. Analyses 1-5 are from an angular xenocryst in the groundmass of a spessartite dyke (Fig. 3a); 1-3 are representative analyses of the center of the xenocryst and 4-5 are from the rim. Analysis 6 is a Zn-rich chromite from spessartite in the Montagne Noire, France (Béziat et al., 1993) and analyses 7-9 are chromite inclusions in phlogopite from ultrapotassic lamprophyres in the District of Keewatin (Peterson and LeCheminant, 1993).

	1 T153 C1	2 T153 C2	3 T153 C3	4 T153 R1	5 T153 R2	6	7 P150	8 T072-X2 R	9 T072-X2 C
SiO_2						0.16	0.18	0.25	0.07
TiO_2	0.49	0.54	0.43	0.66	1.03	0.38	0.23	0.15	0.79
Al_2O_3	9.66	10.05	8.84	8.69	9.23	12.72	7.02	1.85	9.10
Cr_2O_3	53.22	52.88	54.06	50.53	44.76	46.33	57.25	54.05	51.48
FeO	18.41	19.15	20.14	26.13	28.85	27.81	22.93	32.97	28.26
Fe_2O_3	7.15	7.02	6.62	8.00	10.51	6.95			
NiO	0.15	0.15	0.09	0.04	0.12		0.17	0.05	0.10
MnO	0.26	0.35	0.25	1.59	2.15	0.87	1.69	3.53	0.79
MgO	9.58	9.26	8.39	3.80	0.70	1.31	8.52	0.65	6.26
CaO							0.06	0.14	0.13
ZnO	0.20	0.07	0.15	0.34	2.24	3.40	0.15	2.11	1.21
V_2O_3	0.09	0.05	0.05	0.13	0.22		0.02	0.06	0.02
sum	99.21	99.52	99.02	99.91	99.81	99.98	98.22	95.80	98.22

spessartite sills in the Montagne Noire, France (Table 1). Potassium-rich lamprophyres also contain chromite xenocrysts, some with Zn-rich chromites that occur as inclusions in phlogopite (Wagner and Velde, 1985; Peterson and LeCheminant, 1993).

DISCUSSION AND CONCLUSIONS

Well-defined internal zones and strong preferred crystal orientation in the lamprophyre dykes are interpreted to result from crystal sorting by flow differentiation (Bhattacharji and Smith, 1965; Ross, 1986). Effects of flow differentiation are most evident in narrow dyke segments (<30 cm wide), resulting in sharply bounded internal layers containing variable proportions of phenocrysts and xenocrysts. Some dyke margins preserve two chilled zones indicative of closely spaced pulses of magma – the second pulse arrived when the outer glassy chilled zone was still able to interact with phenocrysts in the newly injected magma to produce flow and drag features along an irregular interface. Breccia zones extending out from dyke segments suggest gas-driven fracturing occurred in advance of magma injection. Narrow widths and irregular segmentation of the lamprophyre dykes, and lack of consistent horizontal flow indicators suggest a significant vertical component of magma flow.

The lamprophyric magmas carried chromite and completely altered olivine xenocrysts, along with highly variable proportions of clinopyroxene and amphibole phenocrysts. Complex zoning in the phenocrysts and the presence of resorbed xenocrystic cores and partly disaggregated crystal clusters indicate the magmas underwent fractional crystallization interrupted by mixing with new batches of more primitive magma. Blue quartz and pink microcline xenocrysts, interpreted to be remnants from assimilation of granitic rocks, suggest the magmas were modified by crustal contamination during ascent. Lamprophyres with characteristics similar to the Slave lamprophyres are interpreted to crystallize from magmas derived by volatile-rich melting of a mantle source enriched by subduction-driven fluids (Macdonald et al., 1985; Thorpe et al., 1993). Similarly, eruption of ultrapotassic lamprophyres near Baker Lake in the Churchill Province at about 1.85 Ga is interpreted to have been triggered by subduction-related metasomatism (Peterson et al., 1994). Both the Baker Lake and Slave lamprophyres contain Zn- and Mn-rich chromite xenocrysts, altered by fluid metasomatism that may have occurred during subduction-driven metamorphism of oceanic lithosphere (Schulze, 1986) containing Zn- and Mn-bearing sediments.

An Archean ultramafic lamprophyre, rich in crustal xenoliths ranging up to 3.2 Ga in age, intrudes the Yellowknife greenstone belt at the Con Gold mine (Nikic et al., 1980;

Webb and Kerrich, 1988). The xenoliths indicate old granitoid crust underlies the Yellowknife greenstone belt, and intrusion of the lamprophyre shows that alkaline ultramafic magmas derived from metasomatized upper mantle were generated during the Archean (Webb and Kerrich, 1988). The amphibole-rich lamprophyres west of Yellowknife crosscut Indin diabase dykes and are therefore younger than 2.0 Ga. The underlying mantle, initially altered in the Archean, may have been modified by Paleoproterozoic subduction beneath the western margin of the Slave Province. Lamprophyric magmas originated, perhaps, in metasomatically altered lithospheric mantle shortly after cessation of subduction following 1.91-1.84 Ga collisional events in Wopmay orogen (Hoffman, 1989). Ultrapotassic lamprophyres at Baker Lake erupted from a phlogopitized upper mantle within the interior of an Archean terrane, requiring large horizontal penetration of subducted lithosphere (Peterson et al., 1994). In contrast, the Slave lamprophyres are relatively close to the western margin of the Slave craton (Fig. 1) and shallow east-dipping subduction beneath the Slave margin during generation of the 1.88-1.84 Ga Great Bear arc (Hildebrand et al., 1987) could have produced pockets of metasomatized amphibole-bearing lithospheric mantle.

ACKNOWLEDGMENTS

Thanks are extended to Craig Nicolson and Martin Irving for help in Yellowknife, and to Scott Doehler, Adrienne Jones and Allie Marshall for assistance in the field. I am also grateful to Deborah Lemkow for assistance with figure production; to Gina LeCheminant for microprobe analyses; to Armand Tsai and David Walker for their expertise on the SEM; and to Bill Davis, Bruce Kjarsgaard, Tony Peterson, and John Henderson for discussions and for constructive and timely comments on the manuscript.

REFERENCES

Béziat, D., Joron, J.-L., and Monchoux, P.
1993: Spessartites in the Montagne Noire, France: mineralogical and geochemical data; European Journal of Mineralogy, v. 5, p. 879-891.

Bhattarcharji, S. and Smith, C.H.
1965: Flowage differentiation; Science, v. 145, p. 150-153.

Bowring, S.A., Van Schmus, W.R., and Hoffman, P.F.
1984: U-Pb zircon ages from Athapuscow aulacogen, East Arm of Great Slave Lake, N.W.T.; Canadian Journal of Earth Science, v. 21, p. 1315-1324.

Cavell, P.A. and Baadsgaard, H.
1986: Geochronology of the Big Spruce Lake alkaline intrusion; Canadian Journal of Earth Science, v. 23, p. 1-10.

Folinsbee, R.E.
1949: Lac de Gras, District of Mackenzie, Northwest Territories; Geological Survey of Canada, Map 977A, scale 1" to 4 miles.

Gates, T.M. and Hurley, P.M.
1973: Evaluation of Rb-Sr dating methods applied to the Matachewan, Abitibi, Mackenzie, and Sudbury dike swarms in Canada; Canadian Journal of Earth Science, v. 10, p. 900-919.

Henderson, J.B.
1985: Geology of the Yellowknife-Hearne Lake area, District of Mackenzie: a segment across an Archean Basin; Geological Survey of Canada, Memoir 414, 135 p.

Henderson, J.B. and Chacko, T.
1995: A reconnaissance of the high-grade metamorphic terrane south of Ghost Lake, southwestern Slave Province, Northwest Territories; in Current Research 1995-C; Geological Survey of Canada, p. 77-85.

Hildebrand, R.S., Hoffman, P.F., and Bowring, S.A.
1987: Tectomagmatic evolution of the 1.9 Ga Great Bear magmatic zone, Wopmay orogen, northwestern Canada; Journal of Volcanology and Geothermal Research, v. 32, p. 99-118.

Hoffman, P.F.
1989: Precambrian geology and tectonic history of North America; in The geology of North America – An overview, (ed.) A.W. Bally and A.R. Palmer; Geological Society of America, DNAG v. A, p. 447-511.

LeCheminant, A.N.
1994: Proterozoic diabase dyke swarms, Lac de Gras and Aylmer Lake areas, District of Mackenzie, Northwest Territories; Geological Survey of Canada, Open File 2975, scale 1:250 000.

LeCheminant, A.N., van Breemen, O., and Buchan, K.L.
1995: Proterozoic dyke swarms, Lac de Gras-Aylmer Lake area, N.W.T.; Regional distribution, ages and paleomagnetism; Geological Association of Canada/Mineralogical Association of Canada, Program with Abstracts, v. 20, p. A57.

Leech, A.P.
1966: Potassium-argon dates of basic intrusive rocks of the District of Mackenzie, N.W.T.; Canadian Journal of Earth Sciences, v. 3, p. 389-412.

Macdonald, R., Thorpe, R.S., Gaskarth, W., and Grindrod, A.R.
1985: Multi-component origin of Caledonian lamprophyres of northern England; Mineralogical Magazine, v. 49, p. 485-494.

McGlynn, J.C. and Irving, E.
1975: Paleomagnetism of Early Aphebian diabase dykes from the Slave structural province, Canada; Tectonophysics, v. 26, p. 23-38.

Nikic, Z., Baadsgaard, H., Folinsbee, R.E., Krupicka, J., and Leech, A.P.
1980: Boulders from the basement, the trace of an ancient crust?; in Selected studies of Archean gneisses and Lower Proterozoic rocks, Southern Canadian Shield, (eds.) G.B. Morey and G.N. Hanson; Geological Society of America, Special Paper 182, p. 169-175.

Pell, J.A.
1995: Kimberlites in the Slave Structural Province, Northwest Territories, Canada: a preliminary review; Sixth International Kimberlite Conference, Extended Abstracts, Novosibirsk, Russia, p. 433-435.

Peterson, T.D., Esperança, S., and LeCheminant, A.N.
1994: Geochemistry and origin of the Proterozoic ultrapotassic rocks of the Churchill Province, Canada; Mineralogy and Petrology, v. 51, p. 251-276.

Peterson, T.D. and LeCheminant, A.N.
1993: Glimmerite xenoliths in early Proterozoic ultrapotassic rocks from the Churchill Province; Canadian Mineralogist, v. 31, p. 801-819.

Rock, N.M.S.
1984: Nature and origin of calc-alkaline lamprophyres: minettes, vogesites, kersantites and spessartites; Transactions of the Royal Society of Edinburgh: Earth Sciences, v. 74, p. 193-227.
1991: Lamprophyres; Van Nostrand Reinhold, New York, 285 p.

Ross, M.E.
1986: Flow differentiation, phenocryst alignment, and compositonal trends within a dolerite dike at Rockport, Massachusetts; Geological Society of America Bulletin, v. 97, p. 232-240.

Schiller, E.A.
1994: Success at Lac de Gras; Mining North, NWT Chamber of Mines, v.3, #1, p. 21-29.

Schulze, D.J.
1986: Calcium anomalies in the mantle and a subducted metaserpentinite origin for diamonds; Nature, v. 319, p. 483-485.

Sinclair, W.D., Hunt, P.A., and Birkett, T.C.
1994: U-Pb zircon and monazite ages of the Grace Lake Granite, Blatchford Lake Intrusive Suite, Slave Province, Northwest Territories; in Radiometric Age and Isotopic Studies: Report 8; Geological Survey of Canada, Current Research 1994-F, p. 15-20.

Streckeisen, A.
1979: Classification and nomenclature of volcanic rocks, lamprophyres, carbonatites, and melilitic rocks: Recommendations and suggestions of the IUGS Subcommission on the systematics of igneous rocks; Geology, v. 7, p. 331-335.

Suzuki, K. and Shiraki, K.
1980: Chromite-bearing spessartites from Kasuga-mura, Japan, and their bearing on possible mantle origin andesite; Contributions to Mineralogy and Petrology, v. 71, p. 313-322.

Thorpe, R.S., Gaskarth, J.W., and Henney, P.J.
1993: Composite Ordovician lamprophyre (spessartite) intrusions around the Midlands Microcraton in central Britain; Geological Magazine, v. 130, p. 657-663.

Webb, D.R. and Kerrich, R.
1988: An Archean ultramafic lamprophyre, Yellowknife: implications for tectonics and source regions; in Contributions to the Geology of the Northwest Territories, v. 3, N.W.T. Geology Division, INAC, Yellowknife, p. 115-122.

Wagner, C. and Velde, D.
1985: Mineralogy of two peralkaline, arfvedsonite-bearing minettes. A new occurrence of Zn-rich chromite; Bulletin Minéralogie, v. 108, p. 173-187.

Geological Survey of Canada Project 890011

Stratigraphy of the southern portion of an Archean stratovolcano in the Back River volcanic complex, Slave Province, Northwest Territories

M.B. Lambert
Continental Geoscience Division, Ottawa

Lambert, M.B., 1996: Stratigraphy of the southern portion of an Archean stratovolcano in the Back River volcanic complex, Slave Province, Northwest Territories; in Current Research 1996-C; Geological Survey of Canada, p. 19-28.

Abstract: Innerring and Thlewycho sequences represent an Archean stratovolcano that forms the southern part of the Back River volcanic complex. The Innerring sequence, comprising andesite/dacite lavas overlain by ash-flow tuffs and a rhyolite dome, represents the upper part of an ancestral volcano. The overlying Thlewycho sequence documents the main constructional phase of the stratovolcano. The southern portion of this sequence comprises basal andesitic/basaltic lavas overlain by an extensive volcaniclastic units containing abundant ash-flow tuffs.

Volcanism ended with effusion of large rhyolite/dacite dome complexes, one of which contains seven overlapping lava lobes separated by rhyolitic tuffs and detritus forming a pile about 550 m thick. A rhyolitic detrital apron formed along the southeastern side of this lava/dome where the volcanic complex is overlain by turbidites of the Beechy Lake Group. Carbonate cemented flow breccias, detrital, massive, oolitic and stromatolitic carbonate prevail where rhyolite lavas entered the sea.

Résumé : Les séquences d'Innerring et de Thlewycho sont reliées à un strato-volcan archéen qui s'observe dans la moitié méridionale du complexe volcanique de Back River. La séquence d'Innerring, composée de laves d'andésite-dacite sous-jacentes à des tufs pyroclastiques et un dôme de rhyolite, représente la partie supérieure d'un ancien volcan. Elle est surmontée de la séquence de Thlewycho, qui constitue la principale phase de construction du strato-volcan. La portion méridionale de cette séquence se compose, à la base, de laves andésitiques-basaltiques, lesquelles sont recouvertes de vastes unités volcanoclastiques aux tufs pyroclastiques abondants.

Le volcanisme a pris fin avec l'effusion de grands dômes de rhyolite-dacite, dont l'un se compose de sept lobes de lave se chevauchant, séparés par des tufs et des débris rhyolitiques; le tout atteint une épaisseur d'environ 550 mètres. Un tablier détritique de rhyolite s'est formé le long de la bordure orientale du complexe volcanique, là où il est recouvert de turbidites du Groupe de Beechy Lake. Les brèches de coulée à ciment carbonaté ainsi que les roches carbonatées détritiques, massives, oolitiques et stromatolitiques dominent au endroits où les laves de rhyolite se sont épanchées dans la mer.

INTRODUCTION AND GENERAL STRATIGRAPHY

The Back River volcanic complex is a ca. 2.7 Ga (van Breemen et al., 1987) stratovolcano which lies about 480 km northeast of Yellowknife, Northwest Territories. The complex, which belongs to the Back Group (Frith and Percival, 1978) of the Yellowknife Supergroup (Henderson, 1970), is somewhat anomalous in the Slave Province because it has undergone only a low degree of deformation and metamorphism (generally greenschist grade but locally up to lower amphibolite grade). The southern half of the complex, which is exposed at the crest of a broad structural dome, is essentially an eroded stratovolcano preserved in an upright position with sides steepened by regional deformation. Previous publications provide descriptions of rock units and outline preliminary stratigraphy and structure of the complex (Lambert, 1976, 1977, 1978, 1982a, b; Lambert et al. 1990, 1992).

Stratigraphy of the complex consists of four volcano-sedimentary sequences (Innerring, Thlewycho, Boucher-Regan, and Keish, Fig. 1). The Innerring sequence represents the upper part of an eroded early stage of the volcano that now forms an elliptical area in the south-central part of the complex. It includes andesite lavas overlain by dacite lavas, massive volcaniclastic units interpreted as ash-flow tuffs, and a rhyolite dome complex. All units have features consistent with subaerial deposition. Laminated volcanic siltstone and black sulphide-rich slate and shale and, locally, iron-formation mark the top of this sequence on the northern and eastern sides.

The Thlewycho sequence represents the main constructional phase of the stratovolcano. It forms an outward dipping annular succession around the Innerring sequence. Its stratigraphy, which changes around the volcano, varies from 5 cycles of andesitic to rhyolitic lava effusion followed by deposition of volaniclastic debris on the north side, to effusion of 30 subaerial, dominantly andesitic lava flows and few intermittent pyroclastic and epi-volcaniclastic units on the eastern side. Volcanism in this sequence ended with the eruption of large rhyolite/dacite dome/flow complexes around the periphery of the volcano. This event has been dated at 2692 ± 2 Ma (van Breeman et al., 1987) by U-Pb analysis on zircon from a rhyolite unit related to the Gold Lake dome, on the southern side of the stratovolcano (Fig. 1, 5). A nearly continuous but lithologically variable succession including cherty iron-formation, oolitic/stromatolitic carbonate, magnetite- sulphide- and siderite- iron-formation, sulphidic volcaniclastic rocks and graphitic slate marks the end of major constructive volcanism and beginning of turbidite sedimentation of the Beechy Lake Group.

The Boucher-Regan sequence represents a dominantly subaqueous succession deposited in the northern parts of the complex. It records effusion of basaltic pillow lava followed by andesitic lavas and late stage felsic lava domes. It may include units related to the Thlewycho and Innerring sequences.

The Keish sequence forms a broad apron on the northwest side of the volcanic complex, and is interpreted as a shallow submarine to subaerial clastic fan derived by degradation of the volcanic pile. It comprises volcaniclastic sediments that include epiclastic volcarenite, rhyolite to dacite block breccias (of debris flow, scree or landslide origin), adjacent lava domes, polymict breccia and conglomerate containing andesite and dacite/rhyolite clasts, and andesitic tuffs.

This paper presents new data on: (1) stratigraphy of the previously undivided southern and western parts of the Thlewycho sequence, (2) internal stratigraphy of the Gold Lake rhyolite dome/flow complex, in the southeastern part of the Thlewycho sequence, and (3) a new stromatolite locality.

SOUTHERN PORTION OF THE THLEWYCHO SEQUENCE

Figure 2 shows stratigraphy of the Thlewycho and Innerring sequences and Figure 2A shows details of stratigraphy in two columnar sections across the Thlewycho sequence near Thlewycho Lake and 'Boomerang' lake (See Fig. 2 in Lambert et al., 1992, for comparison with sections near Rusty Lake and Gold Lake).

Thlewycho Lake section

On the western side of the stratovolcano strata dips 45-60° westward. Along most of this side, andesitic pillow lavas form the base of the Thlewycho Sequence. They are overlain by a thick volcaniclastic succession that contains both epiclastic and pyroclastic material, but most is interpreted to be andesitic ash-flow tuffs, including both non-welded and welded varieties. Thick lenticular units of plagioclase- and plagioclase-hornblende-phyric andesite lava interrupt the central parts of this volcaniclastic succession. An extensive rhyolite lava succession about 1.2 km wide (estimated thickness of 800 m) by 10 km long forms the top of the Thlewycho sequence. Thinner (80-200 m thick) parts of this rhyolite succession continue for another 7 km around the southern side of the complex. Rhyolite flows and related coarse carbonate-cemented breccias at the top of the sequence are highly sheared and tectonically brecciated along its western side and intruded by abundant mafic dykes and sills in its northern parts. In spite of this deformation, there are "windows" where spectacular flow layering is preserved (Fig. 3). Basaltic pillow lavas, minor shale and bedded volcaniclastic rocks divide the rhyolite succession longitudinally in the northern parts of this unit.

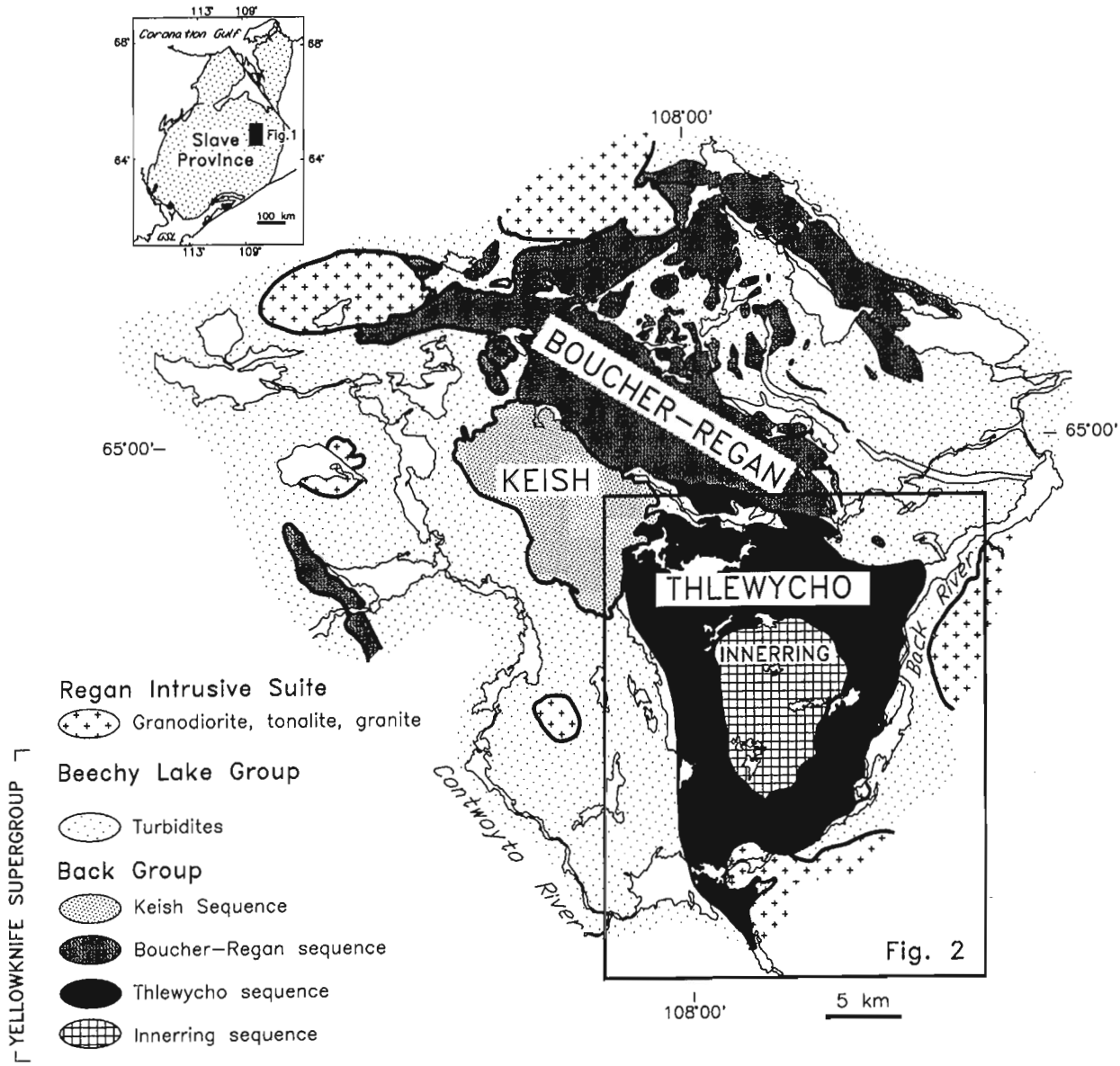

Figure 1. *Stratigraphic sequences of the Back River volcanic complex.*

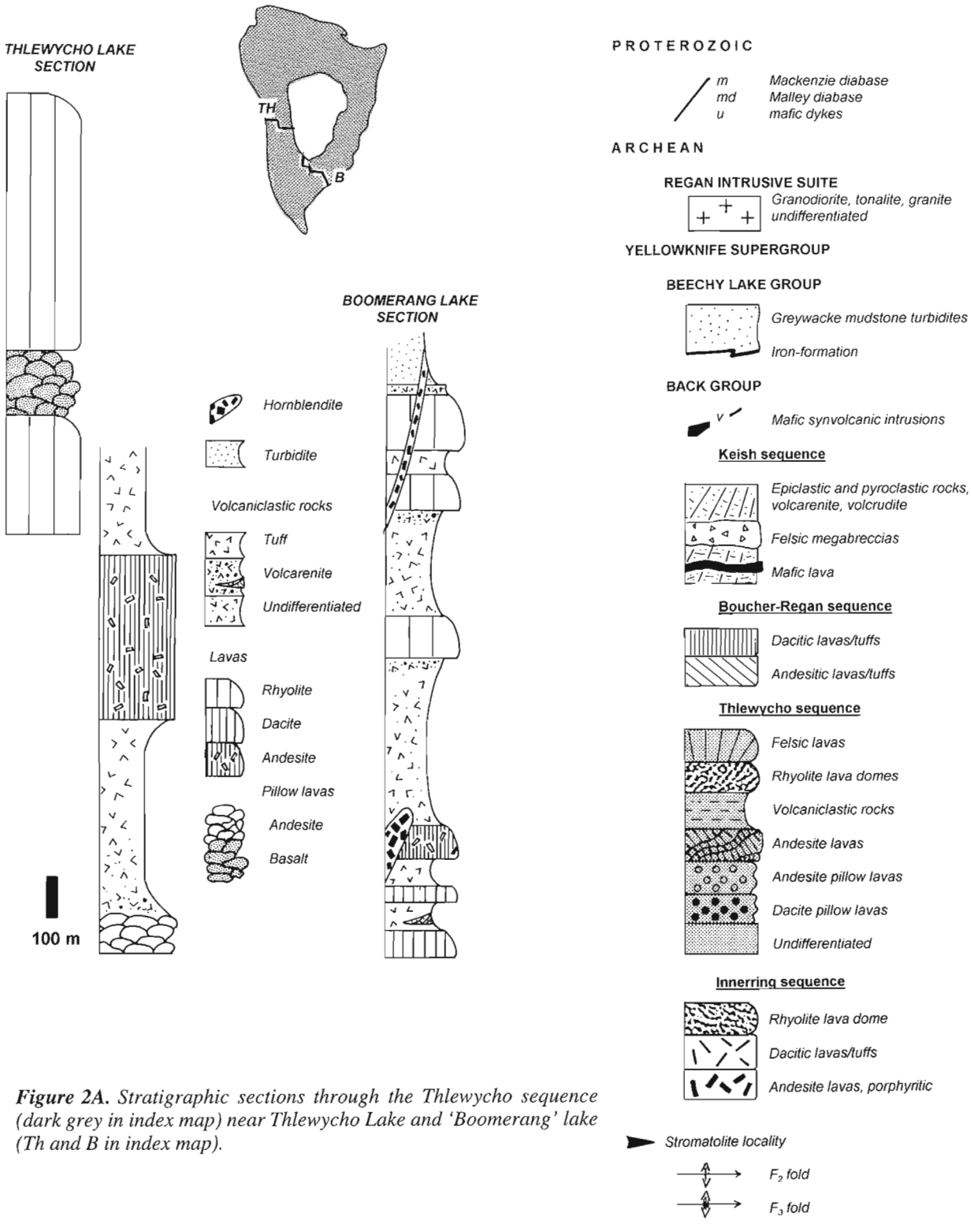

Figure 2A. *Stratigraphic sections through the Thlewycho sequence (dark grey in index map) near Thlewycho Lake and 'Boomerang' lake (Th and B in index map).*

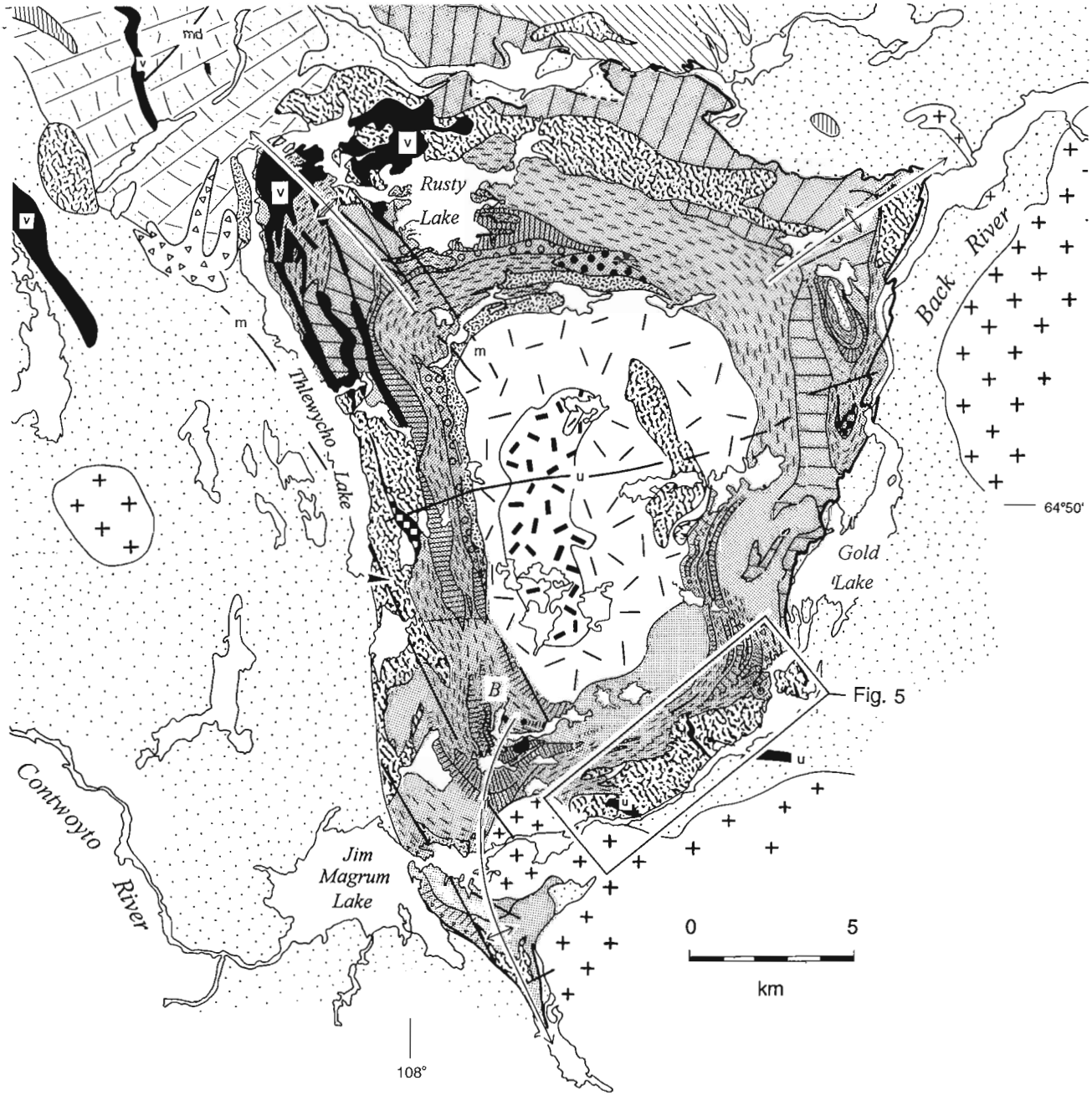

Figure 2. *Generalized geology of the Back River stratovolcano in the southern half of the Back River volcanic complex. B, 'Boomerang' lake.*

'Boomerang' Lake section

The 'Boomerang' lake section is a somewhat diagrammatic stratigraphic column from northeast of 'Boomerang' lake to the Back River southwest of Gold Lake (Fig. 2, 2A). Near the base of this section, strata in the Thlewycho sequence is shallow dipping to almost flat lying where it folds over the crest of a major anticline. Broad areas of andesitic lavas shown on the map (Fig. 2) are in fact relatively thin flows. Thicknesses of the basal units in the section probably are not accurate because of uncertain low angles of dip.

In this area, transition from the Innerring sequence to the Thlewycho sequence is poorly defined. There is no clear sedimentary break between the two volcanic sequences as there is in the northern and eastern sides of the volcano, and both sequences contain major volcaniclastic units interpreted as ash-flow tuffs. In this section the boundary is drawn arbitrarily between massive felsic tuffs, assumed to belong to the Innerring sequence, and porphyritic dacitic to andesitic lavas, presumably of the Thlewycho sequence. This 'boundary' is below or very near units that suggest erosional conditions, such as the braided stream deposits near 'Boomerang' lake (see Lambert et al., 1990) which contain carbonate-fragment breccias and crossbedded coarse carbonate sands indicating erosion from a pre-existing carbonate horizon, lower in the stratigraphy. Carbonate cemented breccias of various sorts are common at about this stratigraphic level. In areas where units are nearly flat lying, lithological contacts probably meander over broad areas (for example, the braided stream deposits near 'Boomerang' lake are less than 10 m thick yet units extend over an area 400 m across).

In general, however, basal units of the sequence comprise a few porphyritic dacite and andesite lavas interlayered with tuffs of similar composition. These units are overlain by a thick (ca. 400 m) succession of non-welded ash-flow tuffs (Fig. 4) and volcaniclastic rocks of epiclastic origin that extend around the southern and southeastern sides of the complex and interfinger with major lobes of the Gold Lake lava dome. The Gold Lake rhyolite dome marks the end of Thlewycho sequence volcanism.

THE GOLD LAKE LAVA DOME COMPLEX

The 1.5 km by 8 km Gold Lake lava dome (Fig. 5) is one of the best exposed and least deformed of the major rhyolite bodies of the Back River complex. Internal stratigraphy, except for major volcaniclastic horizons is variable probably because of the lenticular and overlapping nature of the numerous flow units. In the central part the complex (see columnar section, Fig. 5) comprises at least seven southeasterly dipping, massive, rhyolitic to dacitic lava flows separated by rhyolitic volcaniclastic units. The complex has a clastic apron along its southern side where it makes contact with turbiditic rocks of the generally overlying Beechy Lake Group. The complex ends on the western side in four thick flow lobes. The flows conformably overlie porphyritic andesite lavas and major pyroclastic units to the northwest.

Units of the dome have gentle southeasterly dips. Where interflow clastic units weather in recession and mark flow boundaries, the general inclination of large units, as seen from a distance, is about 10-20 degrees. Dips steepen within the eastern clastic apron, however, where well bedded volcaniclastic units locally show inclinations of about 40 degrees (Fig. 6). In down-dip panoramic views, some of the distinctive, blocky, cliff-forming flow units can be seen to form gentle undulations that define broad open folds. This is F3 folding (Lambert et al., 1992) of the complex about northwesterly trending axes. Assuming average dips, the cumulative thickness of the lava dome complex is about 550 m.

Figure 3. *Flow layering in rhyolite lava at south end of Thlewycho Lake. Exposure is 80 cm high. GSC 1995-244L*

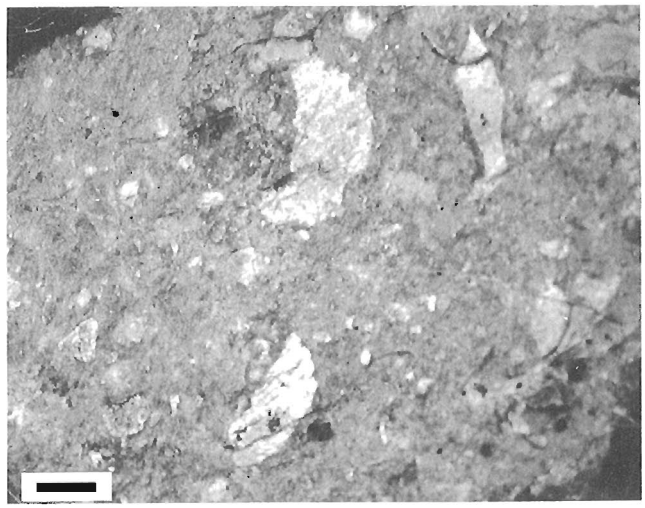

Figure 4. *Coarse, crystal-lithic lapilli tuff in ash-flow tuff unit of the Thlewycho sequence. Scale bar is 2 cm. GSC 1995-244G*

Lavas

Individual lava flow units range from 25 m to 60 m thick. The white, buff and pink weathering massive lavas are aphanitic to quartz and feldspar phyric. Rocks containing abundant coarse phenocrysts (such as the dacite flow unit near the base of the succession that contains 35% phenocrysts up to 5 mm in size) are the only distinctive felsic flow lithologies within the complex. Flow layering (Fig. 7) is rarely visible except in exceptionally clean, smooth, lichen-free exposures. Although coarse flow breccias occur throughout the lava succession, they are mainly along the eastern side of the complex.

Volcaniclastic units

Volcaniclastic units underlie the lava dome complex, form distinctive horizons that mark boundaries between flow units within it, and form an extensive felsic clastic apron along the southern side of the complex. Interflow pyroclastic/epiclastic units have maximum thickness of 30 m.

Pyroclastic rocks within the dome complex vary from very fine grained ash- or crystal-ash-tuffs to crystal-lithic lapilli tuffs. They are hard, white to buff weathering rocks like the massive rhyolite. In general, tuffs form thinner layers than the epiclastic horizons. Coarser tuffs contain relicts of glass shards, lapilli with cuspidate margins suggesting broken bubble walls or pumiceous material, fragments of broken feldspar

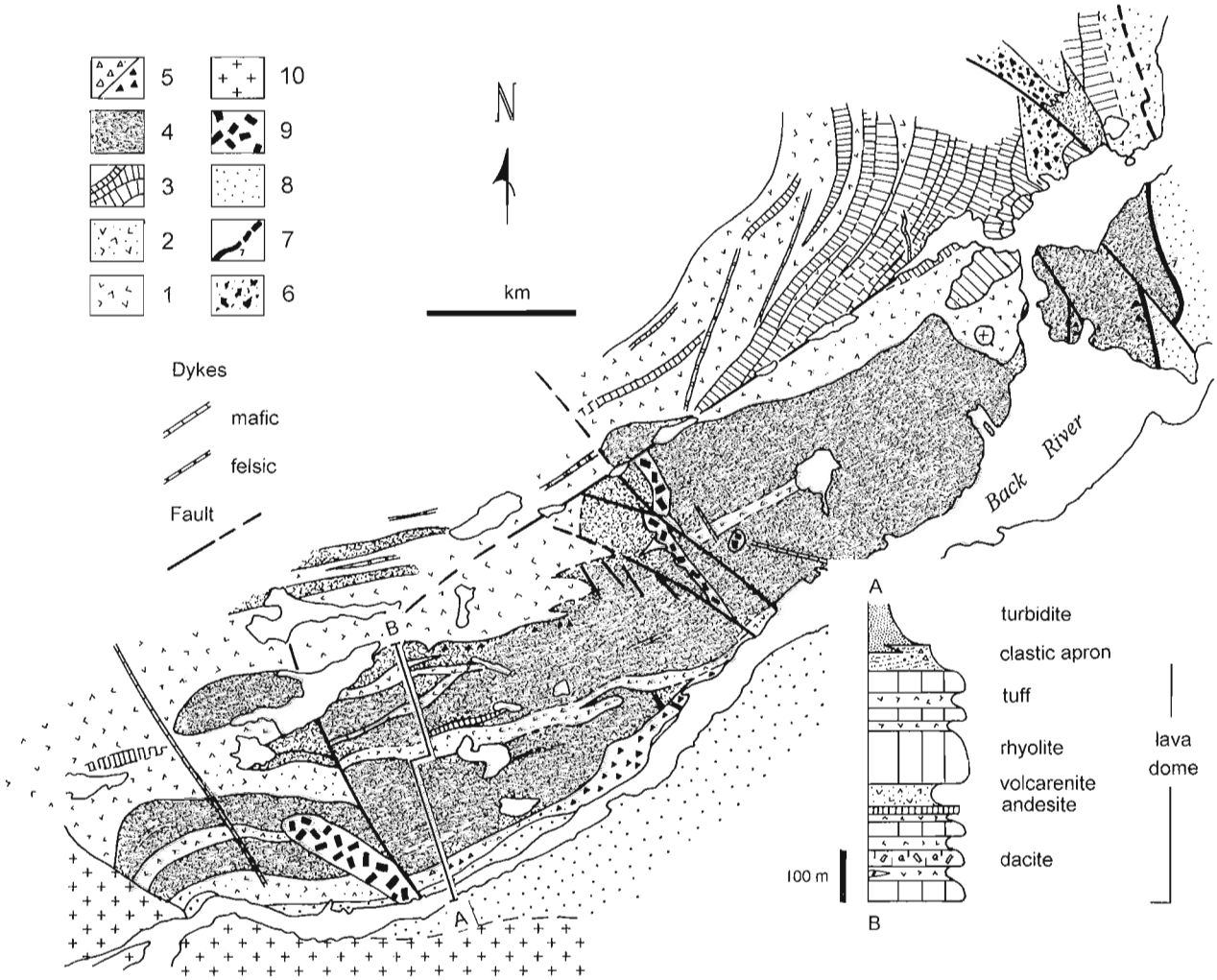

Figure 5. *Gold Lake lava dome complex. Map location shown in Figure 2. 1 – volcaniclastic rocks (dominantly tuff) undifferentiated; 2 – epicastic volcaniclastic rocks; 3 – andesite and dacite lavas; 4 – rhyolite/dacite lavas of the dome complex; 5 – rhyolite breccia / carbonate cemented breccia; 6 – avalanche breccia; 7 – iron-formation; 8 – turbidites of the Beechy Lake Group; 9 – hornblendite; 10 – granodiorite.*

crystals and in some cases lithic lapilli of porphyritic andesite. Clast sizes range from 1-2 mm to 10 cm,with most large clast sizes between 5 mm to 20 mm. Most units are massive and non layered; bedding is rare. Poorly sorted, massive units are interpreted as non welded ash-flow tuffs. Rare fine layered units are probably tuffs of air-fall origin.

Epiclastic rocks that underlie the northeastern and northwestern sides of the rhyolite complex, and form the widest band of volcaniclastic rocks in the central part of the dome complex, are grey, greenish-grey to dark grey weathering, poorly sorted, polymictic volcarenites that have knobby to pitted weathering surfaces. The silty-looking matrix is notably much softer than that of white weathering rhyolitic tuffs.

Figure 6. *Rhyolite turbidite beds in clastic apron on east side of Gold Lake dome, dipping 40° toward southeast. Exposure is about 20 m across. GSC 1995-244A.*

Figure 7. *Flow layering in rhyolite lava flow in the Gold Lake lava dome. Pencil (upper right) is 8 mm thick. GSC 1995-244I*

Clasts of porphyritic andesite (2-5 cm size and locally up to 10 cm across) and feldspar crystal fragments are much more abundant than rhyolitic clasts, except in the wide central band, where rhyolite clasts dominate.

Rocks of the 200-280 m wide (70 and 150 m thick) clastic apron along the southeastern side of the lava dome vary along strike from carbonate-cemented megabreccia (flow breccias), coarse rudite to fine pebbly sandstone and rhyolite turbidites. They are non- to poorly-sorted rocks with clasts derived mainly from adjacent felsic flows. At the northeastern end of the complex, a polymictic pebble breccia contains rounded to angular clasts (5 mm to 15 cm) predominantly of rhyolitic but also abundant angular clasts of dark grey micaceous siltstone (Fig. 8). This unit is interpreted as the distal end of coarse mass-flow deposits that were part of a shallow clastic fan at the edge of the rhyolite complex. At one location, the carbonate-cemented rhyolite flow breccia overlies massive carbonate and crossbedded clastic carbonate beds. Similarly, at the southwestern end of the lava dome rhyolite volcaniclastic rocks overlie Beechy Lake turbidites. At the eastern end of the dome, however, carbonate, iron-formation, and turbidites clearly overlie the rhyolite dome. Thus, the margin of the dome complex probably interfingers with Beechy Lake turbidites.

CARBONATE UNITS

Carbonate occurs throughout the volcanic complex but is most abundant as cement or fracture fillings in rhyolite flow breccias, and as pods and lenses in faults and shear zones. At the top of the Thlewycho sequence carbonate is less common as a primary chemical sediment in the form of interlayers in

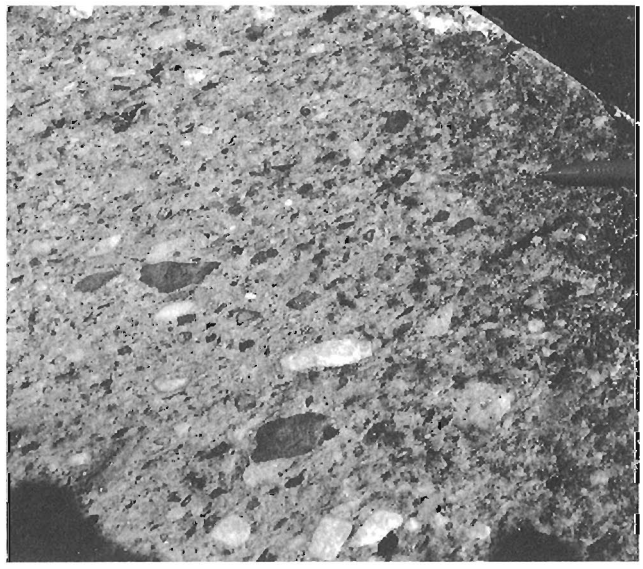

Figure 8. *Polymictic pebble breccia in detrital apron near the northeast end of Gold Lake dome. Pencil is 8 mm thick. GSC 1995-244F*

cherty iron-formation and as stratified clastic carbonate locally containing oolites and stromatolites. Some debris flows near the base of the Thlewycho sequence contain carbonate clasts indicating the presence of primary carbonate strata. Carbonate-cemented flow breccias occur mainly in the south-central and eastern parts of the Gold Lake dome complex.

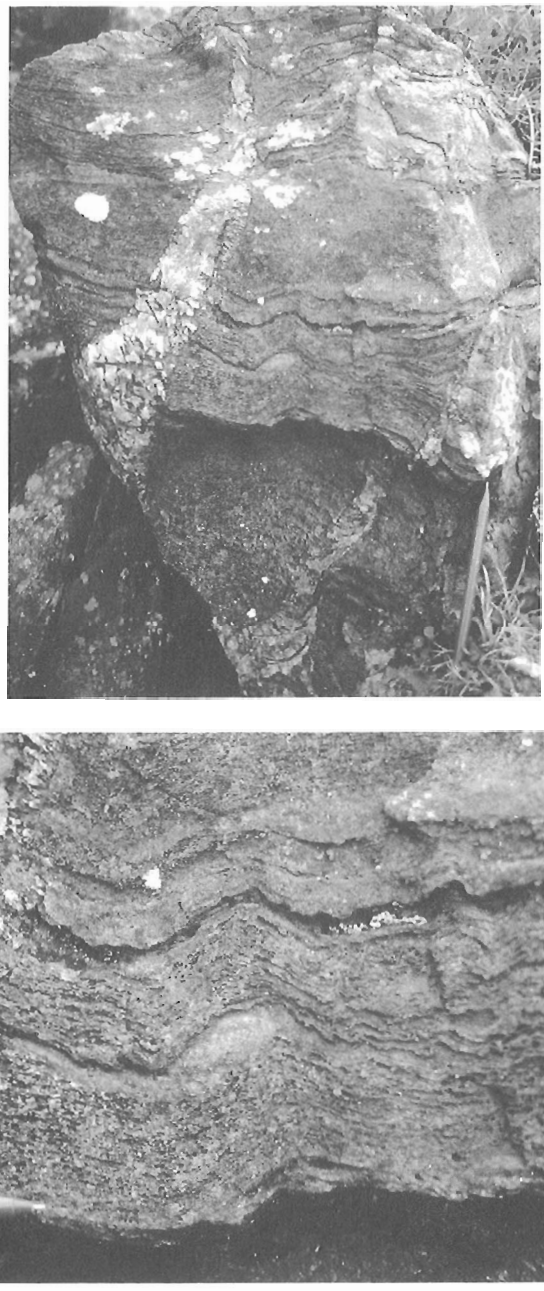

Figure 9. *Carbonate block (top photo) showing beds of wavy laminated carbonate interpreted as stromatolites. Pencil is 15 cm long. GSC 1995-244B. Detail of stromatolite laminations (bottom photo) in centre of block. Pencil (lower left) is 8 mm thick. GSC 1995-244J*

Carbonate is notably lacking amongst the fine rhyolite detritus of the clastic apron where it makes contact with turbidites. Thus it appears that carbonate horizons and the thick rhyolite flow breccias developed where the lavas entered the surrounding sea.

A new stromatolite locality (in addition to the nine localities reported in Lambert et al., 1990,1992) was discovered off the southeast end of Thlewycho Lake at co-ordinates 64°49′N, 108°00′47"W. Stromatolites at this locality were seen only in coarse rubble at the base of a 2.5 metre cliff (30 m east of a northwest-trending Mackenzie dyke that intrudes a major rhyolite lava complex). The cliff exposes brown weathering massive to clastic carbonate. Features interpreted as biogenic structures are 1 mm thick wavy laminations that form 1-4 cm thick beds having aggregate thickness of 10 cm (Fig. 9). Stromatolites were not found in place in the adjacent carbonate cliff. This carbonate unit is within the rhyolite dome/flow complex, that is at the same general stratigraphic position as the previously discovered stromatolite localities. Unlike the other localities, however, it is not at the exact boundary between the rhyolite complex and overlying turbiditic sedimentary rocks of the Beechy Lake Group.

INTERPRETIVE SUMMARY

On the southern and western sides of the stratovolcano, the Thlewycho sequence marks the beginning of major andesitic volcanism expressed by the effusion of porphyritic lavas, followed by explosive eruptions that produced voluminous pyroclastic flows which spread across much of the southern slopes of the volcano.

Thlewycho sequence volcanism ended with effusion of enormous rhyolitic lava fields that extended along the western and southern sides of the volcanic complex. Internal stratigraphy of the Gold Lake rhyolite complex indicates that the dome evolved by effusion of numerous thick lava flows punctuated by intermittent explosive events that produced interflow rhyolitic ash falls and pyroclastic flows. Mass wasting and erosion from the lava dome produced an apron of coarse breccias and felsic volcaniclastic detritus that interfingered with turbidites in the sea along the eastern side of the volcano. Along this side, a close spatial relationship between carbonate units, stromatolites and rhyolite flow breccias (and the general lack of carbonate where epiclastic detritus makes contact with turbidites) suggests that carbonate prevails mainly where the lava flows entered the sea.

ACKNOWLEDGMENTS

Carolyn Davis provided enthusiastic and competent assistance during field work under the NR Canada volunteer program. I thank Robert Baragar and John Henderson for critical review of the manuscript.

REFERENCES

Frith, R.A. and Percival, J.A.
1978: Stratigraphy of the Yellowknife Supergroup in the Mara-Back Rivers area, District of Mackenzie. in Current Research, Part C; Geological Survey of Canada, Paper 78-1C, p. 89-98.

Henderson, J.B.
1970: Stratigraphy of the Archean Yellowknife Supergroup, Yellowknife Bay-Prosperous Lake area, District of Mackenzie; Geological Survey of Canada, Paper 70-26, 12 p.

Lambert, M.B.
1976: The Back River Volcanic Complex, District of Mackenzie; in Report of Activities, Part A; Geological Survey of Canada, Paper 76-1A, p. 363-367.
1977: The southwestern margin of the Back River Volcanic Complex; in Report of Activities, Part A; Geological Survey of Canada, Paper 77-1A, p. 153-158.
1978: The Back River Complex - a cauldron subsidence structure of Archean age; in Current Research, Part A; Geological Survey of Canada, Paper 78-1A, p. 153-158.

Lambert, M.B. (cont.)
1982a: Felsic domes and flank deposits of the Back River volcanic complex, District of Mackenzie; in Current Research, Part A; Geological Survey of Canada, Paper 82-1A, p. 159-164.
1982b: The Back River Volcanic Complex, District of Mackenzie, N.W.T.; Geological Survey of Canada, Open File 848, 1:50 000 scale map.

Lambert, M.B., Burbidge, G., Jefferson, C.W., Beaumont-Smith, C., and Lustwerk, R.
1990: Stratigraphy, facies and structure in volcanic and sedimentary rocks of the Archean Back River volcanic complex, N.W.T.; in Current Research, Part C; Geological Survey of Canada, Paper 90-1C, p. 151-165.

Lambert, M.B., Beaumont-Smith, C., and Paul, D.
1992: Structure and stratigraphic succession of an Archean stratovolcano Slave Province, N.W.T.; in Current Research, Part C; Geological Survey of Canada, Paper 92-1C, p. 189-200.

van Breemen, O., Henderson, J.B., Sullivan, R.W., and Thompson, P.H.
1987: U-Pb, zircon and monazite ages from the eastern Slave Province, Healey Lake area, N.W.T.; in Radiogenic Age and Isotopic Studies: Report 1; Geological Survey of Canada, Paper 87-2, 101-110.

Geological Survey of Canada Project 740011

Regional gravity survey of western Great Slave Lake, Northwest Territories: a GSC contribution to the SNORCLE transect

C. Lowe and D.A. Seemann
GSC Victoria, Sidney

Lowe, C. and Seemann, D.A., 1996: Regional gravity survey of western Great Slave Lake, Northwest Territories: a GSC contribution to the SNORCLE transect; in Current Research 1996-C; Geological Survey of Canada, p. 29-35.

Abstract: In March 1995, 117 new gravity measurements were obtained at an average spacing of 8.5 km on the frozen surface of western Great Slave Lake. The measurements were acquired using a LaCoste and Romberg gravimeter, which was operated in damped mode to overcome oscillations of the lake ice. Station co-ordinates were computed using differential GPS. Water level gauge measurements, tied to local benchmark networks, were used to determine station elevations. Simple Bouguer anomalies, considered accurate to ±0.4 mGal, have been computed for all stations.

Western Great Slave Lake is underlain by Paleozoic cover rocks of the Western Canada Sedimentary Basin. The structure of the Precambrian basement beneath this cover is conjectural, extrapolated largely on the basis of magnetic anomaly data from surrounding regions. A preliminary analysis of the new gravity data reveals distinct anomalies and suggests the basement structure may be more complex than previously inferred.

Résumé : En mars 1995, on a effectué 117 nouvelles mesures gravimétriques sur la surface gelée de la partie occidentale du Grand lac des Esclaves, suivant un espacement moyen de 8,5 kilomètres. On a utilisé pour ce faire un gravimètre LaCoste-Romberg en mode amorti, pour annuler l'effet des oscillations dues à la glace lacustre. Les coordonnées des stations ont été calculées avec un SPG en mode différentiel. Les mesures des niveaux d'eau, rattachées à des repères locaux, ont servi à déterminer l'altitude des stations. On a calculé pour toutes les stations les anomalies simples de Bouguer, selon une précision de ± 0,4 mGal.

La portion ouest du Grand lac des Esclaves est tapissée de roches de couverture paléozoïque du bassin sédimentaire de l'Ouest canadien. La structure du socle précambrien sous cette couverture repose sur des conjectures; elle est principalement extrapolée des données sur les anomalies magnétiques des régions environnantes. Une analyse préliminaire des nouvelles données gravimétriques fait ressortir des anomalies distinctes et incite à supposer que la structure du socle est peut-être plus complexe qu'on ne l'avait inféré.

INTRODUCTION

The Slave Province in the Northwest Territories is presently the focus of major geoscience investigations both from the diamond exploration industry's unprecedented claim staking and from Lithoprobe's Slave Northern Cordilleran Lithospheric Evolution (SNORCLE) transect. Important objectives of SNORCLE which commenced in 1993-1994 are to map the structure of the lithosphere and to examine crustal growth and evolution from the Slave Province to the western limit of the Cordillera. Acquisition of detailed gravity and high resolution seismic reflection data in one of the transect corridors (Corridor 1) is scheduled for 1996. This corridor extends from Nahanni Butte to Fort Providence with a northern extension to Lockhart Lake and a southern extension to Fort Smith (Fig. 1). Gravity data are an integral component of all Lithoprobe transects as they provide valuable information on crustal structure and composition and important constraints on the interpretation of seismic data. Additionally, gravity is one of the primary tools used in the exploration for diamonds. The gravity data acquired over western Great Slave Lake in March 1995, and described in this paper, complete regional coverage within Corridor 1 and provide a new framework for structural studies and exploration programs.

Figure 2 shows the distribution of gravity data in the western Northwest Territories prior to undertaking this survey. The data were acquired between 1966 and 1988 during seven individual surveys. Typically measurements are 10 km apart, although smaller station spacings exist along a few highways (1-2 km), and over the East Arm (~6 km) and North Arm (~3 km) of Great Slave Lake. The latter two areas were surveyed in 1976 to test the interpretation of seismic refraction data (Clee et al., 1974) which suggested that the Yellowknife Greenstone Belt (part of the Slave province) extended offshore in a simple basin structure. Three-dimensional models of the gravity data confirmed the existence of the basin, but showed it was thinner than the initial seismic interpretation and had significant along-axis variation in both the thickness and composition of the basin-fill (Gibb and Thomas, 1980). The budget available during this project permitted acquisition of 117 new measurements (at a station interval of 8.5 km) over the unsurveyed portion of western Great Slave Lake (Fig. 3a). Unfortunately, it did not permit acquisition of data west of Big Island.

REGIONAL SETTING

Figure 1 shows the regional geological setting of Great Slave Lake. The North Arm of the lake is underlain by rocks belonging to the Archean Slave Province, the East Arm is underlain by the Early Proterozoic Athapuscow aulacogen, and much of the central and western portions of the lake are underlain by Devonian and older Paleozoic rocks. The structure of the Precambrian basement beneath these latter areas is conjectural, extrapolated largely on the basis of magnetic anomalies from surrounding regions (note: with the exception of the East Arm there is no aeromagnetic coverage of the lake itself).

The Slave Province is an amalgam of early to late Archean rocks that were assembled over a period of more than a billion years (Card and King, 1992). It is composed primarily of granitic rocks and metaturbidites and to a lesser extent mafic

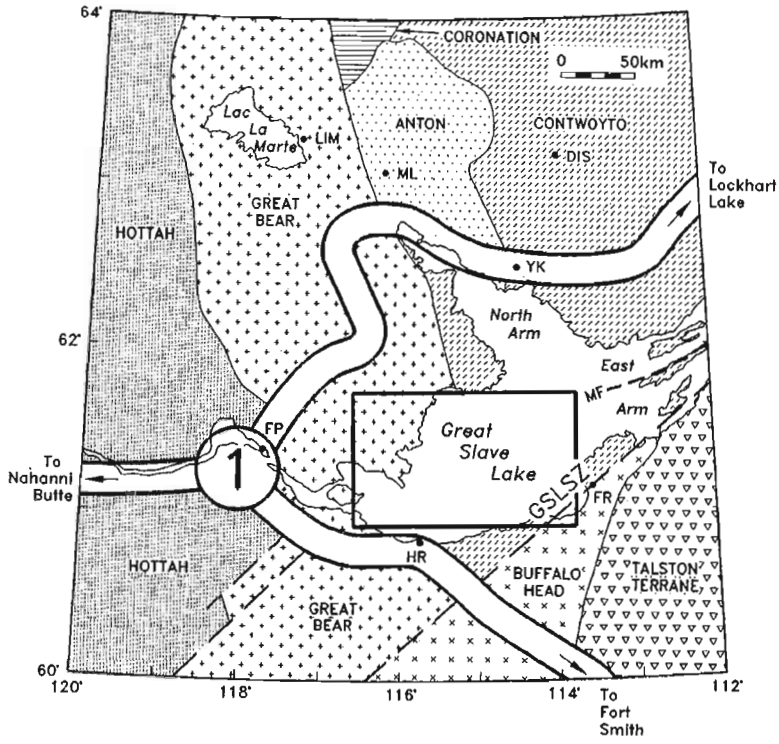

Figure 1.

Regional geological setting of Great Slave Lake showing the main Archean and Proterozoic tectonic elements (after Clowes (1993)). Terranes in the west are overlain by a Late Proterozoic to Phanerozoic cover. Contwoyto and Anton are part of the Early Archean Slave Province. Coronation, Great Bear, Hottah, and Buffalo Head are part of the Early Proterozoic Wopmay Orogen. See "Regional Setting" for age, composition, and tectonic interpretation of individual units. The area surveyed as part of this study is outlined. The proposed location of deep seismic profiles (Corridor 1 of the SNORCLE transect) is shown with parallel solid lines. Abbreviations are as follows: GSLSZ, Great Slave Lake shear zone; MF, McDonald-Wilson Fault.

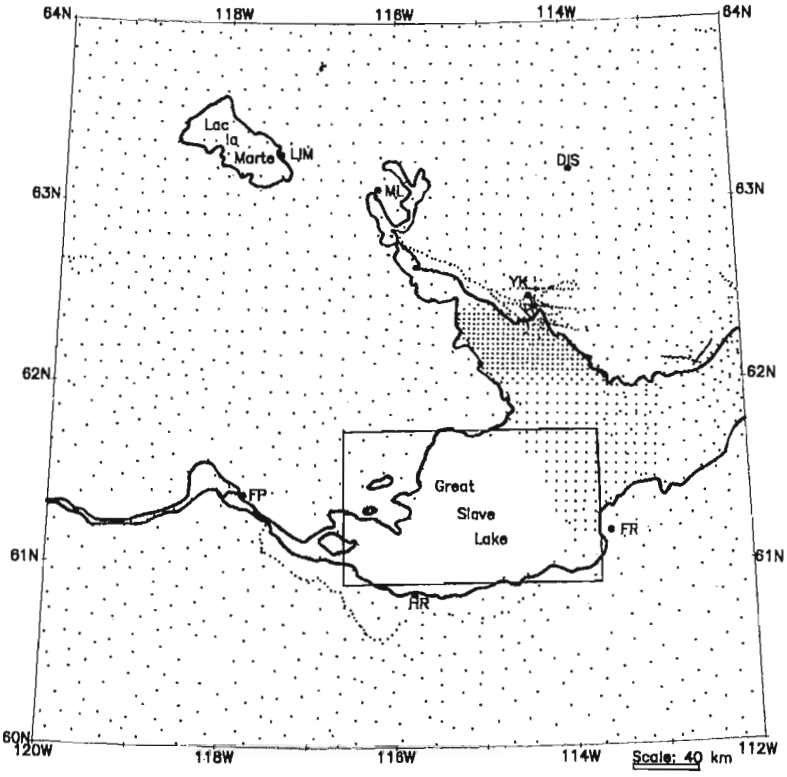

Figure 2.

Distribution of gravity data prior to the 1995 western Great Slave Lake gravity survey. The area surveyed as part of this study is outlined. Population centres are abbreviated as follows: DIS – Discovery; FP – Fort Providence; FR – Fort Resolution; HR – Hay River; LlM – Lac la Marte; ML – Marion Lake; YK – Yellowknife.

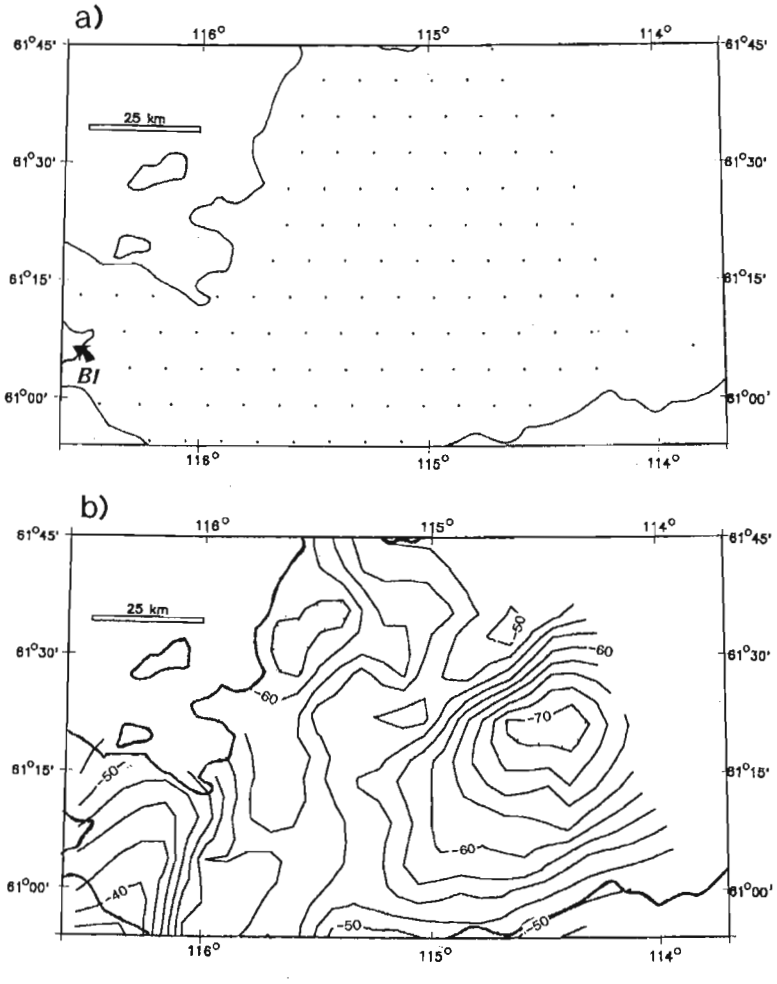

Figure 3.

***a)** Distribution of the 117 new gravity stations acquired on the frozen surface of western Great Slave Lake, see Figure 2 for regional setting. BI – Big Island. **b)** Contoured Bouguer anomaly map of the gravity data acquired at the locations shown in (a).*

to felsic metavolcanic rocks. It has been subdivided into a number of smaller tectonic elements including the Contwoyto and Anton Provinces. The western Slave Province was involved in the Early Proterozoic (2.1-1.8 Ga) Wopmay orogen, major features of which include the Coronation Supergroup, the Hottah Terrane, and the Great Bear Magmatic Zone (Bowring et al., 1989). The Coronation Supergroup is a depositional prism which accumulated between 1.9 and 1.85 Ga on the western margin of the Slave Province and which was subsequently deformed, detached from its basement, and thrust eastward during the Calderian Orogeny (Hoffman and Bowring, 1984; Bowring, 1985). The Hottah Terrane is comprised of amphibolite facies metasedimentary and (intermediate) metavolcanic rocks which were uplifted, unroofed, and intruded by a 1.914-1.902 Ga suite of calc-alkalic plutons (Bowring, 1985). The 1.88-1.84 Ga continental volcano-plutonic Great Bear Magmatic Zone unconformably overlies the Hottah Terrane and the west side of the Coronation Supergroup (Hoffman and McGlynn, 1977; Hildebrand, 1981). It is composed of plutons that range in composition from gabbro to granite.

The Athapuscow aulacogen, which is an Early Proterozoic intracratonic basin, outcrops beneath the East Arm of Great Slave Lake and separates the Slave Province from the northwestern Churchill Province. The western boundary of the aulacogen is obscured by the Paleozoic cover rocks which underlie the central portion of the lake. Nappes in the aulacogen are cut and offset by the McDonald-Wilson Fault system (Fig. 1, Bowring et al., 1984). This fault system which extends for more than 550 km from Great Slave Lake to the Thelon Front has an estimated dextral displacement of 70-125 km based on the correlation of stratigraphic units and aeromagnetic anomalies (Hoffman et al., 1977; Thomas et al., 1976). Motion on the fault system is thought to have occurred between 2.2 and 1.74 Ga (Reinhardt, 1969), but these ages are not well constrained.

The Talston magmatic arc is a belt of 1.99 to 1.92 Ga granitic to dioritic plutons which extends along the transition between the Churchill and Slave Provinces (Bostock et al., 1987; Thériault and Ross, 1991). The Buffalo Head domain, which lies to the west of the Talston arc, is a subsurface crustal domain defined primarily by its distinctive aeromagnetic signature. Drill core samples from hydrocarbon exploration wells show that it is comprised primarily of 1.99-2.32 Ga metaplutonic rocks ranging in composition from gabbro to leucogranite, with less common metavolcanic rocks and paragneisses (Thériault and Ross, 1991).

The Great Slave Lake shear zone, is a 1300 km long northeast-trending belt of granulite to greenschist facies mylonites which preserves records of dextral transcurrent motion of the order of 300-700 km. The shear zone is thought to link deformation in the Thelon magmatic arc (east flank of the Slave Province) to deformation in the Talston magmatic arc and has been interpreted by Hoffman (1987) as an intracontinental transform related to the collision and indentation of the Churchill Province by the Slave Province.

SURVEY LOGISTICS

March was selected as the optimum month to conduct the survey as there is approximately eleven hours of daylight at the latitude of Great Slave Lake, a low probability for winter storms, and typically 1-2 m of ice on the lake (i.e., sufficient to support the weight of a fully loaded helicopter) at that time of year.

The Geodetic Survey of Canada operates a permanent GPS tracker station at the Yellowknife Geophysical Observatory and we were granted permission to use it for the duration of the survey. In addition, the Canadian 206B Helicopter which was chartered for the survey was based in Yellowknife. To maintain an operational helicopter closer to the survey area would have increased survey costs enormously. For these reasons, Yellowknife, rather than Hay River, was selected as the base of operations for the survey, despite its greater distance from the survey area (Fig. 2).

DATA ACQUISITION

At each station, gravity was measured using a model G LaCoste and Romberg gravimeter, station co-ordinates were established using differential GPS, and water depths were determined using a calibrated Edo echo sounder.

Gravity data

The gravimeter was operated in a fully damped mode to slow the meter's response, and allow stable, (i.e. reproducible) readings to be observed on the unstable ice which covered the lake surface. Storm activity during the period March 20-23 (inclusive) made the acquisition of stable readings impossible. In addition, a stable gravity measurement could not be obtained at one particular station close to the western edge of the lake, where a river entered the lake, eroded the base of the ice and decreased its stability. Measurements were successfully observed at all other predetermined station locations. The gravimeter and the echo sounder (see below) were deployed adjacent to the helicopter landing sites and usually less than one metre apart.

Positioning data

Horizontal station co-ordinates were determined using a differential GPS system. Two Turbo Rogue receivers were used, one of which (the base station) was installed at the permanent GPS tracker site in the Yellowknife Geophysical Observatory. This receiver shared the resident tracker's antenna, the co-ordinates of which were well established. The other receiver (the rover) was installed in the helicopter. At each gravity station the rover's antenna, which was mounted on a tripod, was positioned approximately 10 m from the helicopter (and gravity station) so as to have an unobstructed view of the sky. The bearing and the distance to the antenna were recorded so that the location of each gravity station could be determined from that of the GPS antenna.

Both receivers recorded satellite data at 10 second intervals. The base receiver recorded data continuously during the daylight operation, while approximately 6 minutes of satellite observations were recorded at each gravity station (pre-survey tests indicated that 30-36 recordings would be sufficient to obtain a position accuracy of better than a metre).

During the survey period the mean elevation of the lake ice surface at Yellowknife was 156.50 ± 0.03 m and at Hay River (approximately 200 km southwest of Yellowknife) was 156.61 ± 0.03 m, indicating minimal overall variation in the lake ice surface. These values were determined from water level gauges maintained by the Inland Water Directorate (Environment Canada). Both gauges are tied to local benchmarks and are considered accurate to ± 0.01 m. The two sets of values were averaged and an elevation of 156.55 m assigned to all gravity observations taken on the lake surface. Although GPS data also included station elevations, they were considered less accurate than the water gauge data and consequently not used.

Water depth data

The water depth beneath each station was measured using a Model 9040 Edo echo sounder. Prior to its deployment the instrument was calibrated using a reflective target placed at a known depth beneath the ice. In a deep channel, approximately 18 km south of Yellowknife, a hole large enough to accommodate a 0.36 m x 0.36 m metal plate, was augured into the 1.2 m thick ice. The "weighted" metal plate was then lowered to a depth of 50 m and the internal calibration of the sounder adjusted until a reading of 50 m was obtained on the echo sounder's paper chart record. Repeat measurements were taken twice daily at this site to confirm the instruments calibration.

DATA PROCESSING AND ACCURACY

Gravity data

The gravity observations were tied to national base stations at Yellowknife and Hay River, and theoretical gravity values were calculated using the Geodetic Reference System 1967 gravity formula. Simple Bouguer anomalies were computed using a standard density of 2670 $kg \cdot m^{-3}$ and a sea level datum for the Bouguer correction. Terrain corrections were not applied as the topography of the terrain surrounding the surveyed area is for the most part subdued swampland with very gentle gradients (typically <4m/km within a 20 km radius of the shoreline). The Bouguer anomaly at each station has an estimated error of ±0.4 mGal attributable primarily to uncertainties in the station co-ordinates and water depth (see below). A comprehensive description of the acquisition and processing methods together with a full discussion of the data accuracies are given in Seemann and Lowe (unpublished report, 1995).

Positioning data

GPS data were processed using in-house software provided by the Continental Geoscience Division (GSC, Ottawa). Station positions were subsequently corrected for the offset between antenna and gravimeter at each station and the corrected position was converted from the WGS84 reference ellipsoid (used in orbit computations of satellites) to the NAD27 reference ellipsoid (used for archival of data in the National Gravity Data Base). The accuracy of the GPS-derived positions, allowing for errors associated with the offset between the GPS antenna and gravimeter at each station, is estimated to be ±5 m.

Elevation data required no processing. The water level gauges, which were used to provide the elevation of the gravity stations, are tied to local benchmarks and are considered accurate to ±0.01 m.

Water depth data

Water depth information was scaled directly from the paper chart record generated by the Edo Echo Sounder and required no processing. Repeat measurements at the calibration site showed the readings were accurate to ±1%.

PRELIMINARY OBSERVATIONS AND CORRELATIONS

The new data are presented as a contoured Bouguer anomaly map in Figure 3b. The trends observed in the data are discordant with those mapped in the Paleozoic cover rocks suggesting that the latter are quite thin and have little effect on the gravity field. Consequently, we believe that the underlying basement structure and lithologies are primarily responsible for the observed variations. The most prominent feature of the new data set is a northeast-trending Bouguer anomaly low (minimum -74 mGal) which extends over much of the eastern portion of the survey area, that is, the central part of the lake. Regional Bouguer data show that this anomaly is sub-oval with a maximum length of ~120 km and a maximum width of ~55 km (see anomaly "1" in Fig. 4). It terminates to the northeast near Butte Island and has relatively steeper gradients (1 $mGal \cdot km^{-1}$) along its northwestern margin compared with those along its other boundaries (typically <0.6 $mGal \cdot km^{-1}$). It is discordant with the trend of anomalies in both the North and East Arms of the lake. The gravity high (Fig. 4) associated with volcanics of the Kam Formation (Yellowknife Greenstone belt, Slave Province) in the North Arm of Great Slave Lake (Clee et al., 1974; Gibb and Thomas, 1980) is abruptly truncated by the Bouguer low. Similarly, the southwest-trending belt of anomalously high gravity values associated with the Proterozoic sequences of the Athapuscow aulacogen in the East Arm of the Lake (Hornal and Boyd, 1972; Hoffman et al., 1977; Bowring et al., 1984) terminate against the northeastern boundary of the Bouguer low. High Bouger values associated with mafic units in the aulacogen do, however, extend as far as Fort Resolute along

the southeast margin of the Bouguer low (Fig. 4). The magnitude of the low is comparable with those observed over the granodiorite bodies outcropping both to the east and to the west of the Yellowknife Greenstone Belt (Gibb and Thomas, 1980) and with mapped granites in the Talston magmatic arc. These observations suggest that the anomaly may be caused by a granitic body with a relatively steeper contact on the northeast. In addition, they suggest that the emplacement of the body must postdate deposition of the Yellowknife Greenstone Belt and possibly also development of the Athapuscow aulacogen.

Another Bouguer anomaly low of somewhat smaller magnitude (minimum -63 mGal) is observed further to the west (Fig. 3b and anomaly "2" in Fig. 4). This anomaly, which has an average width of 20-25 km, trends northward from Hay River to the north shore of the lake (a distance of ~90 km) before swinging to the east for a further 30 km. Its orientation, geometry, and magnitude are similar to anomalies associated with granitic units in the Contwoyto terrane (western Slave Province (Fig. 1)) suggesting that it too may be due to a buried granite. The Paleozoic cover rocks which underlie the central portion of the lake obscure the western limit of the Athapuscow aulacogen and the westward extent of many of the faults which dissect it (for example, those of the McDonald-Wilson Fault system). The northern limits of this Bouguer low and the more easterly one, described above, lie along strike of the Wilson Fault suggesting that this fault system extends (and offsets) units as far west as the western edge of Great Slave Lake.

A localized gravity high (maximum -38 mGal) is observed to the southeast of Big Island in the southwest corner of the survey area (Fig. 3 and anomaly "3" in Fig. 4). The magnitude and extent (~30 km long x ~20 km wide) of the high suggest it is caused by an excess mass at shallow depths. A more detailed examination of the local geology is required to resolve this feature.

SUMMARY

New gravity measurements acquired on the frozen surface of Great Slave Lake define three distinct anomalies (Fig. 3b, 4):

1. a 120 km long x 55 km wide, sub-oval, northeast-trending Bouguer anomaly low which extends over much of the central portion of the lake. An initial correlation of this anomaly with the mapped geology suggests it may be caused by a granitic body which intruded some time after the Athapuscow aulacogen was emplaced;
2. a predominantly north-trending gravity low which extends from Hay River in the south to the north shore of the lake where it swings east for a distance of about 30 km. This anomaly may also be caused by a buried granitic body;
3. a small (~30 km long x ~20 km wide) sub-oval gravity high which is located southwest of Big Island and which is probably due to an excess mass at shallow depths.

The northerly termination of the Bouguer lows lies along strike of the Wilson Fault system, suggesting that the fault system may offset basement units as far west as the western edge of Great Slave Lake. Future studies are planned to investigate these preliminary correlations more thoroughly.

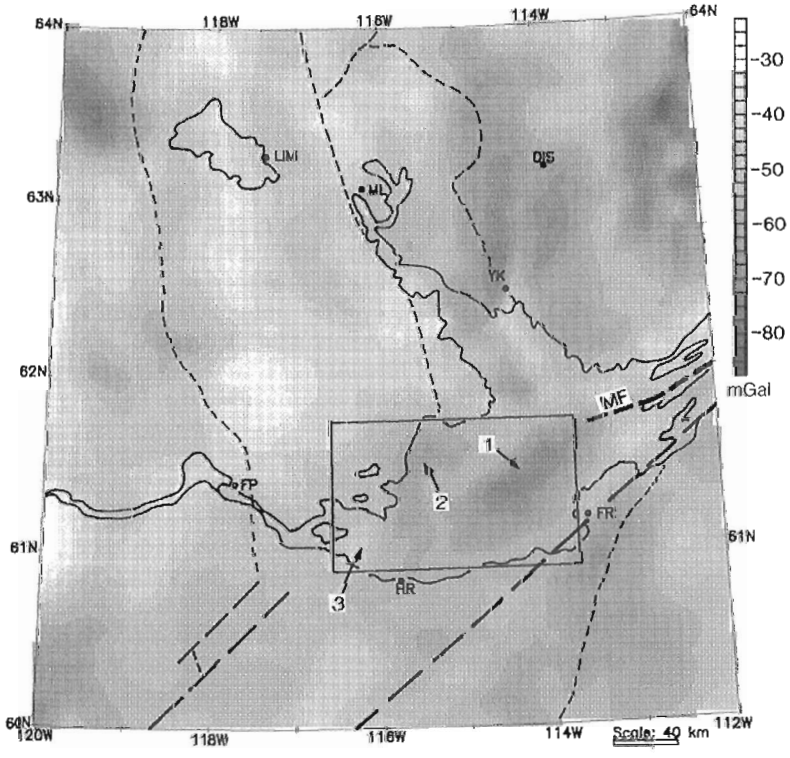

Figure 4.

Regional Bouguer anomaly map of the western Northwest Territories (high values are shown in light shades and low values in dark shades). Boundaries of the main Archean and Proterozoic tectonic elements are indicated with broken lines (see Figure 1 for names of individual tectonic elements). The location of the region in this survey is outlined. Refer to text for a discussion of anomalies labelled "1", "2", and "3".

ACKNOWLEDGMENTS

This project could not have been undertaken without the assistance and support of several individuals and organizations. We thank the Polar Continental Shelf Project and the Continental Geoscience Division (CGD) of the Geological Survey of Canada for financial and logistical support. Thanks to Mike Schmidt, Herb Dragert (Pacific Geoscience Centre), and John Halpenny (CGD) for the loan of GPS receivers, instruction on their operation, and for processing software. Thanks to John Bigger and Rudy Kutello (Canadian Hydrographic Services) for the loan of the Edo echo sounders and instruction on their operation. Kim Epp and Murray Jones (Environment Canada) supplied us with lake level data. We thank Andy Langois and Bill Outhwaite (Yellowknife Geophysical Observatory) for their generous hospitality. Dewayne Hansen (Canadian Helicopters) cheerfully and masterfully piloted the helicopter during the survey. Mel Best and Tark Hamilton (GSC-Victoria) provided critical review of this paper, and Richard Franklin assisted with the preparation of figures.

REFERENCES

Bostock, H.H., van Breemen, O., and Loveridge, W.D.
1987: Proterozoic geochronology in the Talston magmatic zone, Northwest Territories; Geological Survey of Canada, Paper 87-9.

Bowring, S.A.
1985: U-Pb zircon geochronology of early Proterozoic Wopmay orogen, Northwest Territories, Canada: and example of rapid crustal evolution; PhD. thesis, University of Kansas, Kansas City, 148 p.

Bowring, S.A., Van Schmus, W.R., and Hoffman, P.F.
1984: U-Pb zircon ages from the Athapuscow aulacogen, East Arm of Great Slave Lake, N.W.T., Canada; Canadian Journal of Earth Sciences, v. 21, p. 1315-1324.

Bowring, S.A., Williams, I.S., and Compston, W.
1989: 3.96 Ga gneisses from the Slave province, Northwest Territories, Canada; Geology, v. 17, p. 971-975.

Card, K.D. and King, J.E.
1992: The tectonic evolution of the Superior and Slave Provinces of the Canadian Shield: introduction; Canadian Journal of Earth Sciences, v. 29, p. 2059-2065.

Clee, T.E., Barr, K.G., and Berry, M.J.
1974: Fine structure of the crust near Yellowknife; Canadian Journal of Earth Sciences, v. 11, p. 1534-1549.

Clowes, R.M. (ed.)
1993: LITHOPROBE Phase IV proposal – Studies of Evolution of a Continent published by the LITHOPROBE secretariat, University of British Columbia, Vancouver, British Columbia p. 4-23.

Gibb, R.A. and Thomas, M.D.
1980: Correlation of gravity anomalies with Yellowknife Supergroup rocks, North Arm, Great Slave Lake; Canadian Journal of Earth Sciences, v. 17, p. 1506-1516.

Hildebrand, R.S.
1981: Early Proterozoic LaBine Group of Wopmay orogen: remnant of a continental volcanic arc developed during oblique convergence; in Proterozoic basins of Canada, (ed.) F.H.A. Campbell; Geological Survey of Canada, Paper 81-10, 135-156.

Hoffman, P.F.
1987: Continental transform tectonics: Great Slave Lake shear zone (ca. 1.9 Ga), northwest Canada; Geology, v. 15, p. 785-788.

Hoffman, P.F. and Bowring, S.A.
1984: Short-lived 1.9 Ga continental margin and its destruction, Wopmay orogen, northwest Canada; Geology, v. 12, p. 68-72.

Hoffman, P.F. and McGlynn, J.C.
1977: Great Bear batholith: a volcano-plutonic depression; in Volcanic Regimes in Canada, (ed.) R.A. Barager, L.C. Coleman, and J.M. Hall; Geological Association of Canada, Special Paper 16, p. 170-192.

Hoffman, P.F., Bell, I.R., Hildebrand, R.S., and Thorstad, L.
1977: Geology of the Athapuscow aulacogen, East Arm of Great Slave Lake, District of Mackenzie; in Report of Activities, Part A, Geological Survey of Canada, Paper 77-1A, p. 117-129.

Hornal, R.W. and Boyd, J.B.
1972: Gravity measurements in the Slave and Bear Structural Provinces, Northwest Territories; Gravity Map Series No. 89, Earth Physics Branch, Ottawa.

Reinhardt, E.W.
1969: Geology of the Precambrian rocks of Thubun Lakes map-area in relation to the McDonald fault system, District of Mackenzie; Geological Survey of Canada, Paper 69-21, 29 p.

Thériault, R.J. and Ross, G.M.
1991: Nd isotopic evidence for crustal recycling in the ca. 2.0 Ga subsurface of western Canada; Canadian Journal of Earth Sciences, v. 28, p. 1140-1147.

Thomas, M.D., Gibb, R.A., and Quince, J.R.
1976: New evidence from offset aeromagnetic anomalies for transcurrent faulting associated with the Bathurst and McDonald faults, Northwest Territories; Canadian Journal of Earth Sciences, v. 13, p. 1244-1250.

Geological Survey of Canada Project 910027

Thematic structural studies in the Slave Province, Northwest Territories: the Sleepy Dragon Complex

Wouter Bleeker[1]
Continental Geoscience Division

Bleeker, W., 1996: Thematic structural studies in the Slave Province, Northwest Territories: the Sleepy Dragon Complex; in Current Research 1996-C; Geological Survey of Canada, p. 37-48.

Abstract: The geometry of the Sleepy Dragon Complex, a controversial structure in the Yellowknife Domain of the Archean Slave province, is shown to be a mushroom interference pattern between regional F_1 and F_2 folds. Critical evidence in favour of a F_1 fold hinge on the western side of the complex is provided by a change in vergence of the S_1 schistosity and coplanar bulk flattening planes in pillows. The Sleepy Dragon Complex basement uplift was initiated as a high-amplitude F_1 anticline, not as a syn-depositional horst.

A well-preserved quartzite/banded iron-formation assemblage underlies the Cameron River basalt at Patterson Lake. This assemblage is cross-cut by the deformed and metamorphosed dykes that likely fed the Cameron River basalt. It is suggested that the contact between the Cameron River basalt pile and an overlying rhyolite unit represents an intravolcanic, angular unconformity that is laterally equivalent with the unconformity at the base of the Raquette Lake Formation.

Résumé : La géométrie du complexe de Sleepy Dragon, structure controversée du domaine de Yellowknife (Province archéenne des Esclaves), est présentée comme une interférence en champignon entre les plis régionaux P_1 et P_2. Un changement de vergence de la schistosité S_1 et l'observation de plans d'aplatissement essentiellement coplanaires dans les coussins constituent des indices critiques en faveur d'une charnière de pli P_1 sur la portion ouest du complexe. Le soulèvement du socle dans le complexe de Sleepy Dragon a été amorcé par un anticlinal P_1 de forte amplitude plutôt que par un horst synsédimentaire.

Un assemblage composé de quartzite et de formation de fer rubanée a été bien conservée sous les basaltes de Cameron River, au lac Patterson. Cet assemblage est recoupé par les dykes déformés et métamorphisés qui ont probablement alimenté les basaltes de Cameron River. Il est proposé que le contact entre l'édifice basaltique de Cameron River et une unité de rhyolite sus-jacente représente une discordance anguleuse intravolcanique, qui est latéralement équivalente à la discordance située à la base de la Formation de Raquette Lake.

[1] Continental Geoscience Division, 5013-51st Street, Yellowknife, Northwest Territories, X1A 1S5

INTRODUCTION

New results are presented of an ongoing study on the structural geology and tectonic history of the Archean Slave structural province, Northwest Territories. The rationale for this study and some initial results were discussed in Bleeker and Beaumont-Smith (1995) and Bleeker and Villeneuve (1995). In short, the central question comprises the tectonic evolution of Slave province greenstone belts.

Bleeker and Beaumont-Smith (1995) suggested that the Sleepy Dragon Complex, a critical and controversial area for understanding the relationship between basement gneiss and

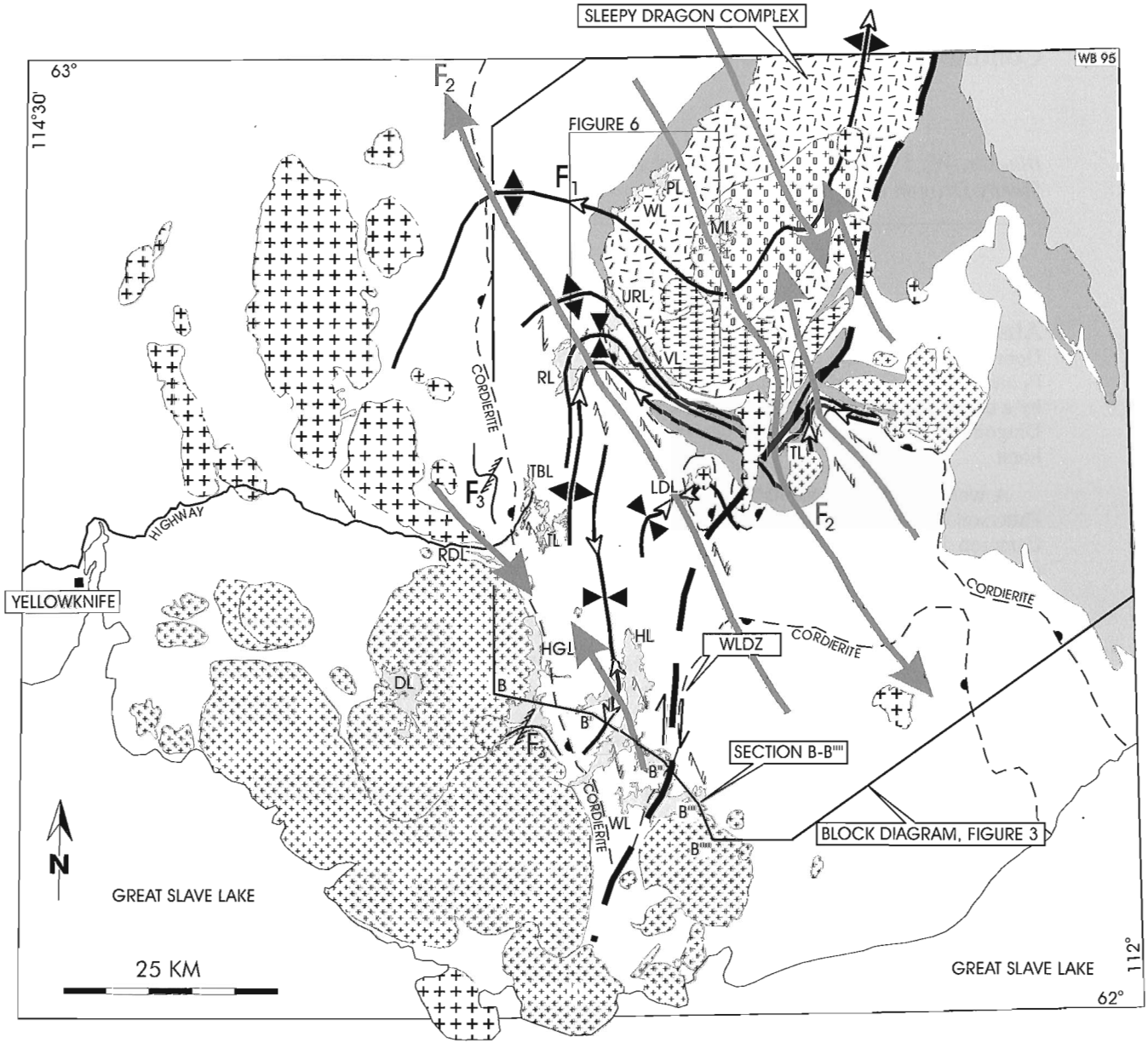

Figure 1. *Simplified geological map (modified after Henderson, 1985 and Bleeker and Beaumont-Smith, 1995), showing the traces of first-order F_1 and F_2 fold structures in and around the Sleepy Dragon Complex, 75 km east-northeast of Yellowknife. Insets show the outlines of the block diagram presented in Figure 3 and a detailed map of the F_1 hinge region in Figure 6. The F_1-F_2 synformal mushroom interference structure at lower Donore Lake (LDL, 20 km east of the end of the highway), an inverted analogue of the Sleepy Dragon structure, is shown in Figure 4. For section B-B'''' through Watta Lake (WL), Hearne Lake (HL), and Harding Lake (HGL), see Figure 2 in Bleeker and Beaumont-Smith (1995). Other localities referred to in the text are: Patterson Lake (PL) and Webb Lake (WL), both along the western flank of the Sleepy Dragon Complex, and Tibbit Lake (TBL), Terry Lake (TL), Reid Lake (RDL) in the central map area.*

greenstone units (Henderson, 1943; Barager, 1966; Davidson, 1972; Baragar and McGlynn, 1976; Henderson, 1985; Henderson et al., 1987; Lambert and van Staal, 1987; Lambert, 1988; Lambert and van Breemen, 1991; Kusky, 1990; James and Mortensen, 1992; Lambert et al., 1992), is a large-scale mushroom interference pattern resulting from first (F_1) and second (F_2) generation regional fold structures. Figure 1 summarizes the structural relationships in the area and provides a framework for further data and discussions presented below.

NEW WORK

From the initial work reported by Bleeker and Beaumont-Smith (1995), the study area has been extended to the central part and the western flank of the Sleepy Dragon Complex, particularly Patterson Lake and Webb Lake (PL and WL, respectively, see Fig. 1) where Kusky (1990) claimed the existence of a tectonic mélange on the contact between basement gneiss and mafic volcanic rocks of the Cameron River greenstone belt. To the west, data collection geared at construction of detailed structural cross-sections (e.g. section B-B'''', see Fig. 2 in Bleeker and Beaumont-Smith, 1995) was extended to Terry Lake, Tibbit Lake, and Reid Lake (TL, TBL, and RDL, respectively, see Fig.1), and onto the "Ingraham Trail" highway where the Lithoprobe SNORCLE seismic reflection line will be shot in the near future (Clowes, 1993).

Significant new results include: 1) preliminary mapping of a well-preserved quartz pebble conglomerate/quartzite/banded iron-formation (BIF) assemblage underlying the Cameron River basalt at Patterson Lake; 2) a detailed re-evaluation of the contact relationships at the base of the Cameron River basalt, which failed to show evidence for a

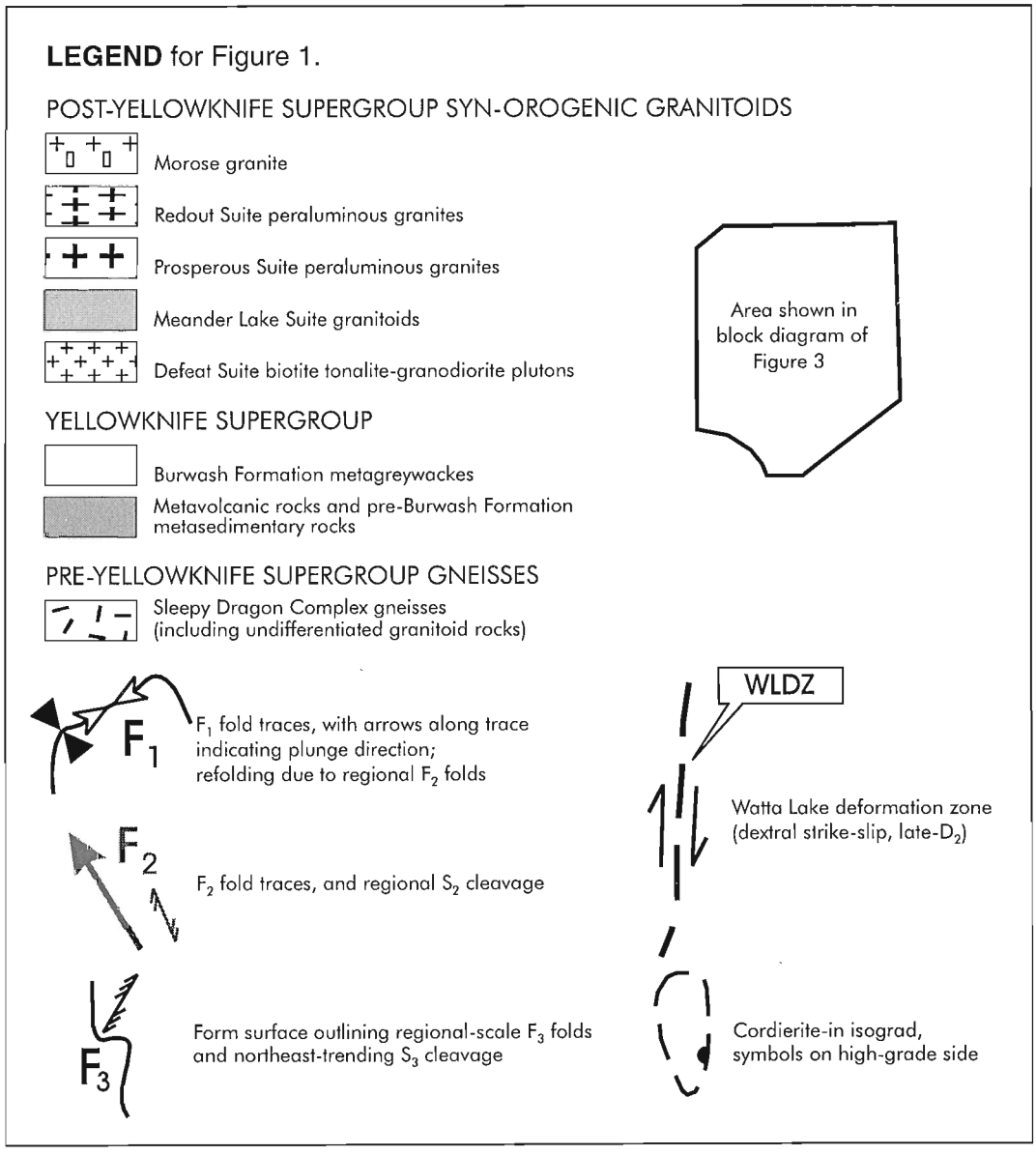

tectonic mélange at this contact; 3) the documentation of felsic tuff layers, similar to the Watta Lake tuff layer (Bleeker and Beaumont-Smith, 1995; Bleeker and Villeneuve, 1995), throughout the Burwash Formation metaturbidite stratigraphy (Fig. 2); 4) preliminary U-Pb zircon data on the Watta Lake tuff layer indicating an age of 2661 ± 2 Ma (Bleeker and Villeneuve, 1995 and unpublished data); and 5) documentation of the folded gabbroic to dioritic sills within the Burwash Formation metaturbidites at Terry and Tibbit lakes. Some of these results are briefly described below.

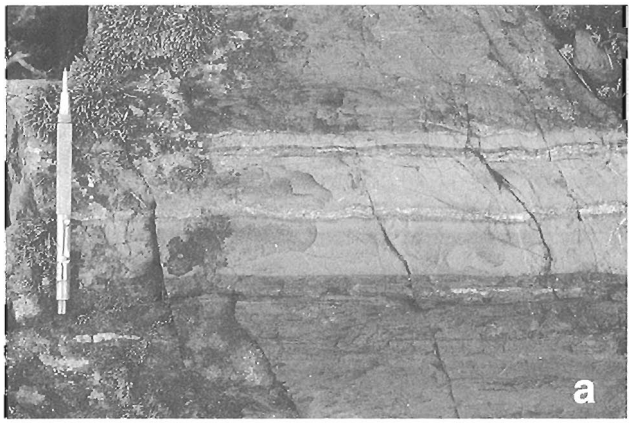

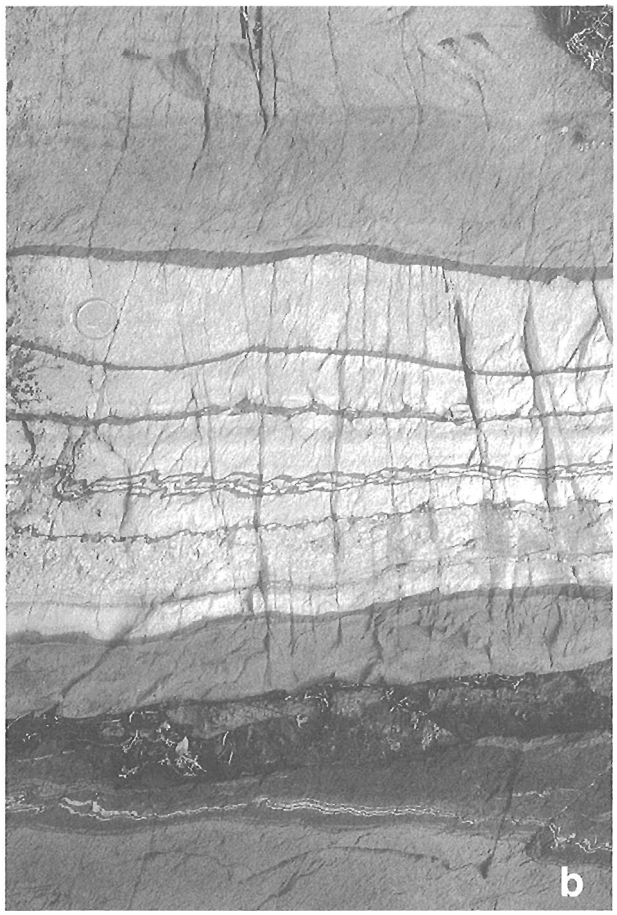

GEOMETRY OF THE SLEEPY DRAGON COMPLEX

Tectonic modelling of complex geological terranes involves the synthesis of a number of different data sets. In structurally complex areas, particularly critical constraints to a tectonic model are provided by geometric analysis (i.e., structural analysis *sensu stricto*) and kinematic analysis. In general, structural analysis should precede kinematic analysis to provide a framework in which the kinematic indicators can be interpreted (e.g. Turner and Weiss, 1963). Without a sufficiently accurate geometrical model an analysis of kinematic indicators may lead to spurious results.

A geometrical synthesis of the structural relationships shown in Figure 1, and discussed in some detail in Bleeker and Beaumont-Smith (1995), is presented as a block diagram in Figure 3. In this diagram, the large-scale structural relationships in and around the Sleepy Dragon Complex are shown as projected from 220°, looking 24° down (azimuth and inclination of the orthographic projection). The three-dimensional structure is based on a well-constrained map view and a large body of structural orientation data throughout the area, collected by the author as well as by previous workers (e.g. Henderson, 1985; Lambert, 1988). Specifically, orientation data were collected on all macroscopic fold structures that are critical to the overall geometry. The diagram (Fig. 3) highlights the fact that the southern termination of the Sleepy Dragon Complex is a steeply plunging F_2 fold hinge, and not the locus of a north-south subhorizontal axis through the complex. Kusky (1990) used such a non-existent subhorizontal axis to unfold his lineation and kinematic data (see discussion in Bleeker and Beaumont-Smith, 1995).

The geometry of the Sleepy Dragon Complex is that of an antiformal, type 2 interference pattern involving steeply plunging, northwest- or southeast-trending F_2 folds overprinting a regional-scale, basement-cored F_1 anticline. The geometry and structural systematics of the Sleepy Dragon

Figure 2. *Felsic tuff layers are found throughout the metaturbidite stratigraphy of the Burwash Formation, always hosted by thin black shale intervals within otherwise sand and silt dominated turbidites. The black shale intervals represent periods of quiescence that "captured" one to several ash fall events from contemporaneous felsic volcanism. Preservation of the delicate tuff layers, over large distances, without evidence of reworking, indicates that the tuffs settled in a deep water setting.* ***a)*** *Thin felsic tuff "layer" at Terry Lake, relatively low within the Burwash Formation, consisting of three, thin, normally graded beds within a ca. 12 cm shale (and tuff) interval (pen for scale).* ***b)*** *Complex felsic tuff layer at Watta Lake (see also Bleeker and Beaumont-Smith, 1995), dated at 2661 ± 2 Ma (Bleeker and Villeneuve, 1995 and unpubl. data). This layer occurs higher up in the Burwash Formation and has now been recognized at several widely spaced localities. (In both figures, stratigraphic tops are towards the top of the page).*

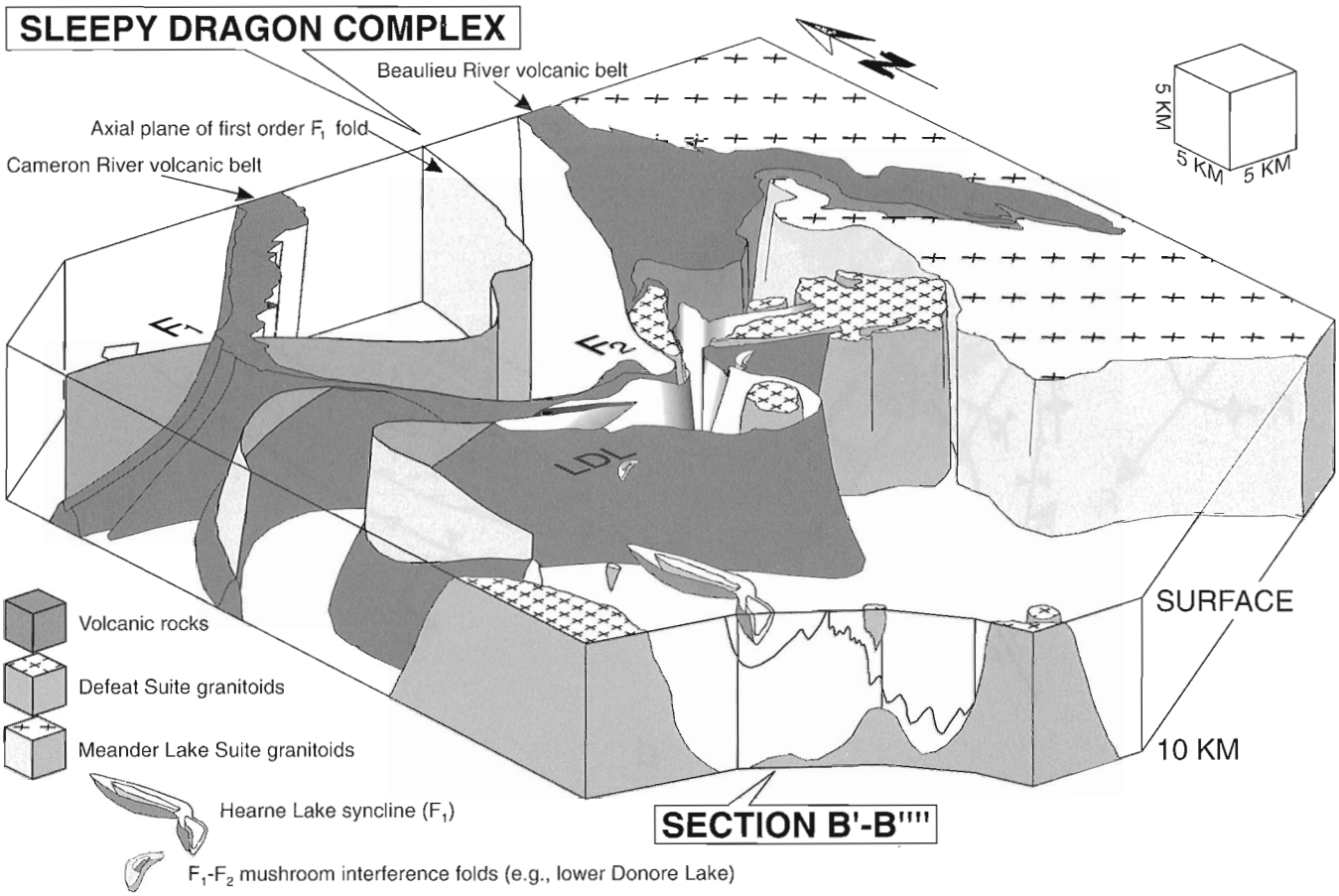

Figure 3. *Orthographic block diagram of the Sleepy Dragon Complex, projected 24° down (inclination) from 220° (azimuth). The area encompassed by the diagram is shown in Figure 1. No vertical exaggeration. Front face of the block is section B-B'''' shown in Figure 2 of Bleeker and Beaumont-Smith (1995).*

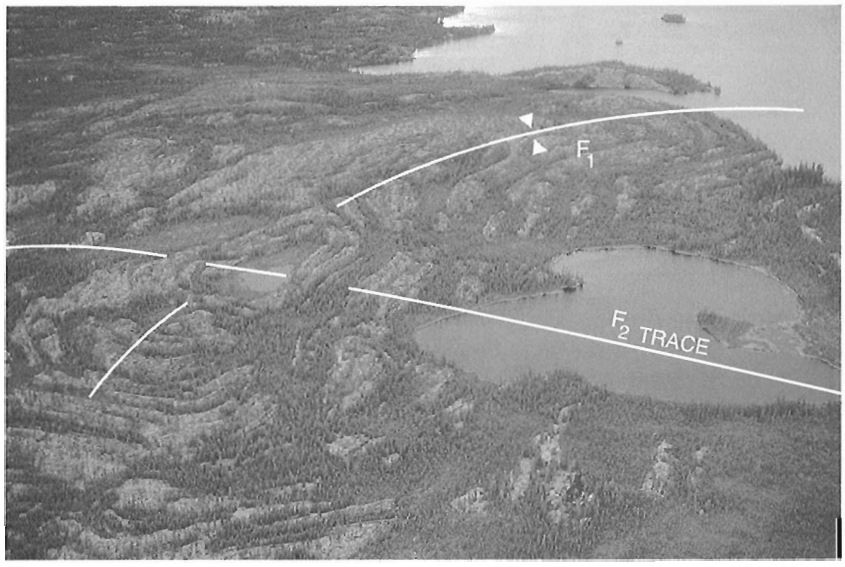

Figure 4.

A kilometre-scale, synformal mushroom interference structure (F_1-F_2) in metaturbidites of the Burwash Formation, at lower Donore Lake (LDL, see Fig. 1; see also Figure 3). View is towards the northeast.

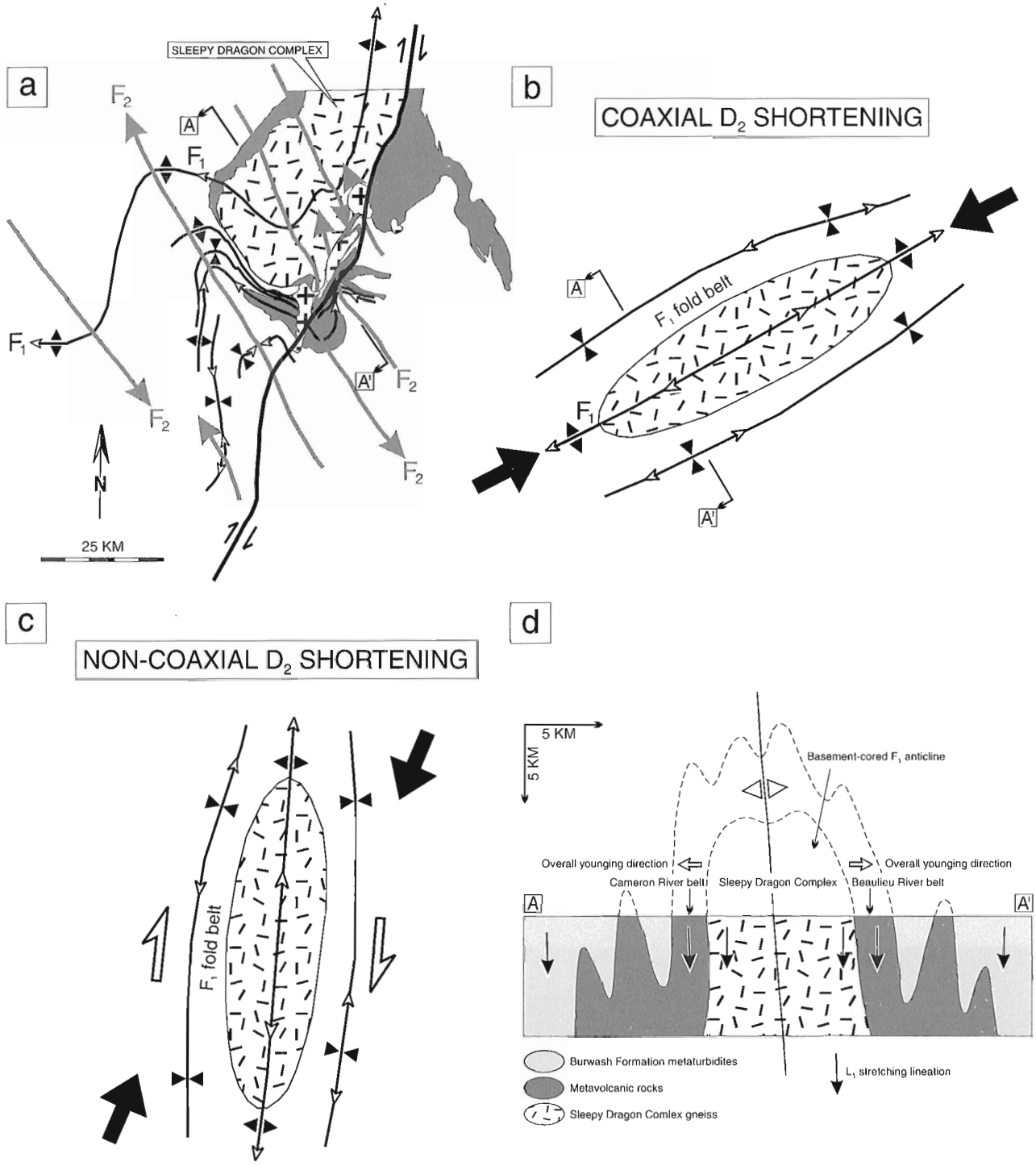

Figure 5. *The Sleepy Dragon Complex unfolded.* ***a)*** *Present interference geometry. Note the F_1 hinge on the west side of the complex.* ***b)*** *Unfolding of the steeply plunging F_2 folds, assuming D_2 was a largely coaxial northeast-southwest shortening event. At this stage, the Sleepy Dragon Complex was a regional scale, basement-cored, doubly plunging F_1 anticline.* ***c)*** *Similar to b) but showing an alternative scenario that assumes D_2 was strongly non-coaxial, resulting in late-stage strike-slip faults (such as the Watta Lake Deformation Zone, see Bleeker and Beaumont-Smith, 1995).* ***d)*** *Qualitative cross-section (A-A′) through the Sleepy Dragon Complex prior to D_2, showing a high-amplitude, basement-cored, upright F_1 anticline. Penetrative strain, including steep stretching lineations, is present throughout the section. The overall geometry, symmetry, and penetrative D_1 strain dictate that the structure is a fold and not a basement "horst". Note the schematic position of section A-A′ in Figures a and b.*

mushroom interference structure are identical to mushroom-type interference structures observed in the Burwash Formation turbidites surrounding the complex (e.g. such as the synformal mushroom structure at lower Donore Lake, Fig. 3, 4). Interpretation of the geometry of the Sleepy Dragon Complex as a F_1-F_2 mushroom interference structure predicts that the "nose" on the western side of the complex is the expression (in map view) of the original F_1 anticlinal hinge. This prediction has been tested in the field, and the results are discussed in the following section.

WHY IS THE SLEEPY DRAGON COMPLEX A BASEMENT-CORED F_1 FOLD?

Workers in favour of ensialic rift models for the development of the Slave province supracrustal sequences have generally adhered to the view that basement culminations such as the Sleepy Dragon Complex reflect to a large extent original basement horsts (i.e. up-faulted basement blocks that predate and survived ductile deformation; Henderson, 1985). According to this view, these horsts subsequently acted as buttresses against which the supracrustal rocks were shortened and folded. This model is incompatible, however, with structural relationships in and around the complex which show that 1) all flanks of the basement complex are ductilely deformed and steeply dipping, 2) all paleo-horizontal indicators such as unconformities and bedding planes in the overlying supracrustals are steeply dipping, and 3) penetrative ductile strain in the form of D_1-related L-S fabrics, as well as F_2 folds, can be recognized not only in the supracrustal flanks of the complex, but also far into its core. The southern F_2 fold hinge of the complex (Fig. 1, 3) is a steeply plunging structure that cannot explain the sub-vertical attitudes of the unconformities and bedding planes around the complex. Prior to F_2, therefore, the Sleepy Dragon Complex must have been an upright, basement-cored structure with subvertical flanks showing steeply dipping, outward younging and correlatable supracrustal sequences (i.e. the Cameron River and Beaulieu River volcanic belts; Fig. 1, 3, 5). Collectively, these characteristics require a F_1 anticline, the axial plane of which is shown in Figures 1, 3, 5, and 6. Since the basement-cored structure terminates towards the south, it must have been a plunging anticline, unless the termination is explained by faulting. No large-scale faults with the required characteristics have been found or documented.

The overall geometry and structural systematics identify the western apex of the complex as the most likely locus for the plunging hinge of the original F_1 anticline. Not surprisingly, this locality shows the most pronounced "nose" to the structure, apart from the southern termination of the complex which is already identified as a F_2 fold hinge (Bleeker and Beaumont-Smith, 1995). That the western "nose" is nevertheless rather broad is consistent with the lobate shape of other well-documented, high-amplitude, basement-cored anticlines in other orogenic belts (e.g. Ramsay, 1967, p. 383-385; or the Exmouth antiform in Wopmay orogen documented by King, 1986, and Hoffman et al., 1988).

Figures 6 and 7 show recent mapping results that indicate that a critical reversal in vergence, of the S_1 schistosity relative to bedding, occurs across the proposed F_1 axial planar trace. In "DOMAIN A" (Fig. 6, 7), the pronounced bulk flattening plane of deformed pillows and coplanar schistosity is consistently clockwise from bedding traces (flow contacts), whereas the opposite vergence is observed in "DOMAIN B" and farther south. Furthermore, in the "nose" region, the bulk flattening plane and S_1 schistosity attain high angles relative to bedding, in itself a strong indication for a hinge region of a regional fold.

It can be shown elsewhere in the area that the bulk flattening plane, in general, tracks the S_1 cleavage direction (e.g. Fig. 8; Bleeker and Beaumont-Smith, 1995; see also Henderson, 1985), and that contributions to the bulk strain by later deformation events are relatively minor, even though on a grain scale S_2 may be a stronger cleavage. Elsewhere around the Sleepy Dragon Complex, the bulk flattening plane and S_1 schistosity are parallel or subparallel to the strike of lithological units, singling out the western "nose" as the only possible F_1 hinge region. Such an interpretation is fully consistent with the map pattern of Figure 1, the overall geometry of Figure 3, and the S_1 vergence relationships illustrated in Figures 6 and 7. Bedding attitudes in the hinge region are all steep ($\geq 70°$, and generally $\geq 80°$ or even weakly overturned). These steep attitudes constrain the macroscopic axis of the F_1 hinge to have a steep plunge, subparallel to the steep stretching lineations throughout the area.

STRETCHING LINEATIONS AND THE SIGNIFICANCE OF THE STEEP F_1 AXIS

Pronounced stretching lineations are present throughout the area and are almost everywhere steeply plunging. Observations on a mesoscopic scale show that the stretching lineations lie in S_1, and formed principally during D_1 (F_1), although the lineation may have been amplified by D_2-related strain (Bleeker and Beaumont-Smith, 1995). The stretching lineation is developed in all rocks, including granitoid rocks several kilometres into the core of the Sleepy Dragon Complex, its volcanic "cover", the Burwash Formation metaturbidites, and in the youngest pre-D_1 rocks such as gabbro sills that intrude the Burwash Formation at Tibbit and Terry lakes. Therefore, the intense deformation seen throughout the area is developed throughout the rock column and is not specifically related to the basement/volcanic contact.

Late-D_1 development of the strong L-fabric is the most likely, and currently the only viable explanation for the steep plunge of the F_1 hinge, which initially must have been plunging more moderately but was subsequently rotated towards the L_1 stretching orientation. The wholesale rotation of this macroscopic hinge is one of the more dramatic indications of the intensity of the regional thick-skinned deformation. Near-parallelism between the macroscopic fold axis and the regional stretching lineation, suggests that the F_1 folds, at least locally, are highly non-cylindrical to almost sheath-like in geometry.

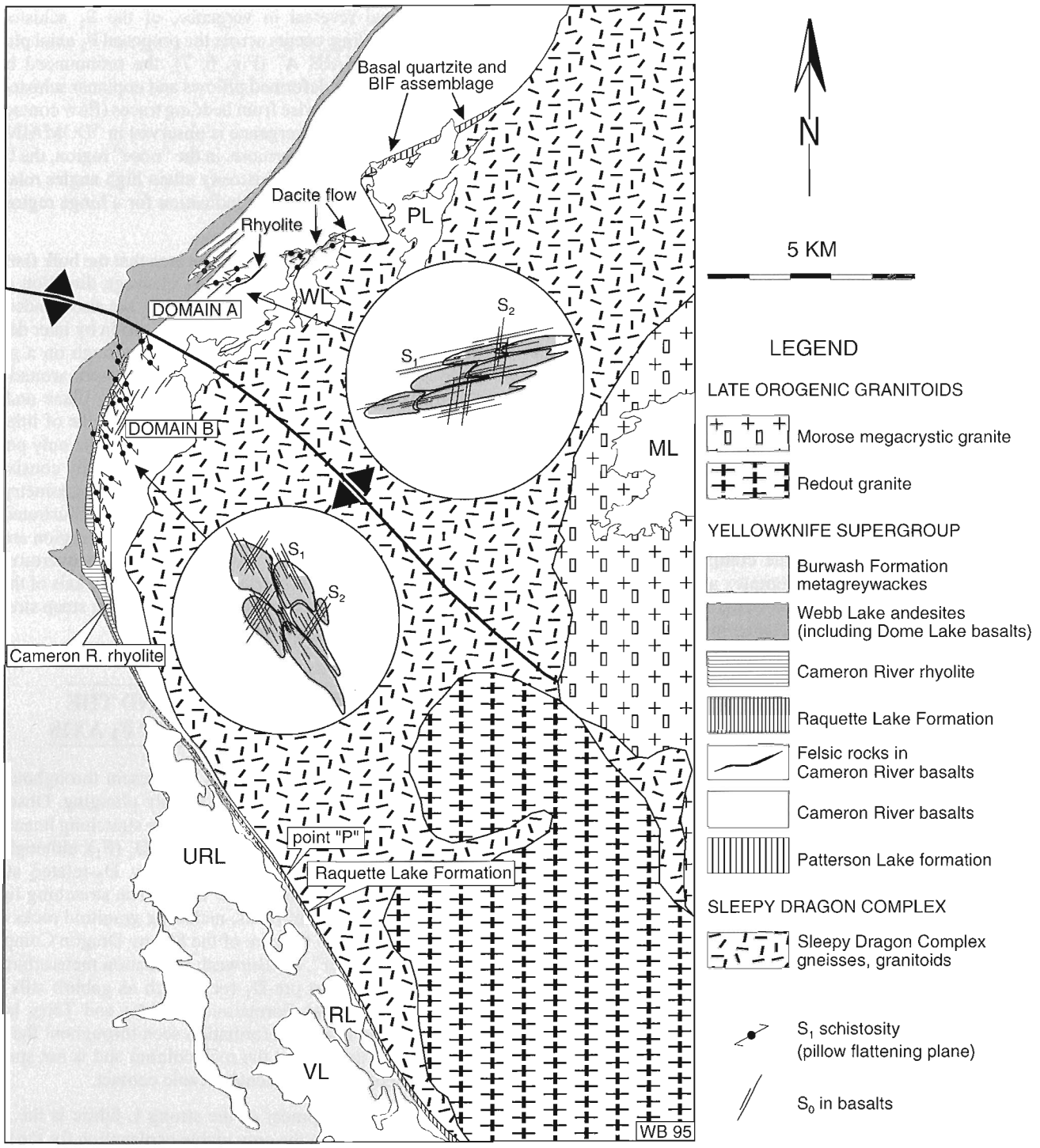

Figure 6. *Map of the western "nose" area of the Sleepy Dragon Complex. Insets show mesoscopic structures in pillowed flows of "DOMAIN A" and "DOMAIN B". Cleavage vergence relationships (S_1 relative to bedding) confirm the existence of a steeply plunging F_1 hinge. Note the presence of a well-preserved basal quartzite and banded iron formation assemblage below the Cameron River basalt at Patterson Lake (PL). Note also that the Cameron River basalt is progressively cut out in "DOMAIN B" by the Cameron River rhyolite and farther south by the clastic rocks of the Raquette Lake Formation. South of point "P", mafic volcanic-dominated conglomerate lies directly on basement rocks. These relationships suggest a low-angle unconformity.*

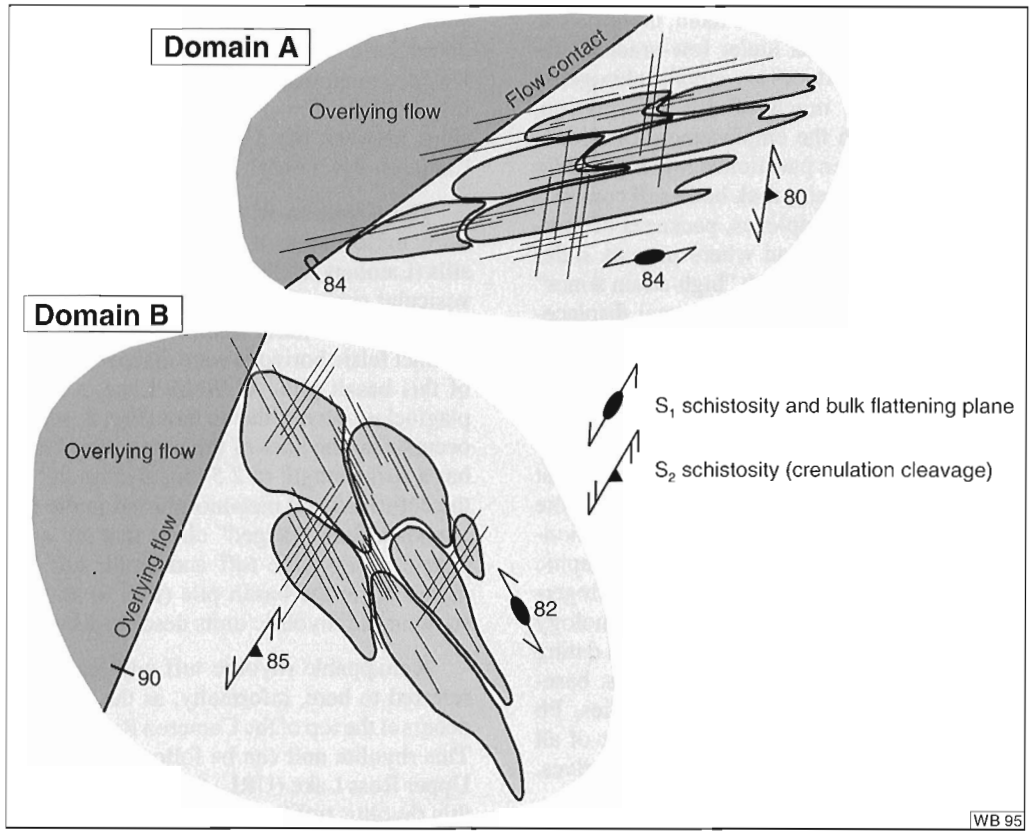

Figure 7. *Detailed sketch of the relationships between the S_1 schistosity (and coplanar bulk flattening plane) and bedding (flow contacts) in "DOMAIN A" and "DOMAIN B" of Figure 6. The regional S_2 schistosity is present in both outcrops and manifests itself as a crenulation cleavage that overprints S_1 but has little effect on the bulk flattening plane of the pillows.*

HIGH-STRAIN ZONES: ARE THEY SIGNIFICANT?

It was argued above and in Bleeker and Beaumont-Smith (1995) that the stretching lineations seen throughout the complex cannot be related to "thin-skinned" obduction of oceanic slivers (cf. Kusky, 1990). Instead, development of the lineations (L_1) appears to have post-dated the assembly of all the major lithological units into their present relative configurations. If the basalt-dominated piles represent obducted oceanic slivers, they must have been emplaced on cryptic thrusts, which are not easily resolved from the present fabrics due to the intensity of subsequent polyphase deformation. In Phanerozoic accretionary settings, cryptic thrusts are probably the norm rather than the exception among structures associated with the emplacement of thin allochthons. Recognition of such thrusts is usually based on stratigraphic rather than structural arguments. Deformation zones specifically related to thrust planes may be vanishingly thin, while the overlying allochthon may show few signs of penetrative strain.

Figure 8. *Field photograph of a quartz-plagioclase-phyric dacitic unit (a flow?) that was observed intercalated near the base of the Cameron River basalt pile. The dacite contains dark, ragged clasts which are sparsely quartz-phyric. Note flattening of the clasts parallel to the S_1 schistosity, as well as the presence of the S_2 schistosity at a high angle to S_1 (25 cent coin for scale).*

In many greenstone belts, on the other hand, deformation of contrasting lithological domains under low-grade metamorphic conditions typically produces extremely heterogeneous strain fields. Invariably, much of the deformation, whether it was associated with the emplacement of allochthons or not, appears to have been partitioned into high-strain zones on the contacts between major rock bodies of contrasting rheology such as volcanic complexes, packages of sedimentary rocks, granitoid plutons, and where present, older basement gneisses. The existence of such "high-strain zones" is of little diagnostic significance unless the total displacement on the zones can be quantified and the timing of displacement(s) established. At best, the zones can provide supporting evidence rather than the primary argument in favour of an allochthonous origin for certain rock packages.

Ultimately, diagnostic evidence in favour of or against emplacement of allochthonous basaltic slabs can only come from reconstructions of the macroscopic structural relationships (e.g. large-scale imbrication, cut-offs), stratigraphic relationships (e.g. absence or presence of primary interfingering of critical rock types), sedimentology and volcanology (e.g. ocean floor versus shallow water setting), zircon dating (e.g. "old over young" relationships, detrital zircons, basement xenocrysts), and geochemistry (e.g. ε_{Nd} studies, Pb isotopes, trace elements). Perhaps the least diagnostic of all the critical relationships are the high-strain zones themselves.

NOTES ON THE STRATIGRAPHIC RELATIONS

One of the major overall aims of the current project is to provide a comprehensive stratigraphic understanding for the Yellowknife Domain. Given the scope of this paper and the fact that much of this work is in progress, a thorough treatment of the subject would be premature. Nevertheless, some of the current results have important stratigraphic implications and are briefly described below.

At Patterson Lake, a well-preserved assemblage of quartz-rich metasedimentary rocks and banded iron-formation can be mapped along the contact of protomylonitic Sleepy Dragon Complex gneiss and the Cameron River basalt (Fig. 6). The assemblage includes quartz pebble conglomerate, quartzite, immature breccias with volcanic clasts, chert, and oxide facies iron-formation. The entire assemblage is cross-cut by numerous deformed and metamorphosed mafic dykes. The simplest interpretation of these dykes is that they correlate with dykes in the underlying gneiss and similar dykes and sills that have been mapped in the overlying Cameron River basalt (Lambert, 1988). Although these correlations need further testing (e.g. Lambert et al., 1992), the dykes at Patterson Lake do show that there was at least one significant dyking event that post-dated deposition of the quartz-rich sedimentary rocks. These dykes have field relationships that are consistent with them representing feeders to the basaltic pile.

Kusky (1990) briefly mentioned the presence of metasedimentary rocks at Patterson Lake, but included them in his "tectonic mélange". Although the rocks are indeed highly strained, the present study has failed to find diagnostic evidence for a mélange (e.g. tectonic breccias, exotic blocks). Detailed mapping of this critical assemblage is in progress and may hold the key to understanding the stratigraphic relationships between the Sleepy Dragon Complex gneiss and the Cameron River basalt.

The Cameron River basalt consist of a ca. 3 km thick, fairly uniform pile of massive and pillowed flows and gabbro sills (Lambert, 1988). Pillowed flows are dominant and show vesicular rims and carbonate-filled pillow interstices, possibly hinting at a fairly shallow depositional environment. Two distinct felsic horizons were discovered that will allow dating of this basalt pile. At Webb Lake, a 5-10 m thick, quartz-plagioclase-phyric dacite unit (Fig. 8; see Fig. 6 for location) occurs near the base of the basalt pile. This unit is stratiform, has a strike length of 2.5 km, is cross-cut by at least some of the deformed and metamorphosed mafic dykes, and contains abundant dark "ragged" clasts that are also sparsely quartz-phyric. A rhyolitic tuff and lapilli tuff horizon was found higher up in the basalt pile (Fig. 6) and may correlate with some of the rhyolitic units described by Lambert (1988).

A mappable rhyolite tuff and lapillistone unit, which is referred to here, informally, as the Cameron River rhyolite, occurs at the top of the Cameron River basalt (Lambert, 1988). This rhyolite unit can be followed from the F_1 hinge area to Upper Ross Lake (URL) farther south where it merges with a thin rhyolitic tuff horizon that overlies or forms the uppermost unit of the Raquette Lake Formation (Henderson, 1985; Lambert, 1988; this study; see Fig. 6). Following the rhyolite unit from the F_1 hinge region, it shows a weak but distinct angular relationship with flow units in the underlying Cameron River basalts, which are progressively cut out towards the south (Fig. 6). At point "P" (Fig. 6), the Cameron River basalts are no longer present and conglomerate of the Raquette Lake Formation, which is dominated by mafic volcanic clasts, directly overlies deformed basement gneiss.

Although an alternative interpretation is possible (see Lambert, 1988), it is suggested here that the field relationships point to the existence of a weak but important unconformity between the Cameron River basalt and the overlying rhyolite unit. The same field relationships also suggest that the coarse clastic Raquette Lake Formation, which is unconformable on basement gneiss, is broadly correlative with the Cameron River rhyolite. The Raquette Lake Formation unconformity is thus intravolcanic in age and post-dates extrusion or emplacement of the Cameron River basalt. Important supporting evidence comes from the observation that neither the Cameron River rhyolite nor the Raquette Lake Formation is cross-cut by the gabbroic dykes and sills that are so numerous in the underlying Cameron River basalt and basement gneiss. Much work remains to be done on the proposed unconformity, but the prediction is made that this unconformity is correlative with the weak angular unconformity documented in the Yellowknife greenstone belt between the Kam Group basalt and Banting Group felsic rocks (Padgham, 1987). Some of the critical answers will come from U-Pb zircon dating of the units in question.

In the F_1 hinge region, the Cameron River rhyolite is overlain and intruded by members of the Webb Lake andesite unit (Lambert, 1988; Fig. 6). Farther south, rhyolite tuffs of the Cameron River rhyolite and correlative tuffs at the top of the Raquette Lake Formation are typically overlain by a thin, sulphidic, black slate unit which forms the transition to metaturbidites of the Burwash Formation. Numerous felsic tuffs layers have now been documented throughout the Burwash Formation, at various stratigraphic levels (Fig. 2), indicating that felsic volcanism remained active during Burwash Formation deposition. One of the tuff layers, at Watta Lake (Fig. 2b; see Bleeker and Beaumont-Smith, 1995), has been dated at 2661 ± 2 Ma (Bleeker and Villeneuve, 1995). The tuff layers are invariably hosted by thin black shale intervals, which probably represent periods of quiescence in the turbidite basin. The quiescent periods appear to have "captured" one or more ash fall events from contemporaneous felsic volcanism. Preservation of the delicate tuff layers, over large distances, without evidence of reworking by current or wave action, indicates that the tuffs settled in a relatively deep water setting.

Gabbroic to dioritic sills at Tibbit Lake and Terry Lake (Henderson, 1985) intruded the Burwash Formation turbidites prior to development of F_1 upright folds. Together with the turbidites, the sills are deformed into doubly plunging F_1 synclines and anticlines that conform to the overall F_1 fold belt of Figure 1. Although clearly intrusive, the sills show complex pillow-like structures and irregularly shaped apophyses on some of their contacts with the surrounding greywacke, suggesting intrusion into a wet, unlithified, sedimentary pile. Thin, pre-F_1 mafic dykes have also been recognized within the Hearne Lake syncline, at a relatively high stratigraphic level within the Burwash Formation (Bleeker and Beaumont-Smith, 1995). Thus both felsic and mafic magmatism accompanied much of the depositional history of the Burwash Formation (Henderson, 1985).

CONCLUSIONS

The overall geometry of the Sleepy Dragon Complex has been documented. The interpretation that it forms a regional-scale mushroom interference structure (Bleeker and Beaumont-Smith, 1995) is confirmed by the present study, particularly by the documentation of the S_1 vergence relationships in the western "nose" of the complex. The S_1 vergence relationships show that this "nose" represents the hinge of a plunging, basement-cored F_1 anticline.

The overall geometry and qualitative unfolding of the F_2 folds indicate that the original F_1 anticline was upright and of high amplitude. Stretching lineations in the area relate to this high-amplitude fold rather than to pre-folding obduction of an oceanic slab. The subvertical stretching is responsible for the steep plunge of the anticlinal axis in the hinge area.

Both the structural and stratigraphic relationships described here and in Bleeker and Beaumont-Smith (1995) disagree with key aspects of the model proposed by Kusky (1990). Although it is still possible that the basaltic piles were emplaced on cryptic thrusts, it is considered unlikely on the basis of the current database. Now that an accurate geometrical model exists for the complex, a detailed study of kinematic indicators will be critical to the resolution of this problem. Other work in progress on the detailed stratigraphic relationships, geochronology and geochemistry of most of the critical units involved will help to fill in gaps in the current database and possibly allow detailed correlations with nearby greenstone belts, such as the Yellowknife greenstone belt proper.

ACKNOWLEDGMENTS

Joseph Macek, Cameron Bowie, Claudia Riveros, and Shoichi Kiyokawa all provided spirited and able field assistance during various parts of the field work. Discussions with John Henderson, both in and out of the field, have been helpful in many ways, particularly so with respect to the tuff layers in the Burwash Formation. Cees van Staal is thanked for his review and constructive critique.

REFERENCES

Barager, W.R.A.
1966: Geochemistry of the Yellowknife volcanic rocks; Canadian Journal of Earth Sciences, v. 3, p. 9-30.

Barager, W.R.A. and McGlynn, J.C.
1976: Early Archean basement in the Canadian shield: a review of the evidence; Geological Survey of Canada, Paper 76-14, 20 p.

Bleeker, W. and Beaumont-Smith, C.
1995: Thematic structural studies in the Slave Province: preliminary results and implications for the Yellowknife Domain, Northwest Territories; in Current Research 1995-C; Geological Survey of Canada, p. 87-96.

Bleeker, W. and Villeneuve, M.
1995: Structural studies along the Slave portion of the SNORCLE transect; in Slave-Northern Cordillera Lithospheric Experiment (SNORCLE), Transect Meeting (April 8-9, 1995), University of Calgary, (comp.) F. Cook and P. Erdmer; LITHOPROBE Report No. 44, p. 8-13.

Clowes, R.M. (ed.)
1993: LITHOPROBE Phase IV Proposal—Studies of the evolution of a continent; Lithoprobe Secretariat, University of British Columbia, Vancouver, British Columbia, 290 p.

Davidson, A.
1972: Granite studies in the Slave province; in Report of Activities, Part A; Geological Survey of Canada, Paper 72-1A, p. 109-115.

Henderson, J.B.
1985: Geology of the Yellowknife-Hearne Lake area, District of MacKenzie: a segment across an Archean basin; Geological Survey of Canada, Memoir 414, 135 p., 1:250,000 map.

Henderson, J.B., van Breemen, O., and Loveridge, W.D.
1987: Some U-Pb zircon ages from Archean basement, supracrustal and intrusive rocks, Yellowknife-Hearne Lake area, District of MacKenzie; in Radiogenic Age and Isotopic Studies: Report 1; Geological Survey of Canada, Paper 87-2, p. 111-121.

Henderson, J.F.
1943: Structure and metamorphism of Early Precambrian rocks between Gordon and Great Slave Lakes, North West Territories; American Journal of Science, v. 241, p. 430-446.

Hoffman, P.F., Tirrul, F., King, J.E., St-Onge, M.R., and Lucas, S.B.
1988: Axial projections and modes of crustal thickening, eastern Wopmay orogen, northwest Canadian shield; in Processes in Continental Lithospheric Deformation, (ed.) S.P. Clark, B.C. Burchfield, and J. Suppe; Geological Society of America, Special Paper 218, p. 1-29.

James, D.T. and Mortensen, J.K.
1992: An Archean metamorphic core complex in the southern Slave Province: basement-cover structural relationships between the Sleepy Dragon Complex and the Yellowknife Supergroup; Canadian Journal of Earth Sciences, v. 29, p. 2133-2145.

King, J.E.
1986: The metamorphic internal zone of Wopmay orogen (Early Proterozoic), Canada: 30 km of structural relief in a composite section based on plunge projection; Tectonics, v. 5, no. 7, p. 973-994.

Kusky, T.M.
1990: Evidence for Archean ocean opening and closing in the southern Slave province; Tectonics, v. 9, no. 6, p. 1533-1563.

Lambert, M.B.
1988: The Cameron River and Beaulieu River volcanic belts, District of MacKenzie, Northwest Territories; Geological Survey of Canada of Canada, Bulletin 382, 145 p., 1:50 000 map.

Lambert, M.B. and van Breemen, O.
1991: U-Pb zircon ages from the Sleepy Dragon Complex and new occurrence of basement rocks within the Meander Lake Plutonic Suite, Slave Province, N.W.T.; in Radiogenic and Isotopic Studies: Report 4, Geological Survey of Canada, Paper 90-2, p. 79-84.

Lambert, M.B., and van Staal, C.R.
1987: Archean granite-greenstone boundary relationships in the Beaulieu River volcanic belt, Slave province, N.W.T.; in Current Research, Part A; Geological Survey of Canada, Paper 87-1A, p. 605-618.

Lambert, M.B., Ernst, R.E., and Dudás, F.Ö.
1992: Archean mafic dyke swarms near the Cameron River and Beaulieu River volcanic belts and their implications for tectonic modelling of the Slave Province, Northwest Territories; Canadian Journal of Earth Sciences, v. 29, p. 2226-2248.

Padgham, W.A.
1987: The Yellowknife volcanic belt: setting and stratigraphy; in Yellowknife Guide Book, A Guide to the geology of the Yellowknife Volcanic Belt and its Bordering Rocks, (ed.) W.A. Padgham; Geological Association of Canada, p. 11-20.

Ramsay, J.G.
1967: Folding and Fracturing of Rocks; McGraw-Hill Book Company, New York, 568 p.

Turner, F.J. and Weiss, L.E.
1963: Structural analysis of metamorphic tectonites; McGraw-Hill Book Company, New York, 545 p.

Geological Survey of Canada Project 870008

Stratabound and stratiform sediment-hosted uranium-copper prospects in the Paleoproterozoic Amer Group, Churchill Structural Province, Northwest Territories[1]

A.R. Miller
Mineral Resources Division, Ottawa

Miller, A.R., 1996: Stratabound and stratiform sediment-hosted uranium-copper prospects in the Paleoproterozoic Amer Group, Churchill Structural Province, Northwest Territories; in Current Research 1996-C; Geological Survey of Canada, p. 49-62.

Abstract: The upper clastic sequence of the Paleoproterozoic Amer Group hosts uneconomic stratabound and stratiform sediment-hosted uranium-copper prospects. The unit of interbedded calcareous sandstone-siltstone-mudstone with minor carbonate which hosts the prospects is underlain by dolomitic limestone and overlain by calcareous feldspathic sandstone. The former, comprising pink, fine grained sandstone and drab siltstone-mudstone, was deposited in an intertidal lagoonal to sabkha environment and it is enriched in Cu, Pb, and Zn along its 140 km strike; mineralized zones are restricted to the lower portion of the sandstone-siltstone-mudstone unit. Anomalous concentrations of euhedral magnetite in sandstone-siltstone are commonly associated with disseminated pitchblende and coffinite, pyrite, chalcopyrite, ±bornite, covellite and chalcocite. Textures and opaque mineral assemblages suggest that the redox reaction of magnetite to hematite and replacement of magnetite by iron and copper sulphides controlled metal deposition. The primary mineralization is interpreted to be diagenetic, being weakly recrystallized and remobilized during Paleoproterozoic lower greenschist thermotectonism.

Résumé : La séquence clastique supérieure du Groupe d'Amer du Paléoprotérozoïque renferme des zones d'intérêt à minéralisation en uranium-cuivre dans des sédiments stratoïdes et stratiformes nonéconomiques. Les interlits de grès, de siltstone et de mudstone calcaires, accompagnés de petites quantités de roches carbonatées et dans lesquels sont situés les zones d'intérêt, sont sus-jacents à un calcaire dolomitique et sous-jacents à un grès feldspathique calcaire. Dans les interlits, les grès rose à grain fin et les siltstones-mudstones ternes ont été déposés dans un milieu allant de la lagune intertidale à la sebkha; ils sont riches en Cu, Pb et Zn sur une longueur de 140 km et les zones minéralisées sont limitées à leur partie inférieure. Les concentrations anomales de magnétite euédrique dans les grès-siltstones sont le plus souvent associées à des disséminations de divers minéraux (pechblende et coffinite, pyrite, chalcopyrite, ± bornite, covellite et chalcocite). Les textures et les associations de minéraux opaques incitent à supposer que la réaction d'oxydo-réduction de la magnétite en hématite et la substitution de la magnétite par des sulfures de fer et de cuivre ont contrôlé la mise en place des métaux. La minéralisation aurait eu lieu durant la diagenèse et il y aurait eu une recristallisation et une remobilisation peu intenses au cours d'un épisode paléoprotérozoïque de thermotectonisme au faciès des schistes verts inférieur.

[1] Contribution to Canada-Northwest Territories Mineral Initiatives (1991-1996), an initiative under the Canada-Northwest Territories Economic Development Cooperative Agreement.

INTRODUCTION

Scattered remnants of Paleoproterozoic supracrustal sequences are preserved across the western Churchill Province. These sequences display contrasting sedimentology, deformation, and metamorphism and are divisible into three time-stratigraphic units: Amer and Hurwitz groups as well as the Kiyuk Group and Chantery belt circa 2.45 to 2.1 Ga; Baker Lake and Wharton groups of the Baker Lake Basin, circa 1.84 to 1.76 Ga; and Barrensland Group, of the Thelon Basin circa 1.72 Ga (Fig. 1). The first is preserved as infolded keels within Archean supracrustal rocks and gneiss, the second as weakly deformed to undeformed graben fill, and the third as extensive flat-lying sheets. Even though these three sequences record three different stages in the thermotectonic evolution that spans over 0.73 billion years, these sequences are united by common metallogenetic theme – uranium mineralization. Several uranium deposit types are recognized in the central Churchill uranium province (Curtis and Miller, 1980; Miller and LeCheminant, 1985), each linked to sedimentary, volcanic, or thermotectonic processes during the Paleoproterozoic and Mesoproterozoic.

This report is part of ongoing regional uranium metallogenetic studies and focuses on the earliest recognized Proterozoic uranium mineralization in the central Churchill Province. Data is presented on the stratabound and stratiform uranium prospects in the Amer Group, the stratigraphic and sedimentological characteristics of the uraniferous unit, petrographic and mineralogical data, and effects of Paleoproterozoic tectonics. This report identifies the deposit type which this mineralization most closely resembles and draws a comparison to other Paleoproterozoic uraniferous sequences and sediment-hosted deposits.

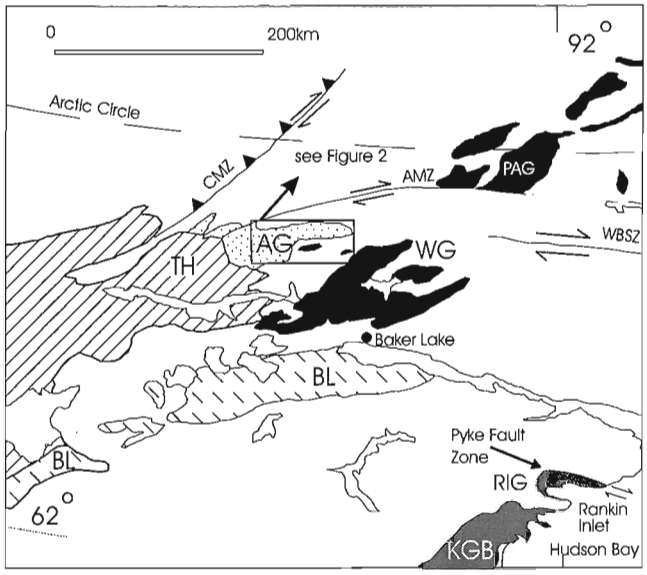

Figure 1. Location of the Amer Group, western Churchill Province.

EXPLORATION HISTORY

In 1969, an initial large-scale reconnaissance airborne radiometric survey was conducted over metasedimentary rocks that comprise the Amer synclinorium in NTS 66H. This survey identified several anomalies and resulted in the acquisition of claim groups and prospecting permits in the Amer Lake area (Frantz, 1969). In 1970, Aquitaine Company of Canada refined the airborne radiometric survey, and completed detailed ground prospecting, geological mapping and 8170 m of exploration diamond drilling on two showings (Chambrias, 1970; Fraser, 1970). Results of this program outlined two lenses of uranium mineralization hosted within laminated psammite-pelite of the upper Amer Group. Narrow uraniferous intersections ranged from 0.6 to 5.5 m with grades between 0.050 and 0.166% U_3O_8.

In 1976-77, Cominco continued exploration on the Aquitaine property. Exploration involved regional-scale geological mapping, detailed geological mapping and radiometric surveys on newly discovered and previously surveyed showings, and 300 m of exploration drilling (Blackwell, 1977). Representative uraniferous intersections assayed 0.041% U_3O_8 over 3.9 m, 0.183% over 1.84 m, 0.021% over 1.4 m and 0.060% over 1.83 m.

From 1978 to 1984, exploration continued in the Amer Group (Petura, 1982; Wiese, 1983; Evoy et al., 1982; Brown, 1982) however the exploration strategy had shifted from evaluation of the stratiform and stratabound uranium in the upper Amer Group to evaluating the potential for basement-hosted unconformity-type uranium deposits near the margin of and beneath the Thelon Basin.

REGIONAL GEOLOGY

Stratigraphy and sedimentology

The Amer Group overlies a heterogeneous polydeformed Archean granitoid basement complex composed of migmatite, layered orthogneiss, paragneiss, granite, and infolded metavolcanic rocks equated with the ca. 2.79 Ga Woodburn Lake Group (Tella, 1994). A granite within the basement complex yielded a U/Pb zircon age of 2617 ± 20 Ma (Tella,

1994). The deformed and metamorphosed Paleoproterozoic Amer Group was intruded by granite/syenite and ultrapotassic dykes that yielded an U/Pb age of 1849 ± 18 Ma.

The Amer Group consists of seven units that are variably exposed for approximately 140 km along the southwest-trending strike of the belt (Tella, 1994; Patterson, 1986; Tippett and Heywood, 1978). This stratigraphic sequence is made up of two clastic sequences and the following description follows the nomenclature of Tella (1994). The lower clastic sequence is massive white, grey, pink, and minor green orthoquartzite (Aq) with subordinate quartz-pebble conglomerate. The upper sequence is black siltstone-sandstone-pyritiferous shale (Aic), feldspathic quartzite (Afq), dolomitic limestone (Ac), feldspathic sandstone-siltstone-mudstone (Ams), and feldspathic sandstone arkose (Afs).

The texture, composition, and sedimentology of the supermature orthoquartzite suggest a fluvial to shallow marine environment (Knox, 1980) and are similar to those of the Kinga Formation, Hurwitz Group (Aspler et al., 1992). In the east portion of the belt, orthoquartzite is conformably and gradationally overlain by a thin, black, iron-rich siltstone-shale-sandstone which thins and is absent in the southwestern portion of the belt (Tippett and Heywood, 1978; Knox, 1980). This stratigraphic thinning is similar to regional wedging-out of the Ameto Formation, Hurwitz Group, in the Griffin Lake area (Aspler and Bursey, 1990). Fine clastic, euxinic sedimentation immediately following mature clastic sedimentation implies rapid deepening of the intracratonic basin. Black pelite is overlain by a thin planar to crossbedded feldspathic quartzite; the latter may be equivalent to below-wave-base and turbidity-like arkosic sedimentation in the upper Ameto Formation.

A heterogeneous, impure carbonate unit consisting of carbonate, chert, and pelitic and siliciclastic rocks overlies the feldspathic quartzite and is comparable to the middle segment of the Watterson Formation, Hurwitz Group, which was deposited in a subtidal setting. The upward increase of pelitic and psammitic interbeds implies shallowing into the overlying sandstone-siltstone-mudstone unit.

The sandstone-siltstone-mudstone unit is best described as a rhythmite or tidalite. The fine grained, calcareous feldspathic sandstones, calcareous siltstones, and mudstones are intercalated in fining upward cycles. Thin, siliciclastic carbonate-rich interbeds are present only in the lower segment of this unit. Cross stratification and parallel stratification with small-scale ripple marks in thin psammite sheets, fining upward cycles, and spheroidal structures in laminated siltstone, possibly concretions, suggest a subaqueous to supratidal setting, possibly a coastal sabkha. This unit appears to be equivalent to the Ducker-Tavanni formations, Hurwitz Group (Miller and Reading, 1993; Aspler et al., 1994).

The uppermost unit of the Amer Group, a feldspathic sandstone-arkose, coarsens upward. Contrasting types of stratification and lithology upward through this unit suggest a transition from near-shore marine to fluvial setting (Knox, 1980). This unit may be equivalent to the Tavanni Formation (Aspler et al., 1992).

Stratigraphic position of uranium mineralization

The Amer Group hosts several types of uranium occurrences, for example Amer-type U-Cu and unconformity-type uranium with or without base and precious metals. Only Amer-type prospects are shown in Figure 2. Amer-type prospects occur at two stratigraphic levels within the tidalite unit in particular to the lower segment of the tidalite that is interbedded with carbonate (Miller and LeCheminant, 1985). The interpreted subaqueous to supratidal sabkha environment combined with the restricted lithostratigraphic distribution of Amer-type mineralization are paramount in the understanding of these mineral occurrences and ore forming processes.

Structure and metamorphism

The polydeformed supracrustal rocks of the Amer Group are exposed in a broad, northeast-trending synclinorium which is characterized by locally overturned shallow, west-southwest plunging folds and by northwest-verging thrust faults (Tella, 1994; Patterson, 1986; Knox, 1980). Thrusting resulted in the repetition of the stratigraphy and juxtaposition of thin slivers of granitoid basement over the supracrustals. Northwest-trending, late brittle faults expose deeper parts of the synclinorium progressively towards the southwest. The intensity of deformation increases from southwest to northeast with a corresponding increase in metamorphic grade from subgreenschist to lower amphibolite.

REGIONAL LITHOGEOCHEMISTRY OF THE AMER GROUP

To evaluate the base metal distribution in the Amer Group metasedimentary rocks, 241 samples were analyzed for Cu, Pb, Zn, Ni, Co, and Cr by XRF pressed powder pellet. Samples are from each stratigraphic unit across and along the trend of the Amer Group from NTS 66H/9 southwestward to H/5. Averages and ranges are listed in Table 1.

A trend of increasing average base metal abundances is present upwards through the Amer stratigraphy. Metal values are lowest in the basal orthoquartzite, Aq, and increase to a maximum in rhythmically interbedded sandstone-silty sandstone-siltstone-carbonate, Ams, which hosts stratiform and stratabound prospects. Lower average copper and lead and comparable Zn, Ni, Co, and Cr values are present in the overlying feldspathic sandstone unit, Afs, when compared to the underlying metal-rich Ams unit. However there is overlap in the range in individual metal abundances between these two units.

Anomalous concentrations of copper to 988 ppm, zinc to 103 ppm, and lead to 57 ppm were found in the dolomitic limestone which is stratigraphically below and conformable with the metal-rich Ams unit. This recognition of anomalous metal contents in a shoaling upward marine to lagoonal mudflat-supratidal environment draws comparison to other Proterozoic sediment-hosted copper environments (Knutson et al., 1983; Lange et al., 1987; Unrug, 1989).

Anomalous metal abundances are present in the basal sericitic schist, unit As, which is interpreted to have been derived from a feldspathic sandstone. These values are significantly greater than in the overlying orthoquartzite. These metal contents may be in part primary and have been derived from Archean Woodburn Lake Group mafic-ultramafic metavolcanic rocks that are part of the basement complex southeast of the Amer belt. Alternatively, some metal may have been introduced during Paleoproterozoic basement-cover infolding. A primary enrichment of metals is suggested by extreme metal concentrations within subunits of the orthoquartzite. Concentrations of Ni, Cr, and Co to 2770, 2060, and 135 ppm respectively are associated with green fuchsite-bearing orthoquartzite. This contrasts with the low metal abundances present in white to pink orthoquartzite (Table 1).

PETROGRAPHY AND MINERAL CHEMISTRY

Unmineralized metasedimentary rocks

The upper clastic sequence of the Amer Group comprises two units. The lower unit is a heterogeneous unit of interstratified sandstone with black to drab green/khaki siltstone and mudstone – unit Ams of Tella (1994). This unit is overlain by a feldspathic sandstone – unit Afs of Tella (1994). Pelitic subunits in the Ams unit contain the diagnostic metamorphic assemblages: biotite+sericite/muscovite+chlorite or sericite/muscovite+chlorite indicative of lower to middle greenschist metamorphism. Accessory to essential phases in pelitic rocks include quartz, plagioclase, microcline, and carbonate.

Quartzofeldspathic rocks locally contain minor to trace quantities of the above metamorphic phyllosilicates. Psammitic rocks in the Ams unit exhibit a uniform grain-size distribution of 0.2 to 0.4 mm, are feldspathic with a feldspar/quartz ratio of 65:35 to 55:45, and are plagioclase-rich with a plagioclase-to-potassic feldspar ratio of 3:1 to 2:1. Disseminated texturally rounded resistate minerals: zircon, tourmaline and apatite, occupy intergranular areas; however neither equant rounded grains of iron nor iron-titanium oxides, nor pseudomorphs are present in psammitic or pelitic units.

Unmineralized sandstones are light to medium pink due to micrometre-scale to very fine grained hematite mantling framework grains and disseminated with authigenic cements. Additional authigenic calcite, albite, and quartz, along with hematite, are responsible for the high induration of the feldspathic sandstone. Carbonate, which is the most ubiquitous authigenic cement, varies from 10% to 25% by volume.

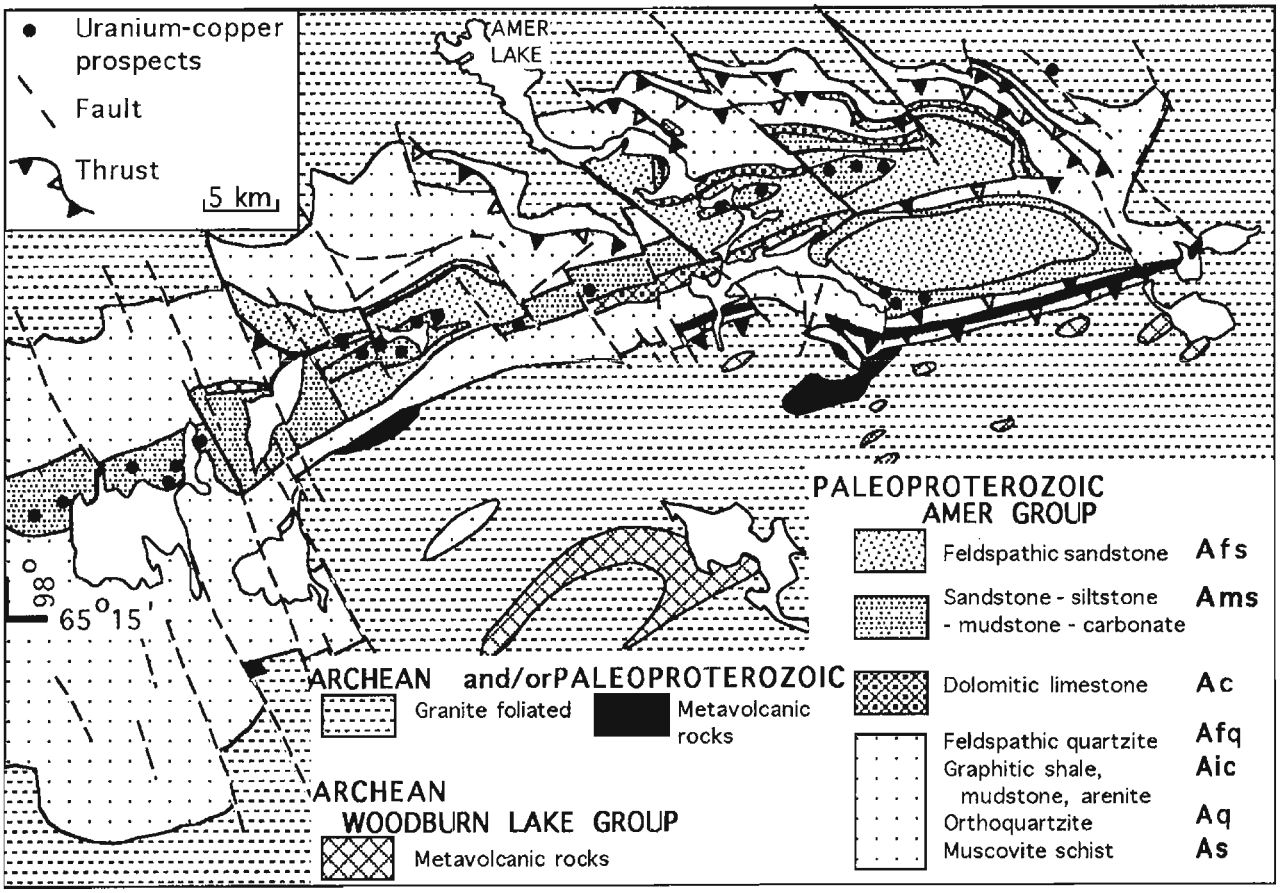

Figure 2. Simplified geology of the Amer Group, part of 66H (modified after Tella, 1994) and the location of sediment-hosted uranium-copper prospects.

Table 1. Base metal contents for each lithostratigraphic unit in the Amer Group.

Stratigraphic Unit	Cu ppm	Pb ppm	Zn ppm	Ni ppm	Co ppm	Cr ppm
Afs* AVERAGE=	10.9	6.66	3.38	24.33	10.31	49.53
N=	65	65	65	65	65	65
# of samples with non- detectible values	4	23	0	4	10	0
Range	3 - 231	2 - 109	6 - 240	2 - 71	1 - 71	8 - 149
Ams* AVERAGE=	16.79	32.04	49.68	26.27	10.89	59.84
N=	31	31	31	31	31	31
# of samples with non- detectible values	3	7	0	1	4	0
Range	4 - 102	2 - 178	3 - 114	3 - 76	1 - 19	4 - 118
Ac* AVERAGE=	7.35	15.43	28.96	10.40	5.00	24.71
N=	28	28	28	28	28	28
# of samples with non- detectible values	11	14	0	8	17	4
Range	4 - 988	2 - 57	4 - 103	2 - 47	2 - 13	2 - 112
Afq* AVERAGE=	13.20	32.81	16.43	13.0	5.39	39.35
N=	28	28	28	28	28	28
# of samples with non- detectible values	3	12	0	3	10	2
Range	3 - 79	1 - 120	2 - 45	1 - 52	1 - 17	5 - 115
Aic* AVERAGE=	12.20	6.00	27.00	6.80	9.00	24.00
N=	5	5	5	5	5	5
# of samples with non- detectible values	0	3	0	0	2	0
Range	3 - 35	6	5 - 83	4 - 9	4 - 14	3 - 64
Aq* AVERAGE=	6.17	25.62	10.94	14.55	5.71	15.17
N=	74	74	74	74	74	74
# of samples with non-detectible values	5	32	0	16	60	9
Range	1 - 237	2 - 101	3 - 109	2 - 2770	1 - 135	1 - 2060
As* AVERAGE=	13.88	65.00	31.38	24.00	13.75	53.29
N=	8	8	8	8	8	8
# of samples with non- detectible values	8	3	8	5	4	7
Range	3 - 66	2 - 111	4 - 91	3 - 69	10 - 19	5 - 106

* Stratigraphic nomenclature (ie. Aq) for the Amer Group from Tella (1994).

Authigenic albite, composition An_0 (Table 2), mantles rounded detrital feldspar; overgrowths are in optical continuity with detrital plagioclase grains. Framework plagioclase grains are distinguished from authigenic overgrowths by round equant to round subequant form and by their partial replacement by ultra-fine grained, unoriented sericite platelets. Similar plagioclase compositions, between detrital plagioclase grains and their respective authigenic rims, suggest that plagioclase grains were homogenized during burial diagenesis (Table 2; Turner, 1980). Authigenic quartz is approximately equal in abundance to authigenic albite and mantles both framework quartz and feldspar. The paragenetic sequence of authigenic cements is: early hematite; albite+quartz+hematite; carbonate+phyllosilicate, the last now represented by chlorite.

Uranium- and copper-bearing strata

In outcrop, the colour of uranium- and copper-bearing sandstone-siltstone differs markedly from that of unmineralized equivalents and is concordant with bedding (Fig. 3). This colour varies from cherry red to red-brown on both weathered and fresh surfaces. It results from the presence of martitized magnetite and a greater proportion of disseminated ultra-fine grained authigenic hematite mantling and staining framework silicates and cements. Elevated magnetite contents in interbedded sandstone-silty arkose-siltstone define weak magnetic anomalies that parallel bedding. Some, but, not all of these anomalies coincide with anomalous radioactivity (Evoy et al., 1982; Brown, 1982). This association of uranium-copper minerals with elevated abundances of magnetite and/or hematite, and the textural relationships between authigenic cements, iron oxides, and sulphides, are critical to interpreting mineralizing processes.

Magnetite and hematite

Magnetite is present in mineralized and unmineralized sandstone-silty sandstone and siltstone and varies from <5% in pelite to 3% in uraniferous psammite and semipelitic psammite. Marked differences in modal proportions between pelitic and psammitic beds suggest that iron distribution may have been controlled by permeability differences. Magnetite is fine grained, ranges from 0.1 to 0.35 mm, and occurs as octahedrons and cubes. Euhedral magnetite contrasts with altered detrital iron oxides commonly present in redbeds and suggests this magnetite is not detrital in origin (Turner, 1980; Morad and Aldahan, 1986). Magnetite is evenly disseminated or forms diffuse bands that parallel primary stratification in sandstone (Fig. 4, 5). Folded magnetite laminations indicate a predeformation origin for the magnetite. Some coarser grains, 0.25-0.35 mm, are poikiloblastic, containing inclusions of authigenic quartz and carbonate. Closely spaced, fine grained magnetite euhedra coalesce to form a polygranular mosaic up to 0.7 mm. In both unmineralized pelite and psammite, a digenetic origin for magnetite is supported by uniform reflectivity across magnetite grains, the absence of textures indicative of magnetite overgrowths on preexisting detrital oxides, uniform core to rim compositions, and the absence of divalent cations commonly present in ulvospinel

Table 2. Representative electron microprobe analyses of authigenic minerals associated with Amer-type mineralization.

	MAGNETITE	HEMATITE	MAGNETITE	HEMATITE	MAGNETITE CORE	MAGNETITE RIM		CHLORITE	CHLORITE		CARBONATE	CARBONATE		ALBITE	ALBITE
	CORE	RIM	CORE	RIM	UNALTERED	UNALTERED								AUTHIGENIC	DETRITAL CORE
	GRAIN 1	GRAIN 1	Grain 2	GRAIN 2	GRAIN 3	GRAIN 3		GRAIN 1	GRAIN 2		GRAIN 1	GRAIN 2		GRAIN 1	GRAIN 1
FeO	92.86	90.02	92. 73	89.52	94.06	93.61	SIO2	29.43	30.63	CaO	51.96	52.71	SIO2	67.85	68.64
TiO2	0.03	0.08	0.10	0.05	0.04	0.12	AL2O3	17.78	16.53	MgO	1.02	1.28	AL2O3	19.87	19.68
Cr2O3	0.09	0.06	0.05	0.04	0.04	0.04	TIO2	0.00	0.02	MnO	0.47	0.50	FEO	0.21	0.07
MgO	0.04	0.03	0.02	0.06	0.04	0.01	CR2O3	0.02	0.01	FeO	1.69	1.87	CAO	0.07	0.06
SiO2	0.08	0.15	0.08	0.12	0.07	0.09	FEO	15.52	18.18	BaO	0.00	0.04	NA2O	12.02	11.73
Al2O3	0.03	0.06	0.03	0.09	0.03	0.05	MNO	0.17	0.06	SrO	0.17	0.17	K2O	0.11	0.09
MnO	0.06	0.00	0.00	0.03	0.04	0.05	MGO	24.43	21.62	TOTAL	55.31	56.57	TOTAL	100.13	100.27
TOTAL	93.19	90.4	93.01	89.91	94.32	93.97	CAO	0.11	0.10						
							NA2O	0.03	0.07		(BASIS 6 OXYGEN)			(BASIS 32 OXYGEN)	
(BASIS	32 OXYGEN)	6 OXYGEN)	32 OXYGEN)	6 OXYGEN)	32 OXYGEN)	32 OXYGEN)	K2O	0.13	0.09						
							TOTAL	88.08	87.56	Ca	5.652	5.602	Si	11.877	11.962
Al	0.011	0.004	0.011	0.006	0.011	0.018				Mg	0.154	0.189	Al	4.099	4.042
Cr	0.022	0.003	0.012	0.002	0.010	0.010		(BASIS 28OXYGEN)		Mn	0.040	0.042	Total	15.976	16.004
Fe+3	15.954	3.975	15.932	3.976	15.960	15.918				Fe	0.143	0.155			
Ti	0.007	0.003	0.023	0.002	0.009	0.028	Si	5.882	6.204	Ba	0.000	0.002	Na	4.080	3.963
Total	15.994	3.993	15.978	3.992	15.990	15.974	Al	2.118	1.796	Sr	0.010	0.010	Ca	0.013	0.011
							Total	8.000	8.000	Total	5.999	6.000	K	0.025	0.020
Fe+2	7.972	0.003	8.012	0.000	7.985	8.009							Total	4.118	3.994
Mg	0.018	0.002	0.009	0.005	0.018	0.005	Al	2.071	2.150		MOL %	MOL %			
Mn	0.016	0.000	0.000	0.001	0.008	0.013	Ti	0.000	0.003	CaCO3	94.22	93.37	Fe	0.031	0.010
Total	8.006	0.005	8.021	0.006	8.011	8.027	Cr	0.003	0.002	MgCO3	2.57	3.15	Total	0.031	0.010
							Fe	2.595	3.080	MnCO3	0.67	0.70			
							Mn	0.029	0.010	FeCO3	2.38	2.58		MOL%	MOL%
							Mg	7.279	6.527	BaCO3	0.00	0.03	Ab	99.08	99.22
							Ca	0.024	0.022	SrCO3	0.17	0.17	An	0.32	0.28
							Na	0.012	0.027				Or	0.61	0.50
							K	0.034	0.023						
							Total	12.047	11.844						
							Fe/Fe+Mg	0.263	0.321						

Figure 3. Outcrop of concordant U-Cu mineralization. Hematitized uraniferous calcareous feldspathic sandstone bed (S_0 outlined by dashed lines) is interbedded within less permeable nonhematitic siltstone-silty sandstone with S_1 cleavage. (Subdivisions on hammer are 5 cm). GSC 1995-236A

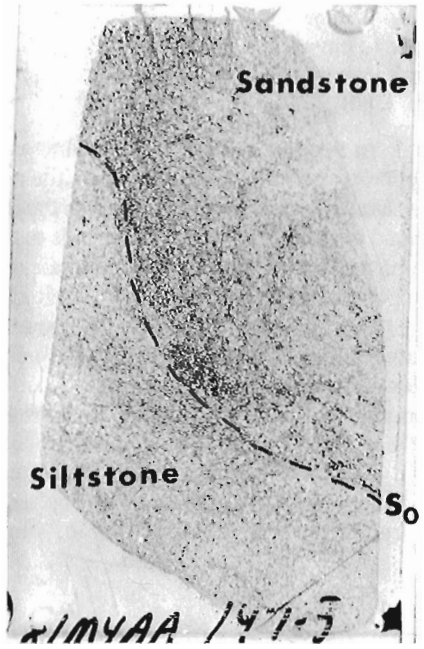

Figure 5. Photograph of thin section, width 26 mm, displaying folded contact between mineralized sandstone and unmineralized siltstone. Disseminated magnetite+ pitchblende are concentrated in the sandstone at the contact. GSC 1995-250A

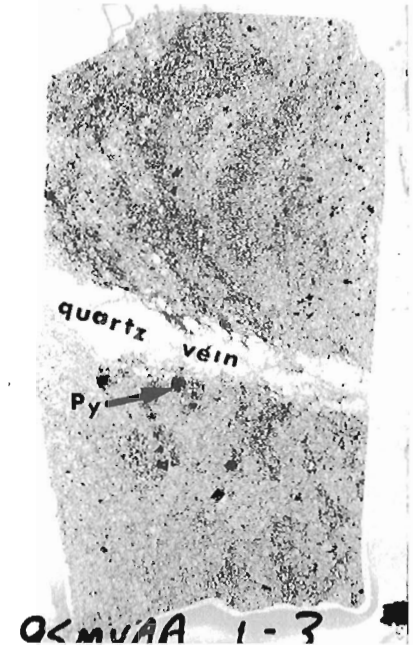

Figure 4. Photograph of thin section, width 26 mm, displaying folded mineralized sandstone. Diffuse dark bands are comprised of altered magnetite and uranium minerals with poikiloblastic pyrite (Py). GSC 1995-250B

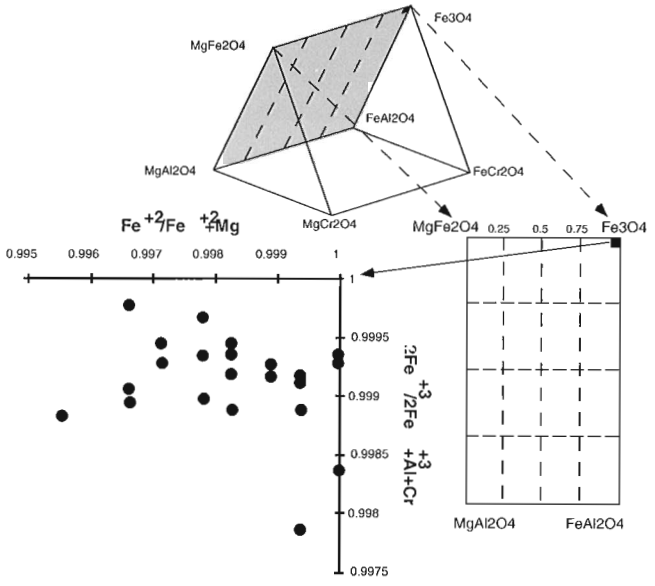

Figure 6. Composition of magnetite from mineralized and unmineralized sandstone-siltstone plotted on the oxidized face of the spinel prism.

formed by igneous processes (Fig. 6; Table 2). The magnetite is interpreted to have formed under reducing conditions similar to processes that formed magnetite during serpentinization (Eckstrand, 1980).

However, in mineralized psammite and to a lesser extent in pelite, replacement of magnetite by hematite and sulphides is common. Martitized magnetite preserves the original idiomorphism and ranges from partial, thin rinds to total replacement. Corona replacement textures are prevalent (Fig. 7) and resemble replacement textures as ferrichromit after chromite (Haggerty, 1991). Similar martitization textures can form during weathering of magnetite (Morris, 1980). Features such as restriction of hematitized magnetite to uraniferous strata, the conformable geometry of hematitization (Fig. 3), and the absence of oxidation on coexisting disseminated sulphides, indicate that the martitization process was related to mineral reactions that precipitated uranium and copper, and not to surficial processes. The composition of hematite after euhedral magnetite and interstitial anhedral hematite lacks divalent cations (Table 2). These plot at the Fe_2O_3 apex in the Fe_2O_3-$FeTiO_3$-$MnTiO_3$ ternary diagram (Fig. 8).

Uranium and sulphide minerals

Amer-type mineralization is characteristically disseminated, comprising complex intergrowths of pitchblende, coffinite, and a Ti-U phase. The intergrowth of uranium minerals with and on authigenic albite and quartz, and their subsequently mantling by carbonate, suggest that uranium precipitation was synchronous with early cementation. Uranium phases are less than 20 μm and coalesce into sooty mats up to 250 μm (Fig. 7). Martitized magnetite is always present near sooty uraniferous aggregates, as is fine grained subhedral pyrite (Fig. 7). Remobilized uranium in axial planar quartz veins is present where prospects are positioned in F_1 hinge zones.

Sulphides include pyrite with subordinate chalcopyrite and trace bornite and chalcocite group minerals. Replacement textures such as chalcopyrite and poikiloblastic pyrite

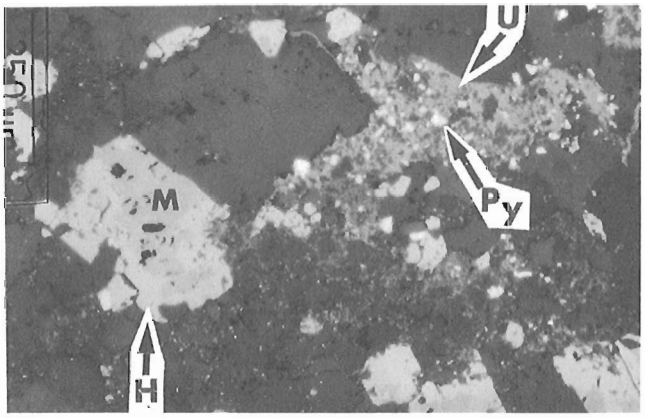

Figure 7. Corona texture produced by light gray hematite (H) after dark gray euhedral magnetite (M). Sooty uranium minerals (U) with pyrite (Py) partially fill interstitial volumes. GSC 1995-250F

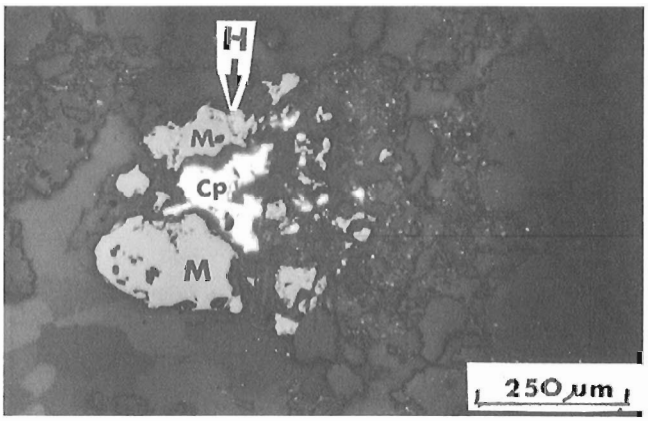

Figure 9. Sulphide replacement of magnetite: chalcopyrite (Cp) associated with weakly martitized (hematite H) anhedral magnetite (M). GSC 1995-250E

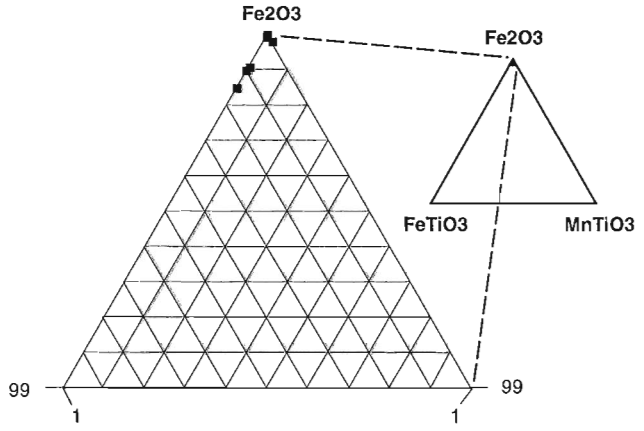

Figure 8. Composition of hematite associated with uranium and sulphide minerals.

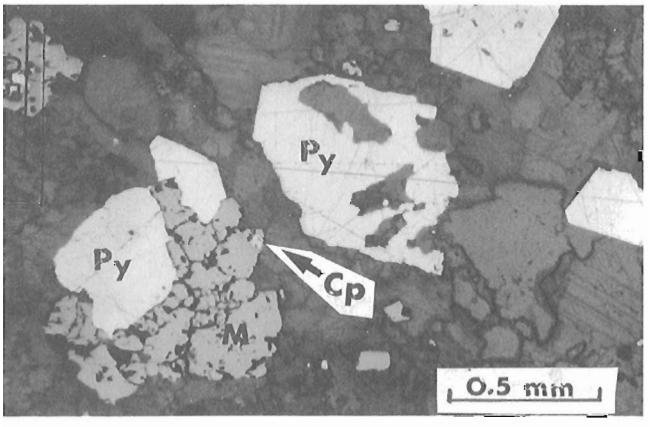

Figure 10. Poikiloblastic pyrite (Py) with chalcopyrite (Cp) replacing magnetite (M). GSC 1995-250D

mantling magnetite (Fig. 9, 10) and islands of chalcopyrite and pyrite in magnetite (Fig. 11), indicate that magnetite is the precursor mineral that was replaced and not Fe-Ti minerals or diagenetic pyrite, both of which are nuclei for copper in sediment-hosted copper deposits. Bornite contains exsolution lamellae of chalcopyrite; this texture may have developed during greenschist metamorphism of S-rich bornite.

Chlorite

Chlorite is an accessory phase, <0.5%, in both mineralized and unmineralized sandstone and silty sandstone. Ultra-fine grained, <0.1 mm, colourless to very pale green platelets of chlorite occur along grain margins of authigenic carbonate and locally replace feldspar in mineralized sandstone. Representative analyses of interstitial chlorite have MgO>FeO and Fe/Fe+Mg ratios that range from 0.08 to 0.32 (Table 2). Chlorite compositions cluster about the pycnochlorite-clinochlore join but extend to Mg-rich penninite field (Fig. 12). This range in composition differs from Fe-rich chlorite compositions common in continental redbeds (Aldahan and Morad, 1986) and may be indicative of shallow marine diagenetic processes.

Carbonate

Carbonate occupies the intergranular volumes and paragenetically follows authigenic albite and quartz. Equigranular polygonal grains up to 0.3 mm exhibit triple point junctions and undulatory extinction. These textures record minor recrystallization during Paleoproterozoic thermotectonism.

The composition of carbonate in both unmineralized and mineralized psammite and pelite plots near the calcite apex (Fig. 13). The substitution of the divalent cations in ferromagnesian calcite is minor and constant along the strike of the Ams unit. Substitutions of iron as high as 1.87 wt.% FeO and magnesium as high as 1.42 wt.% MgO are consistent with associated authigenic minerals, hematite, and Mg-rich chlorite. In addition strontium as high as 0.27 wt.% SrO may have been derived during albitization of detrital plagioclase grains

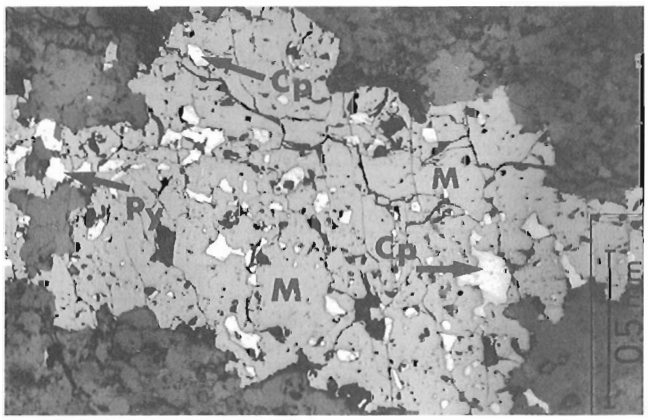

Figure 11. Replacement island texture-chalcopyrite (Cp) and pyrite (Py) after magnetite (M). GSC 1995-250C

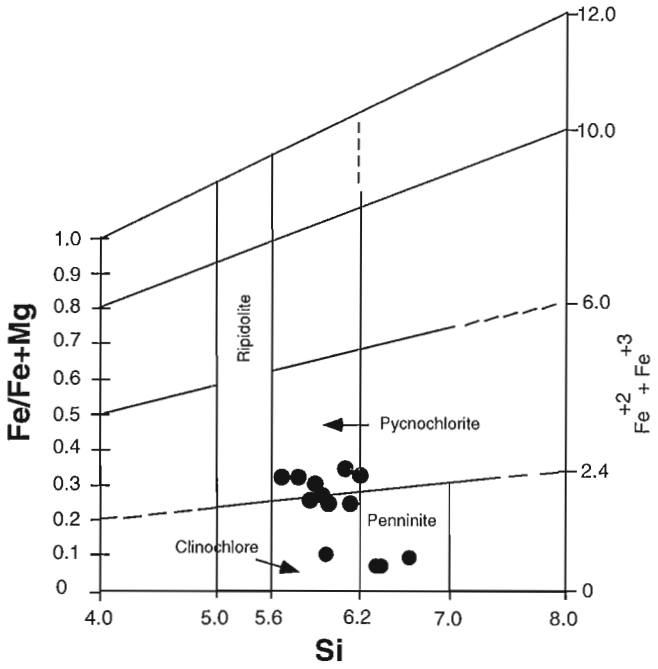

Figure 12. Composition of chlorite from uraniferous sandstone-siltstone, Amer Group.

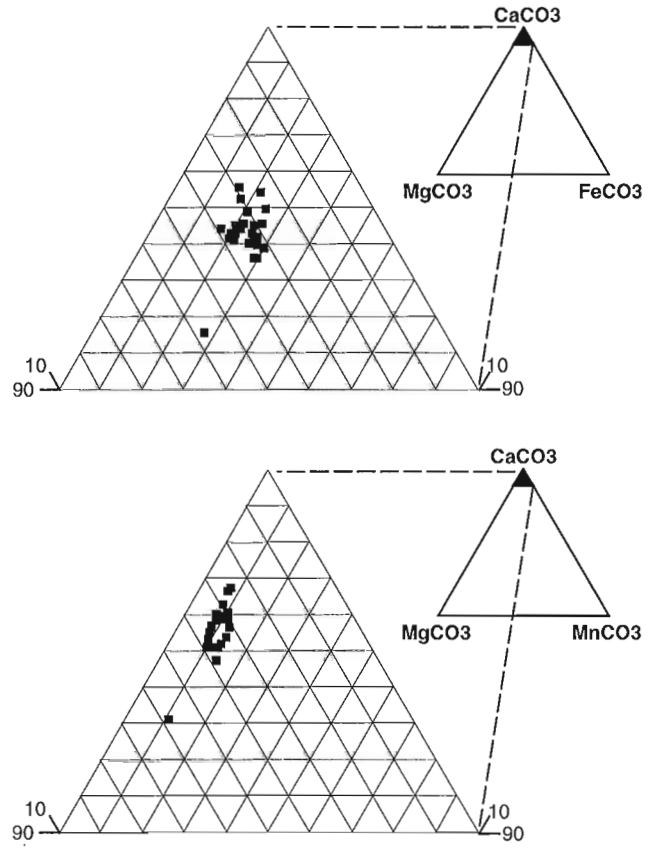

Figure 13. Compositional variation of interstitial carbonate from mineralized and unmineralized feldspathic sandstone-siltstone.

Table 3. Geochemistry of mineralized sandstone and siltstone, Amer Group.

		U	Cu	Pb	Zn	Ni	Co	Cr	Ag	Mo	V
SAMPLE	LITHOLOGY	DNC	ICP	ICP	ICP	ICP	ICP	ICP	ICP	ICP	ICP
	Detection Limit	0.1 ppm	0.5 ppm	2 ppm	0.5 ppm	1 ppm	1 ppm	1 ppm	0.2 ppm	1 ppm	2 ppm
81MYAA146-2	BLACK PHYLLITE	30.7	6.2	23	88	51	17	56	0.3	1	104
81MYAA148-1	BLACK PHYLLITE	22.2	3.8	14	87.2	44	18	42	<0.2	2	114
95MYAA1-13	RED SANDSTONE	191	4.1	53	62.7	47	16	44	1.1	3	103
81MYAA143-1	RED SDSTwBLK PHY	>10000	809	4480	30.4	10	12	44	7.8	29	14
81MYAA143-2	RED SANDSTONE	4400	295	1660	24.3	10	9	22	3.3	19	20
81MYAA147-3	RED SANDSTONE	>10000	30.5	6230	41	38	17	58	7.4	4	42
81MYAA147-1	RED SDSTwBLK PHY	8690	55.9	3550	46	37	18	46	4.4	383	87
81MYAA142-1	RED SANDSTONE	2450	60	1260	25.5	12	7	33	2	5	15
81MYAA150-3	RED SANDSTONE	>10000	132	6240	43.7	36	2	29	7	<1	21
81MYAA249-2	RED SANDSTONE	7150	107	2570	31.3	11	19	25	3.3	3	35
81MYAA249-3	PINK SANDSTONE	582	54.8	373	12.8	7	5	14	0.6	1	23
81MYAA249-8	RED SANDSTONE	1620	187	734	16.9	10	19	26	1.7	12	38
95MYAA1-1	PYRITIC RED SDST	5250	152	1830	16.6	12	16	28	2.5	4	28
95MYAA1-2	PINK SANDSTONE	1240	171	565	10.9	10	8	9	0.7	5	18
95MYAA1-4	RED SANDSTONE	4470	164	1700	9.4	11	13	28	2.5	5	24
95MYAA1-6	RED SDSTwBLK PHY	1030	73	431	17.2	6	6	14	1	10	21
95MYAA1-11	PINK SANDSTONE	207	21.2	29	10.8	5	3	16	0.8	21	22
94MYAA34-2	PINK SANDSTONE	323	7.7	38	8.2	7	3	16	0.4	<1	27
94MYAA34-1	RED SANDSTONE	6380	71.6	398	11.3	21	55	16	3	<1	53

		Ba	Sr	Fe	Ti	Mn	Ca	Mg	Na	K	Al
SAMPLE	LITHOLOGY	ICP	ICP	ICP	ICP	ICP	ICP	ICP	ICP	ICP	ICP
		1 ppm	0.5 ppm	0.01%	0.01%	2 ppm	0.01%	0.01%	0.01%	0.01%	0.01%
81MYAA146-2	BLACK PHYLLITE	1680	111	3.99	0.34	354	1.37	1.65	1.61	3.88	8.67
81MYAA148-1	BLACK PHYLLITE	1700	112	4.02	0.38	493	1.55	1.94	1.48	4.59	9.00
95MYAA1-13	RED SANDSTONE	1560	67.1	5.04	0.33	273	1.25	1.24	1.3	3.71	8.16
81MYAA143-1	RED SDSTwBLK PHY	251	137	6.64	0.08	308	2.41	0.21	1.6	0.74	3.56
81MYAA143-2	RED SANDSTONE	329	131	5.65	0.09	340	2.49	0.29	1.62	0.85	3.79
81MYAA147-3	RED SANDSTONE	904	153	2.28	0.13	856	3.98	1.38	1.04	2.65	5.73
81MYAA147-1	RED SDSTwBLK PHY	1380	91.3	2.61	0.32	461	1.99	1.36	1.25	3.96	8.07
81MYAA142-1	RED SANDSTONE	351	129	1.56	0.06	617	4	0.53	1.19	0.76	3.34
81MYAA150-3	RED SANDSTONE	311	198	6.09	0.06	998	6.7	0.82	1.1	0.72	3.22
81MYAA249-2	RED SANDSTONE	969	177	9.5	0.03	563	5.65	0.15	1.73	0.73	3.48
81MYAA249-3	PINK SANDSTONE	1330	140	0.82	0.10	532	4.34	0.25	2.13	1.39	4.70
81MYAA249-8	RED SANDSTONE	712	227	6.12	0.05	878	7.96	0.26	2.02	0.94	3.58
95MYAA1-1	PYRITIC RED SDST	491	237	3.84	0.05	867	8.68	0.28	1.94	0.95	3.40
95MYAA1-2	PINK SANDSTONE	559	257	1.76	0.05	886	9.65	0.27	2.18	1.41	3.86
95MYAA1-4	RED SANDSTONE	610	212	4.43	0.05	820	7.7	0.19	1.73	1.59	3.39
95MYAA1-6	RED SDSTwBLK PHY	1240	214	0.75	0.10	750	7.51	0.38	2.37	1.72	4.61
95MYAA1-11	PINK SANDSTONE	390	218	1.5	0.09	1320	12.5	0.7	1.44	2.03	4.00
94MYAA34-2	PINK SANDSTONE	723	68.3	0.59	0.15	269	2.32	0.62	2.49	1.72	4.75
94MYAA34-1	RED SANDSTONE	1070	47.9	0.51	0.13	141	0.22	0.66	0.9	4.24	4.65
SDST=SANDSTONE	PHY=PHYLLITE										

(Table 2), and manganese contents range as high as 0.88 wt.% MnO. The presence of one carbonate species and absence of any compositional differences between mineralized and unmineralized rocks suggest that the intraformational fluids were remarkably uniform throughout the interbedded sandstone-siltstone-mudstone unit.

GEOCHEMISTRY OF MINERALIZED SANDSTONE-SILTSTONE

Major- and trace-element geochemistry of mineralized and weakly mineralized sandstone, silty sandstone, and siltstone are tabulated in Table 3. Both the total iron content (up to 9.6 wt.%) and its mineralogical form are unusual for Proterozoic red clastic sedimentary rocks (Turner, 1980). Total iron is positively correlated with uranium even though high uranium is present in iron-poor sandstone. Copper as high as 809 ppm and an average of 125 ppm has a positive correlation with total iron, reflecting the observed textural relationship of sulphides after magnetite and with uranium. Even though silver is not greater than 7.8 ppm, silver correlates with elevated uranium and copper. Anomalous molybdenum is present in uraniferous samples and rare molybdenite grains have been identified in some Amer-type prospects (Curtis and Miller, 1980). The mineralogical site for barium is unexplained but, if present as authigenic barite, this would support the interpreted sabkha environment.

DIAGENESIS AND MINERALIZATION

The timing for metal deposition in most stratiform sediment-hosted deposits is synsedimentary or late diagenetic even though tectonism can modify the distribution of ore minerals. Permeability and redox interfaces control ore localization. Concordant Amer-type mineralization is hosted in laterally continuous, sandstone-silty sandstone beds which are enveloped by less permeable, weakly or nonmineralized siltstone and mudstone. Amer-type mineralization does not display typical replacement textures documented in sediment-hosted deposits.

Table 4. Potential reactions for the formation of Amer-type U-Cu mineralization.

$FE_2O_3 \cdot FeO = Fe_2O_3 + 1/2O_2$

magnetite hematite

$UO_2(CO_3)_3^{4-} + 2Fe^{2+} + 3H_2O = UO_2 + 2Fe(OH)_3 + 3CO2$

U in solution pitchblende geothite

↓

hematite

$4[UO_2(CO_3)_3^{4-}] + 2HS^- + Fe^{2+} + 14H^+ = 4UO_2 + FeS_2 + 12CO_2 + 8H_2O$

The association of oxidized magnetite with uranium and sulphides after magnetite indicates that magnetite rather than Fe-Ti oxides or early diagenetic pyrite acted as the catalyst for metal precipitation. Magnetite authigenesis is recognized in continental clastic and marine chemical sediments. Magnetite in lower Paleozoic carbonates is attributed to late diagenesis related to orogenic fluids (Jackson et al., 1988) and diagenetic magnetite is related to hydrocarbon migration in Triassic red sandstone (Kilgore and Elmore, 1989). During early diagenesis magnetite is stable under reduced, slightly alkaline conditions and would be compatible with authigenic albite and calcite. Alternatively, magnetite may have formed during syntectonic late diagenesis. Reaction of focused oxidized copper- and uranium-bearing fluids with magnetite in sandstone aquifers could account for the observed ore mineral textures (Table 4).

METALLOGENETIC COMPARISONS

Host rock type, depositional setting, metal associations, and the timing of mineralization are attributes of the Amer-type U-Cu prospects that suggest comparison to sediment-hosted copper deposits. Neoproterozoic copper deposits in the Zambia-Zaire and Namibia copperbelts are hosted primarily in near-shore marine, fine clastic, and carbonate rocks that overlie continental clastics (Unrug, 1989; Borg and Maiden, 1989). Metal associations and relative abundances vary between copperbelts as copper-cobalt in the Namibian deposits, but notably uranium associated with stratiform copper-cobalt-nickel in the Zambia-Zaire deposits. In eastern India, uranium and copper deposits are hosted in the Paleoproterozoic Singhbhum schist belt which was metamorphosed during the 2.05-2.0 Ga Singhbhum Orogeny (Sarkar, 1984; Singh et al., 1990; Bhattacharyya, 1992). These schist units, derived from quartzitic, arenaceous to pelitic, and volcanic protoliths are interpreted as having formed in a continental to shallow marine ensialic basin. Uranium and copper deposits are lithostructurally controlled but features such as overlap of each deposit type along a 75-100 km strike of the schist belt, the presence of copper in uranium deposits and vice versa, Ni-Mo-Bi-Co in copper deposits, and Cu-Ni-Mo-Co in uranium deposits suggest that these deposits are stratabound and were possibly originally stratiform. These ores also contain accessory magnetite.

In the Churchill Province north of 60°, sediment-dominated supracrustal sequences such as the Kiyuk, Hurwitz, and Amer groups and Chantery belt have broadly similar stratigraphic sequences, structural style, and appear to be correlative with the highly deformed and metamorphosed northeast-trending Wollaston Group supracrustal rocks in the Churchill Province, south of 60°. Paleoproterozoic siliciclastic rocks of the Wollaston Domain are subdivided into a lower, immature clastic sequence (alluvial fans-rift basin) and a transgressive shallow marine sequence.

The highly deformed and metamorphosed Wollaston Group hosts subeconomic deposits and many mineral occurrences which display a spectrum of metal associations. These associations combined with the host and associated rock

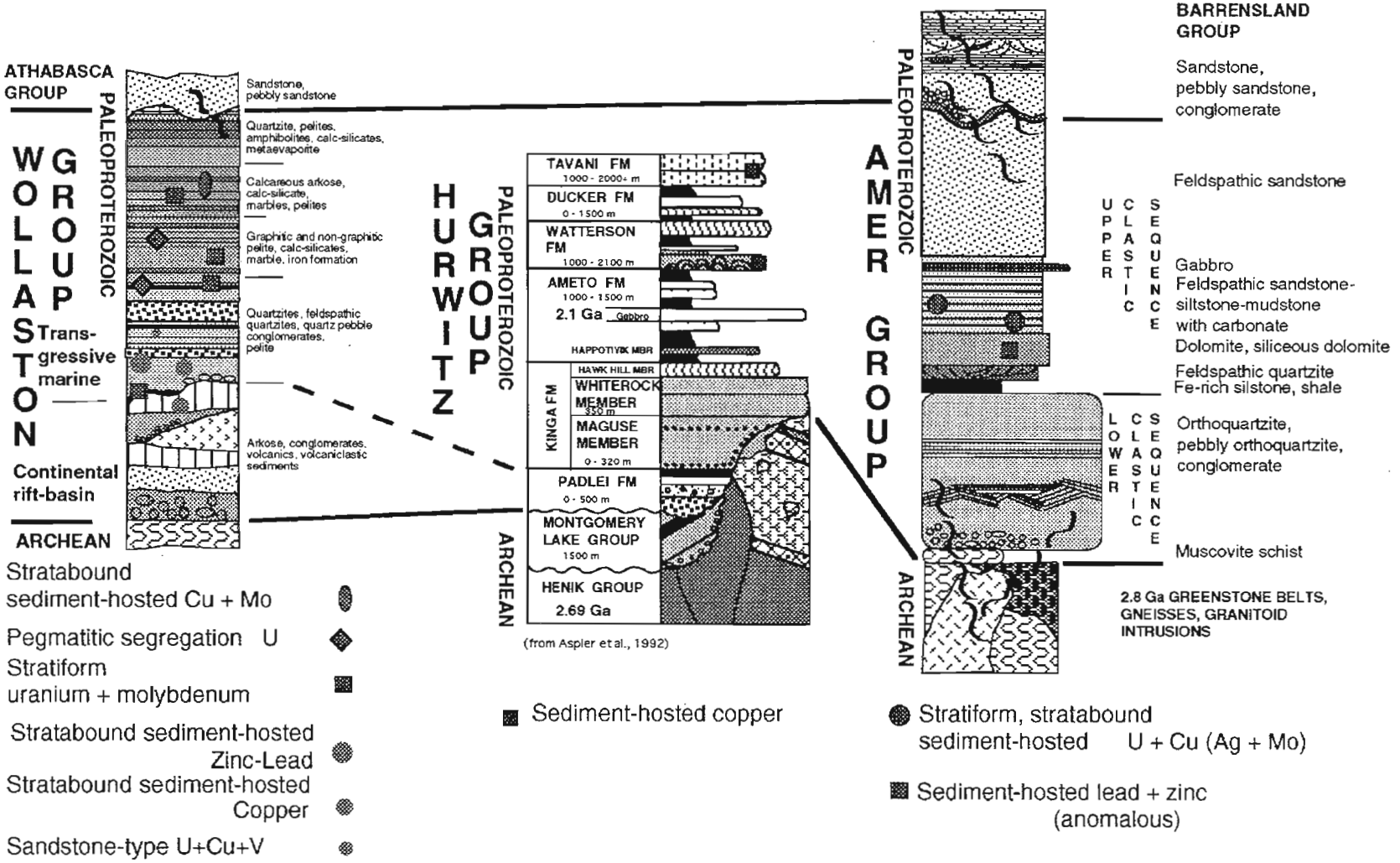

Figure 14. *Stratigraphic and metallogenetic correlations of Paleoproterozoic supracrustal sequences, western Churchill Province.*

units, and their inferred deposition setting, indicate that the Wollaston Group is a metal-rich domain containing a variety of sediment-hosted deposit types (Delaney, 1993, 1994) A schematic stratigraphic column with types of sediment-hosted deposits is presented in Figure 14. This interpreted stratigraphy of the transgressive marine siliciclastic rocks of the Wollaston Group is correlated with the Hurwitz and Amer groups to the north. Importantly, the uranium-copper prospects in lagoonal facies of the Amer Group and a similar depositional setting in the upper Hurwitz Group (Miller and Reading, 1993; Aspler et al., 1994) with copper occurrences (A.R. Miller, unpub. data) strengthens regional metallogenetic correlations. In summary, the Paleoproterozoic sequences distributed across the western Churchill Province, north of 60°, exhibit the sedimentological and depositional attributes with accompanying mineral occurrences that flag terranes as prospective for sediment-hosted mineral deposits.

ACKNOWLEDGMENTS

I am grateful to the following for logistical support and the opportunity to examine their mineral prospects in the Amer belt: Cameco Corporation, 1994-95, Ron McMillan formerly of Westmin Resources Ltd., 1981-82 and Urangesellschaft Canada Ltd., 1981-82. S. Tella is thanked for geological discussions and access to data files; J. Jakop for computer support; J. Stirling for assistance on the microprobe; and C.W. Jefferson and V. Ruzicka for reviewing the manuscript.

REFERENCES

Aldahan, A.A. and Morad, S.
1986: Mineralogy and chemistry of diagenetic clay minerals in Proterozoic sandstones from Sweden; American Journal of Science, v. 286, p. 29-80.

Aspler, L.B. and Bursey, T.L.
1990: Stratigraphy, sedimentation, dome and basin basement-cover infolding and implications for gold in the Hurwitz Group, Hawk Hill-Mountain Lakes area, District of Keewatin, N.W.T.; in Current Research, Part C; Geological Survey of Canada, Paper 90-1C, p. 219-230.

Aspler, L.B., Bursey, T.L., and LeCheminant, A.N.
1992: Geology of the Henik, Montgomery Lake, and Hurwitz groups in the Bray-Montgomery-Ameto lakes area, southern District of Keewatin, Northwest Territories; in Current Research, Part C; Geological Survey of Canada, Paper 92-1C, p. 157-170.

Aspler, L.B., Chiarenzelli, J.R., and Ozarko, D.L.
1994: Geology of Archean and Proterozoic supracrustal rocks in the Otter and Ducker lakes area, southern District of Keewatin, Northwest Territories; in Current Research, Part C; Geological Survey of Canada, Paper 92-1C, p. 165-174.

Bhattacharyya, D.S.
1992: Early Proterozoic metallogeny, tectonics and geochronology of the Singhbhum Cu-U belt, eastern India; Precambrian Research, v. 58, no. 1-4, p. 71-83.

Blackwell, J.D.
1977: Cominco Ltd., Amer Lake area, Keewatin; Indian and Northern Affairs, Yellowknife, Mining Assessment Report #061789.

Borg, G. and Maiden, K.J.
1989: The middle Proterozoic Kalahari copperbelt of Namibia and Botswana; in Sediment-hosted Stratiform Copper Deposits, (ed.) R.W. Boyle, A.C. Brown, C.W. Jefferson, E.C. Jowett and R.V. Kirkham; Geological Association of Canada, Special Paper 36, p. 525-540.

Brown, D.F.
1982: Westmin Resources Ltd., Amer Lake area, Keewatin; Indian and Northern Affairs, Yellowknife, Mining Assessment Report #081448.

Chambrias, G.
1970: Aquitaine Company of Canada Ltd., Amer Lake area, Keewatin; Indian and Northern Affairs, Yellowknife, Mining Assessment Report #019953.

Curtis, L. and Miller, A.R.
1980: Uranium geology in the Amer-Dubawnt-Yathkyed-Baker Lake region, Keewatin District, N.W.T., Canada; in Uranium in the Pine Creek Geosyncline, (ed.) J. Ferguson and A.B. Goleby; Proceedings of the International Uranium Symposium on the Pine Creek Geosyncline, International Atomic Energy Agency, Vienna, p. 595-616.

Delaney, G.D.
1993: A re-examination of the context of U-Cu, Cu and U mineralization, Duddridge Lake, Wollaston Domain; in Summary of Investigations 1993, Saskatchewan Geological Survey, Saskatchewan Energy Mines, Miscellaneous Report 93-4, p. 73-85.
1994: Geological setting of sediment-hosted copper mineralization in the area southwest of Janice Lake, Wollaston Domain; in Summary of Investigations 1994, Saskatchewan Geological Survey, Saskatchewan Energy Mines, Miscellaneous Report 94-4, p. 53-62.

Eckstrand, O.R.
1980: The Dumont serpentinite: a model for control of nickeliferous opaque mineral assemblages by alteration reactions in ultramafic rocks; Economic Geology, v. 70, p. 183-201.

Evoy, R., Kretschmar, K., Stewart, R.A., Fisk, L.F., and Nicholls, P.R.J.
1982: Westmin Resources Ltd., northwest of Baker Lake area, Keewatin; Indian and Northern Affairs, Yellowknife, Mining Assessment Report #081561.

Frantz, R.
1969: Cousins Minerals Ltd., Thelon River area, Keewatin; Indian and Northern Affairs, Yellowknife, Mining Assessment Report #060663.

Fraser, I.
1970: Aquitaine Company of Canada Ltd., Amer Lake area, Keewatin; Indian and Northern Affairs, Yellowknife, Mining Assessment Report #060383.

Haggerty, S.E.
1991: Oxide textures – a mini-atlas in Oxide Minerals: Petrologic and magnetic significance, Chapter 5, (ed.) D.H. Lindsley; Reviews in Mineralogy, v. 25, Mineralogical Society of America, p. 129-219.

Jackson, M., McCabe, C., Ballard, M.M., and Van der Voo, R.
1988: Magnetite authigenesis and diagenetic paleotemperatures across the northern Appalachian basin; Geology, v. 16, p. 592-595.

Kilgore, B. and Elmore, R.D.
1989: A study of the relationship between hydrocarbon migration and the precipitation of authigenic magnetic minerals in the Triassic Chugwater Formation, southern Montana; Geological Society of America Bulletin, v. 101, p. 1280-1288.

Knox, A.W.
1980: Geology and mineralization of the Aphebian Amer Group, southwest of Amer Lake, District of Keewatin, N.W.T.; MSc. thesis, University of Calgary, Calgary, Alberta, 207 p.

Knutson J., Donnelly, T.H., and Tonkin, D.G.
1983: Geochemical constraints on the genesis of copper mineralization in the Mount Gunson area, South Australia; Economic Geology, v. 78, p. 250-274.

Lange, I.M., Moore, J.N., and Krouse, H.R.
1987: Diagenesis and copper mineralization in carbonates in the Spokane Formation, Belt Supergroup, at Wolf Creek, Montana; Economic Geology, v. 82, p. 1334-1347.

Miller, A.R. and LeCheminant, A.N.
1985: Geology and uranium metallogeny of Proterozoic supracrustal successions, central District of Keewatin, N.W.T. with comparisons to northern Saskatchewan; in Geology of Uranium Deposits, (ed.) T.I.I. Sibbald and W. Petruk; Canadian Institute of Mining and Metallurgy, Special Volume 32, p. 167-185.

Miller, A.R. and Reading, K.L.
1993: Iron formation, evaporite, and possible metallogenic implications for the Lower Proterozoic Hurwitz Group, District of Keewatin, Northwest Territories; in Current Research, Part C; Geological Survey of Canada, Paper 93-1C, p. 179-185.

Morad S. and Aldahan, A.A.
1986: Alteration of detrital Fe-Ti oxides in sedimentary rocks; Geological Society of America, v. 97, p. 567-578.

Morris, R.C
1980: A textural and mineralogical study of the relationship of iron ore to banded iron-formation in the Hamersley Iron Province of Western Australia; Economic Geology, v. 75, p. 184-209.

Patterson, J.G.
1986: The Amer Belt: remnant of an Aphebian foreland fold and thrust belt; Canadian Journal of Earth Sciences, v. 23, p. 2012-2023.

Petura, J.
1982: Uranerz Exploration and Mining Ltd., Amer Lake, Keewatin; Indian and Northern Affairs, Yellowknife, Mining Assessment Report #081500.

Sarkar, S.C.
1984: Geology and ore mineralization of the Singhbhum copper-uranium belt, Eastern India; Jadavpur University, Calcutta, 263 p.

Singh, G., Banerjee, D.C., Dhana Raju, R., and Saraswat, A.C.
1990: Uranium mineralization in the Proterozoic mobile belts of India; Exploration and Research for Atomic Minerals, v. 3, p. 83-101.

Tella, S.
1994: Amer Lake (66H), Deep Rose Lake (66G) and parts of Pelly Lake (66F); Geological Survey of Canada, Open File 2969.

Tippett, C.R. and Heywood, W.W.
1978: Stratigraphy and structure of the northern Amer Group (Aphebian), Churchill structural province, District of Keewatin, in Current Research, Part B; Geological Survey of Canada, Paper 78-1B, p. 7-11.

Turner, P.
1980: Continental Red Bed; in Developments in Sedimentology 29, Elsevier Scientific Publishing Co., 562 p.

Unrug, R.
1989: Landsat-based structural map of the Lufilian fold belt and the Kundelunga Aulacogen, Shaba (Zaire), Zambia and Angola and the regional position of Cu, Co, U, Au, Zn and Pb mineralization; in Sediment-hosted Stratiform Copper Deposits, (ed.) R.W. Boyle, A.C. Brown, C.W. Jefferson, E.C. Jowett, and R.V. Kirkham; Geological Association of Canada, Special Paper 36, p. 519-524.

Wiese, C.
1983: Urangesellschaft Canada Ltd., Deep Rose Lake area, Keewatin; Indian and Northern Affairs, Yellowknife, Mining Assessment Report #081731.

Geological Survey of Canada Project 810024

Geology of the Meta Incognita Peninsula, south Baffin Island, Northwest Territories: tectonostratigraphic units and regional correlations

M.R. St-Onge, S. Hanmer[1], and D.J. Scott
Terrain Sciences Division, Ottawa

St-Onge, M.R., Hanmer, S., and Scott, D.J., 1996: Geology of the Meta Incognita Peninsula, south Baffin Island, Northwest Territories: tectonostratigraphic units and regional correlations; in Current Research 1996-C; Geological Survey of Canada, p. 63-72.

Abstract: Tectonostratigraphic domains in southern Baffin Island contain units which can be correlated with those in northern Quebec (Cape Smith Belt – Ungava Orogen) or central Baffin Island (Baffin Orogen). A grey tonalite gneiss is identified as possible Archean Superior Province basement. Siliciclastic-mafic-ultramafic rock sequences are correlated with the Povungnituk Group (Quebec). Carbonate and siliciclastic units of the Lake Harbour Group may be in part equivalent to the Sugluk Group (Quebec). Large felsic plutonic units comprise the southern extension of the Cumberland Batholith (central Baffin Island). Finally, panels of tonalite and monzogranite are correlated with the Narsajuaq arc (Quebec). Such correlations do not support suggestions that orthogneisses on southern Baffin Island constitute the southeastern arm of the Archean Rae craton. Correlations with the Povungnituk Group highlight the economic potential of the area.

Résumé : Les domaines tectonostratigraphiqus de la partie sud de l'île de Baffin contiennent des unités lithologiques qui ressemblent à celles que l'on trouve au Québec (ceinture de Cape Smith, orogène de l'Ungava) ou dans la partie centrale de l'île de Baffin (orogène de Baffin). Un gneiss tonalitique est identifié comme faisant peut-être partie de la province archéenne du lac Supérieur. Des séquences silicoclastiques-mafiques-ultramafiques sont corrélées au Groupe de Povungnituk (Québec). Des roches silicoclastiques et carbonatées du Groupe de Lake Harbour sont en partie équivalentes au Groupe de Sugluk (Québec). Des unités plutonqiues felsiques représentent le prolongement vers le sud du batholite de Cumberland (partie centrale de l'île de Baffin). Ces corrélations contredisent les suggestions selon lesquelles les gneiss de l'île de Baffin représenteraient la partie sud-est du craton archéen de Rae. Quant aux corrélations avec le Groupe de Povungnituk, elles soulignent le potentiel économique de la partie sud de l'île de Baffin.

[1] Continental Geoscience Division, Ottawa

INTRODUCTION

Fieldwork in Meta Incognita Peninsula, southern Baffin Island, was initiated in June 1995. This marks the first phase of a proposed three-year multidisciplinary project to investigate the geology of Lake Harbour (NTS 25K), Big Island (NTS 25L), Markham Bay (NTS 25M), and Armshow River (NTS 25N) map areas. Field aspects of the project in 1995 included bedrock geological mapping of 15 000 km^2 at 1:100 000 scale between Lake Harbour and Iqaluit (Fig. 1), mapping of surficial deposits at 1:250 000 scale, and rock/mineral identification for local residents and Inuit carvers.

Previous bedrock geological investigations include mapping of Baffin Island south of 66°N at 1:506 880 scale by Blackadar (1967), and detailed work in the vicinity of Lake Harbour by Scott and Godin (1995). Geological work in the area prior to 1965 is summarized in Blackadar (1967).

This report presents an overview of the supracrustal and plutonic units in the project area and proposes a number of tectonostratigraphic interpretations and regional correlations. A second report (Hanmer et al., 1996) describes the principal structural elements of the transect area. A third report (Scott, 1996) documents the geology of an east-west corridor across the Hall Peninsula that adjoins the project area. Finally, the reader is referred to GSC colour Open File maps #3191-3193 which document the detailed distribution of the tectonostratigraphic elements described below (Hanmer et al., in press; Scott et al., in press; St-Onge et al., in press).

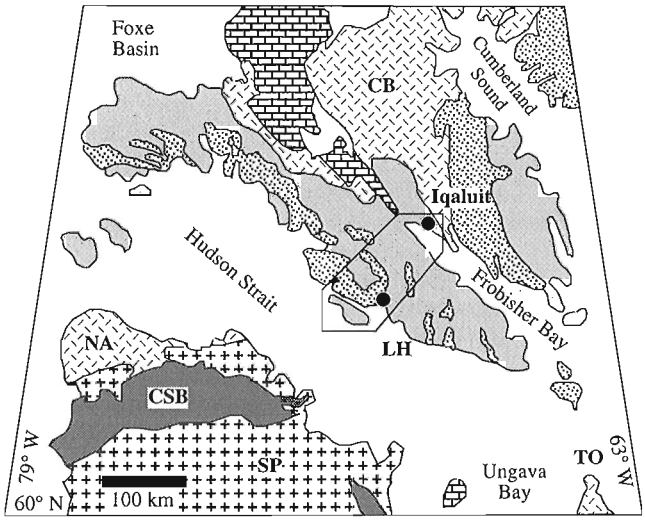

Figure 1. Geology of northern Quebec and southern Baffin Island (after Scott and Godin, 1995) highlighting area mapped in 1995. Metasedimentary units shown in coarse stippled pattern, Ordovician cover in brick pattern and orthogneisses in fine stippled pattern. CB – Cumberland batholith, CSB – Cape Smith Belt, LH – Lake Harbour, NA – Narsajuaq arc, SP – Superior Province, TO – Torngat Orogen.

TECTONOSTRATIGRAPHIC DOMAINS

Five tectonostratigraphic domains were identified (Fig. 2) and are described from south to north.

Big Island domain

The Big Island domain (Fig. 2) is underlain by (Archean?) tonalite and monzogranite orthogneisses which are separated from (Paleoproterozoic?) layered tonalite gneisses by relatively thin thrust-bound panels of supracrustal rocks (Hanmer et al., 1996, in press).

Biotite±hornblende tonalite

Biotite±hornblende±orthopyroxene±clinopyroxene±garnet tonalite is the dominant lithology. It is grey, medium grained, and equigranular. The tonalite displays a well developed gneissic foliation (Fig. 3) and in some outcrops granulite-facies minerals (orthopyroxene, clinopyroxene) are replaced by amphibolite-facies assemblages (hornblende, garnet). Mafic enclaves are locally abundant and entrained within the gneissic foliation. Massive to deformed concordant veins and sheets of biotite monzogranite comprise up to 20-25% of the gneiss.

Biotite±hornblende monzogranite

Biotite±hornblende±orthopyroxene granites vary in composition from granodiorite to syenogranite, although monzogranite is overwhelmingly the most common rock type. The kilometre-scale granite bodies are medium- to coarse-grained, grey or pink, and vary from equigranular to K-feldspar megacrystic. The plutons are generally foliated and can contain centimetre- to kilometre-scale inclusions of tonalite, quartz diorite, and amphibolite. The massive to deformed granitic veins observed in tonalite gneiss are interpreted as being related to emplacement of the granitic plutons.

Layered hornblende±biotite tonalite/quartz diorite

Mafic tonalite, pervasively interlayered with quartz diorite at the metre scale, occurs separately from the more leucocratic tonalite and monzogranite described above. The medium grained tonalite is hornblende±biotite±orthopyroxene-bearing, and volumetrically composes 60 to 70% of the layered unit. Layers of hornblende-biotite±orthopyroxene±clinopyroxene quartz diorite range in thickness from 1-5 m and are often boudined. Replacement of granulite-facies minerals (orthopyroxene, clinopyroxene) by amphibolite-facies minerals (hornblende, garnet) is common. Metre-scale amphibolite, hornblendite, and particularly pyroxenite enclaves occur locally. All components of the layered tonalite/quartz diorite gneiss unit are crosscut by concordant pink biotite monzogranite to syenogranite veins. The granite veins vary from relatively massive to well foliated and range in thickness from several millimetres to over ten metres.

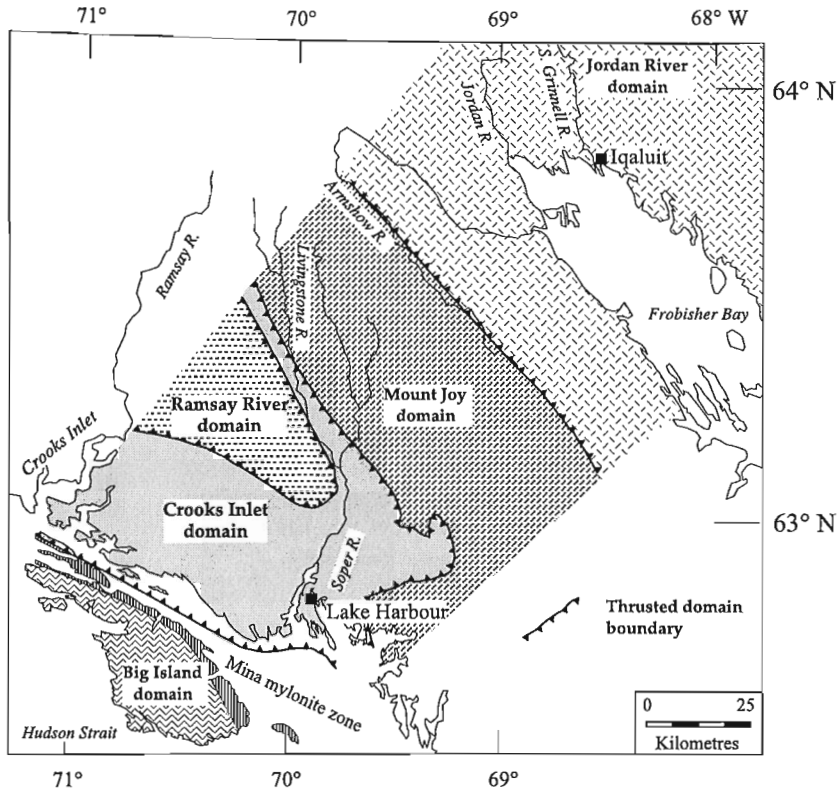

Figure 2.

Principal tectonostratigraphic domains of map area.

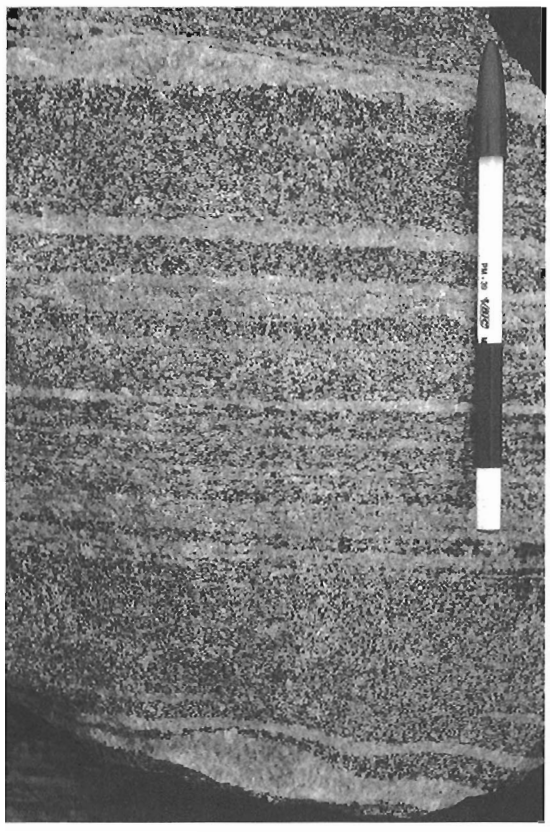

Figure 3. *Layered tonalite gneiss, Big Island domain. Pen is 15 cm long.*

Amphibolite/quartzite/semipelite assemblage

Panels of supracrustal rocks occur in abrupt contact with the orthogneisses (Fig. 4) and separate the biotite±hornblende tonalite and granite from the more mafic tonalite/quartz diorite unit. The panels, often several hundred metres in width, generally contain both siliciclastic rocks and hornblende-biotite-garnet±clinopyroxene mafic rocks. The siliciclastic rocks comprise biotite±garnet quartzite (Fig. 5), garnet-biotite semipelite, and sillimanite-K-feldspar- biotite±graphite pelite. Layering in the sedimentary rocks is assumed to be transposed bedding. In general, the mafic rocks are fine- to medium-grained, homogeneous amphibolites interpreted as mafic flows or intrusive units. These are locally interlayered with bands of medium grained amphibolite which display internal compositional layering, and are interpreted as layered mafic sills. Layers and pods of metaperidotite and pyroxenite several metres in thickness are associated with the supracrustal units and are interpreted as dismembered ultramafic sills.

Tectonostratigraphic interpretation

Contacts between supracrustal and orthogneiss units are interpreted as tectonic based on the following observations. The contacts are abrupt and intrusive relationships are not observed. Late intrusive phases such as the monzogranite component in the orthogneisses are not found within the supracrustal panels. Finally, fabric gradients (flaggyness) locally characterize the bounding plutonic rocks. The lithological association (siliciclastic-mafic-ultramafic) and field

characteristics of the supracrustal rocks are similar to the thrust-bound panels of the Paleoproterozoic lower Povungnituk Group in Ungava Orogen (Lucas and St-Onge, 1992). The supracrustal rocks of the Povungnituk Group have been interpreted by St-Onge et al. (1992) and previous workers as a record of continental rifting along the north margin of the Superior Province.

Based on the lithological association, field characteristics and granulite/amphibolite overprinting mineral assemblages (cf. St-Onge and Lucas, 1995), the biotite±hornblende tonalite and monzogranite are interpreted as comprising possible Archean basement units. These plutonic rocks are very similar to units in northernmost Quebec (Fig. 1) which were interpreted by St-Onge et al. (1992) as belonging to an Archean magmatic arc within the northeast Superior Province. In contrast, the hornblende±biotite tonalite/quartz diorite gneisses are similar to the Paleoproterozoic Narsajuaq arc units in Ungava Orogen (St-Onge et al., 1992). Such correlations will be tested by U-Pb geochronology.

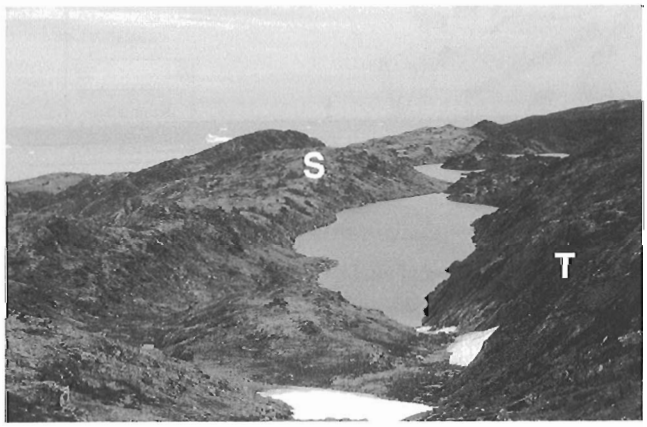

Figure 4. *Fault-bound panel of supracrustal rocks (S) juxtaposed against tonalite gneiss (T), Big Island domain. Lake is 15 m wide.*

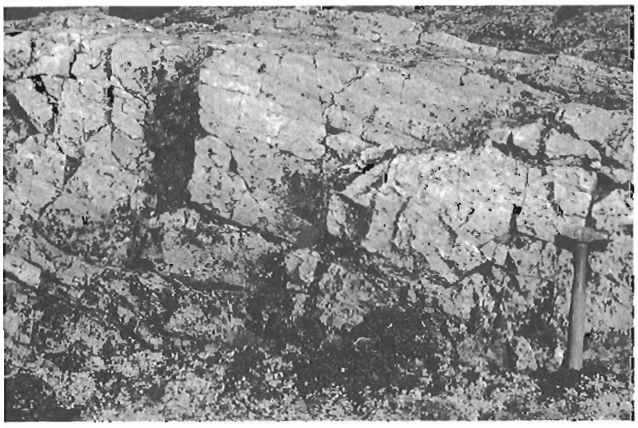

Figure 5. *Quartzite, Big Island domain. Hammer is 39 cm long.*

Crooks Inlet domain

Crooks Inlet domain is separated from the Big Island domain by a major thrust fault (Fig. 2; Hanmer et al., 1996). The domain comprises predominantly siliciclastic and carbonate metasedimentary units structurally interleaved with tonalite-quartz diorite gneiss along thrust faults (Hanmer et al., 1996, in press; St-Onge et al., in press).

Psammite, quartzite, and semipelite

Biotite-garnet-feldspar psammite (Fig. 6) is the dominant unit. The rusty-weathering rock ranges in composition from quartzite and feldspar-rich arkose (Fig. 7) to micaceous psammite. Layering varies from a few to tens of metres in thickness, and individual bands can be traced for up to hundreds of metres. Psammitic and quartzitic layers contain up to 20% lilac garnet. Sillimanite is observed in more micaceous intervals. Sandy layers generally contain abundant graphite, with individual books/flakes up to 5 mm across. Layers of biotite-garnet±cordierite semipelite are generally rusty, thinly layered at the centimetre-scale, and characterized by abundant graphite. Pyrite and chalcopyrite occur as accessory minerals.

Marble and calc-silicate

Calcareous and calc-silicate rocks form numerous prominent light-coloured ridges (Fig. 6, 8) that are laterally continuous but vary greatly in thickness. The thickest bands (several hundred metres) occur in the Crooks Inlet area and along the southwest coast of Meta Incognita Peninsula, and thin in general towards the north and east. The marble is generally medium-to coarse-grained, with compositional layering outlined by metamorphic minerals (e.g. wollastonite, forsterite, humite, diopside, spinel, tremolite, phlogopite, and grunerite). Individual layers range from centimetres to metres in thickness and can be traced for tens of metres (Fig. 9). Graphite, apatite, and titanite are common accessory minerals. Disseminated pyrite and pyrrhotite are present.

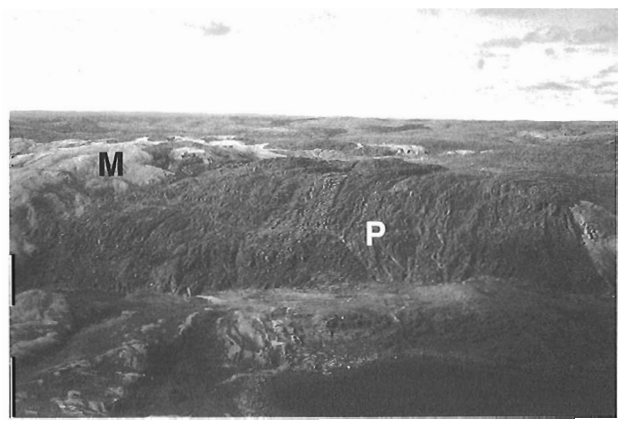

Figure 6. *Psammite (P) and marble (M), Crooks Inlet domain. Psammite section is 1 km wide.*

Calc-silicate and siliciclastic units are interlayered with the calcite marble bands and occur as boudined inclusions in the marble (Hanmer et al., 1996).

White monzogranite

White monzogranite is commonly associated with the clastic units. The monzogranite is leucocratic, garnet-biotite± cordierite±sillimanite-bearing (Fig. 10), and occurs as small tabular bodies or more diffuse, irregular pods and seams. Both feldspars are invariably white. The intimate association with the clastic rocks, the aluminous mineral assemblage and the reduced nature of the feldspars suggests a derivation by anatexis from a graphite-rich metasedimentary source.

Orthopyroxene-biotite tonalite/quartz diorite

Several panels of foliated tonalite (Fig. 11) and quartz diorite gneiss are present within the Crooks Inlet domain and are similar to the layered tonalite/quartz diorite unit inferred to be Proterozoic in age within the Big Island domain. The orthopyroxene-biotite±hornblende tonalite is medium- to coarse-grained and tan-weathering. Hornblende-orthopyroxene-clinopyroxene±biotite±garnet constitutes the dominant granulite-facies assemblage in the quartz diorite. Both tonalite and quartz diorite are crosscut by concordant biotite monzogranite to syenogranite veins. Contacts between the gneissic rocks and adjacent siliciclastic and carbonate units are interpreted as thrust faults based on the following observations (see also Hanmer et al., 1996). At the outcrop scale, contacts are abrupt and intrusive relationships are not observed. Supracrustal rocks are not crosscut by even the youngest granitic phase. Down-dip stretching lineations are

Figure 8. *Marble ridge, Crooks Inlet domain. Height of cliff is 30 m.*

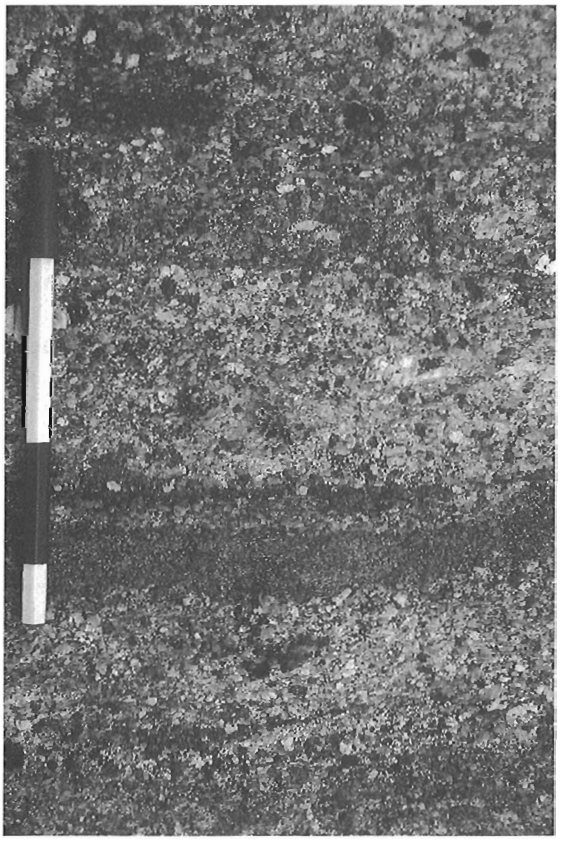

Figure 7. *Arkosic grit, Crooks Inlet domain. Pen is 15 cm long.*

Figure 9. *Compositional layering in marble, Crooks Inlet domain. Hammer is 39 cm long.*

locally preserved within the granulite-facies foliation. At the regional scale, the supracrustal and plutonic panels are characterized by marked along-strike continuity (~100 km), generally narrow widths (several hundred metres to a few kilometres), multiple tectonostratigraphic repetitions, and along-strike truncations of units (cf. ramp structures) (Hanmer et al., in press; St-Onge et al., in press).

Tectonostratigraphic interpretation

The siliciclastic and carbonate rocks of the Crooks Inlet domain belong to the Paleoproterozoic Lake Harbour Group (Davison, 1958; Jackson and Taylor, 1972). Although the sequence is internally imbricated with distinct tectonostratigraphic units (marble, quartzite, psammite, etc.) repeated by thrusting (Hanmer et al., 1996), an overall upward progression from coarse to fine siliciclastic units (quartzite-psammite-semipelite) and ultimately carbonate is indicated from the map distribution of units (Hanmer et al., in press; St-Onge et al., in press). This sequence is interpreted in terms of the construction of a carbonate shelf sequence on a dominantly siliciclastic sedimentary wedge. The tectonostratigraphic equivalent to the Lake Harbour Group in the Ungava Orogen is the Sugluk Group (St-Onge et al., 1992). Although dominated by semipelite, quartzite, and pelite, the Sugluk Group also contains rare carbonate and calc-silicate layers on Digges Island and along the southern shore of Hudson Strait. However, in apparent contrast to the Lake Harbour Group, the Sugluk Group is both in fault and intrusive contact with adjacent plutonic units (Lucas and St-Onge, 1992).

Based on field characteristics, and preliminary geochronology indicating tonalite emplacement during the period ca. 1840-1830 Ma (Scott and Godin, 1995), the gneissic rocks within the Crooks Inlet domain are interpreted as correlative with the Narsajuaq arc (St-Onge et al., 1992) and are similar to the layered tonalite/quartz diorite unit of the Big Island domain.

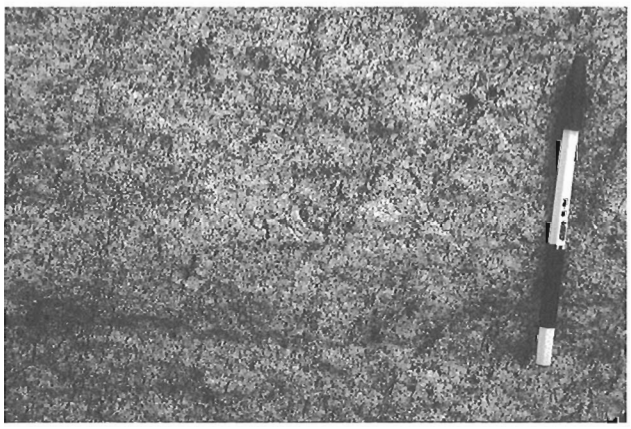

Figure 10. *Garnet-biotite white monzogranite, Crooks Inlet domain. Pen is 15 cm long.*

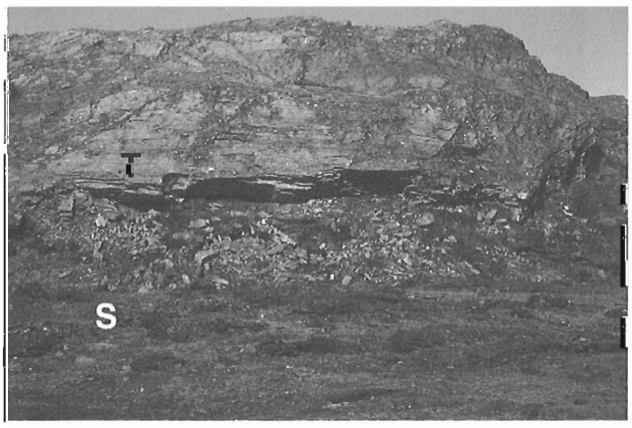

Figure 11. *Fault-bound panel of tonalite gneiss (T) overlying semipelite (S), Crooks Inlet domain. Height of cliff is 25 m.*

Ramsay River domain

The Ramsay River domain occurs structurally above the Crooks Inlet domain (Fig. 2) and is separated from the latter by regionally extensive thrust faults (Hanmer et al., 1996). The domain comprises a distinct sequence of siliciclastic, mafic, and ultramafic units interleaved with tonalite gneiss panels and intruded by monzogranite plutons (St-Onge et al., in press).

Quartzite and semipelite

Fine- to medium-grained, biotite±feldspar quartzite forms prominent grey-weathering ridges up to several hundred metres in thickness. The quartzite typically occurs as 0.5-2 m layers, commonly alternating with thinner bands of psammitic or pelitic compositions. Primary depositional features such as crossbedding or graded bedding were not observed. Fine grained, disseminated chalcopyrite and pyrite are locally present. Interlayered with the quartzite are rusty intervals of finely layered (centimetre-scale) semipelite which contain abundant biotite and lesser garnet and pyrite. In general the semipelite is associated with sillimanite±cordierite pelitic layers. The predominance of thick, mature quartzite layers suggests a proximal tectonostratigraphic facies.

Mafic-ultramafic units

Numerous mafic-ultramafic bands are present within the clastic sequence (Fig. 12). The bands vary from 10 to 300 m in thickness and range in composition from metaperidotite and metapyroxenite to hornblende±orthopyroxene±clinopyroxene amphibolites. The thicker mafic bands preserve gabbroic to leucogabbroic textures, whereas others are fine grained and massive. Contacts with the siliciclastic rocks are conformable and the mafic-ultramafic bands are interpreted as layered sills or thick flows.

Orthopyroxene-biotite tonalite/quartz diorite

Panels of orthopyroxene-biotite±hornblende±clinopyroxene tonalite gneiss and associated quartz diorite are similar to those within the Big Island and Crooks Inlet domains. The

tonalite is medium- to coarse-grained, foliated to locally gneissic. The quartz diorite contains hornblende-orthopyroxene-clinopyroxene and occurs as inclusions or boudined layers within the tonalite gneiss. The bands of plutonic rocks display sharp contacts with the supracrustal units and show no intrusive or entrapment relationships. Tonalite or quartz diorite are not observed crosscutting the supracrustal units. Based on theses observations, the contacts are interpreted to be tectonic.

Orthopyroxene-biotite monzogranite

Massive, locally foliated, orthopyroxene-biotite monzogranite is associated with and emplaced into the tonalite/quartz diorite gneiss panels. Dykes and veins crosscutting the older rocks are commonly observed, as are rafts and inclusions of tonalite/quartz diorite within and near the margin of the monzogranite plutons. The monzogranite plutons are generally medium- to coarse-grained and locally K-feldspar megacrystic. Locally they grade into granodioritic and tonalitic compositions. Monzogranite plutons are also emplaced into the siliciclastic supracrustal rocks.

Tectonostratigraphic interpretation

The siliciclastic, mafic and ultramafic units of the Ramsay River domain are similar in appearance, lithological association, and structural context to the lower Povungnituk Group of northern Quebec (St-Onge et al., 1992) and in the Big Island domain. The gneissic tonalite-quartz diorite panels and the crosscutting foliated orthopyroxene monzogranites are similar to Narsajuaq arc gneisses and plutons found in Ungava Orogen (St-Onge et al., 1992) as well as inferred for the Big Island and Crooks Inlet domains.

Mount Joy domain

Rocks of the Mount Joy domain (Fig. 2) are dominantly plutonic with subordinate amounts of siliciclastic and mafic rocks (St-Onge et al., in press). The domain is separated from the Crooks Inlet domain by thrust faults (Hanmer et al., 1996a).

Orthopyroxene-biotite tonalite

Granulite-facies orthopyroxene-biotite tonalite gneiss is medium- to coarse-grained, buff-weathering and characterized by minor amounts of hornblende and clinopyroxene. The orthogneisses are generally foliated, relatively homogeneous, and in contrast to the Big Island, Crooks Inlet, and Ramsay River domains, contain much less included mafic material (Fig. 13). A massive to weakly foliated pink-weathering syenogranite, generally medium grained but locally pegmatitic, occurs as dykes and sheets within the tonalite, and also forms intrusive bodies hundreds of metres across.

Semipelite

In abrupt contact with the foliated tonalite gneiss are packages of clastic sedimentary rocks. These comprise dominantly rusty biotite semipelite which locally contains red garnet, graphite, and pyrite. The semipelite is layered at the centimetre-scale. Garnet-sillimanite±cordierite pelite is commonly interlayered with the semipelitic bands. Relatively thin (<1 m thick) layers of psammite, quartzite, and minor carbonate are also present. Garnet-biotite white monzogranite, similar to that described in the Crooks Inlet domain, is spatially associated with the metasedimentary rocks, and may represent a product of anatexis.

Mafic rocks

Amphibolite, gabbro, and leucogabbroic units are intimately associated with the siliciclastic packages in the Mount Joy domain. The mafic and gabbroic sequences vary in thickness from 300 to 900 m, are generally well layered, and are characterized by hornblende-orthopyroxene-clinopyroxene granulite-facies assemblages. The mafic and gabbroic bands are interpreted to comprise intrusive and extrusive units including layered sills. Rare, thin (<1 m) layers of fine grained felsic gneiss (metarhyolite?) are also present. A metre-scale band of anorthositic gabbro has a strike continuity of several kilometres.

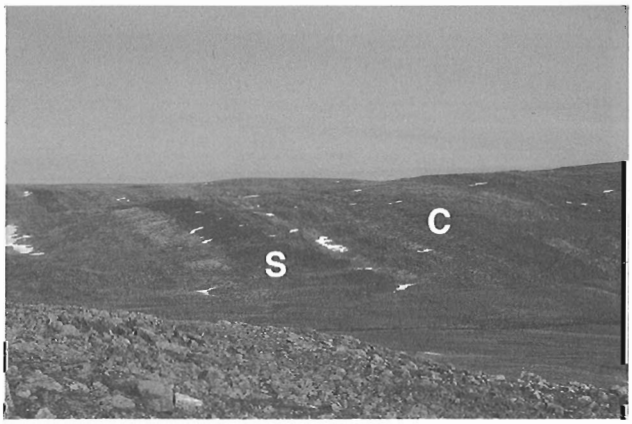

Figure 12. *Layered mafic/ultramafic sill (S) within clastic sedimentary sequence (C), Ramsay River domain. Sill is 200 m wide.*

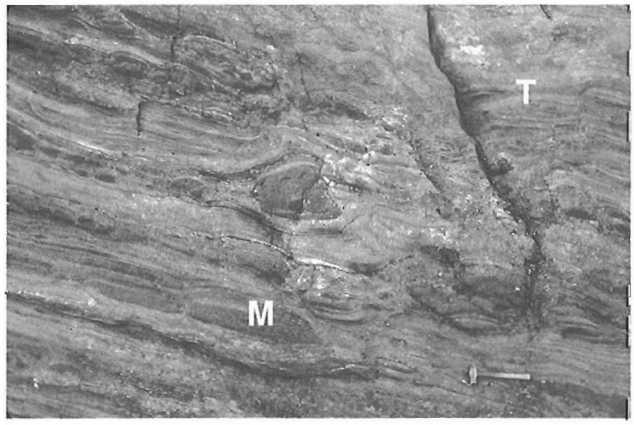

Figure 13. *Tonalite (T) with mafic enclaves (M), Mount Joy domain. Hammer is 39 cm long.*

Tectonostratigraphic interpretation

The foliated orthopyroxene-biotite tonalite gneiss is physically similar to ca. 1830 Ma tonalite dated in the Lake Harbour area (Scott and Godin, 1995) and is interpreted as correlative with similar units in the Big Island, Crooks Inlet, and Ramsay River domains. As well, it presents common field characteristics and occurs in a similar structural context to tonalites of the Narsajuaq arc (Lucas and St-Onge, 1992). The clastic and mafic rocks within the Mount Joy domain are correlated with those of Ramsay River domain. Based on the predominance of semipelitic material and the general absence of quartzite and psammitic layers (i.e. in contrast to the Ramsay River domain), the clastic and mafic rocks are interpreted as deeper water units of the lower Povungnituk Group. The absence of intrusive relationships with adjacent plutonic units, or within the supracrustal packages, suggests tectonic contacts.

Jordan River domain

The dominantly plutonic Jordan River domain is separated from the Mount Joy domain by a set of southwest-verging thrust faults (Fig. 2) (Hanmer et al., 1996).

Orthopyroxene-biotite monzogranite

Massive to foliated, orthopyroxene-biotite monzogranite is the dominant plutonic unit. The granulite-facies granite is tan and may contain hornblende, clinopyroxene, and garnet. The terrain underlain by the monzogranite is generally rugged with large outcrops typically characterized by steeply-dipping faces (Fig. 14). In the northeastern portion of the domain, the granite is massive, coarse grained, often K-feldspar megacrystic, and devoid of supracrustal or tonalite inclusions. In contrast, on the southwest side of the Sylvia Grinnell River (Fig. 2), and particularly in the zone adjacent to the southwestern domain boundary, the monzogranite contains numerous inclusions of tonalite, quartz diorite (Fig. 15), and clastic metasedimentary rock. The monzogranite clearly intrudes foliated tonalite in the southwestern portion of the domain and, with the notable concentration of included material, is interpreted as delineating the intrusive margin of a batholithic mass.

Garnet-biotite monzogranite

White monzogranite occurs both northeast and southwest of the Sylvia Grinnell River. The monzogranite is foliated to gneissic, can be K-feldspar megacrystic and contain abundant garnet as well as orthopyroxene, sillimanite, graphite, and/or metasedimentary inclusions. Mafic inclusions were not observed. In general, the garnet monzogranite is very coarse grained in the northeast (with garnet megacrysts up to 5 cm in diameter) and finer grained in the southwest.

Mafic sills

At the boundary with the Mount Joy domain, a swarm of mafic sills is emplaced in the orthopyroxene-biotite granite. The sills are generally less than 2-3 m in width, continuous along strike for several hundred metres, and are commonly boudined. Hornblende-orthopyroxene-clinopyroxene±garnet constitutes the mineral assemblage within the dykes whereas hornblende±clinopyroxene±biotite characterizes the margins.

Clastic and mafic supracrustal rocks

Supracrustal units occur in two settings: 1) as xenolithic material within plutonic bodies, and 2) as narrow, strike-continuous panels. The xenolithic material includes clastic metasedimentary rocks and amphibolite, and varies in size from metre- to kilometre-scale, the latter forming rafts or screens of country rock. The strike-continuous bands (generally 50-100 m in width) display sharp contacts with the adjacent plutonic rocks, are not crosscut by monzogranitic material, and are interpreted as tectonic. Two sequences of fault-bound supracrustal material were identified; 1) semipelite, quartzite and amphibolite, tentatively interpreted as lower Povungnituk Group; and 2) marble plus quartzite, tentatively interpreted as Lake Harbour Group.

Figure 14. *Monzogranite, Jordan River domain. Height of outcrop is 40 m.*

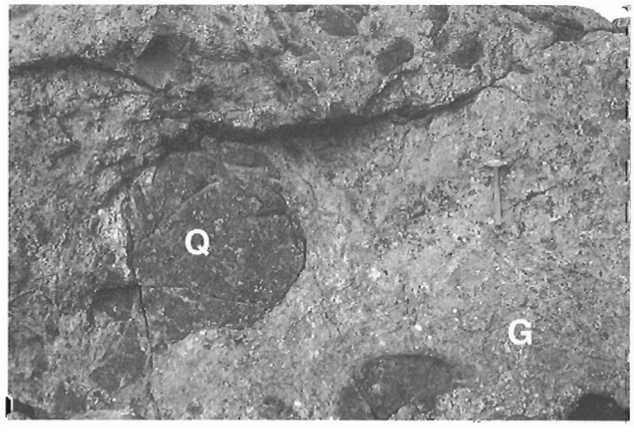

Figure 15. *Monzogranite (G) with quartz diorite inclusions (Q), Jordan River domain. Hammer is 39 cm long.*

Tectonostratigraphic interpretation

The plutonic rocks north and east of Iqaluit were mapped by Blackadar (1967) and interpreted by Jackson et al. (1990) as part of the Paleoproterozoic Cumberland Batholith (see also Scott, 1996). A sample of pink monzogranite from Iqaluit was dated by Jackson et al. (1990) at 1857 Ma. Observations this summer indicate that units of the batholith extend further to the southwest than previously noted and effectively underlie the bulk of the Jordan River domain (Fig. 2). Spatial variations within the batholith suggest that an intrusive contact with country rocks lies in the southwestern portion of the domain.

REGIONAL CORRELATIONS

Major lithological units of southern Baffin Island can be correlated with units in northern Quebec or elsewhere on Baffin Island based on lithological association, field characteristics, mineral assemblages, preliminary U-Pb geochronology, and structural/tectonic context. In the Big Island domain, tonalite and monzogranite are interpreted as possible Archean units similar to those in the Archean Superior Province of northern Quebec; tonalite/quartz diorite gneisses are similar to rocks of the Paleoproterozoic Narsajuaq arc and siliciclastic-mafic-ultramafic supracrustal units are correlated with the lower Povungnituk Group in Ungava Orogen (St-Onge et al., 1992).

The Crooks Inlet domain contains clastic and carbonate units of the Paleoproterozoic Lake Harbour Group which appears to extend as far west as the southern Foxe Basin (Fig. 1; Jackson and Taylor, 1972; Jackson et al., 1990). These rocks may be tectonostratigraphically equivalent to the Sugluk Group of Ungava Orogen (St-Onge et al., 1992). However, the predominance of carbonates in the Lake Harbour Group and the apparent absence of intrusive tonalitic bodies distinguish it from the Sugluk Group. Foliated tonalite gneiss panels, dated at ca. 1830 Ma (Scott and Godin, 1995) are imbricated with the Lake Harbour Group and correlated with the Narsajuaq arc. Within the Ramsay River domain siliciclastic, mafic, and ultramafic units are similar to the Povungnituk Group in the southern part of the Cape Smith Belt. Spatially associated tonalite/quartz diorite gneiss imbricates (as yet undated) and crosscutting foliated monzogranites are similar to gneisses and plutons of the Narsajuaq arc.

The tonalite gneiss in the Mount Joy domain presents the same field characteristics as tonalites of the Narsajuaq arc. The clastic and mafic rocks are correlated with those of Ramsay River domain and interpreted as more distal (deeper water) units of the lower Povungnituk Group. Plutonic units within the Jordan River domain are correlated with the Cumberland Batholith of central Baffin Island (Jackson et al., 1990) and show intrusive relationships into units of the Mount Joy domain in the southwest and with possible northern Labrador supracrustals to the east (Scott, 1996).

If the tectonostratigraphic correlations proposed above are correct, then available observations and preliminary geochronology (Scott and Godin, 1995) calls into question the suggestion that Archean rocks (Jackson et al., 1990) form the metaplutonic basement on Meta Incognita Peninsula at current exposed structural levels. As well, the available data do not support the suggestion that orthogneisses on the peninsula constitute the southeastern arm of the Rae craton (Hoffman, 1989). In contrast, the only convincing Archean basement units (within the Big Island domain) are tentatively correlated with similar units in the Superior Province basement of northern Quebec.

ECONOMIC POTENTIAL

The correlation of tectonostratigraphic units with the lower Povungnituk Group is of potential significance for mineral exploration work. Within the Cape Smith Belt of northern Quebec, Fe-Ni-Cu mineralization (Raglan-type) is associated with the emplacement of ultramafic and differentiated mafic-ultramafic units in siliciclastic rocks of the Povungnituk Group (St-Onge and Lucas, 1994; and references therein). The occurrence of clastic sedimentary rocks and mafic/ultramafic assemblages in Meta Incognita Peninsula occurring in thrust-bound panels similar to those of the Cape Smith Belt (St-Onge and Lucas, 1994), extends the Raglan-type deposit range substantially.

ACKNOWLEDGMENTS

We thank Polar Continental Shelf Project for logistical support during the field season. Natasha Wodicka (GSC) and David Cobb Copeland, Christopher Herd, Julius Ruechel, and Ian Russell are acknowledged for their high-quality, independent geological mapping. Dugald Carmichael (Queen's University) and Joe White (University of New Brunswick) provided many critical observations. Debbie Guilfoyle did an outstanding job as camp cook and radio operator. Dale Flemming, David Kennedy, Howard Sheppard, and Bruce Wentzell of Canadian Helicopters provided professional support and humour. Fred Alt of Bradley Air facilitated logistics from Iqaluit, and Lynn Peplinski and Julie Beauchesne of the Iqaluit Research Centre took care of communications. Steve Lucas is thanked for critically reviewing a first version of the manuscript.

REFERENCES

Blackadar, R.G.
1967: Geological reconnaissance, southern Baffin Island, District of Mackenzie; Geological Survey of Canada, Paper 66-47, 32 p.

Davison, W.L.
1958: Lake Harbour, Northwest Territories; Geological Survey of Canada, Map 29-1958, with marginal notes.

Hanmer, S., St-Onge, M.R., and Scott, D.J.
1996: Structural geology of the Meta Incognita thrust belt, south Baffin Island; in Current Research 1996-C; Geological Survey of Canada.
in press: White Strait, southern Baffin Island, Northwest Territories; Geological Survey of Canada, colour Open File Map 3192, with marginal notes.

Hoffman, P. F.
1989: Precambrian geology and tectonic history of North America; in The Geology of North America - An Overview, (ed.) A.W. Bally and A.R. Palmer; Geological Society of America, The Geology of North America, v. A, p. 447-512.

Jackson, G.D. and Taylor, F.C.
1972: Correlation of major Aphebian rock units in the northeastern Canadian Shield; Canadian Journal of Earth Sciences, v. 9, p. 1650-1669.

Jackson, G.D., Hunt, P.A., Loveridge, W.D., and Parrish, R.R.
1990: Reconnaissance geochronology of Baffin Island, N.W.T.; in Radiogenic Age and Isotopic Studies: Report 3; Geological Survey of Canada, Paper 89-2, p. 123-148.

Lucas, S.B. and St-Onge, M.R.
1992: Terrane accretion in the internal zone of the Ungava orogen, northern Quebec. Part 2: Structural and metamorphic history; Canadian Journal of Earth Sciences, v. 29, p. 765-782.

Scott, D.J.
1996: Geology of the Hall Peninsula east of Iqaluit, southern Baffin Island, Northwest Territories; in Current Research 1996-C; Geological Survey of Canada.

Scott, D.J. and Godin, L.
1995: Preliminary geological investigation of the Lake Harbour Group and surrounding gneissic rocks near Lake Harbour and Markham Bay, southern Baffin Island, Northwest Territories; in Current Research 1995-C; Geological Survey of Canada, p. 67-76.

Scott, D.J., St-Onge, M.R., and Hanmer, S.
in press: Frobisher Bay, southern Baffin Island, Northwest Territories; Geological Survey of Canada, colour Open File Map 3193, with marginal notes.

St-Onge, M.R. and Lucas, S.B.
1994: Controls on the regional distribution of iron-nickel-copper-platinum group element sulfide mineralization in the eastern Cape Smith Belt, Quebec; Canadian Journal of Earth Sciences, v. 31, p. 206-218.
1995: Large-scale fluid infiltration, metasomatism and re-equilibration of Archaean basement granulites during Palaeoproterozoic thrust belt construction, Ungava Orogen, Canada; Journal of Metamorphic Geology, v. 13, p. 509-535.

St-Onge, M.R., Hanmer, S., and Scott, D.J.
in press: Soper River, southern Baffin Island, Northwest Territories; Geological Survey of Canada, colour Open File Map 3191, 2 sheets with marginal notes.

St-Onge, M.R., Lucas, S.B., and Parrish, R.R.
1992: Terrane accretion in the internal zone of the Ungava orogen, northern Quebec. Part 1: Tectonostratigraphic assemblages and their tectonic implications; Canadian Journal of Earth Sciences, v. 29, p. 746-764.

Geological Survey of Canada Project 950033

Structural geology of the Meta Incognita thrust belt, south Baffin Island, Northwest Territories

S. Hanmer[1], M.R. St-Onge, and D.J. Scott
Terrain Sciences Division, Ottawa

Hanmer, S., St-Onge, M.R., and Scott, D.J., 1996: Structural geology of the Meta Incognita thrust belt, south Baffin Island, Northwest Territories; in Current Research 1996-C; Geological Survey of Canada, p. 73-81.

Abstract: The principal structural components of Meta Incognita Peninsula, south Baffin Island, include a widespread penetrative foliation, four arrays of kinematically linked thrusts, and southwest-vergent folds up to tens of kilometres in wavelength. These structures collectively comprise the southwest-vergent Meta Incognita thrust belt. The thrusts are intruded and structurally overlain to the northeast by the Cumberland Batholith. The generalized structural sequence starts with formation of a low-angle foliation, followed by regional thrusting, folding, and localized strike-slip shearing. All preserved deformation structures formed at granulite facies. The Meta Incognita thrust belt is interpreted as the high temperature equivalent of the Cape Smith thrust belt, Ungava Orogen, northern Quebec.

Résumé : La géologie structurale de la péninsule de Meta Incognita (partie sud de l'île de Baffin) comprend une schistosité pénétrative généralisée, quatre réseaux de chevauchements cinématiquement reliés et des plis décakilomètriques déversés vers le sud-ouest, qui forment ensemble la ceinture de chevauchement de Meta Incognita. Dans la partie nord-est, les réseaux de chevauchement sont à leur tour surmontés du batholite de Cumberland. La séquence structurale est la suivante : schistosité à pendage faible, chevauchement régional, plissement et cisaillement en décrochement, ce dernier étant localisé. Toutes les structures conservées ont évolué au faciès des granulites. La ceinture de chevauchement de Meta Incognita représente l'équivalent, formé à haute température, de la ceinture de Cape Smith (orogène de l'Ungava, Québec septentrional).

[1] Continental Geoscience Division, Ottawa

INTRODUCTION

A new programme of geological mapping has been initiated by the Geological Survey of Canada on Meta Incognita Peninsula, south Baffin Island (Fig. 1; see St-Onge et al., in press). A transect from Big Island to Hall Peninsula was mapped at 1: 100 000 scale during the 1995 field season (Fig. 2; Hanmer et al., in press; St-Onge et al., 1996; Scott et al., in press). From southwest to northeast, the transect is divided into five tectonostratigraphic domains, composed of potential equivalents to Archean Superior Province basement, and Early Proterozoic supracrustal and plutonic rocks of the Povungnituk Group, Sugluk Group, and Narsajuaq arc (see St-Onge et al., in press for descriptions, regional correlations, and reference to previous work). In this contribution, we will show that the structural geology of Meta Incognita Peninsula comprises three first order elements: widespread penetrative foliation, thrusts, and folds up to tens of kilometres in wavelength, which collectively comprise the Meta Incognita thrust belt.

Meta Incognita thrust belt is structurally and tectonostratigraphically divided into Big Island, Crooks Inlet, Ramsay River, Mount Joy, and Jordan River domains (Fig. 2A; St-Onge et al., in press). At the regional scale, lithological contacts, faults, fold axial planes, and foliations of the Meta Incognita thrust belt dip variably to the northeast (Fig. 2B). Longitudinal (strike-parallel) folds and coaxial extension lineations plunge moderately to the northwest. All of the preserved structural elements of the Meta Incognita thrust belt developed at granulite facies (St-Onge et al., in press). This contribution will outline the geometry of the thrust belt from southwest to northeast, the relative timing of thrusting and folding, and the localization of discrete thrust faults within hot, nominally viscous crust. The reader is referred to Geological Survey of Canada colour Open File maps 3191, 3192, and 3193 for detailed documentation (Hanmer et al., in press; St-Onge et al., in press; Scott et al., in press).

META INCOGNITA THRUST BELT

Big Island domain

In the northeast of Big Island, thin panels of Povungnituk Group rocks (St-Onge et al., in press) dip moderately to the northeast and extend the length of the island, separating panels of tonalite up to several kilometres thick (Hanmer et al., in press). Concordant, penetrative foliations in the Povungnituk Group rocks and the tonalites are parallel to the map unit boundaries. With few exceptions, extension lineations plunge up to 30° to the northwest. Rarely, local extension lineations are closer to dip-parallel. Lithological contacts are sharp, and are generally not associated with shear zones. Within the Povungnituk Group rocks, the same stratigraphic assemblage is repeated from panel to panel, and no evidence (veins or xenoliths) was found to indicate that they had been intruded by the tonalites. The lateral continuity and stratigraphic repetition of the Povungnituk Group panels, and the absence of intrusive relationships, suggest that the map unit contacts are faults, while the repetition of the Povungnituk Group stratigraphy suggests that they are thrusts. Furthermore, in the southern part of the island, tonalite/quartz diorite of probable Narsajuaq arc affinity is separated from tonalite of possible Archean (Superior Province?) basement by panels of Povungnituk Group rocks (St-Onge et al., in press). Geochronological confirmation of the presence of fault-bound panels of Archean basement structurally overlying younger rocks will test our argument for thrusting.

In the northern part of the island, lithological contacts, thrusts, and foliation surfaces are deformed by a train of southwest- vergent, kilometre-scale, 'S' folds, plunging gently to the northwest parallel to the extension lineation. A steeply to moderately northeast-dipping, 2-3 km wide belt of penetratively developed ribbon mylonites, forms the northern edge of the island (Fig. 3A and B). The mylonites are part of the 7 km wide Mina mylonite zone (Fig. 2), extending halfway across White Strait, and derived at the expense of tonalite, Povungnituk Group, and monzogranite protoliths. The mylonites carry a gently northwest-plunging extension lineation, which in places porpoises about the horizontal. Rare, but spectacular shear-sense indicators demonstrate dextral strike-slip movement along the extension lineation (Fig. 3C). The mylonite zone is markedly asymmetrical; the penetrative Big Island fabrics are flanked to the southwest by a 10-500 m progressive strain gradient, in stark contrast to a 4 km wide braided zone of about 100 m thick mylonite strands to the northeast. The mylonites are themselves deformed by gently northwest-plunging, lineation-parallel folds. These include upright, regional-scale folds at the

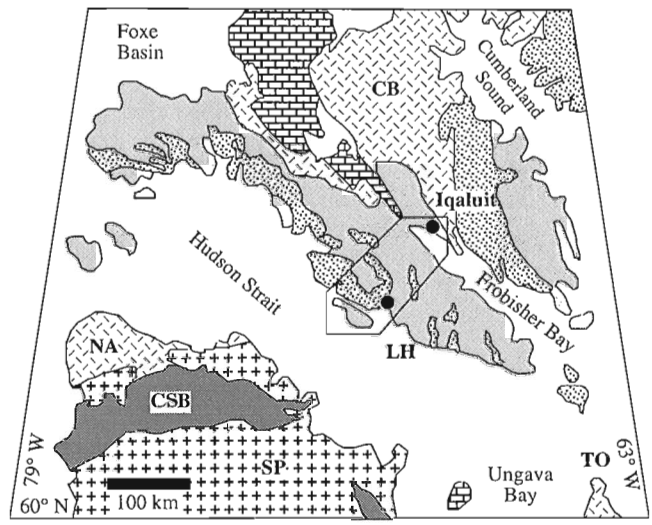

Figure 1. *Generalized geology of northern Quebec and southern Baffin Island, showing the limits of regional mapping in the current project. Lake Harbour (LH) and Iqaluit are indicated for reference. Rocks of the Lake Harbour Group are shown in stippled pattern along the south coast of Baffin Island, CB – Cumberland Batholith, Ordovician sedimentary rocks are shown in brick pattern. Cape Smith Belt (CSB) and Narsajuaq magmatic arc (NA) are shown in northern Quebec, and Torngat orogen (TO) in northernmost Labrador. SP – Superior Province. After Scott and Godin (1995).*

latitude of North Bay, which refold rare outcrop-scale southwest-verging 'S' folds which occur throughout the mylonite zone (Fig. 3D).

Direct kinematic evidence for thrusting is rare. Within the potential Archean basement, hornblende-pyroxene tonalite and diorite (St-Onge et al., in press) are progressively deformed into steeply northeast-dipping strands of granoblastic hornblende-bearing straight gneiss (Hanmer, 1988), 500 m thick by up to 15 km long, one of which occurs adjacent to the Mina mylonite zone. In this strand, a northeastward gradient from the protolith into the fine grained straight gneiss is marked by (i) development of a coarse grained flaggy gneiss, (ii) formation of trains of open to close 'S' folds, about 10-25 cm in wavelength, pitching steeply to the northwest in the plane of the flaggy gneissosity they deform, (iii) progressive tightening of the folds and rotation of the axes towards a steeply to moderately southeast-pitching extension lineation, and (iv) transposition of the folds into the straight gneisses. The constant symmetry of the folds and their relationship to the finite extension direction of the deformation are indicative of oblique, northeast-side-up thrust sense of shear along the lineation, associated with formation of the straight gneiss.

Crooks Inlet-Ramsay River domains

A network of branching and linking layers of Lake Harbour Group marble (Fig. 4A), alternating with panels and lenses of Lake Harbour Group siliciclastic metasediments and Narsajuaq arc tonalite (Crooks Inlet domain; St-Onge et al., in press) outlines a southwest-verging, moderately

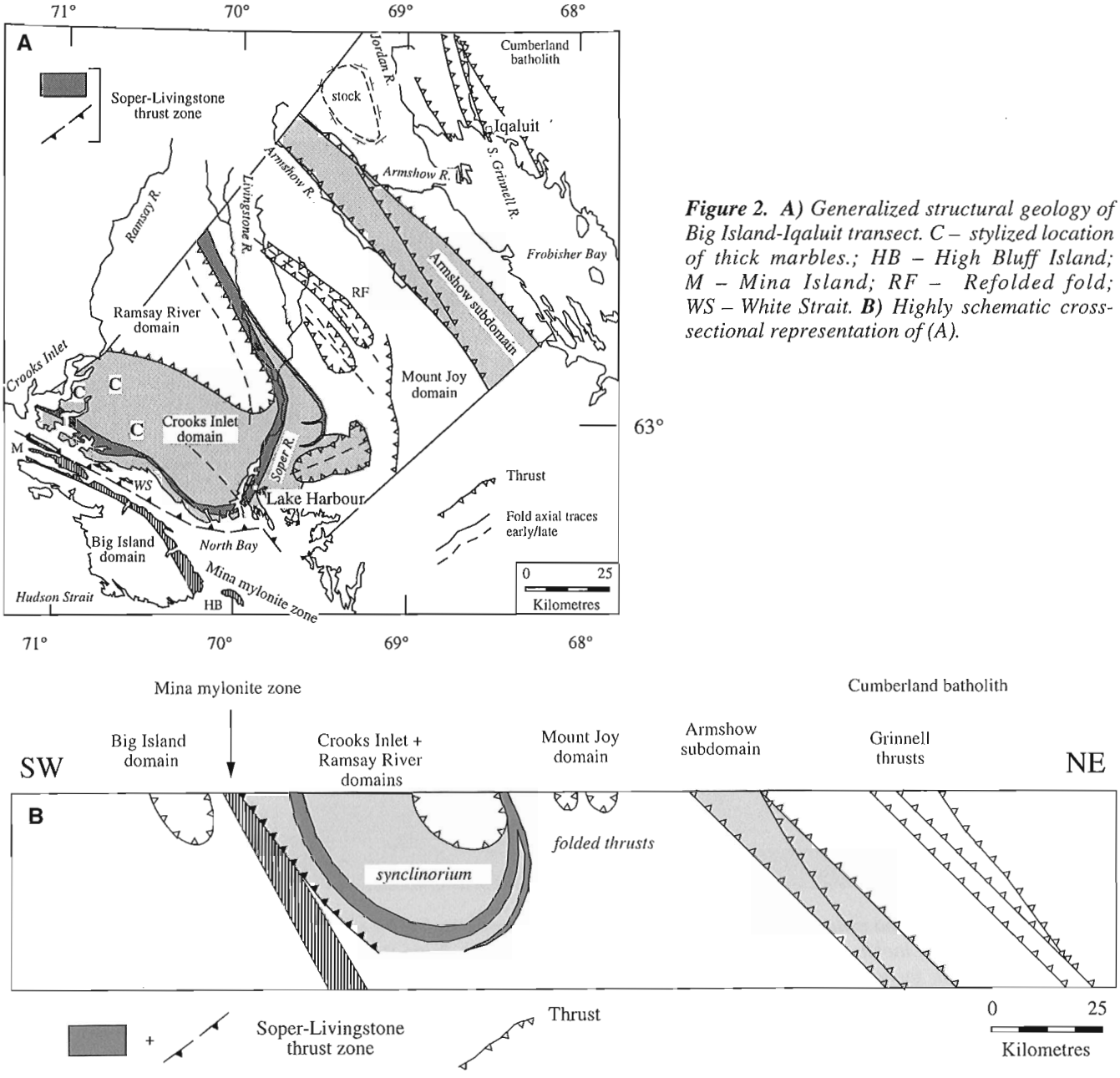

Figure 2. *A) Generalized structural geology of Big Island-Iqaluit transect. C – stylized location of thick marbles.; HB – High Bluff Island; M – Mina Island; RF – Refolded fold; WS – White Strait.* ***B)*** *Highly schematic cross-sectional representation of (A).*

northwest-plunging synclinorium, 75 km in outcrop width (Fig. 2; Hanmer et al., in press; St-Onge et al., 1996). The marbles are often separated from the overlying tonalite-monzogranite panels by a thin (<10 m) horizon of clastic metasediment. With the exception of certain panels of tonalite and monzogranite, all map units share a common, penetratively developed foliation and/or tectonic layering concordant with the regional lithological contacts. Throughout the synclinorium, the extension lineation is generally parallel to fold axes at all scales, although locally the lineation is close to dip-parallel. Because lineations are only patchily preserved, the relationship between the two orientations is not directly observed. The upper structural level of the synclinorium is cored by a synform of panels of tonalite and monzogranite, separated by a branching and linking network of Povungnituk Group rocks (Ramsay River domain, St-Onge et al., in press). Smaller scale (1-5 km wavelength) disharmonic minor folds occur throughout the synclinorium and reflect its overall geometry (Fig. 4B, C, and D). However, they are often isoclinal (Fig. 4C) and, at least locally, strongly noncylindrical (Fig. 4D), e.g. in the northeast limb of the synform of Povungnituk Group rocks.

The dispositions of both the synclinorium and the Lake Harbour Group sediments are markedly asymmetrical (Fig. 2). First, the width (35 km) of the Lake Harbour Group sediments southwest of the Povungnituk Group synform is much greater than on the northeast side (<5 km). Second, the thick marbles, with their abundant silicate inclusions east of Crooks Inlet and at the hamlet of Lake Harbour in the southwest, pass into narrow, parallel-sided layers of relatively clean marble along the Livingstone River to the northeast (Fig. 2A).

As on Big Island, the lateral continuity and stratigraphic repetition of the Lake Harbour Group and Povungnituk Group panels, and their alternation with exotic tonalites, indicates that the map unit contacts are faults. Shear-sense indicators are rare, but in the southwest limb of the synclinorium asymmetrical extensional shear band foliation and rotated pressure

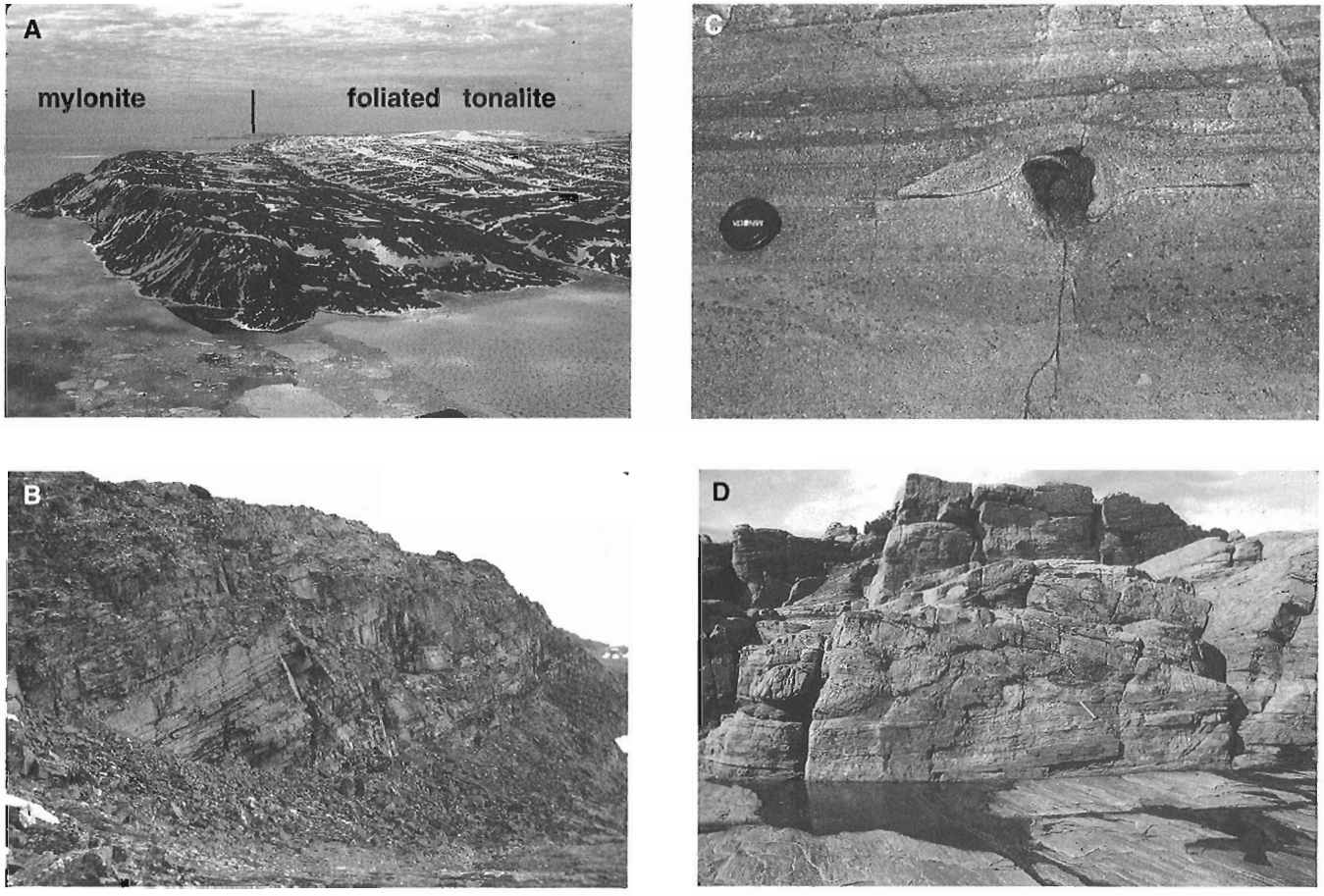

Figure 3. *Mina mylonite zone.* ***A)*** *3 km wide belt of penetratively developed mylonite along north shore of Big Island, looking southeast.* ***B)*** *Northeast-dipping mylonites, Mina Island. Vertical relief about 100 m.* ***C)*** *Mafic inclusion with 'in-plane' wings set in granite mylonite, indicates dextral strike-slip shear; subhorizontal XZ surface, Mina Island.* ***D)*** *Flat-lying ribbon fabric in tonalite mylonite, High Bluff Island, North Bay. Note northwest-trending horizontal extension lineation in foreground, coaxial with 'S' fold axes in mafic layer exposed on vertical face to left of hammer.*

shadows point to northeast-side-up movement along a steeply southeast-pitching extension lineation. However, this could as readily be attributed to flexural slip related to the synclinorium as to thrusting. More to the point, the above noted asymmetry of the synclinorium and its component parts corresponds to the geometry of a folded imbricate fan or duplex with a trailing branch line to the northeast (see Fig. 2). This geometry is indicative of southwest directed thrusting at the scale of the Crooks Inlet and Ramsay River domains (e.g. Boyer and Elliot, 1982). The network of branching and linking marble layers constitute the floor and lower levels of the stack (Fig. 2) and show abundant evidence for the tectonic incorporation of fragments and rafts of wall rock (Fig. 5; cf. Hanmer, 1988). We refer to them as the Soper-Livingstone thrust zone.

A smaller scale equivalent of the Crooks Inlet-Ramsay River thrust stack occurs to the east of the Soper River (Fig. 2A; Hanmer et al., in press). It appears to be an outlier or klippe of the Crooks-Ramsay imbricate fan or duplex, but its floor is marked by a single, thin and discontinuous marble layer, quite distinct from the nearby Soper-Livingstone thrust zone. If indeed it is related to the Crooks-Ramsay structure, we suggest that it may represent a more proximal set of faults which was later over-ridden as the main stack was emplaced along the Soper-Livingstone thrust zone.

Mount Joy domain

North of the Crooks Inlet and Ramsay River domains, Povungnituk Group rocks form an array of thin (about 100 m), subparallel, northwest-striking panels, separated by Narsajuaq tonalite (Mount Joy domain; St-Onge et al., 1996, in press). The supracrustal panels are continuous along strike and do not commonly branch or link. The Povungnituk Group rocks and the tonalites share a common penetrative, concordant foliation. As to the southwest, the lateral continuity of the Povungnituk Group rocks, their alternation with the tonalites and the absence of intrusive relationships, combine

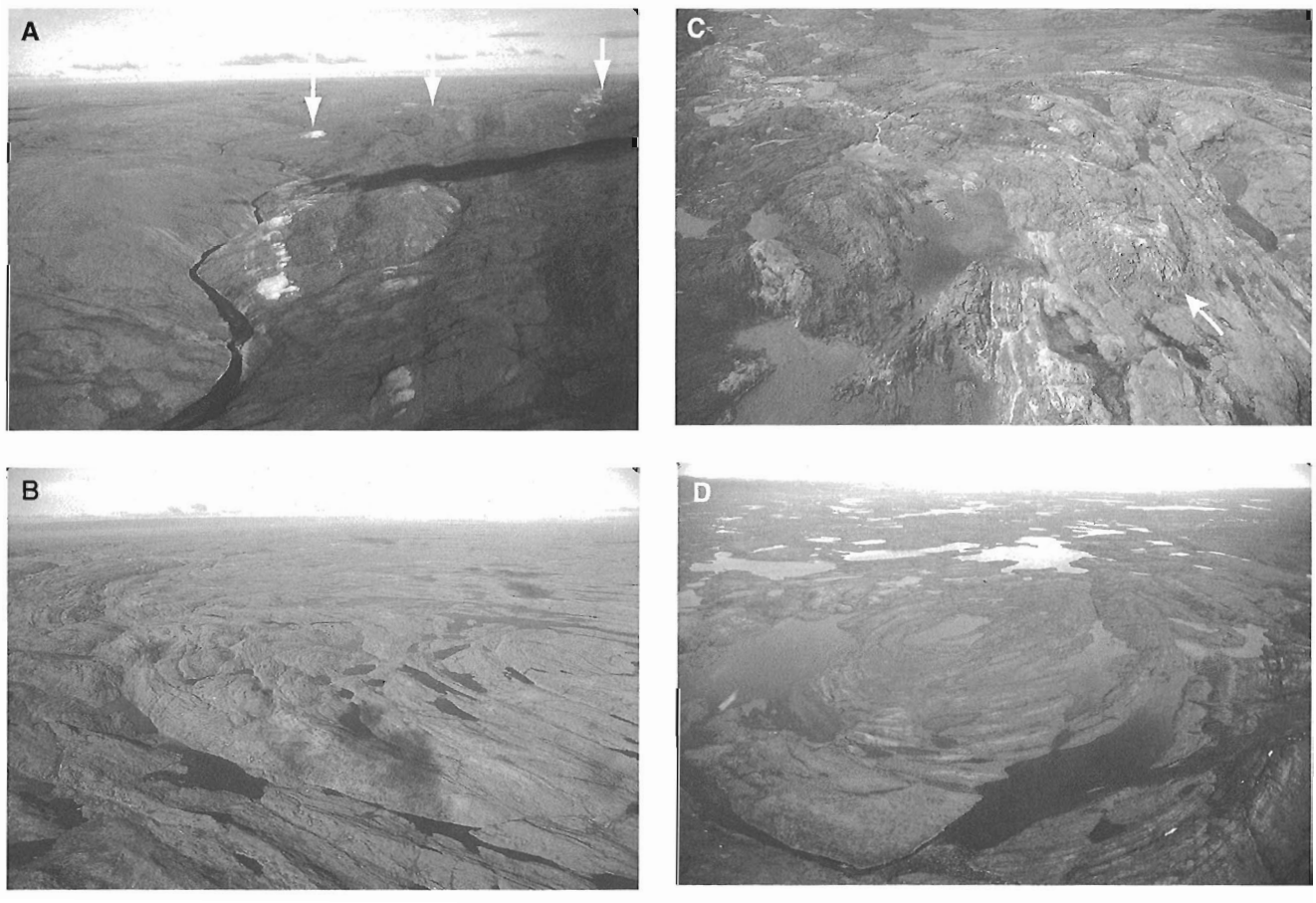

Figure 4. *Crooks Inlet domain.* ***A)*** *3 bands of marble tectonite (arrows), part of the Soper-Livingstone thrust zone, separating thrust imbricated panels of siliciclastic metasedimentary rocks and tonalite, Livingstone River. Arrows span 10 km.* ***B)*** *Regional synformal closure folding lithological contacts, thrust faults, and regional foliation, west of Lake Harbour, looking west toward White Strait.* ***C)*** *Refolded axial trace of isoclinal fold deforming lithological contacts and regional foliation (arrow indicates closure) west of Lake Harbour.* ***D)*** *Open, upright, doubly-plunging fold of lithological contacts and regional foliation, northwest of Lake Harbour. Fold structure about 2.5 km across.*

to indicate that the map-unit contacts are faults. In the absence of other criteria, local interpretation of these faults as thrusts is principally based on stratigraphic repetition. The composite regional enveloping surface, representing the lithological contacts, thrusts, and foliation surface, dips moderately to the northeast throughout much of the domain. However, in the south of the map area it is gently southwest- to west-dipping.

A set of mildly noncylindrical, lineation-parallel folds, up to 8 km in wavelength, deforms lithological contacts and foliation, and refolds a single example of a map-scale postfoliation isocline (Fig. 2, 6). The map-scale folds involving the Povungnituk Group rocks are mostly synforms, ranging from open, upright and symmetrical, to isoclinal and southwest-verging. Folds with intermediate asymmetrical geometries have northeast-dipping axial planes and steep to vertical northeast limbs.

Jordan River domain

The Jordan River domain is considered in two parts. The bulk of the domain is underlain by rocks of the Cumberland Batholith, flanked to the southwest by the Armshow subdomain.

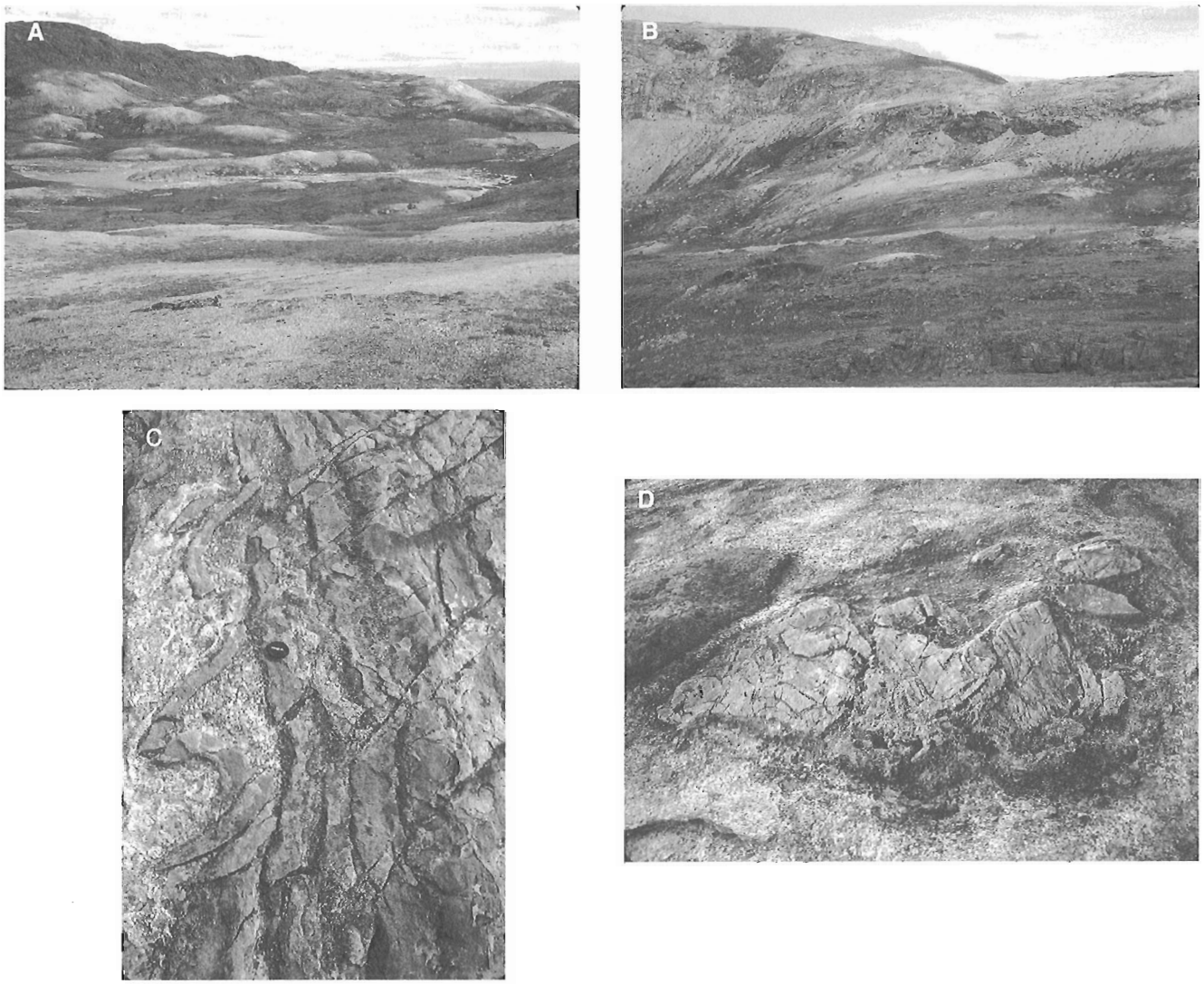

Figure 5. *Details of marble tectonites, Crooks Inlet domain.* ***A)*** *Marble (light) adjacent to siliciclastic metasedimentary rocks (dark, far left), contain abundant large rafts of included foliated wall rock. View about 1 km wide.* ***B)*** *Marble (light) with isolated included rafts of foliated and misoriented siliciclastic metasedimentary rock (dark). Cliff height at left about 200 m.* ***C)*** *Detail of quartzite inclusion (medium grey) in marble (light) to illustrate the mobility of the carbonate, its ability to intrude and spawl off thin slivers, and the folding of quartzite slabs in the flowing marble.* ***D)*** *Isolated quartzite inclusion in marble to illustrate fracturing, plucking, and rotation of included material in the highly mobile, flowing carbonate. A) and B) from east of Crooks Inlet, C) and D) from lowermost Soper River.*

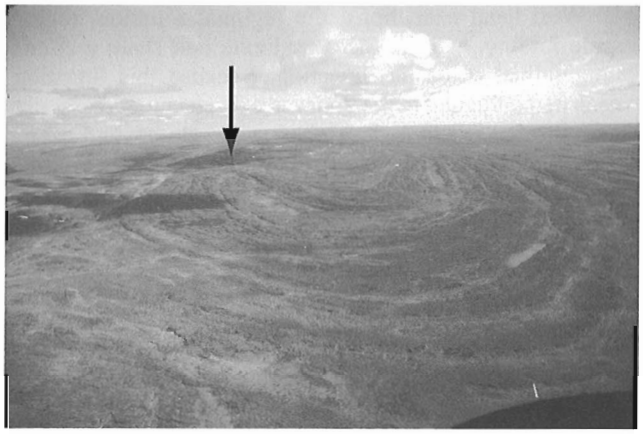

Figure 6. Looking southeast at southwest-vergent moderate open fold (8 km across) of axial trace of earlier isoclinal fold (arrow), itself deforming lithological contacts and regional foliation in metasedimentary rocks of the Povungnituk Group. Mount Joy domain, located at RF in Figure 2A.

Armshow subdomain

The Mount Joy domain is overlain by a zone of closely spaced, relatively narrow panels of clastic metasedimentary rocks of the Povungnituk Group, and associated anatectic garnetiferous white granite, bounding panels of tonalite and monzogranite (St-Onge et al., in press). With the exception of some of the monzogranite, all lithologies share a common, concordant, variably developed foliation. Although generally poorly preserved, a widespread extension lineation plunges gently to the northwest. Some of the panels of Povungnituk Group rocks are folded on a 1-5 km scale along axes coaxial with the extension lineation. However, most are straight and dip moderately to the northeast. Some of the more laterally continuous panels show evidence of branching, and truncate the folded panels of Povungnituk Group rocks. Other, less continuous panels of Povungnituk Group rocks occur in closely spaced arrays. Taken together, these features resemble a network of linked faults. As in the case of the Mount Joy domain, local interpretation of the faults as thrusts is principally based upon on stratigraphic repetition of the Povungnituk Group rocks from panel to panel.

In the panels between the faults, pervasively foliated tonalite is intruded by variably foliated monzogranite. Despite the weak development of its foliation, some of the monzogranite has a markedly streaky structure due to the presence of disrupted, initially concordant synplutonic mafic sills (see McLelland et al., 1992 and references therein), some of which are preserved in a pristine state (Fig. 7). The mafic sills which cut the tonalites and streaky monzogranite do not extend into the Povungnituk Group rocks, emphasising the faulted nature of the contacts between supracrustal and plutonic rocks. However, sheets of orthopyroxene granite, which represent veins of the Cumberland Batholith intruded into its already deformed tonalite wall rock (St-Onge et al., in press), cut and are cut by faults of the Armshow subdomain.

Cumberland Batholith

The orthopyroxene granites northeast of the Armshow River (Jordan River domain; St-Onge et al., in press; Scott, 1996) are divided into two parts by a set of closely spaced, narrow, subparallel bands of clastic and carbonate metasedimentary rocks, centred on the Sylvia Grinnell River, and separated from each other by panels of weakly foliated orthopyroxene granite (Scott et al., in press). To the northeast, the coarse grained, nearly isotropic granite is associated with two large panels of garnetiferous white granite. To the southwest, the variably foliated orthopyroxene granite is locally charged with xenoliths and elongate, concordantly foliated rafts of tonalite and diorite, with minor associated clastic metasediments. For the most part, the foliation and inclusions in the orthopyroxene granite dip moderately to steeply to the northeast. However, northwest of Frobisher Bay, a discontinuous train of map-scale rafts of diorite, tonalite and clastic metasedimentary rocks outlines an upright symmetrical dome, 30 km by 15 km, cored by isotropic orthopyroxene granite (Scott et al., in press; Fig. 2A). The postfoliation, intrusive relationship of the granite with respect to the inclusions is locally well exposed, and the dome appears to be a stock within the batholith. Accordingly, the foliation in the inclusions would have been shallow dipping to horizontal prior to entrainment in the stock. In contrast, the bands of metasedimentary rocks in the vicinity of the Sylvia Grinnell River show no evidence of having been intruded by the granite (Fig. 2). Their lateral continuity, subparallel geometry, and alternation with the granite suggests that the metasedimentary rocks were intercalated with the batholith rocks by postmagmatic faulting. The observation that the faults place the more internal northeastern parts of the batholith over more external southwestern

Figure 7. Streaky aspect to monzogranite due to disruption of aligned mafic sills (left), Armshow subdomain. The relatively high degree of disruption, the moderate intensity of the foliation and the presence of pristine subconcordant mafic sills (right) cutting the streaky structure of the granite combine to suggest that the sills were emplaced while the granite host was still in a magmatic state (McLelland et al., 1992).

parts (St-Onge et al., in press), as well as repeating the same stratigraphic assemblage, argues in favour of thrusting. Hence, we refer to them as the Sylvia Grinnell thrusts (Fig. 2).

Structural sequence

First order observations indicate that southwest-directed thrusting in the Meta Incognita thrust belt was succeeded by regional-scale folding with southwest vergence, and that the Mina mylonite zone, discordant to the regional-scale folding, is itself folded. Accordingly, these observations indicate the sequence (i) regional thrusting, (ii) regional folding, (iii) localized strike-slip shearing, (iv) localized folding.

The early stages of the evolution of the Meta Incognita thrust belt are apparent after qualitative removal of the geometrical effects of the regional-scale folding. The penetrative, concordant foliation present in most map units represents an extensive, shallow northeast-dipping, prefolding enveloping surface. Such fabrics, generated at granulite facies through a significant crustal thickness, are characteristic of distributed subhorizontal shearing deformation e.g. Davidson, 1984). In the Mount Joy domain, we have identified a single example of a map-scale nappe-like isoclinal fold which deforms the foliation, but is itself deformed by the regional, southwest-verging folds (St-Onge et al., 1996). The isoclinal fold may represent an older stage of deformation intermediate between the early foliation and the later displacements along discrete surfaces.

Throughout the map area, southwest of the Armshow subdomain, panels of penetratively foliated tonalite are cut by sheets of variably deformed monzogranite, late- to synkinematic with respect to the foliation. The abrupt absence of such intrusive sheets from the overwhelming majority of the intervening supracrustal panels indicates that thrust intercalation of the latter with the tonalite occurred after regional foliation development had ceased. Similar reasoning may be applied to the relative timing of the emplacement of the Cumberland Batholith. The initially flat-lying foliated tonalite and diorite inclusions outlining the stock northwest of Frobisher Bay indicate that the early stage of distributed subhorizontal shearing had already occurred by the time of magmatic emplacement of the batholith. Moreover, the crosscutting relationships in the Armshow subdomain, combined with the Sylvia Grinnell thrusts, indicate that the Cumberland Batholith was emplaced into a dynamic, evolving thrust belt.

The sequence of structural events in the Meta Incognita thrust belt can therefore be summarized as follows:

i) Penetrative subhorizontal shearing, with formation of a regional foliation.

ii) Localization of deformation on calcareous thrust zones and discrete brittle thrusts, possibly associated with the initiation of nappe-like folds.

iii) Regional folding of the thrusts, with southwest vergence.

iv) Localization of dextral, strike-slip shearing and mylonitization.

v) Magmatic and tectonic emplacement of the Cumberland Batholith could have occurred at any time after or during (ii).

With local exceptions, the regional foliation, regional-scale folding, and the Mina mylonite belt share a common longitudinal extension lineation. Because this lineation is near-perpendicular to the transverse displacements associated with thrusting, and is developed at a scale beyond even the largest fold structures, we suggest that it reflects long-lived far-field boundary conditions beyond the scope of our present mapping.

Localization

During the development of the granulite facies Meta Incognita thrust belt, deformation became localized into surprisingly narrow carbonate shear zones and brittle faults. The occurrence of brittle faulting, intermediate in time between the formation of regionally extensive granulite facies foliation and tight to isoclinal folds, raises two possibilities. Either brittle deformation occurred during the same thermal event as the granulite facies structures, or it occurred at much lower temperatures. The latter scenario would imply significant cooling, followed by a second heating event. However, there is no indication in the metamorphic assemblages of such cooling (St-Onge et al., in press). Alternatively, brittle deformation at elevated granulite facies temperatures implies that localization of deformation was due to change in variables other than temperature, e.g. pH_2O or strain rate. The observation that brittle thrusts form regional-scale kinematically linked systems, such as the imbricate fan or duplex structure of the Crooks Inlet and Ramsay River domains, implies that such variation was contemporaneous throughout an extensive volume of rock. Tight to isoclinal folding of the brittle thrusts, and postfold mylonitization, indicate a return to conditions of viscous flow, suggesting that the brittle behaviour was transient. We suggest that these considerations tend to favour strain rate as the controlling variable.

Regional correlations

Tectonostratigraphic considerations suggest that the map units of the Meta Incognita thrust belt are correlative with the Archean basement, Povungnituk Group, Sugluk Group, and Narsajuaq arc rocks of the Ungava Orogen in northern Quebec (see St-Onge et al., in press). Here, we further suggest that the Meta Incognita thrust belt represents the high-temperature equivalent of the Cape Smith thrust belt, the external part of the Ungava Orogen (Lucas, 1989; Lucas and St-Onge, 1992). Without necessarily equating the individual events, there are certain first order similarities in the structural histories of the internal and external parts of the orogen. First, they are thrust belts with displacements directed toward the Superior Province. Secondly, early and later stages of thrusting are recognized. Thirdly, the thrusts are deformed by regional-scale longitudinal folds verging toward the Superior Province. However, there are also important differences. Initial thrusting in the Cape Smith thrust belt preceded peak metamorphic temperatures, whereas all preserved structures in the Meta Incognita thrust belt formed at granulite facies. By analogy with Cape Smith and other thrust belts elsewhere, we suggest that direct evidence of pre-granulite facies events which gave rise, or contributed, to the initial crustal

thickening and consequent elevated temperatures, have been obliterated. Therefore, it is perhaps more appropriate to consider the structural events documented in the Meta Incognita thrust belt as comparable with the second phase of thrusting and subsequent folding in the Cape Smith Belt (Lucas and Byrne, 1992).

ACKNOWLEDGMENTS

We wish to thank our colleague Natasha Wodicka, our assistants David Copeland, Ian Russell, Julius Ruschel, and Chris Herd, and our cook Debbie Guilfoyle, for their splendid collective and personal efforts, without which this work would have been neither possible, nor as enjoyable as indeed it was. We are also indebted to our Canadian Helicopter crews Dale Flemming, Bruce Wentzel (pilots) and Dave Kennedy and Howard Sheppard (engineers), and to Lynn Peplinski and Julie Beauchesne of the Iqaluit Research Centre. We thank Steve Lucas for perceptive critical comments on the manuscript.

REFERENCES

Boyer, S.E. and Elliot, D.
1982: Thrust systems; Bulletin of the American Association of Petroleum Geologists, v. 66, p. 1196-1230.

Davidson, A.
1984: Identification of ductile shear zones in the southwestern Grenville Province of the Canadian Shield; in Precambrian Tectonics Illustrated, (ed.) A. Kroner and R. Greiling; Stuttgart, E. Schweitz. Verlags, p. 207-235.

Hanmer, S.
1988: Ductile thrusting at mid-crustal level, southwestern Grenville Province; Canadian Journal of Earth Sciences, v. 25, p. 1049-1059.

Hanmer, S., St-Onge, M.R., and Scott, D.J.
in press: White Strait, southern Baffin Island, Northwest Territories; Geological Survey of Canada, Open File 3192, colour map with marginal notes, scale 1: 100 000.

Lucas, S.B.
1989: Structural evolution of the Cape Smith thrust belt and the role of out-of-sequence faulting in the thickening of mountain belts; Tectonics, v. 8, p. 655-676.

Lucas, S.B. and Byrne, T.
1992: Footwall involvement during arc-continent collision, Ungava orogen, northern Canada; Journal of the Geological Society of London, v. 149, p. 237-248.

Lucas, S.B. and St-Onge, M.R.
1992: Terrane accretion in the internal zone of the Ungava orogen, northern Quebec. Part 2: structural and metamorphic history; Canadian Journal of Earth Sciences, v. 29, p. 765-782.

McLelland, J.M., Chiarenzelli, J., and Perham, A.
1992: Age, field, and petrological relationships of the Hyde School Gneiss, Adirondack Lowlands, New York: criteria for an intrusive origin; Journal of Geology, v. 100, p. 69-90.

Scott, D.J.
1996: Geology of the Hall Peninsula east of Iqaluit, southern Baffin Island, Northwest Territories; in Current Research 1996-C; Geological Survey of Canada.

Scott, D.J. and Godin, L.
1995: Preliminary geological investigation of the Lake Harbour Group and surrounding gneissic rocks near Lake Harbour and Markham Bay, southern Baffin Island, Northwest Territories; in Current Research 1995-C; Geological Survey of Canada, p. 67-76.

Scott, D.J., St-Onge, M.R., and Hanmer, S.
in press: Frobisher Bay, southern Baffin Island, Northwest Territories; Geological Survey of Canada, Open File 3193, colour map with marginal notes, scale 1: 100 000.
1996: Geology of the Meta Incognita Peninsula, south Baffin Island, Northwest Territories: tectonostratigraphic units and regional correlations; in Current Research 1996-C, Geological Survey of Canada.

St-Onge, M.R., Hanmer, S., and Scott, D.J.
in press: Soper River, southern Baffin Island, Northwest Territories; Geological Survey of Canada, Open File 3191, colour map with marginal notes, scale 1: 100 000.

Geological Survey of Canada Project 950033

Geology of the Hall Peninsula east of Iqaluit, southern Baffin Island, Northwest Territories

David J. Scott
Terrain Sciences Division, Ottawa

Scott, D. J., 1996: Geology of the Hall Peninsula east of Iqaluit, southern Baffin Island, Northwest Territories; in Current Research 1996-C; Geological Survey of Canada, p. 83-91.

Abstract: A corridor east of Iqaluit has been mapped and sampled for U-Pb geochronology in order to evaluate the hypothesis that the rocks of the Hall Peninsula represent in part the along-strike continuation of the Torngat Orogen (northern Labrador), and to determine the relationship of these rocks to those of the Cumberland Batholith. The metaplutonic rocks of the western part of the corridor appear to represent the southern continuation of the Cumberland Batholith. These rocks intrude the central metasedimentary gneisses that are interpreted as the northward continuation of the Tasiuyak gneiss of the Torngat Orogen. An orthopyroxene tonalite that intrudes the central metasedimentary rocks has been dated at 1890 ± 2 Ma. The eastern metaplutonic rocks are enigmatic; they may represent the northward continuation of ca. 1.9 Ga metaplutonic rocks of the Torngat Orogen.

Résumé : Un corridor à l'est d'Iqaluit a été cartographié et échantillonné pour la géochronologie U-Pb, afin d'évaluer l'hypothèse selon laquelle les roches de la péninsule Hall constitueraient le prolongement de l'orogène de Torngat (Labrador septentrional), mais aussi de déterminer leur relation avec les roches du batholite de Cumberland. Les roches de la partie occidentale du corridor représenteraient le prolongement vers le sud du batholite de Cumberland. Elles ont fait intrusion dans les gneiss supracrustaux du centre, qui sont interprétés comme le prolongement vers le nord des gneiss de Tasiuyak de l'orogène de Torngat. Une tonalite à orthopyroxène, qui recoupe les gneiss supracrustaux du centre, a été datée à 1 890 ± 2 Ma. Les roches métaplutoniques de l'est sont énigmatiques; elles pourraient s'avérer être le prolongement des roches métaplutoniques (env. 1,9 Ga) de l'orogène de Torngat.

INTRODUCTION

The Precambrian geology of southern Baffin Island comprises possible Archean metaplutonic rocks, and Paleoproterozoic metaplutonic and metasedimentary rocks. The bedrock geology of the area was investigated at reconnaissance scale in 1965 (Blackadar, 1967). This investigation clearly outlined the major lithological packages on the Hall Peninsula (Fig. 1). Correlations were suggested between the carbonate and siliciclastic metasedimentary rocks of the Lake Harbour Group and similar rocks in northeastern Quebec (Jackson and Taylor, 1972). Hoffman (1989) has suggested that the Tasiuyak paragneiss, which parallels the hinterland of the Torngat Orogen, may continue northward onto the Hall Peninsula. More recent projects have begun to investigate the tectonic history in further detail, focusing on the Lake Harbour-Iqaluit area (Jackson et al., 1990; Scott and Godin, 1995; St-Onge et al., 1996; Hanmer et al., 1996).

The present fieldwork was initiated in order to evaluate the hypothesis that the rocks of the Hall Peninsula represent in part the along-strike continuation of the Torngat Orogen, and to determine the relationship of these rocks with the southern continuation of the Cumberland Batholith (Fig. 1). Geological mapping along a well-exposed corridor east of Iqaluit (Fig. 1) will be combined with detailed U-Pb geochronological investigations of the metaplutonic and metasedimentary rocks. This work contributes to the Geological Survey of Canada's Northeast Laurentia program, the LITHOPROBE Eastern Canadian Shield Onshore-Offshore Transect (ECSOOT), and will facilitate a more detailed comparison of geological events in southern Baffin Island with those in northernmost Labrador and northern Quebec.

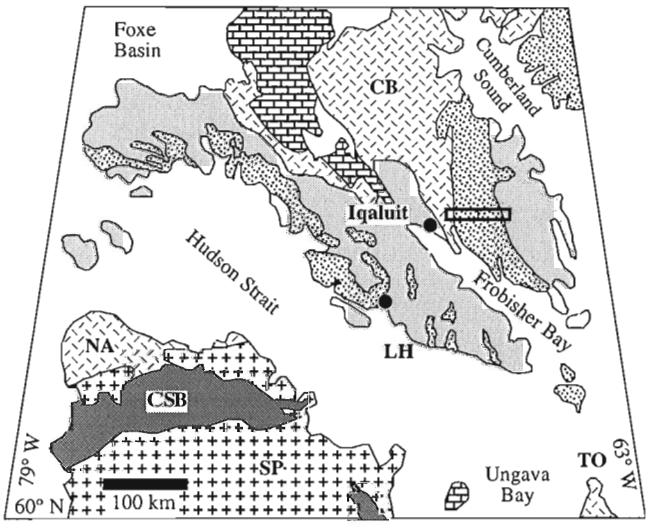

Figure 1. Location of study area on Hall Peninsula. CB – Cumberland Batholith; CSB – Cape Smith Belt; LH – community of Lake Harbour; NA – Narsajuaq Arc; SP – Superior Province; TO – Torngat Orogen.

GEOLOGY OF THE HALL PENINSULA (NTS 25O)

A three-part division of the rocks of the Hall Peninsula is clear from Blackadar's (1967) reconnaissance: a western domain is dominated by orthopyroxene- and garnet-bearing monzogranites, a central domain comprises siliciclastic metasedimentary rocks and subordinate metaplutonic rocks, and an eastern domain consists of tonalitic gneisses, monzogranite, and minor metasedimentary rocks (Fig. 2).

Western plutonic domain

The metaplutonic rocks of this domain have been identified as the southernmost exposures of the ca. 1.85 Ga Cumberland Batholith (Jackson and Taylor, 1972; Jackson et al., 1990), and are the eastward continuation of the rocks examined by St-Onge et al. (1996) and Scott et al. (in press).

Orthopyroxene-biotite monzogranite

Medium- to coarse-grained orthopyroxene-biotite monzogranite is the dominant rock type in the western plutonic domain (Fig. 3A). This buff-weathering rock locally contains hornblende after orthopyroxene, small amounts of clinopyroxene, or finely disseminated lilac garnet. It is massive to weakly foliated, and has developed a distinctively rugged, craggy topography (Fig. 3B). Decametre- to kilometre-scale rafts of garnet±sillimanite psammite (described below) were identified in the easternmost exposures of this unit (Fig. 2), indicating that the monzogranite has an intrusive relationship to the metasedimentary rocks of the central domain. A representative sample of this monzogranite was collected for U-Pb geochronology.

Garnet-biotite monzogranite

Monzogranite characterized by the presence of biotite and deep-red garnet is locally present. This fine- to medium-grained rock weathers light grey-brown, and is massive to weakly foliated. It occurs as discordant sheets within panels of foliated metasediment, and as larger bodies that commonly contain irregular rafts of metasedimentary rock. The relationship between this unit and the orthopyroxene-biotite monzogranite was not directly determined, although it appears as though the two units may be compositional variants of a single magmatic suite. A representative sample of this unit was collected for U-Pb geochronology.

Psammite

Rusty-weathering quartz-feldspar-biotite psammite which contains ubiquitous lilac garnet are found in the eastern part of the monzogranite unit as decametre- to kilometre-scale inclusions and panels (Fig. 2). Heterogeneous compositional layering, defined by variations in proportions of quartz, feldspar, and biotite, ranges from 1-2 mm to tens of centimetres

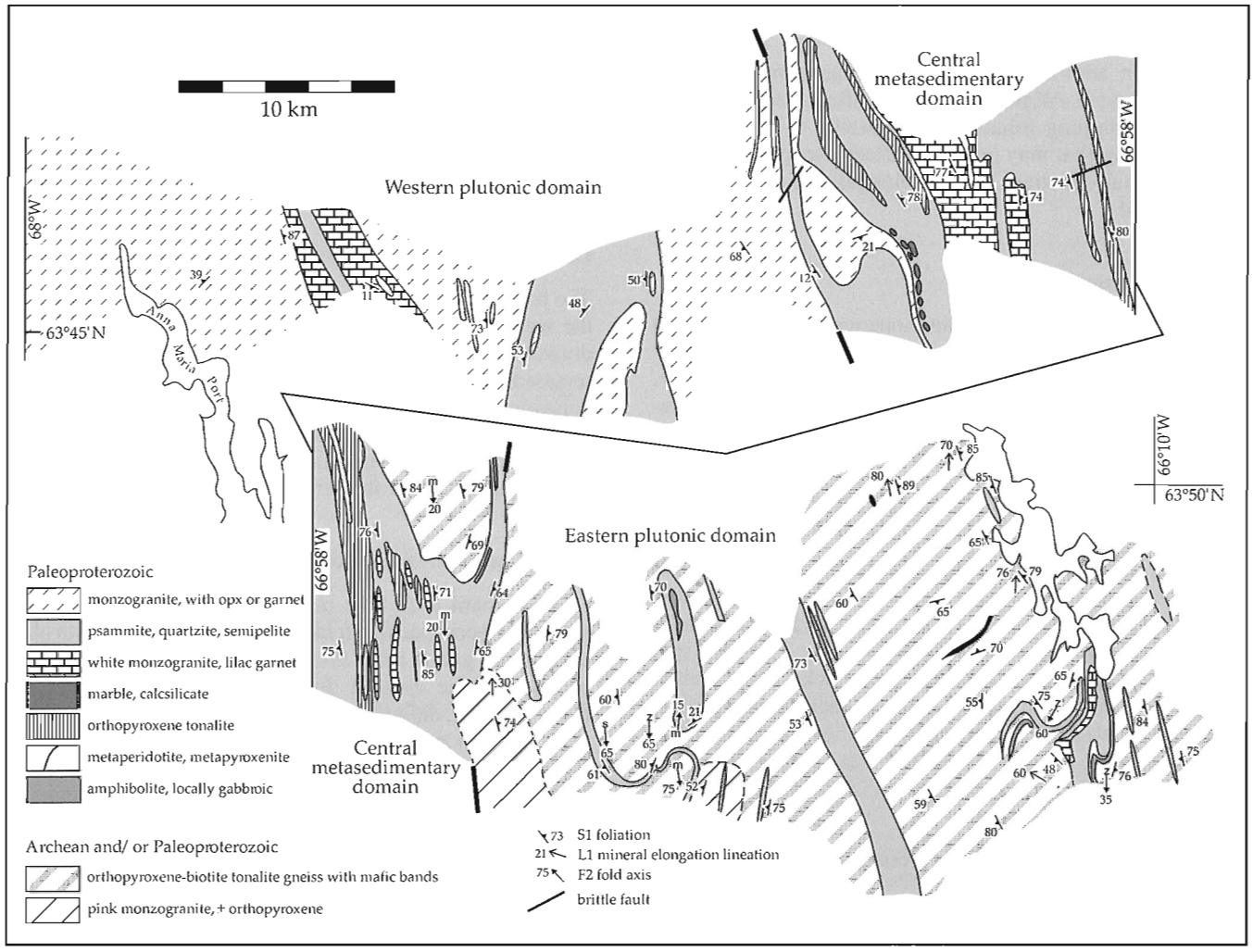

Figure 2. *Geological map of the study area, eastern Hall Peninsula.*

Figure 3A. *Homogeneous orthopyroxene-biotite monzogranite, western plutonic domain. Pocket knife is 2 cm across.*

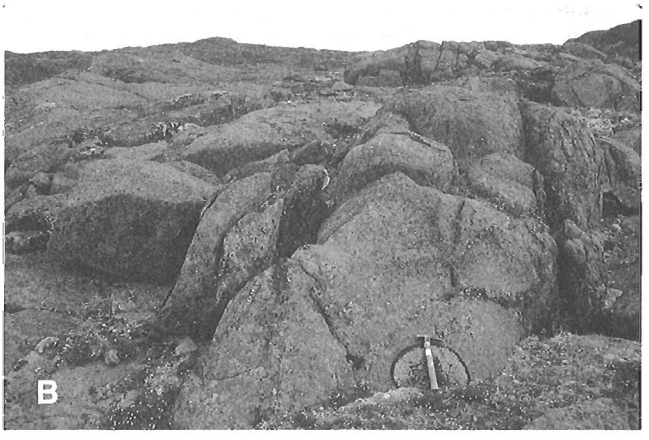

Figure 3B. *Typical craggy outcrop of orthopyroxene-biotite monzogranite. Hammer is 35 cm long.*

in thickness. Rare quartz-rich layers up to several decimetres thick are present locally. Sillimanite was only rarely observed, in addition to biotite and lilac garnet, in more micaceous layers. Alignment of mica defines a strong, generally steeply-dipping foliation (S_1), parallel to the compositional layering that may possibly reflect transposed primary compositional variation. Mineral elongation lineations were not observed.

White monzogranite

A distinctive, white-weathering monzogranite characterized by the presence of abundant lilac garnets, is intimately associated with the metasedimentary rocks of the western domain. This generally fine grained rock only rarely contains sillimanite or potassium feldspar megacrysts. The monzogranite occurs as diffuse, irregular seams or pods generally parallel to compositional layering and foliation in the clastic rocks, and as discrete, tabular bodies locally discordant to layering. In the central part of the western domain, kilometre-scale bodies of white monzogranite contain inclusions of lilac-garnet psammite. The westernmost occurrence is spatially associated with a large raft of psammite (Fig. 2), and intrudes orthopyroxene-biotite monzogranite (Fig. 4). The close spatial relationship to the metasedimentary rocks, and the ubiquitous presence of lilac garnets, suggest that the monzogranite may be derived locally by anatexis of the host metasediments. A representative sample of this unit was collected for U-Pb geochronology.

Tectonic interpretation of the western plutonic domain

The orthopyroxene-biotite and garnet-biotite monzogranite units represent the southern continuation of the Cumberland Batholith, interpreted as a Paleoproterozoic magmatic arc (e.g. Hoffman, 1990). Whereas the petrogenesis of these rocks, which form one of the most extensive plutonic belts in the northeastern Canadian Shield, is not well known, the present investigation shows that they have a clearly intrusive relationship to the metasedimentary rocks of the central domain on the Hall Peninsula. The southwestern margin of the batholith is in tectonized intrusive contact with rocks of the Meta Incognita Peninsula (St-Onge et al., 1996). The presence of intrusive sheets of white, garnetiferous monzogranite in both the metasediments and the orthopyroxene-biotite and garnet-biotite monzogranite units suggests that generation of the white monzogranite by partial melting of the metasedimentary rocks followed emplacement of the orthopyroxene-biotite and garnet-biotite monzogranites.

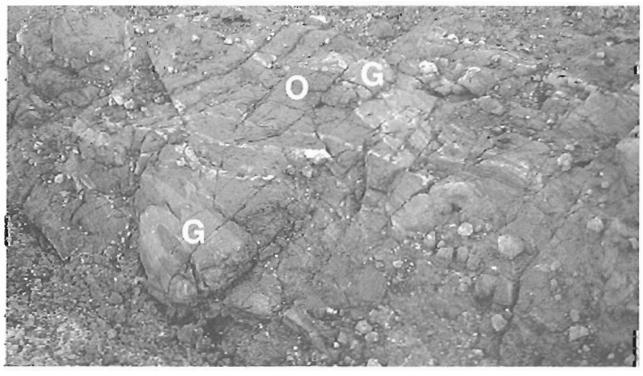

Figure 4. *White-weathering, lilac-garnet monzogranite (G) intrusive into buff, orthopyroxene-biotite monzogranite (O). Width of view is ~10 m.*

Central metasedimentary domain

The boundary between the dominantly metaplutonic rocks of the western domain and the rocks of the central domain is drawn at the westernmost occurrence of continuous panels of metasedimentary rocks (Fig. 2). The boundary also broadly coincides with the topographic break between the deeply-incised region underlain by the western plutonic rocks and the approximately 600 m plateau underlain by the metasedimentary rocks of the central domain.

Psammite, quartzite, and semipelite

The dominant rock type in the central domain (Fig. 2) is rusty-weathering quartz-feldspar-biotite psammite with ubiquitous lilac garnet (Fig. 5A). It is identical to that found as enclaves in the western domain. Heterogeneous compositional layering, defined by variations in biotite content, ranges from 1-2 mm to tens of centimetres in thickness (Fig. 5B). Rare quartz-rich layers up to several metres thick can be traced along strike for tens of metres (Fig. 5C). Semipelite layers, generally less than several centimetres thick, commonly contain sillimanite and 3-4 mm flakes of graphite, in addition to biotite and lilac garnet.

Alignment of mica defines a strong, generally north-striking, steeply-dipping foliation (S_1), parallel to the compositional layering that is interpreted as transposed primary compositional variation. Garnet poikiloblasts, locally up to 5 mm in diameter, overgrow S_1. Sillimanite generally occurs as mats of randomly oriented needles on S_1; alignment of needles was not observed. Fold closures defined by compositional layering with S_1 parallel to the fold axial plane (F_1) were only rarely noted, whereas folds of S_1 (F_2) are observed at all scales (Fig. 5D). The F_2 fold axes are generally shallowly south-plunging, although northerly plunges were also noted. Steeply plunging F_2 fold axes are rare.

White-weathering monzogranite that contains lilac garnet is present locally as discrete, tabular bodies and as more diffuse, irregular seams (Fig. 6) or pods. Garnet monzogranite bodies of both types are generally parallel to compositional layering, and comprise up to 30% of some outcrops, and are interpreted as the products of local anatectic melting. A representative sample of a tabular monzogranite body was collected for U-Pb geochronology.

Pb-isotopic compositions of detrital zircons extracted from a representative sample of psammite have been analyzed using the Laser Ablation Microprobe ICP-MS technique (Scott and Gauthier, in press). The $^{207}Pb/^{206}Pb$ ages of fifty-three individual grains were determined; about 60% are younger than ca. 2.0 Ga, and none are older than 2.4 Ga. These

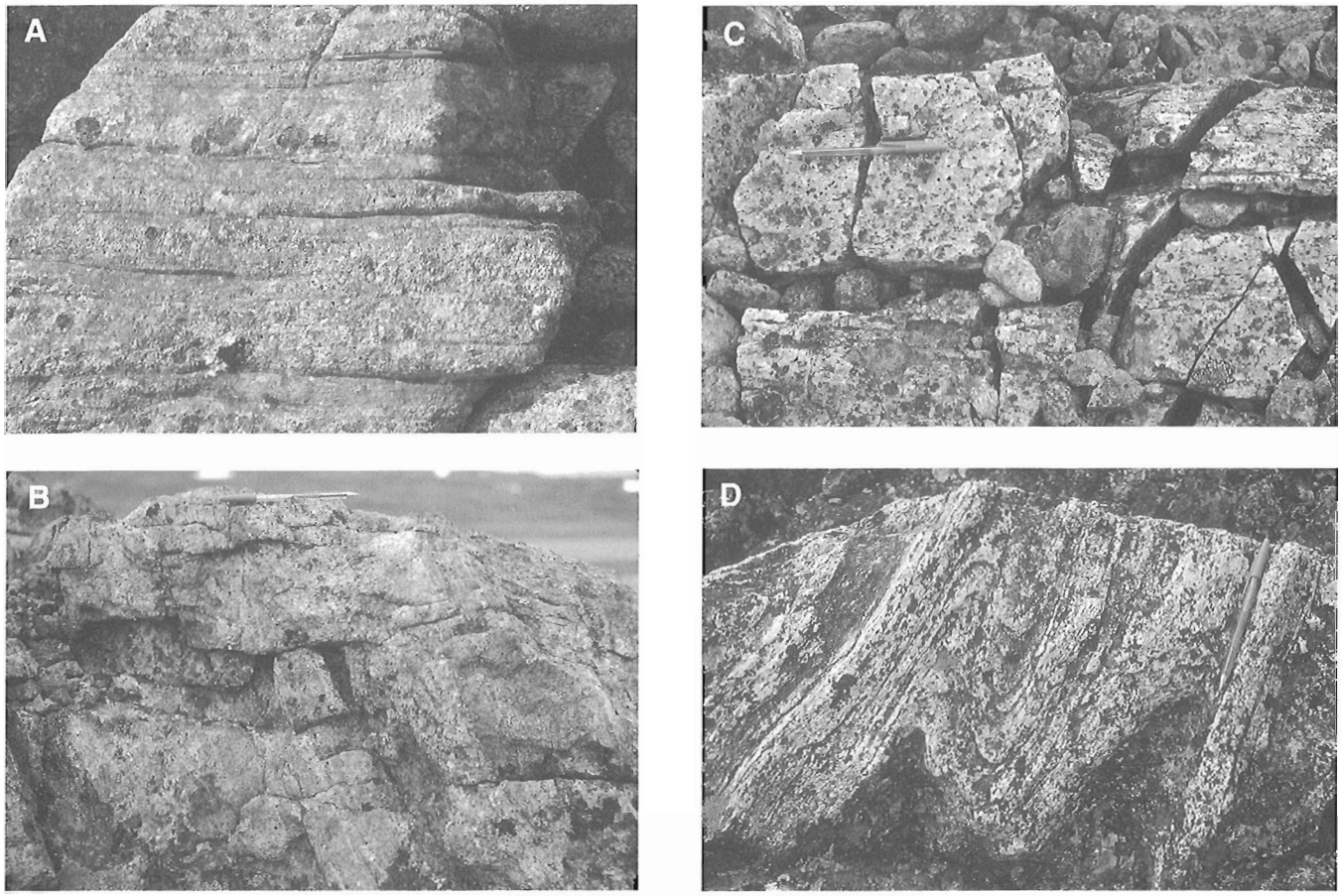

Figure 5. *A) Typical lilac-garnet psammite, central metasedimentary domain. Pen is 15 cm long.* ***B)*** *Compositional layering, defined by darker biotite-rich and lighter psammitic bands.* ***C)*** *20-30 cm thick quartzite layers.* ***D)*** *F_2 folds of S_1 in quartzite (light) interlayered with semipelite (dark).*

data indicate a depositional age younger than 2.0 Ga, and suggest that extensive Archean material was not available in the source region during sedimentation. Two zircon overgrowths removed from rounded, detrital grains have been analyzed individually using the conventional isotope dilution thermal ionization technique (U-Pb); one is concordant at 1852 ± 2 Ma, the other is slightly discordant with a $^{207}Pb/^{206}Pb$ age of 1850 Ma (Scott and Gauthier, in press). The timing of the thermal peak of metamorphism at this location is thus interpreted as ca. 1852 ± 2 Ma. It may coincide with the generation of the white, garnetiferous monzogranites, and be related to the emplacement of the Cumberland Batholith.

Marble, mafic and ultramafic rocks

Rare occurrences of marble as well as mafic and ultramafic rocks are found within the siliciclastic metasedimentary package. A series of decametre-scale lenses of forsterite+diopside

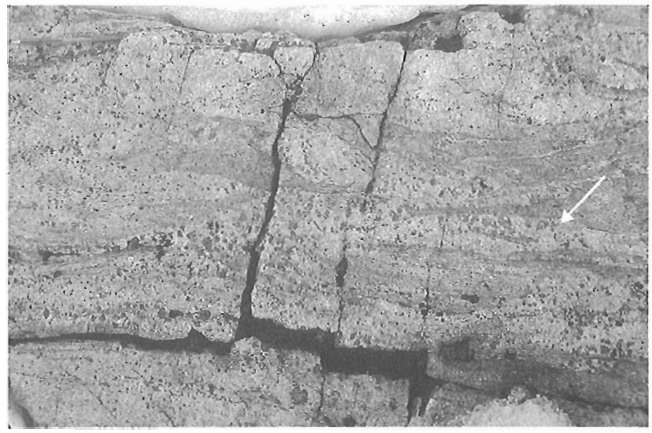

Figure 6. *Irregular seams (at arrow) of white-weathering, lilac-garnet monzogranite in psammite.*

calcsilicate was identified (Fig. 2). Poor exposure of the contacts of the lenses precludes direct observation, but the outcrop pattern is suggestive of a single marble layer which has been boudined at map scale.

Isolated pods of fine- to medium-grained metaperidotite, up to several metres thick and tens of metres in length, are rare but occur throughout the central metasedimentary domain. These bodies are parallel to the principal compositional layering in the host rocks, and may represent disrupted sills, although primary evidence, such as chilled margins, is no longer preserved.

Mafic rocks are present as thin layers within the clastic rocks, generally 1-2 m thick, and less than 10 m in length. Whereas they are dominantly composed of fine grained hornblende and plagioclase, rare clinopyroxene and possibly orthopyroxene were observed as cores in coarser hornblende crystals. Gabbroic textures were only rarely noted (Fig. 7). These rocks may originally been massive volcanic flows and/or thin intrusive sills, as is suggested by the gabbroic-textured rocks.

Orthopyroxene-biotite tonalite

The metasedimentary rocks of the central domain are cut by sheets of fine- to medium-grained orthopyroxene-biotite-bearing tonalite up to one kilometre thick and several kilometres long (Fig. 2). These rusty-brown- to buff-weathering intrusions are in general only weakly foliated. Deep-red garnet is present within several metres of the margins of some of the tonalite bodies, suggesting possible incorporation of material from the host metasedimentary rocks. An intrusive age of 1890 ± 2 Ma has been determined for one of these bodies (D.J. Scott, unpub. data, 1995), providing a younger bracket on the timing of sedimentation.

Tectonostratigraphic interpretation of the central metasedimentary domain

Based on similarities in lithological assemblage, metamorphic grade, along-strike continuity of aeromagnetic anomaly patterns (Hoffman, 1989), and detrital zircon ages (Scott and Gauthier, in press), it seems reasonable to concur with Hoffman's (1989) suggestion that the rocks of the central domain may represent the northern continuation of the Tasiuyak gneiss complex of the Torngat Orogen (northern Labrador). The orthopyroxene-biotite tonalite intrusions in the metasedimentary rocks, one of which was emplaced at 1890 ± 2 Ma, are identical in age to similar rocks which intrude the Tasiuyak gneiss in northern Labrador (Scott and Machado, 1995; Scott, in press b). Although this is consistent with the suggestion that the Torngat Orogen continues northward onto the Hall Peninsula, these preliminary observations and conclusions need to be further evaluated with additional U-Pb geochronology.

The tectonostratigraphic significance of these rocks is unclear, as pervasive deformation has destroyed any primary, internal depositional structures. In the more extensively-studied northern Labrador segment, contact relations between the Tasiuyak paragneiss and the surrounding gneisses are tectonic. Goulet and Ciesielski (1990) have proposed that the Tasiuyak gneiss represents a distal stratigraphic equivalent of the shelf sedimentation recorded by the Lake Harbour Group. Alternatively, it may represent a more highly deformed, distal equivalent of the rift-related Ramah Group which rests unconformably on the Nain craton, although the extant detrital zircon ages appear to preclude this. The currently preferred hypothesis is that the source of the Tasiuyak paragneiss is neither associated with the Lake Harbour Group nor the Ramah Group, and that it was deposited in an axially-fed offshore trench parallel to the ancient margin of the Nain craton (Scott, in press c).

Eastern plutonic domain

The boundary between the metasedimentary rocks of the central domain and the metaplutonic rocks of the eastern domain is drawn at the easternmost occurrence of continuous panels of metasedimentary rocks (Fig. 2). Similar metasedimentary rocks also occur within the eastern domain.

Orthopyroxene-biotite tonalite

Fine- to medium-grained orthopyroxene-biotite tonalite is the dominant rock type in the eastern plutonic domain. This pale-brown-weathering rock is commonly finely layered, weakly to moderately foliated, and characterized by the presence of disrupted mafic layers or xenoliths (Fig. 8A). Pegmatitic granitic veining, predominantly parallel to layering but locally discordant, contributes to the overall streaky, gneissic appearance of this unit. The tonalitic phase commonly contains hornblende after orthopyroxene, whereas the mafic layers contain clinopyroxene and hornblende. Folds of

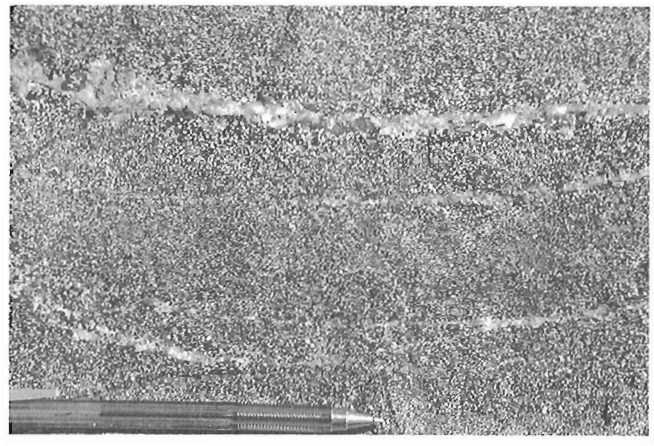

Figure 7. *Gabbroic texture in amphibolite.*

compositional layering (F_1), with the principal foliation (S_1) as axial planar, were only rarely observed. Steeply northwest-plunging minor folds of compositional layering and foliation (F_2) are common, as are mineral elongation lineations defined by quartz-feldspar aggregates (Fig. 8B) and more rarely by orthopyroxene. Where present in the same outcrop, F_2 fold axes and mineral elongation lineations are typically collinear. The principal foliation is only rarely mylonitic; in such cases, mylonites occur as narrow bands that are several metres wide and discontinuous along strike.

Monzogranite

Grey- to pink-weathering monzogranite is common in the western part of the domain. In contrast to the orthopyroxene-biotite tonalite, this fine- to medium-grained unit is more massive and only locally strongly foliated. Disseminated clinopyroxene and/or hornblende, as well as discrete mafic layers up to several metres in thickness, are present locally. Minor folds of foliation were only rarely observed; where present the are generally steeply plunging. Intrusive relationships between this unit and the orthopyroxene-biotite tonalite were not observed, although the more homogeneous nature of the monzogranite suggests that it may be younger than the tonalite.

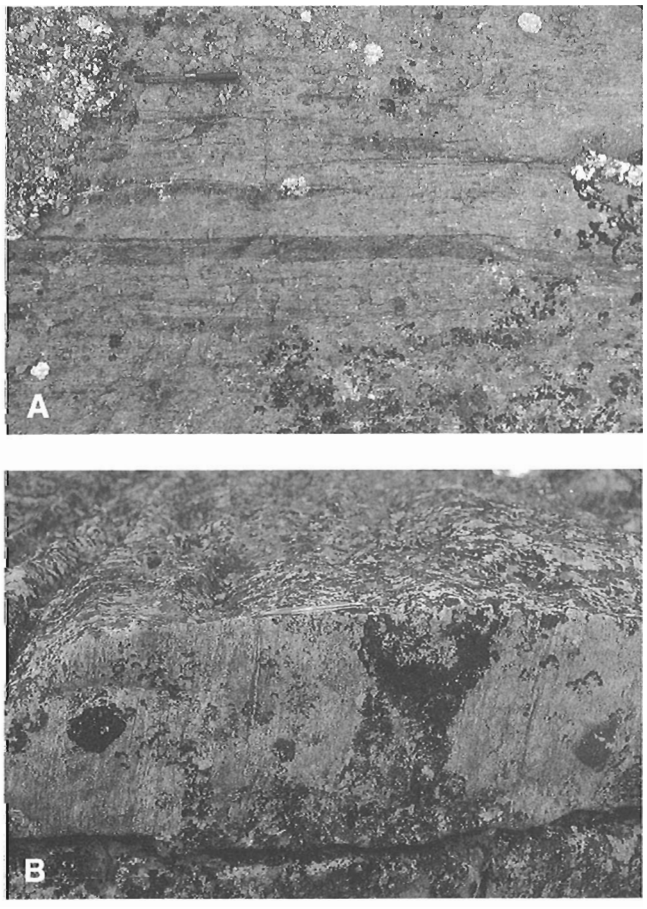

Figure 8. A) Discontinuous mafic layers in orthopyroxene-biotite tonalite, eastern plutonic domain. B) Quartz-feldspar elongation lineation on S_1 in tonalite.

Quartzite, psammite, and semipelite

A 1.5 km thick panel of quartzite, psammite, and semipelite was mapped (Fig. 2), and represents the largest continuous occurrence of metasedimentary rocks examined in the eastern domain. Whereas the variety and nature of these rocks is very similar to those of the central and western domains, the relative proportions of the various components is somewhat different. Decimetre-thick layers of lilac-garnetiferous quartzite are more common than either psammite or semipelite. Sillimanite is abundant in the semipelitic rocks, and is present in many quartzite layers.

Numerous thinner panels of metasedimentary rocks occur throughout the metaplutonic rocks of the eastern domain. Near the western edge of the domain, a package of semipelite, quartzite, and rare amphibolite is preserved in a spectacular doubly-plunging F_2-F_3 synform (Fig. 2). To the east, panels of semipelite and quartzite tens to hundreds of metres in thickness can be traced along strike for up to several kilometres. Where exposed, the contacts with the surrounding metaplutonic rocks are invariably sharp. Evidence of primary depositional relationships, such as an unconformity or basal conglomerate, was not observed, suggesting either intrusive and/or tectonic contacts. The provenance and depositional age(s) of these metasediments will be investigated by the Pb-Pb and U-Pb techniques.

Mafic rocks

Concordant layers of fine grained amphibolite are associated with metasedimentary rocks throughout the eastern domain. The generally massive, weakly to moderately foliated rocks are composed of clinopyroxene, hornblende, and plagioclase. Individual layers are generally less than 5 m thick, but can be traced along strike for up to hundreds of metres. Rare, coarser grained examples preserve gabbroic textures. The finer grained sheets may represent metavolcanic rocks or thin sills, whereas the gabbroic bodies may be sills.

Ultramafic rocks

Several isolated localities of pods of fine- to medium-grained metaperidotite, up to 5 m thick and tens of metres in length, have been identified (Fig. 2). These nonlayered bodies are typically parallel to the principal compositional layering in the host rocks, and may represent disrupted sills. This interpretation is speculative, as poor exposure of the contacts of the lenses and the general deformed nature of the rocks precludes direct observation of primary features such as chilled margins.

A concordant clinopyroxenite sheet several decametres thick and greater than one kilometre long was identified within the tonalitic orthogneisses in the central part of the domain (Fig. 2). This massive, fine- to medium-grained rock contains orthopyroxene and garnet, in addition to trace amounts of plagioclase.

Tectonic interpretation of the eastern plutonic domain

The tectonic significance and origin of the metaplutonic rocks of the eastern domain are not clear, but several possibilities can be suggested. These rocks may represent: 1) a distinct Archean microcontinent (Hoffman, 1989); 2) reworked Archean gneisses of the Nagssugtoqidian Orogen of west Greenland (Jackson et al., 1990); 3) the northern continuation of the Archean Nain craton (Scott and Campbell, 1993); and/or 4) ca. 1.9 Ga metaplutonic rocks of the Torngat Orogen (Scott and Machado, 1995; Scott, in press a). The metasedimentary rocks, although similar to the Paleoproterozoic units of the central domain, are of unknown age and affinity. U-Pb and Pb-Pb analytical work on representative samples from this domain is required before more direct comparisons can be made. The interpretations of the eastern domain are further discussed in the "Regional correlations" section.

DISCUSSION

Metamorphism and deformation

Metamorphic assemblages in the quartzofeldspathic metasedimentary rocks of the Hall Peninsula (Fig. 2) contain biotite, garnet, sillimanite, and melt pods, indicative of at least upper-amphibolite facies conditions, as has been identified across much of southern Baffin Island (Jackson and Morgan, 1978; Scott and Godin, 1995; St-Onge et al., 1996). Orthopyroxene-biotite assemblages in tonalitic rocks across the study area record granulite-facies conditions.

Garnet porphyroblasts and sillimanite needles that overgrow S_1 and L_1 suggest that peak thermal conditions postdated this phase of deformation. Early deformation led to the development of S_1, followed by thermal re-equilibration and culmination possibly associated with emplacement of the Cumberland Batholith ca. 1.85 Ga.

The S_1 is folded into a series of open to tight F_2 folds at all scales. A map-scale doubly-plunging synform (eastern domain, Fig. 2), and variations in plunge of north-south F_2 fold axes suggests that the entire area may have been subjected to a later, roughly west-trending folding event. Discrete faults or high-strain zones, such as the thrusts mapped on the Meta Incognita Peninsula (Hanmer et al., 1996) or the transcurrent Abloviak shear zone (Taylor, 1979; Hoffman, 1989), have not been documented in the present area. It is possible that significant deformation may have occurred within the study area, although its importance cannot presently be fully evaluated.

Regional correlations

The metaplutonic rocks of the western domain represent the southern continuation of the ca. 1.85 Ga Cumberland Batholith (Jackson and Taylor, 1972; Jackson et al., 1990). The eastern limit of the batholith is an intrusive contact with the metasedimentary rocks of the central domain; the southwest margin is a tectonized intrusive contact with gneisses of the Meta Incognita Peninsula (St-Onge et al., 1996; Scott et al., in press). Precise U-Pb dating is required to determine the timing of emplacement and tectonic context.

Based on lithological similarities, field relationships, and limited U-Pb results, the metasedimentary rocks and 1.89 Ga orthopyroxene-biotite tonalite plutons of the central domain are interpreted to represent the northern continuation of the Tasiuyak gneiss and Burwell plutonic rocks of the Torngat Orogen of northern Labrador, respectively. This preliminary interpretation requires testing with further analytical work.

The tectonic significance of the rocks of the eastern domain remains problematic. Hoffman (1989) has suggested that these rocks represent the Archean Burwell microcontinent. As the southern extent of this postulated entity has been shown to comprise rocks of the Nain craton and 1.91-1.87 Ga intrusions (Scott, in press a, in press c), the existence of a discrete Burwell craton is considered doubtful. Scott and Campbell (1993) have suggested that the Archean Nain craton may continue northward onto the Hall Peninsula. However, discordant mafic dykes, characteristic of the Nain/North Atlantic craton in Labrador and Greenland, have not been observed in the study area. Jackson et al. (1990) have correlated the rocks of the eastern domain with reworked Archean gneisses of the Nagssugtoqidian Orogen in west Greenland. Recent work in west Greenland by Kalsbeek and Nutman (1995) has begun to document the extent of ca. 1.9 Ga metaplutonic rocks in the ca. 2.9-2.6 Ga gneisses. The preferred hypothesis for the eastern domain is that the metaplutonic rocks are the along-strike equivalents of the 1.91-1.87 Ga Burwell magmatic suite that intrudes the Nain craton in northern Labrador, and the panels of metasedimentary rocks represent the northern continuation of the Tasiuyak gneiss.

Based on the present field observations and preliminary geochronological results, the western Hall Peninsula appears to be underlain by rocks of the ~1.85 Ga Cumberland Batholith. The central and eastern regions are underlain by rocks which represent the along-strike continuations of the Tasiuyak paragneiss and 1.91-1.87 Ga Burwell magmatic suite of the Torngat Orogen (northern Labrador). This does not support the hypothesis of Hoffman (1989) that this region is underlain by Archean crust. Complimentary investigations southwest of Iqaluit (Scott and Godin, 1995; St-Onge et al., 1996) suggest that the rocks of the Meta Incognita Peninsula are Paleoproterozoic, rather than part of the southeast arm of the Archean Rae craton (cf. Hoffman, 1989). Thus, significant re-evaluation of existing models for the Paleoproterozoic tectonic development of the northeast Laurentia is required, and forms the goal of ongoing geological and geochronological studies.

Economic potential

The proposed continuation of the Tasiuyak gneiss northward onto the Hall Peninsula is of potential economic significance. The recently discovered Voisey Bay Ni-Cu-PGE deposit in northern Labrador is associated with anorthosite-mangerite-charnockite-granite suite rocks of the Mesoproterozoic Nain Plutonic Suite, and is situated near the intrusive contact with the metasedimentary Tasiuyak gneiss. As a result, much of the exposed strike length of the Tasiuyak gneiss in Labrador has now been staked. The occurrence of a similar assemblage of metasedimentary gneisses on the Hall Peninsula thus may be prospective for additional Ni-Cu-PGE deposits if associated Nain Plutonic Suite-type rocks can be identified. Whereas the present investigation has examined only a very restricted portion of this unit, Blackadar's (1967) reconnaissance work suggests that these metasedimentary rocks have more than 300 km of exposed strike length on the Hall Peninsula, although Nain Plutonic Suite-type rocks were not specifically identified.

ACKNOWLEDGMENTS

Fieldwork during 1994 would not have been possible without the dedicated assistance and camaraderie of Laurent Godin (Carleton University), the logistical support of the Polar Continental Shelf Project (PCSP) and the Science Institute of the Northwest Territories (SINT), and the financial support of LITHOPROBE. Dick Deblicquy (Bradley Air Services), as well as Lynn Peplinski and Julie Beauchesne (Iqaluit Research Centre) are sincerely thanked for their enthusiastic involvement. The completion of fieldwork (1995) was facilitated by the continued support of PCSP (Bruce Wentzell, Canadian Helicopters), LITHOPROBE, and SINT, and through co-operation with the Geological Survey of Canada's South Baffin project. Marc St-Onge is thanked for his assistance in the collection of field data, and discussion of numerous aspects of this project. Reviews of this manuscript by Steve Lucas, Marc St-Onge, and Simon Hanmer have improved the clarity of the ideas presented.

REFERENCES

Blackadar, R.G.
1967: Geological reconnaissance, southern Baffin Island, District of Franklin; Geological Survey of Canada, Paper 66-47, 32 p.

Goulet, N. and Ciesielski, A.
1990: The Abloviak shear zone and the NW Torngat Orogen, eastern Ungava Bay, Québec; Geoscience Canada, v. 17, p. 269-272.

Hanmer, S., St-Onge, M.R., and Scott, D.J.
1996: Structural geology of the Meta Incognita thrust belt, south Baffin Island, Northwest Territories; in Current Research 1996-C; Geological Survey of Canada.

Hoffman, P.F.
1989: Precambrian geology and tectonic history of North America; in The Geology of North America – An Overview, (ed.) A.W. Bally and A.R. Palmer; Geological Society of America, The Geology of North America, v. A, p. 447-512.
1990: Dynamics of the tectonic assembly of northeast Laurentia in geon 18 (1.9-1.8 Ga); Geoscience Canada, v. 17, p. 222-226.

Jackson, G.D. and Morgan, W.C.
1978: Precambrian metamorphism on Baffin and Bylot Islands; in Metamorphism in the Canadian Shield, (ed.) J.A. Fraser and W.W. Heywood; Paper 78-10, p. 249-267.

Jackson, G.D. and Taylor, F.C.
1972: Correlation of major Aphebian rock units in the northeastern Canadian Shield; Canadian Journal of Earth Sciences, v. 9, p. 1650-1669.

Jackson, G.D., Hunt, P.A., Loveridge, W.D., and Parrish, R.R.
1990: Reconnaissance geochronology of Baffin Island, N.W.T.; in Radiogenic Age and Isotopic Studies: Report 3; Geological Survey of Canada, p. 123-148.

Kalsbeek, F. and Nutman, A.
1995: Reconnaissance SHRIMP U-Pb dating: assistance for lithological mapping and understanding the tectonothermal evolution of the Nagssugtoqidian orogen; in Proceedings of the DLC Workshop "Nagssugtoqidian Geology 1995", (ed.) F.C. Mengel, M. Marker, and J. van Gool; p. 29-33.

Scott, D.J.
in press a: U-Pb geochronology of a Paleoproterozoic continental magmatic arc on the western margin of the Archean Nain craton, northern Labrador, Canada; Canadian Journal of Earth Sciences, v. 32.
in press b: An overview of the U-Pb geochronology of the Torngat orogen and evolution of northeastern Laurentia; in Precambrian Crustal Evolution in the North Atlantic Region, (ed.) T.S. Brewer and B.P. Atkin; Special Publication.
in press c: U-Pb geochronology of the Nain craton on the eastern margin of the northern Torngat Orogen, Labrador; Canadian Journal of Earth Sciences, v. 32.

Scott, D.J. and Campbell, L.M.
1993: Evolution of the Paleoproterozoic Torngat orogen, Labrador Canada: Recent advances using U-Pb geochronology and Nd isotopic systematics (abstract); Geological Society of America, v. 25, p. A-237.

Scott, D.J. and Gauthier, G.
in press: Ages of detrital zircons in Paleoproterozoic sediments from northeastern Laurentia using TIMS (U-Pb) and Laser Ablation Microprobe ICP-MS (Pb): Comparison of techniques and implications for the tectonic evolution of the region; Chemical Geology.

Scott, D.J. and Godin, L.
1995: Preliminary geological investigation of the Lake Harbour Group and surrounding gneissic rocks near Lake Harbour and Markham Bay, southern Baffin Island, Northwest Territories; in Current Research 1995-C; Geological Survey of Canada, p. 67-76.

Scott, D.J. and Machado, N.
1995: U-Pb geochronology of the northern Torngat Orogen, Labrador Canada: a record of Paleoproterozoic magmatism and deformation; Precambrian Research, v. 70, p. 169-190.

Scott, D.J., St-Onge, M.R., and Hanmer, S.
in press: Frobisher Bay, southern Baffin Island, Northwest Territories; Geological Survey of Canada, Colour Open File Map #3193.

St-Onge, M.R., Hanmer, S., and Scott, D.J.
1996: Geology of the Meta Incognita Peninsula, south Baffin Island, Northwest Territories: tectonostratigraphic units and regional correlations; in Current Research 1996-C; Geological Survey of Canada.

Taylor, F.C.
1979: Reconnaissance geology of a part of the Precambrian Shield, northeastern Quebec, northern Labrador, and Northwest Territories; Geological Survey of Canada, Memoir 393, 99 p.

Geological Survey of Canada Project 950033

Structural geology of the Flin Flon area, Manitoba and Saskatchewan[1]

D. Gale[2], S.B. Lucas, and J.M. Dixon[2]
Continental Geoscience Division, Ottawa

Gale, D., Lucas, S.B., and Dixon, J.M., 1996: Structural geology of the Flin Flon area, Manitoba and Saskatchewan; in Current Research 1996-C; Geological Survey of Canada, p. 93-103.

Abstract: The structure of the Flin Flon area, host to the Flin Flon and Callinan Cu-Zn orebodies, has been examined through mapping of mesoscopic and macroscopic structures in both the ca. 1.90 Ga Flin Flon arc assemblage volcanic basement and its 1.845 Ga continental sedimentary cover (Missi suite). The volcanogenic massive sulphide orebodies occur within the basalt-dominated basement stratigraphy in close proximity to a major regional unconformity. The unconformity cuts through a significant amount of basement section and is markedly angular, suggesting that the basement was deformed prior to erosion and sedimentation, consistent with regional constraints. The cover sequence, comprising fluvial sandstones interspersed with conglomeratic units, records three principal folding and foliation-forming events. As a result of F_1-F_2 folding, the cover rocks are preserved in fold interference basins. Significant low-angle overlap of basement on cover is attributed to F_1 north- or northeast-verging nappe development and subsequent shear displacement on the overturned basement-cover contact.

Résumé : Le style structural de la région de Flin Flon, où s'observent les massifs minéralisés cuprozincifères de Flin Flon et de Callinan, a fait l'objet d'une analyse basée sur la cartographie des structures mésoscopiques et macroscopiques à la fois dans le socle volcanique d'assemblage d'arc de Flin Flon (env. 1,90 Ga) et dans sa couverture sédimentaire continentale (1,845 Ga, suite de Missi). Les sulfures massifs volcanogènes sont associés aux strates du socle surtout composées de basalte qui se trouvent à une faible distance d'une discordance régionale majeure. La discordance en question, au pendage remarquablement fort, recoupe une portion importante du socle; ce dernier a donc été déformé avant l'érosion et la sédimentation, comme l'indiquent aussi les déformations régionales. La séquence de couverture, composée de grès fluviatiles intercalés d'unités conglomératiques, témoigne de trois événements principaux de plissement et de foliation. À la suite du plissement P_1-P_2, les roches de couverture ont été conservées dans des bassins d'interférence de type 1. Le vaste chevauchement peu incliné du socle sur la couverture est attribué à la formation d'une nappe à vergence nord P_1 et à un déplacement de cisaillement subséquent sur le contact socle-couverture déversé.

[1] Contribution to the Shield Margin NATMAP Project
[2] Department of Geological Sciences, Queen's University, Kingston, Ontario K7L 3N6

INTRODUCTION

The Paleoproterozoic Flin Flon Belt (Fig. 1) is host to numerous Cu-Zn volcanogenic massive sulphide deposits, the largest of which occurs at Flin Flon itself (Fig. 2) within the volcanic strata the ca. 1.9 Ga Flin Flon arc assemblage (formerly Amisk Group; Price, 1977; Syme and Bailes, 1993). Detailed examination of the structural geology of the Flin Flon area was initiated in 1994 to build on the geological mapping and structural interpretations of Ambrose (1936a), Stockwell (1960), Byers et al. (1965), Stauffer and Mukherjee (1971), Bailes and Syme (1989), Thomas (1992, 1994), and Fedorowich et al. (1995). The present study represents an MSc. thesis project by the first author at Queen's University, undertaken in collaboration with Hudson Bay Mining and Exploration Co. Ltd. and the Geological Survey of Canada. Fieldwork was initiated during 1994 and was completed during the summer of 1995. The objectives of the project are (1) to determine the regional distribution and geometry of structural elements and develop a three-dimensional structural model for the area; and (2) to determine the relative and, where possible, the absolute timing and kinematic framework for structures in the Flin Flon area.

To accomplish these objectives, mapping was undertaken in both the ca. 1.9 Ga volcanic basement and a ca. 1.845 Ga sedimentary cover sequence (approximate study area shown by Fig. 3). This report summarizes the structural elements mapped in both basement and cover stratigraphy.

REGIONAL GEOLOGY

The Flin Flon Belt (Fig. 1) is a collage of distinct tectonostratigraphic assemblages that was assembled at a relatively early stage in the tectonic evolution of the Paleoproterozoic Trans-Hudson Orogen (Stern et al., 1995a, b; Lucas et al., in press). Tectonic boundaries have been identified between major assemblages and are demonstrably long-lived (1.88-1.69 Ga; Fedorowich et al., 1995; Lucas et al., in press). Recent detailed geochronological, geochemical, and isotopic studies of the volcanic stratigraphy in the Flin Flon mine area (Fig. 2) have yielded a U-Pb zircon age for the Mine rhyolite of 1904+7/-4 Ma (Fig. 2; David et al., 1993) and shown that the mine sequence occurs within a tectonostratigraphic package of primitive, isotopically juvenile island arc tholeiites (Syme and Bailes, 1993; Stern et al., 1995a). The tholeiitic suite forms part of

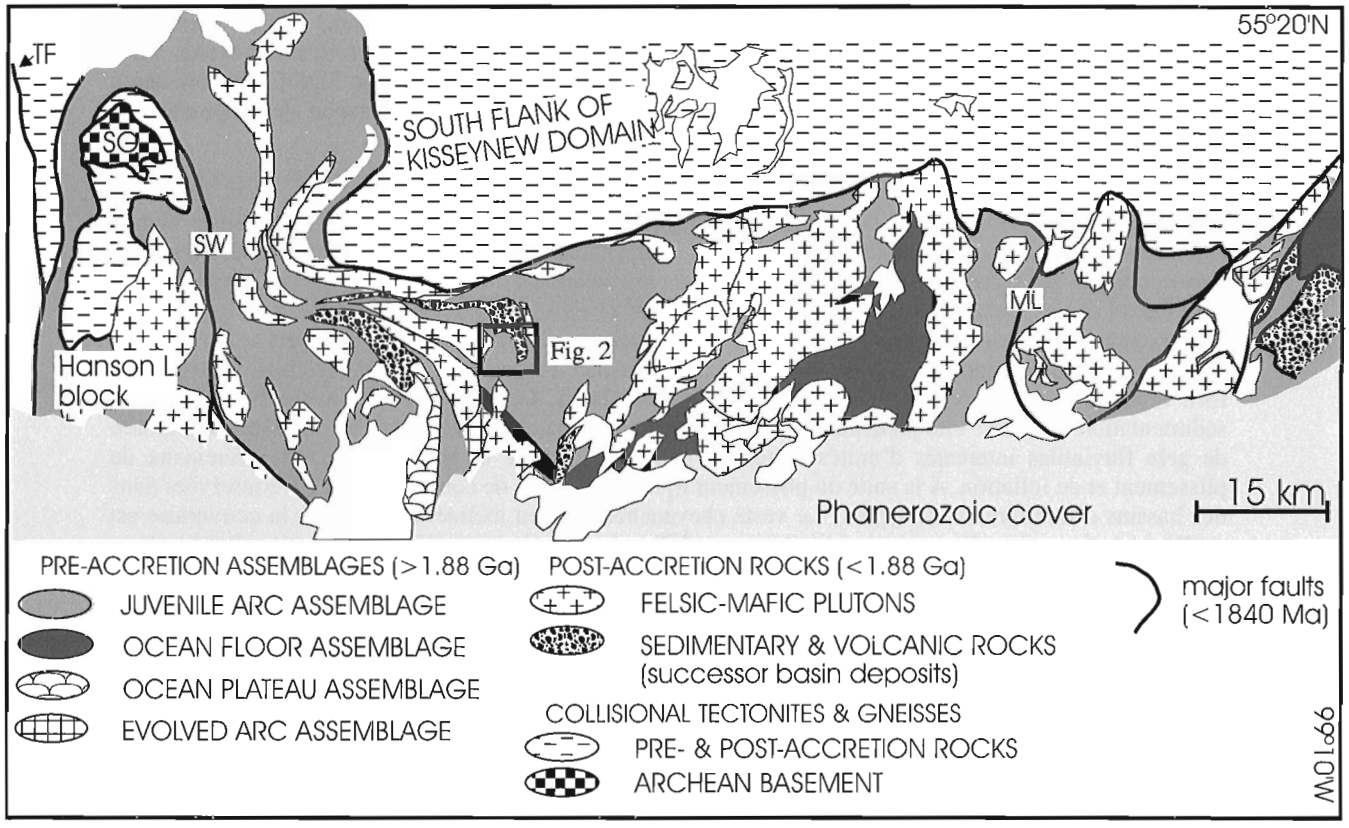

Figure 1. *Map of the Flin Flon Belt showing major tectonostratigraphic assemblages and plutons. The Flin Flon Belt is structurally sandwiched between the overriding south flank of the Kisseynew Domain and Snow Lake arc assemblage and the underlying Hanson Lake Block. The location of Figure 2 is indicated. ML – Morton Lake fault; SW – Sturgeon-weir shear zone; SG – Sahli granite; TF – Tabbernor fault.*

the Flin Flon arc assemblage and is unconformably overlain by continental (alluvial-fluvial) sedimentary rocks of the Missi suite (Bailes and Syme, 1989; Stauffer, 1990; Fig. 2).

The Missi sandstones at Flin Flon were deposited at ca. 1845 Ma, bracketed by the age of the youngest detrital zircon (1847 Ma; Ansdell et al., 1992; Ansdell, 1993) and the oldest crosscutting intrusion (1842 ± 3 Ma Boundary Intrusion; Heaman et al., 1992). The unconformity cuts through a significant amount of basement section and is markedly angular (Stockwell, 1960; Bailes and Syme, 1989), suggesting that the basement was deformed prior to or during erosion and sedimentation, consistent with regional constraints (Lucas et al., in press). The volcanic basement and sedimentary cover rocks at Flin Flon were deformed and metamorphosed at greenschist to lower amphibolite grade conditions (Ambrose, 1936b; Bailes and Syme, 1989; Digel and Gordon, 1995). Fedorowich et al. (1995) present biotite and hornblende Ar-Ar data that indicate peak metamorphism at 1820-1790 Ma in the Flin Flon area, coeval with regional peak metamorphism and deformation across the Trans-Hudson Orogen (e.g., Gordon et al., 1990; Ansdell and Norman, 1995; David et al., in press).

STRUCTURAL RELATIONS – COVER SEQUENCE (MISSI SUITE)

The Missi cover rocks are preserved in a large fold interference basin that is cut by north-northwest-trending faults (Fig. 2, 3). Stauffer and Mukherjee (1971) documented two generations of folds and one regional foliation in the Missi cover sequence within the study area (Fig. 3), as well as a number of dominantly north-northwest-trending, steeply-dipping oblique slip faults. The oblique slip faults are associated with both ductile (e.g., Channing Fault) and brittle-ductile (e.g., Ross Lake fault) fault zone structures and range in age from 1.82 to 1.69 Ga (Fedorowich et al., 1995). Our structural studies document three generations of folds and associated foliations in the southern part of the Missi basin (Table 1).

The S_1 foliation is not extensively developed throughout the study area and tends to be preserved in isolated lenses of fine grained shale or thinly laminated tuff beds (Fig. 4). A number of F_1 folds have been identified on the basis of facing reversals, map pattern, and overprinting by the S_2 regional foliation; only one macroscopic F_1 fold has a well developed S_1 axial planar foliation (Missi outlier, Fig. 3; see below). Examples of F_1 folds include the Ross Creek syncline and the Flin Flon Creek syncline (Fig. 3; Stauffer and Mukherjee, 1971).

The S_2 foliation is a penetrative cleavage that generally strikes north to northeast and dips shallowly to moderately to the east (Fig. 4, 5). In the southern portion of the Missi basin, S_2 has a northerly attitude with a steeper eastward dip. Throughout the area, S_2 represents the principal flattening fabric in the Missi cover sequence (Stauffer and Mukherjee, 1971), and developed at peak metamorphic conditions (Ambrose, 1936b; Bailes and Syme, 1989; Fedorowich et al., 1995). S_2 is axial planar to the F_2 Pipeline syncline (described below) and Mud Lake syncline (Fig. 3; Stauffer and Murkerjee, 1971).

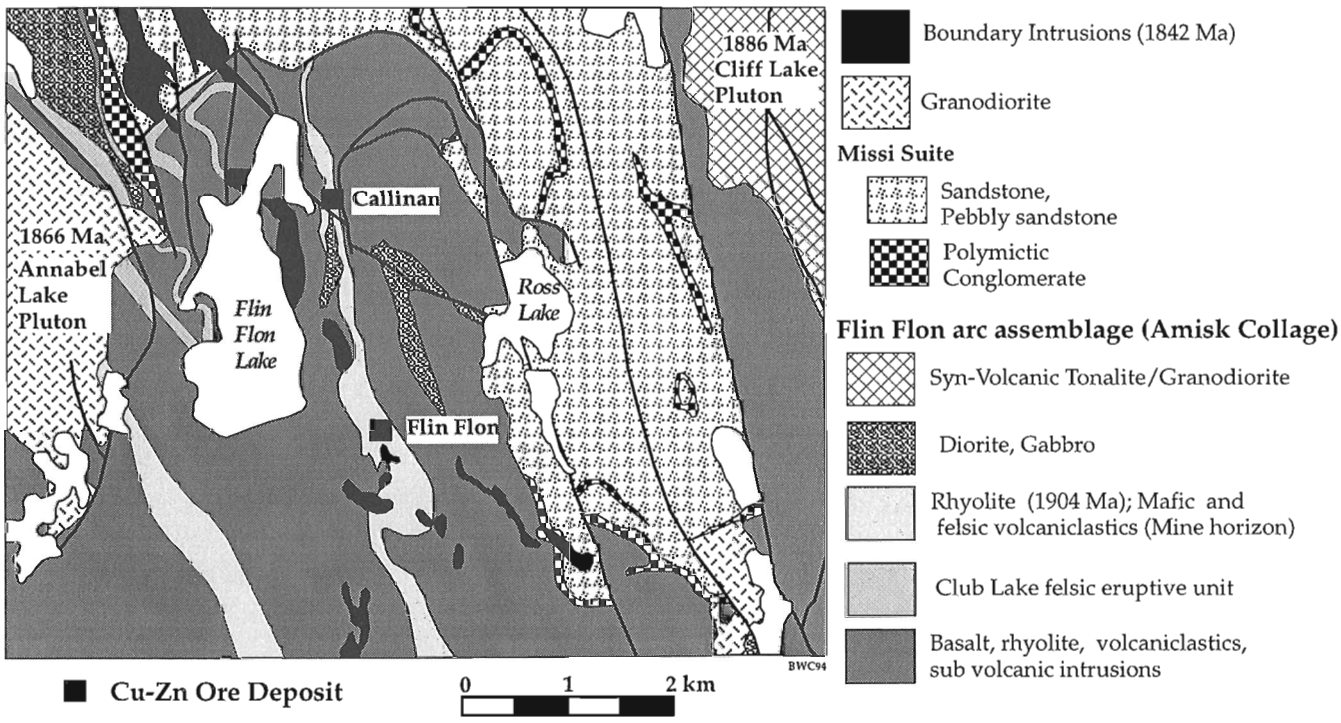

Figure 2. *Geology of the Flin Flon area (after Stockwell, 1960; Bailes and Syme, 1989; Syme et al., 1993; Thomas, 1992, 1994).*

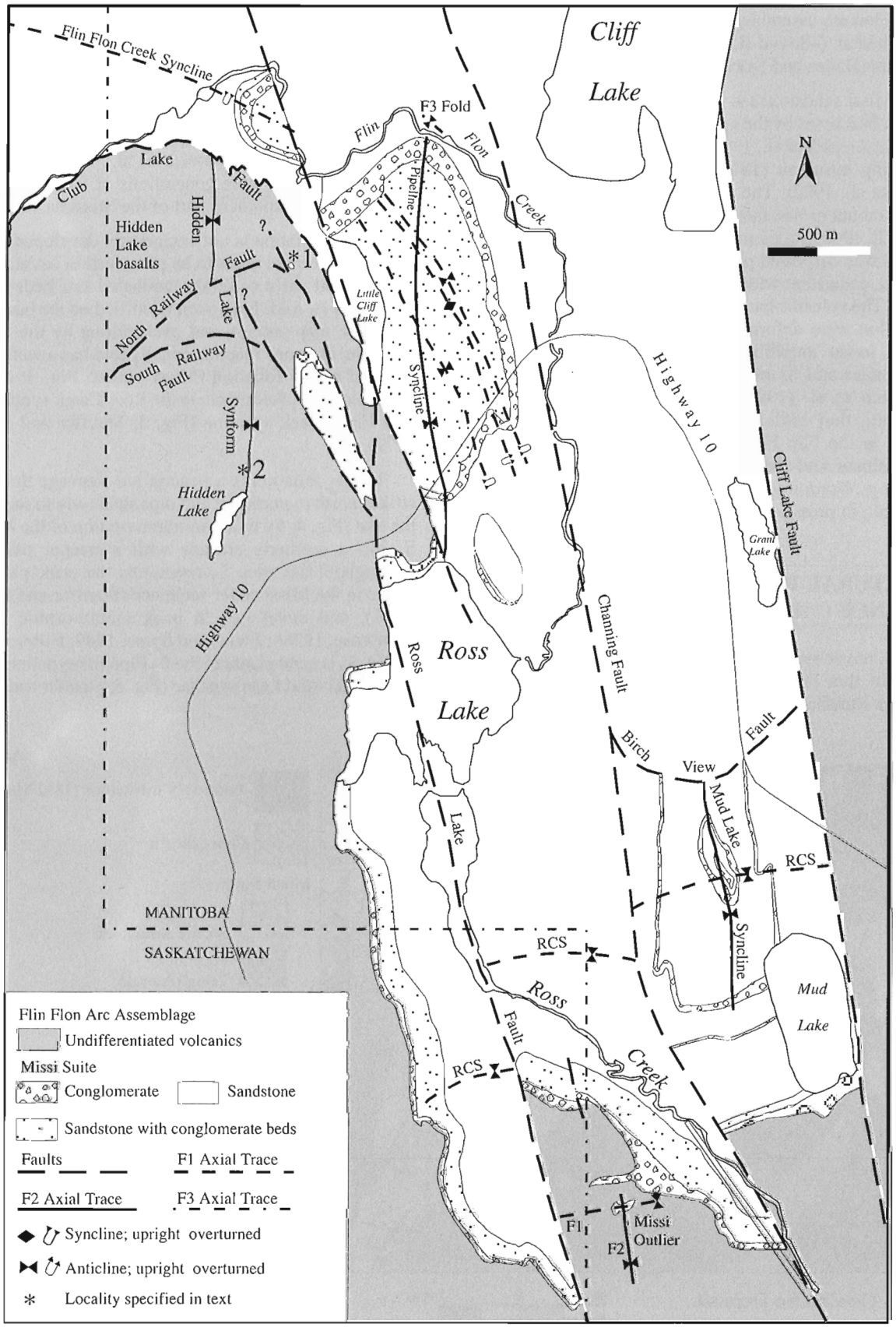

Figure 3. *Structural geology of the study area. Location of fold axes from this study, Stockwell (1960), Bailes and Syme (1989), Stauffer and Mukherjee (1971), and Thomas (1992). RCS – Ross Creek syncline.*

The S_3 foliation is a spaced, domainal cleavage that strikes northwest, dips steeply to moderately northeast, and is heterogeneously developed throughout the area (Fig. 4, 6). It is axial planar to rare F_3 folds.

A regional lineation was mapped throughout the northern half of the study area in both the sedimentary cover and volcanic basement (Stauffer and Mukherjee, 1971; Bailes and Syme, 1989). It is defined by the elongation of pillows, clasts within the conglomerate and volcaniclastic beds, and quartz and feldspar grains in the matrix of the sandstones and granites. In areas where the lineation is well developed, conglomerate clasts display aspect ratios of up to 7:1 (Fig. 7; cf. Stauffer, 1990). We suggest that the lineation formed during D_2 deformation (i.e. L_2), consistent with the interpretations of Stauffer and Mukherjee (1971) and Fedorowich et al. (1995), who associate the lineation with S_2 and growth of peak metamorphic assemblages. However, the extension lineation is also subparallel to F_1, F_2, and F_3 fold axes and the intersection of S_2 and S_3. Detailed thin section study is required to establish the age of all lineations relative to the S_2 and S_3 foliations.

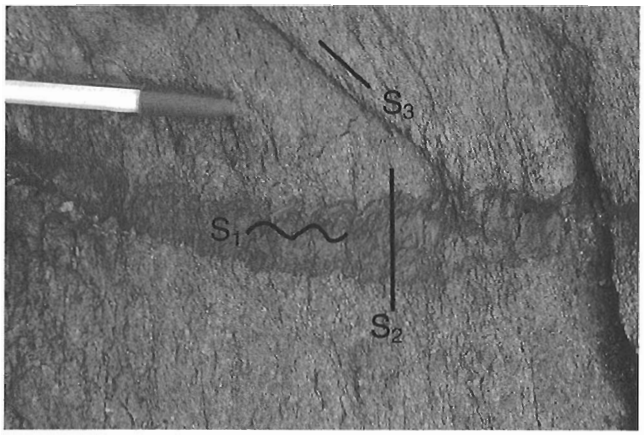

Figure 4. *Overprinting cleavage relations (S_1, S_2 and S_3) in the Missi outlier (Pen=15 cm).*

Missi outlier

A small outlier of Missi suite sedimentary rocks occurs just to the south of the principal Missi basin (Fig. 3) and contains evidence for all three deformation events (Fig. 4). Macroscopic folds are easily delineated by tracing two distinctive conglomerate units in the dominant pebbly sandstone facies (Fig. 8), while mesoscopic folds are well developed in beds with centimetre-scale hematite laminations (Fig. 9). S_1 is a bedding-parallel cleavage that is axial planar to an east-trending F_1 fold but is only developed in rare, fine grained shale lenses between sandstone beds (Fig. 4) and within the regolith developed at the unconformity. S_2 crenulates S_1 (Fig. 4) and is axial planar to open to tight folds which trend north and have axial planes that dip moderately to the east (Fig. 8). S_3 cleavage strikes northwest and dips steeply to the northeast but is not obviously related to any macroscopic folds in the outlier. Clasts within the sandstone and conglomerate beds are flattened in S_2 where S_3 is absent, but are aligned in S_3 where it is developed. The Missi units in the outlier do not contain an extension lineation.

We infer that the outlier's basinal shape is a result of a type 1 interference pattern (Ramsay, 1967) caused by F_1 and F_2 folding. The macroscopic F_1 syncline trends east (Fig. 3) and has an overturned northern limb and a steeply north-dipping axial plane. The southern limb generally dips moderately to the north but is locally overturned to the south due to F_2 folding. These observations suggest that the F_1 fold has a southward vergence, although it is most likely a second-order fold on the flanks of a larger F_1 anticline that closes to the south.

Pipeline structure

The Pipeline structure, located just east of Little Cliff Lake and outlined by a conglomerate horizon, is a southeast-plunging fold interference basin (Stauffer and Mukerjee, 1971). F_1 folds are found in the core of the interference basin (Fig. 3) and are recognized by reversals of facing direction as indicated by crossbedding. There is no field evidence for an S_1 foliation associated with these folds. The F_1 folds in the central domain of the Pipeline structure are generally tight,

Table 1. Summary of deformation events.

Deformation Event	Description	Associated Fabric Elements
D_1	N/NE-verging F_1 folds of basement and cover (Flin Flon Creek syncline, Ross Creek syncline, Missi outlier)	S_1 (rare cleavage in fine grained units).
D_2	Development of the Hidden Lake synform	None observed.
	Westward-verging F_2 folds of basement and cover (Mud Lake and Pipeline structures)	S_2 (well-developed axial-planar cleavage associated with all folds). L_2 (well-developed lineation).
D_3	Upright F_3 folds (Missi 'wedge' west of Ross Lake fault)	S_3 (spaced domainal cleavage).
D_4	High angle, oblique slip faulting (Ross Lake fault, Cliff Lake fault)	Ductile to brittle fault-related fabrics.

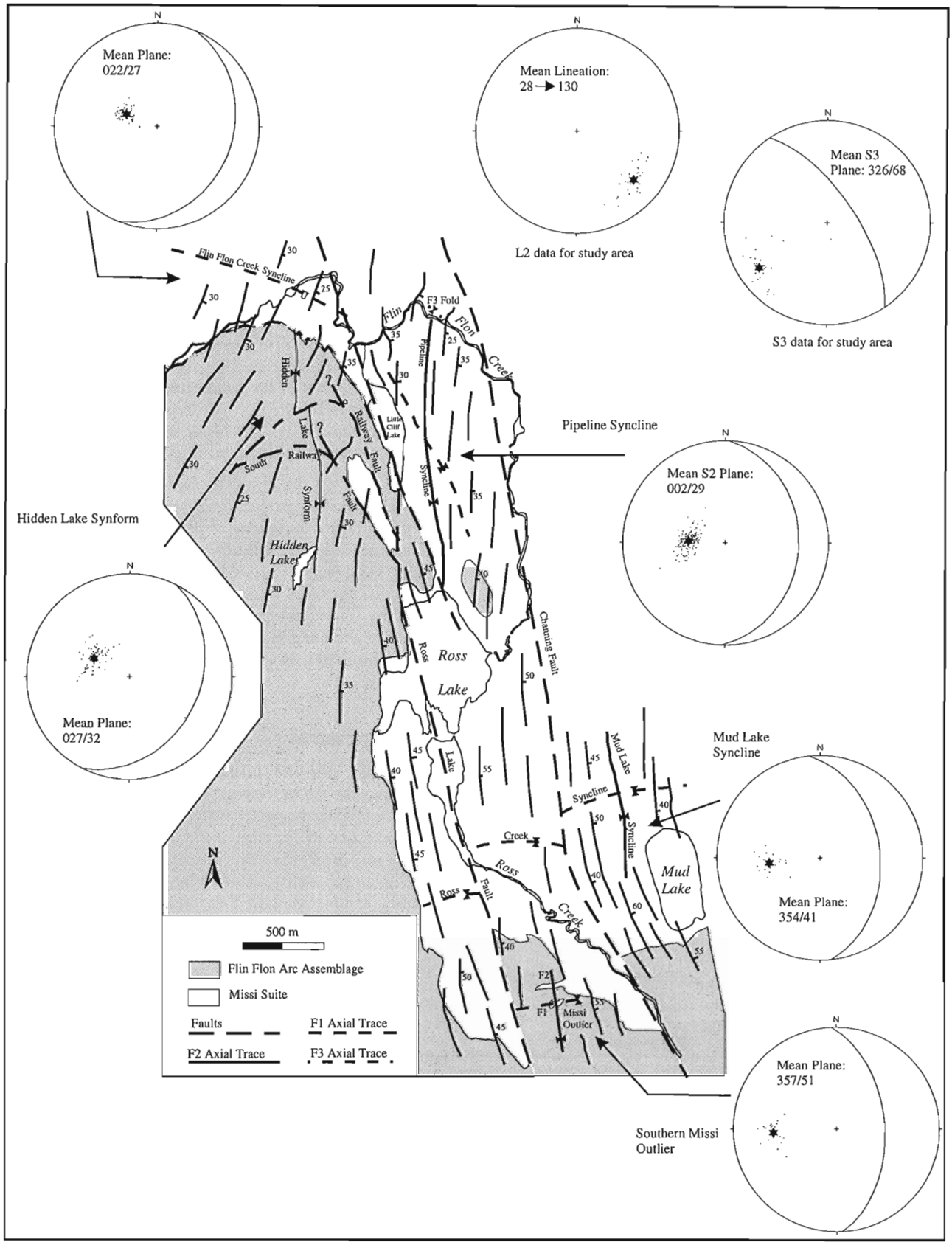

Figure 5. *S_2 cleavage traces (with dip indicated) for the study area, with associated lower hemisphere equal area plots for specified domians. Summary stereonet plots are shown for L_2 and S_3 with data from across the study area.*

plunge 23° towards 138° and have moderately east-dipping axial planes. Bedding is overturned on the eastern and southern portions of the Pipeline structure. The S_2 foliation maintains a northerly strike across these folds (Fig. 5), consistent with their interpretation as F_1 structures.

The major F_2 fold in the Pipeline structure is a tight to isoclinal, west-verging map-scale syncline outlined by the conglomerate horizon (Fig. 3) . Its eastern limb is overturned, dipping 60°-80° towards the east, and its western limb dips 25°-40° to the east. The F_2 axial plane dips shallowly to the east and the fold axis at the northern closure plunges 29° towards 132°, while the fold axis for the southern portion of the structure plunges 45° towards 115°. The mean orientation of S_2 (Fig. 5) is parallel to the synform's axial plane, thus implying an F_2 age for this fold (cf. Stauffer and Mukherjee, 1971). Interference between asymmetric F_1 and F_2 folds produced the Pipeline structure's southeast-plunging basinal shape (Stauffer and Mukherjee, 1971).

To the north of the Pipeline syncline, on the north shore of the Flin Flon Creek (Fig. 3), there is an isolated fold of decametric scale. This structure is an open, upright fold that has an axial plane of 311°/70°, which corresponds to the average orientation of the S_3 foliation (Fig. 5). The S_2 foliation is folded around the hinge of this fold. These two relationships suggest that it is a F_3 structure, the only mapped expression of F_3 in the Pipeline area. Elsewhere, S_3 transects the F_1-F_2 Pipeline structure. A well developed clast elongation lineation (L_2) occurs in the conglomerate bed that outlines the Pipeline structure (mean orientation is 28° towards 131°), as noted by previous workers (cf. Stauffer and Mukherjee, 1971).

STRUCTURAL RELATIONS – BASEMENT (FLIN FLON ARC ASSEMBLAGE)

Within the Flin Flon arc assemblage, the Hidden Lake basalts occur east of and conformably overlie the Flin Flon ore horizon (Fig. 2), and comprise a package of feldspar-phyric

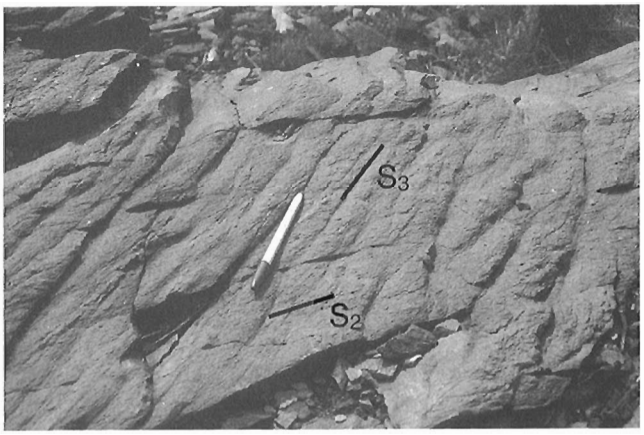

Figure 6. *S_3 cleavage (pen=15 cm, defining strike) overprinting S_2; southeastern corner of the F_2 Pipeline syncline.*

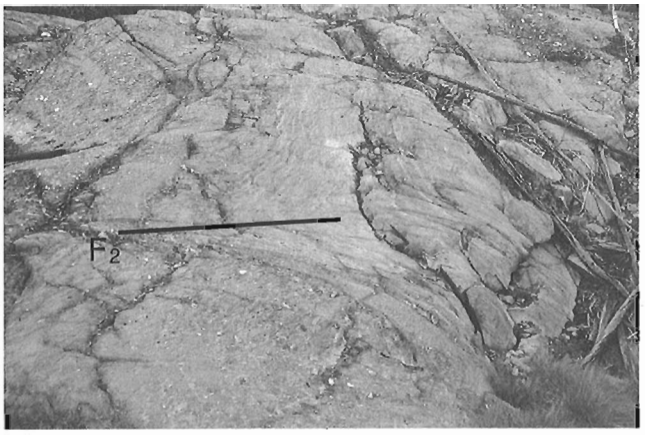

Figure 8. *Macroscopic F_2 fold (S-asymmetry) from the Missi outlier (width of photo is 8 m).*

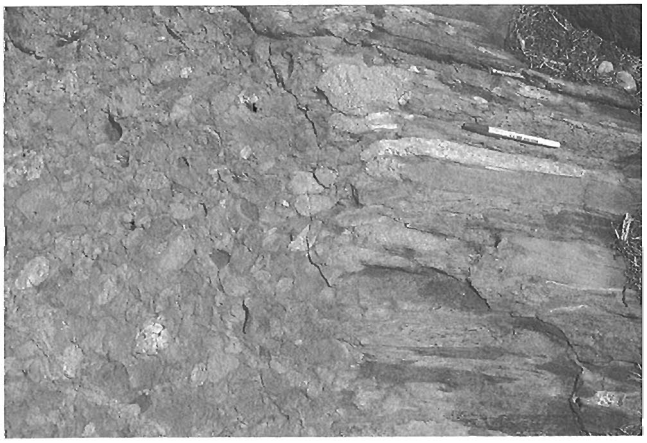

Figure 7. *L_2 from the conglomerate bed on western limb of F_2 Pipeline syncline (pen=15 cm).*

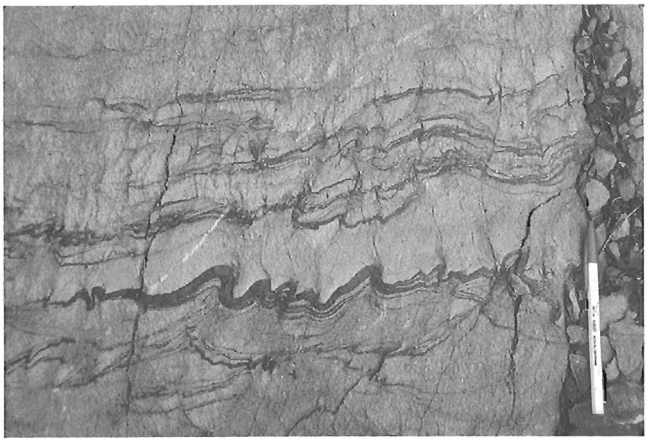

Figure 9. *Mesoscopic F_2 folds (Z-asymmetry) of hematite laminations from the Missi outlier (pen=15 cm).*

pillowed flows (Stockwell, 1960; Bailes and Syme, 1989; Thomas, 1992). The basalts are folded around the southeast-plunging, upright Hidden Lake synform (Fig. 3; Stockwell, 1960), attributed by Bailes and Syme (1989) to post-F_1 (i.e., post-Missi) folding. However, Bailes and Syme did indicate that the Hidden Lake synform could predate deposition of the Missi sediments. The basement-cover contact to the north and northeast of the Hidden Lake synform in the study area has long been interpreted as a thrust fault (Club Lake fault, Fig. 3), as the Hidden Lake basalts structurally overlie Missi sedimentary rocks (Bruce, 1918; Ambrose, 1936a; Stockwell, 1960; Stauffer and Mukherjee, 1971; Bailes and Syme, 1989; Thomas, 1992; Fedorowich et al., 1995). Previous workers have extended the Club Lake fault from the western end of basement-cover contact in Saskatchewan, where it is cut by a north-northwest-trending fault, to the position where the contact is cut by the Ross Lake fault in Manitoba (Fig. 2). The basement-cover contact to the south of Ross Lake (Fig. 3) is considered to be a folded and locally sheared unconformity, as it generally dips east or north towards the Missi basin. The high-angle Cliff Lake fault forms the eastern boundary to the Missi basin (Fig. 2, 3; Stauffer and Mukerjee, 1971; Bailes and Syme, 1989). Both the Hidden Lake synform and Club Lake fault were re-examined in this study with the aim of correlating basement and cover structures and deformation histories.

Hidden Lake synform

The Hidden Lake synform (Fig. 3) is defined by flow contacts, tuff layers, and pillow facing directions (Stockwell, 1960; Bailes and Syme, 1989). Bedding on the western limb dips 30°-40° to the southeast whereas it dips 65°-80° to the southwest on the eastern limb. Beds are locally overturned on the eastern limb of the fold. The poles to bedding define a fold axis of 41° towards 146°. Two regional foliations are observed within the volcanic rocks of the Hidden Lake synform. The first is a northeast-striking, shallowly to moderately southeast- dipping foliation that is subparallel to S_2 in the Missi sediments (Fig. 5). The foliation in the volcanic rocks has the same penetrative, synmetamorphic nature as S_2 in the Missi (Fig. 10), and is thus interpreted as S_2. It is noteworthy that this foliation maintains a roughly constant strike across the core of the Hidden Lake synform (Fig. 5). The second regional foliation in the volcanic basement is a northwest-striking, moderately to steeply northeast-dipping spaced cleavage, with a mean orientation of 327°/73°, parallel to S_3 in the Missi rocks (Fig. 5). It overprints the penetrative S_2 foliation in the basalts (Fig. 10) and is thus correlated with S_3 in the Missi rocks. Elongated quartz amygdules, pillows, and clasts in volcaniclastic beds define a well developed linear fabric element with an average orientation of 28° towards 135°, parallel to L_2 in the rocks of the Missi suite.

Basement-cover contact and the Club Lake fault

Study of the Club Lake 'fault' in the northeast part of the study area (Fig. 2, 3) has shown that it is a sheared, overturned unconformity (Fig. 11, 12) and not simply a major thrust fault juxtaposing basement on cover. Deformed and metamorphosed regolith has been mapped sporadically along much of the contact in the study area (Fig. 11, 12), thus providing strong evidence for an unconformity. Individual outcrops of regolith are discontinuous, generally 1-3 m thick and extend for no more than 35 m along strike at any one locality. Sections of the basement-cover contact without regolith may represent paleochannels in which weathered horizons were removed, or alternatively, may represent a tectonic contact in which the unconformity has either been cut out or is no longer discernible due to the intensity of deformation.

Where the basement-cover contact strikes east-west, it dips 45° to the south and the rocks on either side are strongly schistose but still preserve evidence for the unconformity. Outcrop-scale fold interference patterns (at least 3 generations of folding) require early recumbent folds (F_1?) with axial surfaces that parallel a south-dipping foliation developed parallel to the contact. Compilation of S_2 orientations in the

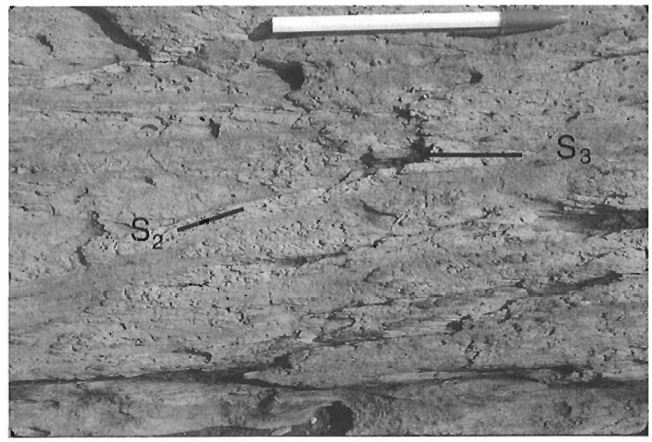

Figure 10. *S_2 and S_3 cleavage relations in basement rocks from Hidden Lake synform area. Pen for scale is 15 cm.*

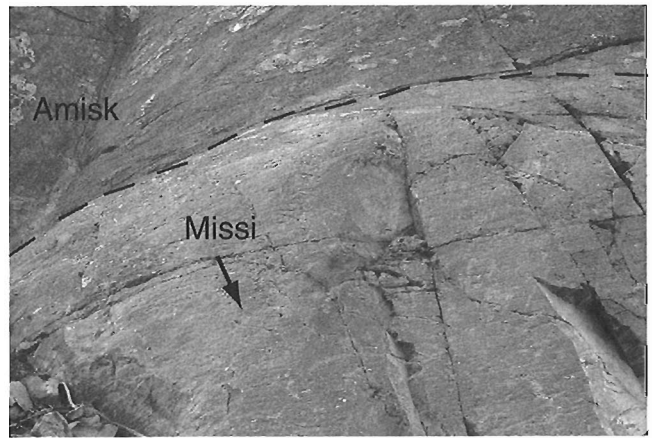

Figure 11. *Contact between Amisk basalt sequence and regolith with light coloured epidosite 'clasts' (top) and Missi sandstones (bottom). Photograph taken from near top of cliff section above Flin Flon Creek. Missi rocks face down, and Amisk rocks face up. Contact is the Club Lake 'fault'.*

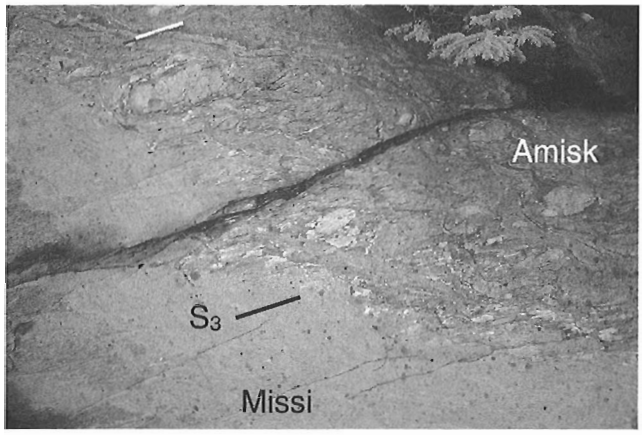

Figure 12. *F_3 folding (Z-asymmetry) of unconformity along the Club Lake fault (pen=15 cm). Missi sandstones are light coloured rock. Amisk refers to the Hidden Lake basalts and regolith derived from them (light coloured blocks are epidosite 'clasts').*

study area (Fig. 5) indicates that this initial deformation of the basement-cover contact must have preceded F_2/S_2. As the basement-cover contact turns to the southeast, it is deformed by map and outcrop-scale Z and S folds that include F_1, F_2, and F_3 structures (based on relationship to S_2 and S_3) and that all plunge to the southeast. The F_1 folds are metre- to decametre-scale Z folds that are transected by S_2. At least three decametre-scale S folds with S_2 subparallel to their axial planes are interpreted as F_2 structures, and suggest that an antiformal syncline lies to the east and closes to the south. S_2 is deformed into relatively open F_3 Z folds with S_3 as the axial planar cleavage (Fig. 12). Locally, post-F_3/S_3 high-strain zones containing sinistral shear bands deform the northwest-trending basement-cover contact, and are probably related to D_4 faulting (Table 1). The basement-cover contact is truncated by the Ross Lake fault in Little Cliff Lake (Fig. 3).

A well developed linear fabric, trending 33° towards 125° and defined by both mineral alignment and stretched clasts, is found along the trace of the Club Lake fault. This lineation is parallel with the regional L_2 lineation and to the fold axis defined by the poles to the Club Lake basement-cover contact (29° towards 130°).

Railway faults

The North and South Railway faults are a prominent set of bedding-parallel shear zones within the Hidden Lake basalts (Fig. 2, 3; Stockwell, 1960; Bailes and Syme, 1989; Thomas, 1992). They appear to juxtapose different units within the Hidden Lake strata (i.e., volcaniclastics on pillow basalts), but do not have any significant displacement. In detail, they are marked by centimetre- to metre-scale ductile shear zones, multiple generations of folding and foliations, and quartz-carbonate-chlorite veining. There are locally up to five strands of the South Railway fault, ranging from 1-5 m in width. These shear zones contain centimetre- to metre-scale aphyric felsic dykes which are often boudined. The dykes are not commonly found in the Hidden Lake sequence outside of the shear zones, suggesting that they may be syntectonic.

Field examination of the shear zones bounding the Missi wedge in the eastern portion of the Hidden Lake synform (Fig. 3) indicates that they are of S_3 age (or younger) and deform the S_2 foliation in both basement and cover rocks. In contrast to previous interpretations, we suggest that these shear zones may truncate the Railway faults to the north (Fig. 3).

DISCUSSION

The three generations of folds and foliations observed in the Missi sedimentary rocks in this study (Table 1) match in general the sequence established by Stauffer and Murkerjee (1971). The principal advance in the present study has been the correlation of deformation structures between basement and cover. An important feature of the Flin Flon area structures is the parallelism of virtually all linear features, including mesoscopic and macroscopic fold axes, elongation lineations, mineral lineations, and intersection lineations. Observations to date indicate that the parallelism of these structures is independent of strain intensity, suggesting that the fold hinges have not been rotated into parallelism with the extension direction.

Two packages of Missi rocks have been mapped on the eastern limb of the Hidden Lake synform, isolated from the principal Missi basin to the east and south. A small (10 m diameter) outlier of Missi rocks, consisting of conglomerate and sandstone overlying regolith, is preserved at locality 1 on Figure 3 (D. Price, pers. comm., 1995). The second package of Missi rocks forms a wedge-shaped basin (Fig. 3) previously thought to lie between strands of the Railway fault system (Stockwell, 1960; Bailes and Syme, 1989). The Missi rocks unconformably overlie the Hidden Lake basalts on the northwest and southeast ends of this basin, and are in fault contact along the northwest-trending east and west margins. The S_3 cleavage is axial planar to northwest-trending upright folds of the unconformity and S_2 that are well developed at the northwest and southeast ends of this basin. Documentation of the unconformity at the base of the two Missi outliers, as well as along the Club Lake fault, suggests that the basement-cover contact may not project significantly above the current erosion surface on the eastern limb of the Hidden Lake synform.

The Club Lake fault is best interpreted as a deformed unconformity. Its geometry in the study area requires early recumbent folding of the basement-cover contact, which we ascribe to F_1. The inferred geometry of the unconformity between the Missi outlier (locality 1, Fig. 3) and the Club Lake fault trace suggests north or northeast vergence on the F_1 basement-cored nappe, consistent with the asymmetry of the F_1 Flin Flon Creek syncline (Ambrose, 1936a). Thrust-sense (i.e., northward) shear may have occurred along the overturned contact, but it is difficult to distinguish between basement on cover overlap due to folding or faulting. Post-F_1 deformation was localized along appropriately oriented

portions of contact during succeeding deformation episodes. Minor folds related to all three post-Missi fold generations deform the basement-cover contact throughout the study area.

Stauffer and Mukherjee (1971) estimated about 1067-1830 m of northwestward thrust displacement on the Club Lake fault. Recently, Hudson Bay Exploration and Development Co. Ltd. have drilled into Missi sandstones structurally beneath the Hidden Lake basalts in several holes (T. Baumgartner and D. Price, pers. comm., 1995). At locality 2 (Fig. 3), the basement-cover contact was encountered at a depth of 2100 m. Further drill hole information suggests that the contact dips moderately to the south or southeast, consistent with its dip along the east-west segment of the Club Lake fault. The amount of fold/fault overlap of basement on cover depends on the kinematics of deformation, which have not been fully resolved to date. However, if basement on cover overlap is primarily the result of F_1 folding (north- or northeast-verging), then overlap is in the range of 500-2000 m.

The geometry of the Hidden Lake synform is not consistent with that of either the Flin Flon Creek or Pipeline F_1 folds, implying that the folding event responsible for the synform either predates or postdates F_1. There does not appear to be an expression of the Hidden Lake fold in the sedimentary strata to the north of the Club Lake 'fault', although the F_1 Flin Flon Creek syncline has a concave-to-the-south axial trace (Stauffer and Mukherjee, 1971). The concave-to-the-south shape of the Club Lake contact, coupled with the southeast plunge of all basement and cover structures in the area (Fig. 2, 3), requires that development of the Hidden Lake synform postdated F_1. However, as illustrated in Figure 5, S_2 cuts across the hinge of the Hidden Lake synform. We thus interpret the synform as an early D_2 structure, possibly coeval with initation of the D_2 folds in the Missi suite, that is subsequently transected by the S_2 regional cleavage. The geometry of the F_2 mesoscopic S folds of the Club Lake basement-cover contact northwest of Little Cliff Lake (Fig. 3) is consistent with an synformal anticline to the west, which describes the F_1-F_2 fold interference pattern affecting the Hidden Lake basalts. The map pattern for the preserved Railway fault segments (Fig. 3) suggests that they initiated as D_1 thrust faults and were folded during early D_2 development of the Hidden Lake synform. The apparent presence of two adjacent F_2 synforms (Hidden Lake and Pipeline) without an intervening antiform probably results from post-D_2 faulting (e.g., Ross Lake-Little Cliff Lake faults, Fig. 3).

The structural studies to date show no evidence for major faults along the Flin Flon-Callinan ore horizon (Fig. 2). Although deformed and disrupted by mesoscopic and map-scale structures related to all deformation episodes, the stratigraphy of the ore horizon sequence appears to be essentially 'intact' from footwall to hanging wall (cf. Thomas, 1994). The significance of this is that Mine horizon (Fig. 2) can be traced from Callinan along strike past the Flin Flon mine and to the south, where it is folded by a large southeast-plunging Z fold (F_3?) and is cut by a number of discrete faults (Thomas, 1994).

ACKNOWLEDGMENTS

Special thanks are extended to Kevin Reid and Shannon Balzer for excellent assistance in the field in 1995 and 1994 respectively. Thanks also go out to Dave Thomas for an introduction to volcanology and the rocks of the Flin Flon area. Fieldwork for this project is jointly funded by Hudson Bay Exploration and Development Co. Ltd., through the GSC's Industrial Partner's Program, and the GSC's NATMAP Shield Margin Project. The project would not have gone ahead without the invaluable co-operation and assistance of Don Birak, Ted Baumgartner, and Dave Price (Hudson Bay Exploration and Development). We thank Simon Hanmer and Cees van Staal for their comments on the manuscript.

REFERENCES

Ambrose, J.W.
1936a: Structures in the Missi Series near Flin Flon, Manitoba; Transactions of the Royal Society of Canada (Third Series), v. 30, sec. 4, p. 81-98.
1936b: Progressive kinetic metamorphism in the Missi Series, near Flin Flon, Manitoba; American Journal of Science, v. 32, p. 257-286.

Ansdell, K.
1993: U-Pb constraints on the timing and provenance of fluvial sedimentary rocks in the Flin Flon and Athapapuskow Basins, Flin Flon Domain, Trans-Hudson Orogen; in Radiogenic Age and Isotopic Studies: Report 7; Geological Survey of Canada, Paper 93-2, p. 49-57.

Ansdell, K., Kyser, K., Stauffer, M., and Edwards, G.
1992: Age and source of detrital zircons from the Missi Group: a Proterozoic molasse deposit, Trans-Hudson Orogen, Canada; Canadian Journal of Earth Sciences, v. 29, p. 2583-2594.

Ansdell, K.M. and Norman, A.R.
1995: U-Pb geochronology and tectonic development of the southern flank of the Kisseynew Domain, Trans-Hudson Orogen, Canada; Precambrian Research, v. 72, p. 147-167.

Bailes, A.H. and Syme, E.C.
1989: Geology of the Flin Flon-White Lake area; Manitoba Energy and Mines, Geological Report GR87-1, 313 p.

Bruce, E.L.
1918: Amisk-Athapapuskow Lake district; Geological Survey of Canada, Memoir 105, 91 p.

Byers, A.R., Kirkland, S.J.T., and Pearson, W.J.
1965: Geology and mineral desposits of the Flin Flon area, Saskatchewan; Saskatchewan Department of Mineral Resources, Report 62, 95 p.

David, J., Bailes, A.H., and Machado, N.
in press: Evolution of the Snow Lake portion of the Paleoproterozoic Flin Flon and Kisseynew belts, Trans-Hudson Orogen, Manitoba, Canada; Precambrian Research.

David, J., Machado, N., Bailes, A., and Syme, E.
1993: U-Pb geochronology of the Proterozoic Flin Flon Belt-Snow Lake Belt: new results; in Trans-Hudson Orogen Transect, LITHOPROBE Report No. 34, p. 84-87.

Digel, S. and Gordon, T.M.
1995: Phase relations in metabasites and pressure-temperature conditions at the prehnite-pumpellyite to greenschist facies transition, Flin Flon, Manitoba, Canada; in Low-Grade Metamorphism of Mafic Rocks, (ed.) P. Schiffman and H.W. Day; Boulder, Colorado, Geological Society of America, Special Paper 296, p. 67-80.

Fedorowich, J.S., Kerrich, R., and Stauffer, M.R.
1995: Geodynamic evolution and thermal history of the central Flin Flon Domain Trans-Hudson Orogen: constraints from structural development, $^{40}Ar/^{39}Ar$, and stable isotope geothermometry; Tectonics, v. 14, p. 472-503.

Gordon, T.M., Hunt, P.A., Bailes, A.H., and Syme, E.C.
1990: U-Pb ages from the Flin Flon and Kisseynew belts, Manitoba: chronology of crust formation at an Early Proterozoic accretionary margin; in The Early Proterozoic Trans-Hudson Orogen of North America, (ed.) J.F. Lewry and M.R. Stauffer; Geological Association of Canada, Special Paper 37, p. 177-199.

Heaman, L.M., Kamo, S.L., Ashton, K.E., Delaney, G.D., Harper, C.T., Reilly, B.A., Sibbald, T.I.I., Slimmon, W.L., and Thomas, D.J.
1992: U-Pb geochronological investigations in the Trans-Hudson Orogen, Saskatchewan; in Summary of Investigations 1992, Saskatchewan Geological Survey, Saskatchewan Energy and Mines, Miscellaneous Report 92-4, p. 120-123.

Lucas, S.B., Stern, R.A., and Syme, E.C.
in press: Intraoceanic tectonics and the development of continental crust: 1.92-1.84 Ga evolution of the Flin Flon Belt (Canada); Geological Society of America Bulletin.

Price, D.P.
1977: Geology and economic potential of the Flin Flon-Snow Lake areas; University of Manitoba, Center for Precambrian Studies, Annual Report 1977, p. 52-83.

Ramsay, J.G.
1967: Folding and Fracturing of Rocks; Pergamon Press, New York.

Stauffer, M.R.
1990: The Missi Formation: an Aphebian molasse deposit in the Reindeer Lake Zone of the Trans-Hudson Orogen, Canada; in The Early Proterozoic Trans-Hudson Orogen of North America, (ed.) J.F. Lewry and M.R. Stauffer; Geological Association of Canada, Special Paper 37, p. 121-142.

Stauffer, M.R. and Mukherjee, A.C.
1971: Superimposed deformations in the Missi metasedimentary rocks near Flin Flon, Manitoba; Canadian Journal of Earth Sciences, v. 8, p. 217-242.

Stern, R.A., Syme, E.C., Bailes, A.H., and Lucas, S.B.
1995a: Paleoproterozoic (1.90-1.86 Ga) arc volcanism in the Flin Flon Belt, Trans-Hudson Orogen, Canada; Contributions to Mineralogy and Petrology, v. 119, p. 117-141.

Stern, R.A., Syme, E.C., and Lucas, S.B.
1995b: Geochemistry of 1.9 Ga MORB- and OIB-like basalts from the Amisk collage, Flin Flon Belt, Canada: evidence for an intra-oceanic origin; Geochimica et Cosmochimica Acta, v. 59, p. 3131-3154.

Stockwell, C.H.
1960: Flin Flon-Mandy, Manitoba and Saskatchewan; Geological Survey of Canada, Map 1078A, scale 1:12 000.

Syme, E.C. and Bailes, A.H.
1993: Stratigraphic and tectonic setting of volcanogenic massive sulfide deposits, Manitoba; Economic Geology, v. 88, p. 566-589.

Syme, E.C., Thomas, D.J., Bailes, A.H., Reilly, B., and Slimmon, W.
1993: Geology of the Flin Flon area, Manitoba and Saskatchewan (parts of NTS 63K and 63L); Geological Survey of Canada, Open File 2658, 1 sheet, scale 1:50 000.

Thomas, D.J.
1992: Highlights of investigations around the Flin Flon mine: reassessment of the structural history; in Summary of Investigations, Saskatchewan Geological Survey, Miscellaneous Report 92-4, p. 1-15.
1994: Stratigraphic and structural complexities of the Flin Flon mine sequence; in Summary of Investigations, Saskatchewan Geological Survey, Miscellaneous Report 94-4.

Geological Survey of Canada Project 910035

The structural anatomy of the central Flin Flon Belt, northern Manitoba[1]

James J. Ryan[2] and Paul F. Williams[2]
Continental Geoscience Division

Ryan, J.J. and Williams, P.F., 1996: The structural anatomy of the central Flin Flon Belt, northern Manitoba; in Current Research 1996-C; Geological Survey of Canada, p. 105-116.

Abstract: The structural geology of the Elbow-Cranberry-Iskwasum lakes area in the central Flin Flon Belt records a complex, episodic deformation history for this portion of the Trans-Hudson Orogen. Structural elements developed during two episodes of metamorphism and are divided into six generations of ductile deformation features and a generation of brittle-ductile to brittle features. Structural analysis, coupled with isotope geochemistry and geochronology, indicates significant changes in tectonic regimes at successive stages during a developmental history in excess of 100 Ma.

Résumé : La géologie structurale de la région des lac Elbow, Cranberry et Iskwasum (partie centrale de la ceinture de Flin Flon) révèle une déformation épisodique complexe dans cette portion de l'orogène trans-hudsonien. Les éléments structuraux se sont formés pendant deux épisodes de métamorphisme; ils sont divisés en six générations d'éléments de déformation ductile et une génération d'éléments de déformation cassante-ductile à ductile. L'analyse structurale, combinée à des analyses géochimiques et géochronologiques d'isotopes, indique des changements significatifs de régime tectonique à des stades successifs durant un processus de formation d'une durée dépassant 100 Ma.

[1] Contribution to the Shield Margin NATMAP Project

[2] Centre for Deformation Studies in the Earth Sciences, Department of Geology, University of New Brunswick, P.O. Box 4400, Fredericton, New Brunswick E3B 5A3

INTRODUCTION

The Elbow-Iskwasum-Cranberry lakes area encompasses a large portion of the central Flin Flon Belt (Fig. 1) of the Paleoproterozoic Trans-Hudson Orogen, and affords much insight into its orogenic evolution. Recent collaborative investigations concerning regional stratigraphy (Syme and Whalen, 1992; Syme, 1993; Syme and Morrison, 1994), isotope geochemistry (Stern et al., 1995a, b) and geochronology (Whalen and Hunt, 1994) indicate that the study area comprises a complex collage of tectonostratigraphic assemblages that were stitched together by large granitoid plutons (1.88-1.83 Ga). Detailed structural analysis provides a critical link in the understanding of how and when this collage was assembled and subsequently partially dismembered. The Elbow Lake shear zone, the single most regionally significant structure in the central Flin Flon Domain, has had a long-lived deformation history (Ryan and Williams, in press a) and separates different tectonostratigraphic assemblages (Syme, in press).

The 1995 field season concluded three summers of field work in the Elbow Lake area (Fig. 2), towards the first author's PhD. dissertation at the University of New Brunswick. Building on the work of Syme (1993, 1994), reconnaissance mapping was extended into the Cranberry lakes (Fig. 3) and Iskwasum Lake (Fig. 4) areas in an attempt to extrapolate the tectonometamorphic history interpreted for Elbow Lake to the southern extremity of the exposed Flin Flon Belt. Geochronological study of felsic dykes in the Elbow Lake area is part of a collaborative effort with the Geological Survey of Canada and Kevin Ansdell (University of Saskatchewan).

TECTONOSTRATIGRAPHIC ASSEMBLAGES

The Elbow-Cranberry-Iskwasum lakes area hosts three of the major tectonostratigraphic assemblages (arc, ocean floor, and ocean island assemblages) that comprise the Amisk Collage (Stern et al., 1995a, b; Lucas et al., in press). Metavolcanic and related sedimentary rocks (1.92-1.88 Ga) that comprise these assemblages are geochemically and lithologically diverse. They are intruded by both extensive synvolcanic mafic intrusions and voluminous 1.88-1.83 Ga calc-alkaline plutons that were emplaced following juxtaposition of the tectonostratigraphic assemblages (Stern and Lucas, 1994; Whalen and Hunt, 1994; Lucas et al., in press).

The Elbow-Athapap ocean floor assemblage comprises about 80% of the supracrustal rocks in the map area (Fig. 1), and is subdivided (in order of aerial extent) into the MacDougalls Point, Claw Bay, Moen Bay, and Athapapuskow basalt formations (Stern et al., 1995b; Syme, in press). These subaqueous pillowed and massive basalt flows are exclusively tholeiitic with geochemical similarities to modern N- and E-type MORBs (Stern et al., 1995b), contain synvolcanic sediments and are spatially associated with mafic-ultramafic complexes (Syme, 1992, 1993, 1994). Collectively, the basalts and related rocks of the Elbow-Athapap ocean floor assemblage are interpreted to have formed in a back-arc setting (Stern et al., 1995b).

Arc rocks (part of the Flin Flon assemblage) are exposed only on the northeast side of Elbow Lake (Fig. 1 and 2). The Flin Flon arc assemblage contains tholeiitic, transitional tholeiitic-calc-alkaline and much lesser shonshonitic volcanic rocks (Syme, 1990; Stern et al., 1995a). These rocks are readily distinguished from the ocean floor rocks by their compositional and lithological diversity (pillowed and massive flows, rhyolite breccias, massive rhyolite, and hyaloclastite flows; Syme, 1991).

The ocean island assemblage (Long Bay formation) is one of the most lithologically and geochemically distinct packages in the Flin Flon Belt (Syme, 1991; Stern et al., 1995b). It is exposed only on the northeast side of Long Bay and on Webb Island in northeast Elbow Lake (Fig. 1). The Long Bay formation is a mafic conglomerate interpreted as a series of submarine debris flows. Basalt clasts, which form the bulk of the conglomerate, are geochemically similar to the E-MORB's and most closely resemble Hawaiian tholeiites (Stern et al., 1995b). The ocean island basalts within the Long Bay formation are interpreted as having erupted subaerially, possibly upon a rifted arc basement (Stern et al., 1995b), and then deposited as subaqueous debris flows. This summer's mapping indicates that minor chert and rhyolite occur in the Long Bay formation, and that this unit may extend northward along the Elbow Lake shear zone as a thin, continuous unit.

Granitoid plutons make up 60-70% of the map area (Fig. 1). The plutons grade, with age, from tonalite-hornblende granodiorite (e.g. Gants Lake batholith) to granite (Anvil Lake pluton). The suite of calc-alkaline plutons is interpreted as representing post-accretion (successor) arc magmatism that contributed to the development of continental crust in the Flin Flon Belt (Lucas et al., in press). Whalen and Hunt (1994) provided U/Pb zircon age dates for several of the plutons in the Elbow Lake area (Fig. 2). Most notable are: an early phase of the composite Gants Lake batholith (1876+7/-6 Ma); the Elbow Lake tonalite stock (1864 ± 3 Ma); Elbow Lake tonalite (1864+5/-3 Ma); and the Big Rat Lake pluton (1845 ± 3 Ma). Shear zone deformation was preferentially concentrated within the intervening panels of supracrustal rocks. Dykes of variable composition and orientation occur throughout the supracrustal rocks, but are more abundant along the shear zones, especially in the Elbow Lake area. Crosscutting relationships between dykes and the shear zone fabrics provide excellent geochronology targets to bracket the timing of shear zone deformation (see below).

STRUCTURAL HISTORY AND RELATIVE TIMING OF METAMORPHISM

Metamorphism

Supracrustal rocks in the central Flin Flon Belt record two episodes of metamorphism: (1) M_1 hornblende grade contact metamorphism related to the voluminous 1876-1864 Ma plutonism; (2) M_2 regional metamorphism, which probably peaked in the Flin Flon Belt between 1820 and 1805 Ma (e.g. Ansdell and Norman, 1995; David et al., 1993, in press). Detailed metamorphic study has only been completed for

rocks from the Elbow Lake area. Ryan and Williams (1994) reported early hornblende occurring up to 3 km away from the nearest plutons, illustrating the widespread nature of M_1. The grade of M_2 on the east side of the Elbow Lake shear zone is epidote-amphibolite, as indicated by mafic rocks that contain pargasitic hornblendes to ferro-tschermakites (amphiboles). Plagioclase compositions grade from albite to oligoclase eastward towards the Gants Lake batholith (Fig. 2), coinciding with the disappearance of chlorite.

On the west side of the Elbow Lake shear zone, the grade of M_2 varies from amphibolite in the north, to actinolite-bearing upper greenschist facies rocks around Long Bay, and middle greenschist along the southwest side of Elbow Lake. Samples from the Cranberry lakes and Iskwasum Lake have not yet been analyzed, but appear to record greenschist facies metamorphism. Mafic tectonites on the south side of First Cranberry Lake (Fig. 3) are overgrown by coarse grained hornblende (~15 mm).

Structural history

Most folds, shear zones, and related fabrics are vertical across the map area. Structural elements can be broadly divided into six ductile deformation generations and later brittle-ductile to brittle features. Regional-scale folding appears to have been responsible for the pervasive, upright regional foliation, but shear zone deformation has played a more important role in the present distribution and strain state of the host lithologies. The trajectories of the various fabrics are illustrated by form surface maps of the Elbow Lake, the Cranberry lakes and Iskwasum Lake areas (Fig. 2, 3, and 4). A tectonometamorphic synthesis for the study area is presented in Figure 5, and is discussed in the following sections.

First generation structures

The earliest fabric recognized in the map area consists of mafic mylonites (S_1) in the southern Elbow Lake area derived from basalts and gabbro. The foliation is overgrown by amphibole and is crosscut by a suite of pink, quartz-phyric tonalite dykes (Fig. 6) that are similar in character to the Elbow Lake tonalite. One of these crosscutting dykes yielded a U/Pb zircon age of ~1868 Ma (K. Ansdell and J.J. Ryan, unpub. data), within analytical uncertainty of the 1864 Ma age of the tonalite plutons. These mylonites represent a pre-1868 Ma shear zone that may be related to early accretionary tectonics. The zone separates the MacDougalls Point basalt on the west from Claw Bay basalt on the east, but the zone has been

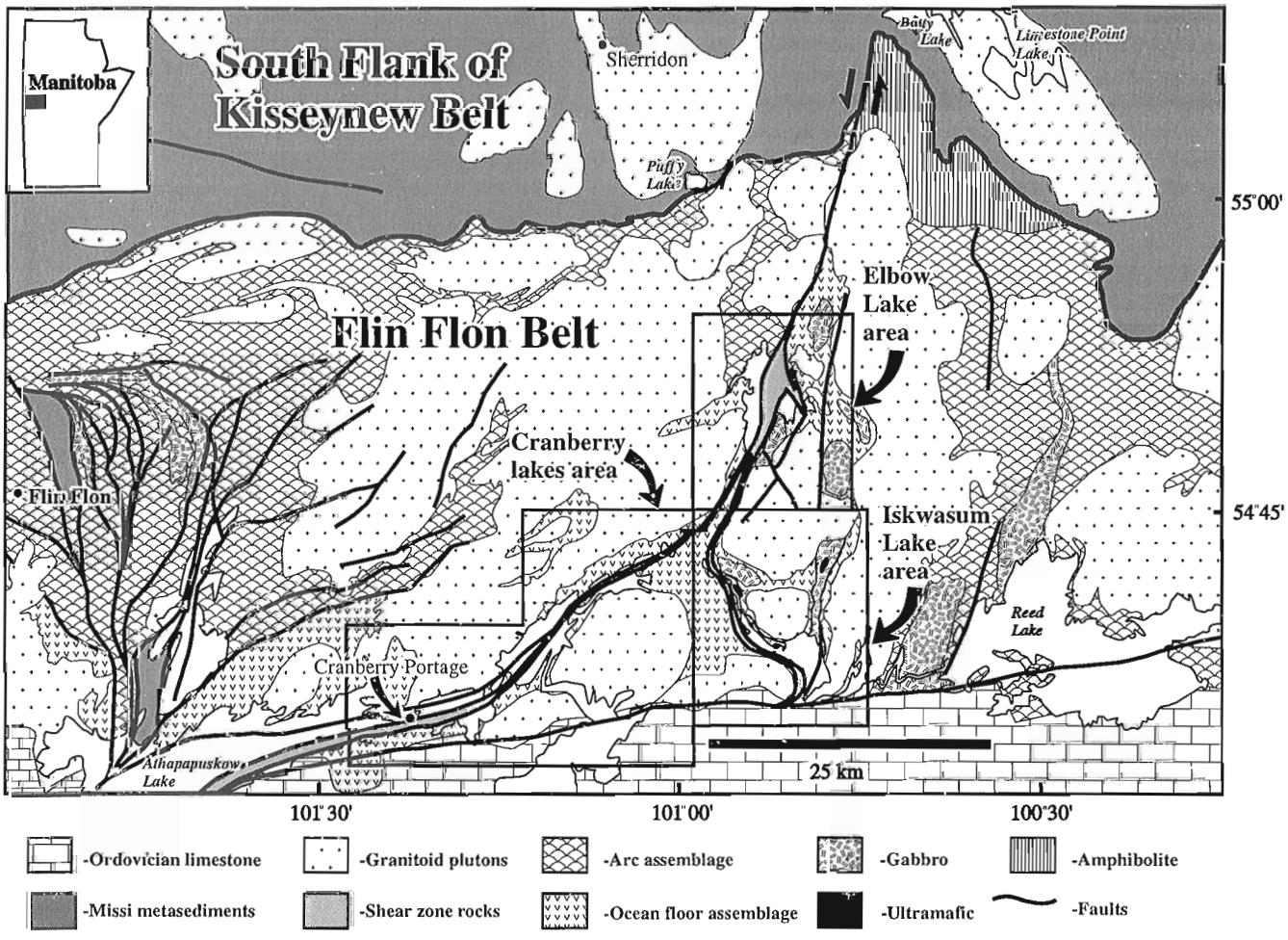

Figure 1. *Simplified overview map of the central Flin Flon Belt outlining the study areas.*

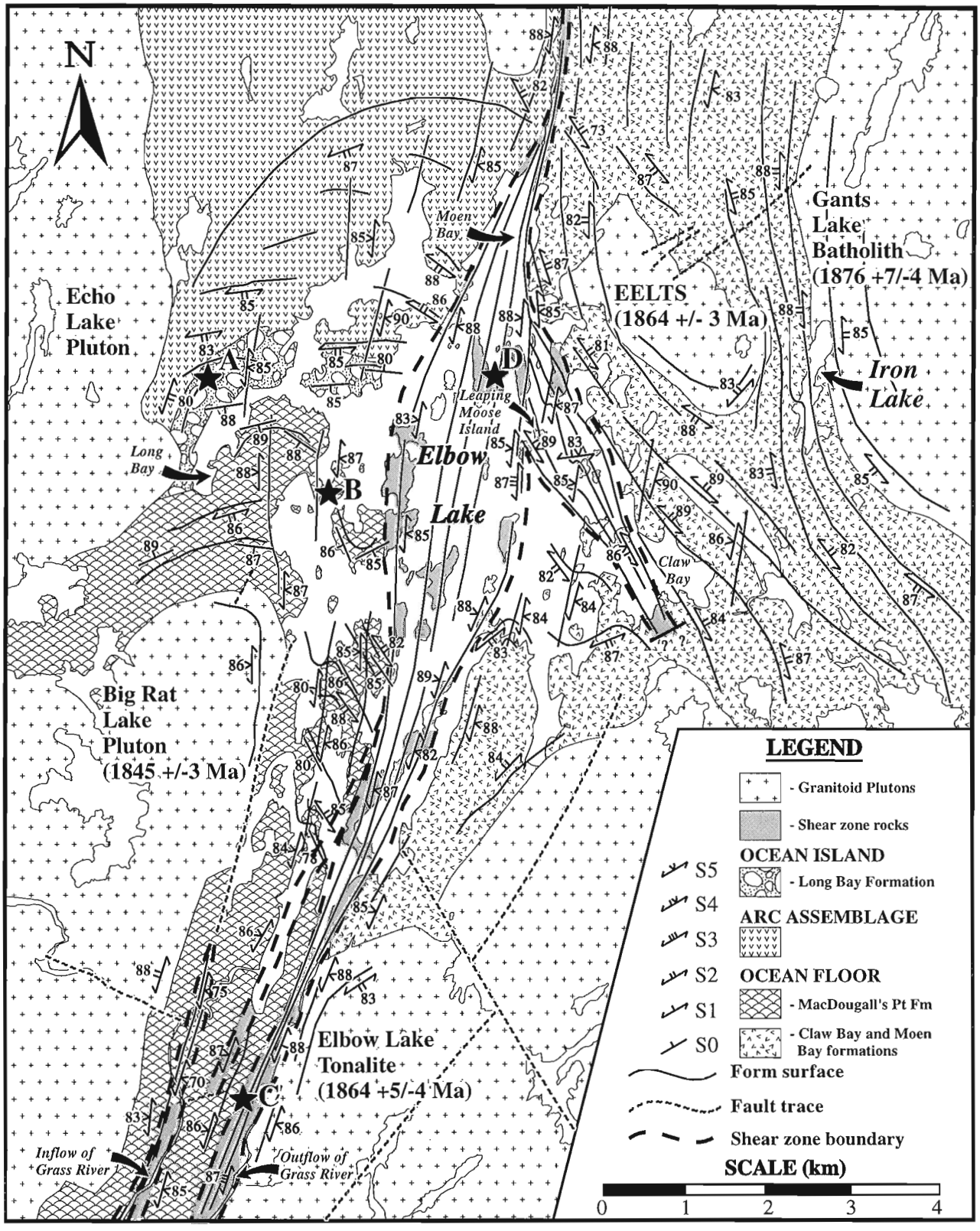

Figure 2. *Simplified geological map of the Elbow Lake area illustrating form surface trajectories and representative structural data.*

affected by significant post-S_1 shear zone deformation, making the timing of juxtaposition unclear. Intervolcanic sediments on the western side of Elbow Lake and the eastern side of Iskwasum Lake contain bedding-parallel tectonic fabrics that are considered to be S_1 in age.

Second generation structures

The S_2 "regional foliation" is ubiquitous throughout the map area and is most intensely developed around large plutons. The S_2 is well developed along the eastern side of the Elbow Lake shear zone from northeast Elbow Lake (Fig. 2) through to the southern exposed margin of the Flin Flon Belt. It is prevalent in the northwest portion of Elbow Lake and decreases in intensity southward. The S_2 is moderately to weakly developed along the Cranberry lakes (intensely around plutons) but strongly developed on the south side of First Cranberry Lake. Where S_2 overprints bedding or an S_1 fabric, it typically forms a differentiated crenulation cleavage (Fig. 7). In previously undeformed massive rocks, S_2 typically developed as a flattening fabric. The orientation of S_2 is controlled largely by the shape of plutons, the orientation of intervening volcanic packages and by later, large-scale folds. Taking into account the effects of the later folding and pluton shapes at their north and south ends, S_2 has a general north-south orientation, indicating significant east-west shortening of the belt during F_2. The S_2 is less intensely developed adjacent to the north- or south-facing ends of plutons as compared to the areas adjacent to the east and west sides of plutons, consistent with this interpretation.

A long-standing issue in the Flin Flon Belt has been how and when stratigraphy was tilted upright (e.g. Lucas et al., in press). Large scale isoclinal F_2 folds can be mapped out within the Long Bay formation and in pillowed flow sequences in the arc rocks, but these folds typically plunge vertically, parallel to F_5 fold axes. One location in the Long Bay formation, however, exhibits large scale (tens of metres), subhorizontally plunging, upright asymmetric isoclinal F_2 folds. Figure 8 illustrates the hinge area of one of these F_2 isoclinal S-folds in laminated mafic sandstone, plunging 12° towards the southeast. The present axial trend of this fold is a consequence of F_5 folding. We conclude that F_2 folds were generally shallow plunging, and have been vertically reoriented during F_5 deformation, and with only local preservation of shallow structures. For this reason, we interpret F_2 as being

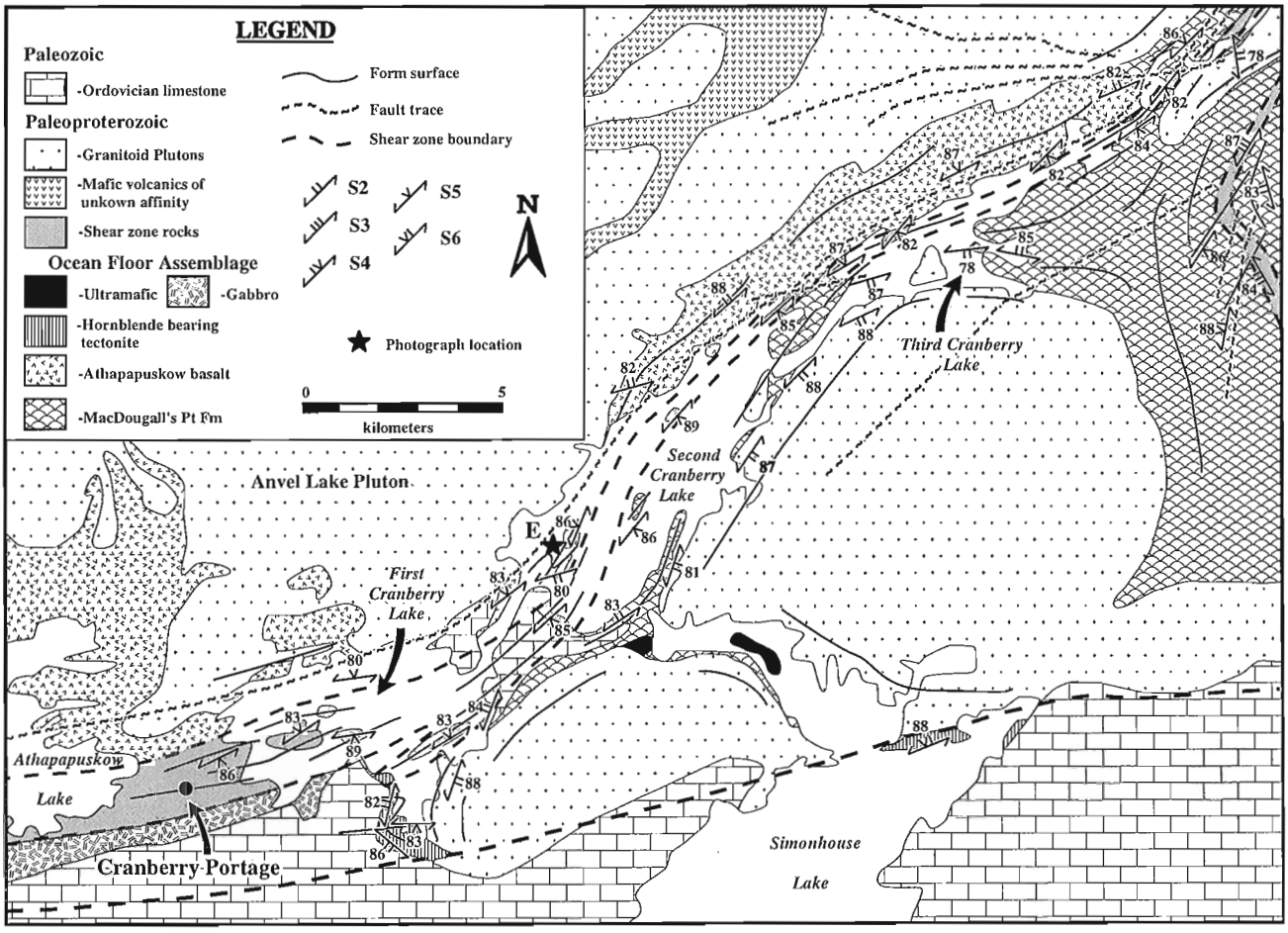

Figure 3. *Simplified geological map of the Cranberry lakes area illustrating form surface trajectories and representative structural data (modified from Syme, 1993).*

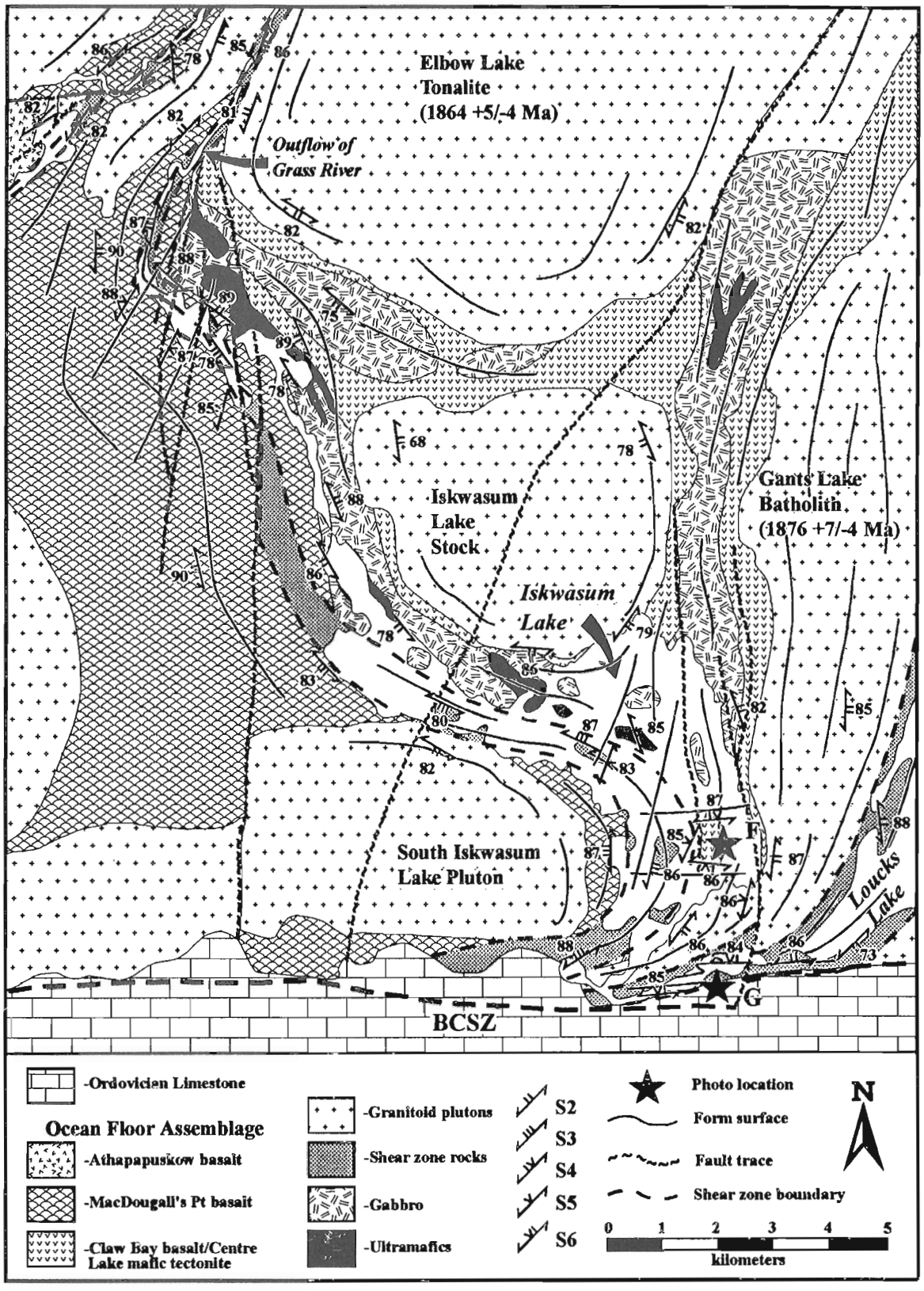

Figure 4. *Simplified geological map of the Iskwasum Lake area illustrating form surface trajectories and representative structural data (modified from Syme and Morrison, 1994).*

the deformation episode responsible for steepening the stratigraphy. Subsequent deformation has intensified the transposed foliation.

The development of S_2 can be bracketed between 1868 Ma, the age of tonalitic dykes that cut S_1 but contain S_2, and the crosscutting Little Swan Lake pluton, which yielded an U/Pb titanite age of 1826 ± 5 Ma (Whalen and Hunt, 1994). The S_2 likely developed closer to 1864 Ma while the rocks were still at elevated temperatures. The suite of 1845 Ma plutons are much more weakly foliated (S_2) than the older plutons. The S_2 foliation is similar in orientation and style to pervasive foliations recorded from Reed Lake (Syme et al., in press) to Flin Flon (Fig. 1; Lucas et al., in press) and is interpreted here to be the same foliation. The age of this foliation relative to metamorphism and to plutons of known age is consistent along the Flin Flon Belt.

Third generation structures

An S_3 manifestation of the Elbow Lake shear zone trends south-southwest from Elbow Lake (Fig. 2) and southeast through Iskwasum Lake (Fig. 4). At Elbow Lake, S_3 is only locally preserved due to the effects of later overprinting deformation. In the Leaping Moose Island area (Fig. 2), S_3 trends south-southeast and has intrafolial S-verging drag folds with vertical axes. In the Iskwasum Lake area, the S_3 shear zone is almost completely intact, but is folded on the map scale by later deformation. The mylonitic S_3 fabric appears to be annealed, indicating that it developed prior to and/or during the peak of M_2 (prior to about 1820-1805 Ma). The S_3 fabric is weakly developed in a conglomerate on Iskwasum Lake that has a character and composition similar to the Missi suite conglomerates (Ryan and Williams, in press b). At Flin Flon, the Missi suite was deposited prior to 1845 Ma (Ansdell, 1993), thus suggesting that S_3 developed between 1845 Ma and 1820-1805 Ma. The S_3 fabric does not extend very far into the wall rocks of the S_3 shear zone.

Structures Developed			Meta-morphism	Inferred Age and Setting
Elbow Lake	**Cranberry lakes**	**Iskwasum Lake**		
S1: early shear zone foliation		S1: Bedding-parallel cleavage	M1 contact meta-morphism	**Early accretionary tectonism** (Predates 1868 Ma dyke)
F2: folds of stratigraphy, pervasive upright S2 regional foliation	S2 differentiated layering and regional foliation	F2: folds of S0 andS1, S2 differentiated crenulation cleavage, regional foliation		**Arc magmatism** (1876-1864 Ma) **Intra-arc deformation** (1864-1826 Ma) **Missi sedimentaion** (~1845 Ma)
S3: NNE-trending ELSZ shear zone, with sinistral shear drag folds		S3: NW-trending ELSZ shear zone, of unknown shear sense		**Continentalization** (Kisseynew thrust over Flin Flon ~ 1830 Ma)
S4a: NNW-trending CBSZ (dextral)		S4b: Axial plane fabric to F4 folds trending E-W, related to dextral shear along BCSZ	M2 peak regional meta-morphism	**Peak M2** (1820-1805 Ma)
S5: NNE-trending ELSZ (sinistral transpression), vertical lineation, km-scale folds in wall rocks	S5: ENE to NE-trending ELSZ with steep SW-plunging lineation	S5: Pervasive crenulation cleavage, axial-planer to large F5 folds of S2 and S3		**Intra-continental deformation** and segmentation (post-1805 Ma)
	S6: Axial plane fabric to irregular, E-W trending F6 folds associated with BCSZ	F6: S-verging folds with E-W trending axial plane fabric related to sinistral reactivation of BCSZ	Retrograde meta-morphism	
D7: Dextral ductile to brittle shear bands, kink bands, brittle faults	D7: Kink bands and brittle faults	D7: kink bands, N-S faults that offset S6		**Brittle-ductile transition** (~1760 Ma)

Figure 5. *Tectonometamorphic synthesis of the central Flin Flon Belt. ELSZ = Elbow Lake shear zone; CBSZ = Claw Bay shear zone; BCSZ = Berry Creek shear zone.*

The MacDougalls Point formation and the Claw Bay basalt are not separated by the Elbow Lake shear zone in the Iskwasum Lake area (Fig. 4) as they are in the Elbow Lake area, but by a poorly exposed narrow, brittle feature farther to the east (Syme, 1994). The age of this feature is unknown, but must predate F_5 folding.

Fourth generation structures

In the Leaping Moose Island area in Elbow Lake (Fig. 2), the S_3 fabric is Z-folded by the south-southeast-trending S_4 Claw Bay shear zone, indicating dextral shear (Ryan and Williams, 1993). Fold axes and stretching lineations in the Claw Bay shear zone are vertical. Where S_4 and S_2 are parallel, they are difficult to differentiate in outcrop. The distinction is more readily apparent in thin section because S_4 developed syn- to post-peak M_2 conditions (Ryan and Williams, 1994).

In the Iskwasum Lake area, the southern portion of the Elbow Lake shear zone (S_3) is folded by a map scale east-trending F_4 fold (Fig. 4) related to a dextral deflection of fabrics along an F_4 manifestation of the Berry Creek shear zone. There are no S_4 shear zone rocks associated with the Berry Creek shear zone exposed in the map area, but they are interpreted to occur under the Phanerozoic cover just to the south of the map area. The Berry Creek shear zone is a mappable feature from Wekusko Lake (southeast of Snow Lake) westward to Athapapuskow Lake (Fig. 1). The S_4 fabric at Iskwasum Lake persists for about 3 km north of the Berry Creek shear zone. The F_4 structures at Elbow Lake and Iskwasum Lake cannot be correlated and may be unrelated. They postdate S_3 and predate S_5, and are therefore designated S_4a and S_4b.

Fifth generation structures

The D_5 structures are well developed throughout the map area. An S_5 shear zone (Elbow Lake shear zone-S_5) can be mapped from north of Elbow Lake (Fig. 2) to west of Cranberry Portage (Fig. 3). At Elbow Lake, transcurrent kinematic indicators, the presence of intense vertical stretching lineations (typically 1:3:20), and a horizontal plane of symmetry led Ryan and Williams (1994) to conclude that S_5 developed in transpressional shear. Kinematic indicators are predominantly sinistral. Figure 9 shows a vertically-plunging sinistral drag fold, which are relatively common features of the Elbow Lake shear zone. The S_5 Elbow Lake shear zone reaches a maximum width of about 2.5 km in central Elbow Lake, and an intense S_5 crenulation cleavage extends across a zone at least 8 km wide, further supporting the transpressive nature of this shear zone.

The S_5 fabric crenulates hornblende (the peak metamorphic mineral) and biotite grows along S_5, indicating that S_5 developed shortly after the M_2 thermal peak (Ryan and Williams, 1994). Because S_5 developed under retrograde metamorphic conditions, it is relatively easy to differentiate from early fabrics, even where they are subparallel. The S_5 is ubiquitously phyllonitic where developed in metavolcanic rocks but typically forms a finely spaced fracture cleavage with narrow (1-20 cm) mylonitic bands in the more competent intrusive rocks. Abundant intrafolial carbonate and iron oxide staining are generally associated with S_5 fabrics. Figure 10 illustrates the overprinting relations between S_3 and a retrograde S_5 zone. S_3 at this locality is a composite S_1-S_2-S_3 fabric which is fairly homogeneously mylonitic and has been annealed. Strain in the S_5 zone, which contains abundant centimetre-scale intrafolial sinistral shear drag folds, is heterogeneous. The intersection geometry between S_3 and S_5 in Figure 10 (and several other examples) is problematic. The

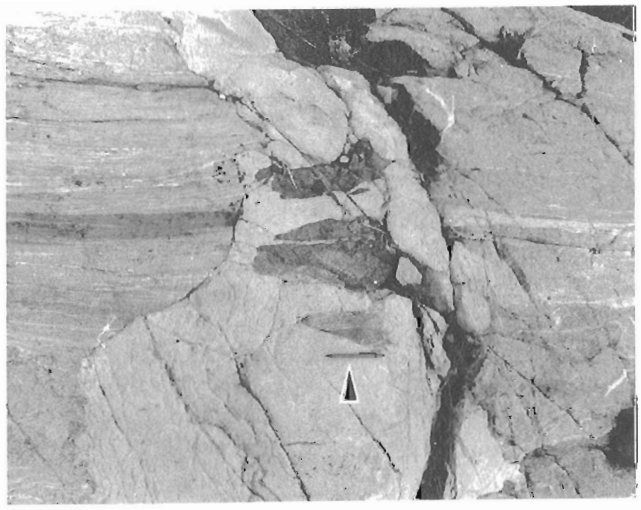

Figure 6. *Tonalite dyke crosscutting S_1 shear zone foliation (location C, Fig. 2). Pencil (by arrow) points towards 010° parallel to a weak S_2 fabric in the dyke.*

Figure 7. *S_2 differentiated layering overprinted by S_5 and a set of later kink folds trending 350° (location E, Fig. 3). Pencil points toward 205°.*

apparent sweep of S_3 should indicate dextral shear, however, this is inconsistent with the ubiquitous sinistral folds occurring there, and sinistrally sheared dykes (marked by an arrow in Fig. 10). The S_5 foliation may record both sinistral and dextral displacements, or perhaps S_3 at this locality rotated slightly anticlockwise and folded during sinistral shear.

Certain outcrops in the map area record multiple fabrics, indicating the relative deformational sequence. The outcrop illustrated in Figure 11 comprises a mafic turbiditic sequence in which bedding is well preserved despite subsequent intense deformation. The outcrop occurs ~700 m east of the eastern boundary of the S_3 Elbow Lake shear zone, and no effects of S_3 are recognized there. The relative orientation of fabrics in this outcrop is the same as on the map scale (Fig. 4).

Sixth generation structures

The D_6 structures are restricted to the southern extremity of the map area, and are interpreted as being related to reactivation of the Berry Creek shear zone. At Iskwasum Lake (Fig. 4), the westward deflection and thinning of rock units and early structures was attributed to F_4 dextral shear along the Berry Creek shear zone. Along the very southern exposures, the reoriented fabric is intensely S-folded with a well developed axial plane cleavage (Fig. 12). The fold vergence is inconsistent with dextral shear during F_4, and the folds are not overprinted by S_5, which is ubiquitous across the rest of the area. For these reasons, the S-folds are interpreted

Figure 8. *F_2 fold in laminated sandstone of the Long Bay formation (location A, Fig. 2), looking south-southeast.*

Figure 9. *F_5 sinistral shear drag fold in the Elbow Lake shear zone (location D, Fig. 2). Pencil points 020°. Note that as the S_5 layer folded and rotated, an S_5 crenulation cleavage (by the tip of the pencil) overprinted the initial S_5 fabric.*

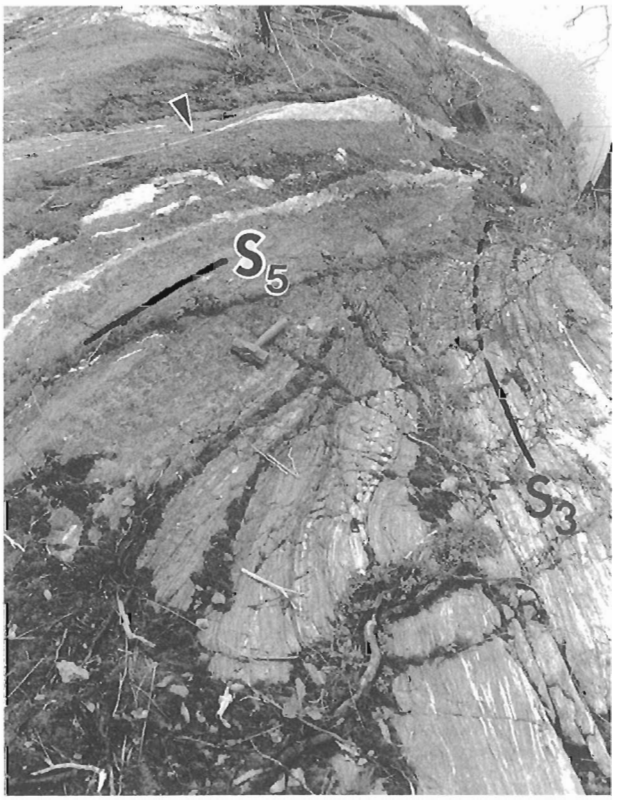

Figure 10. *Overprinting of S_3 by S_5 fabric of the Elbow Lake shear zone (location C, Fig. 2). Note sinistrally sheared dyke marked by arrow. Hammer handle points towards 025°.*

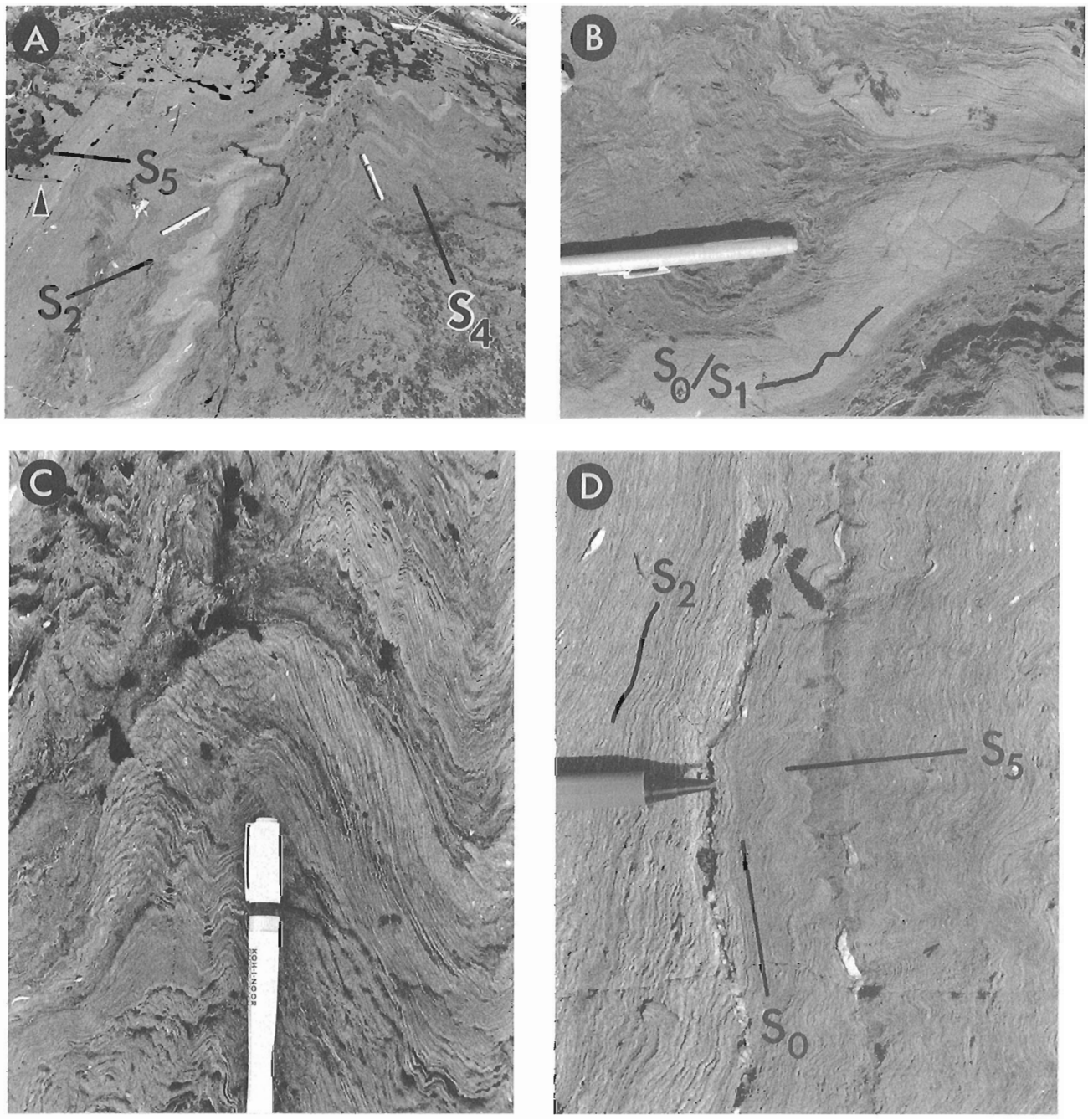

A) *Overview of the overprinting relationship in which bedding is defined by a light coloured sandy layer, the elongate eraser trends north along S_2, the rapidiograph drafting pen trends east along S_4 and the pencil (marked with an arrow) trends north-northeast along S_5. The S_2 and S_4 are almost orthogonal. The pencil (marked by arrow) points towards 195°.*

B) *Bedding (S_0) and an S_0-parallel S_1 fabric are folded by F_2, with an intensely developed axial plane differentiated crenulation cleavage (S_2), parallel to the eraser which points towards 160°.*

C) *Close-up of F_4 closure overprinting S_2 which is oblique to S_0. The F_4 fold closure superbly illustrates how S_2, inclined to S_0/S_1, is in a stretching direction on the south limb and in a shortening direction on the north limb. The S_4 is a spaced crenulation cleavage parallel to the drafting pen, which points towards 085°.*

D) *Close-up of S_5 crenulation cleavage overprinting S_0 and S_1. The S_5 overprints the entire outcrop.*

Figure 11. *Overprinting relationships among S_0, S_1, S_2, S_4, and S_5 in southeast Iskwasum Lake (location F, Fig. 4).*

as F_6 folds, representing a sinistral reactivation of the Berry Creek shear zone, shortening the S_4 foliation. Unlike F_4 deformation, F_6 only affects a narrow zone in the study area, and probably represents the last significant ductile deformation episode recognized in the central Flin Flon Belt.

In the southern part of First Cranberry Lake and the northern part of Simonhouse Lake (Fig. 3), folding is more irregular than at Iskwasum Lake. Both S- and Z-folds with east-west axial planes occur there but are difficult to divide into fold generations because they are parasitic on larger structures, and the vergence of the larger folds cannot be established due to a lack of continuous outcrop. Realistically, the folds are probably a mixture of F_4 and F_6 as at Iskwasum Lake.

Seventh generation structures

A variety of late features are grouped as D_7 structures, which likely developed during protracted deformation under brittle-ductile and brittle conditions. The most significant D_7 structures occur as ductile-brittle shear bands, kink bands, and brittle faults. In the Elbow Lake area, a set of southeast-trending, south-verging kink folds overprint S_5, and may be related to very local east-trending minor folds, with a subtle axial plane fabric that indicates late north-south shortening of the Elbow Lake shear zone. A conjugate set of brittle kink bands also indicates late north-south shortening. The region between southern Elbow Lake and northern Third Cranberry and Iskwasum lakes is overprinted by a set of pervasive ductile-brittle dextral shear bands. The shear bands are intrepreted as being associated with dextral steps in the S_5 Elbow Lake shear zone that have been mapped in this region. These offsets do no appear to affect the margin of the Elbow Lake tonalite (Fig. 2), and slip planes likely sole into the S_5 shear zone to alleviate the space problem. A series of straight north-, north-northeast, and north-northwest-trending brittle faults are the latest features mapped in the area. These faults are rarely exposed. Minor associated faults are typically very narrow (0.5-15 cm) and exhibit cataclastic brecciation.

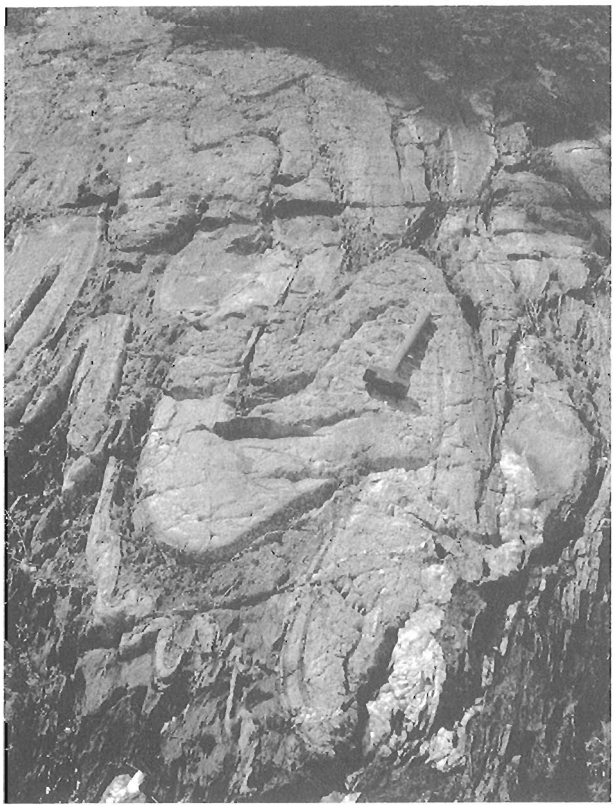

Figure 12. *East-trending south-verging F_6 folds related to the Berry Creek shear zone (location G, Fig. 4). Hammer points towards 090°.*

DISCUSSION AND CONCLUSIONS

The timing of initial juxtaposition of distinct tectonometamorphic assemblages at Elbow Lake is unclear because of the effects of later deformation. The S_1 mylonites, only locally preserved, developed prior to 1868 Ma, consistent with relations documented in the Flin Flon area to the west by Lucas et al. (in press). The development of S_2 is interpreted to be coeval 1.87-1.84 Ga arc magmatism and thus represents intra-arc deformation (Ryan et al., 1995). The S_2 foliation is consistent in style and orientation throughout the entire Flin Flon Belt, and therefore provides a useful time marker for structural studies. The intense east-west shortening during F_2 folding should have contributed significantly to the crustal thickening that was ongoing at that time, and may also have contributed to the exhumation of the 1876-1845 Ma plutonic rocks that are incorporated in Missi sediments (cf. Lucas et al., in press).

Metasedimentary rocks of the Kisseynew Belt were initially thrust over Amisk collage rocks at 1.84-1.83 Ga, resulting in crustal thickening and subsequent regional metamorphism (1820-1805 Ma; Ansdell et al., in press; Connors, in press; David et al., in press). The Flin Flon Belt behaved as a rigid block within the deforming orogen (Norman et al., 1995) and deformed internally along shear zones, thus recording intracontinental deformation (S_3-S_6). Displacements along these shear zones was restricted by the dimensions of the belt. For example, the S_5 transpression zone (Elbow Lake shear zone) that can be mapped for about 55 km along strike, may not have had large displacements. The termination of the Elbow Lake shear zone to the north is contentious due to a lack of exposure. An apparent 10 km sinistral offset in the Kisseynew-Flin Flon thrust boundary aligns well with the probable northward extension of the Elbow Lake shear zone (north portion of Fig. 1). Such an offset along the Elbow Lake shear zone would be adequate to develop features observed at Elbow Lake.

The timing of brittle-ductile and brittle deformation cannot be well-constrained in the central Flin Flon Belt. Whalen and Hunt (1994) presented K-Ar and $^{40}Ar/^{39}Ar$ mineral ages for biotite and hornblende in plutonic rocks from Elbow Lake that cluster around 1760 Ma. These ages may reflect the occurrence of a metamorphic pulse (M_3) at this time, resetting the K and Ar systematics, although there is no textural evidence to support an M_3 pulse. Alternńikely, and more

likely, the 1760 Ma ages represent the time at which these minerals cooled from the peak of M_2 through their blocking temperatures during regional uplift. Brittle deformation in the Elbow Lake area, associated with the final stages of exhumation of the Flin Flon Belt, may significantly postdate 1760 Ma.

The structural anatomy of the central Flin Flon Belt clearly illustrates a complex, episodic deformation history that developed during significant changes in tectonic regime. It spans from intra-arc to intracontinental deformation, and finally to deformation during postorogenic exhumation (Ryan et al., 1995), and represents a history of structural development in excess of 100 Ma.

ACKNOWLEDGMENTS

Sandra MacDougall, Natasha Connell, and Scott Gilliss provided very capable field assistance during the summers of 1993, 1994, and 1995 respectively. The mapping of Ric Syme (Manitoba Energy and Mines) from 1990 to 1994 laid much of the foundation for the present study. Ric has made significant contributions over the past three years including field trips, base maps, and sound geological discussion. Manitoba Energy and Mines are thanked for partial logistical support, and many of the staff are thanked for geological discussions. Duane Morrison (University of Ottawa) led a field trip in the Iskwasum Lake area in 1994. Steve Lucas (Geological Survey of Canada) is thanked for initiating the project, logistical support, and for enthusiastic geological discussions. Jack Henderson and Steve Lucas are acknowledged for their critical reviews of the manuscript.

REFERENCES

Ansdell, K.M.
1993: U-Pb constraints on the timing and provenance of fluvial sedimentary rocks in the Flin Flon and Athapapuskow basins, Flin Flon domain, Trans-Hudson Orogen, Manitoba and Saskatchewan; in Radiogenic Age and Isotopic Studies: Report 7; Geological Survey of Canada, Paper 93-2, p. 49-57.

Ansdell, K.M. and Norman, A.R.
1995: U-Pb geochronology and tectonic development of the southern flank of the Kisseynew Domain, Trans-Hudson Orogen, Canada; Precambrian Research, v. 72, p. 147-167.

Ansdell, K.M., Lucas, S.B., Connors, K.A., and Stern, R.A.
in press: Kisseynew metasedimentary gneiss belt, Trans-Hudson Orogen (Canada): Back-arc origin and collisional inversion; Geology.

Connors, K.A.
in press: Unravelling the boundary between turbidites of the Kisseynew Domain and volcano-plutonic rocks of the Flin Flon Domain, eastern Trans-Hudson Orogen, Canada; Canadian Journal of Earth Sciences.

David, J., Bailes, A.H., and Machado, N.
in press: Evolution of the Snow Lake portion of the Paleoproterozoic Flin Flon and Kisseynew belts, Trans-Hudson Orogen, Manitoba, Canada; Precambrian Research.

David, J., Machado, N., Bailes, A.H., and Syme, E.
1993: U/Pb geochronology of the Flin Flon -Snow Lake Belt: new results; in Proceedings, Lithoprobe Trans-Hudson Orogen Transect meeting, Regina, Report No. 38, p. 84-87.

Lucas, S.B., Stern, R.A., and Syme, E.C.
in press: Intraoceanic tectonics and the development of continental crust: 1.92-1.84 Ga evolution of the Flin Flon Belt (Canada); Geological Society of America Bulletin.

Norman, A.R., Williams, P.F., and Ansdell, K.M.
1995: Early Proterozoic deformation along the southern margin of the Kisseynew gneiss blet, Trans-Hudson Orogen: a 30 Ma progressive deformation cycle; Canadian Journal of Earth Sciences, v. 32, p. 875-894.

Ryan, J.J. and Williams, P.F.
1993: Structural mapping in the Elbow Lake area, Flin Flon-Snow Lake belt, central Manitoba; in Manitoba Energy and Mines, Minerals Division, Report of Activities, 1993, p. 84-85.
1994: Tectonometamorphic history of the Elbow Lake Shear Zone, Flin Flon-Snow Lake greenstone belt, Manitoba, in Proceedings, Lithoprobe, Trans-Hudson Orogen Transect, Report No. 38, p. 221-229.
in press a: The Elbow Lake area: a long-lived deformation corridor; in Proceedings, Lithoprobe, Trans-Hudson Orogen Transect, Report.
in press b: Structural mapping in the Elbow Lake-Cranberry lakes-Iskwasum Lake area, Flin Flon belt, Manitoba, in Manitoba Energy and Mines, Minerals Division, Report of Activities, 1995.

Ryan, J.J., Williams, P.F., and Lucas, S.B.
1995: Intra-arc to intercontinental deformation along the Elbow Lake shear zone, southeastern Trans-Hudson Orogen; Geological Association of Canada, Program with Abstracts, v. 20, p. A92.

Stern, R.A. and Lucas, S.B.
1994: U-Pb zircon constraints on the early tectonic history of the Flin Flon accretionary collage, Saskatchewan; in Radiogenic Age and Isotopic Studies: Report 8; Geological Survey of Canada, Current Research 1994-F, p. 75-86.

Stern, R.A., Syme, E.C., Bailes, A.H., and Lucas, S.B.
1995a: Paleoproterozoic (1.90-1.86 Ga), arc volcanism in the Flin Flon Belt, Trans-Hudson Orogen, Canada; Contributions to Mineralogy and Petrology, v. 119, no. 213, p. 117-141.

Stern, R.A., Syme, E.C., and Lucas, S.B.
1995b: Geochemistry of 1.9 Ga MORB- and OIB-like basalts from the Amisk collage, Flin Flon Belt, Canada: evidence for intra-oceanic origin; Geochimica et Cosmochimica Acta, v. 59, no. 15, p. 3131-3154.

Syme, E.C.
1990: Elbow Lake project (parts of NTS 63K/15W); in Manitoba Energy and Mines, Minerals Division, Report of Activities, 1990, p. 49-57.
1991: Elbow Lake project - Part A: supracrustal rocks and their structural setting; in Manitoba Energy and Mines, Minerals Division, Report of Activities, 1991, p. 14-27.
1992: Elbow Lake project - Part A: supracrustal rocks and their structural setting; in Manitoba Energy and Mines, Minerals Division, Report of Activities, 1992, p. 32-46.
1993: Cranberry-Simonhouse reconnaissance; in Manitoba Energy and Mines, Minerals Division, Report of Activities, 1993, p. 61-66.
1994: Supracrustal rocks of the Iskwasum Lake area (63K/10W), in Manitoba Energy and Mines, Minerals Division, Report of Activities 1994, p. 47-56.
in press: 1.9 Ga arc and ocean floor assemblages and their bounding structures in the central Flin Flon belt; in Proceedings, Lithoprobe, Trans-Hudson Orogen Transect, Report.

Syme, E.C. and Morrison, D.
1994: Iskwasum Lake (NTS 63K/10W); Manitoba Energy and Mines, Preliminary Map 1994F-1, scale 1:50 000.

Syme, E.C. and Whalen, J.B.
1992: Elbow Lake (part of NTS 63K/15), Manitoba Energy and Mines, Preliminary Map 1992F-1; scale 1:20 000.

Syme, E.C., Bailes, A.H., and Lucas, S.B.
in press: Geology of the Reed Lake area (Parts of 63K/9 and 10), in Manitoba Energy and Mines, Minerals Division, Report of Activities 1995.

Whalen, J.B. and Hunt, P.A.
1994: Geochronological study of granitoid rocks in the Elbow Lake map area, Manitoba: a portion of the Flin Flon Domain of the Trans-Hudson Orogen; in Radiogenic Age and Isotopic Studies: Report 8; Geological Survey of Canada, Current Research 1994-F, p. 87-96.

Geological Survey of Canada Project 910035

The application of digital geophysical data to the restoration of crustal deformation in the Canadian Shield, Ontario

R.T. Bird, W.R. Roest, M. Pilkington, R.E. Ernst[1], and K.L. Buchan
Continental Geoscience Division, Ottawa

Bird, R.T., Roest, W.R., Pilkington, M., Ernst, R.E., and Buchan, K.L., 1996: The application of digital geophysical data to the restoration of crustal deformation in the Canadian Shield, Ontario; in Current Research 1996-C; Geological Survey of Canada, p. 117-124.

Abstract: Digital geophysical data have been used recently for plate tectonic reconstructions in oceanic settings, and we demonstrate a similar approach here for the restoration of crustal deformation in a continental regime. The technique accounts for nonuniformly distributed strain and enables our reconstruction of two gridded data sets as examples. First, we use the deformed Matachewan dyke swarm as a primary strain marker for deformation in the central Superior Province associated with the Kapuskasing structural zone. Reconstructed aeromagnetic data reveal the three subswarms of linear Matachewan dykes radiating from a broad focal region, indicative of dyke injection from a mantle plume. Second, we reconstruct gravity data from the Sudbury Structure and illustrate its near circular geometry prior to deformation, which supports an impact origin for this feature. Restored data sets may be used to examine the continuity of other geological features, refine estimates of deformation, and identify other possible tectonic events.

Résumé: Des mouvements de plaques tectoniques en milieu océanique ont récemment été modélisés à l'aide de données géophysiques numériques. Dans le présent article, une méthode semblable est utilisée pour reconstituer la déformation crustale en milieu continental. Cette technique rend compte d'une déformation non uniforme et permet d'utiliser deux ensembles de données maillées. L'essaim de dykes déformés de Matachewan est d'abord considéré comme marqueur de déformation primaire dans la zone structurale de Kapuskasing (centre de la Province du lac Supérieur). Les données aéromagnétiques révèlent les trois sous-essaims des dykes linéaires de Matachewan, rayonnant à partir d'une large région focale; cela indique que l'injection des dykes est attribuable à un panache du manteau. Sont ensuite mises en contexte les données gravimétriques de la Structure de Sudbury pour illustrer sa géométrie quasi circulaire avant la déformation, ce qui appuie l'hypothèse d'un impact comme origine de cette structure. Les ensembles de données restaurées peuvent servir à analyser la continuité d'autres éléments géologiques, à affiner les estimations des déformations et à identifier d'autres événements tectoniques possibles.

[1] Department of Earth Sciences, University of Western Ontario, London, Ontario N6A 5B7

INTRODUCTION

Digitized structural and magnetic lineations and gridded geophysical data have been used recently in oceanic settings to reconstruct the tectonic histories of rigid lithospheric plates (e.g., Verhoef et al., 1990). In continental regimes, however, deformation is often distributed heterogeneously over large areas. Such deformation may be described by a continuous strain pattern, rather than by Euler rotation vectors typically used for rigid plate motions. This strain pattern then may be used to transform a region to its predeformation geometry.

We present two examples where this approach is used to restore digital geophysical data from deformed regions of the Canadian Shield. First, we reconstruct the central Superior Province (Fig. 1) in the region of the Kapuskasing structural zone. In this case, the deformed Matachewan dyke swarm (2.47-2.45 Ga) serves as the primary strain marker for production of a digital strain map (West and Ernst, 1991). Second, we illustrate the use of this technique in the reconstruction of the Sudbury Structure, located within the Southern Province (Fig. 1), which has undergone deformation likely associated with the Penokean Orogeny (Rousell, 1984). A recent Lithoprobe seismic reflection profile across the Sudbury Structure (Milkereit et al., 1992) has provided additional constraints on its deformation and a strain map has been assembled consistent with structural observations (Roest and Pilkington, 1994).

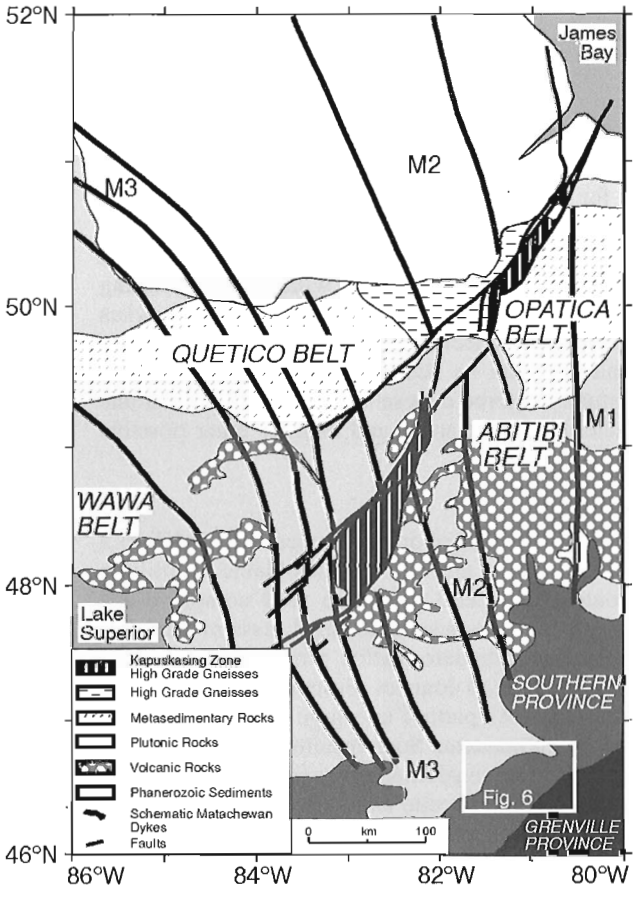

Figure 1. *Map illustrating the general geology of the study area. Thick black lines are representative dykes of the Matachewan dyke swarm which may be divided into three subswarms labelled M1, M2, and M3. These subswarms cut high-grade gneisses of the Kapuskasing structural zone and are crosscut by a series of faults. The Sudbury Structure is located in the lower right hand corner of the map within the Southern Province. The white box outlines the boundaries of a simplified geological map of the Sudbury Structure shown in Figure 6.*

METHOD

In order to reconstruct nonuniform deformation, a continuous strain pattern is constructed and used to map "paleolatitude" and "paleolongitude" as a function of the present-day geographic co-ordinates (Fig. 2). Both paleolatitude and paleolongitude values are gridded at a spacing appropriate for the digital data that are to be reconstructed. From these strain-map grids, any geological or geophysical data set possessing present-day geographic co-ordinates may be assigned corresponding paleoco-ordinates. Therefore, reconstruction of the paleoco-ordinate system involves a simple transformation (Fig. 2). A fundamental assumption in the process is that deformation is restricted to the horizontal plane, or if the strain pattern does not preserve the horizontal area, the horizontal projection of more complicated tectonics is modelled. For example, the Kapuskasing structural zone includes crustal blocks from paleodepths of 30 km, and is interpreted, at least in part, as an intracratonic thrust related to Hudsonian

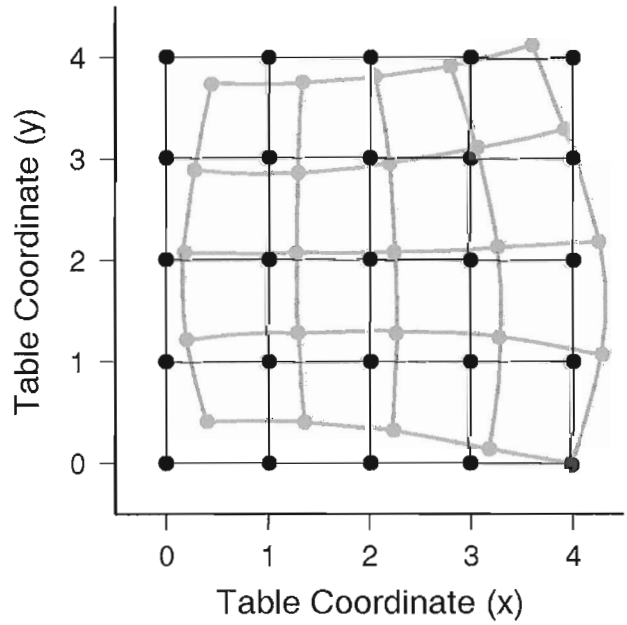

Figure 2. *Transformation of paleolatitude and paleolongitude lines in a deformed grid (grey) to the grid's undeformed geometry (black).*

collision (West and Ernst, 1991; Percival and West, 1994). However, only the horizontal component of this thrusting is modelled here.

Interpretation of reconstructed geophysical data requires extreme care. For reconstructed potential field data, zones of compression (such as the thrusts of the Kapuskasing structural zone) or extension will display distorted anomalies. For example, a zone of compression will expand to its original horizontal dimensions requiring the data to be stretched to fill the void. Thus, the anomalies are distorted but are useful because they illustrate the amount of deformation in the horizontal plane, when compared with the original data. It is important to remember that potential field data for geological features that postdate deformation are also reconstructed and therefore deformed in the process, unless these data have been removed.

CENTRAL SUPERIOR PROVINCE RECONSTRUCTION

Matachewan dyke swarm and Kapuskasing structural zone

The Matachewan dykes constitute a deformed, giant radiating dyke swarm which extends over an area of 250 000 km^2 (Halls, 1991). Aeromagnetic maps have been used to define the full extent of the swarm (Fig. 3) and show it to be

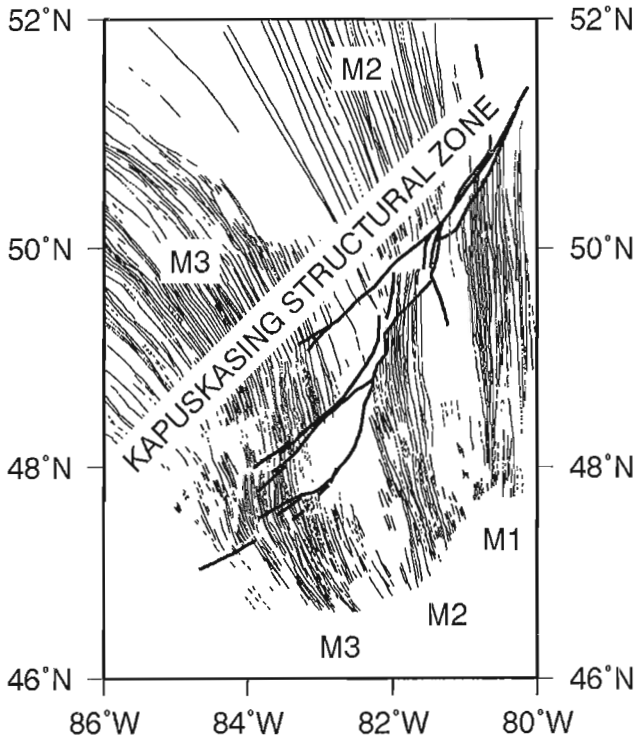

Figure 3. *Present-day distribution of Matachewan dykes in the central Superior Province (after West and Ernst, 1991). The Kapuskasing structural zone crosscuts these dykes and is delineated here by a series of faults.*

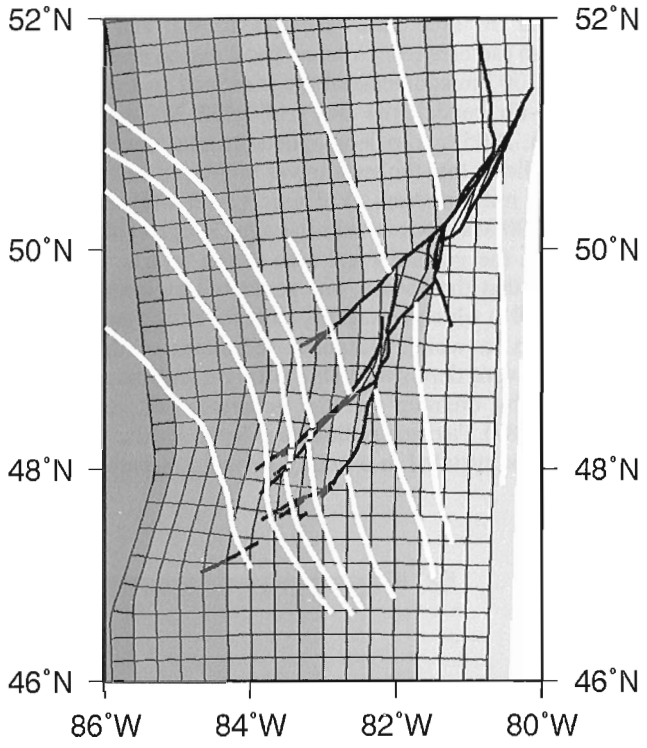

Figure 4a) *Strain map for the central Superior Province. Narrow black lines join points of equal paleolatitude or paleolongitude (after West and Ernst, 1991). Thick black lines are faults, and white lines are representative dykes of the Matachewan swarm.*

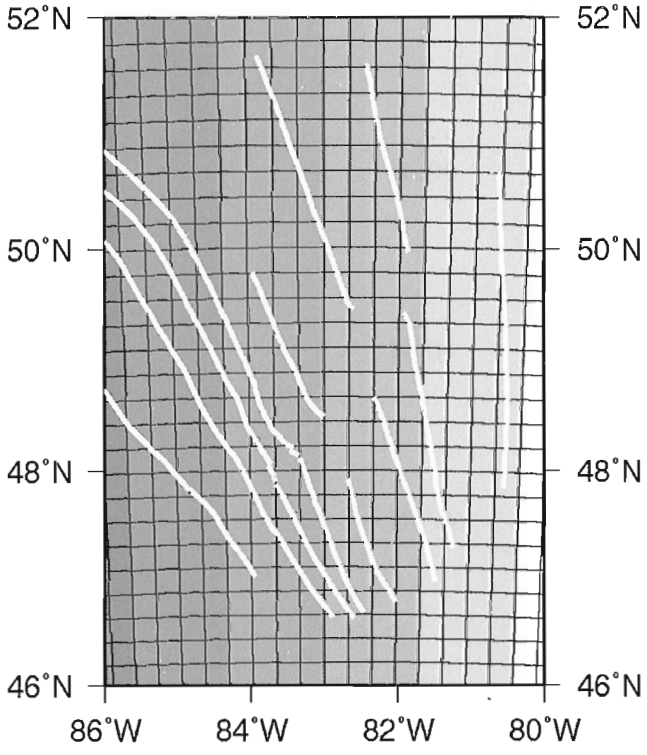

Figure 4b) *Recontructed strain map for the central Superior Province.*

composed of three subswarms (M1, M2, and M3). Each subswarm radiates from a broad focal region centred approximately 200 km southeast of the truncated swarm's southern limit. U-Pb baddeleyite dates of 2473 Ma and 2446 Ma (Heaman, 1995) and paleomagnetic results (Bates and Halls, 1991) indicate that the swarm was emplaced over a period of about 30 million years. Volcanic (2450 Ma) and plutonic (2480-2490 Ma) rocks of similar age (Krogh et al., 1984) are located in the general focal area of the swarm. It has been proposed that the swarm was generated by a mantle plume (Halls, 1991) which was responsible for rifting and formation of a basin in which Huronian sediments of the Southern Province were deposited. This rifting event may have been followed by breakup and the generation of oceanic crust (Fahrig, 1987). Paleomagnetic data indicate that the Matachewan swarm was intruded in a nearly perfect fan pattern but was subsequently distorted during dextral transcurrent deformation and uplift along the Kapuskasing structural zone (~1.9 Ga; Bates and Halls, 1991; Percival and West, 1994). In the northeast portion of the Kapuskasing structural zone the deformation is discontinuous and concentrated along a fault with a horizontal displacement of about 60-80 km, whereas in the southwest portion of the Kapuskasing structural zone this deformation is distributed over an approximate 80 km wide zone (West and Ernst, 1991).

Strain map reconstruction

To reconstruct the Matachewan dyke swarm, the strain pattern published by West and Ernst (1991) is used. Figure 4a illustrates this strain pattern in terms of lines of paleolatitude and paleolongitude. The original strain pattern (West and Ernst,

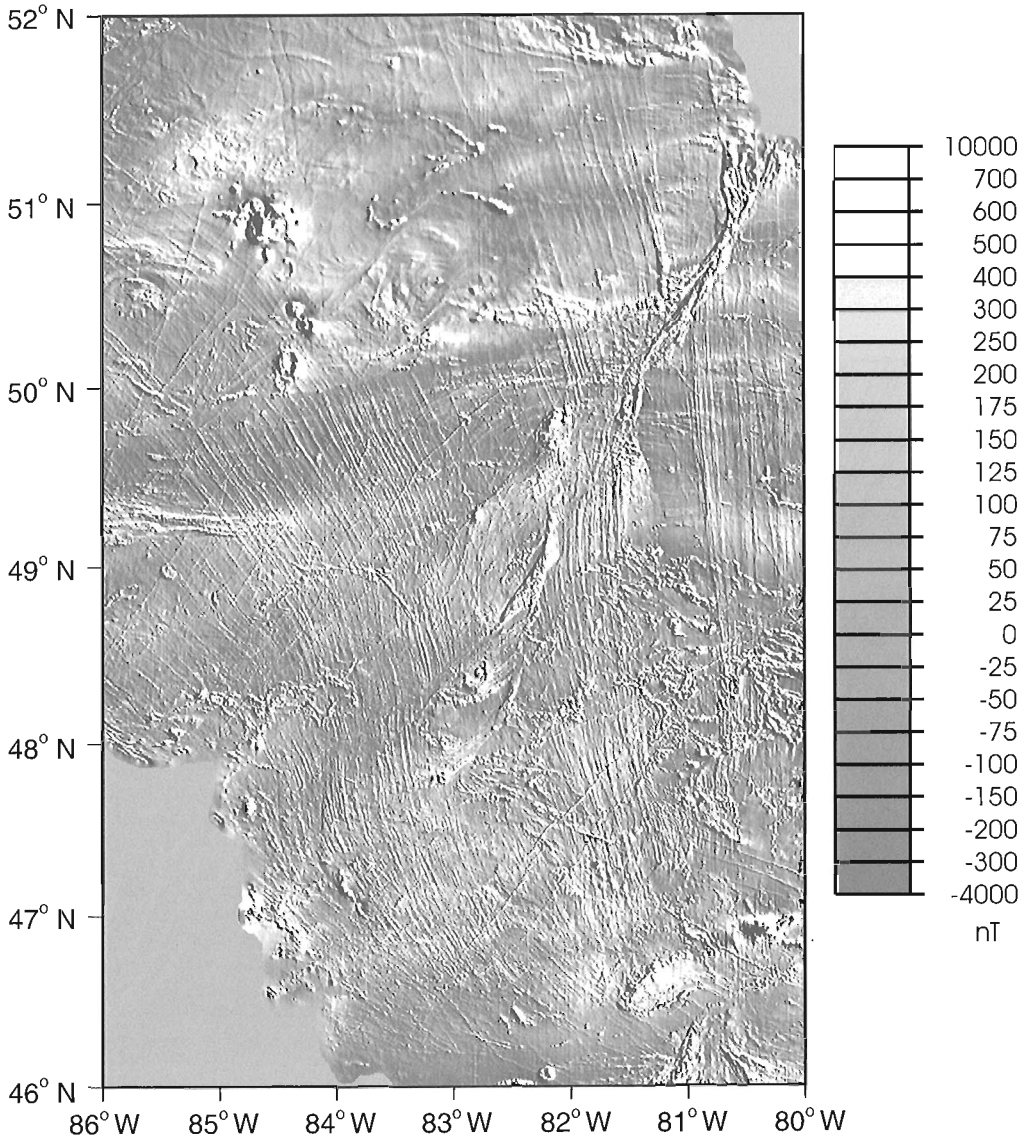

Figure 5a) *Shaded-relief aeromagnetic map of the study area. Illumination azimuth is N75°E.*

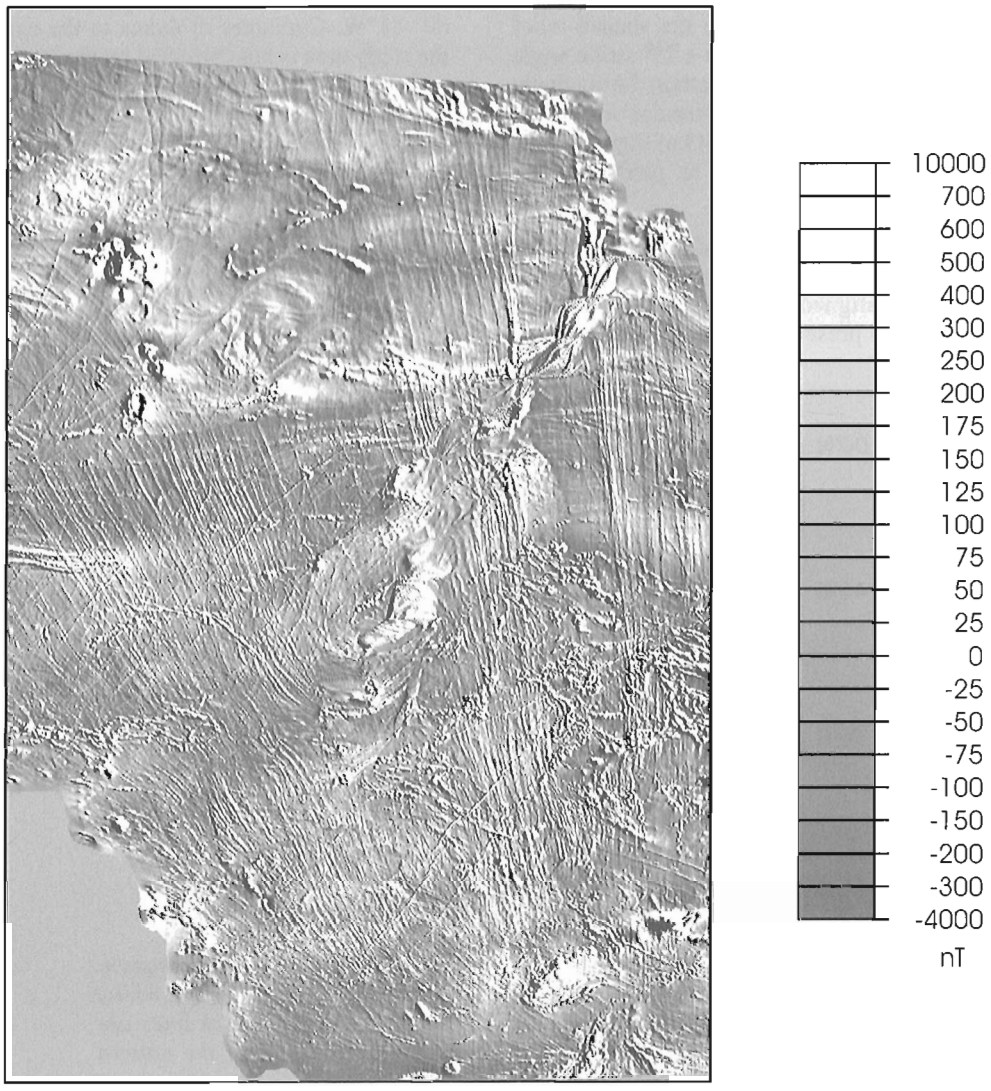

Figure 5b) *Shaded-relief aeromagnetic map after reconstruction. Illumination azimuth same as in (a).*

1991) is a deformed, rectangular grid superimposed on a map with a universal transverse mercator projection. Therefore, the lines of paleolatitude and paleolongitude on our strain map appear curved when plotted with a standard mercator projection. The Kapuskasing structural zone is evident in the highly strained region trending southwest across which the representative Matachewan dykes are offset. Restoration of this strain map is shown in Figure 4b.

Aeromagnetic data reconstruction

In the same way that we restored the strain map for this area (Fig. 4), we can reconstruct the aeromagnetic data (Fig. 5) or any other digital data set. Figure 5a displays total magnetic field intensity anomalies for the study area. These data are part of the new, relevelled 200 m aeromagnetic grid of Ontario retrieved from the National Aeromagnetic Data Base (Geological Survey of Canada Geophysical Data Centre). The

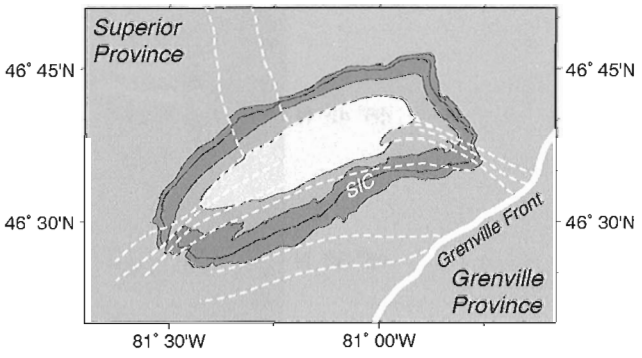

Figure 6. *Simplified geological map of the Sudbury Structure (after Roest and Pilkington, 1994). The Sudbury Igneous Complex (SIC) is darkly shaded. Dashed white lines are major faults.*

Matachewan dykes are clearly visible in the shaded-relief maps (Fig. 5), which are illuminated from a 75° strike angle to highlight north-trending structures. Together, the magnetic lineaments of these dykes form three broad bands corresponding to the three subswarms, M1, M2, and M3 of Figure 3. The Kapuskasing structural zone is evident as predominantly high-amplitude magnetic anomalies.

After reconstruction (Fig. 5b), the radial pattern of the Matachewan dyke swarm becomes evident. The boundaries of each subswarm are realigned, and the three subswarms converge to a focal region presently located near 40°-41°N, 80°-81°W. Curvature of dykes to the extreme northwest of the study area is not corrected by the strain pattern, however, and may represent additional deformation or primary curvature related to the regional stress field present during dyke injection. Dykes immediately adjacent to the Southern Province boundary are also somewhat curved, and may reflect deformation possibly associated with the Penokean Orogeny. Thrusting related to the Kapuskasing uplift is evident in the artificial stretching of anomalies which are related to Archean geology in the Kapuskasing structural zone vicinity. In the southwest portion of the zone, detailed examination of the restored data shows that some dykes retain a small measure

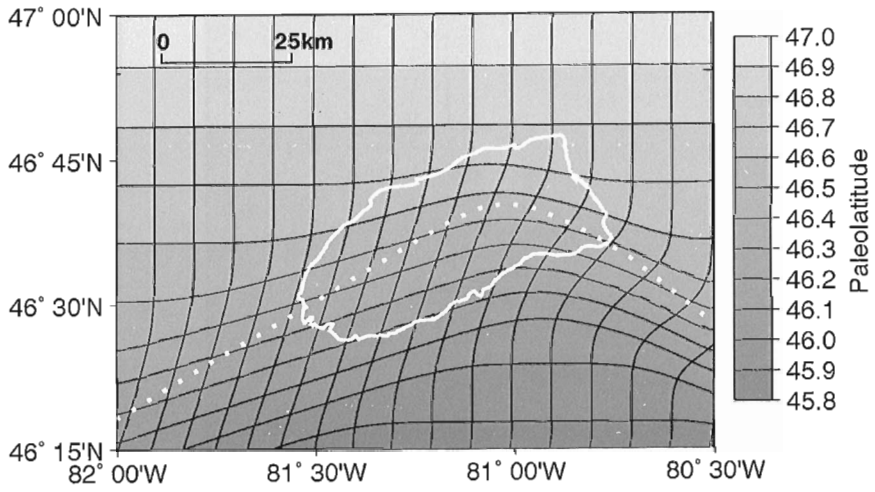

Figure 7. *Strain map for Sudbury deformation (after Roest and Pilkington, 1994). The present outer limit of the Sudbury Structure is outlined in white, and the deformation axis is the dotted white line. Narrow black lines are lines of paleolatitude and paleolongitude. Decompression of the pattern restores a grid of uniform rectangles.*

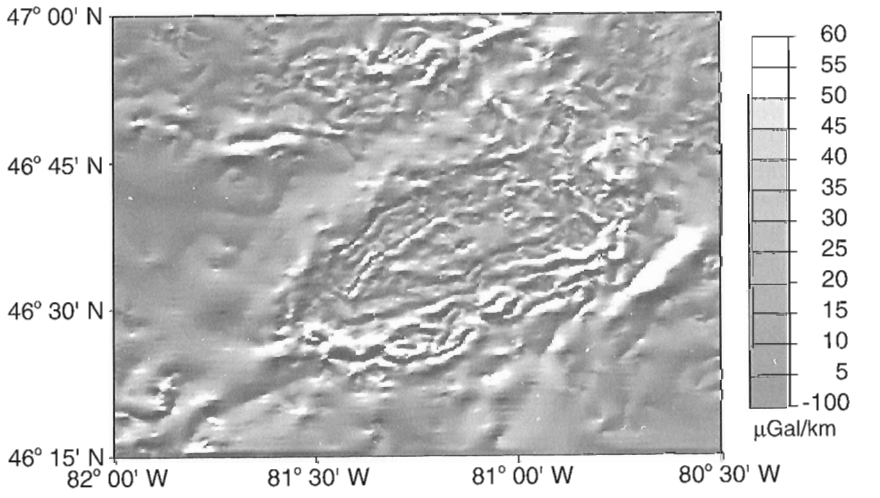

Figure 8. a) *Shaded-relief map of horizontal gravity gradient over the Sudbury Structure. Illumination azimuth is N20W°.*

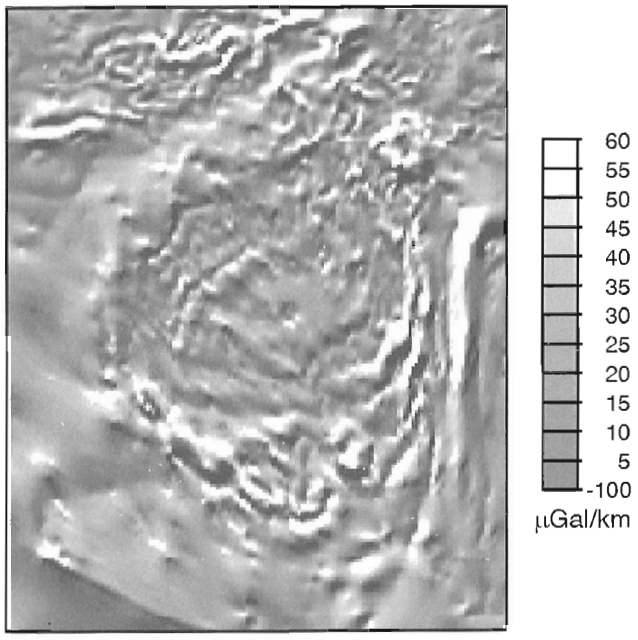

Figure 8. b) *Shaded-relief map of horizontal gravity gradient after reconstruction. Illumination azimuth same as in (a).*

of curvature or are slightly rotated from a linear trend. This same curvature and rotation is evident in the representative dykes of Figure 4b. Thus, the strain pattern (West and Ernst, 1991) used in the reconstruction may be inadequate for data restoration of the southwest Kapuskasing structural zone at small scales. Certainly, for larger scale geological features, the strain pattern appears to provide an adequate basis for reconstruction.

SUDBURY STRUCTURE RECONSTRUCTION

The Sudbury Structure

A second example of the application of this reconstruction technique is the restoration of the Sudbury Structure's predeformation geometry. This structure is well known for its mineral wealth, and its origin has been the topic of debate for many years. The most widely accepted model is that of an impact origin (Dietz, 1964), although the present geometry of the structure is not circular (Fig. 6) as the model predicts. There is substantial evidence that this area was significantly deformed during the Penokean Orogeny (Rousell, 1984), and a recent Lithoprobe seismic reflection profile (Milkereit et al., 1992) suggests the structure is asymmetric at depth. Crustal shortening of the Sudbury Igneous Complex (SIC) is estimated at about 30 km, and the direction of strain at about 20°W (Shanks and Schwerdtner, 1991).

Strain map and gravity data reconstruction

Based on existing geological observations, Roest and Pilkington (1994) define a simple strain pattern for the Sudbury Structure (Fig. 7). With this pattern, potential field data over the Sudbury Structure may be reconstructed to investigate its predeformation geometry. Figure 8a shows the horizontal gradient of the Bouguer gravity anomalies for an area encompassing the structure. In this map, the Sudbury Igneous Complex is quite evident as an oval-shaped band of higher-amplitude anomalies.

From the strain map for this region, data points in Figure 8a can be assigned paleolatitudes and paleolongitudes. These co-ordinates can then be used to render a new undeformed version of the data. Figure 8b displays the reconstructed map of the horizontal gravity gradient. This figure reveals the near-circular geometry of the restored Sudbury Igneous Complex which has a diameter of about 60 km. The Sudbury Igneous Complex has been interpreted to represent the impact melt sheet (Grieve et al., 1991) of a crater that was at least 150 km in diameter prior to erosion (Roest and Pilkington, 1994).

SUMMARY

We have demonstrated a technique for the reconstruction of digital geophysical data in deformed continental settings. In the central Superior Province, the cumulative strain pattern of West and Ernst (1991) appears adequate for the reconstruction of a variety of geological and geophysical digital data sets. Restored grids of aeromagnetic or other data may be used to better correlate faults, shear zones, and other geological features offset by deformation associated with the Kapuskasing structural zone. For reconstruction of the Sudbury Structure, a simple strain pattern incorporating about 30 km of compression in a northwest-southeast direction is sufficient to restore a nearly circular geometry, as delineated by the Sudbury Igneous Complex. This reconstruction supports a model for the formation of the Sudbury Structure by impact. The technique used in these two reconstructions may be applied in other deformed regions to restore digital data to a predeformation configuration, given adequate geological and geophysical data. With the continued acquisition of aeromagnetics and gravity data throughout the world, this method may provide a powerful tool for reconstruction of deformed terranes.

REFERENCES

Bates, M.P. and Halls, H.C.
1991: Broad-scale Proterozoic deformation of the central Superior Province revealed by paleomagnetism of the 2.45 Ga Matachewan dyke swarm; Canadian Journal of Earth Sciences, v. 28, p. 1780-1796.

Dietz, R.S.
1964: Sudbury structure as an astrobleme; Journal of Geology, v. 72, p. 412-434.

Fahrig, W.F.
1987: The tectonic settings of continental mafic dykes: failed arm and early passive margin; in Mafic Dyke Swarms, (ed.) H.C. Halls and W.F. Fahrig; Geological Association of Canada, Special Paper 34, p. 331-348.

Grieve, R.A.F., Stöffler, D., and Deutsch, A.
1991: The Sudbury Structure: constroversial or misunderstood; Journal of Geophysical Research, v. 96, p. 22753-22764.

Halls, H.C.
1991: The Matachewan dyke swarm, Canada: an early Proterozoic magnetic field reversal; Earth and Planetary Science Letters, v. 105, p. 279-292.

Heaman, L.M.
1995: U-Pb dating of mafic rocks: past, present and future; Geological Association of Canada/Mineralogical Association of Canada, Program and Abstracts, v. 20, A-43.

Krogh, T.E., Davis, D.W., and Corfu, F.
1984: Precise U-Pb zircon and baddeleyite ages for the Sudbury Structure; in The geology of ore deposits of the Sudbury Structure, (ed.) E.G. Pye, A.J. Naldrett, and P.E. Giblin; Ontario Geological Survey, Special Volume 1, p. 431-445.

Milkereit, B., Green, A.G., et al.
1992: Deep geometry of the Sudbury Structure from seismic reflection profiling; Geology, v. 20, p. 807-811.

Percival, J.A. and West, G.F.
1994: The Kapuskasing uplift: a geological and geophysical synthesis; Canadian Journal of Earth Sciences, v. 31, p. 1256-1286.

Roest, W.R. and Pilkington, M.
1994: Restoring post-impact deformation at Sudbury: a circular argument; Geophysical Research Letters, v. 21, p. 959-962.

Rousell, D.H.
1984: Structural geology of the Sudbury Basin; in The geology and ore deposits of the Sudbury Structure, (ed.) E.G. Pye, A.J. Naldrett, and P.E. Giblin; Ontario Geological Survey, Special Volume 1, p. 83-95.

Shanks, W.S. and Schwerdtner, W.M.
1991: Crude quantitative estimates of the original northwest-southeast dimension of the Sudbury Structure, south-central Canadian Shield; Canadian Journal of Earth Sciences, v. 28, p. 1677-1686.

Verhoef, J., Usow, K.H., and Roest, W.R.
1990: A new method for plate reconstructions: the use of gridded data; Computers and Geosciences, v. 16, p. 51-74.

West, G.F. and Ernst, R.E.
1991: Evidence from aeromagnetics on the configuration of Matachewan dykes and the tectonic evolution of the Kapuskasing Structural Zone, Ontario, Canada; Canadian Journal of Earth Sciences, v. 28, p. 1797-1811.

Geological Survey of Canada Project 930023

Geological investigations in the Swayze greenstone belt, southern Superior Province, Ontario: a final field update[1]

Kevin B. Heather, Geoff T. Shore, and Otto van Breemen
Continental Geoscience Division, Ottawa

Heather, K.B., Shore, G.T., and van Breemen, O., 1996: Geological investigations in the Swayze greenstone belt, southern Superior Province, Ontario: a final field update; in Current Research 1996-C; Geological Survey of Canada, p. 125-136.

Abstract: This report summarizes the results of the final year of lithological and structural mapping within the Swayze greenstone belt. In addition, 14 preliminary U-Pb zircon and titanite age dates and one refined age are reported.

Granitoid rocks in the southwestern portion of the Kenogamissi Batholith consist of sheet-like dioritic and tonalitic intrusions which are interpreted to be synvolcanic. These foliated intrusions contain thin screens of amphibolitized mafic volcanic rocks and are folded about regional F_2 folds.

A poorly preserved mafic-felsic volcanic cycle occupies the core of the Woman River Anticline, stratigraphically below the 2729 Ma Marion volcanic package. It also underlies the easternmost extension of the 2731 Ma Shunsby volcanic package, north and west of the 2740 Ma Chester granitoid complex (CGC). Felsic volcanic rocks north of the complex exhibit REE patterns characteristic of FII-type felsic rocks known to be associated with base-metal mineralization elsewhere in the Superior Province (e.g., Sturgeon Lake, northwestern Ontario).

Résumé : Le présent article est un résumé des résultats de la dernière année consacrée à la cartographie lithologique et structurale de la zone de roches vertes de Swayze. Il fait aussi état de 15 datations U-Pb sur zircon et titanite, lesquelles ne sont que préliminaires, de même que d'une datation précise.

Les roches granitoïdes observées dans la portion sud-ouest du Batholite de Kenogamissi sont composées d'intrusions dioritiques et tonalitiques stratiformes que l'on considère synvolcaniques. Ces intrusions foliées, incluant des lames minces de métavolcanites mafiques amphibolitisées, sont déformées par les plis P_2 régionaux.

Un cycle volcanique mafique-felsique mal conservé occupe le noyau de l'anticlinal de Woman River, situé stratigraphiquement au-dessous de l'ensemble volcanique de Marion (2 729 Ma), mais aussi sous-jacent au prolongement d'extrême est de l'ensemble volcanique de Shunsby (2 731 Ma), au nord et à l'ouest du complexe granitoïde de Chester (CGC, 2 740 Ma). Les volcanites felsiques au nord du complexe présentent des spectres des ÉTR caractéristiques de roches felsiques de type FII, que l'on sait être associées à une minéralisation en métaux communs ailleurs dans la Province du lac Supérieur (p. ex. Sturgeon Lake, partie nord-ouest de l'Ontario).

[1] Contribution to Canada-Ontario Subsidiary Agreement on Northern Ontario Development (1991-1995), under the Canada-Ontario Economic and Regional Development Agreement.

INTRODUCTION

The Swayze greenstone belt and surrounding granitoid rocks represent the western extension of the mineral-rich Abitibi greenstone belt (Fig. 1). This summary is the fourth and final installment of field results from the Swayze bedrock mapping program being conducted by the Geological Survey of Canada under the auspices of the Northern Ontario Development Agreement (NODA) for minerals. Geological, structural, and radiometric age data are reported in Heather (1993), Heather and van Breemen (1994) and Heather et al. (1995). Powell et al. (1995) stated that all of the Archean supracrustal rocks (>2677 Ma) in the Rouyn-Noranda have undergone regional metamorphism, the age of which they constrain at between 2677 and 2643 Ma. As all of the rock types within the Swayze greenstone belt are older than 2680 Ma and likely metamorphosed, with the exception of the ca. 2660 Ma biotite granite suite, the prefix 'meta' will not be used. Nomenclature of the granitoid units follows Streckeisen (1976) and is based on field estimates of proportions of quartz, plagioclase, potassium feldspar, and mafic minerals.

GENERAL GEOLOGY

The Swayze greenstone belt contains a varied collection of volcanic, sedimentary, and igneous rock types which are summarized in Heather (1993), Heather and van Breemen (1994), and Heather et al. (1995). The Swayze greenstone belt is bounded to the west by the Kapuskasing structural zone and by the Nat River granitoid complex to the north, the Kenogamissi batholithic complex to the east, and the Ramsey-Algoma granitoid complex to the south (Fig. 2a, b). Volcanic and sedimentary rocks range in age from 2731 to 2690 Ma, whereas the intrusive rocks range from 2740 to 2660 Ma (Heather and van Breemen, 1994; Heather et al., 1995). The volcanic and sedimentary rocks form an upward-facing, upward-younging stratigraphic sequence that is complexly folded and faulted (Heather et al., 1995). The following section highlights the geology of selected areas within the Swayze greenstone belt that have been recently mapped.

Dale stock

The Dale stock is a small, intra-greenstone-belt, felsic intrusive body located in north-central Dale Township (Fig. 2a, b). The stock is a hornblende granodiorite with a potassium feldspar megacrystic core and a massive equigranular margin. Both phases are moderately to strongly hematitic and contain hornblendic enclaves. The Dale stock is of similar texture and mineralogy as the 2680 Ma Hillary and 2682 Ma Neville plutons (Fig. 2a, b) and therefore interpreted to be part of the same suite.

Southwestern Kenogamissi batholith

The large Kenogamissi batholithic complex (KBC) separates the Swayze greenstone belt from the main Abitibi greenstone belt (Fig. 1, 2). The geology of the main part of the complex is described in Heather (1993) and Heather and van Breemen (1994). Field mapping during the 1995 season concentrated on completing coverage in the southwestern part of the

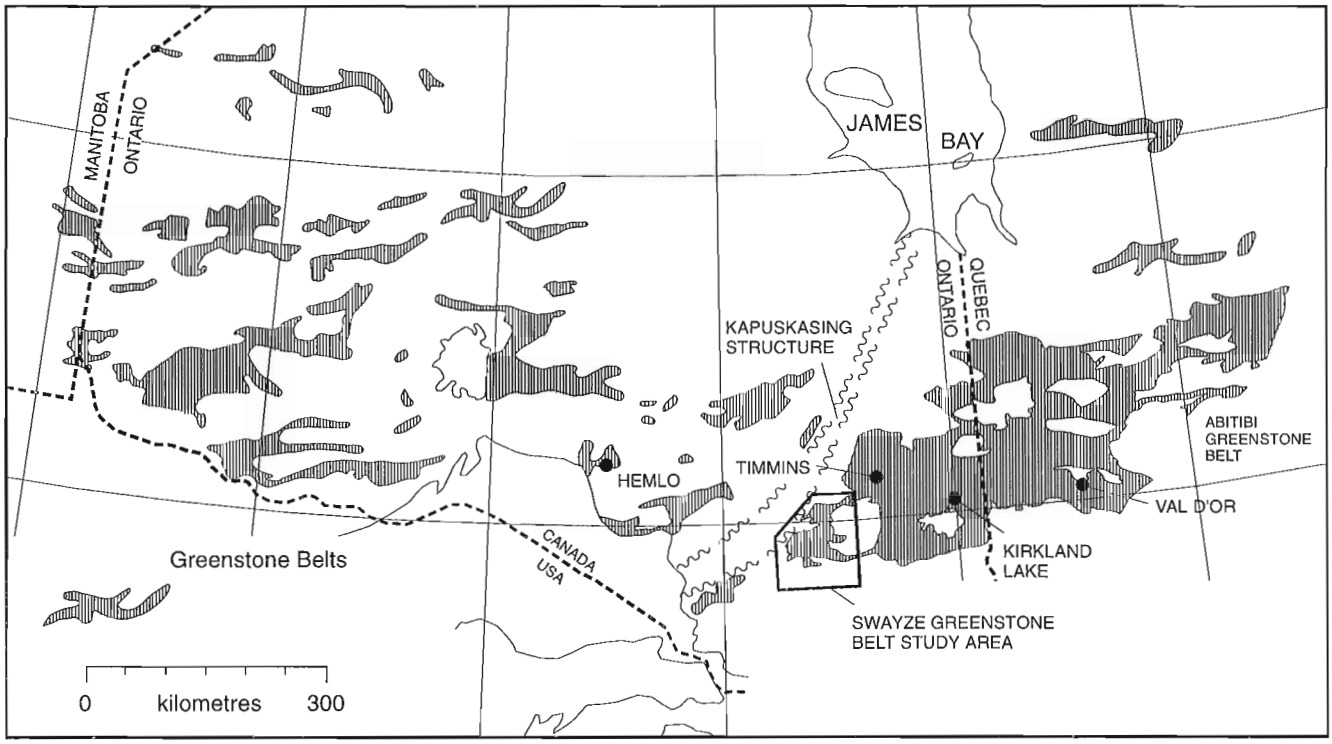

Figure 1. *Regional setting of the Swayze greenstone belt.*

Kenogamissi batholith complex in the vicinity of Rush, Rice, and Pebonishewi lakes (Fig. 3). This portion of the Kenogamissi batholithic complex contains granitoid rocks similar to those described by Heather and van Breemen (1994) from the northern and central portions of the complex. The granitoid phases are described from oldest to youngest based on known crosscutting relationships.

Remnants of foliated amphibolite occur as decametre-scale screens and xenoliths within granitoid phases proximal to the synformal lobe of greenstone in the vicinity of Northpoint Lake (Fig. 3). Fine grained amphibolites in the northern Rice Lake area are interpreted to be mafic volcanic rocks. Fine- to medium-grained amphibolites located in the vicinity of the Rush River are interpreted to have both mafic extrusive and intrusive protoliths.

Foliated diorite to monzodiorite also occurs as xenoliths within the younger phases of the southwestern Kenogamissi batholithic complex and is spatially associated with the screens of amphibolite (Fig. 3). The diorite varies from mesocratic to melanocratic, medium- to coarse-grained, and

Figure 2. a) *Townships, major lakes, and roads (heavy black lines) for the Swayze project area. The distribution of greenstone belt rocks and major intrusions is indicated by the fine dashed lines. This figure is to be used in conjunction with Figure 2b.*

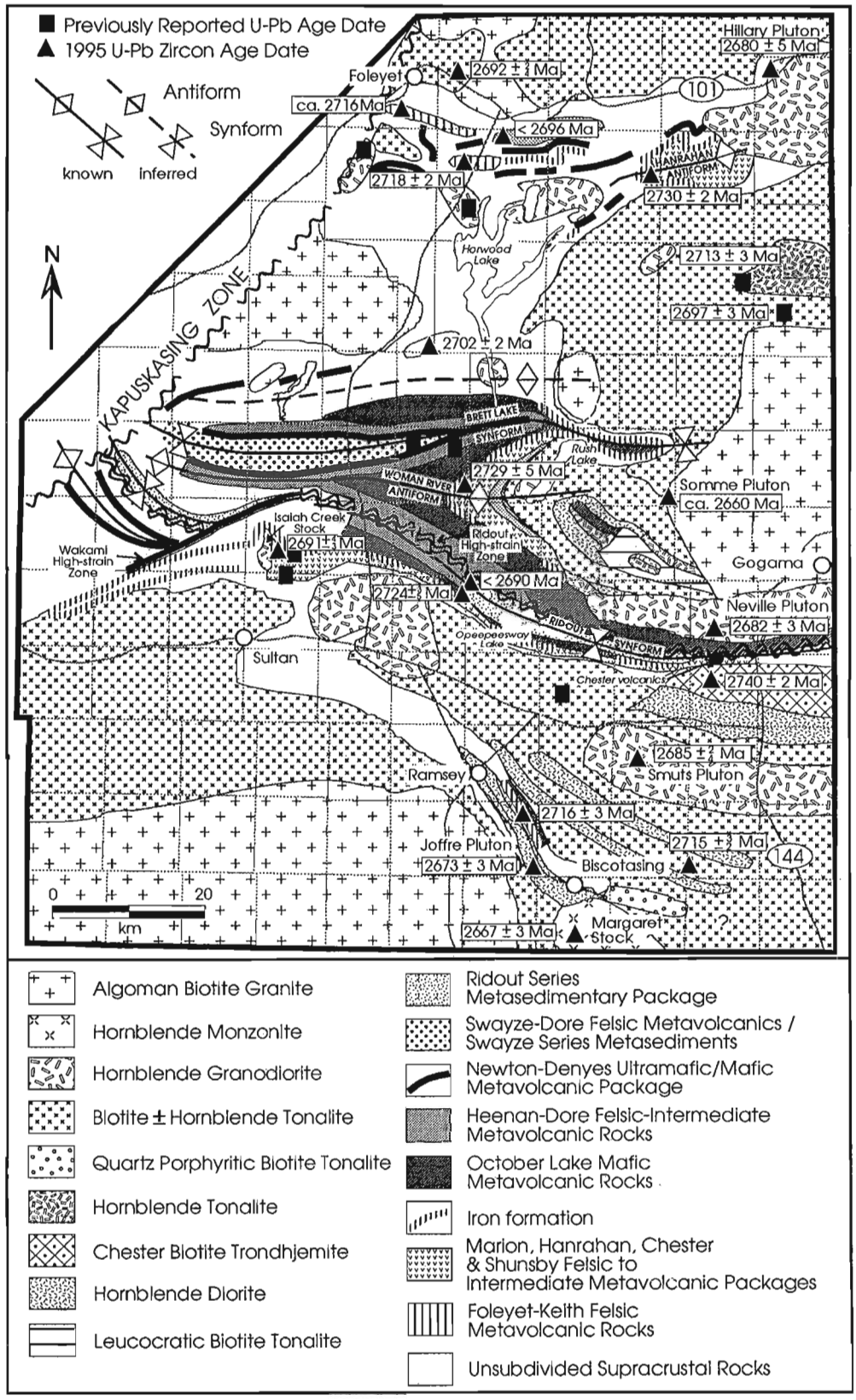

Figure 2. b) *Simplified bedrock and structural geology of the Swayze greenstone belt depicting major F_2 fold axes and high-strain zones. The locations of new U-Pb age dates are indicated. Late diabase dykes have been omitted for clarity.*

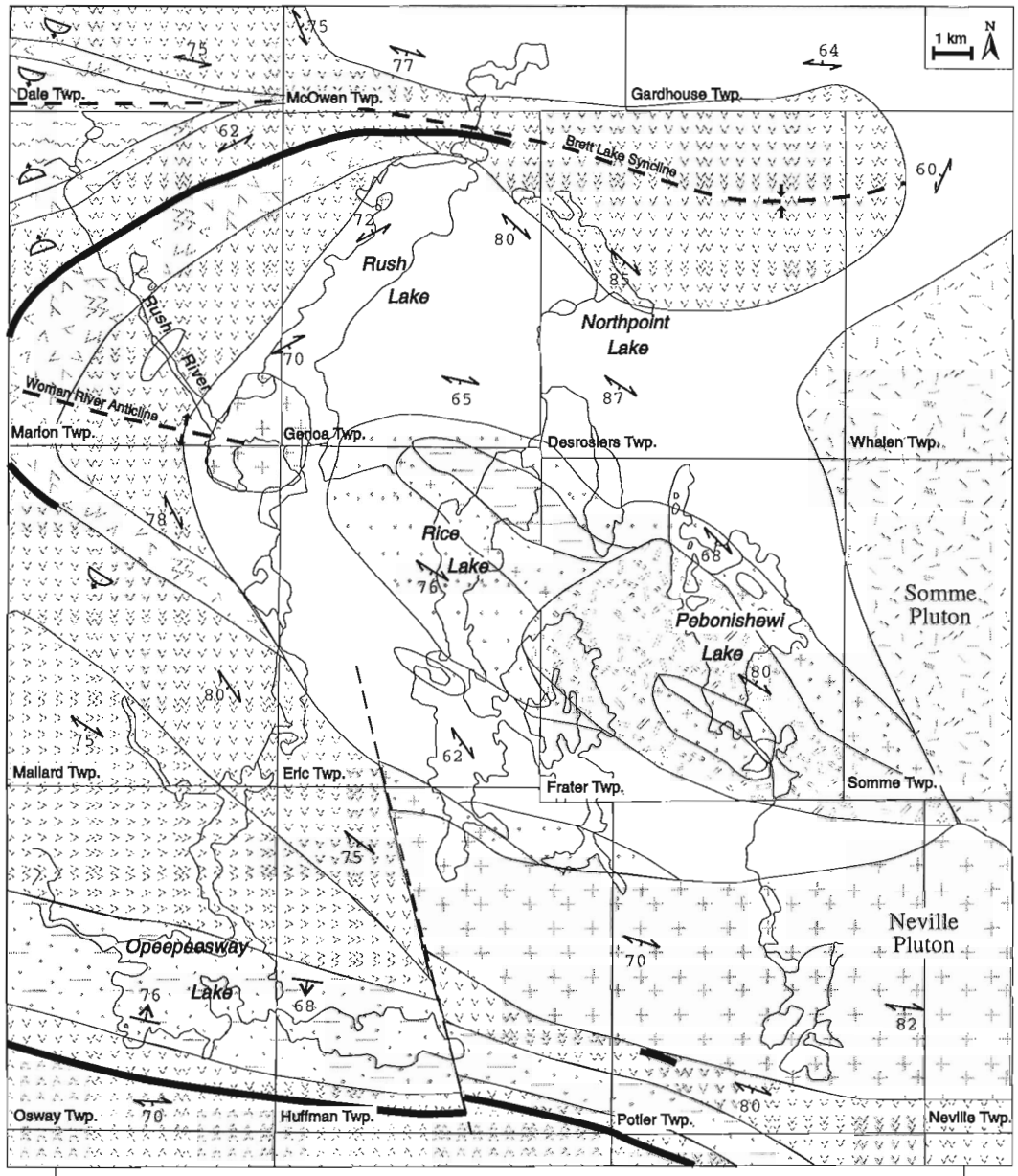

Figure 3. *Simplified geology map for the southwestern lobe of the Kenogamissi batholithic complex.*

is locally hornblende porphyritic. Where feldspar is locally hematized, the diorite may display an overall pinkish hue. These diorite zones are similar to those within the Ramsey Algoma Granitoid Complex (RAGC) in Biscotasi and Alcona townships (Heather et al., 1995).

Foliated hornblende±biotite tonalite to granodiorite and associated pegmatitic and aplitic dykes occur spatially related to, and locally intrude, map-scale screens and xenoliths of amphibolite and diorite (Fig. 3). Detailed relationships between this unit and xenoliths of amphibolite and diorite suggest that the hornblende±biotite tonalite to granodiorite may have been derived by contamination of a tonalitic to granodioritic magma through disaggregation and assimilation of mafic xenoliths.

Foliated biotite tonalite to granodiorite and associated pegmatitic and aplitic dykes are the dominant unit in the southwestern Kenogamissi batholithic complex (Fig. 3). This unit varies from medium- to coarse-grained, leucocratic to mesocratic, weakly or extensively hematized, and maybe mineralogically and texturally similar to biotite tonalite described elsewhere in the Kenogamissi batholithic complex and in the Ramsey Algoma Granitoid Complex (Heather and van Breemen, 1994; Heather et al., 1995).

Foliated, leucocratic biotite tonalite with accessory magnetite and titanite occurs mainly in the vicinity of Rice Lake (Fig. 3). This unit is characterized by homogeneous, medium grained, equigranular texture, and the presence of mesoscopic magnetite and titanite. The relative timing between this and other units in the area is not well constrained, however it is interpreted to be younger than the amphibolite, diorite, and hornblende tonalite based on its crosscutting map pattern (Fig. 3).

Massive to weakly foliated (possibly layered) hornblende granodiorite to monzonite occurs in a homogeneous sheet-like body on the southern margin of the Kenogamissi batholithic complex (Fig. 3). This unit is characterized by the local development of potassium feldspar megacrysts and rounded hornblende-rich clots/autoliths. The body represents the westward extension of the Neville pluton described by Heather and van Breemen (1994) and dated at 2682 ± 3 Ma. Smaller intrusions of massive hornblende monzonite to quartz monzonite occur in the vicinity of southern Rush Lake (Fig. 3) and share mineralogical and textural characteristics with the Neville pluton.

The Somme pluton (ca. 2660 Ma) is the youngest unit in the southwestern Kenogamissi batholithic complex and consists of massive to weakly foliated biotite granite to granodiorite and associated pegmatitic and aplitic dykes. This unit cuts older granitoid units at outcrop scale and truncates the eastward extension of dioritic and tonalitic bodies in the Rice and Pebonishewi lakes area (Fig. 3). The Somme pluton is mineralogically and texturally similar to Algoman granite and granodiorite identified elsewhere in the Swayze, both in the Kenogamissi batholithic complex and the Ramsey Algoma Granitoid Complex (Heather and van Breemen, 1994).

Granitoid rocks in the southwestern Kenogamissi batholithic complex occur as sheet-like bodies with dominantly northwest-southeast foliations. Foliations in the vicinity of Rush Lake vary from east-west to southwest-northeast and appear to be folded about the F_2 Woman River anticline (Fig. 3). Screens and megaxenoliths of amphibolite and diorite generally parallel the granitoid trends.

Hotstone Lake-Ridout Lake-Little Ridout Lake area

Detailed structural and lithological mapping in the Hotstone, Ridout, and Little Ridout lakes area, southwestern Swayze greenstone belt, has better established the character and kinematics of the D_3 Wakami high-strain zone (Heather et al., 1995). Highly strained, variably altered, and locally Au mineralized rocks in the Hotstone Lake and Ridout Lake areas are part of a semi-continuous corridor that can be traced westward through southern Halcrow Township and eastward through parts of northern Cunningham, southern Swayze, central Garnet, Benton, Osway, Huffman, Potier and Chester townships (Fig. 2a, b). This anomalously strained and altered corridor, known informally as the Ridout high-strain zone, is interpreted to represent either, the western extension of the Kirkland Lake-Matachewan-Shiningtree regional structure or, a new subparallel structure (Heather et al., 1995). In the vicinity of Little Ridout and Ridout lakes, the Ridout high-strain zone is sinistrally deflected along the northeast-striking Wakami high-strain zone (Heather et al., 1995).

Timiskaming-type conglomerate and sandstone occur along Little Ridout Lake and southwest along the Wakami River, coincident with both the Ridout and Wakami high-strain zones. Timiskaming-type rocks have been traced discontinuously northwest through southern Halcrow Township. Timiskaming-type rocks are also preserved on Travel Lake and to the east in central Garnet Township as small erosional outliers. Intermediate to felsic volcanic tuff and crystal tuff on southeastern Little Ridout Lake are compositionally similar and spatially related to the conglomerate and sandstone, suggesting they are also Timiskaming-type. Limited facing data from these rocks on Little Ridout Lake indicate tops to the south. Farther to the west, in the vicinity of Sylvanite Creek and north of Betty Lake, facing data indicate tops to the north. Upright F_2 folds of these rocks, such as those in the vicinity of Hotstone Lake, may explain the facing reversals.

Kinematic indicators and weakly developed lineations within the Ridout high-strain zone suggest a component of oblique, dextral movement, however there is a significant component of flattening also associated with this zone. Mineral and elongation lineations in rocks west of the Wakami zone are moderately to shallowly southeast plunging. These lineations are progressively re-oriented into a shallowly northeast-plunging attitude within the Wakami high-strain and then return to moderately to shallowly southeast-plunging on the east side of the zone. Both the regional F_2 folds and associated S_2 axial planar cleavages, as well as the moderate to strong S_2 schistosity associated with the Ridout high-strain zone, are re-oriented within the Wakami high-strain zone. The Wakami high-strain zone can be characterized as a greenstone-belt-scale, sinistral, extensional shear band (Heather et al., 1995) made up of numerous northeast-striking, brittle-ductile structures along which the cumulative apparent horizontal displacement is approximately 10 to 15 km. The

outcrop-scale shear bands have a limited strike length and tend to become strata/foliation parallel at their ends. Regionally, the Wakami zone appears to have the geometry of a megascopic shear band, as it too becomes strata-parallel to the northeast of Little Ridout Lake and likely does not continue north of the Cree Lake area. To the southwest, thick glacial sedimentary cover precludes the accurate delineation of the zone and hence the map presented by Heather et al. (1995) showing an extrapolated extension several tens of kilometres to the southwest is possibly incorrect. The zone more likely becomes strata-parallel, similar to its northeast end (Fig. 2a, b).

Hellyer-Biggs-Raney-Rollo townships

During the 1995 field season, coverage was completed on Hellyer, Biggs, Raney and Rollo townships (Fig. 2a, b) which had been mapped previously at a reconnaissance scale (Heather, 1993). The area consists of ultramafic flows, pillowed mafic volcanic rocks and later granitoid intrusive phases.

Pillowed mafic volcanic flows occur in northern Raney and southern Hellyer townships at amphibolite grade. The flows are well foliated (approximately east-west) but become more strongly deformed and epidotized towards the north where they are intruded by a granite to granodiorite body in central Hellyer township. Medium- to coarse-grained amphibolites are interpreted to be coarse-grained flows or sills. Rusty-weathering selvages and pillow breccias are locally developed. Feldspar is present locally as phenocrysts within pillow cores. Owing to the high state of deformation, no consistent tops indicators could be identified within the package.

Heather (1993) first identified and described ultramafic rocks in northwestern Raney Township (Fig. 2a, b). These rocks display an orangy-brown weathering and are highly magnetic. Metre-scale flows exhibiting massive, fine- to medium-grained bases with well-developed olivine spinifex texture towards the top have now been identified. Olivine crystals in the spinifex zone vary from 1-5 cm in length and locally form radiating fans. Polyhedral jointing marks the flow tops, while contacts between flows are gently scalloped. Polysutured flow tops and downward fanning of spinifex crystals indicate tops to the south, locally overturned. Aeromagnetic maps (Ontario Geological Survey, 1982a, b) suggest the komatiites are folded into a doubly-closing structure, but this could not be confirmed due to poor outcrop.

Several outcrops of massive, coarse grained, potassium feldspar megacrystic hornblende granite, granodiorite, and quartz monzonite occur in northern Raney Township. They are characterized by homogeneous texture and grain size, low quartz content (<15%), and the presence of rounded hornblende-rich clots. These bodies are similar in texture and mineralogy to the ca. 2680 Ma suite of intrusions seen elsewhere within the Swayze greenstone belt.

The Biggs pluton, a massive, pink coloured, medium- to coarse-grained biotite granite to granodiorite, occurs in Biggs and Hellyer townships (Fig. 2a, b). The pluton is distinctly variable in grain size; medium grained, coarse grained, and pegmatitic patches were identified at most outcrops. Sinuous biotite granite to granodiorite pegmatite dykes with diffuse margins occur throughout the pluton. They are characterized by reddish quartz (hematite stained), graphic intergrowths of quartz and potassium feldspar, large (2-3 cm) biotite flakes and large (1 cm) interstitial magnetite crystals. Garnet occurs rarely within pegmatitic patches and dykes in close proximity to the mafic volcanic rocks to the south. Intrusion breccias consisting of angular enclaves of mafic amphibolite and diorite to quartz diorite within a granitic to granodioritic matrix occur locally in northern Hellyer Township. The Biggs pluton is mineralogically and texturally similar to Algoman intrusions (ca. 2660 Ma) within the Kenogamissi batholithic complex and the Ramsey Algoma Granitoid Complex.

Halcrow-Denyes-Swayze townships

Sedimentary rocks of the 'Swayze Series' (Furse, 1932) consist of intercalated quartz- and/or feldspar-rich sandstone, siltstone, polymictic conglomerate, wacke, and mudstone (Fig. 4, 5, 6). Felsic to intermediate crystal tuff, lapilli tuff and volcanoclastic rocks of the Swayze-Dore package (Heather, 1993; Heather et al., 1995) are intimately intercalated with and of similar composition to the sedimentary rocks, which makes distinguishing the two somewhat difficult. Graded bedding, crossbedding, and channel scours are common features in the sandy and silty sedimentary rocks. Ripped-up clasts of bedded mudstone commonly occur within felsic volcanoclastic beds (Fig. 5). The polymictic conglomerate is typically matrix supported and dominated by felsic to intermediate volcanic clasts of similar texture and composition to the intercalated volcanic rocks (Fig. 6). No iron-formation or tonalite clasts were observed. The conglomerates typically exhibit reverse graded bedding whereas adjacent sandstones are normally graded. The sedimentary rocks have a felsic character and composition and are interpreted to be felsic turbidite aprons on the flanks of felsic volcanic edifices of the Swayze-Dore package. Facing information from graded beds

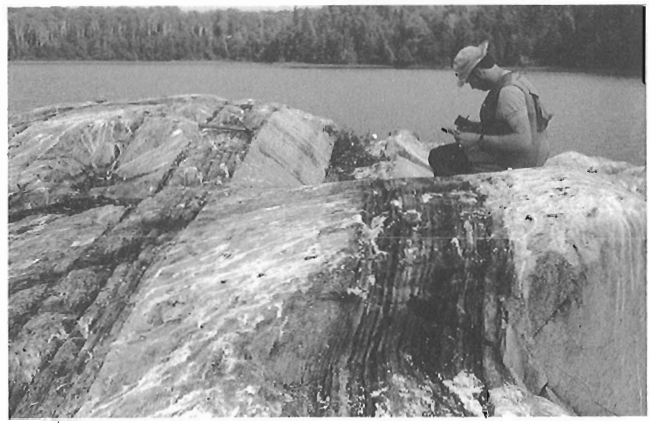

Figure 4. *North-dipping, south-facing, overturned beds of conglomerate, sandstone, and mudstone within the Swayze Series sedimentary package, Denyes Lake. G. Shore for scale. GSC 1995-259A*

and crossbeds supports Furse's (1932) conclusion that the Swayze series sediments have a synclinal geometry. However new data also indicate that the north limb of that syncline is overturned to the south. North of the Swayze series sediments, facings from pillow tops and flow tops in mafic volcanic rocks and flow tops in spinifex-textured komatiites all indicate that they are overturned to the south. This is consistent with these mafic and ultramafic rocks being part of a fold repeated Newton-Denyes package (Heather et al., 1995), located stratigraphically below the Swayze-Dore package.

GEOCHRONOLOGY

New U-Pb geochronological results are presented for 14 samples collected during the 1994 field season (Fig. 2a, b). All ages are derived from zircon analyses unless indicated otherwise. In addition, a refined age is given for a sample reported in Heather et al. (1995), and a second sample's location in the stratigraphy is re-interpreted.

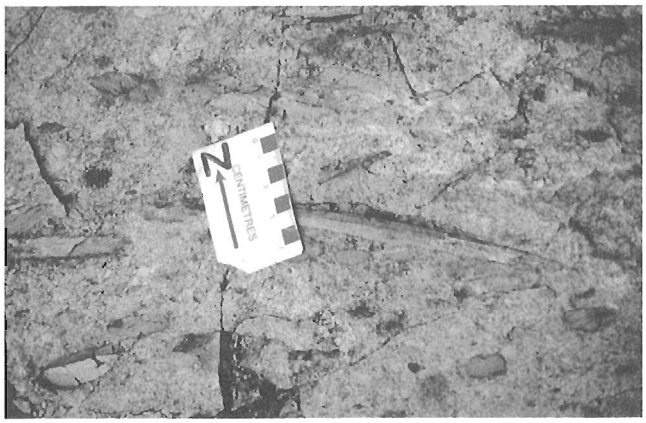

Figure 5. *Bedded mudstone rip-up clasts within a felsic volcanoclastic matrix, Swayze Township. Note the angular/tabular shape of the clasts suggesting minimal transport. Scalecard for north. GSC 1995-259C*

Figure 6. *Reversally-graded (tops to the left), north-dipping conglomerate/sandstone bed, Denyes Lake. View is looking east towards a vertical surface. Scalecard for scale. GSC 1995-259D*

The age for the Isaiah Creek stock has been refined to 2691 +3/-5 Ma. A felsic volcanoclastic tuff dated at 2724 ± 2 Ma was incorrectly reported (Heather et al., 1995) as occurring in the stratigraphic footwall of the Shunsby base-metal occurrence. The tuffs are actually intercalated between the upper and lower chert-dominated iron-formations that host the base-metal mineralization at the Shunsby. A 2731 ± 2 Ma felsic lapilli tuff (Heather et al., 1995) occurs stratigraphically below the lowest iron-formation, thereby constraining the age of the lower iron-formation to between 2733 Ma and 2722 Ma.

An intermediate lapilli tuff in the Hanrahan volcanic package near the footwall of the Nat River iron-formation is dated at 2730 ± 2 Ma. A quartz-eye bearing rhyolite breccia from the upper part of the Marion volcanic package, in the immediate footwall of the Woman River iron formation, yields a preliminary age of 2729 ± 5 Ma, with indications of approximately 2750-2740 Ma inherited zircons.

A massive, quartz-eye porphyritic felsic volcanic rock from the Biscotasing arm (Heather et al., 1995), southern Swayze greenstone belt, is dated at 2716 ± 3 Ma. A large body of foliated, medium- to coarse-grained, biotite±hornblende tonalite located east of the Biscotasing arm yields a similar age of 2715 +3/-2 Ma. In Foleyet Township, northern Swayze greenstone belt, an aphanitic rhyolite exhibiting autoclastic breccia textures yields an imprecise age of ca. 2716 Ma. A quartz-eye phyric felsic volcanic rock in Keith Township is dated at 2718 ± 2 Ma. In Silk Township, a foliated, felsic volcanoclastic tuff, with lapilli-sized fragments, is dated at 2702 ± 2 Ma.

A feldspar-quartz porphyry (FQP) body in Esther Township, bounded immediately to the north by a polymictic conglomerate of the Ridout Series, is dated at 2724 +4/-3 Ma. Detrital zircons from a quartz- and feldspar-rich sandstone within the Ridout Series provides a maximum age of sedimentation of 2690 Ma, which is consistent with it being of Timiskaming-type as previously interpreted. These results also indicate that an unconformable and/or structural contact must exist between the Ridout Series sediments and the Esther Township porphyry body. The majority of the detrital zircons from the Ridout sandstone yield ages between 2745-2735 Ma, which is consistent with a source dominated by older rocks as found in the southern Swayze greenstone belt (Heather et al., 1995). Detrital zircons from a sandstone within the Muskego sedimentary package, Keith Township northern Swayze greenstone belt, provide a maximum age of sedimentation of 2696 Ma. The majority of the detrital zircons ages cluster between 2702-2696 Ma, with one 2720 Ma grain, which is similar to results obtained for greywacke turbidite sedimentary rocks in the Kidd Creek area and the Porcupine Group near Timmins (Bleeker and Parrish, in press). Therefore, the sandstone in Keith Township appears to be more akin to Porcupine turbiditic sedimentary rocks rather than the younger Timiskaming-type Ridout series.

In Muskego Township, a biotite granodiorite to tonalite in the Nat River granitoid complex (Heather, 1993) yields a preliminary age of 2692 +2/-4 Ma. A massive, feldspar-phyric felsic rock from the Hanrahan package yields an age of 2689 ± 3 Ma, suggesting that it is a high-level intrusion into the 2730 Ma Hanrahan volcanic rocks. A massive, medium grained, biotite granodiorite from the Smuts pluton (Heather et al., 1995) yields a preliminary age of 2685 +2/-4 Ma. A hornblende quartz diorite phase of the Joffre pluton (Heather and van Breemen, 1994; Heather et al., 1995) yields an age of 2673 ± 3 Ma, based on both zircons and titanites. The hornblende monzonitic Margaret stock (Heather et al., 1995) yields an igneous titanite and zircon crystallization age of 2667 ± 3 Ma.

STRATIGRAPHIC RELATIONSHIPS

Heather et al. (1995) presented evidence for the presence of a coherent, continuously upward facing D_1 lithotectonic stratigraphic sequence (see Fig. 5 in Heather et al., 1995) preserved in a low-strain domain on the north limb of the regional F_2 Woman River anticline[1] (Fig. 2a, b). The D_1 deformation event is cryptically preserved as a regional S_1 foliation that is approximately strata-parallel and folded around the F_2 folds. There is neither structural repetition of the stratigraphic sequence, nor any 'old-over-young' (i.e. thrust) geometries apparent within the stratigraphic sequence. The base of that stratigraphic sequence was thought to be the 2729 ± 5 Ma Marion felsic to intermediate volcanic package, however recent mapping has identified poorly preserved mafic and felsic volcanic rocks stratigraphically below the Marion package, in the core of the antiform. The mafic volcanic rocks are massive to pillowed flows which are interpreted to be the base of the Marion volcanic cycle. Stratigraphically below the mafic volcanic unit is a discontinuous, poorly preserved felsic volcanic package which is cut by abundant tonalitic and dioritic intrusions.

South of the Ridout synform (Fig. 2a, b), felsic to intermediate volcanic rocks associated with large iron-formations in the Cunningham Township (Shunsby) area have been traced discontinuously for nearly 50 km to the east into Chester Township (Heather et al., 1995). This felsic to intermediate volcanic package, informally referred to here as the Chester volcanic package, has been regionally correlated with the 2731 to 2724 Ma Shunsby package to the west and with the 2729 Ma Marion and 2730 Ma Hanrahan packages to the north (Heather et al., 1995). In Chester, Yeo, and Potier townships a package of mafic volcanic rocks occurs south of, or stratigraphically below, the Chester felsic volcanic rocks and iron-formation. These pillowed and massive mafic volcanic rocks are interpreted to be the base of the Chester volcanic cycle. South of the Chester mafic-felsic volcanic cycle are vestiges of another mafic-felsic volcanic cycle which is interpreted to be stratigraphically lower and hence older. This lower volcanic package is intruded by the 2740 Ma Chester granitoid complex which constrains their age to ≥2740 Ma.

[1] Heather et al. (1995) referred to this as an antiform; however, now the stratigraphic sequence is known with the oldest rocks occurring in the core of the fold and therefore anticline is the correct terminology.

GEOCHEMISTRY

An integral part of the Swayze project is the lithogeochemical characterization of all the major volcanic, sedimentary, and plutonic rock packages. The purpose of the discussion here is not to present all the details of this geochemistry, but rather to highlight facets that may have direct implications for mineral exploration.

Characterization of felsic volcanic rocks using chondrite-normalized REE (Rare Earth Element) patterns can aid in distinguishing 'barren' versus 'base-metal mineralized' suites (Campbell et al., 1981, 1982; Lesher et al., 1986). Lesher et al. (1986) distinguished three main types of felsic volcanic rocks (i.e. FI, FII, and FIII) based on their REE patterns. The majority of the base-metal deposits in the Superior Province are preferentially associated with FIII-type felsic volcanic rocks and to a lesser extent with FII-type felsic rocks (Lesher et al., 1986). The FIII-type is rhyolite and high-silica rhyolite characterized by relatively flat REE patterns with negative Eu anomalies. The FII-type includes rhyodacite and rhyolite characterized by gentle sloping REE patterns with variable Eu anomalies. The FI-type has dacite and rhyodacite characterized by steep REE patterns with weakly negative to moderately positive Eu anomalies.

All the major felsic volcanic packages from the Swayze greenstone belt have been analyzed and classified according to the aforementioned scheme. Presently all the samples from the Marion, Hanrahan, Shunsby, Heenan-Dore and Swayze-Dore felsic packages can be characterized as FI-type, exhibiting steep REE patterns and no negative Eu anomalies. An exception to this is the Chester felsic volcanic rocks (Fig. 7) located north of the Chester granitoid complex in Chester Township (Fig. 2a, b). These are interpreted to be the eastern extension of the 2731 to 2724 Ma Shunsby package (Heather et al., 1995). The rhyolite and rhyodacite of the Chester

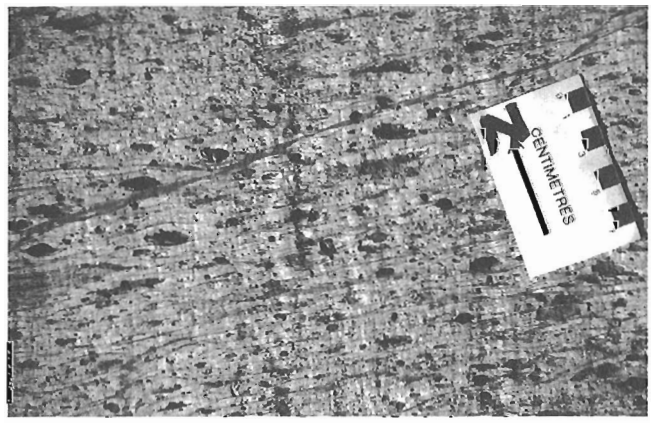

Figure 7. *Highly-strained rhyolite from the Chester volcanic package, Chester Township. Scalecard for north. GSC 1995-259B*

volcanic package show gently sloping REE patterns with negative Eu anomalies indicative of the FII-type (Fig. 8A). In addition, three of the four samples analyzed are high-silica rhyolites (i.e., SiO_2 = 79-82 wt.%) which are known to be associated with many of the major volcanogenic base-metal sulphide deposits in the Superior Province (Barrie, 1995).

To the south of the Chester volcanic rocks is the 2740 Ma Chester granitoid complex, a trondhjemite-diorite intrusion exhibiting magma mingling textures and opalescent blue quartz eyes (Heather, 1993; Heather et al., 1995). Locally within the trondhjemitic phase of the complex there is strongly developed, fracture-controlled (i.e. stockwork) magnetite-chlorite-epidote±quartz±sericite alteration (Fig. 9). The alteration is interpreted as syn-magmatic based on the observation that trondhjemite dykes of similar composition are both pre- and post-alteration. The Chester trondhjemite has a similar REE pattern to the Chester felsic volcanic rocks (Fig. 8B, C) suggesting a genetic link, whereas the dioritic phases show no negative Eu anomaly. Campbell et al. (1981) described a similar relationship between felsic volcanic rocks and plutonic rocks of the Beidelman Bay complex in the Sturgeon

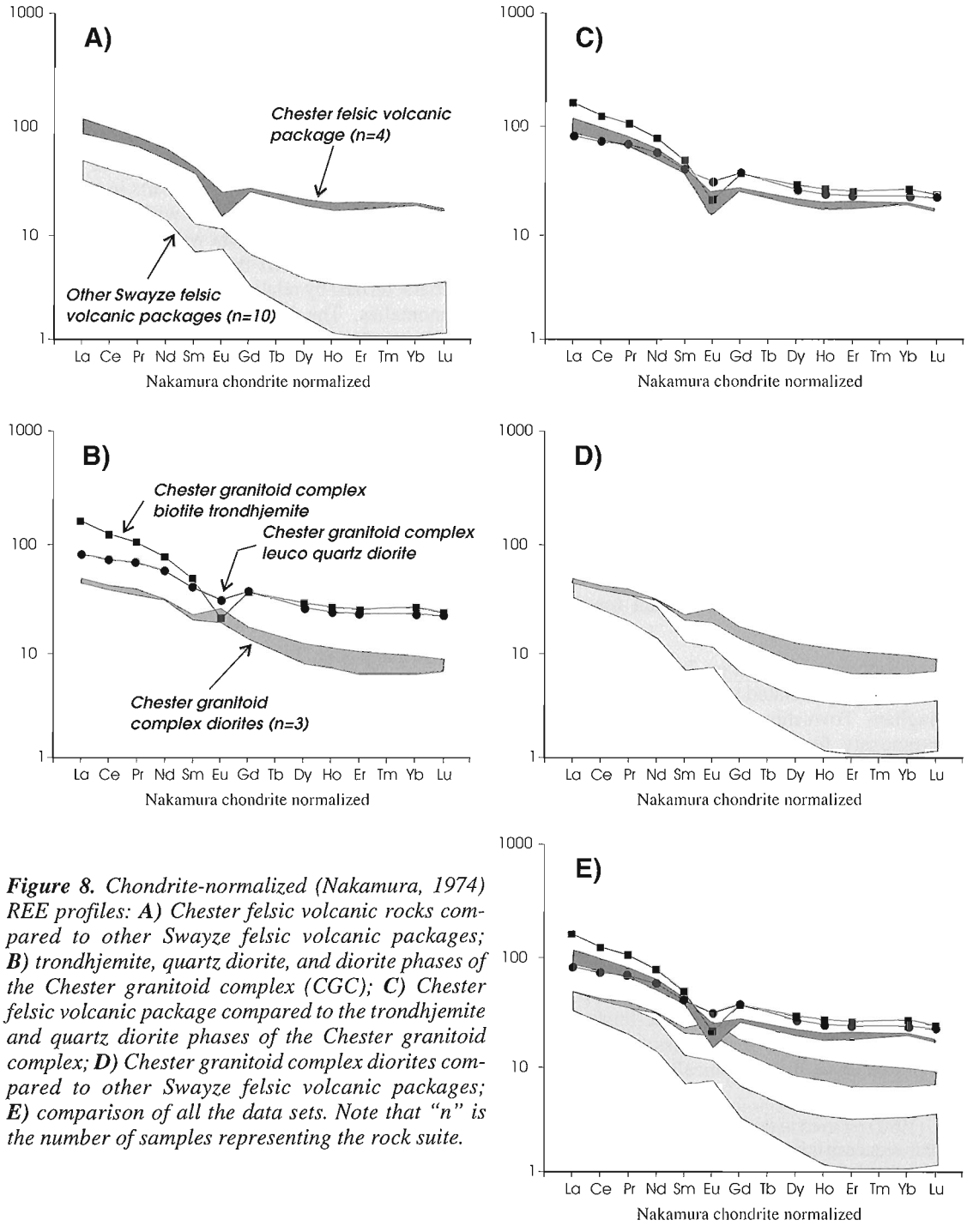

Figure 8. *Chondrite-normalized (Nakamura, 1974) REE profiles:* ***A)*** *Chester felsic volcanic rocks compared to other Swayze felsic volcanic packages;* ***B)*** *trondhjemite, quartz diorite, and diorite phases of the Chester granitoid complex (CGC);* ***C)*** *Chester felsic volcanic package compared to the trondhjemite and quartz diorite phases of the Chester granitoid complex;* ***D)*** *Chester granitoid complex diorites compared to other Swayze felsic volcanic packages;* ***E)*** *comparison of all the data sets. Note that "n" is the number of samples representing the rock suite.*

Lake area, northwestern Ontario. The base-metal deposits at Sturgeon Lake are associated with FII-type felsic volcanic rocks (Lesher et al., 1986) dated at 2735.5 ± 1.5 Ma (Davis et al., 1985). The Beidelman Bay complex, dated at 2733.8 ± 1.4 Ma (Davis et al., 1985), is a quartz diorite to trondhjemite (Franklin, 1978) containing intrusive breccias (magma mingling ?) and opalescent blue quartz eyes (Trowell, 1974).

DISCUSSION AND IMPLICATIONS FOR EXPLORATION

Granitoid rocks within the southwestern Kenogamissi batholithic complex consist of sheet-like bodies of dioritic to tonalitic composition. Screens of amphibolite are interpreted to be vestiges of mafic volcanic rocks preserved in structural outliers from the main greenstone belt. There is a spatial association between dioritic rocks, screens of amphibolite and hornblende±biotite tonalites, suggesting that at least some of the diorites are the product of assimilation/contamination. Heather et al. (1995) documented a similar relationship within the Ramsey-Algoma granitoid complex. Foliations in the tonalite and diorite are parallel to the greenstone belt contact and are folded about the regional F_2 Woman River anticline along with a strata-parallel, S_1 foliation within the volcanic stratigraphy. The southwestern lobe of the Kenogamissi batholithic complex is an anticlinal culmination, related to the F_2 Woman River anticline, which has exhumed synvolcanic diorite and tonalite sheets. The linear geometry of these intrusive sheets, their relative crosscutting relationships, and the fact they are folded by F_2 folds, all argue against a diapric origin. Instead, the entire Kenogamissi batholithic complex is made up of several anticlinal culminations (e.g. Hanrahan Lake anticline) separated by synclinal septa of greenstone belt rocks (e.g. Brett Lake syncline). The 2682 Ma Neville pluton intrudes along the contact between the greenstone and the synvolcanic diorite/tonalite, but is not demonstrably folded around the F_2 Woman River anticline. The non-foliated, ca. 2660 Ma Somme pluton, a biotite granite, crosscuts all of the aforementioned intrusions and truncates the regional foliation, indicating that it is post-tectonic.

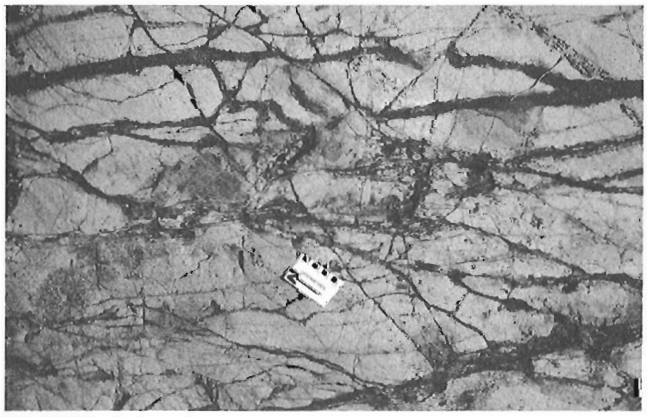

Figure 9. *Fracture-controlled magnetite-chlorite-epidote± quartz±sericite alteration within a biotite trondhjemite of the Chester granitoid complex, Chester Township. Scalecard for north. GSC 1995-259E*

Sedimentary rocks occurring in northern Halcrow, Raney, Denyes and Swayze townships (Fig. 2a, b) were provisionally designated by Furse (1932) as the Swayze series and interpreted to be different in lithology and age from the Timiskaming-type Ridout series sediments to the south. Rickaby (1935) concluded that the Swayze series and Ridout series were the same age and were merely opposite limbs of a major northwest-plunging anticline. Current mapping indicates that the Swayze series sediments are turbidites of felsic composition spatially related to, and intercalated with, rocks of the Swayze-Dore felsic to intermediate volcanic package. The conglomerates are dominated by felsic to intermediate volcanic clasts and contain no tonalite or iron-formation clasts typical of the Timiskaming-type Ridout series sediments. The Swayze series and Muskego sediments are interpreted to be more analogous to the < 2699 Ma Porcupine Group turbiditic greywackes in the Timmins area. In addition, the 2697 Ma Swayze-Dore package (Cattell et al., 1984) is of similar composition and age to the 2698 Ma Krist felsic fragmental unit in Timmins, which is spatially related to the Porcupine sediments. Data collected during the current mapping support Furse's (1932) conclusion that the Swayze and Ridout series are likely of different age and derived from different source regions.

Several important ideas and conclusions can be developed based on the new U-Pb zircon and titanite age dates. Three major felsic to intermediate volcanic packages, the 2730 ± 2 Ma Hanrahan package (Nat River iron-formation), the 2729 ± 5 Ma Marion package (Woman River iron-formation), and the 2731 ± 2 Ma Shunsby package (Shunsby iron-formation) are separated by several hundred kilometres and are all capped by significant, regionally extensive iron-formations. All of the iron-formations are overlain by mafic to ultramafic volcanic rocks. The iron-formations are closely related to the felsic volcanism as evidenced by the strong chlorite alteration of the footwall volcanic rocks to the iron-formations and by the felsic tuffaceous beds intercalated with the chert-magnetite beds. An intercalated tuff between the lower and upper iron-formations at the Shunsby is dated at 2724 ± 2 Ma while the footwall volcanics to the lower iron-formation are 2731 ± 2 Ma, thereby indicating that the lower iron-formation formed in a 4 to 11 Ma period. These particular iron-formations are at least a time marker, if not a time-stratigraphic marker, within the Swayze greenstone belt.

The huge Kidd Creek Cu-Zn deposit is associated with 2717 to 2710 Ma felsic volcanic rocks (Bleeker and Parrish, in press). Recognition of two ca. 2717 Ma felsic volcanic rock packages in the northern Swayze greenstone belt represents the first documented occurrence of Kidd Creek-like ages south of the Destor-Porcupine fault zone. The presence of 2716 ± 3 Ma felsic volcanic rocks and 2715 +3/-2 biotite tonalites in the Biscotasing arm portion of the southern Swayze greenstone belt significantly increases the southward extent of these potentially important rocks of this age.

The recognition of FII-type high-silica rhyolites in Potier and Chester townships (Chester volcanic rocks) and the presence of magnetite-chlorite-epidote±quartz±sericite alteration within the 2740 Ma Chester trondhjemite are interpreted as positive indications for base-metal mineralization. The similarity of these felsic volcanic rocks and synvolcanic intrusive rocks to those in the Sturgeon Lake area, host to several base-metal deposits, is significant and requires further evaluation.

ACKNOWLEDGMENTS

The authors would like to acknowledge the continued support of the mineral exploration community for the ongoing studies in the Swayze greenstone belt. B. Youngman (Northern Dynasty Minerals Ltd.), A. Sexton (WMC International Ltd.), M. Collison (Falconbridge Ltd.) and D. Patrie (prospector) provided information on their properties in the southern Swayze belt. Geological discussions with J. Ayer, M. Bernier, S. Jackson, and A. Fyon of the Ontario Geological Survey proved fruitful. Visits to the field by C. van Staal, W. Bleeker, and M. Lambert of the GSC and J. Winchester (Keele University) provided valuable perspectives on many geological problems. J. Harris (GSC) is thanked for providing reconnaissance-scale, sampling and ground follow-up gamma-ray spectrometer work in the external granitoid rocks.

REFERENCES

Barrie, C.T.
1995: Zircon thermometry of high-temperature rhyolites near volcanic-associated massive sulphide deposits, Abitibi subprovince, Canada; Geology, v. 23, no. 2, p. 169-172.

Bleeker, W. and Parrish, R.
in press: Stratigraphy and U-Pb zircon geochronology of Kidd Creek: implications for the formation of a giant VMS deposit and the tectonic history of the Abitibi greenstone belt; Canadian Journal of Earth Sciences.

Campbell, I.H., Coad, P., Franklin, J.M., Gorton, M.P., Scott, S.D., and Thurston, P.C.
1982: Rare earth elements in volcanic rocks associated with Cu-Zn massive sulphide mineralization: a preliminary report; Canadian Journal of Earth Sciences, v. 19, p. 619-623.

Campbell, I.H., Franklin, J.M., Gorton, M.P., Hart, T.R., and Scott, S.D.
1981: The role of subvolcanic sills in the generation of massive sulphide deposits; Economic Geology, v. 76, p. 2248-2253.

Cattell, A.C., Krogh, T.E., and Arndt, N.T.
1984: Conflicting Sm-Nd whole-rock and U-Pb zircon ages for the Archean lavas from Newton Township, Abitibi Belt, Ontario; Earth and Planatary Science Letters, v. 70, p. 280-290.

Davis, D., Krogh, T.E., Hinzer, J., and Nakamura, E.
1985: Zircon dating of polycyclic volcanism at Sturgeon Lake and implications for base-metal mineralization; Economic Geology, v. 80, p. 1942-1952.

Franklin, J.M.
1978: Petrochemistry of the South Sturgeon Lake volcanic belt; in Proceedings of the 1978 Archean Geochemistry Conference, (ed.) I.E.M. Smith and J.G. Williams; University of Toronto Press, Toronto, p. 161-180.

Furse, G.D.
1932: Geology of the Swayze area; Ontario Department of Mines, Annual Report, 1932, v. 41, pt. 3, p. 35-53.

Heather, K.B.
1993: Regional geology, structure, and mineral deposits of the Archean Swayze greenstone belt, southern Superior Province, Ontario; in Current Research, Part C; Geological Survey of Canada, Paper 93-1C, p. 295-305.

Heather, K.B. and van Breemen, O.
1994: An interim report on geological, structural, and geochronological investigations of granitoid rocks in the vicinity of the Swayze greenstone belt, southern Superior Province, Ontario; in Current Research 1994-C; Geological Survey of Canada, p. 259-268.

Heather, K.B., Shore, G.T., and van Breemen, O.
1995: The convoluted "layer-cake": an old recipe with new ingredients for the Swayze greenstone belt, southern Superior Province, Ontario; in Current Research 1995-C, Geological Survey of Canada, p. 1-10.

Lesher, C.M., Goodwin, A.M., Campbell, I.H., and Gorton, M.P.
1986: Trace-element geochemistry of ore-associated and barren, felsic metavolcanic rocks in the Superior Province, Canada; Canadian Journal of Earth Sciences, v. 23, p. 222-237.

Nakamura, N.
1974: Determination of REE, Ba, Fe, Mg, Na, and K in carbonaceous and ordinary chondrites; Geochimica et Cosmochimica Acta, v. 38, p. 757-775.

Ontario Geological Survey
1982a: Airborne electromagnetic and total intensity magnetic survey, Swayze Area, Ivanhoe Lake Sheet, District of Sudbury; Ontario Geological Survey, Geophysical/Geochemical Series, Map 80 537, scale 1:20 000.
1982b: Airborne electromagnetic and total intensity magnetic survey, Swayze Area, Rollo Lake Sheet, District of Sudbury; Ontario Geological Survey, Geophysical/Geochemical Series, Map 80 537, scale 1:20 000.

Powell, W.G., Carmichael, D.M., and Hodgson, C.J.
1995: Conditions and timing of metamorphism in the southern Abitibi greenstone belt, Quebec; Canadian Journal of Earth Sciences, v. 32, p. 787-805.

Rickaby, H.C.
1935: Geology of the Swayze gold area, District of Sudbury; Ontario Department of Mines, Annual Report, 1934, v. 43, pt. 3, p. 1-36, accompanying 1:63 360 scale Map 43b.

Streckheisen, A.
1976: To each plutonic rock its proper name; Earth-Science Reviews, v. 12, p. 1-33.

Trowell, N.F.
1974: Geology of the Bell Lake-Sturgeon Lake Area, Districts of Kenora and Thunder Bay; Ontario Division of Mines, Geological Report 114, 67 p., accompanying 1:31 680 scale Maps 2268 and 2269.

Geological Survey of Canada Project 850014FF

Arsenic in surface waters, Cobalt, Ontario

J.B. Percival, C.G. Dumaresq[1], Y.T.J. Kwong[2], K.B. Hendry[3], and F.A. Michel[4]

Mineral Resources Division

Percival, J.B., Dumaresq, C.G., Kwong, Y.T.J., Hendry, K.B., and Michel, F.A., 1996: Arsenic in surface waters, Cobalt, Ontario; in Current Research 1996-C; Geological Survey of Canada, p. 137-146.

Abstract: Water samples from the Farr Creek drainage basin, Cobalt, Ontario, were collected to study the aqueous transport of As and other metals in a weakly alkaline environment. New data on downstream changes in total As, As(III), and As(V) concentrations are presented. Temporal (1991-1995) changes in aqueous As distribution in the study area are also examined. Total dissolved As concentrations in surface waters range from 11 to 20 000 µg/L. Arsenic concentration generally decreases downstream, especially through wetlands, and appears to decrease with time. Widespread mine waste is undoubtedly the primary source of As in surface waters, but natural background levels in groundwater may also contribute and need to be assessed. Without mitigation, however, exposed tailings and waste rock will continue to release significant amounts of As and associated trace elements to the drainage system.

Résumé : Des échantillons d'eau ont été prélevés dans le bassin de drainage du ruisseau Farr (Cobalt, Ontario), dans le but d'étudier le transport par l'eau de l'arsenic (As) et d'autres métaux dans un milieu faiblement alcalin. De nouvelles données sur les changements en aval des concentrations totales en As, As(III) et As(V) sont présentées. Les variations temporelles (1991-1995) pour ce qui est de la distribution dans l'eau de l'As dans la région à l'étude sont également analysées. Les concentrations totales en As dissous dans les eaux superficielles varient entre 11 000 et 20 000 µg/L. Elles sont généralement moindres vers l'aval, en particulier à travers les terres humides; elles semblent également diminuer avec le temps. L'abondance des résidus miniers est sans aucun doute la principale source d'As dans les eaux superficielles, mais les concentrations de fond naturelles dans les eaux souterraines pourraient également y contribuer et doivent être, de ce fait, évaluées. Sans mesure de réduction, cependant, les stériles et les terrils continueront de libérer des quantités importantes d'As et d'éléments traces associés dans le réseau de drainage.

[1] AQUAMIN Secretariat, Evaluation and Interpretation Branch, Environment Canada, Ottawa, Ontario K1A 0H3
[2] Environmental Sciences Division, National Hydrology Research Institute, 11 Innovation Boulevard, Saskatoon, Saskatchewan S7N 3H5
[3] Department of Geology, University of New Brunswick, Fredericton, New Brunswick E3B 5A3
[4] Department of Earth Sciences, Carleton University, Ottawa, Ontario K1S 5B6

INTRODUCTION

Cobalt, located in northeastern Ontario in the district of Timiskaming, is historically renowned for its silver production. By 1971 more than 600 million ounces (1.698×10^7 kg) of silver were mined from the Cobalt area deposits (Petruk et al., 1971). Numerous tailings deposits, waste rock dumps, and mine workings are testimony to the early prosperity of the region (Fig. 1). Mining continues on a smaller scale today, with Co as the main commodity. Mitigation efforts to date have been limited to fencing of obvious mine hazards (shafts, pits, and some mill foundations), reprocessing of tailings from some of the tailings deposits, and some revegetation efforts on at least two tailings deposits.

Arsenic contamination of the surface waters in the Cobalt region has been documented previously (OWRC, 1967; Boyle et al., 1969; Hawley, 1980; Dumaresq, 1993). On the basis of surface water chemistry and stream flow data, Dumaresq (1993) estimated that the mean annual discharge of As from Farr Creek to Lake Timiskaming is about 18 000 kg. The present study is concerned with the transport and fixation of As in the surficial environment from the mine waste sites (tailings and waste rock) through surface waters to wetlands. This is part of a larger study which includes lithogeochemistry and mineralogy of tailings sample sites and chemistry of surface and groundwaters in the Farr Creek drainage basin which drains into Lake Timiskaming (Fig. 1). Understanding the behaviour of As in natural waters is important because As and its compounds are potentially toxic to humans and to aquatic organisms (Government of Canada et al., 1994).

In this progress report, we present new data on the general water chemistry of the study area. Special emphasis is placed on the downstream changes in total As, As(III), and As(V)

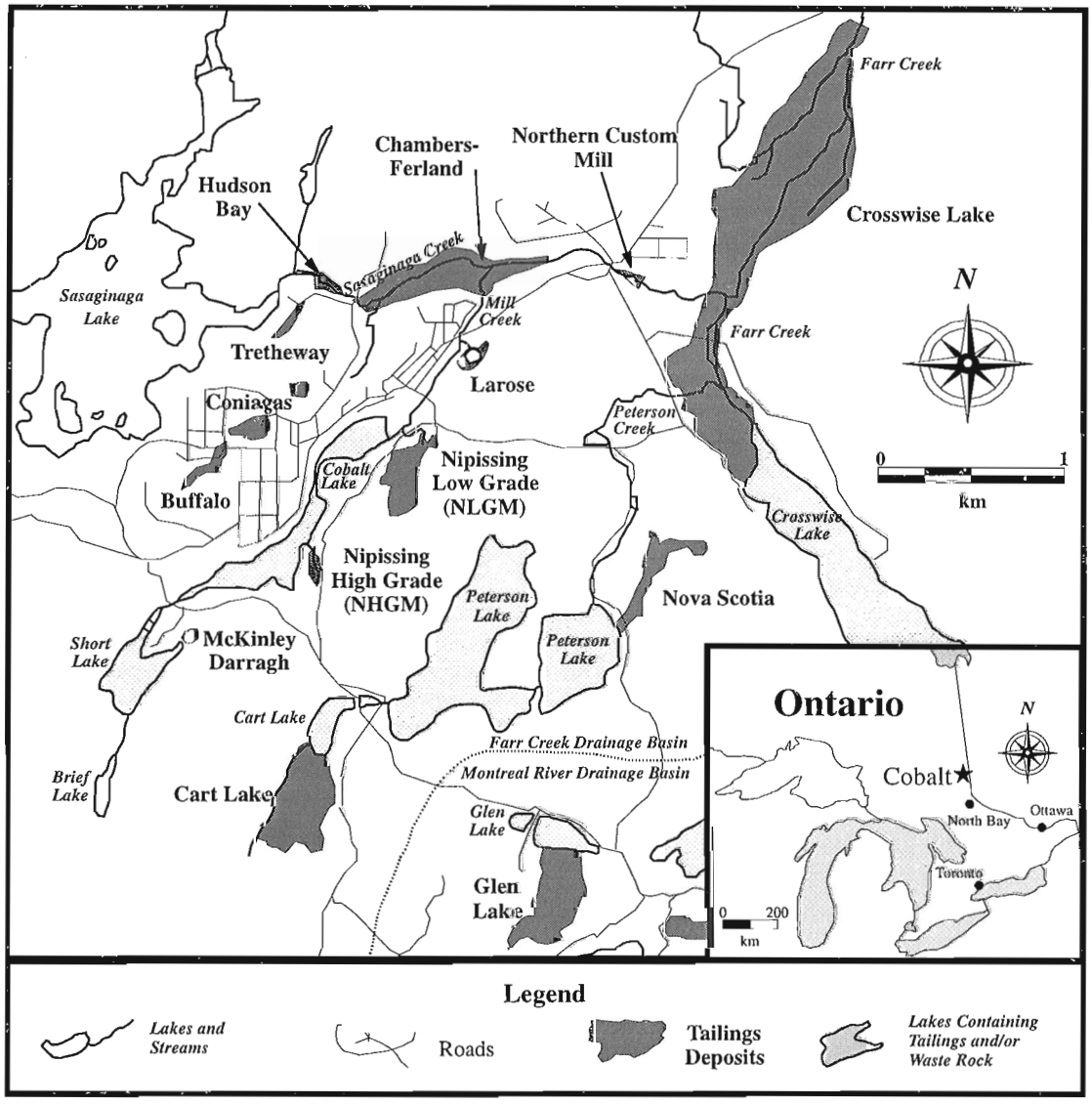

Figure 1. *Location map of Cobalt, Ontario showing details of the Farr Creek drainage basin and location of tailings deposits and waste rock dumps (after Dumaresq, 1993).*

concentrations in relation to other chemical and physical water parameters. Where appropriate, the current data set is also compared with that of Dumaresq (1993) to discern temporal changes in aqueous As distribution in the study area.

GENERAL GEOLOGY

In the Cobalt area Archean volcanic and sedimentary rocks are overlain unconformably by Proterozoic sediments of the Cobalt Group. The oldest unit of this group, the Coleman Member of the Gowganda Formation, is composed of conglomerate, greywacke, quartzite, and arkose. The Coleman Member is overlain by argillite of the Firstbrook Member and both are overlain by arkose and quartzite of the Lorrain Formation. All units are cut by early Proterozoic Nipissing diabase (Boyle, 1968; Jambor, 1971), with which the Ag-Co-Ni-As deposits are spatially associated.

Native Ag occurs in veins associated with native Au, As, and Bi, as well as arsenides, sulpharsenides, and sulphides such as nickeline, cobaltite, safflorite, loellingite, rammelsbergite, gersdorfite, skutterudite, arsenopyrite, tetrahedrite, chalcopyrite, bornite, galena, sphalerite, pyrite, and marcasite (Petruk, 1971). Gangue minerals include calcite, dolomite, quartz, and chlorite. Oxidation of the primary ore minerals produces secondary minerals, in particular, erythrite, annabergite, and scorodite. Sulphates (e.g., gypsum and thenardite), Fe and Mn oxides and oxyhydroxides, as well as clay minerals are also present (Boyle and Dass, 1971).

ARSENIC CYCLE

Arsenic is stable in four oxidation states: (-III), (O), (III), and (V). Arsenic (-III) is found only in gaseous AsH_3 (arsine). Arsenic can occur in the metallic state in some mineral deposits, but usually occurs in compounds with S and a variety of other metals (Boyle and Jonasson, 1973). In natural waters, dissolved As is present as inorganic As(III) and As(V) species, or as methylated As(V) compounds (Cullen and Reimer, 1989). Arsenic is mobile in both acid and alkaline waters due to its amphoteric nature (Boyle et al., 1969).

Arsenate ($As^{V}O_4^{3-}$) species predominate in aerobic waters whereas arsenite ($As^{III}O_3^{3-}$) occurs under anaerobic conditions (Ferguson and Gavis, 1972; Cullen and Reimer, 1989). Ferguson and Gavis (1972) noted that arsenite can be found in surface waters if the Eh is less than 0.1 V or if oxidation to As(V) is incomplete. Removal of As from solution can result by co-precipitation with hydrous Fe and Al oxides, adsorption onto clays or through chelation by organic matter. Increases in pH, Eh, salinity, temperature, or biological activity help to increase the rate of oxidation of arsenite to arsenate. This is important because arsenite is more toxic than arsenate.

Organisms bioaccumulate As from water but As is not biomagnified through the foodchain (CCREM, 1987). The decreasing order of toxicity is: arsine(-III) > organo-arsine derivatives > inorganic arsenite(+III) > organic As(III) compounds > arsenoxides(+III) > arsenates(+V) > organic As(V) compounds > metallic As(O) (Penrose, 1974; NRCC, 1978; Eisler, 1988). In general, inorganic arsenical compounds are higher in toxicity than organic compounds and the trivalent As-species is more toxic than the pentavalent As-species (NRCC, 1978).

METHODS

Surface water samples were collected in July and September 1994, and in May 1995. Sample sites are shown in Figure 2 and numbered consecutively from the southwest to the northeast in the direction of drainage. Groundwater samples were collected from a pipe draining a mineshaft near Sasaginaga Creek (GW1), overflow from a shaft near Cobalt Lake (GW2), and from a well house and taps from the Bucke Park campground (GW3-GW7). Temperature, pH, Eh, and electrical conductivity were determined in the field using a Cole-Parmer Water Test meter. Water samples were filtered in the field through a 0.45 μm Millipore filter paper (type HAWP). One sample was acidified to 0.4% in HNO_3 (using Seastar double sub-boiling distilled) for cation determinations, one to 0.4% in HCl (using Merck Suprapur) for As speciation, and one remained unacidified for anion determinations. Major and trace elements were determined on the HNO_3-treated sample by inductively-coupled plasma-atomic emission spectrometry (ICP-AES) and inductively-coupled plasma-mass spectrometry (ICP-MS) (note that "total" in this paper implies total "dissolved"; i.e., through 0.45 μm filter). Total As and As(III) were determined by hydride generation quartz tube AAS using $NaBH_4$ as a reducing agent. With sample adjusted to a pH of 5 with citric acid, arsine (AsH_3) was generated only from As(III), As(V) being nonreactive. A separate aliquot was then prereduced with 5% KI and ascorbic acid to determine total As. Arsenic(V) was then determined as the difference between total As and As(III). Anions (SO_4^{2-} reported here only) were determined using a Dionex ion chromatograph.

RESULTS AND DISCUSSION

Water quality

Selected physical and chemical parameters of surface and groundwaters are shown in Tables 1 and 2, respectively. Surface water conditions observed during the 1994 and 1995 surveys included temperatures of 21.7 to 27.8°C for July (1994), 9.8 to 21.5°C for September (1994), and 11.1 to 18.5°C for May (1995). The low temperature of 9.8°C was more representative of groundwater conditions as this sample was taken from the decant pond during dewatering of a mine (Cobatec operation). All surface waters were alkaline with an average pH of 7.9, well-oxygenated (Eh from +67 to +208mV), and had dissolved oxygen levels (data not shown) at or near saturation. Overall, conductivity was high but with peak values corresponding to drainage from exposed tailings (e.g., from Nipissing high-grade mill (NHGM), LaRose tailings etc.). Groundwaters were cooler (6.4 to 14.8°C), slightly

less alkaline (mean pH 7.4), with higher conductivities, but they were reducing (Eh from -57 to -72 mV). One exception was sample GW1 (Eh = +252 mV) that was taken from a mine shaft discharging from a pipe into Sasaginaga Creek.

Arsenic

Relative to the guidelines for Canadian drinking water quality (25 µg/L; Health and Welfare Canada, 1989), As concentrations in surface waters in the Cobalt region are excessive (note: with the exception of Sasaginaga Lake, surface waters in the study area are not used for drinking water). Only 6 samples contain less than 100 µg/L total As (Table 2). The highest concentrations, 15 000-20 000 µg/L, are associated with drainage from a small area that contains Nipissing high-grade mill tailings. This drainage discharges into Cobalt Lake at sites 6 and 7 (Fig. 2A). Water from the outlet of the LaRose tailings site (site 15, Fig. 2C) is also characterized by high total As (>3000 µg/L). Conversely, some samples that contain greater than 1000 µg/L total As are not associated with tailings (e.g., sites 14 and 20, Fig. 2B) whereas others that contain less than 500 µg/L are (e.g., sites 18 and 19, Fig. 2C). This suggests that tailings from different mines vary in composition and that the tailings may not be the only source of As in the study area.

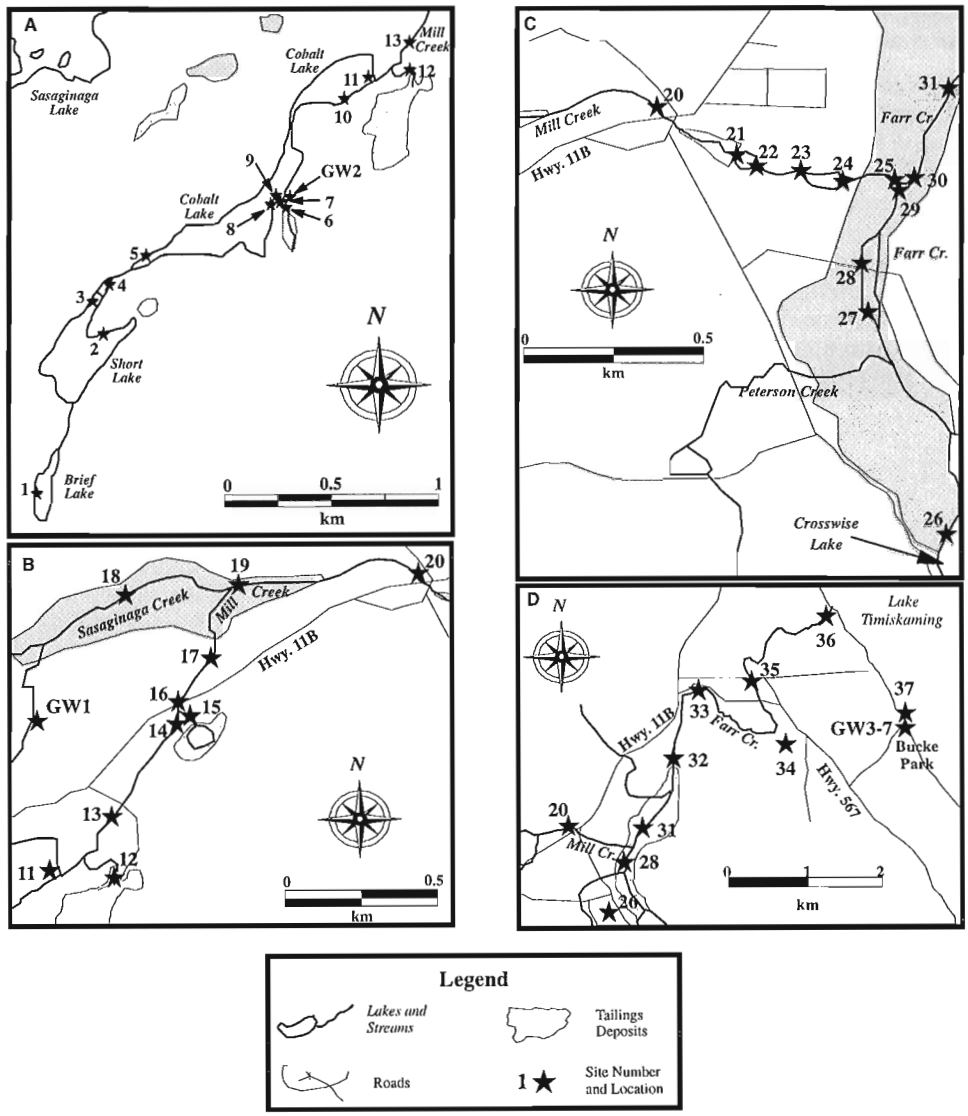

Figure 2. *Site locations of all sampling stations used in 1991-1992, 1994, and 1995 surveys:* ***A)*** *Cobalt Lake area;* ***B)*** *Sasaginaga Creek and Mill Creek confluence;* ***C)*** *Mill Creek and Farr Creek confluence; and* ***D)*** *Bucke Park campground. Drainage of the Farr Creek basin is to the northeast to Lake Timiskaming.*

The trend of As concentration within the Farr Creek drainage system is plotted as the mean concentration for all data (1991 to 1995) per sampling site in Figure 3. Low concentrations (e.g., <300 µg/L) are observed in Brief Lake, Short Lake, Sasaginaga Creek, Crosswise Lake, and Farr Creek. Brief Lake is located at the head of the Mill Creek system and does not contain any tailings whereas Short Lake contains at least two waste rock piles along its shores. These waste rock piles appear to make only a small contribution (e.g., ~50 µg/L) to the As budget. Both Sasaginaga and Farr Creeks contain submerged tailings and meander through wetlands situated on tailings upstream from the Mill Creek confluence. Metal fixation processes such as adsorption or chelation may occur in the wetlands to account for the lower total As than is observed in Mill Creek.

The As concentration rises downstream from Short Lake, in Cobalt Lake. Several mills deposited tailings in Cobalt Lake, and the lake was drained from 1914 to 1932 to recover some of the tailings for reprocessing. The south end of the lake was also drained in the early 1950s and in the mid 1960s. It is estimated that about 250 000 t of tailings remain submerged in Cobalt Lake (Dumaresq, 1993). The drainage from the Nipissing high-grade mill although extremely high in As, is low in volume and becomes insignificant when it mixes with the large volume of water in Cobalt Lake. To investigate

Table 1. Characteristics of surface water and some groundwaters from Cobalt, Ontario. Site locations shown on Figures 2A to 2D.

SITE	DATE	TEMP °C	pH	Eh mV	COND µS/cm
1	09/94	15.3	7.4	+185	181
2	91-92	na	7.7	na	170
3	09/94	15.9	8.1	+181	174
4	09/94	16.6	7.6	+171	176
5	09/94	17.3	8.1	+171	345
6	91-92	na	8.4	na	360
	07/94	27.8	8.8	+130	542
	09/94	17.7	8.5	+133	439
	05/95	18.5	8.1	+134	424
7	05/95	13.1	8.0	+159	332
8	91-92	na	8.3	na	175
	05/95	13.7	8.0	+140	354
9	05/95	12.8	8.0	+143	349
10	91-92	na	8.1	na	243
	07/94	23.5	8.5	+173	387
11	05/95	13.9	8.0	+125	372
12	91-92	na	7.4	na	228
13	91-92	na	8.0	na	242
	07/94	23.0	8.2	+189	364
14	91-92	na	7.5	na	265
	07/94	23.6	9.6	+121	494
	09/94	21.5	8.6	+94	341
15	91-92	na	7.3	na	480
	07/94	24.7	7.6	+182	584
	09/94	19.2	7.0	+207	573
16	91-92	na	7.9	na	410
	07/94	24.2	8.4	+167	469
	09/94	19.6	8.0	+148	454
17	91-92	na	8.0	na	285
	07/94	24.7	8.7	+154	584
18	91-92	na	7.6	na	185
19	91-92	na	7.6	na	270
20	91-92	na	7.4	na	260
	07/94	22.6	7.5	+191	440293
	05/95	16.3	8.3	+159	
21	09/94	16.5	7.4	+118	439
22	05/95	14.7	8.1	+117	288
23	05/95	15.2	8.2	+94	290
24	05/95	11.1	7.9	+208	297
25	07/94	21.7	7.5	+187	421
	05/95	12.2	8.1	+136	291
26	91-92	na	8.0	na	110
27	07/94	25.3	8.0	+151	188
28	91-92	na	7.6	na	153
	07/94	26.6	8.1	+142	172
	05/95	15.0	7.9	+173	169
29	07/94	26.2	7.9	+165	173
	05/95	13.6	7.8	+133	192
30	07/94	25.3	7.7	+200	254
	05/95	12.6	7.7	+104	218
31	07/94	24.0	7.9	+202	247
32	91-92	na	7.6	na	475
	07/94	22.9	6.9	+243	250
33	91-92	na	7.9	na	217
	09/94	18.2	8.3	+114	317
34	09/94	9.8	7.8	+110	416
35	09/94	17.5	7.9	+118	379
	05/95	13.9	7.7	+148	216
36	91-92	na	8.5	na	290
37	09/94	17.2	7.6	+67	181
GW1	91-92	na	7.2	na	420
	09/94	6.4	7.2	+252	290
GW2	91-92	na	7.7	na	280
GW3	91-92	na	7.5	na	537
	07/94	11.3	8.1	-72	513
	09/94	7.5	7.4	-71	463
GW4	09/94	9.4	7.5	-61	477
GW5	09/94	na	na	na	na
GW6	09/94	12.2	7.2	-70	491
GW7	09/94	14.8	7.1	-57	526

Note – na: not analyzed

possible localized effects near the Nipissing high-grade mill outlet in Cobalt Lake, determination of As in pore waters and sediments sampled from the vicinity are in progress. On the other hand, the contributions from the Nipissing low-grade mill (NLGM) and LaRose tailings give rise to an increase in downstream As concentration as they mix with a smaller volume of water in Mill Creek. The source of contamination leading to the higher As concentration at site 20 is unclear. Samples collected upstream in Sasaginaga Creek contain low As concentrations (<300 µg/L) despite the fact that this creek is underlain by tailings. Higher As concentration at site 20 may suggest that there is an unidentified groundwater discharge in this area. The concentration generally decreases across a wetlands area (between sites 16 and 32), with some minor fluctuations, but increases again slightly before entering Lake Timiskaming. Some of these minor fluctuations are easily explained. For example, the increase just before the Mill Creek-Farr Creek confluence (site 25, Fig. 2C) reflects contribution from an unknown volume of tailings that were discovered in Mill Creek in September 1994. These tailings were not reported in Anderson (1993) and probably were discharged from the nearby Northern Customs mill. Arsenic concentrations are higher in Farr Creek at site 35 than at site 32. In September 1994 Farr Creek was receiving decant (site 34; Fig. 2D) from the settling pond at Cobatec during dewatering of the Pan Silver mine. Although the decant may be a contributing factor to the increase in As concentration at site 35, it is not the major factor, as a similar trend was reported by Dumaresq (1993). The Farr Creek basin contains no mine wastes downstream of site 32. Thus, the probable source of contamination leading to increased As concentrations between sites 32 and 36 is groundwater discharge along

Table 2. Chemistry of surface waters and some ground waters from Cobalt, Ontario. Site locations shown on Figures 2A to 2D. Data for total As, As(III), As(V), Co, and Ni in µg/L; Ca, Mg, and SO_4 in mg/L.

SITE	DATE	As(T)	As(III)	As(V)	Co	Ni	Ca	Mg	SO_4
1	09/94	11.1	5.7	5.4	1.0	2.6	38	6.3	3.3
2	91-92	48	na	na	nd	nd	32	9	14
3	09/94	51	2.7	48	0.5	2.6	35	6.0	9.6
4	09/94	93	3.6	89	2.1	5.3	36	6.1	9.5
5	09/94	877	7.8	869	3.6	19	50	9.9	17
6	91-92	17470	na	na	364	293	75	26	55
	07/94	20238	1470	18768	410	330	78	17	43
	09/94	17018	411	16607	450	340	80	18	42
	05/95	15799	266	15533	440	390	37	14	32
7	05/95	7981	95	7886	370	230	52	12	26
8	91-92	638	na	na	20	nd	47	14	18
	05/95	819	46	773	29	28	47	8.7	18
9	05/95	602	29	573	23	25	47	8.7	17
10	91-92	695	na	na	nd	nd	42	14	44
	07/94	1056	10	1046	3.0	12	45	9.9	19
11	05/95	653	41	612	14	23	49	9.2	18
12	91-92	534	na	na	217	152	39	8	24
13	91-92	834	na	na	25	nd	46	12	16
	07/94	1459	132	1327	23	26	46	9.5	17
14	91-92	1280	na	na	41	nd	53	16	20
	07/94	1106	130	976	19	29	43	7.3	106
	09/94	1147	11.8	1135	20	26	43	9.5	16
15	91-92	3210	na	na	2028	643	63	5.2	87
	07/94	3477	84	3393	1300	440	62	13	89
	09/94	3004	21	2983	1500	660	60	12	95
16	91-92	1180	na	na	296	107	56	4.4	27
	07/94	2303	136	2167	460	160	48	10	77
	09/94	2074	29	2045	680	300	51	11	50
17	91-92	792	na	na	nd	nd	45	12	40
	07/94	2137	137	2000	380	160	62	9.2	128
18	91-92	217	na	na	nd	nd	45	6	21
19	91-92	515	na	na	69	nd	33	2.6	14
20	91-92	1421	na	na	159	101	47	13	19
	07/94	1281	15	1266	140	73	51	10	32
	05/95	605	43	562	90	76	37	7.6	17
21	09/94	1119	22	1097	220	110	54	11	26

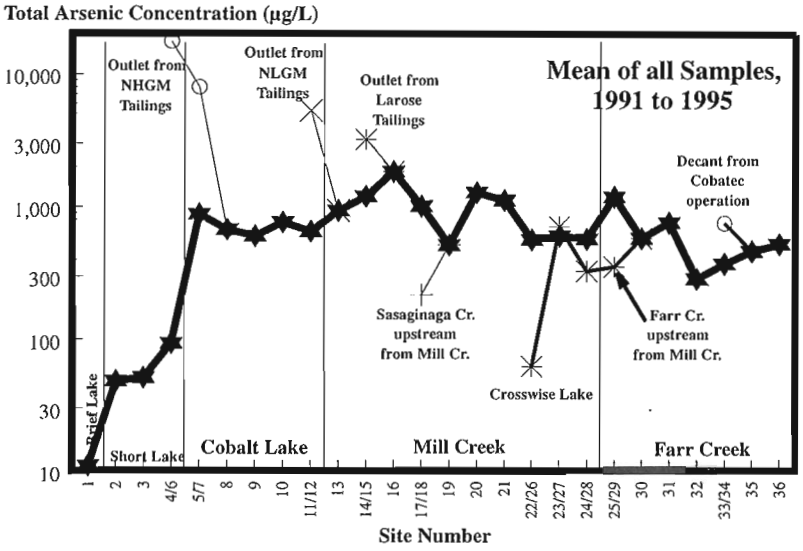

Figure 3.

Mean total dissolved As for all samples (1991-1995) plotted against relative distance downstream for each sampling site.

Table 2. (cont.)

SITE	DATE	As(T)	As(III)	As(V)	Co	Ni	Ca	Mg	SO_4
22	05/95	565	32	533	84	63	36	7.5	16
23	05/95	602	30	572	88	57	36	7.5	17
24	05/95	571	34	537	88	83	37	7.7	16
25	07/94	1815	14	1801	110	68	53	10	21
	05/95	573	30	543	90	64	37	7.7	16
26	91-92	62	na	na	nd	nd	21	8	7.9
27	07/94	710	18	692	5.9	5.4	29	7.1	9.1
28	91-92	324	na	na	nd	nd	47	21	18
	07/94	416	15	401	3.4	3.8	25	6.1	8.4
	05/95	252	27	225	6.4	27	25	6.3	9.9
29	07/94	393	29	364	4.0	5.2	26	6.1	8.5
	05/95	312	15	297	25	36	27	6.4	11
30	07/94	823	8.6	814	35	23	33	7.4	13
	05/95	334	16	318	40	41	29	6.6	12
31	07/94	761	8.2	753	17	21	34	7.4	12
32	91-92	313	na	na	nd	nd	43	11	18
	07/94	231	14	217	14	9.2	37	8.3	2.1
33	91-92	406	na	na	nd	nd	39	10	13
	09/94	265	3.2	262	24	11	44	9.4	10.6
34	09/94	755	115	640	83	34	67	25	64
35	09/94	522	3.7	518	19	10	51	13	23
	05/95	397	9.1	388	33	53	30	6.8	11
36	91-92	522	na	na	nd	nd	42	11	19
37	09/94	30	6.5	23	4.0	3.5	6.7	2.0	6
GW1	91-92	880	na	na	144	83	76	nd	32
	09/94	750	4.6	745	140	100	71	13	29
GW2	91-92	2090	na	na	235	100	47	11	25
GW3	91-92	6970	na	na	1673	458	77	50	32
	07/94	9707	6032	3675	1700	440	80	35	27
	09/94	9693	7531	2162	1800	450	82	36	25
GW4	09/94	9452	7268	2184	1700	440	81	35	25
GW5	09/94	8869	3874	4995	1700	440	82	36	25
GW6	09/94	9933	7117	2816	1800	450	82	36	25
GW7	09/94	9168	5629	3539	1700	440	81	35	25

NOTE: na: not analyzed; nd: not detectable

fault zones. The course of Farr Creek near site 33 is controlled by two faults which intersect just north of the creek, and another fault crosses the creek at site 36. Previous studies (MOE, 1977) have shown that groundwaters, particularly those originating in the Coleman Formation, do contain elevated concentrations of As and other metals.

The variation of total As with time is shown in Figure 4 for eight sites. These sites were selected as they had been sampled repeatedly during the 1991-1992 and 1994-1995 sampling programs. Only three sites, 6, 20, and 28, are relatively complete in terms of the number of data points. Sites 8, 10, and 13 show a general increase in total As with time. Sites 8 and 10 are located in Cobalt Lake site; 8 is south of the Nipissing high-grade mill drainage adjacent to a waste rock pile and site 10 is about 50 m north of the park that separates the lake into two basins. Site 13 is located near the Right of Way mine, just downstream from the Nipissing low-grade mill drainage. Site 8 is unlikely influenced by the Nipissing high-grade mill drainage but is influenced by the waste rock pile and the submerged tailings. The data for 1991-1992 show a slight, continual increase which levels off between 1992 and 1995. Sites 10 and 13 follow a similar trend with peak concentrations in 1994. Arsenic released from the submerged tailings in Cobalt Lake is probably gradual and continual. Release from the Nipissing low-grade mill tailings may also be continual but would peak during periods of high surface runoff due to the dissolution of efflorescent salts which form on the surface of the tailings during the summer months. Analyses of these salts by Dumaresq (1993) showed that they contained very high concentrations of As and other metals. At these three sites, the increase in total As with time may be related to the type of source material rather than as a consequence of seasonal variations during the sampling events. The tailings will continue to release significant amounts of As to the drainage system for many years.

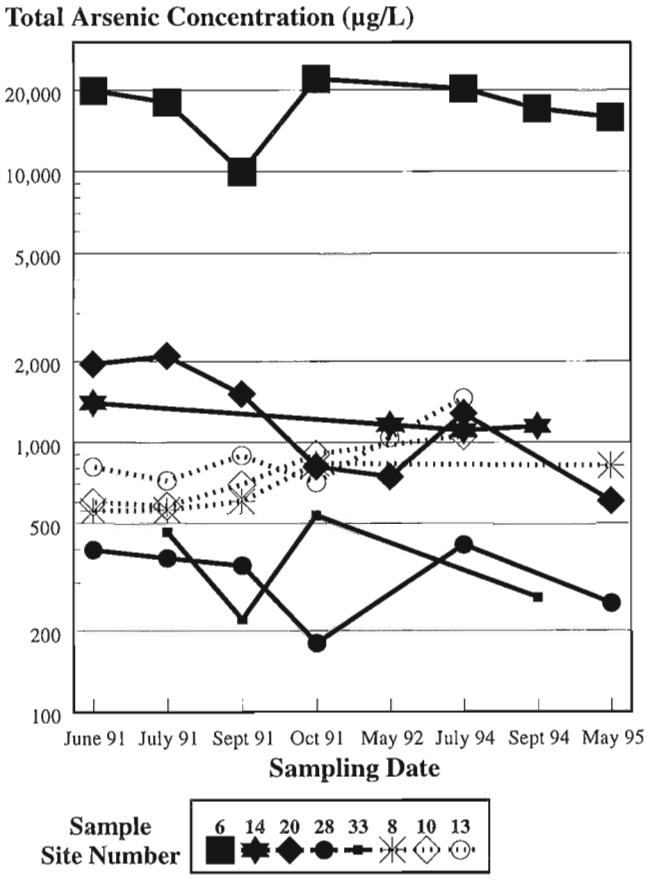

Figure 4. Temporal variation in total dissolved As for selected sample sites.

In general, As concentrations at sites 6, 14, 20, 28, and 33 show a decreasing trend with time. Samples from site 6 were taken from the Nipissing high-grade mill drainage, hence the very high total As concentrations. The other sites are located progressively downstream in either Mill or Farr Creek. At most of these sites there is an initial decrease within the first sampling period (1991-1992) that may be seasonally related. For example, efflorescent salts would first dissolve, flushing As and other metals into the drainage system. As the fall season progresses and the area becomes wetter, dilution would occur due to increased runoff and groundwater discharge.

During the 1994 sampling period, rainfall was, on average, about 70 mm per month from May to October. During this period a decrease in concentration was observed at site 6. The wetlands in 1994 were saturated and difficult to walk through. In May 1995, a total of 134 mm of rain fell, 104 mm of which occurred days before the sampling period. During this period, however, the wetlands downstream from the Farr Creek-Mill Creek confluence were dry and easily traversed on foot. The higher rainfall and lower total As concentrations in May 1995 relative to 1994 suggests dilution through increased runoff, yet water levels in the creeks were lower in 1995. It is possible that the antecedent heavy rain in May 1995 had thoroughly depleted the source area of accumulated, readily-soluble oxidation products prior to the sampling event. Rapid transport of the released As through the surface drainage system rendered low analyses in the samples subsequently collected.

Arsenic speciation data are also shown in Table 2. For surface waters sampled in July 1994, As(III) constitutes 0.8 to 11.8% of total As; for September 1994, 0.7 to 51.4%; and for May 1995, 1.2 to 10.7%. The two high values (51.4 and 21.7%) for September 1994 correspond to total As concentrations of only 11.1 (site 1; Brief Lake) and 30 µg/L (site 37; Lake Timiskaming), respectively. The high proportion of As(III) in the Lake Timiskaming sample appears to reflect the mixing of the well water from Bucke Park with surface waters. At Brief Lake, groundwater may be mixing with the surface waters. If these data are spurious and these samples are not considered, then As (III) content ranges from 0.7 to 15.2% of total As. These values indicate that strongly oxidizing conditions prevail in the surface waters. In contrast, in the more reducing groundwater samples As(III) constitutes 43.7 to 77.7% of total As. The high proportion of the more toxic species is of concern as these samples represent drinking water from the Bucke Park campground (note: as of early summer, 1995, the well was closed to the public by the

Timiskaming Health Unit, New Liskeard; S. Deegan, pers. comm., 1995). Dumaresq (1993) measured As in 39 samples from 23 private wells in the area and found that "total dissolved" As ranged from 1 to 13 µg/L (mean of 3 µg/L). The Bucke Park well, therefore, is an anomaly.

At sites where two or more samples were taken during the 1994-1995 period the As(III) content decreased for half of the samples and increased in the rest. The increase in As(III) relative to As(V) may reflect a greater groundwater input at the time of sampling or may indicate that less secondary minerals are being dissolved. All these factors must be considered along with the seasonal variations to determine the mechanisms of As release from the tailings sites.

Cobalt and nickel

The concentrations of dissolved Co and Ni in the samples are highly variable (Table 2). Cobalt ranges from less than detection to more than 3000 µg/L and Ni from less than detection to more than 600 µg/L. High concentrations are found in the Nipissing high-grade mill (sites 6 and 7) and LaRose (site 15) surface samples and in the Bucke Park groundwater samples (GW3-GW7) and correlate well with total As. The LaRose samples are more enriched in Co relative to the Nipissing high-grade mill samples confirming the heterogenous nature of the tailings. The high concentrations observed at Bucke Park suggests that the Coleman Formation (and related nearby Agaunico mineralization) is the source of the groundwater in this well. Previous studies have shown that groundwater from the Coleman Formation contain the highest average concentrations of As, Co, and Ni of any groundwaters in the area (MOE, 1977). For surface water samples, high Co and Ni contents can be related to the dissolution of secondary minerals such as erythrite and annabergite that are produced and stable during drier periods. Cobalt and nickel in the groundwater samples, however, may be derived directly from primary ore minerals such as cobaltite or nickeline.

The concentrations of Co and Ni observed in this study are comparable to those documented in Boyle et al. (1969), except that the Co content from LaRose and Bucke Park determined in this study are an order of magnitude greater. Boyle et al. (1969) observed that both Co and Ni were relatively mobile up to pH 8 and that Ni has a greater mobility in waters associated with the Palaeozoic (carbonate-rich) rocks. The dramatic decrease in concentrations for both Co and Ni observed in Mill Creek (e.g., from sites 15 to 20, Table 2) indicates that co-precipitation or sorption processes are occurring.

Surface water quality objectives for drinking water have not been established for Co but maximum values of 1000 µg/L for livestock and 500 µg/L for irrigation have been set elsewhere (e.g., Saskatchewan Environment and Public Safety, 1988). Most of the surface water samples are well below these limits. For Ni, a maximum of 50 µg/L is set for drinking water and variable amounts for freshwater aquatic life based on the hardness of water (CCREM, 1985; Saskatchewan Environment and Public Safety, 1988). Some of the surface water samples are within the guidelines, others may be considered hazardous.

Calcium, magnesium, and sulphate

Calcium and magnesium concentrations are given in Table 2. Calcium ranges from 21 to 82 mg/L and Mg from less than detection to 50 mg/L. The higher concentrations of Mg (e.g., 35 to 50 mg/L) are only observed in the groundwater samples from Bucke Park. There is no apparent relationship between Ca and Mg with the other metals reported. Based on the hardness calculation (total hardness = $2.5(Ca^{2+}) + 4.1(Mg^{2+})$) of Freeze and Cherry (1979), these waters would be considered hard with values greater than 100 mg/L (m-eq $CaCO_3$; data not shown). The data reflect the extent of carbonate weathering in the study area. Boyle and Dass (1971) reported that waters leaching the ore veins are mainly bicarbonate-sulphate-rich waters.

Sulphate contents range from about 3 to 130 mg/L (Table 2). Sulphate may be derived from primary sulphide minerals or sulphosalts or from secondary efflorescent salts such as gypsum and thenardite. Higher metal levels appear to correspond to elevated levels of SO_4^{2-} (e.g., sites 6, 14, 15, and 17). These concomitant increases probably reflect dissolution of the secondary alteration products.

SUMMARY AND CONCLUSIONS

Water samples from the Farr Creek drainage basin, Cobalt, Ontario, were collected to study the aqueous transport of As and other metals in a weakly alkaline environment. The Cobalt area, once renowned for its bonanza silver deposits, is now characterized by numerous tailings deposits, waste rock piles, and remnant historical mine workings. Very limited mitigation has been undertaken since mining ceased and thus contamination of the surface drainage system from leaching of the widespread mine waste continues. Currently, concentrations of total dissolved As exceed water quality criteria for drinking (25 µg/L) and sustaining aquatic life (50 µg/L) by, in some cases, 2 to 3 orders of magnitude. There is some attenuation downstream through the wetlands but drainage with high As concentrations (300-500 µg/L) still enters Lake Timiskaming, the receiving water body of the Farr Creek system. Increases in As concentration downstream from the wetlands area suggest that a groundwater contribution to the drainage system must be considered.

With weakly alkaline pH (average 7.9) and Ca and Mg as the dominant cations, the overall water chemistry in the study area reflects a major influence by the carbonate-equilibria. Cobalt and nickel appear to correlate well with total As in the surface waters, suggesting that the source of the metals is likely ephemeral secondary minerals produced by weathering of Co and Ni arsenides and sulpharsenides. The weathering products are readily dissolved during wet periods and the metals flushed into the drainage system. Submerged tailings probably also release metals to the surface waters but at a slower rate. Thus, mitigation of exposed surfaces will certainly help abate this situation but will not eliminate it.

ACKNOWLEDGMENTS

The authors are grateful to G.E.M. Hall, G. Gauthier, and W.H. Nelson of Method Development Laboratory (GSC) for As speciation data; to R.A. Meeds and N.B. Bertrand of Analytical Chemistry (GSC) for ICP-AES and ICP-MS data; to C. Veys of Analytical Chemistry for anion determinations; to the graphics unit of Environment Canada for digitizing maps; and to K. Mooney (GSC) for preparation of the tables. Thanks are due to Agnico Eagle for permission to sample in the Cobalt area, and for logistical support in 1995, and to S. Forsyth (Agriculture Canada) and C. MacDonald (Environment Canada) for their continued support of C.G. Dumaresq. G.E.M. Hall and I.R. Jonasson provided helpful reviews of the manuscript.

REFERENCES

Anderson, P.
1993: Cobalt mining camp tailings inventory, Cobalt, Ontario; unpublished report, Ministry of Northern Development and Mines, 196 p.

Boyle, R.W.
1968: The geochemistry of silver and its deposits; Geological Survey of Canada Bulletin 160, 264 p.

Boyle, R.W. and Dass, A.S.
1971: The geochemistry of the supergene processes in the native silver veins of the Cobalt-South Lorrain area, Ontario; in The Silver-arsenide Deposits of the Cobalt-Gowganda Region, Ontario, (ed.) L.G. Berry; Canadian Mineralogist, v. 11, p. 358-390.

Boyle, R.W. and Jonasson, I.R.J.
1973: The geochemistry of arsenic and its use as an indicator element in geochemical prospecting; Journal of Geochemical Exploration, v. 2, p. 251-296.

Boyle, R.W., Dass, A.S., Church, D., Mihailov, G., Durham, C., Lynch, J., and Dyck, W.
1969: Research in geochemical prospecting methods for native silver deposits, Cobalt area, Ontario, 1966; Geological Survey of Canada, Paper 67-35, 91 p.

Cullen, W.R. and Reimer, K.J.
1989: Arsenic speciation in the environment; Chemical Reviews, v. 89, p. 713-764.

CCREM (Canadian Council of Resource and Environment Ministers)
1985: Canadian Water Quality Guidelines; prepared by the Task Force on Water Quality Guidelines of the Canadian Council of Resource and Environment Ministers.
1987: Canadian Water Quality Guidelines; prepared by the Task Force on Water Quality Guidelines of the Canadian Council of Resource and Environment Ministers.

Dumaresq, C.
1993: The occurrence of arsenic and heavy metal contamination from natural and anthropogenic sources in the Cobalt area of Ontario; MSc. thesis, Carleton University, Ottawa, 326 p.

Eisler, R.
1988: Arsenic hazards to fish, wildlife, and invertebrates: a synoptic review; Biological Report 85 and Contaminant Hazard Reviews, Report No. 12, United States Fish and Wildlife Services, Laurel, Maryland, 92 p.

Ferguson, J.F. and Gavis, J.
1972: A review of the arsenic cycle in natural waters; Water Research, v. 6, p. 1259-1274.

Freeze, R.A. and Cherry, J.A.
1979: Groundwater; Prentice-Hall, Inc., Englewood Cliff, New Jersey, 604 p.

Government of Canada, Environment Canada, and Health and Welfare Canada
1994: Arsenic and its compounds; Canadian Environmental Protection Act, Priority Substances List Assessment Report, Ottawa, 56 p.

Hawley, J.
1980: The chemical characteristics of mineral tailings in the province of Ontario, 1979; Ontario Ministry of the Environment, Toronto, 234 p.

Health and Welfare Canada
1989: Guidelines for Canadian drinking water quality, supporting documentation; Monitoring and Criteria Division, Health and Welfare Canada, Ottawa, 9 p.

Jambor, J.L.
1971: General geology; in The Silver-Arsenide Deposits of the Cobalt-Gowganda Region, Ontario, (ed.) L.G. Berry; Canadian Mineralogist, v. 11, p. 12-33.

MOE (Ministry of the Environment)
1977: A report on the continued investigations into the occurrence of metals and arsenic in private drinking water supplies of the Tritown area; Report No. 2, Toronto, 91 p.

NRCC (National Research Council of Canada)
1978: Effects of arsenic in the Canadian environment; Associate Committee on scientific Criteria for Environmental Quality, National Research Council of Canada No. 15391, Ottawa, 349 p.

OWRC (Ontario Water Resources Commission)
1967: The Cobalt camp: a preliminary assessment of water pollution by mining wastes in the Cobalt area; Government of Ontario, Toronto, 106 p.

Penrose, W.R.
1974: Arsenic in the marine and aquatic environments: analysis, occurrence and significance; CRC Critical Reviews in Environmental Control, v. 4, p. 465-482.

Petruk, W.
1971: General characteristics of the deposits; in The Silver-Arsenide Deposits of the Cobalt-Gowganda Region, Ontario, (ed.) L.G. Berry; Canadian Mineralogist, v. 11, p. 76-107.

Petruk, W., Jambor, J., and Boyle, R.W.
1971: History of the Cobalt and Gowganda area; in The Silver-Arsenide Deposits of the Cobalt-Gowganda Region, Ontario, (ed.) L.G. Berry; Canadian Mineralogist, v. 11, p. 1-7.

Saskatchewan Environment and Public Safety
1988: Surface water quality objectives; Water Quality Branch, Saskatchewan Environment and Public Safety, WQ 110, 33 p.

Geological Survey of Canada Project 680023-ZC

Geometric aspects of a large extensional vein, Donalda deposit, Rouyn-Noranda, Quebec

François Robert, Anne-Marie Boullier[1], and Karima Firdaous[1]
Mineral Resources Division, Ottawa

Robert, F., Boullier, A.-M., and Firdaous, K., 1996: Geometric aspects of a large extensional vein, Donalda deposit, Rouyn-Noranda, Quebec; in Current Research 1996-C; Geological Survey of Canada, p. 147-155.

Abstract: The Donalda gold deposit in the Noranda district of the Abitibi belt is an unusually extensive shallow-dipping quartz vein covering nearly 0.5 km^2. A detailed structural analysis of the vein shows that it consists of dominant shallowly south-dipping arrays of extensional veins, moderately south-dipping, east-west reverse shear zones, and a poorly developed conjugate set of north-dipping reverse shear zones. Local continuity of vein quartz between the three types of structures indicates their contemporaneity. The shallow-dip arrays consist of overlapping first-order extensional veins linked by moderately dipping second-order extensional veins; the shallow-dip arrays are interpreted as "extensional" arrays formed perpendicular to the minimum external strain axis. The kinematics and nature of the different structures indicate that the Donalda deposit formed as a result of north-south shortening and subvertical elongation, common to many gold-quartz vein deposits in southern Abitibi belt.

Résumé : Le gisement d'or de Donalda du district de Noranda dans la ceinture de l'Abitibi consiste en une veine de quartz à pendage faible, couvrant près de 0,5 kilomètre carré, ce qui est rare pour une telle entité. Une étude structurale détaillée a montré que la veine se compose principalement de segments à pendage faible vers le sud, constitués de veines d'extension, mais aussi de zones de cisaillement inverse d'orientation est-ouest à pendage modéré vers le sud et d'un jeu conjugué faiblement développé de zones de cisaillement inverse à pendage modéré vers le nord. Une continuité locale du quartz entre les veines des trois types de structures atteste de leur contemporanéité. Les segments à pendage faible combinent plusieurs veines d'extension de premier ordre disposées en relais, reliées par des veines d'extension de deuxième ordre à pendage plus fort; ces segments à pendage faible représentent des structures en extension formées perpendiculairement à l'axe externe d'allongement. La cinématique et la nature des différentes structures indiquent que le gisement de Donalda s'est formé par raccourcissement nord-sud et allongement subvertical, comme c'est le cas de nombreux gisements d'or filonien de la partie sud de la ceinture de l'Abitibi.

[1] Centre de Recherches Pétrographiques et Géochimiques, Conseil national de la recherche scientifique, B.P. 20, 54501 Vandoeuvre-les-Nancy, Cedex, France

INTRODUCTION

Extensional veins are common components of shear-zone-related quartz-carbonate vein networks (Hodgson, 1990; Robert, 1990). In most cases, they are subhorizontal and fringe laminated fault-fill veins occurring in the central parts of moderately- to steeply-dipping reverse shear zones. Extensional veins are components of arrays at the lateral, up- and down-dip terminations of fault-fill veins, or of planar tabular bodies extending in low strain rocks away from fault-fill veins over significant distances (Robert, 1990). In the latter case, veins may occur over large areas, either as continuous single bodies or as combinations of distinct, overlapping, and interconnected segments.

Such tabular subhorizontal extensional veins developed in greenschist grade rocks during crustal shortening have also been used as evidence for lithostatic fluid pressures at mid-crustal levels (Sibson et al., 1988; Sibson, 1990). Thus, understanding their detailed geometry and mode of propagation also has bearing on the phenomenon of fluid overpressures and on the scale at which it may occur.

This note presents the preliminary results of a structural analysis of a large, shallow-dipping extensional vein at the Donalda deposit near Rouyn-Noranda, Quebec, described by Riverin et al. (1990). This vein covers an area of approximately 0.5 km^2 and is well exposed on walls and pillars of accessible mine workings. It provides a unique opportunity to examine the detailed geometric configuration of the vein and its relations with moderately dipping shear zone-hosted veins.

GEOLOGY OF THE DONALDA DEPOSIT

The geology of the Donalda deposit has previously been described in detail by Riverin et al. (1990), and only the key points are presented here. The deposit occurs in the southern part of the Noranda mining camp, less than 1 km northeast of the town of Rouyn-Noranda (Fig. 1). It straddles the contact between two volcanic formations separated by the Horne Creek fault, a major fault striking east-west and dipping 70° to the north. The Quemont rhyolite occurs on the north side of the fault and the Wilco andesite to the south. The deposit comprises two auriferous quartz veins, dipping shallowly (No. 1 vein) to moderately (No. 2 vein) to the south (Fig. 2). The No. 1 vein contributed the bulk of the ore and was the only vein accessible during the present study. This vein cuts both the Wilco andesite and the Quemont rhyolite, but is offset by the Horne Creek fault. Both volcanic formations and the No. 1 vein are cut by the D'Eldona diabase dyke, striking east-northeast and 20 m thick; the diabase dyke is also offset by the Horne Creek fault (Fig. 1, 2). The Donalda deposit also occurs in proximity to the Horne and Quemont auriferous volcanic-associated massive sulphide (VMS) deposits (Fig. 1)

The No. 1 vein strikes east and has an overall dip of 20° to the south. As shown in Figure 1, the vein occurs on both sides of the Horne Creek fault, covering a minimum area of 0.5 km^2, over which its thickness averages 20-30 cm. As described by Riverin et al. (1990), it consists of alternating moderately-dipping and dominant shallowly-dipping mineralized vein segments (Fig. 2), the latter being fringed by common low-angle splays. The vein and its numerous splays have sharp planar walls and are internally banded parallel or subparallel to their walls.

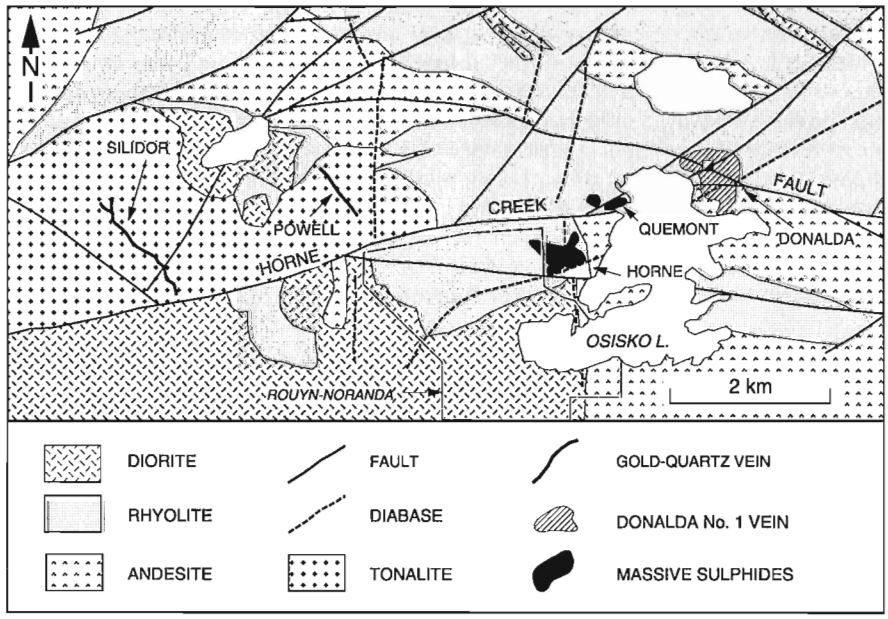

Figure 1. *Simplified geological map of the Noranda area, showing the surface projection of the Donalda and other nearby base metal and gold deposits. Modified from Riverin et al. (1990).*

GEOMETRIC ELEMENTS OF THE NO. 1 VEIN

At the mine scale, the geometry of the No. 1 vein is defined by alternating vein segments of shallow and moderate dips to the south (Riverin et al., 1990). The shallowly dipping segments are more extensive than the moderately dipping ones, resulting in a stepped vein with an overall dip of 20° to the south (Fig. 3A). By virtue of their more restricted dimensions, the moderate-dip segments form relays between larger shallow-dip segments. As illustrated in Figure 3, this type of pattern is observed at kilometre to metre scales.

The shallow-dip segments of the No. 1 vein in turn comprise two sets of connected extensional veins: "first-order" veins, the most extensive ones, fringed by "second-order" veins of more restricted dimensions (Fig. 4A). The first-order veins are relatively continuous and form an array of overlapping veins parallel to the shallow-dip segments in which they occur. Second-order veins have varied dimensions and orientations; they form a series of splays branching off the first-order veins and linking them in relay zones (Fig. 4). Our observations suggest that, in contrast, the moderate-dip segments of the No. 1 vein contain very few, if any, second-order veins. In many cases, the arrangement of first- and second-order veins in shallow-dip segments of the No. 1 vein is very similar to that observed at the mine scale (Fig. 3, 4), suggesting a fractal character of the geometry of the vein.

In addition, a small number of vein-bearing, moderately north-dipping shear zones were recognized as geometric elements probably related to the No. 1 vein. In the following paragraphs, we describe successively the detailed geometry of shallow-dip and moderate-dip segments of the No. 1 vein and their main components, followed by that of the moderately north-dipping shear zones.

Shallow-dip vein segments

As indicated above, each significant shallow-dip segment of the No. 1 vein consists of a number of first-order veins, generally subparallel to the segment but of slightly different orientations, linked to each other by second-order veins.

First-order veins

First-order veins in shallow-dip segments vary in dip from 10 to 40° to the south and range in strike from 025 to 140° (Fig. 5A). Their average orientation is 090-20° (right-hand rule), parallel to the average orientation of shallow-dip segments (Riverin et al., 1990). In a given local area of the mine, the first-order veins show a consistent parallel orientation. However, other areas of the mine are characterized by slightly different orientations of first-order veins, which may correspond to independant vein segments propagating in slightly different directions (see below). First-order veins range in thickness from 10-100 cm, and their dip lengths generally exceed 5 m.

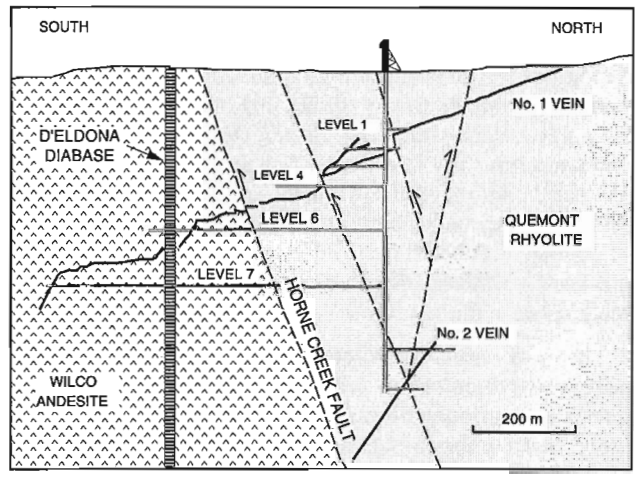

Figure 2. *Geological north-south cross-section through the shaft of the Donalda deposit. Adapted from Riverin et al. (1990).*

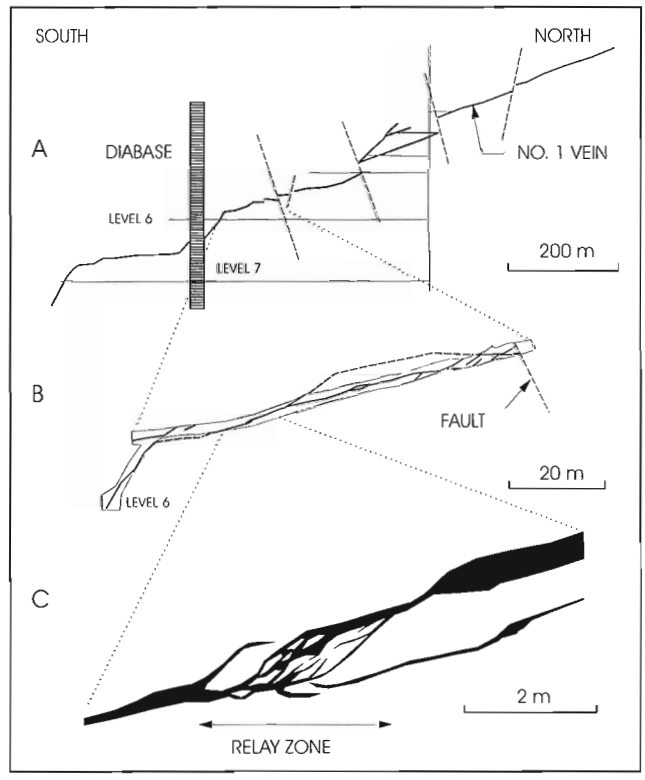

Figure 3. *Geometry of the No. 1 vein at different scales as seen on north-south cross-sections.* ***A)*** *Simplified cross-section through the shaft, modified from Figure 2.* ***B)*** *Cross-section showing details of a shallow-dip segment of the vein.* ***C)*** *Detail of the relay zone between two first-order veins.*

Second-order veins

Second-order veins are all systematically linked to first-order veins. They are generally planar (Fig. 4B), but in a few areas they have clear sigmoidal shapes (Fig. 4C). Second-order veins are typically less than a few tens of centimetres thick and their continuity along the dip is less than a few metres. Although they occur both in the hangingwalls and footwalls of dilatant en échelon first-order veins, second-order veins do not have a uniform distribution: they are more abundant in relay zones at the terminations of en échelon first-order veins.

In most cases, intersections between first- and second-order veins do not show crosscutting relationships but rather quartz is continuous beween the two vein orders. Furthermore, in a number of cases, the total vein thickness remains approximately constant in the transition from a single first-order vein to a relay area containing mostly second-order veins, as is the case in Figure 4C. Such relationships suggest that each second-order vein represents an increment of development of the first-order vein.

In north-south cross-section, second-order veins display a range of angular relations with the first-order veins. They have dips that are either shallower, or more commonly steeper, than those of first-order veins, and in some cases dips in the opposite direction (Fig. 4A, 5A). Second-order veins have the same range of strikes as the first-order veins, and their dips vary between those of first-order veins in shallow- and moderate-dip segments of the No. 1 vein (Fig. 5A). A significant number of second-order veins are in fact parallel to the moderate-dip first-order veins, suggesting that moderate-dip segments of the No.1 vein may in fact be well developed equivalents of second-order veins.

As discussed below, the intersections between pairs of first- and second-order veins may yield information on the propagation directions of the vein segments. We have therefore measured wherever possible, but most commonly calculated, the orientations of intersections between such pairs of

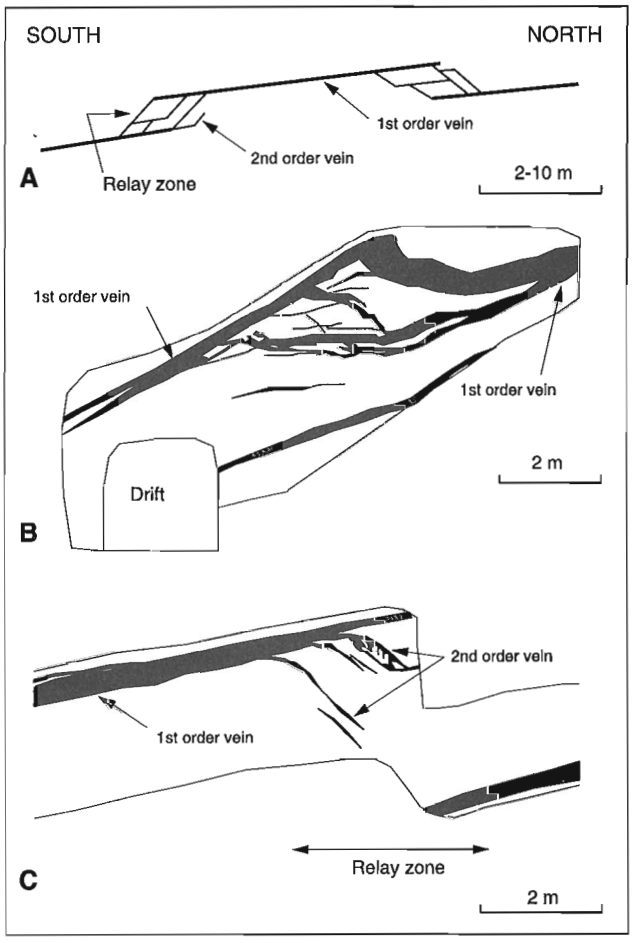

Figure 4. *Geometric relations between first- and second-order veins in shallow-dip segments of the No. 1 vein.* ***A)*** *Schematic representation of observed elements and their relationships.* ***B)*** *Relay zone showing abundant, relatively planar second-order veins between two first-order ones; Level 2.* ***C)*** *Sigmoidal second-order veins in a relay zone; slightly above Level 1.*

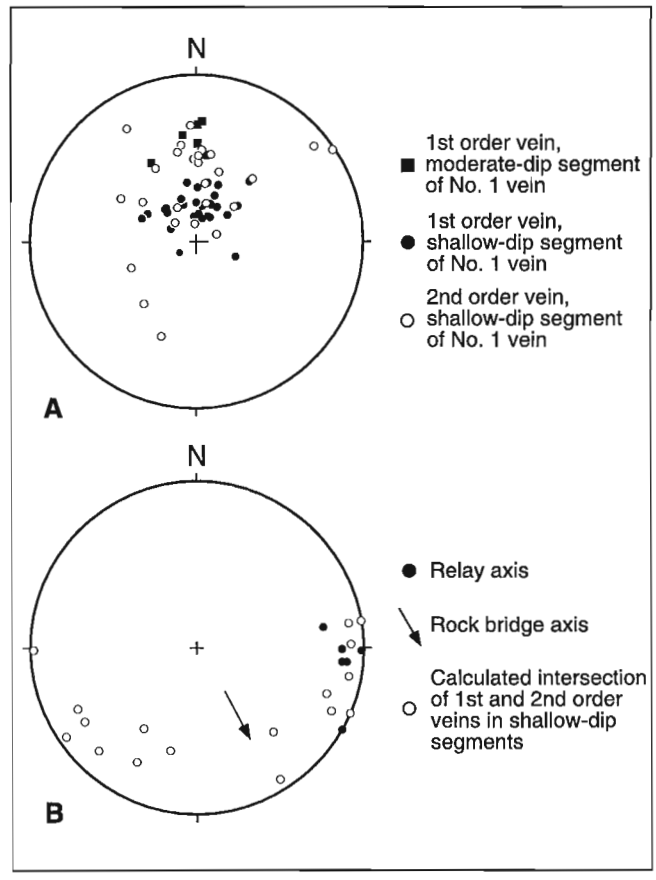

Figure 5. *Stereographic projections of structural elements of the No. 1 vein, equal area, lower hemisphere.* ***A)*** *Poles to first- and second-order veins in shallow-dip segments and to first-order veins in moderate-dip segments.* ***B)*** *Vein intersections and other linear elements of the veins.*

veins. The intersections between pairs of first- and second-order veins have shallow plunges and are grouped around two main directions: 090° and 225° (Fig. 5B). However, one should keep in mind that calculated intersections are in most cases less accurate than ones that have been measured directly. The 090° intersections are also parallel to measured axes of relay zones between overlapping first-order veins (see below).

Relay zones between first-order veins

Relay zones of variable sizes have been observed at several localities between dilatant first-order veins in shallow-dip segments. The vertical spacing between adjacent overlapping first-order veins ranges from a few tens of centimetres (Fig. 3C) to a few metres (Fig. 4C). The first-order veins show limited overlap (Fig. 3C, 4C), and they are typically connected by a network of second-order veins. They grade into incipient breccias where these linking second-order veins are particularly abundant (Fig. 3C).

The axes of a number of relay zones have been measured directly (e.g. Fig. 6). They mainly trend east-west and have subhorizontal plunges (Fig. 5B), parallel to one of the groups of intersections between first- and second-order veins. The relay zones do not present any systematic sense of stepping along a given shallow-dip segment of the No. 1 vein. Both upward steps (Fig. 3C, 6) and downward steps (Fig. 4C, 6) were observed, but upward steps must dominate, given the overall 20° dip to the south of the shallow-dip segments.

Moderate-dip vein segments

Our observations indicate that moderate-dip segments of the No. 1 vein are composed of single continuous first-order veins, a few tens of centimetres thick, with very few, if any, fringing second-order veins. The first-order veins dip moderately to the south (Fig. 2) and have a relatively constant orientation of 090-50° (Fig. 5A)

Intersections between shallow-dip and moderate-dip segments of the No. 1 vein have only been observed at one locality. Here, first-order veins of both segments are simply continuous into one another, without any apparent discontinuity, indicating that they are contemporaneous. This is similar to the relation observed between first- and second-order veins in shallow-dip segments.

In the Wilco andesite, the walls of moderate-dip vein segments are moderately foliated over a few tens of centimetres, in contrast to those along shallow-dip segments. Some foliation planes contain striations with a steep rake to the west. In thin section cut perpendicular to foliation and parallel to striations, well-developed "C-S" structures indicate reverse movement along the vein walls (Fig. 7).

Moderate-dip shear zones

Vein-bearing shear zones, not previously documented, have been observed at two localities. They strike east-west, dip 50-65° to the north, and are 0.5-1.0 m thick. These shear zones are defined by well-developed foliation, subparallel to their

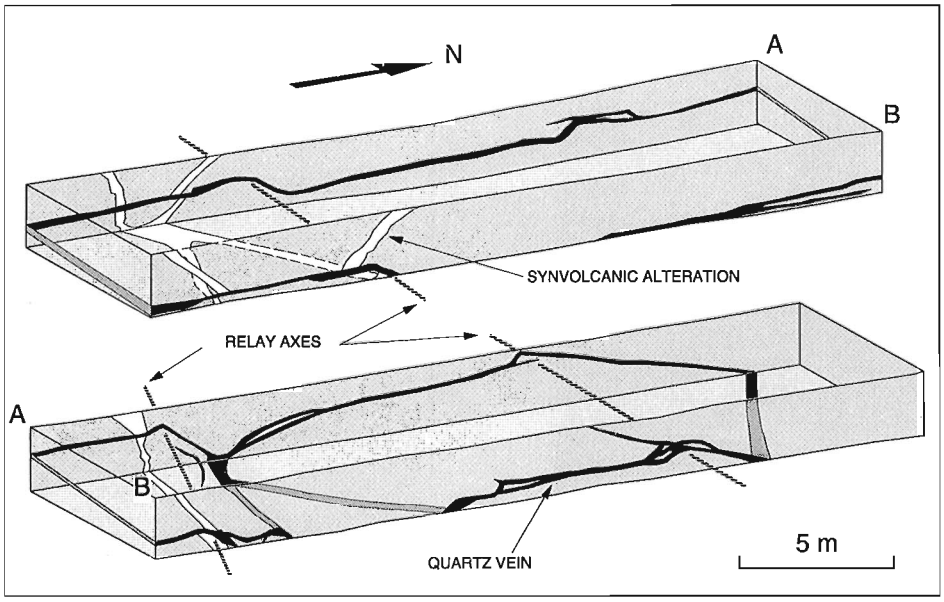

Figure 6. *Three-dimensional representation of a portion of a shallow-dip vein segment mapped in detail. It shows the geometry of the vein, axes of relays, and offsets of synvolcanic alteration bands along the vein; low-angle raise above Level 7.*

envelope, and they contain massive to laminated central, fault-fill veins. In both cases, down-dip striations on foliation planes indicate that vertical movements took place along the shear zones. In one case, the obliquity of the foliation with the shear zone boundary indicates reverse movement (Fig. 8). It is not clear how much of the total reverse vertical offset of the No. 1 vein is related to the shear zone, to the overprinting gougy fault (Fig. 8), or both. In the other case, deflection of the No. 1 vein indicates reverse movement in the order of a few metres. Besides the late structural complications, these north-dipping shear zones are similar in many respects to auriferous ones present in many other deposits in the Abitibi greenstone belt (Robert, 1990).

The age relationships observed between the No. 1 vein and the moderately north-dipping shear zones are different at the two locations. In one case (Fig. 8), the No. 1 vein segment in the footwall of the shear zone clearly cuts the foliation and merges without discontinuity with the vein central to the shear zone. Such relations suggest that the No.1 vein and that in the shear zone are contemporaneous and have formed during or after shear zone development. At the other location, the shear zone and its central laminated quartz vein cut and offset the No. 1 vein.

The conflicting crosscutting relationships documented between the No. 1 vein and the two north-dipping shear zones can be interpreted to indicate broadly coeval development of the two types of structures but the number of observations is rather limited. The continuity of vein quartz between the two types of structures provides a stronger case for this interpretation.

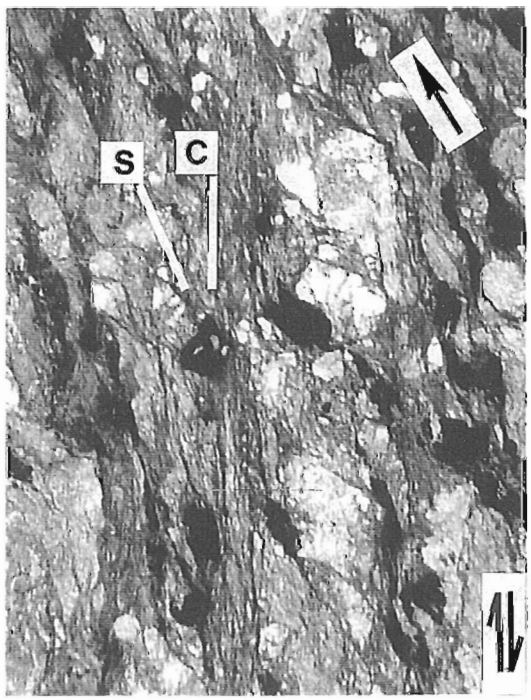

Figure 7. Photomicrograph of foliated wallrocks adjacent to a moderate-dip vein segment (Level) looking west, showing "C-S" structural fabrics; Level 6. Double arrows indicate the inferred sense of shear; the single arrow points to the top of the sample. Photo is 3.4 mm wide.

INTERNAL STRUCTURE OF THE NO. 1 VEIN

Internal structures and textures of vein yield important information on the details of vein development. Preliminary mesoscopic and microscopic observations and their implications are presented here.

Rock bridges

Rock bridges are a common feature of extensional veins: they consist of elongate bands of wallrock separating en échelon extensional veins which can be incorporated as oblique fragments within the veins (Pollard et al., 1982; Foxford et al., 1991). Rock bridges result from local stress perturbations at the tip of a propagating extensional fracture, and their long axes are parallel to the local propagation direction of the fracture (Foxford et al., 1991). The long axes of only two rock bridges could be determined; they trend at 150° (Fig. 5B).

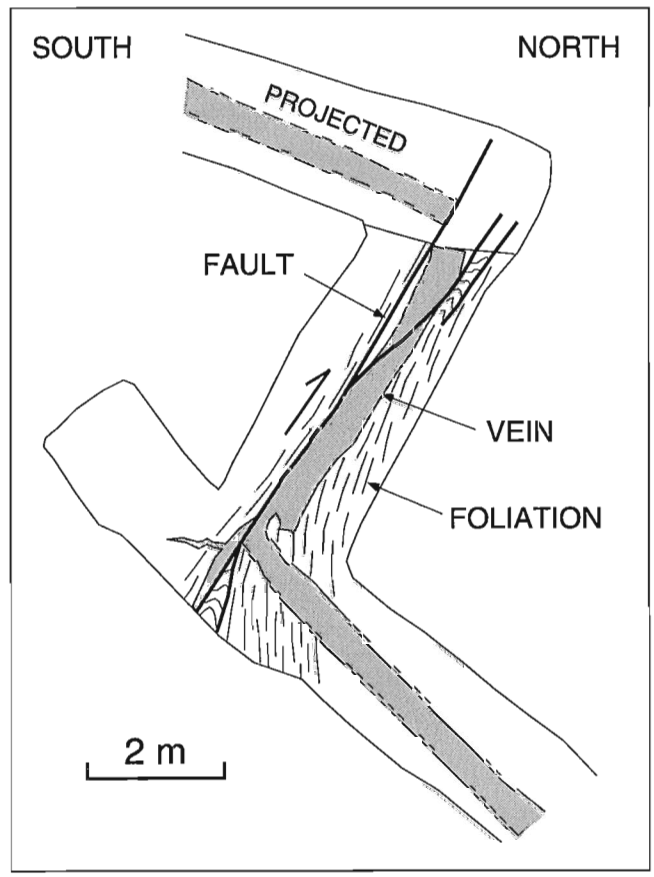

Figure 8. Detailed sketch of the intersection between a moderately north-dipping shear zone and the No. 1 vein; slightly below Level 3.

Internal layering

A dominant feature of both shallow-dip and moderate-dip vein segments is their internal layering. It is defined by alternating 1-10 cm thick layers of milky massive quartz, comb quartz and laminated quartz characterized by abundant millimetre-scale grey quartz laminae (Fig. 9). The layering is parallel to subparallel to the vein walls and is best developed in the shallow-dip vein segments. Such layering results at least in part from incremental vein growth (Fig. 9A).

Comb quartz layers are relatively common in shallow- and moderate-dip segments of the No. 1 vein. They consist of centimetre-scale, euhedral quartz crystals showing internal growth zones, at high angle to the walls of the vein or of their host layer (Fig. 10) and indicative of open-space filling. The interstices between crystals are filled with very fine grained quartz, accompanied by small amounts of chlorite, sericite, pyrite, tellurides, and gold. The coexistence of comb and very fine grained quartz in these layers probably results from sharp variations in precipitation rates, and fluid pressure variations provide on possible explanation for these contrasting textures.

Grey quartz laminae, which locally truncate quartz crystals, consist of angular clastic quartz embedded in a matrix of very fine grained quartz. They are generally parallel to the vein walls but may also dip moderately to the east (Fig. 9B), in which case small, top-to-the-west movements are indicated by offsets of other laminae. The fine grained quartz in such grey laminae does not display any preferred lattice orientations as it should if it originated by plastic deformation and dynamic recrystallization of larger quartz crystals. Although the presence of angular clastic quartz along the laminae probably reflects cataclastic processes, the very fine grained quartz matrix is best explained in the same way as the fine grained quartz interstitial to comb quartz crystals.

Movements along the vein

Two broad sets of striations have been observed along the walls of the No. 1 vein: a southerly trending set (190-220°) indicating dip-slip, north-south movements, and a westerly trending set (250-290°) indicating lateral movements. Dip-slip striations are best developed along the moderate-dip segments of the No. 1 vein where they rake steeply to the west, consistent with the reverse movements indicated by "C-S" structural fabrics. Similar striations occur locally in shallow-dip segments on the walls of first- and second-order veins, along which small reverse slips are indicated by offsets of truncated veins. Such dip-slip movements are likely related to the vein development history.

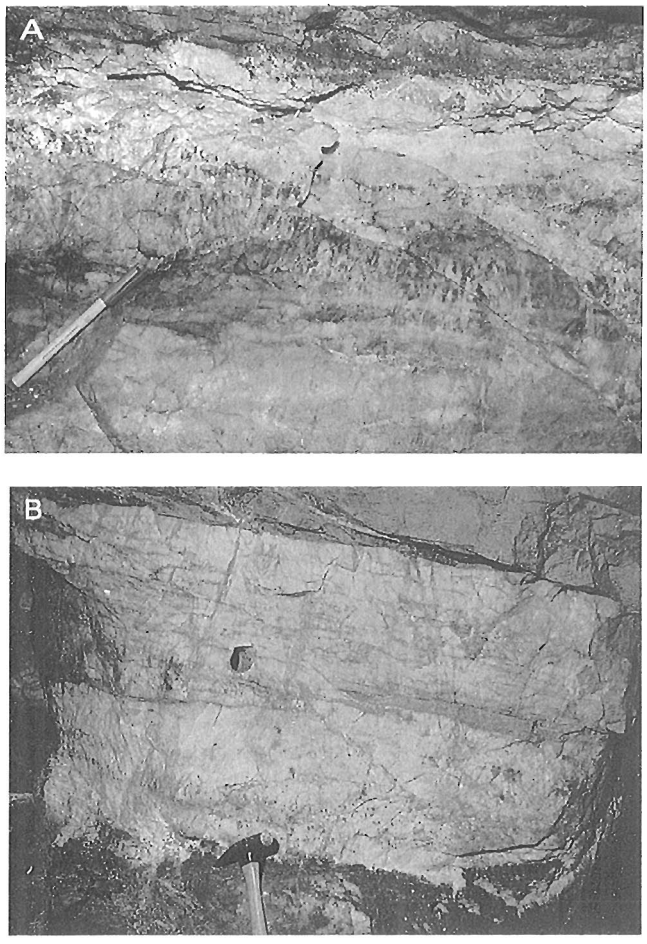

Figure 9. *Details of internal layering of first-order veins in shallow-dip segments.* ***A)*** *Massive and comb quartz layers; note thin massive quartz layers cutting comb quartz in the lower part of the vein; above Level 1. View looking east; 20 cm long pen for scale.* ***B)*** *Laminated and massive quartz layers, above Level 1. View looking north; hammer for scale. Note east-dipping shear fractures cutting the layering in both A and B.*

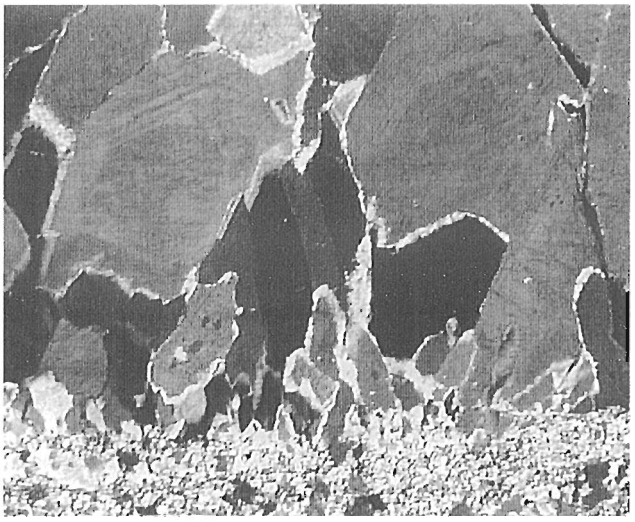

Figure 10. *Photomicrograph showing details of comb quartz developed on a lamina of microcrystalline quartz. Width of photo is 3.8 mm.*

The lateral movements indicated by the second set of striations have a top-to-the-east sense of slip based on offsets of a pair of divergent, pre-vein synvolcanic quartz-epidote alteration bands (Fig. 6, upper left). In contrast, the east-dipping reverse shear fractures observed within the veins (Fig. 9B) indicate thrusting to the west. The significance of such complex east-west movements is not understood, but some reactivation of the No. 1 vein may have occurred during late movements along the Horne Creek fault.

The opening vector along the various segments of the No. 1 vein could not be determined due to the absence of mineral fibres and to complicating effects of late lateral slip along the vein walls. However, despite minor lateral offsets along the vein, the synvolcanic alteration bands described above (Fig. 6) match relatively well above and below the vein. Such a close match suggests that the opening vector must be nearly perpendicular to the vein and precludes any significant north-south thrusting along it.

INTERPRETATIONS

Structural interpretation of the No. 1 vein

Several new observations support the interpretation of Riverin et al. (1990) that the No. 1 vein is largely an extensional vein, as opposed, for example, to a vein occupying a low angle thrust. In shallow-dip segments, individual first- and second-order veins have many attributes of extensional veins: planar walls, matching wall irregularities and rock bridges.

As described above, shallow-dip segments consist of overlapping first-order veins which in fact represent arrays of en échelon veins. An important question to address in restoring related strain axes is whether such an array is an extensional or a shear structure. The arrays defined by the first-order veins have the characteristics of "extensional arrays" as defined by Rothery (1988), in which extensional veins are at a very low angle to the array and show limited overlap, as opposed to those of "shear arrays" in which veins lie at higher angles to the array and show significant overlap. Extensional arrays are interpreted as forming perpendicular to the external extension or minimum strain direction (Rothery, 1988), in contrast to shearing arrays which form at an angle to the external shortening or maximum strain direction. Thus at Donalda, the shallow-dip segments of the No. 1 vein are interpreted as extensional arrays perpendicular to the minimum external strain direction (X), as shown in Figure 11. This interpretation is further supported by the fact that the first-order veins defining the array display relay zones of opposite sense in cross-section (Fig. 4A, 6) and by the lack of significant offset of synvolcanic alteration bands (Fig. 6), both of which are incompatible with reverse shearing along the shallow-dip segments.

As indicated above, moderate-dip segments of the No. 1 vein occupy south-dipping reverse shear zones. The veins themselves within these segments are well laminated and contain slivers of foliated wallrocks, as is typical of fault-fill veins (Robert et al., 1994), but the presence of comb quartz layers within them also indicates significant dilation during vein formation. The moderately north-dipping reverse shear zones also contain fault-fill veins, some of which are continuous with shallow-dip segments of No. 1 vein (Fig. 8). The continuity of veins observed between shallow-dip segments and the north- and south-dipping shear zones suggests that the three types of structures are broadly contemporaneous. The north- and south-dipping shear zones can thus be regarded as conjugate reverse shear zones, reflecting north-south, subhorizontal maximum shortening direction (Z) and vertical minimum shortening direction (X), compatible with the orientation of shallow-dip segments of the vein (Fig. 11). All three types of structures are compatible with their development in a north-south compressional regime.

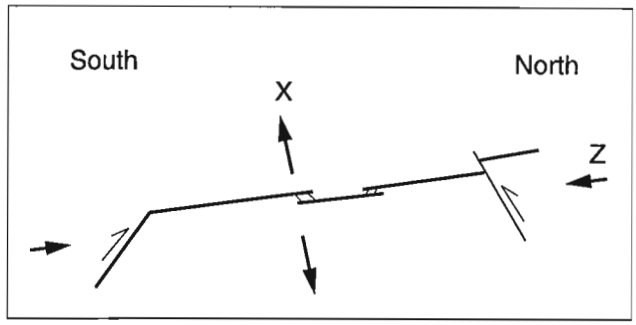

Figure 11. *Schematic diagram showing the main structural elements associated with the No. 1 vein and the interpreted external bulk strain axes.*

Development and propagation of the No. 1 vein

As outlined in the preceeding paragraphs, the No. 1 vein clearly did not result from the propagation of a single continuous extensional fracture. It rather formed by the coalescence of several first-order extensional veins linked by second-order ones to produce shallow-dip segments, which are in turn linked by moderate-dip fault-fill veins.

In a number of relay zones, the north and south terminations of overlapping first-order veins have a sigmoidal shape (Fig. 3C, 4C). Such a pattern is identical to that predicted for the interaction between two extensional cracks propagating toward each other, as a result of stress refraction at crack tips (Pollard et al., 1982). In three dimensions, one can consider that the axis of the relay zone between the two propagating cracks will be perpendicular to their local propagation directions. By analogy, the intersections between first- and second-order veins in relay zones should also be at high angles to the local propagation direction. Thus, axes of relay zones, intersection between first- and second-order veins, as well as axes of rock bridges could all tentatively be used to approximate the propagation direction of individual first-order extensional veins. The orientation of these structural elements (Fig. 5B) indicates propagation of first-order extensional veins along northeast and north directions. These very preliminary results suggest that one can use such structural features to understand the development of large extensional veins as at Donalda.

DISCUSSION

The overall geometry of the Donalda deposit, combining moderately dipping reverse shear zones and shallowly dipping extensional veins is similar to that of other shear-zone-related quartz-carbonate vein gold deposits. The interpreted north-south compressional regime at Donalda is also common to many other deposits of this type in southern Abitibi, where it is generally ascribed to a D2 increment of crustal shortening (Robert, 1990). This suggests that, despite the unique extensive development of extensional structures, the Donalda belongs to shear-zone-related quartz-carbonate vein type of gold deposits. This similarity is further supported by a fluid inclusion study (Chi et al., 1992), which shows that fluids at Donalda are typical of those found in this class of gold deposit: H_2O-CO_2, low salinity fluids, CO_2-rich fluids, and aqueous saline inclusions.

Like at many other shear-zone-related gold deposits, the Donalda vein is spatially associated with a major fault zone, the Horne Creek fault. However, field relations indicate that there are no temporal nor genetic relations between the two types of structures. There is a major kilometric stratigraphic offset along this fault (Fig. 1; Riverin et al., 1990), but the offset of the Donalda vein by the fault is only in the order of a few tens of metres at most (Fig. 2). This indicates that most of the movement along the Horne Creek fault pre-dates the vein and that there was minor post-vein reactivation of the fault, after intrusion of the diabase dyke. Furthermore, the nearly complete absence of veins and alteration within the Horne Creek fault at Donalda indicates that it did not serve as a major conduit for migration of hydrothermal fluids. As noted above, the Donalda deposit occurs in the vicinity of the Horne and Quemont auriferous VMS deposits (Fig. 1). The temporal relationships between the Donalda vein and the Horne Creek fault indicate that the vein is decidedly post-volcanic and has no genetic relation to the VMS deposits. However, it cannot be excluded that some of the Donalda gold was derived from these auriferous VMS deposits.

Finally, it is worth noting the geometric similarities between the Donalda deposit and those of Norseman, Western Australia (O'Driscoll, 1953). The main mineralized veins at Norseman (Mararoa, Crown and Royal) dip 45° and, as at Donalda, they consist of en échelon moderate-dip veins, hosted in reverse shear zones, linked by shallow-dip extensional veins (McKinstry, 1942). The difference at Norseman is that the shallow-dip extensional segments are less extensive than the moderate-dip shear-zone-hosted segments and define a "shear-link" geometry, in which extensional veins link more continuous fault-fill veins (McKinstry, 1942). An opposite situation occurs at Donalda, where the shear-zone-hosted veins are the links between extensional veins.

ACKNOWLEDGMENTS

We would like to express our appreciation to Gérald Riverin and Bernard Boily, of Inmet Mining Corporation, for their logistic and scientific support, without which this project would have not been possible. We also thank G.-X. Chi for his participation in the field work, as well as K.H. Poulsen and C.W. Jefferson for their critical reviews of the manuscript.

REFERENCES

Chi, G.-X., Guha, J., Riverin, G., and Trudel, F.
1992: Examination of an enigmatic flat gold-quartz vein deposit in the Abitibi greenstone belt – A fluid inclusion approach; Fourth Biennal Pan-American Current Research on Fluid Inclusions, Lake Arrowhead, California, Program with Abstracts, p. 23.

Foxford, K.A., Nicholson, R., and Polya, D.A.
1991: Textural evolution of W-Cu-Sn-bearing hydrothermal veins at Minas da Panasqueira, Portugal; Mineralogical Magazine, v. 55, p. 435-445.

Hodgson, C.J.
1990: An overview of the geological characteristics of gold deposit in the Abitibi Subprovince; in Gold and Base Metal Mineralisation in the Abitibi Subprovince, Canada, with Emphasis on the Quebec Segment, (ed.) S.E. Ho, F. Robert, and D.I. Groves; Geology Key Centre and University Extension, The University of Western Australia, Volume Publication 24, p. 63-100.

McKinstry, H.E.
1942: Norseman mine, Western Australia; in Ore Deposits as Related to Structural Features, (ed.) W.H. Newhouse; Princeton University Press, p. 224.

O'Driscoll, D.
1953: Operations on the Norseman field; in Geology of Australian Ore Deposits, (ed.) A.B. Edwards; Australasian Institute of Mining and Metallurgy, Volume Publications – Volume 1: Melbourne p. 138-149.

Pollard, D.D., Segall, P., and Delaney, P.T.
1982: Formation and interpretation of dilatent echelon cracks; Geological Society of America Bulletin, v. 93, p. 1291-1303.

Riverin, G., Bernard, D., and Boily, D.
1990: The Donalda gold deposit, Rouyn-Noranda, Quebec; in The Northwestern Quebec Polymetallic Belt: A Summary of 60 years of Mining Exploration, (ed.) M. Rive, P. Verpaelst, Y. Gagnon, J.M. Lulin, G. Riverin, and A. Simard; Volume Special Volume 43, Canadian Institute of Mining and Metallurgy, p. 199-209.

Robert, F.
1990: An overview of gold deposits in the Eastern Abitibi Subprovince; in The Northwestern Quebec Polymetallic Belt: A Summary of 60 years of Mining Exploration, (ed.) M. Rive, P. Verpaelst, Y. Gagnon, J.M. Lulin, G. Riverin, and A. Simard; Canadian Institute of Mining and Metallurgy, Special Volume 43, p. 93-105.

Robert, F., Poulsen, K.H., and Dubé, B.
1994: Structural analysis of lode gold deposits in deformed terranes; Geological Survey of Canada, Open File 2850. 140 p.

Rothery, E.
1988: En échelon vein array development in extension and shear; Journal of Structural Geology, v. 10, p. 63-71.

Sibson, R.H.
1990: Faulting and fluid flow; in Short Course on Fluids in Tectonically Active Portions of the Crust, (ed.) B.E. Nesbitt; Mineralogical Association of Canada, p. 93-129.

Sibson, R.H., Robert, F., and Poulsen, K.H.
1988: High-angle reverse faults, fluid-pressure cycling and mesothermal gold-quartz deposits; Geology, v. 16, p. 551-555.

Geological Survey of Canada Project 940003
Contribution CNRS-INSU, Fluides et failles #29

Granite-greenstone terranes of the northern Minto block, northeastern Superior Province, Quebec

J.A. Percival, T. Skulski, and L. Nadeau[1]
Continental Geoscience Division, Ottawa

Percival, J.A., Skulski, T., and Nadeau, L., 1996: Granite-greenstone terranes of the northern Minto block, northeastern Superior Province, Quebec; in Current Research 1996-C; Geological Survey of Canada, p. 157-167.

Abstract: The northern Minto block contains greenstone belts consisting primarily of basalt, greywacke-pelite, and andesite, with some iron-formation. Rare conglomerate and quartzite are associated with unconformities against tonalitic basement and synvolcanic plutons. The kilometre-thick belts extend for tens of kilometres along strike. Initial stratigraphy was disrupted by faults, folds, and pluton emplacement. Foliated granodiorite and less deformed granite underlie large areas and enclose older anorthosite and tonalite. Steep, northwest-striking foliation (S_2) and associated downdip mineral and stretching lineations (L_2) dominate all belts. Earlier (D_1) structures are recognized in the Payne Lake area. The map pattern of the Duquet belt is attributed to tight F_3 folds overprinted by open F_4 crossfolds. Mineral assemblages in metapelite indicate low-pressure, amphibolite-facies, syn-D_2 regional metamorphism. Sulphide-bearing oxide- and silicate-facies iron-formations have elevated Au levels (<1000 ppb); fold hinge zones could host economic mineralization.

Résumé : La portion nord du bloc de Minto contient des ceintures de roches vertes composées principalement de basalte, de grauwacke-pélite et d'andésite; des formations de fer s'observent par endroits. De rares conglomérats et quartzites sont associés à des discordances au niveau du socle tonalitique et de plutons synvolcaniques. Les ceintures de puissance kilométrique mesurent des dizaines de kilomètres parallèlement à la direction des couches. La stratigraphie initiale a été perturbée par des failles, des plis et la mise en place de plutons. De la granodiorite foliée et du granite moins déformé s'étendent sur de vastes zones et englobent des anorthosites et des tonalites plus anciennes. Une foliation (S_2) à pendage fort d'orientation nord-ouest et, en aval-pendage, des linéations (L_2) minérales et d'étirement associées caractérisent toutes les ceintures. On observe dans la région du lac Payne des structures (D_1) plus précoces. La figuration cartographique de la ceinture de Duquet est attribuée à des plis P_3 serrés auxquels se surimpriment des plis ouverts transversaux P_4. Les associations minérales des métapélites indiquent un métamorphisme régional à faible pression du faciès des amphibolites, lequel est synchrone de D_2. Les formations de fer à sulfures (faciès oxydés et silicatés) ont des concentrations élevées en Au (< 1 000 ppb); les zones de charnière de plis pourraient être le site de minéralisations économiques.

[1] Quebec Geoscience Centre, Sainte-Foy

INTRODUCTION

Reconnaissance-scale study of the Minto block of northern Quebec is underway to establish a geological framework for this largely unexplored region. Until recently (Percival et al., 1994), this northeastern part of the Superior Province had not been considered in regional-scale syntheses, primarily due to lack of information. Following discovery of well preserved volcano-sedimentary belts (Percival et al., 1992; Percival and Card, 1994) with significant potential for Archean greenstone-belt-hosted mineralization, mapping has focused on a north-south corridor containing supracrustal remnants, enclosed within a broad negative aeromagnetic anomaly (Percival et al., 1995a). Although volumetrically minor, the greenstone belts are key to understanding the regional tectonic history by virtue of their stratigraphic (Percival et al., 1993; Skulski et al., 1994; Skulski and Percival, in press) and structural (Lin et al., 1995, in press) records, not present in the generally younger granitoid units (Stern et al., 1994).

This report presents information on supracrustal and associated plutonic rocks in the region between Payne and Ikirtuuq lakes (Fig. 1, 2). Parts of the Qalluviartuuq belt (Percival et al., 1995b) were revisited to provide stratigraphic and structural detail. A separate report (Skulski et al., in press) provides geochemical and geochronological control for interpretations of the Kogaluc and Qalluviartuuq belts. Preliminary descriptions of the Duquet and associated belts in the northern part of the area form the main body of the report.

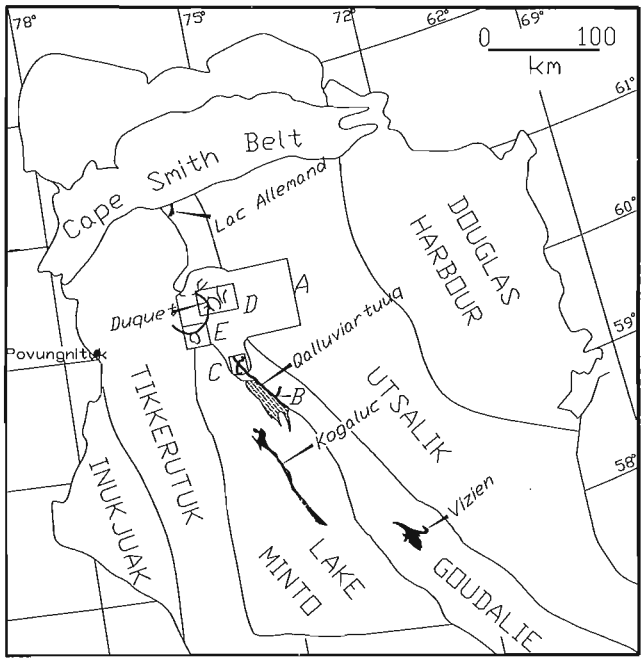

Figure 1. Regional map of Ungava Peninsula showing location of supracrustal belts and detailed maps: A: Qalluviartuuq-Duquet Lake area (Fig. 2); B: Payne Lake area (Fig. 3); C: northern Qalluviartuuq belt (Fig. 4); D: Duquet belt (Fig. 5); E: Akuaraaluk belt (Fig. 6).

REGIONAL GEOLOGY

The northern Minto block in the map area can be divided into three north-trending domains, from west to east the Lake Minto, Goudalie, and Utsalik (Fig. 1). All contain a high proportion of plutonic rocks and are distinguished on the basis of the nature and volume of supracrustal rocks. Lake Minto domain contains variably metamorphosed, dispersed supracrustal remnants, preserved as linear enclaves in plutonic units and elongate belts up to a few kilometres wide. Its supracrustal sequence is dominated by paragneiss, mafic gneiss, and associated iron-formation. Relatively low-grade belts such as the Kogaluc in eastern Lake Minto domain are dominated by steep shear fabrics (Lin et al., 1995) and contain a relatively high proportion of volcanic and associated rocks, including andesite, dacite, and gabbro. These units are interpreted as continental arc remnants and dated at 2779-2757 Ma (U-Pb zircon ages; Skulski et al., in press). Plutonic rocks include a coarse grained, melanocratic, calc-alkaline suite of quartz diorite, tonalite and granodiorite, and peraluminous suites including diatexite, granodiorite, and granite. Rare small bodies of medium grained biotite tonalite are isotopically older (Stern et al., 1994; Skulski et al., in press).

As defined in the Leaf River area (southern part of Fig. 1), Goudalie domain consists of tonalitic rocks (>2.9 Ga) and well preserved supracrustal sequences, including the Vizien greenstone belt (Percival et al., 1992, 1993). The Vizien belt contains a mafic-ultramafic oceanic sequence (2786 Ma; Skulski and Percival, in press), thrust onto younger continental arc (2725 Ma), arc-rift (~2722 Ma), and forearc (<2718 Ma) volcanic-sedimentary sequences. The belt was subsequently deformed in four ductile events (Lin et al., 1995 in press), mainly prior to 2693 Ma. Along strike to the north of extensive drift cover, the aeromagnetic low coincides with the Qalluviartuuq belt, comprising amphibolite-facies basaltic, andesitic, and dacitic rocks with associated intrusions, all with primitive isotopic character (Skulski et al., in press). Rare tonalitic bodies locally form basement to the supracrustal rocks which are in intrusive and/or shear contact with the dominant granodiorites.

Utsalik domain in the east consists of homogeneous plutonic rocks without supracrustal remnants. It contains subequal proportions of granodiorite and granite with ages in the range 2755-2720 Ma (Percival and Card, 1994), and sparse enclaves of pyroxenite, gabbro and diorite. In the Leaf River area, hornblende-biotite-bearing granitoid rocks grade into kilometre-scale patches containing ortho- and clinopyroxene (Percival et al., 1992). To the north, the domain is characterized from west to east by hornblende-biotite±epidote-, clinopyroxene- and orthopyroxene-bearing zones.

SUPRACRUSTAL ROCKS

Supracrustal rocks occur in linked or isolated anastomosing belts containing well preserved sequences up to a few kilometres thick, and narrow, sinuous branches of amphibolite separated by large plutonic masses (Fig. 2). In spite of generally intense deformation and metamorphism to amphibolite

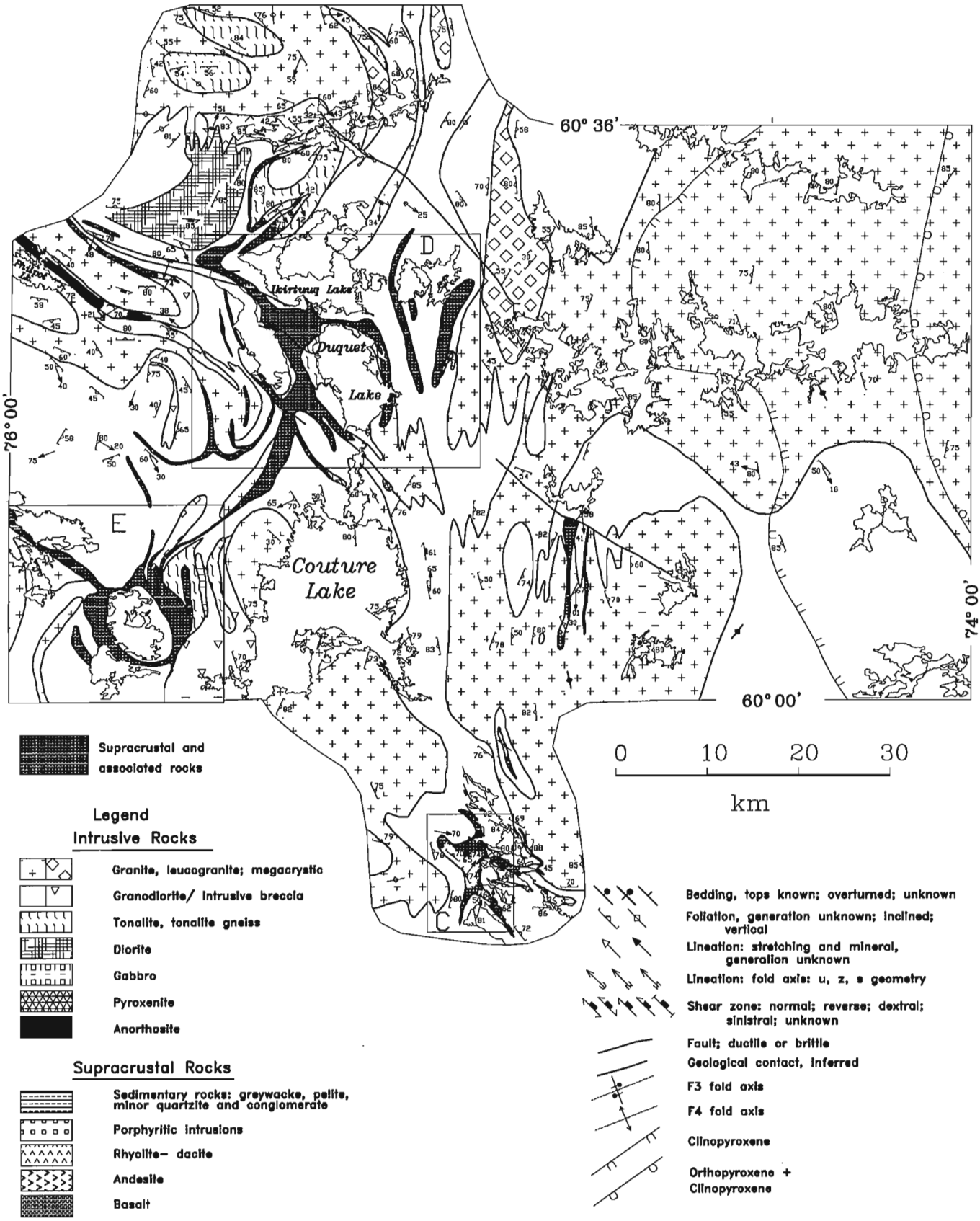

Figure 2. *Regional geological compilation map of the northern Qalluviartuuq Lake-Duquet Lake area, showing location of detailed maps: C: northern Qalluviartuuq belt (Fig. 4); D: Duquet belt (Fig. 5); E: Akuaraaluk belt (Fig. 6). Legend applies to this and subsequent maps.*

facies, stratigraphic relationships are preserved in the thickest parts of the belts. From south to north, the three main belts are referred to as Payne Lake, Qalluviartuuq Lake, and Duquet Lake (Fig. 2).

Payne Lake

In the western Payne Lake area, supracrustal units of the Qalluviartuuq belt broaden into a 5 km wide zone with locally preserved primary features in the lower amphibolite facies. The belt defines a triple junction, with arms extending to the northwest, northeast, and southeast (Fig. 1, 3). Conglomerates were recognized in this area (Percival et al., 1995a, b) and more detailed work revealed a basal unconformity against tonalite. Tonalite-boulder-supported conglomerate passes upward to sandstone, which is overlain by mafic volcanics, the main constituent of the Qalluviartuuq belt. Basalts commonly have preserved pillows, pillow breccias, and carbonate amygdules and veins; abundant gabbro sills also have carbonate veins. Pods of layered siderite may represent carbonate-facies iron-formation and metre-thick layers of dolostone may also be sedimentary in origin. Silicate-facies iron-formation is abundant in the mafic section near the contact with a unit of clastic and chemical sedimentary rocks (Fig. 3). The contact occurs within a 5 m wide high-strain zone that is folded about the dominant regional foliation and overgrown by regional metamorphic minerals. The adjacent pelite-greywacke sequence includes silicate-, oxide-, and sulphide- facies iron-formation in proximity to the contact.

To the southwest, a distinct package of upper amphibolite facies intermediate rocks and minor sedimentary schists occurs in fault contact with the lower-grade pelites (Fig. 3). These include andesitic tuff breccias and plagioclase-porphyritic flows, diorites, and muscovite-sillimanite schists.

Northern Qalluviartuuq Lake

Complex stratigraphic relationships are evident in the northern Qalluviartuuq belt, where Winsky et al. (1995) documented an unconformity between granodioritic basement and sedimentary cover. Further work (Fig. 4) has provided more detail on both the basement and cover sequences, leading to the conclusion that the unconformity represents a significant time break.

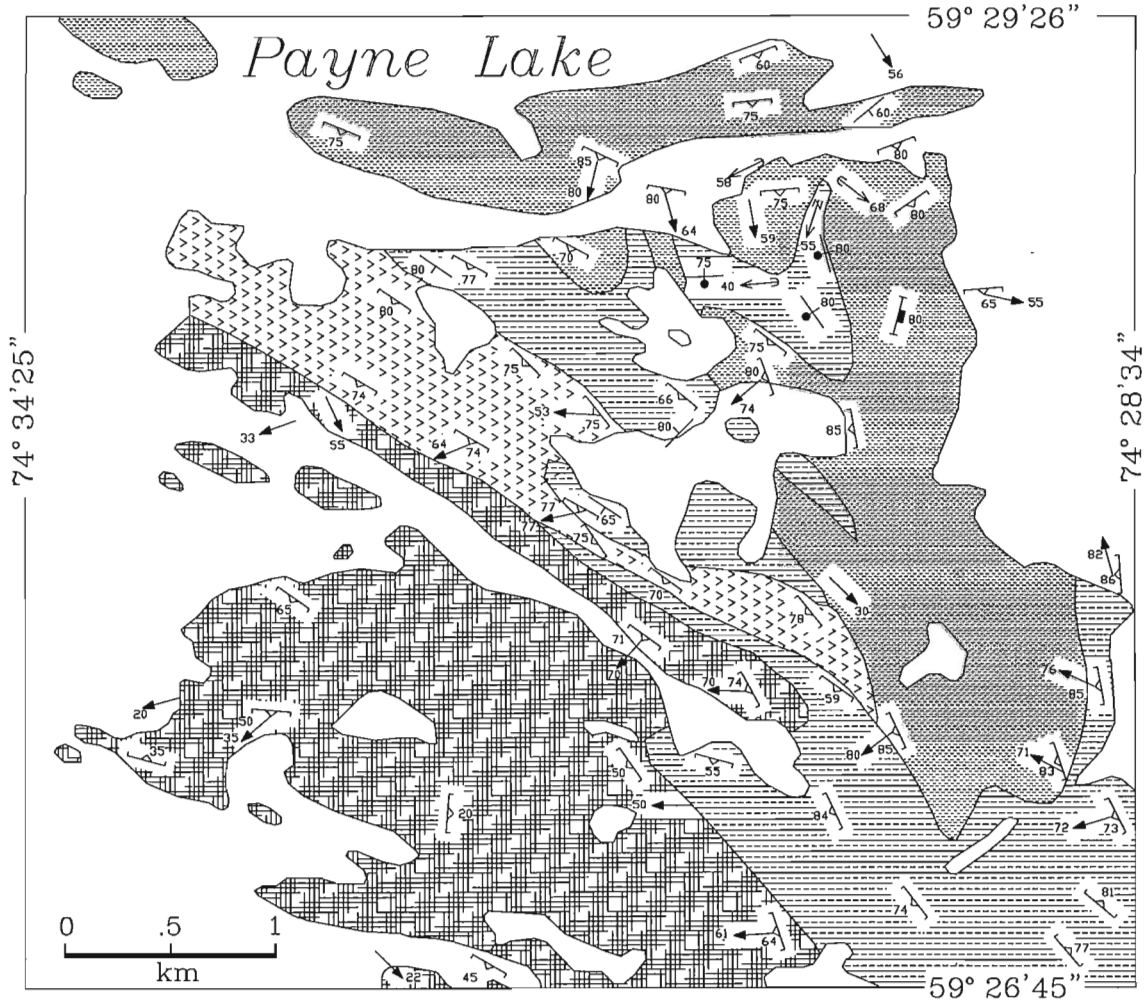

Figure 3. *Geology of the southwestern Payne Lake area. See Figure 2 for legend.*

Intense tectonic fabrics characterize the marginal 500 m of the belt such that primary structures and facing directions are preserved only within the widest, central corridor where the steeply-dipping sequence appears to face west. The inferred base of the sequence in the east is a mafic schist unit that interfingers along strike with pelitic and psammitic schists. Both units are cut by a stratiform intrusive complex of granodiorite (2832 Ma; Skulski et al., in press) and diorite which display abrupt grain size variations and mutual cross-cutting relationships suggestive of magma-mingling processes. Parts of the body have tourmaline-cemented crackle-breccia textures characteristic of high level intrusions. Along strike to the south, the granodiorite becomes porphyritic and then fine grained, suggesting that the complex may have had hypabyssal equivalents. The complex is overlain unconformably by a thin unit of monomict granodiorite-cobble conglomerate containing clasts as young as 2768 Ma (Skulski et al., in press) and quartzite that grades along strike southward into psammitic schist. To the north, sediments are cut by sheets of deformed diorite which, together with foliated, lineated gabbro, constitutes most of the northern end of the belt (Fig. 4). A small peridotite body has an enriched LREE profile like the enclosing andesites. Pillowed and porphyritic rocks overlie the sedimentary sequence. Where observed, the sedimentary-volcanic contact appears depositional. In one example over 50 cm of section, bedded

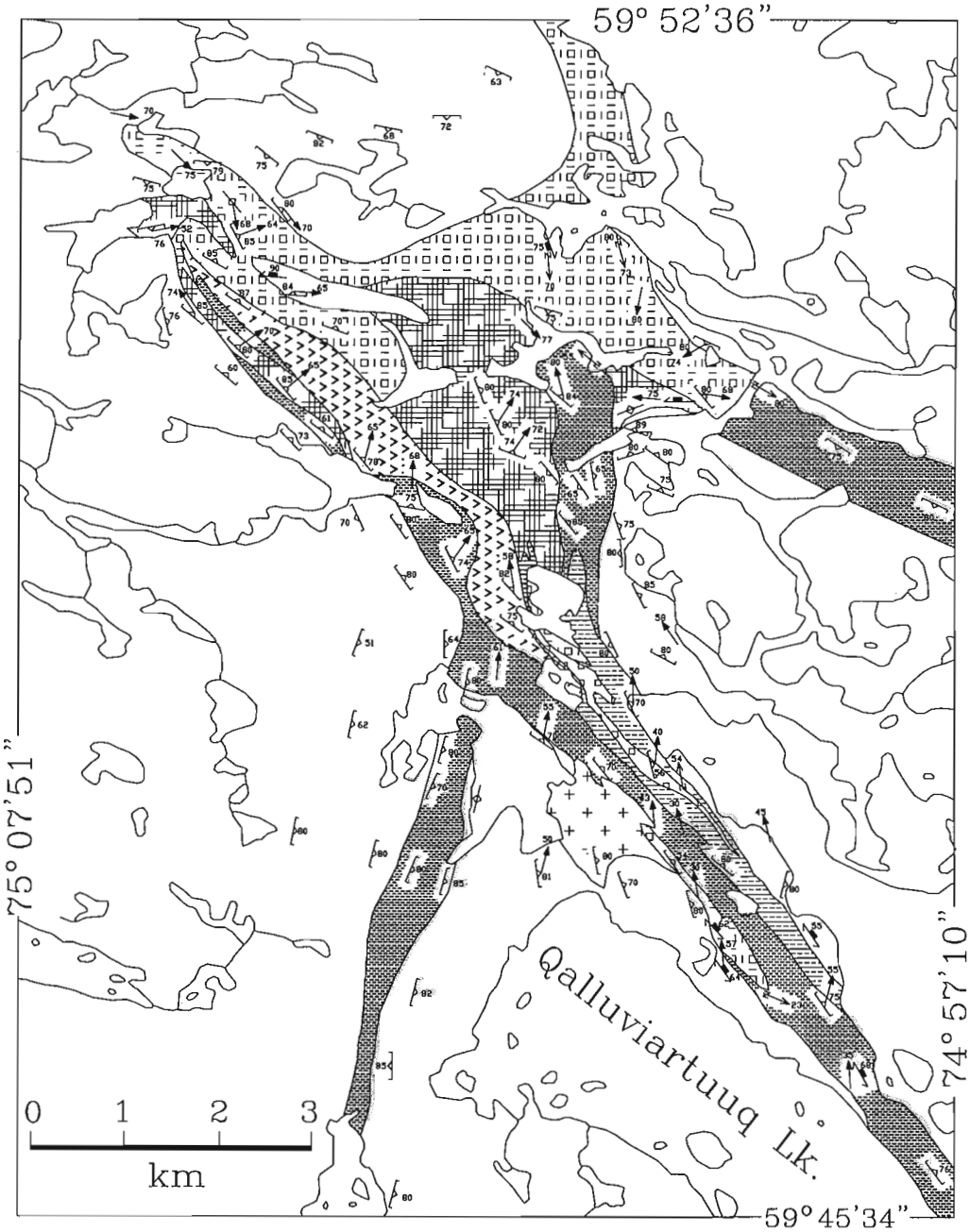

Figure 4. *Geology of the northern Qalluviartuuq belt. See Figure 2 for legend.*

psammites give way to layered calc-silicates, which are in turn overlain by carbonate-altered andesite. Epidote alteration pods are a characteristic feature of the andesitic unit, indicating pervasive premetamorphic hydrothermal alteration, probably in a seafloor environment. Rocks of mafic to intermediate composition dominate the structurally higher, western margin of the belt where primary features are not preserved.

Duquet Lake

A steeply-dipping belt varying in width from 1 to 6 km surrounds Duquet Lake and extends to the northwest and southwest. In spite of a generally high state of strain, stratigraphic sequences can be defined locally. Primary facies variations are rapid across strike and individual units appear to have limited strike extent, due partly to disruption by a set of west-northwest-striking shear zones (Fig. 2, 5).

In the western arm of the Duquet belt (Fig. 5), sedimentary rocks including conglomerate and quartzite locally sit unconformably on tonalite. They are structurally overlain by carbonatized basalt and andesite, interlayered with pelite, rusty biotite schist, and iron-formation, which generally occurs at volcanic-sedimentary contacts. Further north, a west-facing basaltic unit is interlayered with and overlain by slate, pelite, siltstone, and conglomerate. A kilometre-thick lens of quartz-porphyritic dacite associated with plagioclase-porphyritic andesite shows abrupt grain size variations and complex crosscutting relationships characteristic of hypabyssal intrusions. Overlying the sedimentary unit is a lens of intermediate volcanic rocks, mainly plagioclase-porphyritic andesite. Further north, a panel of well preserved basaltic rocks is separated from porphyritic granodiorite to the west by a high-angle reverse ductile shear zone. The northernmost segment of the belt is an east-plunging synform consisting of a basaltic unit structurally overlain by sandstone, pelite, and slate. Both units contain stratiform iron-formations:

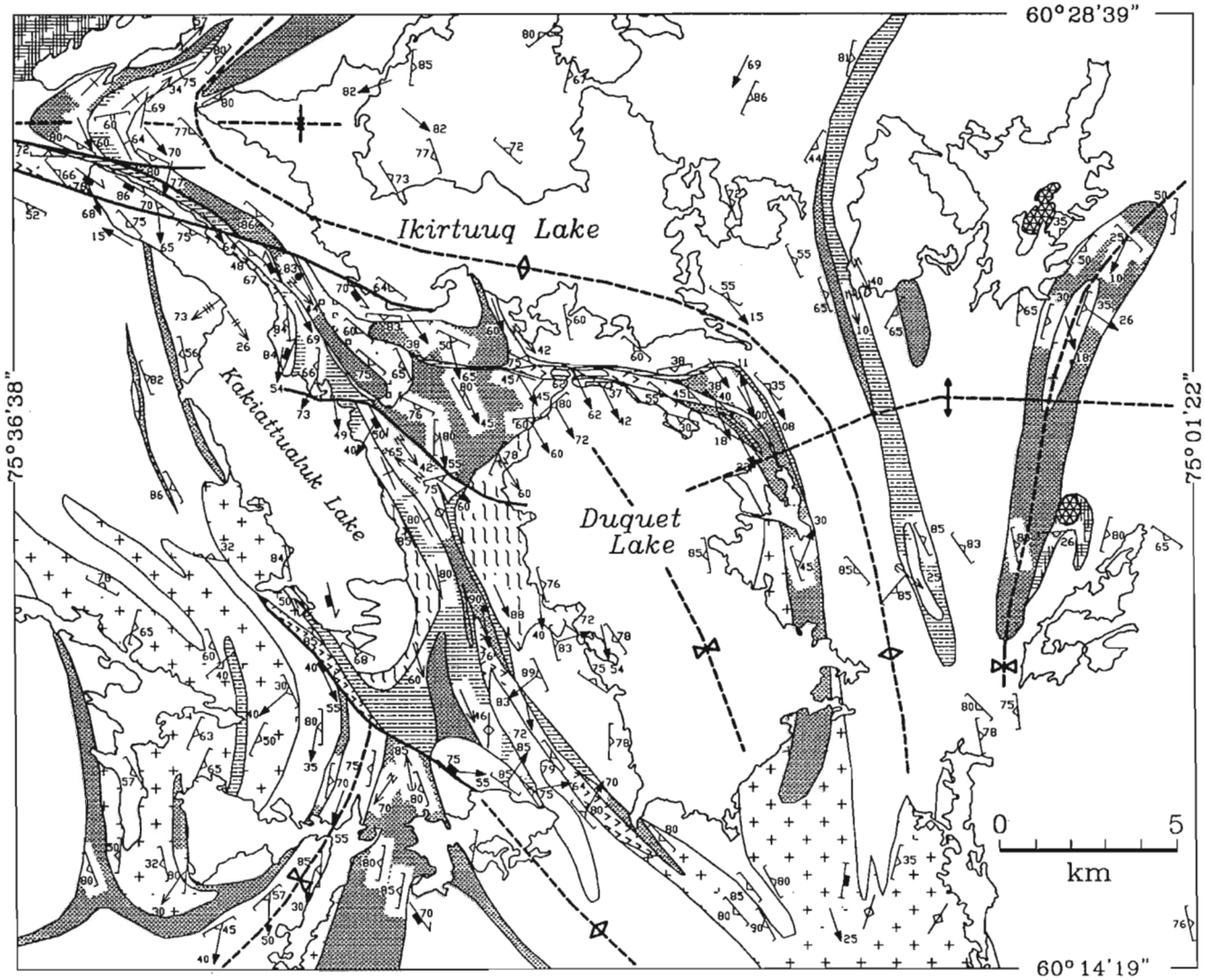

Figure 5. *Geology of the Duquet Lake area. See Figure 2 for legend.*

magnetite-quartz in the western section and garnet-quartz in the sedimentary rocks to the east. The northern arm of the Duquet belt contains all of the main rock types present on the western limb, but in an attenuated state with little strike continuity and poorly preserved stratigraphic relationships.

Lithological units of the Duquet belt may be present in a thin extension to the north. A belt of paragneiss, silicate-facies iron-formation, and amphibolite defines a complex outcrop pattern (Fig. 2). Similarly, part of the Duquet belt may have been offset to the west along faults (Fig. 2), where small remnants of supracrustal rocks are preserved.

Approximately 40 km to the southwest of the Duquet belt and connected by a thin septum of amphibolite is the Akuaraaluk belt, which has a similar geometry (Fig. 2, 6). A mafic unit, comprising amphibolite, mafic gneiss, and rare pillow basalt, forms a discontinuous rim to the belt. Diorite and andesite are abundant on the east and greywacke is common in the north and west. Where observed, the volcanic-sedimentary contact is marked by a rusty-weathering zone, locally containing up to 40% sulphides. One gossan (#19-22, Table 1) measures 150 by 500 m and carries minor anomalies in Cu and Au. Rare rhyolite from the northwestern arm of the belt has fragmental textures. An intrusive complex made up of tonalite with diorite enclaves of variable scale defines the eastern margin of the belt.

Isolated occurrences of supracrustal remnants in the Duquet Lake area testify to severe dismemberment of the volcano-sedimentary complexes during pluton emplacement,

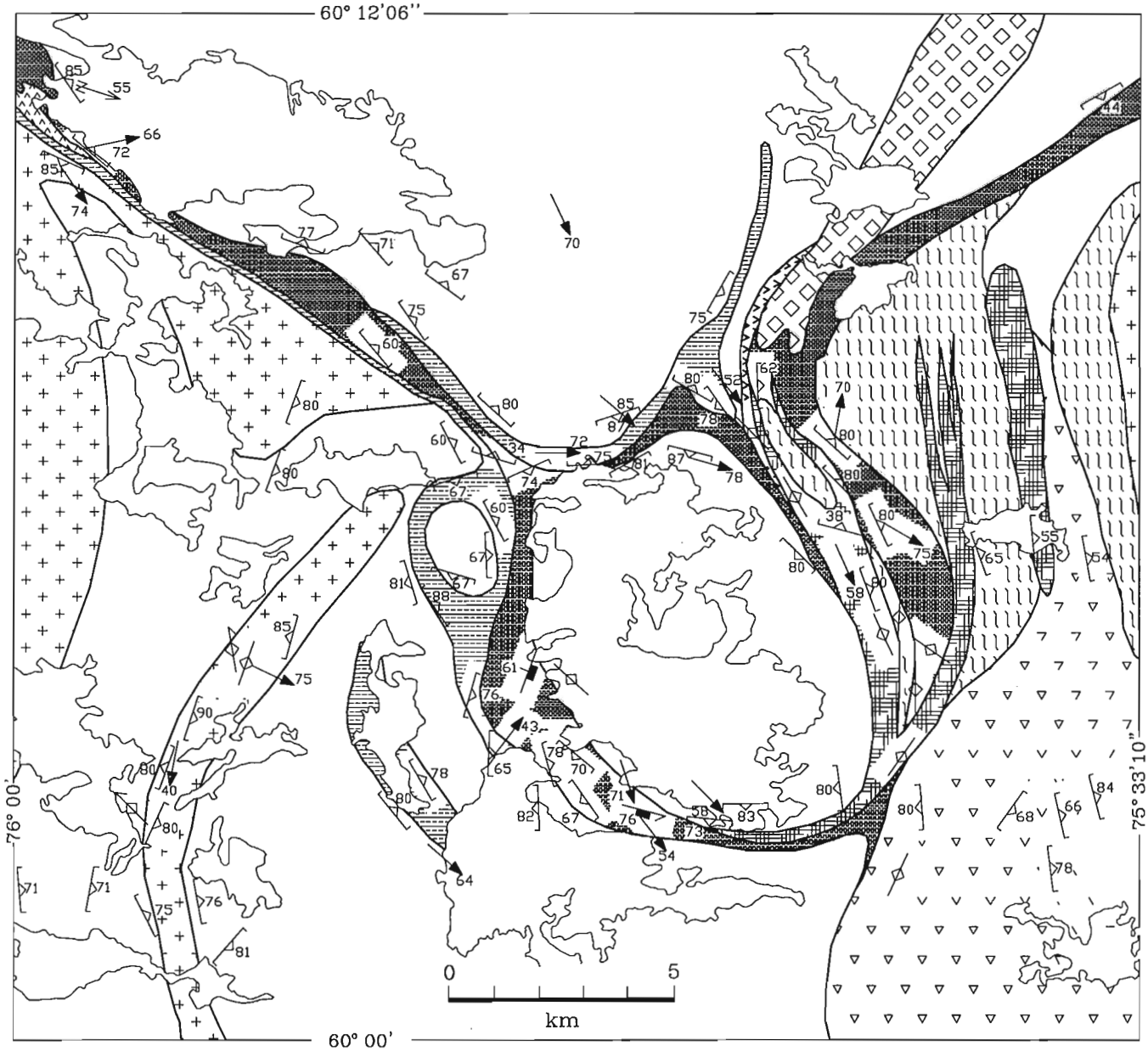

Figure 6. *Geology of the Akuaraaluk belt. See Figure 2 for legend.*

Table 1. Location and partial analyses of gossans.

No.	Easting	Northing	Au ppb	Cu ppm	Zn ppm
1)	508792	6659873	7	33	78
2)	508792	6659873	9	80	90
3)	474309	6675596	2	63	56
4)	474309	6675596	3	29	29
5)	484505	6671790	4	53	185
6)	505071	6616264	130	633	83
7)	505071	6616264	1140	7043	176
8)	475353	6694945	33	750	113
9)	482011	6695286	8	128	101
10)	472214	6686122	9	92	31
11)	527152	6591740	4	39	66
12)	526796	6593388	4	187	486
13)	527990	6593176	9	29	11
14)	528024	6593257	1	10	75
15)	528164	6593316	6	149	29
16)	527616	6593277	2	282	73
17)	528441	6593894	2	51	26
18)	460276	6667159	6	220	157
19)	460205	6666857	45	1013	116
20)	460205	6666857	79	1379	105
21)	460205	6666857	21	859	69
22)	460205	6666857	7	105	23
23)	460251	6667438	4	366	145
24)	446538	6670792	11	396	121
25)	446037	6671408	3	259	380
26)	490827	6697002	12	1246	94
27)	490827	6697002	9	462	92
28)	479851	6695390	7	403	373
29)	480169	6695231	12	174	124
30)	477888	6708641	4	126	125
31)	527281	6593368	4	93	64
32)	452370	6599610	74	1098	46
33)	478043	6689411	72	156	72
34)	491347	6690425	100	329	40
35)	480448	6694012	6	59	435
36)	478406	6686483	6	757	16
37)	475106	6707834	1	33	26
38)	487166	6728071	20	88	65
39)	528885	6590908	2	676	25
40)	458163	6664442	2	17	48
41)	455957	6658646	2	606	31
42)	453982	6704335	68	2700	2255
43)	454999	6705990	6	797	71
44)	468165	6703007	53	196	30
45)	469192	6703532	2	59	35
46)	469192	6703532	65	371	15
47)	478187	6687561	33	116	19
48)	478402	6686911	14	163	571
50)	478336	6686946	2	161	46

uplift, and erosion. Among them, a less than 2 km wide belt of amphibolite located approximately 40 km southeast of Duquet Lake hosts a string of gossans which extends over a strike length of 13 km. A belt less than 2 km wide of amphibolite and paragneiss about 10 km east of the Duquet belt is associated with pyroxenite pods (Fig. 5). A thin mafic belt west of Kakiattualuk Lake is associated with peridotite.

PLUTONIC ROCKS

Plutonic rocks in the Duquet Lake area can be grouped into two major and several minor suites. Voluminous granite and granodiorite suites occur throughout the region whereas some of the minor suites are areally restricted. Apart from rare gneissic tonalites which feature abundant evidence for polyphase deformation, most of the plutonic rocks are homogeneous, medium- to coarse-grained, and moderately foliated to massive.

Tonalitic gneisses occur in the northwestern corner of the area (Fig. 2). They are complex, polyphase hornblende-biotite gneisses with a millimetre-scale, variably folded and boudinaged layering intruded by concordant, centimetre-thick granite veins. The oldest rock component consists of thin mafic schlieren; small layers and pods of gabbroic anorthosite may also predate the dominant tonalitic gneiss phase. Sheets of foliated tonalite cut tonalitic gneiss but are themselves cut by granite. Further south, similar dykes of foliated tonalite cut foliated granodiorite.

Anorthositic rocks are a widespread but volumetrically minor component of the granitoid complex west of Duquet Lake. The largest single body is a less than 2 km by about 10 km sheet northeast of Philpot Lake (Fig. 2). Dominated by anorthositic gabbro, the body includes gabbro and anorthosite. In the same region, enclaves of anorthositic rock define discrete zones in granodiorite and granite.

Pyroxenite occurs as sporadic discrete masses up to 2 km wide within granodiorite and granite east of Duquet Lake. These coarse grained, massive bodies are generally homogeneous clinopyroxenite and hornblendite with accessory orthopyroxene, biotite, and plagioclase. Some bodies have finer grained, foliated margins and are cut by dykes of granodiorite. Peridotite bodies of similar scale, locally with cumulate layers, also occur west of the Duquet belt.

Granodiorite and associated rocks are the predominant rock type in the eastern part of the map area. They are generally homogeneous, medium- to coarse-grained and contain up to 30% combined hornblende, biotite, and epidote. Clinopyroxene cores in hornblende are common in the far eastern part of the area (Fig. 2). With increasing mafic content the composition grades to quartz diorite and diorite. K-feldspar megacrystic varieties form discrete kilometre-scale zones and grade to true granite. Granodiorites contain enclaves (cognate xenoliths?) of quartz diorite and diorite as well as inclusions of supracrustal rocks, locally in large enough quantities to form map-scale intrusive breccia complexes. Granodiorites are generally foliated, with higher strain intensity adjacent to supracrustal belts.

A large body of diorite in the northwestern part of the area may be part of the granodiorite suite. It has gradational contacts with granodiorite, as well as similar grain size and texture. In contrast, the body displays mutually crosscutting relationships with a finer grained to porphyritic diorite phase, including enclaves and dykes of the fine grained rock and indistinct lobate contacts suggesting magma mingling.

Granite occurs throughout the region, on the centimetre to batholith scale. It is generally the youngest intrusive phase in both granitoid regions and supracrustal belts. Its composition ranges from leucogranite, with less than 5% biotite, to mafic varieties with up to 20% hornblende and biotite. One body of muscovite granite was noted near the western edge of the area and pyroxenes are present in granites in the east (Fig. 2). Granites are commonly massive to weakly foliated; K-feldspar megacrystic varieties may contain an igneous flow fabric. Most granites are distinguished by their pink colour imparted by hematite-stained K-feldspar; perthite granites weather white. In some areas, sheets of granite cut granodiorite, on scales ranging from hundreds of metres to centimetre-scale lit-par-lit migmatites.

A small body of massive, coarse grained nepheline syenite was noted southwest of the Akuaraaluk belt. Its age with respect to other units is unknown. A 10 by 800 m, north-striking carbonatite dyke cuts granitoid rocks 30 km southwest of Duquet Lake. This unique coarse grained, massive to flow-layered dolomitic carbonatite contains magnetite phenocrysts and sporadic ultramafic xenoliths.

Two sets of diabase dykes represent the youngest intrusive units in the region. The sparse, west-northwest- and northwest-trending bodies rarely attain 50 m in width. The west-northwest-trending dykes have sigmoidal form, whereas the northwest-trending bodies are straight; crosscutting relationships were not observed. The dykes are probably members of the Paleoproterozoic Payne Lake and New Quebec swarms.

STRUCTURAL GEOLOGY

The region is dominated by northwest structural trends, expressed in the elongate shape of supracrustal belts, their internal structure, and foliation in plutonic rocks. For consistency with areas to the south, the dominant, penetrative, synmetamorphic fabrics are termed D_2 (Lin et al., 1995), although earlier tectonic fabrics are rarely recognized. In contrast to areas further south, northeasterly trends are also present and map-scale structural domes are evident in the western part of the Duquet Lake area (Fig. 2).

In the southwestern Payne Lake area, primary textures and structures are locally well preserved in an area of lower amphibolite facies rocks. Normal and reversed graded bedding in pelites locally provide facing directions (Fig. 3). The dominant regional foliation (S_2) in this region strikes west-northwest and dips moderately to steeply southwest. It locally crenulates an older foliation (S_1) in high-strain zones developed at the contact of pelitic and mafic volcanic units. Facing directions in pelites suggest that the mafic unit structurally overlies it, but facing criteria were not observed within the generally highly strained volcanic rocks. Mylonites are present locally along the folded contact. Lineations include prominent down-dip stretching and mineral lineations as well as small fold axes of uncertain generation. They plunge dominantly southwest in the western part of the region and to the north or east in the east. The variability of the lineation attitudes contrasts with the fairly regular orientation of the strong foliation (S_2), which is disturbed only by gentle warps. The complex map pattern and the fact that lithological contacts define map-scale fold interference patterns suggest early (D_1) structures.

The northern Qalluviartuuq belt is characterized by strong planar and linear fabric (Winsky et al., 1995), named D_2 for regional consistency; older tectonic fabrics have not been recognized in this part of the belt. The foliation parallels the margins of the belt and consistently dips steeply (60-90°) northeast. Within a few hundred metres of the belt margins S_2 foliation is intense and obliterates primary structures; only in the widest part of the belt are earlier features preserved. In the south the S_2 foliation is in general a shear fabric with normal displacement. It is accompanied by moderate (30°) to steep downdip stretching and mineral lineations whose trend and plunge vary systematically along the length of the belt. Moderate northerly plunges in the south increase through a plunge reversal zone in the north which corresponds to the widest part of the belt and, possibly, to the hinge of an open, east-trending F_3 fold. In the southern Qalluviartuuq Lake area, S_2 fabrics of mylonitic intensity are developed at the contact between supracrustal and intrusive rocks. Mylonite, ultramylonite, and pseudotachylite with associated moderately north-plunging stretching lineations are folded into a map-scale "z" fold, probably late D_2 in age as suggested by the coincidence of stretching lineations and z-fold axes.

Plutonic rocks in proximity to the belt generally carry foliations and lineations concordant to those within the belt. A pluton in the east has a marginal quartz diorite phase with strong shear fabrics and a moderately foliated to massive granodioritic interior. In one location along the western margin, a small granite body intrudes along the contact between sheared mafic rocks and granodiorite. Weaker, concordant foliations and lineations in the granite suggest a late syntectonic age of emplacement. Sheets of peraluminous pegmatite are unfoliated but locally occur in map-scale sigmoidal dyke sets, suggesting late intrusion possibly related to the D_2 strain event and regional metamorphism.

Supracrustal belts in the Duquet Lake area, as elsewhere, are characterized by strong tectonic fabrics including steep foliations, and stretching and mineral lineations. As in the northern Qalluviartuuq belt, pre-main foliation structures have not been recognized. For consistency with the Payne Lake area and belts further south (Lin et al., 1995; Percival et al., 1995a) the main fabric elements in this area are also termed S_2 and L_2. Carbonate-altered volcanic rocks and pelites carry stronger fabrics than adjacent units, including mylonitic structures, indicating that D_2 strain is significantly partitioned according to rock type. In the northern Duquet belt, lithological units, S_2 foliations, and L_2 lineations define a moderately south-plunging, tight, symmetrical F_3 synform

(Fig. 5). No associated axial plane fabric has been recognized. Asymmetric minor fold axes have geometry inconsistent with formation as second-order F_3 folds. Rather, these lineation-parallel folds may have formed during the penetrative D_2 event and been subsequently folded (F_3). The D_2 deformation led to the development of mylonitic fabric and more locally, narrow ductile shear zones. The belt is segmented by at least three ductile shear zones that cut stratigraphy and S_2 foliations at low angles (Fig. 5). Although similar in plunge, associated lineations diverge from the average L_2 trend by up to 90°. It is possible that these structures formed during a late increment of D_2 strain and reflect a component of oblique movement. Plunge variations and reversals of L_2 are attributed to a set of open F_4 folds with east-west axes (Fig. 5). An upright, east-west S_4 crenulation cleavage is developed sporadically in fissile rocks throughout the belt. Late west-northwest-trending, brittle fault zones cross both the Duquet belt and plutonic rocks. One brittle fault (Fig. 5) extends at least 20 km to the west-northwest as a zone of fault breccia, cataclasite, and pseudotachylite.

The broad map-scale geometry of the Duquet belt may also be viewed as an interference pattern, developed through contact strain imposed by rising plutonic masses. The plutonic bodies carry strong marginal foliations concordant to S_2 within the belts, consistent with this interpretation. However, away from the supracrustal belts, the foliation pattern in plutonic rocks also defines a folded pattern more consistent with F_3-F_4 interference than to diapiric rise (Fig. 5). A clear illustration is given in the western part of the map area where a domal structure over 30 km in diameter is outlined in plutonic domain (Fig. 2).

The Akuaraaluk belt has similar overall geometry to that of the Duquet belt (Fig. 2, 6). Steep S_2 foliations define an upright or steeply dipping closed structure; associated lineations plunge moderately to steeply southeast but have more variable trends than in the Duquet belt. Surrounding plutonic rocks contain concordant foliations (S_2), which together with those in the Akuaraaluk belt define regional F_3-F_4 interference patterns.

In summary, assuming that the main (D_2) penetrative fabric has a similar origin and age in each belt, similar structural chronologies are apparent in separate areas. Differences in map patterns are attributed to sporadic preservation of older fabric elements, such as at Payne Lake, to variable intensity of D_2 strain, and to the effects of later (F_3, F_4) folds.

METAMORPHISM

Metapelite units in the supracrustal belts provide the most visible monitors of metamorphic grade which varies regionally, from granulite facies northwest of Payne Lake (Percival et al., 1995b) to lower amphibolite facies in southwestern Payne Lake. In all areas, peak metamorphic minerals generally define the principal penetrative tectonic fabric (D_2). This constitutes mainly alignment of amphibole in metavolcanic rocks and phyllosilicates in metasedimentary units.

Metapelite units in the southwestern Payne Lake area (Fig. 3) are characterized by local preservation of bedding and the assemblage andalusite-staurolite-garnet-biotite-muscovite-plagioclase-quartz. Porphyroblasts of andalusite and staurolite up to 2 cm overgrow bedding and rare S_1 high-strain fabrics, but are wrapped by phyllosilicates defining S_2. Peak metamorphic conditions associated with D_2 are estimated at 550-600°C, 100-200 MPa based on petrogenetic grids.

Relict kyanite and staurolite occur with sillimanite, garnet, and cordierite in localities approximately 30 km to the northwest and south of the andalusite-bearing rocks. The assemblage containing kyanite suggests a higher pressure P-T trajectory and equilibration conditions in the range 600-700°C, 350 MPa.

In the northern Qalluviartuuq belt, metasedimentary rocks commonly contain sillimanite with garnet, biotite, and rare staurolite. Cordierite- and anthophyllite-bearing assemblages occur within a thin sedimentary unit.

Andalusite, staurolite, and garnet are common in pelites of the Duquet belt, generally in association with sillimanite. This low-variance assemblage limits conditions to about 600°C, 200 MPa. Slate in the northwestern Duquet belt may indicate local preservation of greenschist facies. An unquantified contrast in metamorphic grade is evident across a west-northwest-striking fault in the northern Duquet belt. To the north are fine grained, white mica-rich slates whereas volcanic rocks to the south are medium grained amphibolites.

REGIONAL CORRELATION

A common tectonostratigraphic assemblage can be recognized discontinuously along 125 km of strike length, from Payne Lake to the northern Duquet belt. The greenstone belts consist of a structurally lower basalt-gabbro sequence with carbonate alteration and glomeroporphyritic units, locally (e.g., southwestern Payne Lake) in D_1 sheared contact with a pelite-rich unit including iron-formation, and andesite-diorite complexes. Supracrustal rocks of the Lake Minto domain to the west (Percival et al., 1995a) include paragneiss, iron-formation, and mafic to intermediate volcanic rocks and gneisses. Low-grade equivalents of this assemblage may be present in the sedimentary and andesitic components of the Qalluviartuuq and Duquet belts. If it is this assemblage that is juxtaposed against primitive basaltic rocks along D_1 structures at Payne Lake, D_1 faults could be significant accretionary structures. In terms of structural style and chronology, the eastern Lake Minto domain (Lin et al., 1995) has a similar history to that of the Qalluviartuuq and Duquet belts, including dominant north-northwest-trending S_2 foliation, south-plunging F_3 folds, and elongate dome and basin geometry. It is likely that these two regions, distinguished primarily on the basis of metamorphic grade, share a similar structural evolution.

Although there are similarities between belts in the Payne Lake-Duquet Lake area and the Vizien belt in the Goudalie type area in terms of supracrustal rock assemblage, structural

chronology, and metamorphic grade, based on available geochronology, little correlation appears possible. Primitive oceanic assemblages in the north are older (~2832 Ma; Skulski et al., in press) than those to the south (2786 Ma; Skulski and Percival, in press), as are calc-alkaline sequences (2832 vs. 2725 Ma). Furthermore, large areas of tonalitic basement have not been recognized in the north. Tectonism in the Vizien belt (~2700 Ma) postdated major granodiorite magmatism (2725 Ma), whereas in the north, tectonism, regional metamorphism, and granodioritic magmatism are inferred to be broadly contemporaneous.

Utsalik domain was defined in the Leaf River area as a homogeneous plutonic terrain lacking supracrustal relics. The region east of the Duquet belt, consisting of homogeneous granodiorite and granite, including pyroxene-bearing varieties in the far east, corresponds well with the type area 300 km to the south.

ECONOMIC POTENTIAL

Supracrustal belts contain many gossans, mainly stratiform silicate- and oxide-facies iron-formations with minor sulphide. These less than 10 metre-scale layers expand locally into pods containing massive sulphide (northern Akuaraaluk belt; Pauline Lake zone). Approximately 50 samples were analyzed for gold and base metals (Table 1) with modest results (<1000 ppb Au). It is evident that concentration from high background levels would be necessary to form economic levels. Structural controls, including unit thickening in fold hinges, are critical in iron-formation-hosted gold deposits such as Lupin (Kerswill, 1993). In this context, fold hinges involving stratiform iron-formations in southwestern Payne Lake and the northern Duquet belt warrant exploration.

ACKNOWLEDGMENTS

Efficient logistic support was provided by Aliva Tulugak (Povungnituk), Johnny May's Air Charters (Kuujjuaq), and Heli-North (Sudbury). Exploration companies active in the region are thanked for logistic collaboration. Katherine Venance, Pauline Orr, and Eric Poirier contributed capable field assistance and some independent mapping. Katherine Venance prepared figures for publication. Jack Henderson and Steve Lucas provided helpful comments on the manuscript.

REFERENCES

Kerswill, J.A.
1993: Models for iron-formation-hosted gold deposits; in Mineral Deposits Modeling; (ed.) R.V. Kirkham, W.D. Sinclair, R.I. Thorpe, and J.M. Duke; Geological Association of Canada, Special Paper 40, p. 171-199.

Lin, S., Percival, J.A., and Skulski, T.
in press: Structural constraints on the tectonic evolution of a late Archean greenstone belt in the northeastern Superior Province, northern Quebec (Canada); Tectonophysics.

Lin, S., Percival, J.A., Winsky, P.A., Skulski, T., and Card, K.D.
1995: Structural evolution of the Vizien and Kogaluc greenstone belts in Minto block, northeastern Superior Province, northern Quebec; in Current Research 1995-C, Geological Survey of Canada, p. 121-130.

Percival, J.A. and Card, K.D.
1994: Geology, Lac Minto-Rivière aux Feuilles, Québec; Gelogical Survey of Canada, Map 1854A, scale 1:500 000.

Percival, J.A., Card, K.D., and Mortensen, J.K.
1993: Archean unconformity in the Vizien greenstone belt, Ungava Peninsula, Quebec; in Current Research, Part C; Geological Survey of Canada, Paper 93-1C, p. 319-328.

Percival, J.A., Mortensen, J.K., Stern, R.A., and Card, K.D.
1992: Giant granulite terranes of northeastern Superior Province: the Ashuanipi complex and Minto block; Canadian Journal of Earth Sciences, v. 29, p. 2287-2308.

Percival, J.A., Skulski, T., Card, K.D., and Lin, S.
1995b: Geology of the Rivière Kogaluc-Lac Qalluviartuuq region (parts of 34J and 34O), Quebec; Geological Survey of Canada, Open File 3112, scale 1:250 000.

Percival, J.A., Skulski, T., Lin, S., and Card, K.D.
1995a: Granite-greenstone terrains of the northern Goudalie domain, northeastern Superior Province, Quebec; in Current Research 1995-C; Geological Survey of Canada, p. 141-150.

Percival, J.A., Stern, R.A., Skulski, T., Card, K.D., Mortensen, J.K., and Begin, N.J.
1994: Minto block, Superior Province: Missing link in deciphering assembly of the craton at 2.7 Ga; Geology, v. 22, p. 839-842.

Skulski, T. and Percival, J.A.
in press: Allochthonous 2.78 Ga oceanic plateau slivers in a 2.72 Ga continental arc sequence: Vizien greenstone belt, northeastern Superior Province, Canada; Lithos.

Skulski, T., Percival, J.A., and Stern, R.A.
1994: Oceanic allochthons in an Archean continental margin sequence, Vizien greenstone belt, northern Quebec; in Current Research 1994-C, Geological Survey of Canada, p. 311-320.
in press: Archean crustal evolution in the central Minto block, northern Quebec; in Radiogenic Age and Isotopic Studies: Report 9; Geological Survey of Canada, Current Research 1996-F.

Stern, R.A., Percival, J.A., and Mortensen, J.K.
1994: Geochemical evolution of the Minto block: a 2.7 Ga continental magmatic arc built on the Superior proto-craton; Precambrian Research, v. 65, p. 115-153.

Winsky, P.A., Kusky, T.M., Percival, J.A., and Skulski, T.
1995: Archean unconformity in the Qalluviartuuq greenstone belt, Goudalie domain, northern Quebec; in Current Research 1995-C, Geological Survey of Canada, p. 131-140.

Geological Survey of Canada Project 890009

Ground penetrating radar survey to define fractures in bedrock, Little French River, Ontario

Jean Pilon, John Scaife[1], Peter Gerabek[2], Eric Timoshenko[1], and Pavel Kurfurst

Terrain Science Division, Ottawa

Pilon, J., Scaife, J., Gerabek, P., Timoshenko, E., and Kurfurst, P., 1996: Ground penetrating radar survey to define fractures in bedrock, Little French River, Ontario; in Current Research 1996-C; Geological Survey of Canada, p. 169-176.

Abstract: This paper presents the results of a ground penetrating radar survey to delineate fractures in gneissic rock outcrops at the site of a future containment dam on the Little French River near Dokis, Ontario. This technique proved to be highly successful for the detection of jointing planes, fractures, and faults to a minimum depth of 15 m. Discussion of the survey set-up and the interpretation techniques used to analyze the field data are also included.

Résumé : Le présent article fait état des résultats d'un levé géoradar effectué pour définir la position et la densité des fractures dans des affleurements rocheux de gneiss, au site d'un futur barrage de retenue sur la rivière Little French, près de Dokis en Ontario. La technique du géoradar s'est avérée très efficace pour la détection des plans de diaclase, des fractures et des failles jusqu'à une profondeur d'au moins 15 mètres. On présente aussi les modalités techniques utilisées pour effectuer les levés géoradar ainsi que les techniques d'interprétation qui ont servi à l'analyse des résultats.

[1] multiVIEW Geoservices Inc., 1091 Brevik Place, Mississauga, Ontario L4W 3R7

[2] Public Works and Government Services Canada, Architectural and Engineering Services, Sir Charles Tupper Building, Riverside Drive, Ottawa, Ontario K1A 0M2

INTRODUCTION

In the fall of 1994, Public Works and Government Services Canada (PWGSC) retained the services of Terrain Sciences Division (TSD) of the Geological Survey of Canada to supervise and manage a ground penetrating radar survey on the site of the Little Chaudiere Dam. The purpose of the survey was to (1) assess the general integrity of the rock under the dam and (2) identify areas of discontinuities in the rock which should be further investigated by conventional drilling and testing methods.

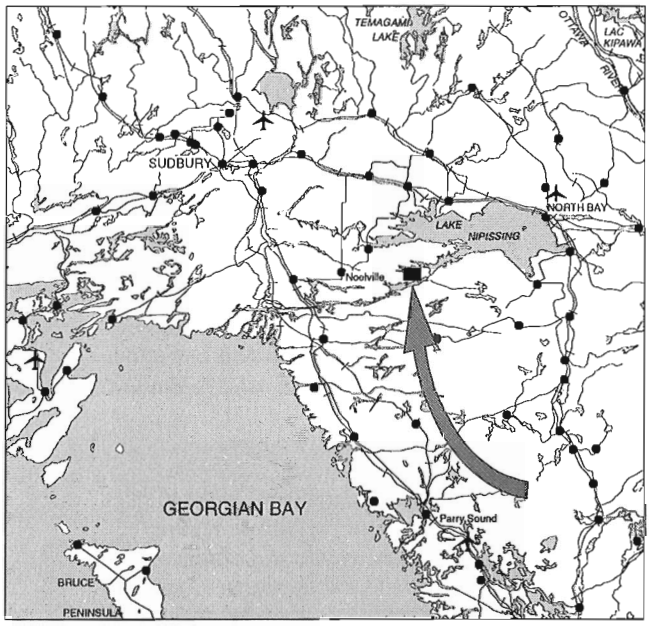

Figure 1. *Map showing the location of the survey area.*

The survey site is located immediately to the west of the Dokis Indian Reservation, approximately 15 km downstream of the village of Dokis, Ontario, near the southwest end of Lake Nipissing. The local geology consists of essentially bare, gently rolling, weathered Precambrian gneissic bedrock.

The Little Chaudiere Dam is one of three structures controlling the water level on the lake. The dam was built in 1915 and has undergone several repairs since. Recent inspection of the Little Chaudiere Dam concluded that the existing dam is in a deteriorated state and will have to be replaced in the near future. It was proposed to build a new structure just downstream of the existing dam in the rock cut channel.

Because of the urgency to complete the investigation, Terrain Sciences Division issued a contract to multiVIEW Geoservices Inc. to carry out the detailed ground penetrating radar (GPR) survey of the Little French River site, as this geophysical method is known for detailed fracture mapping in bedrock (Holloway, 1992; Grasmueck, 1994; Piccolo, 1992; Shikun et al., 1994; Stevens et al.,1994).

This paper describes the site, details of the radar field program and survey procedures, the data compilation and processing procedures along with an interpretation and discussion of the results. This information was used by PWGSC as part of their geotechnical site investigation to select the site of a new dam to be constructed immediately downstream from the existing dam.

SITE DESCRIPTION

The survey area over the proposed dam site measured roughly 39 m north-south and 19 m east-west. These site boundaries were established on site by the radar survey crew using a transit and fibreglass tape. The corners of the survey area were surveyed in by a locally contracted surveyor from North Bay, Ontario. Figure 1 shows the location of the survey area. Figure 2 presents a detailed site map showing the spatial location and extent of each of the radar survey lines with respect to the existing Little Chaudiere Dam.

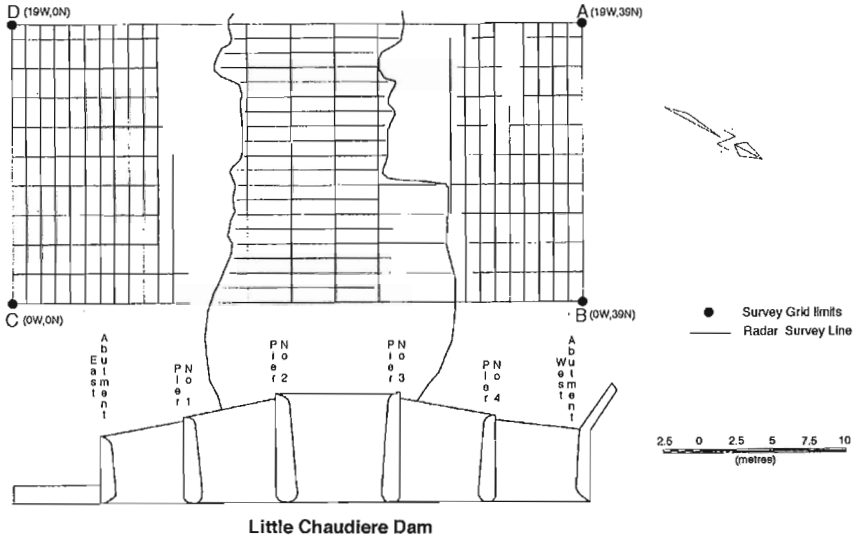

Figure 2.

Site map showing the radar survey lines.

FIELD PROGRAM AND SURVEY PROCEDURES

The following describes the generalized field program and procedures which were followed in order to acheive the objectives of this investigation.

INSTRUMENTATION

A pulseEKKO IV Ground Penetrating Radar system was used for the survey program. Ground penetrating radar is similar to seismic and sonar techniques. The radar produces a short duration pulse of high frequency (10 to 1000 MHz) electromagnetic energy which is transmitted into the ground. The reflected signals are detected and amplified at the receiver. The received signals are digitized and stored on disk on a field computer for post-survey processing.

Radar penetration into geological material is controlled by the electrical conductivity of the material. As the electrical conductivity increases, the radar (electromagnetic) signal is dissipated as heat in the material. Geological horizons that exhibit different conductivities from those above can be delineated by the radar because of their contrast in electrical properties (dielectric constant). Similarly, man-made objects and subsurface voids can be detected as these objects will have markedly different electrical properties than the host material.

Field procedures and system optimization

Prior to starting the production survey work, 50 and 100 MHz test data were acquired along line 36 N and line 39 N using a variety of acquisition parameters. The plots of some of these surveys of line 39 N are presented in Figure 3. A comparison of the two surveys show that the 50 MHz data provided greater signal penetration but sacrificed resolution of the smaller features. Based on these tests, it was decided that the 100 MHz antennas would be utilized to conduct the survey of the site.

Radar survey

For the production ground penetrating radar survey, the pulseEKKO IV system was deployed with 100 MHz antennas oriented in the broadside mode, with the antenna axes set perpendicular to the survey line direction. The transmitting and receiving antennas were 1 m apart. Soundings were acquired at 0.25 m intervals along each survey line; their positioning was achieved through the chained pickets previously established by the survey crew. Figure 4 shows a photograph of the radar system and survey crew during the acquisition of the radar data on land.

Radar data were also acquired across the site-dividing stream immediately downstream of the existing Little Chaudiere Dam. This portion of the survey utilized two inflatable rafts, one housing the 100 MHz antennas and the other supporting the radar console electronics, field computer

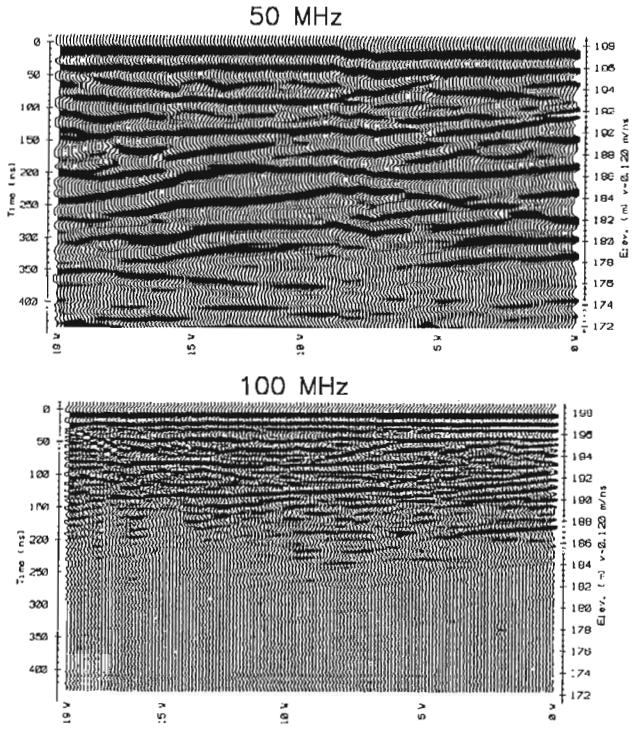

Figure 3. *Comparative results of 50 and 100 MHz radar data along line 39 N.*

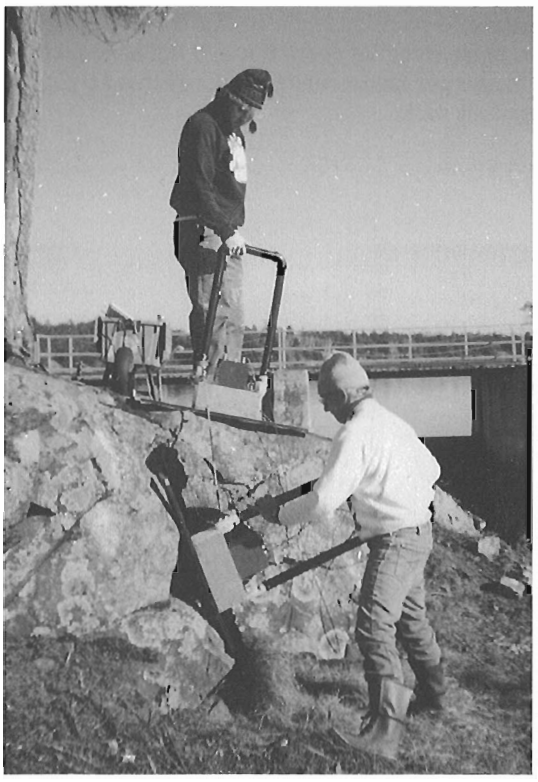

Figure 4. *Photograph of radar data acquisition on land.*

and operator. Due to size restrictions imposed by the inflatable rafts on the water borne portion of the survey, the 100 MHz antennas were only 0.7 m apart.The position of the radar sounding was obtained with the use of chained ropes to record incremental steps in the north-south direction and by restraining ropes in the east-west direction. Due to the nature of the steep banks along the water's edge, no radar data were acquired at the transition zones (from water to land and vice versa) on either side of the river. Figure 5 shows a photograph of the radar system and operator during acquisition of the radar data over the water.

A total of 4136 radar profile data traces were acquired over a linear distance of 1034 line-metres during the course of the survey. During the radar data acquisition, comments regarding position and observed features were stored along with the corresponding individual radar traces. The radar survey commenced on November 15, 1994, and was completed on November 17, 1994, during unseasonably warm conditions.

Radar velocity measurements

Two (2) common mid-point (CMP) velocity soundings were completed on land to determine the radar signal propagation velocity in the local rock. These common mid-points were acquired after a review of the radar survey data had been completed. The common mid-points were positioned on the basis of features observed within the radar data. Both of the common mid-point velocity soundings were completed with 100 MHz antennas. Figure 6a presents the results of the CMP 2 sounding, while Figure 6b present the velocity stack of the CMP 2 sounding. As can be seen from Figure 6, the processed common mid-point data indicate that the propagation velocity of the radar signal at depth through the local rock averages 0.12 metres per nanosecond (m/ns), which is a typical velocity for gneissic rock.

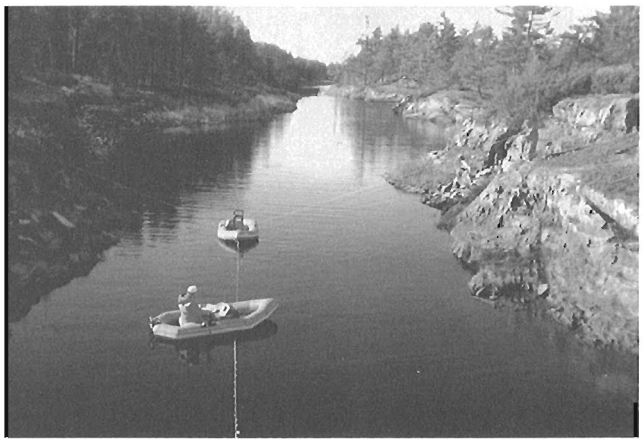

Figure 5. *Photograph of radar data acquisition on water.*

DATA PROCESSING AND PRESENTATION

The following discussion describes the procedures and methodology used for the compilation and presentation of the radar data. Every effort was made to ensure data quality and integrity during the course of both the field work and the post-survey processing.

The initial processing task was editing the header files and comments of each file. After these were completed, other editing functions were applied to the data including deleting traces acquired for quality assurance purposes, merging several files into single files for each survey line, correcting trace positions and reversing the profiles as applicable.

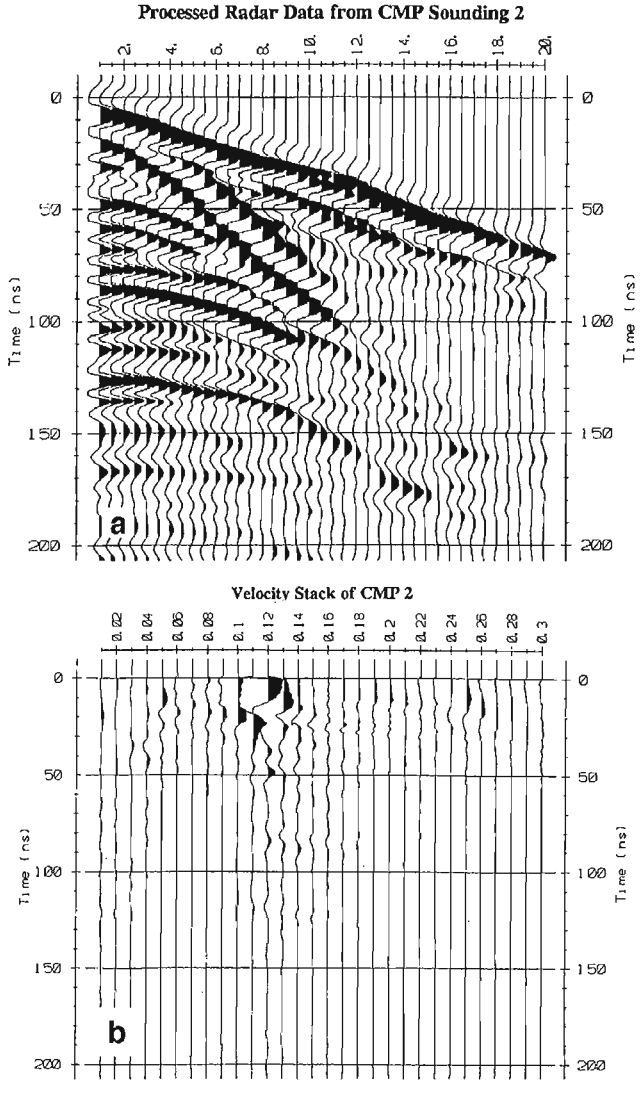

Figure 6. a) *Ground penetrating radar data from the CMP 2 sounding;* ***b)*** *the velocity stack of CMP 2.*

Each of the files were then augmented by interpolating one new radar trace between each recorded radar trace to improve the continuity of the profiles. These files were then processed with gain functions to enhance the data and allow better visual observation of the data in a plotted format.

Upon review of these preliminary data, additional editing was including corrections to annotations, deleting traces from overlapping sections, merging of data files along individual survey lines, time zero drift corrections, correcting starting positions for reverse profile plotting and other minor presentation inconsistencies. All such identified occurrences were corrected prior to the application of a topographic correction to the data based on the topographic data file for the site provided by PWGSC.

Profile plots shown in Figures 7 and 8 are presented at an approximate scales of 1:100 horizontal and 1:250 vertical, resulting in a vertical exaggeration of approximately 2.5.

The presentation of the processed radar data could not be compensated for the variation in radar signal propagation velocity caused by the freshwater in the stream channel. Radar signal propagates at a velocity of 0.033 m/ns in freshwater, or approximately 27.5% of that in the granitic rock. An average velocity of 0.12 m/ns was used to create the elevation axis on each of the processed radar profiles and, therefore, the elevation axes are not relevant for the processed radar data presented within the stream channel.

INTERPRETATION AND DISCUSSION

The interpretation of any geophysical data is always somewhat subjective and based on the experience of the interpreter, available ground truth information, and the overall quality of the data itself. In this case, the data quality was excellent and the interpretation of bedrock features was completed using the following generalized approach which has been evolved historically from reviewing radar data from this and similar environments.

Philosophy of interpretation

The majority of radar reflections from horizontal to sub-horizontal bedding planes, fractures, geological contacts, and stratigraphic sequences produce relatively flat-lying continuous events whereas the majority of radar reflections from physically weathered and heavily fractured rock appear as broken, discontinuous events, generally characterized by hyperbolae and scattered and diffracted signals. Radar reflections from sub-vertical to vertical fractures may produce a series of hyperbolae, or local apparent signal scattering, within the radar profile. The presence of faults can be inferred from breaks in the radar reflection stratigraphy.

This interpretive approach was applied to the radar data acquired during this survey program. Examples of the radar profiles are presented in Figures 7a and 8a where the majority of the radar reflectors are laterally continuous, strong events indicating a relatively continuous fracture network across the area of investigation. Examples of the integrated interpretation of these radar profiles are presented in Figures 7b and 8b as cross-sections showing the bedrock surface and events mapped within the rock. These events have been loosely categorized into three types: minor fractures, major fractures, and inferred faults. Any of these features may not be a single isolated occurrence, but rather a group, or system of occurrences. A uniform marking scheme was applied to all the collected ground penetrating radar sections.

The categorization of the fractures is based on relative signal amplitude and strength recorded on the various radar profiles. This categorization remains a strictly subjective judgment by the interpreting scientists. Changes in radar signal amplitude and strength between those fractures deemed major versus those deemed minor are likely due to any, or all, of the following factors: nature of the infilling material within the fracture (i.e. water, air or soil will produce a stronger contrast in dielectric properties and thus a higher amplitude reflection than a fracture filled with fragments of local rock); fractures that are oriented or positioned at a more favourable location to maximize radar signal returns; and/or the size of the fracture.

The central part of Figure 7b show the top of bedrock roughly corrected for the change of radar signal propagation velocity (0.033 m/ns) caused by the fresh water in the channel. The interpreted cross sections shown in Figures 7b and 8b represent the actual bedrock topography indicating the spatial position of the categorized radar responses.

Radar frequency and amplitude analysis

Along with the GPR profile data, amplitude and frequency spectra for each of the survey lines were computed. Data from one representative line were selected to illustrate this process. Figure 9 presents the amplitude and frequency data computed along line 39 N. These data are representative of the general response along the entire line, not any individual station. This line was chosen based on average radar signal attenuation characteristics at this site.

The amplitude spectra shown in Figure 9a show a response before time zero which represents the average background radar noise level recorded for the entire survey line. This background noise is caused by internal instrument noise and radio-frequency clutter present in the atmosphere in the vicinity of the survey area. Near time zero, the approximately 50 000 microvolt transmit pulse can be identified, which represents the signals received directly through the air and those refracted through near surface ground.

Beyond time zero, the amplitude spectrum analyses show a natural amplitude decay of the response with time. Figure 9a shows that signal is present above the noise level to beyond a delay-time of 250 (ns), which indicates that along line 39 N, coherent radar data indicative of the subsurface geology was obtained to 250 ns or approximately 15 m, when a radar wave velocity of 0.12 m/ns is assigned. It is important to note that these depth estimate values are average values for each of the lines, not specific values for any individual station.

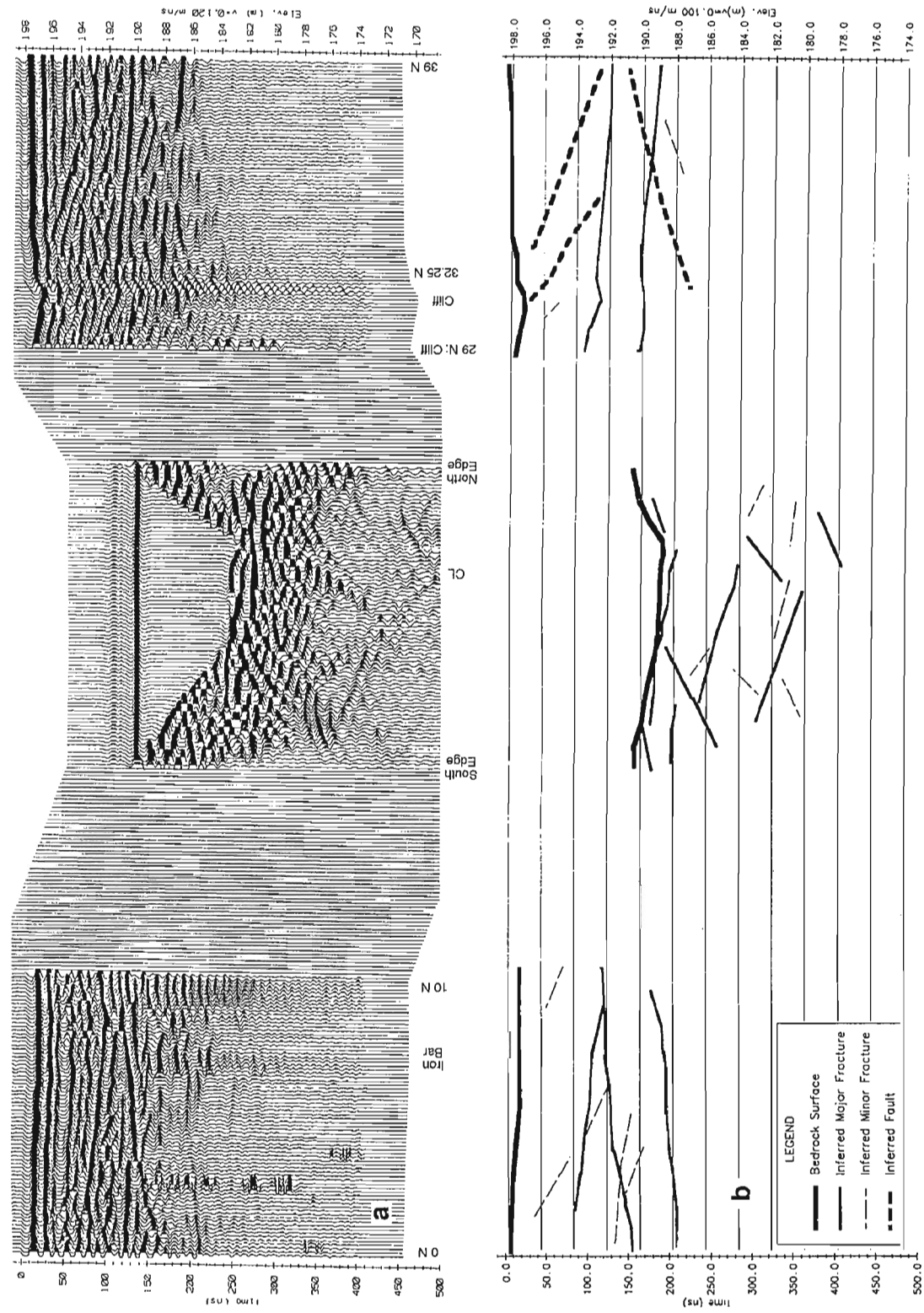

Figure 7. a) Example of ground penetrating radar data along line 10 W; b) Interpretation diagram of the data along line 10 W.

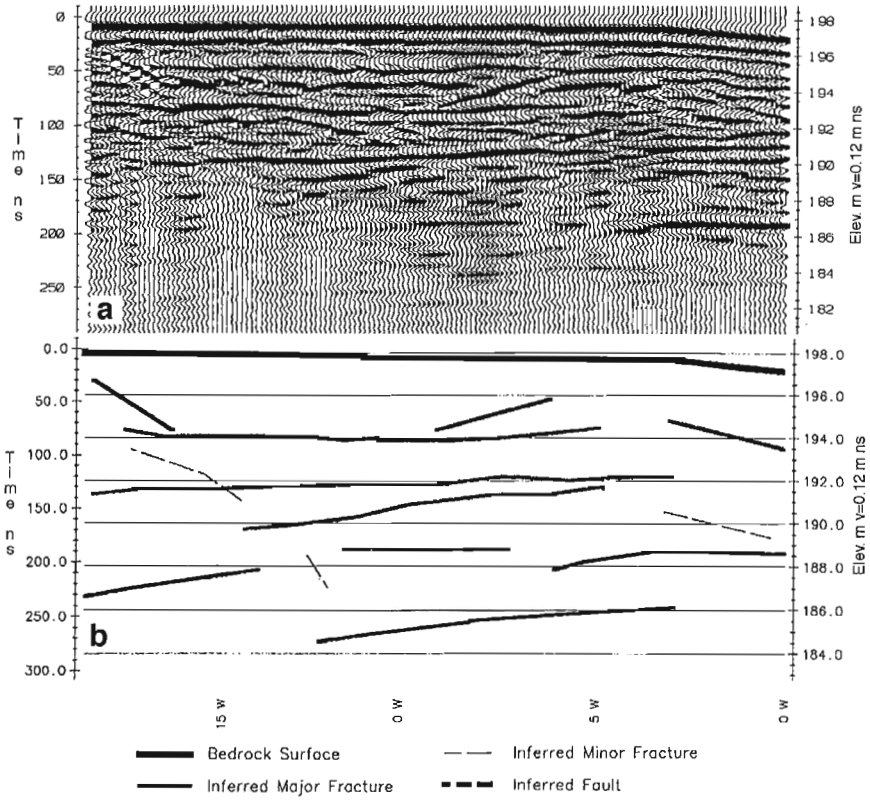

Figure 8. *a) Example of ground penetrating radar data along line 39 N; b) Interpretation diagram of the data along line 39 N.*

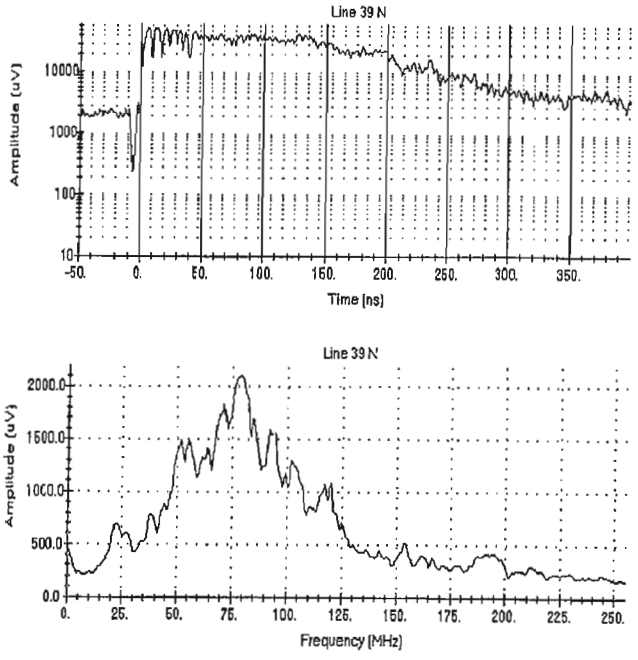

Figure 9. *Amplitude and frequency spectra of line 39 N.*

The corresponding frequency spectrum analysis shown in Figure 9b displays a received broadband response varying from 20 MHz to greater than 130 MHz for the nominal 100 MHz system. These data indicate that a dominant frequency of slightly less than 100 MHz was recorded from the manufactured 100 MHz centre frequency antennae. This type of response is typical since the signals change frequency and character when travelling through media with differing electrical properties, such as rock.

Vertical accuracy and resolving capability

The accuracy of the radar system is dependent on the system performance, the attenuation characteristics of the host material, and the contrast in electrical properties between the host material and the target, or fractures. Given that the host material, gneissic rock, is fairly uniform, and has very low signal attenuation characteristics, it should be possible to detect fractures in the order of millimetres or less in thickness, since the small amount of energy reflected by these tiny fractures should not be attenuated beyond the recording capability of the pulseEKKO IV radar system.

The absolute accuracy of the radar is technically determined by the wavelength of the recorded signals, regardless of the depth to the reflecting horizon. The frequency

spectra in Figure 9 indicate a frequency of slightly less than 80 MHz, which corresponds to a wavelength of slightly greater than 1.25 m in air. Since it is almost always possible to pick the onset of pulse of radar energy to 0.25 of the wavelength, the absolute technical accuracy of these radar data is in the order of 0.33 m, independent of depth. Typically, the theoretical resolving capability of the radar system is in the order of 1/100th of the wavelength of the recorded signals, which at this site, is in the order of 2 cm or less.

The absolute plotted accuracy of the inferred fracture positions is dependent on the variability of the vertical and horizontal changes in radar wave propagation velocity, which is directly related to the complexity of local geological conditions. The presentation of the interpretation in Figures 7b and 8b was completed using the average rock velocity determined by the analysis of the common mid-point soundings. Should significant vertical velocity changes be encountered at any given location, or lateral velocity changes not be adequately defined from the common mid-point data, errors in the inferred fracture elevation may be present. Although minor fluctuations in the absolute fracture elevation values may occur, the general trends indicated by the profile data will be correct.

The radar surveys were conducted with an antenna spacing of 1 m and, therefore, where the features are within 1 m of surface the radar system cannot reliably measure these features as the length of the radar wave ray path will be greater than the depth to the feature.

CONCLUSION

A ground penetrating radar survey procedure that allowed the acquisition of high quality, high resolution three dimensional data at the survey site has been successfully established. The data acquired along 57 survey lines were interpreted to locate discontinuities in the rock mass, thus successfully mapping a series of bedrock fractures and discontinuities in three dimensions at the proposed containment dam construction site. It was also shown that the equipment used for acquiring the data was capable of defining geological conditions in the rock mass to average delay times in excess of 250 ns, or to depth in excess of 15 m using an average propagation velocity of 0.12 m/ns measured at the site.

As the dam site is currently being excavated, it will allow review of the data collected at the site and its interpretation and comparison with drill cores and the excavated faces.

ACKNOWLEDGMENTS

The principal author wishes to acknowledge the help of Richard Laframboise and Douglas Grant of Terrain Sciences Division in teaching him how to make digital figures, as used in this paper.

REFERENCES

Grasmueck, M.
1994: Application of seismic processing techniques to discontinuity mapping with Ground Penetrating Radar in crystalline rock of the Gotthard Massif, Switzerland; Proceedings of the Fifth International Conference on Ground Penetrating Radar, Kitchener, Ontario, p. 1135-1149.

Holloway, A.R.
1992: Fracture mapping in granitic rock using Ground Probing Radar; in Ground Penetrating Radar, (ed.) J. Pilon; Geological Survey of Canada, Paper 90-4, p. 85-100.

Piccolo, M.
1992: GPR application for the definition of unconformities in a carrara marble quarry (Massa Carrara-Italy); in Fourth International Conference on Ground Penetrating Radar June 8-13,1992. Rovaniemi, Finland, (ed.) P. Hänninen and S. Autio; Geological Survey of Finland, Special Paper 16, p. 223-228.

Shikun Deng, Shengrong Zuo, and Huilian Wang
1994: The application of Ground Penetrating Radar to detection of shallow faults and caves; Proceedings of the Fifth International Conference on Ground Penetrating Radar, Kitchener, Ontario, p. 1115-1120.

Stevens, K.M., Everitt, R.A., Street, P.J., and Lodha, G.A.
1994: Litho-structural characterization in granitic rocks using single hole and crosshole radar techniques; Proceedings of the Fifth International Conference on Ground Penetrating Radar, Kitchener, Ontario, p. 625-638.

Geological Survey of Canada Project 920039JP

Un kame sur la batture aux Alouettes, près de l'embouchure du Saguenay, Québec

Jean-Claude Dionne[1]
Division de la science des terrains

Dionne, J.-C., 1996 : Un kame sur la batture aux Alouettes, près de l'embouchure du Saguenay, Québec; dans Recherches en cours 1996-C; Commission géologique du Canada, p. 177-182.

Résumé : Contrairement à la majorité des îles du Saint-Laurent estuarien, la petite île du Chafaud aux Basques, à l'extrémité sud de la vaste batture aux Alouettes, à l'embouchure du Saguenay, est entièrement constituée de matériaux meubles sablo-graveleux stratifiés avec des couches diamictiques caillouteuses. Il s'agit d'un kame sis à la limite des basses mers et reposant sur un estran silto-argileux au pied de l'escarpement du Bouclier laurentidien. Essentiellement précambriens, les matériaux proviennent de l'arrière-pays. L'écoulement glaciaire dans l'anse du Chafaud aux Basques est orienté 95°-105°. À peine modifié par les eaux de la Mer de Goldthwait, ce kame résiduel indique fort probablement la position du front glaciaire dans ce secteur de la côte nord lors de la récurrence de Saint-Narcisse, datée de 11 -10,6 ka.

Abstract: Although most islands in the St. Lawrence estuary are rocky, the islet called Île du Chafaud aux Basques, located at the southern end of the large tidal flat aux Alouettes, at the mouth of the Saguenay fjord, is composed entirely of unconsolidated stratified sand and gravel with bouldery diamict layers. This islet is a true kame occurring at low tide level on a silty-clayey flat that extends from the foot of the Laurentides Shield escarpment. Rock debris are essentially from the inland Precambrian substrate. Late glacial flow directions in Chafaud aux Basques cove are 95°-105°. Slightly modified by wave action during the Goldthwait Sea episode, this relict kame most likely indicates the ice front position during the St. Narcisse event dated at 11-10.6 ka in the area.

[1] Département de géographie et Centre d'études nordiques, Université Laval, Québec, Québec G1K 7P4

INTRODUCTION

Aucun exemple de kame sur les rivages du Saint-Laurent, en aval de Québec, n'étant connu, il s'avère utile de signaler celui de l'anse du Chafaud aux Basques découvert récemment (Dionne, 1994a) et de proposer une interprétation préliminaire.

OBSERVATIONS

L'île du Chafaud aux Basques est située en face de l'anse du même nom (69°45'50"W, 48°01'30"N), soit à l'extrémité sud de la vaste batture aux Alouettes, sise du côté sud-ouest de l'embouchure du Saguenay (fig. 1), à une vingtaine de kilomètres de Pointe-Noire. À cet endroit, on trouve une petite anse découpant la ligne de rivage taillée à même le grand escarpement rocheux du Bouclier laurentidien.

Située à la limite des basses mers (fig. 2), la petite île, de forme triangulaire et cônique, s'élève à 25 m environ au-dessus de l'estran environnant. Elle se trouve dans le prolongement de la ligne du rivage rocheux, de part et d'autre de l'anse. Elle mesure environ 150 m de longueur (axe a) et 90 m de largeur (axe b). Elle est caractérisée par des pentes escarpées mais rarement taillées en falaise vive, car elle est ceinturée par un

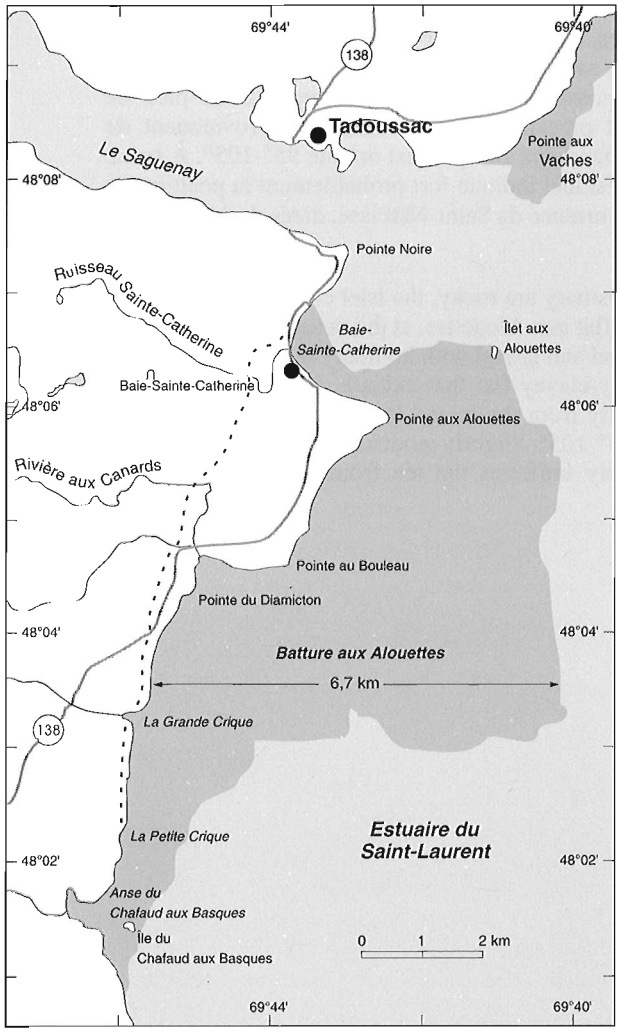

Figure 1. Carte de localisation et noms de lieux.

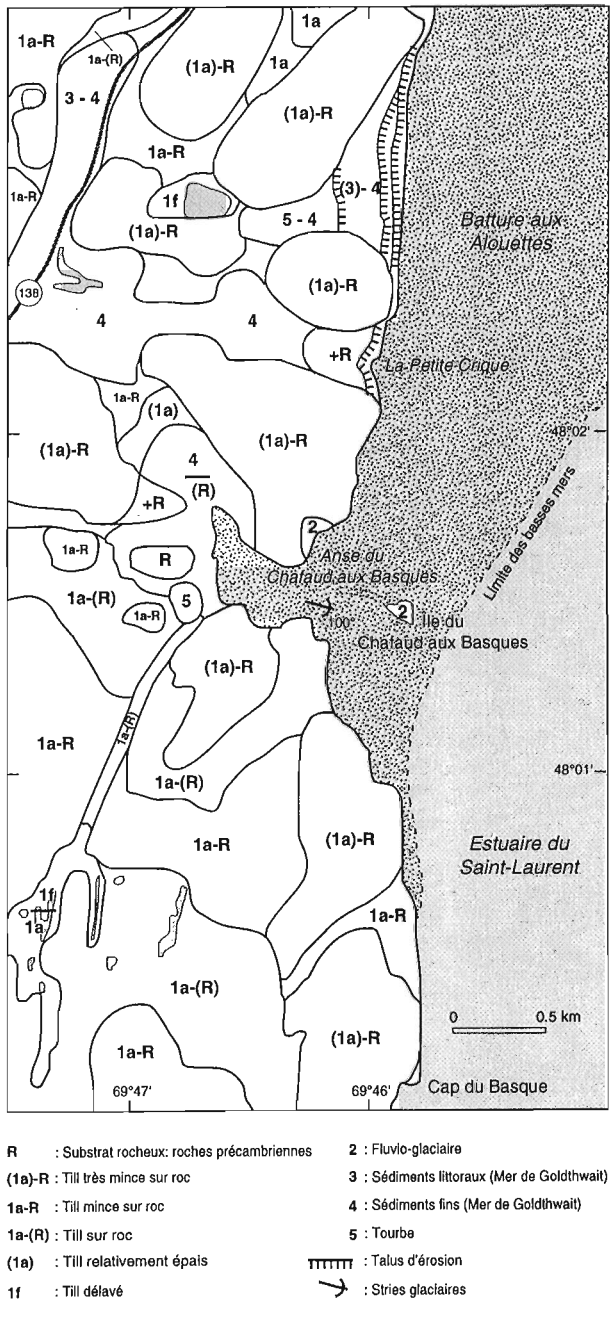

Figure 2. Extrait de la carte des formations meubles de Tadoussac (Dionne, 1972), dans le secteur de l'anse du Chafaud aux Basques.

cordon de gros blocs (fig. 3). Du côté est, exposé aux vagues, les blocs sont presque tous de taille métrique, les plus gros excédant 2 m (L). Les cailloux représentent diverses lithologies ignées et métamorphiques du Bouclier laurentidien d'âge précambrien, situé à proximité (Miller, 1973). Du côté de la mer, on observe un beau replat d'érosion vers 15 m d'altitude. Le sommet de l'îlot est relativement plat.

Sur la photo aérienne prise en 1976 (fig. 4), l'îlot est entièrement boisé. Il y avait alors un beau couvert de résineux et de feuillus comprenant des épinettes (*Picea* sp.), des sapins (*Abies* sp.) et des bouleaux (*Betula papyrifera*). Lorsque nous avons visité l'îlot pour la première fois en 1989, le couvert végétal arborescent avait été détruit par une colonie de cormorans à aigrettes (*Phalacrocorax auritus*). Des reprises d'érosion à quelques endroits sur les versants escarpés ont alors permis d'examiner la nature du dépôt.

Le dépôt comporte essentiellement des matériaux détritiques grossiers (rudites et arénites) stratifiés avec des couches de galets et des blocs, les couches ayant un pendage général vers l'est, c'est-à-dire vers la vallée du Saint-Laurent. Sont associés aux sédiments fluvioglaciaires des masses de diamicton sableux de tailles variées. L'analyse granulométrique d'un échantillon de diamicton provenant de la partie sommitale du côté sud de la butte a révélé que la matrice contenait 19 % de petit gravier, 68,9 % de sable, 9,5 % de silt et 2,6 % d'argile. Le trie est faible, l'indice de Trask étant de 2,984. La teneur en carbonates (calcite) est à peu près nulle : 0,3 % seulement. On n'y a observé aucun cailloux carbonaté (calcaire de Trenton ou dolomie du Protérozoïque). Il n'y en a pas non plus sur le haut de plage au pied du rivage rocheux environnant. Les premiers éléments carbonatés sur le rivage actuel ont été observés après la Petite Crique, à plus de 3,5 km au nord (Dionne, 1994b).

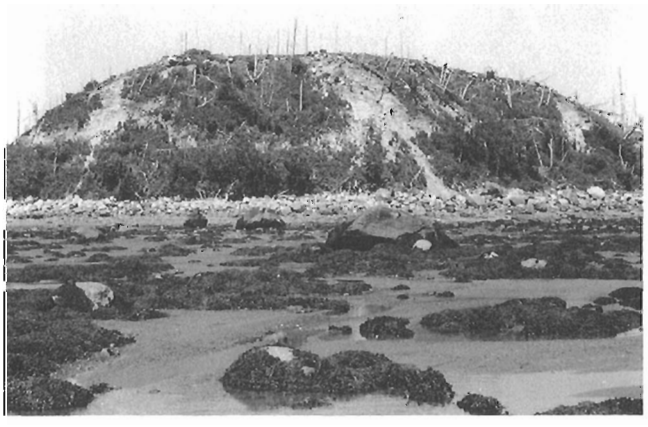

Figure 3. *Vue générale du kame de l'anse du Chafaud aux Basques, à marée basse. À remarquer le couvert forestier détruit par les cormorans et les cicatrices d'érosion apparues par la suite. La butte, d'environ 25 m de hauteur, est ceinturée par un cordon de gros blocs précambriens (6-10-89).*

Le cordon de gros blocs ceinturant l'îlot atteste de l'abondance des blocs dans la butte, ce qui indique la présence d'une source située à faible distance ou encore d'un agent de transport puissant lors de leur dépôt.

Une belle flèche en queue de comète (fig. 4), constituée de sable et de petit gravier, s'est formée du côté ouest de l'île du Chafaud aux Basques, c'est-à-dire du côté abrité. Ce cordon d'environ 250 m de longueur sur une quinzaine de mètres de largeur se prolonge vers le fond de l'anse, en direction d'un îlot rocheux. Ce dernier montre un façonnement glaciaire bien conservé avec une surface polie et striée indiquant un écoulement de la glace selon une direction de 95°-105°, soit grossièrement parallèle à l'axe central de l'anse. Cette direction se retrouve ailleurs dans la région de Tadoussac (Dionne et Occhietti, 1996).

L'estran ceinturant la butte est constitué essentiellement de silt et d'argile stratifiés de couleur gris pâle. À proximité de l'îlot, la surface de l'estran est en grande partie masquée par de minces placages de sable et gravier et des blocs épars. À maints endroit, cependant, la surface argileuse affleure. La flèche en queue de comète repose d'ailleurs sur l'argile. Fait intéressant à signaler, le poids de la masse sédimentaire provoque une surcharge, de sorte que l'argile sous-jacente injectée vers le haut forme des bourrelets diapiriques en bordure de la flèche. La grande batture, qui s'élargit jusqu'à 5,5 km en direction nord vers l'embouchure du Saguenay (fig. 1), est elle aussi, du moins en surface, composée de silt et d'argile stratifiés (Dionne et Occhietti, 1996).

Sur la rive nord, à la sortie de l'anse du Chafaud aux Basques, on a observé un petit dépôt résiduel de type diamictique grossier accroché au versant rocheux. Le matériau sablo-graveleux contient beaucoup de cailloux dont plusieurs de taille métrique. Il s'agit vraisemblablement d'un dépôt apparenté au kame.

Dans les environs de l'anse du Chafaud aux Basques, les collines rocheuses dominent partout et sont en grande partie dénudées. Plutôt mince, le till est concentré dans les dépressions (fig. 2). À l'instar de la dépression de la Petite Crique, au nord, la dépression qui entaille le bouclier à la tête de l'anse du Chafaud aux Basques a un fond rocheux couvert d'une mince couche de till et de sédiments fins silto-argileux laissés par la Mer de Goldthwait; cette dernière a atteint une altitude maximale d'environ 140-145 m dans le secteur. Il ne semble pas y avoir eu de communication entre les deux dépressions.

INTERPRÉTATION

Première interrogation : s'agit-il vraiment d'un kame? Si on se fonde sur les caractéristiques du dépôt, la butte de l'anse du Chafaud aux Basques correspond exactement à la définition d'un kame offerte dans l'ouvrage «Vocabulaire de la géomorphologie» (Conseil international de la langue française, 1979, p. 110): «Dépôt hydro-glaciaire dont les matériaux sont semblables aux moraines d'ablation, mis en place dans des dépressions d'obturation soit entre des lobes d'un glacier, soit en position juxtaglaciaire». La butte de

l'anse du Chafaud aux Basques correspond aussi à la définition d'un kame offerte dans le Glossary of Geology (Bates et Jackson, 1987, p. 354). Il s'agit bien d'un dépôt juxtaglaciaire.

Le deuxième aspect concerne la signification précise du kame de la batture aux Alouettes. D'une part, s'agit-il d'un fragment de moraine frontale appartenant à une langue glaciaire (glacier de piedmont) canalisée dans la dépression de l'anse du Chafaud aux Basques et étalée sur le rivage en face, ou s'agit-il plutôt du front de l'Inlandsis laurentidien formant un grand arc à l'embouchure du Saguenay (Dionne et Occhietti, 1996)? D'autre part, à quel événement se rattache cette butte résiduelle? S'agit-il d'une butte mise en place au Wisconsinien supérieur ou antérieurement ou bien d'un dépôt frontal lié à la récurrence de Saint-Narcisse au tardiglaciaire?

En raison de l'échelle, les cartes de Prest (1969) et de Dyke et Prest (1987) retraçant les fronts glaciaires de l'Inlandsis laurentidien sont peu utiles pour résoudre le problème. La série de cartes de la position du front glaciaire de LaSalle et al. (1977) montre le tracé de l'Inlandsis laurentidien dans le secteur de l'embouchure du Saguenay entre 11 et 10,5 ka (fig. 5). Sur la figure 5A, on constate que vers 11,3-11 ka, le front de l'Inlandsis laurentidien, sur la rive nord du moyen

Figure 4. *Vue aérienne verticale de l'île et de l'anse du Chafaud aux Basques, littoral est de Charlevoix (Photo aérienne Q76317-66; échelle 1 10 000; Photocartothèque du Québec).*

estuaire, occupait une position à l'intérieur des terres légèrement méridionale par rapport au tracé de la moraine de Saint-Narcisse. Toutefois, dans le secteur oriental du moyen estuaire, on note qu'une langue glaciaire occupait la vallée de La Malbaie et s'étalait en un lobe arrondi (glacier de piedmont) dans le Saint-Laurent au droit du banc des Anglais. Cet événement avait d'ailleurs été mis en évidence par Poulin (1977, voir sa carte hors texte en particulier). Plus en aval, le front glaciaire, à la même époque, occupait encore la moitié du chenal Nord entre Saint-Siméon et Tadoussac. La batture aux Alouettes était donc entièrement recouverte par le glacier.

La figure 5B (LaSalle et al., 1977) présente la position du front glaciaire lors de la récurrence de Saint-Narcisse entre environ 11 ka et 10,5 ka. L'ensemble de la rive nord du Saint-Laurent entre Québec et Saint-Siméon était alors déglacé et le rebord du Bouclier laurentidien était submergé par les eaux de la Mer de Goldthwait.

À l'embouchure du Saguenay, cependant, la masse de glace avait changé de configuration, prenant la forme d'un lobe circulaire étalé sur la plate-forme continentale jusqu'aux hauts-fonds de l'île Rouge (Dionne et Occhietti, 1996). La batture aux Alouettes et l'anse du Chafaud aux Basques étaient donc sous la glace à cette époque. Nous ignorons sur quels éléments de terrain LaSalle et al. (1977) se sont basés pour établir le tracé du front glaciaire entre Saint-Siméon et Tadoussac, car ils ne mentionnent pas la seule carte des formations meubles (Dionne, 1972) existant à l'époque pour le secteur en question.

L'âge exact de l'accumulation du kame de l'anse du Chafaud aux Basques n'est pas connu. En première approximation, nous pensons que cette butte a été édifiée par un lobe local lié à la réavancée de Saint-Narcisse, soit entre 11 et 10,6 ka, d'après la chronologie établie pour la région de Tadoussac (Dionne et Occhietti, 1996). Or, il subsiste des questions qu'il convient d'évoquer brièvement.

D'une part, nous ignorons la nature du substrat sur lequel repose le kame. Repose-t-il vraiment sur la surface silto-argileuse environnante ou y est-il enfoui, sa base reposant plutôt sur un substrat de nature inconnu mais peut-être morainique? Si le kame surmonte le dépôt argileux, il lui est forcément postérieur; il correspondrait alors aux événements de Saint-Narcisse, car une partie des sédiments silto-argileux de la batture aux Alouettes semble attribuable à une phase précoce de la Mer de Goldthwait antérieure à la récurrence de Saint-Narcisse. Toutefois, comme l'ont évoqué ailleurs Dionne et Occhietti (1996), la vaste batture aux Alouettes pourrait avoir un âge pré-goldthwaitien. D'autre part, ce kame peut-il être corrélé avec la butte de till de la pointe du Diamicton ou encore avec le dépôt sableux relique de la pointe aux Alouettes qui remonte à environ 35 ka (Dionne et Occhietti, 1996)? Dans l'état actuel des connaissances, il est difficile de répondre de façon satisfaisante à ces interrogations.

Il faut donc poursuivre les recherches sur le Quaternaire du secteur de l'embouchure du Saguenay, qui jusqu'à récemment avait été largement négligé. Des travaux de géophysique et même un sondage par carottier permettraient de connaître la nature et l'épaisseur des formations meubles de la batture aux Alouettes, qui occupe une position étrange à l'embouchure du fjord du Saguenay. La découverte récente à la pointe aux Alouettes d'un dépôt fossilifère relique qui date d'au moins 35 ka permet de penser qu'il subsiste dans le secteur de Tadoussac des traces d'événements géologiques survenus au cours du Wisconsinien moyen ou inférieur. Cela revêt donc une importance majeure pour reconstituer la stratigraphie et l'évolution de la vallée moyenne du Saint-Laurent.

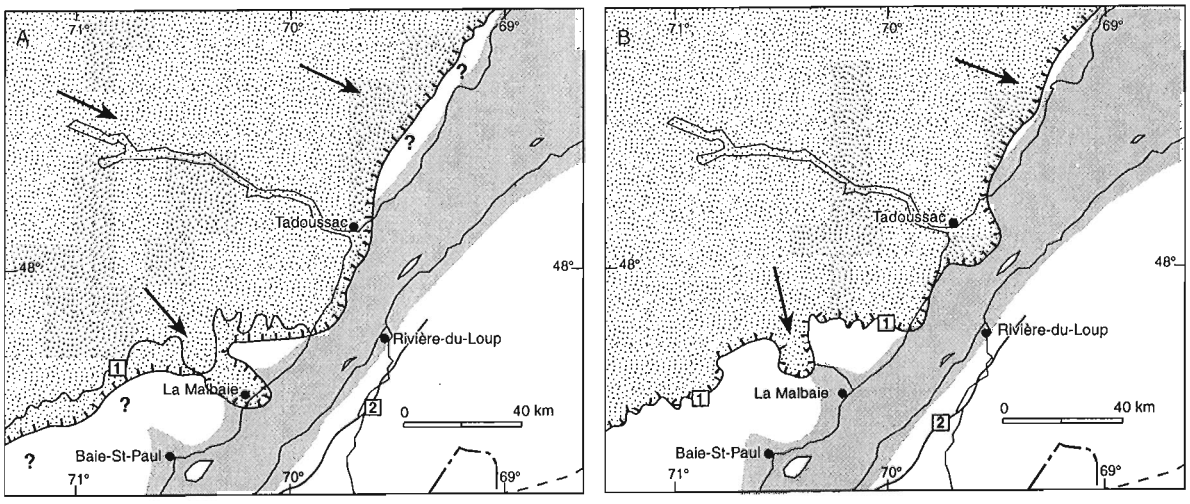

Figure 5. *Tracé du front de l'Inlandsis laurentidien, entre Baie-Saint-Paul et le Saguenay, d'après LaSalle et al. (1977);* ***A****) front glaciaire vers 11,3-11 ka;* ***B****), front glaciaire entre 11 et 10,5 ka.*

REMERCIEMENTS

Cette contribution s'inscrit dans un projet de recherche sur le Quaternaire du Saguenay subventionné par la Commission géologique du Canada. Deux anciens étudiants du Département de géographie de l'Université Laval (Stéphen Poitras et Robert Bonenfant) nous ont accompagné à l'île du Chafaud aux Basques, en 1989 et 1991. Les figures au trait ont été réalisées au Laboratoire de cartographie du Département de géographie, Université Laval. L'analyse granulométrique de l'échantillon du diamicton a été effectuée à la Commission géologique du Canada (Ottawa).

RÉFÉRENCES

Bates, R.L. and Jackson, J.A.
1987: Glossary of Geology; American Geological Institute, Alexandria Virginia, 786 p.

Conseil International de la Langue française
1979: Vocabulaire de la Géomorphologie; Paris, Hachette et la Maison du Dictionnaire, 219 p.

Dionne, J.C.
1972: Cartes morpho-sédimentologiques du Saguenay/Lac-Saint-Jean, Québec; Direction des Terres, Environnement Canada, série de cartes manuscrites à l'échelle de 1 50 000.

Dionne, J.C. (suite)
1994a: Découverte d'un kame sur la batture aux Alouettes (Saguenay). Colloque annuel du Centre d'études nordiques (décembre 1994), résumés, p. 14.
1994b: Les erratiques lointains de l'embouchure du Saguenay; Géographie physique et Quaternaire, vol. 48, p. 179-194.

Dionne, J.C. et Occhietti, S.
1996: Aperçu du Quaternaire à l'embouchure du Saguenay; Géographie physique et Quaternaire, vol. 50, p.

Dyke, A.S. and Prest, V.K.
1987: Late Wisconsinan and Holocene history of the Laurentide Ice Sheet; Géographie physique et Quaternaire, v. 41, p. 237-263.

LaSalle, P., Martineau, G. et Chauvin, L.
1977: Morphologie, stratigraphie et déglaciation dans la région de Beauce - Monts Notre-Dame - Parc des Laurentides; Ministère des Richesses naturelles, Québec, rapport DPV-516, 74 p.

Miller, M.L.
1973: Région de Saint-Siméon - Tadoussac; Ministère des Richesses naturelles, Québec, rapport géologique 159, 94 p.

Poulin, P.
1977: Le complexe morainique de Saint-Narcisse dans le secteur sud de la rivière Malbaie; Département de géographie, Université Laval, Québec, thèse de maîtrise, 83 p.

Prest., V.K.
1969: Retreat of Wisconsin and Recent ice in North America; Geological Survey of Canada, Map 1257A, scale 1: 5 000 000.

Programme des conventions de recherche d'EMR 242-4-92
Commission géologique du Canada projet 920073

Troctolitic rocks of the Reid Brook intrusion, Nain Plutonic Suite, Voisey Bay area, Labrador[1]

Ronald F. Emslie
Continental Geoscience Division, Ottawa

Emslie, R.F., 1996: Troctolitic rocks of the Reid Brook intrusion, Nain Plutonic Suite, Voisey Bay area, Labrador; in Current Research 1996-C; Geological Survey of Canada, p. 183-196.

Abstract: This contribution provides preliminary petrographic, mineralogical, and geochemical data on a set of six samples collected in 1991 from the Reid Brook intrusion of the Nain Plutonic Suite, the nearest spatially-associated troctolitic rocks to the Voisey Bay Ni-Cu-Co sulphide deposit. Although the samples are few, some time likely will elapse before additional detailed published information is forthcoming, so this opportunity is taken to present and discuss the available data in light of other information on basic rocks associated with the Nain Plutonic Suite.

The samples of the Reid Brook intrusion comprise mainly fresh melatroctolite, but also include leucotroctolite and gabbronorite. Mineral chemistry and major and trace element rock geochemistry of the Reid Brook intrusion are consistent with it being a significant potential source for the metals present in the Voisey Bay ores. The source of the sulphur however, may lie elsewhere and the Tasiuyak gneiss is a favourable potential candidate.

Résumé : Le présent article fait état des données pétrographiques, minéralogiques et géochimiques préliminaires sur un ensemble de six échantillons prélevés en 1991 dans l'intrusion de Reid Brook de la suite plutonique de Nain; il s'agit des roches troctolitiques les plus étroitement associées dans l'espace aux sulfures de Ni-Cu-Co de Voisey Bay. Les échantillons sont peu nombreux, mais il s'écoulera probablement du temps avant que d'autres informations détaillées soient publiées. L'occasion est donc saisie pour présenter et traiter les données actuelles à la lumière d'autres informations recueillies sur les roches basiques associées à la Suite plutonique de Nain.

Les échantillons de l'intrusion de Reid Brook se composent surtout de mélatroctolite non altérée, mais également de leucotroctolite et de gabbronorite. La chimie minérale de même que la géochimie des éléments majeurs et traces de l'intrusion de Reid Brook corroborent les grandes possibilités que celle-ci soit la source des métaux qui composent les minerais de Voisey Bay. La source du soufre, cependant, pourrait être située ailleurs et le gneiss de Tasiuyak s'avère un candidat plausible.

[1] Contribution to Canada-Newfoundland Cooperation Agreement on Mineral Development (1990-1994), a subsidiary agreement under the Canada-Newfoundland Economic and Regional Development Agreement.

INTRODUCTION

The recent discovery of economically important Ni-Cu-Co sulphide deposits at Voisey Bay in Labrador makes characterization of the host rocks of some interest for future mineral exploration. The nearest exposed mafic rocks to the deposit are troctolitic rocks of the Reid Brook intrusion. In the summer of 1991, six samples from different parts of the Reid Brook intrusion were collected as part of an overall study of the Nain Plutonic Suite. This report presents petrographic, mineralogical, and geochemical details of the samples in the context of the mineral deposits and makes comparisons with other mafic rocks of the Nain Plutonic Suite.

Principal features of the Nain Plutonic Suite

The Nain Plutonic Suite underlies an area of about 20 000 km^2 on the northern Labrador coast. It is one of the great anorthosite-mangerite-charnockite-granite igneous complexes of the middle Proterozoic. This and other similar complexes are widely considered to represent continental magmatic activity under anorogenic conditions.

Roughly subequal areas of granitoid rocks and basic plus anorthositic rocks underlie the Nain Plutonic Suite and U-Pb dating has revealed a time span of at least 1343 to 1290 Ma for intrusion of rocks of the suite (Hamilton et al., 1994; Connelly and Ryan, 1994). Most of the large granitoid bodies flanking the western side of the suite tend to be older than many of the presently dated basic and anorthositic intrusions in the eastern part of the complex, but both silicic and basic members intruded throughout the development of the suite.

The fact that the parent magma of the Kiglapait intrusion, the largest Nain Plutonic Suite mafic intrusion, did not attain sulphide saturation until a large part of it had crystallized suggests that Nain Plutonic Suite basic magmas may have been typically undersaturated in sulphide. If so, an external source of S was prerequisite to formation of massive volumes of early-precipitated sulphide melts as at Voisey Bay. The bulk of the monosulphide melt for the Voisey Bay deposit was FeS, so S may have been added as the element or as sulphide.

Unlike Ni-rich komatiitic or picritic magmas associated with some sulphide deposits (e.g. Keays, 1994), the parental magma for the Voisey Bay sulphides likely had a relatively low nickel concentration. A key factor in genesis of the deposit may therefore have been access of the magma to an abundant source of sulphur. The metasedimentary Tasiuyak gneiss outcrops along the eastern margin of the Churchill Province in the vicinity of the Nain Plutonic Suite and for several hundred kilometers to the north and is a potential sulphur source.

MAFIC ROCKS OF THE NAIN PLUTONIC SUITE

Mafic rocks associated with the Nain Plutonic Suite include two main rock groups, both subordinate in volume to the dominant anorthositic and granitoid rocks (Fig. 1). Mafic rocks of the first group are dominantly olivine gabbro, troctolite, leucotroctolite, and gabbronorite, and include intrusions such as Kiglapait, Hettasch, Barth Island, Newark Island, and Jonathon; the rock compositions indicate parent magmas ranging from relatively primitive to somewhat evolved. The second group of mafic rocks is subordinate in volume and has a compositional range centred on ferrodiorite; they are typically highly evolved (Mg# near 30) and will not be considered further as potential parental magmas to significant Ni-Cu-Co sulphide concentrations.

Troctolitic and leucotroctolitic rocks occur widely in the Nain Plutonic Suite, mostly but not entirely in the eastern part of the anorthositic complex. The rocks weather deep buff to reddish-brown with more intense rusty brown associated with those rocks richer in olivine. On fresh surfaces the rocks are dark grey to black with greenish-black olivine.

The least-evolved troctolitic rocks of the Nain Plutonic Suite have olivine compositions near Fo_{70} and plagioclase near An_{70}; this also appears to be true for the Reid Brook troctolites. These cannot be considered as very primitive compositions and have crystallized from relatively fractionated melts saturated with both olivine and plagioclase. This fact appears to rule out involvement with komatiitic or picritic melts currently in favour as hosts for major Ni-Cu sulphide deposits (Keays, 1994). Although the presence of picritic melts in the Nain Plutonic Suite has been inferred (Berg, 1980), there is little reason to suggest their significant presence in the suite. Additional support for their absence from the Voisey Bay setting is provided by the relatively low Ni content and high Co:Ni of the massive sulphide ores. The metal concentrations in these ores are not consistent with ore-forming magmas as Ni-rich and primitive as picrite (e.g. Naldrett, 1989).

The following brief descriptions of several of the more prominent mafic intrusions of the Nain Plutonic Suite are drawn largely from summaries in Berg et al. (1994); original references cited therein should be consulted for further details.

Kiglapait intrusion

The Kiglapait intrusion (Morse, 1969, 1979, 1981) has an upright, elongate bowl-shape and underlies an area of about 560 km^2. A U-Pb zircon age of 1306 ± 2 Ma by Krogh has been reported from the Upper Zone of the intrusion. In

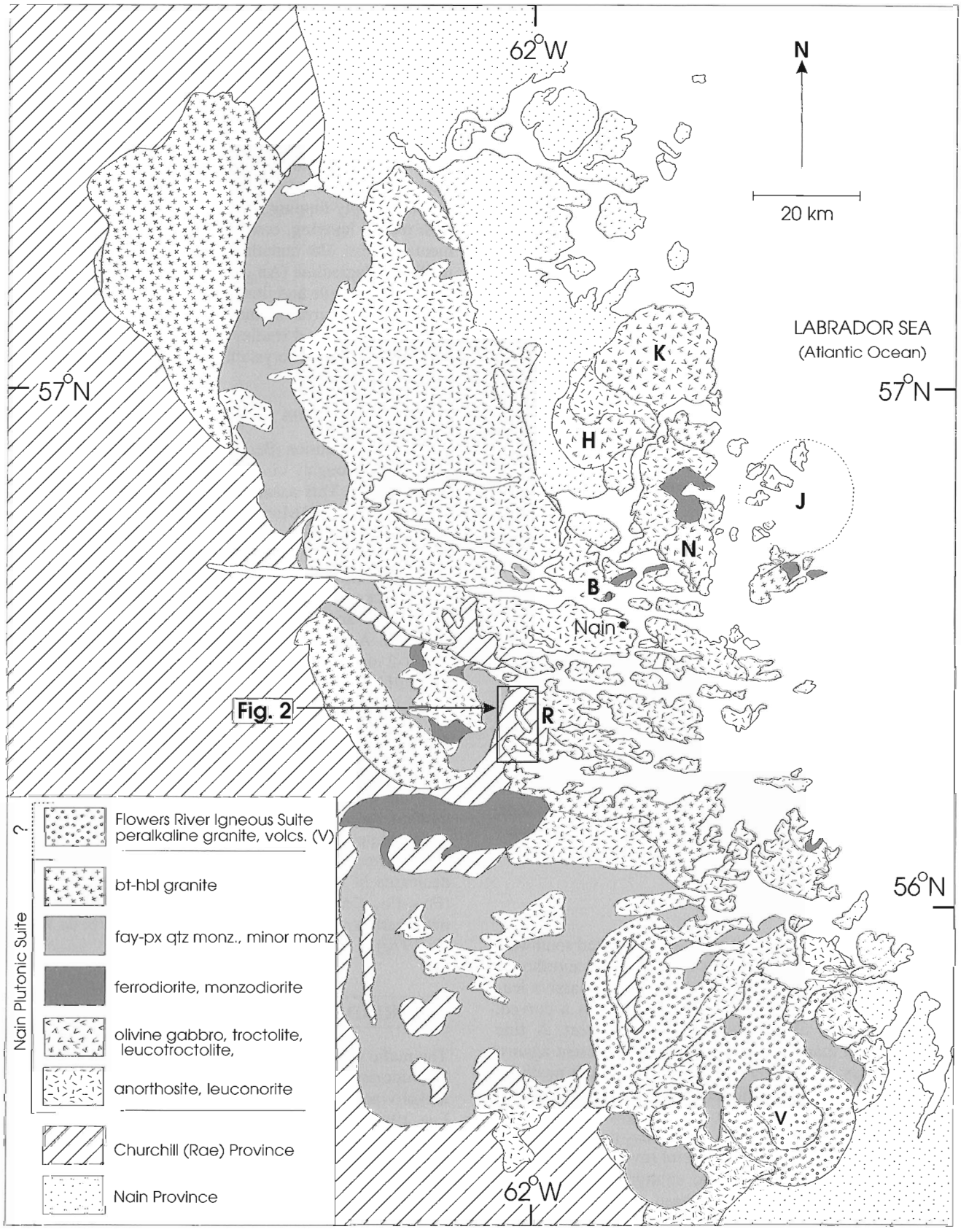

Figure 1. *Simplified geological map of the Nain Plutonic Suite showing the principal rock units. The area of Figure 2 is indicated. Adapted from Emslie et al. (1994). Intrusions referred to in the text are labeled: K – Kiglapait, H – Hettasch, J – Jonathon, N – Newark Island, B – Barth Island, R – Reid Brook.*

excellent agreement, a Sm-Nd whole rock and mineral isochron (De Paolo, 1985) yielded 1305 ± 22 Ma with initial $\varepsilon_{Nd} = -4.7 \pm 0.2$. Initial Nd isotopic compositions for samples from the intrusion span a range from ε_{Nd} = -1.6 to -5.6 (De Paolo, 1985). The Kiglapait intrusion is the largest mafic intrusion, and one of the younger basic members of the Nain Plutonic Suite. The parent magma was an anhydrous aluminous basaltic melt that crystallized over a temperature range of about 300°C. Plagioclase varies from An_{67} to An_{10}, olivine from Fo_{69} to Fo_0, and augite from En_{73} to En_0.

The intrusion has persistent, steep, inward-dipping layers whose attitudes appear to have been primary. Troctolite makes up some 80% of the lower part of the Layered Group. A sulphide-bearing horizon high in the intrusion (Morse, 1969) argues for late sulphide saturation, after most of the nickel, copper, and cobalt had been removed in earlier crystallized silicate minerals.

The inferred initial S content of the Kiglapait magma was 280 ± 70 ppm (weight) and reached sulphide saturation at 2900 ± 900 ppm S above the 80% crystallized level (Shirey, 1975a, b). Shirey also noted the sporadic occurrence of cobaltian pentlandite.

The preferred estimate for the Ni content of the initial Kiglapait liquid is 125 ± 25 ppm and olivine from early troctolitic cumulates of the Kiglapait intrusion (10-20 per cent solidified) contains 463 to 828 ppm Ni (Morse et al. 1991). Two samples, each with about 30% modal olivine from about 15 per cent solidified, have nickel contents for whole rock and olivine of 252 ppm, 828 ppm and 203 ppm, 621 ppm respectively. An estimate of 4.0 (range 3.3 to 5.0) has been made for the partition coefficient of Ni (weight) between olivine and liquid by Morse et al. (1991).

Pyrrhotite-rich sulphide grains from a sample of olivine gabbro from the Upper Zone of the Kiglapait intrusion yielded $\delta^{34}S$(‰) values of -3.0, -0.6, -3.6, -1.6, and -1.4 (Chaussidon et al., 1989). These values fall within the range of mantle-derived sulphides surveyed by Chaussidon et al. (1989).

Hettasch intrusion

The Hettasch intrusion (~200 km^2) was emplaced southwest of the Kiglapait intrusion against older, foliated anorthosite and gneiss and has been intruded by younger massive leucogabbronorite (Berg, 1980). The intrusion has a curved, trough-like form, convex toward the southwest. A fine grained chilled margin of olivine gabbro is present against Archean gneiss. The Lower Zone of the intrusion is medium- to coarse-grained leucotroctolite and anorthosite; the Upper Zone is very coarse grained olivine leucogabbronorite. Plagioclase compositions decrease from An_{72} near the base of the Lower Zone to An_{59}, show several reversals, then fall to An values in the low 50s in the stratigraphically highest cumulates. Olivine is Fo_{69} at the base of the Lower Zone, exhibits reversals, and falls to Fo_{60}.

Newark Island intrusion

The Newark Island intrusion (Weibe, 1988; Weibe and Snyder, 1993; Snyder et al., 1993) is a composite layered intrusion underlying an area of about 150 km^2. A lower layered series of troctolite, olivine gabbro, and oxide-rich cumulate rocks is overlain by an upper hybrid series comprising a wide range of mafic, granitic, and hybrid cumulates with interspersed layers of chilled mafic rocks. The layered series forms a steeply-dipping sheet about 3 km thick at maximum with trough layering, crossbedding, and slumped and fragmental layers. The cumulate rocks are composed predominantly of plagioclase (An_{60}-An_{40}), olivine (Fo_{60}-Fo_{10}), with subordinate augite and ilmenite. Several episodes of magma recharging occurred in the intrusion (Wiebe and Snyder, 1993). Experimental studies by Snyder et al. (1993) defined the T-fO_2 path in the crystallizing intrusion.

Jonathon Intrusion

The Jonathon Intrusion (Berg and Briegel, 1983) is 400-450 km^2 in area, and roughly circular in plan view, as portrayed by Ryan (1990). This assumes that the anorthositic rocks on Orton, Barham, and Marshall Islands (to the east of David and Akulaitualuk Islands), are part of the intrusion but details of those three islands are largely unknown. The Savage Islands, in the extreme east, are at least partly underlain by leucotroctolitic rocks. The largely unlayered rocks are mostly leucotroctolite and leuconorite and plagioclase lamination is common. A chilled margin is typically present and grades over 1-2 m into a zone of coarser leucotroctolite with a color index of 20-30.

Barth Island troctolite

The intrusion has been sliced into three main segments by east-trending faults with modest left-hand offsets. Upon restoration, the troctolite intrusion displays a broadly concentric inward-dipping, basin-like layered structure, about 6 x 9 km in diameter. The intrusion exhibits more or less regular decreases in An in plagioclase (An_{69}-An_{45}), Fo in olivine (Fo_{72}-Fo_{50}), and En in orthopyroxene (En_{74}-En_{51}) from the outer parts toward the middle (de Waard, 1976; de Waard et al., 1976).

THE REID BROOK INTRUSION

The mafic rocks most closely associated with the Ni-Cu-Co sulphide deposits at Voisey Bay are troctolite, leucotroctolite, and olivine leuconorite of the Reid Brook intrusion (Ryan and Lee, 1986; Ryan, 1990). These comprise a number of bodies, dismembered by faults and perhaps, in part, separately intruded (Fig. 2). This contribution presents the scant petrological and geochemical data now available for these rocks, and compares them with the much larger database available for other mafic rocks of the Nain Plutonic Suite. Six samples from the Reid Brook intrusion collected during the 1991 field season are described below.

The Reid Brook troctolitic rocks were identified by Ryan and Lee (1986) as well-layered troctolite, melatroctolite, and massive leucotroctolite. The bodies appear to represent fault-segmented remnants of one or more easterly-dipping layered intrusions; low dips occur at western contacts against gneiss but steepen toward the east (Fig. 2).

Petrographic notes

The minerals and textures of the samples are, for the most part, extremely fresh. Olivine and plagioclase compositions collected from the stratigraphically-uncontrolled traverse revealed olivine $Fo_{68.5}$ to $Fo_{48.2}$ coexisting with plagioclase $An_{63.5}$ to $An_{46.8}$. A texture closely resembling "snowflake texture" occurs in some of the coarse grained troctolites. The rocks are all olivine-plagioclase cumulates with the exception of one gabbronorite.

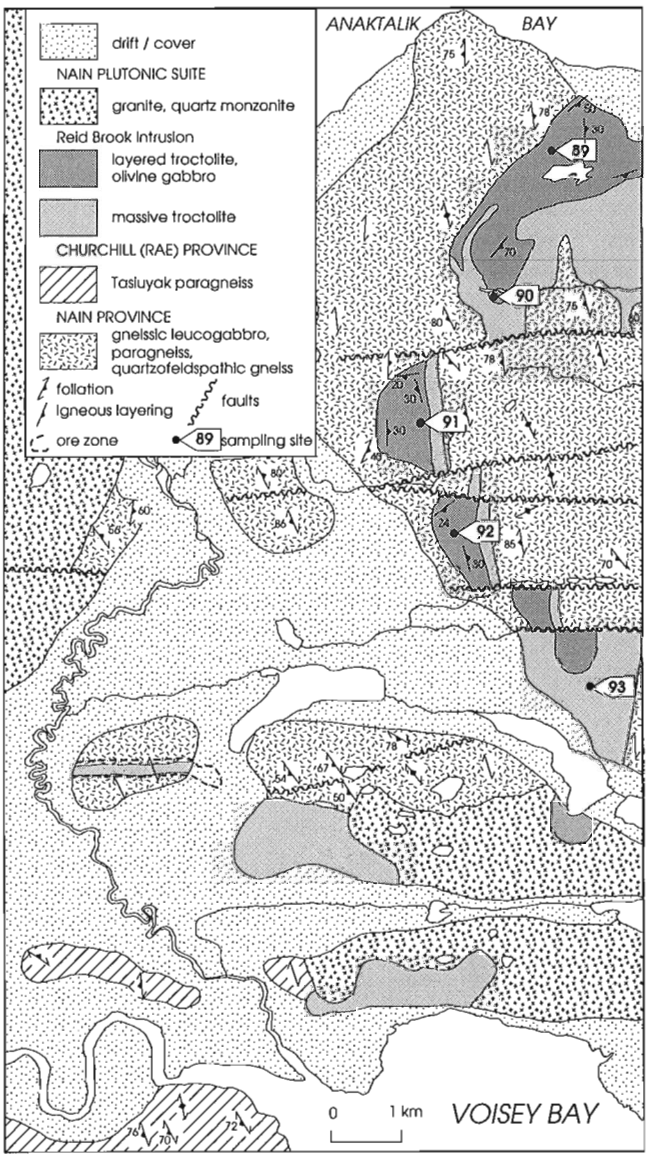

Figure 2. *Geology of the Voisey Bay area, adapted from Ryan et al. (1995), with additions.*

EC91-89 – medium grained melatroctolite has well-formed plagioclase laths with exsolved opaque oxide rodlets. Tabular plagioclase megacrysts up to 0.5 x 3.0 cm are scattered through the section. Rare large prismatic orthopyroxene crystals with dusty exsolution are up to 0.5 x 1.0 cm; these enclose small plagioclase laths. Olivine grains tend to be elongate parallel to the plagioclase lamination. Small, interstitial scraps of deep brown biotite are present. Opaque oxide minerals occur as rare, small grains.

EC91-89A – medium grained, weakly laminated gabbronorite with rare, larger plagioclase crystals. This 2-3 m thick layer is enclosed by melatroctolite EC91-89. Opaque oxides are rare and traces of interstitial sulphide are present.

EC91-90 – medium grained melatroctolite with well-formed plagioclase laths ranging from small delicate ones to rare individuals up to 30 x 60 mm. This rock is interlayered with troctolite and leucotroctolite.

EC91-91 – medium grained melatroctolite with local plagioclase lamination. In thin section, small, subophitic patches of rosy clinopyroxene have abundant fine exsolved opaque oxide minerals. This 200-300 m thick section grades rapidly upward into coarse grained snowflake troctolite with plagioclase laths up to 0.5 x 5.0 cm in rosettes more than 6 cm across.

EC91-92 – medium grained melatroctolite with moderate to strong plagioclase lamination and scattered plagioclase tablets up to 0.3 x 2.0 cm. Weak fracturing and possibly slight shearing lie subparallel to the lamination. Minor opaque oxides and clinopyroxene are interstitial.

EC91-93 – medium grained, dark pyroxene leucotroctolite with some scattered larger plagioclase grains. The larger plagioclase grains display exsolved, oriented, opaque oxide rods, similar to many anorthositic rocks of the Nain Plutonic Suite. Partial, local, symplectic rims occur on olivine. Also present are local chloritic rims on olivine. Scattered rare blocky opaque oxide grains have associated scraps of deep brown biotite. Small interstitial shreds of brown hornblende are present locally.

Geochemistry

Analyses were performed by XRF, AES, and ICP-MS methods in the laboratories of the Geological Survey of Canada. Major- and trace-element data for the Reid Brook samples are presented in Table 1 with comparative mafic rocks of the Nain Plutonic Suite.

Rare earth element plots of rocks from the Reid Brook intrusion are shown in Figure 3. The samples with strongest positive Eu anomalies are the more extreme cumulate examples; those with lesser anomalies probably had a higher trapped liquid component. The divergence between modal olivine-plagioclase compositions and REE enrichment for

Table 1. Whole rock chemistry, Reid Brook intrusion and some comparisons.

		Reid Brook intrusion						Hettasch intrusion			Barth Island intrusion				Jona-thon	Wyatt Harbor	NW of Kingur.	N of Webb B.
	Sample name	EC91 -89	EC91 -89A	EC91 -90	EC91 -91	EC91 -92	EC91 -93	EC91 -103	EC91 -104	EC92 -97	EC91 -4	EC91 -5	EC91 -23	EC91 -35	EC92 -51A	EC90 -223	EC91 -113	EC92 -158
	Sample type	mela-troct.	gabbro -norite	mela-troct.	mela-troct.	mela-troct.	leuco-troct.	troct-olite	troct-olite	mela-troct.	troct-olite	troct-olite	troct-olite	troct-olite	oliv. gabbro	mela-gabbro	mela-troct.	oliv. gabbro
wt %	SiO2	44.0	52.1	42.2	42.0	40.6	49.2	51.6	46.3	42.0	45.5	45.4	47.8	45.2	45.2	49.8	42.1	47.2
	TiO2	0.19	0.93	0.12	0.57	0.25	0.60	0.74	0.30	0.33	0.8	0.63	0.32	0.92	0.42	0.46	0.4	0.71
	Al2O3	10.9	12.1	10.2	9.80	7.80	24.4	9.20	4.80	9.20	18.7	19.0	21.2	16.8	15.0	3.20	9.40	19.5
	Fe2O3	1.6	1.2	1.8	1.7	3.1	1.2	2.8	4.3	4.0	1.4	1.6	0.7	1.5	2.0	....	4.3	1.7
	FeO	18.8	12.4	19.3	16.9	19.0	5.7	10.3	8.0	7.4	9.0	8.5	7.6	10.5	12.8	22.8	7.6	7.6
	MnO	0.25	0.24	0.26	0.23	0.28	0.09	0.22	0.26	0.17	0.13	0.14	0.10	0.15	0.20	0.42	0.20	0.12
	MgO	17.3	11.4	19.1	21.7	22.9	4.10	15.7	21.20	22.20	12.0	11.8	8.85	13.1	13.4	17.0	20.9	11.1
	CaO	4.54	6.79	4.31	4.64	3.49	10.90	6.30	13.6	7.48	9.14	9.15	9.32	8.27	6.97	3.96	8.44	8.78
	Na2O	1.80	2.20	1.60	1.50	1.10	3.30	1.40	0.20	0.60	2.30	2.20	2.90	2.20	2.40	0.50	0.30	2.70
	K2O	0.16	0.33	0.09	0.17	0.09	0.27	0.95	<0.05	0.68	0.27	0.24	0.27	0.34	0.24	0.04	0.96	0.26
	P2O5	0.03	0.11	0.03	0.09	0.05	0.10	0.18	0.02	0.03	0.12	0.09	0.06	0.13	0.03	0.02	0.03	0.13
	H2O	0.3	0.4	0.5	0.5	1.2	0.7	0.5	0.5	5.2	0.4	0.9	0.6	0.7	0.6	....	4.6	0.8
	CO2	0.1	0.1	0.1	0.1	0.1	0.1	0.1	0.3	0.3	0.1	0.2	0.1	0.2	0.2	0.2	0.3	0.1
	Total	99.97	100.30	99.61	99.90	99.96	100.66	99.99	99.78	99.59	99.86	99.85	99.82	100.01	99.46	98.40	99.53	100.70
	Mg #	60.4	60.1	61.9	67.7	65.2	51.9	68.6	76.1	74.7	67.6	67.9	65.7	66.3	62.1	57.1	76.5	68.4
ppm	Cr	48	130	45	45	44	18	820	1800	2500	40	43	42	56	76	250	1500	47
	Ni	420	150	440	600	540	83	570	850	1000	310	320	130	320	340	330	650	200
	Co	150	73	150	150	170	37	66	100	94	72	71	66	81	100	110	82	70
	V	21	150	<5	38	17	34	99	170	120	47	35	15	58	32	140	170	33
	Cu	<10	19	<10	16	<10	20	18	64	<10	22	21	68	25	53	320	16	13
	Zn	140	120	140	130	150	55	210	95	100	80	79	58	94	120	200	100	62
	Rb	0.80	4.5	0.50	2.2	1.0	2.5	....	0.37	33	2.5	3.2	3.2	5.1	1.5	8	44	1.7
	Ba	110	190	50	140	70	160	560	50	150	190	160	160	210	120	80	310	180
	Sr	270	300	240	210	180	560	100	33	100	420	440	490	380	350	65	110	510
	Nb	0.46	3.3	0.32	2.4	0.95	2.8	8.3	0.25	0.96	3.3	2.5	1.5	3.6	0.64	....	0.85	1.9
	Zr	<10	56	<10	37	12	42	60	<10	16	45	39	18	69	35	6	13	65
	Y	1.9	14	1.2	8.8	3.7	9.5	16	9.9	13	12	8.9	5.0	13	2.3	7.7	17	7
	La	1.6	9.2	1.3	5.0	2.2	6.4	24	1.4	5.1	8.5	6.6	5.2	9.5	1.7	2.2	3.2	5.0
	Ce	3.2	21	2.5	12	5.1	15	59	5.3	12	19	15	11	22	3.2	4.7	7.9	12
	Nd	1.6	11	1.2	6.5	2.8	7.7	33	5.8	5.6	10	7.4	4.9	11	1.7	<5	5.3	6.7
	Sm	0.23	2.4	0.20	1.5	0.60	1.7	6.1	1.5	1.2	2.0	1.5	0.81	2.4	0.36	1.2	1.4	1.4
	Eu	0.46	0.97	0.36	0.66	0.39	1.1	1.0	0.51	0.28	1.1	0.91	0.88	1.1	0.54	0.4	0.60	0.86
	Gd	0.31	2.4	0.16	1.5	0.60	1.7	4.6	2.0	1.7	2.2	1.5	0.89	2.4	0.40	1.0	2.2	1.4
	Dy	0.25	2.2	0.18	1.5	0.60	1.6	3.1	1.8	1.9	2.0	1.5	0.86	5.9	0.38	1.5	2.9	1.1
	Ho	0.06	0.48	0.04	0.31	0.12	0.31	0.58	0.38	0.47	0.44	0.33	0.17	0.50	....	0.4	0.66	0.21
	Er	0.19	1.4	0.11	0.80	0.34	0.86	1.4	1.0	1.3	1.1	0.86	0.49	1.4	....	1.3	1.9	0.58
	Tm	0.03	0.22	0.02	0.14	0.06	0.14	0.24	0.16	0.24	0.16	0.15	0.07	0.22	....	0.2	0.31	0.09
	Yb	0.26	1.4	0.16	0.79	0.41	0.77	1.2	0.90	1.4	1.0	0.89	0.49	1.3	0.25	1.2	1.7	0.58
	S	53	139	25	185	65	203	354	105	....	....	....	500	....	....	14800	175	200
	F	81	190	25	86	90	159	1619	189	....	137	98	175	228	79	63	2162	200
	Cl	145	253	233	445	585	199	406	125	....	1029	453	145	140	137	188	847	139

.... = not determined.

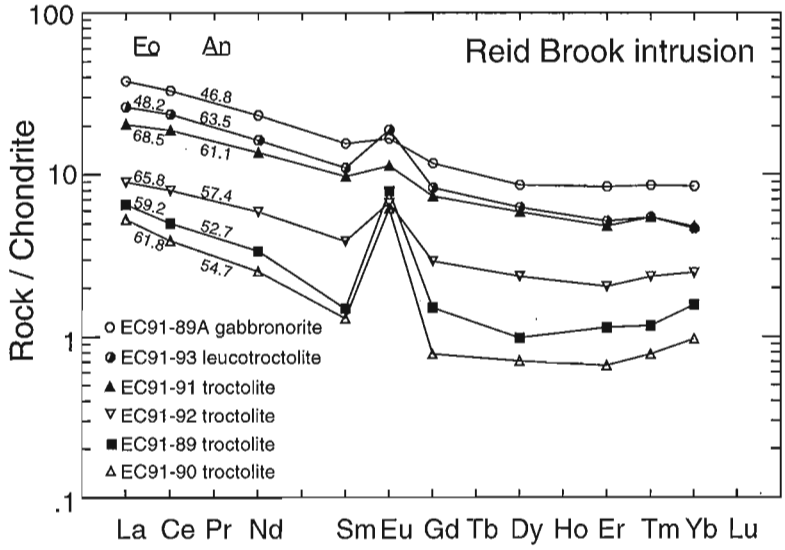

Figure 3.

Chondrite-normalized rare-earth element diagrams for samples from the Reid Brook intrusion. Modal compositions of olivine and plagioclase are indicated for the samples.

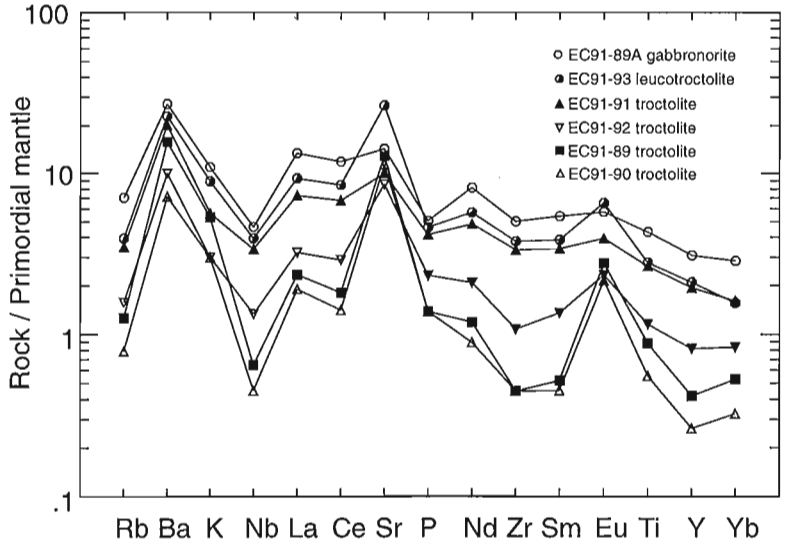

Figure 4.

Extended elemental plot of the samples of the Reid Brook intrusion.

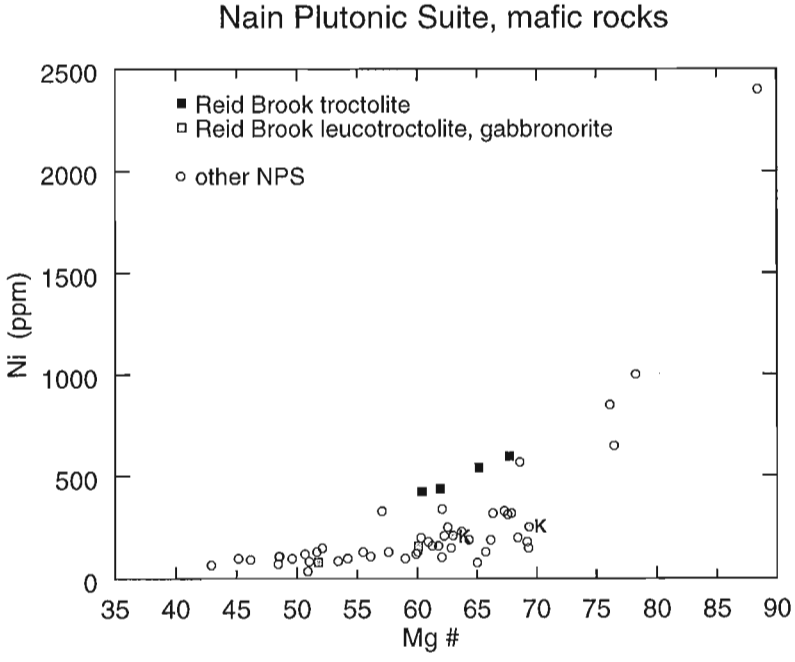

Figure 5.

Nickel contents of whole rocks from the Reid Brook intrusion vs. Mg# ($Mg/(Mg+Fe_{total})$). Two rock samples from Kiglapait mentioned in the text, each with about 30% modal olivine from about 15 PCS, have whole rock-252 ppm Ni, olivine-828 ppm Ni, Mg# 69.5, and whole rock-203 ppm Ni, olivine-621 ppm Ni, Mg# 63.1, respectively and are identified by K.

some samples could be consistent with magma-mixing or separate magma batches. The significance of magma-mixing processes in sulphide ore formation may be worth investigation.

A multi-element plot for the samples is displayed in Figure 4. The positive Eu anomalies are apparent here as are positive Sr anomalies; both elements are enriched in plagioclase and support the cumulate character of the rocks. The low Rb content of the rocks is a widely developed feature of basic and anorthositic rocks of the Nain Plutonic Suite and is also consistent with the cumulate nature of the rocks. The prominent negative Nb anomalies are usually correlated with influence of calc-alkalic crustal components in a source or a subsequent contaminant.

Nickel concentrations in mafic whole rocks of the Nain Plutonic Suite are plotted against whole rock Mg number ($Mg/(Mg+Fe_{total})$ in Figure 5. The Reid Brook troctolitic rocks exhibit the highest nickel concentrations in their Mg# range; nickel is much lower in the less mafic samples. Two rock samples from the Kiglapait intrusion, with the highest nickel contents reported by Morse et al. (1991) are identified by K in Figure 5. Lower Ni in the Kiglapait samples may reflect lower olivine contents, higher trapped liquid components, or both.

Cobalt concentrations in mafic whole rocks of the Nain Plutonic Suite are plotted against whole rock Mg number in Figure 6. The four Reid Brook melatroctolite samples with high Ni concentrations in Figure 5 also have very high Co

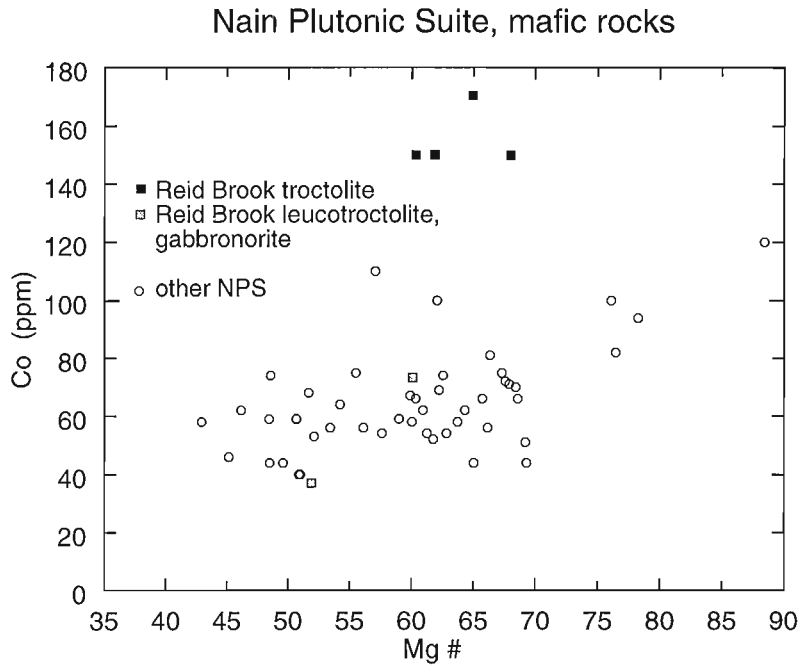

Figure 6.

Cobalt contents of whole rocks from the Reid Brook intrusion vs. Mg# ($Mg/(Mg+Fe_{total})$. The same four Reid Brook melatroctolite samples with high Ni concentrations in Figure 5, have very high Co concentrations. Note that the general decrease in Co as Mg# decreases, is much less rapid than Ni.

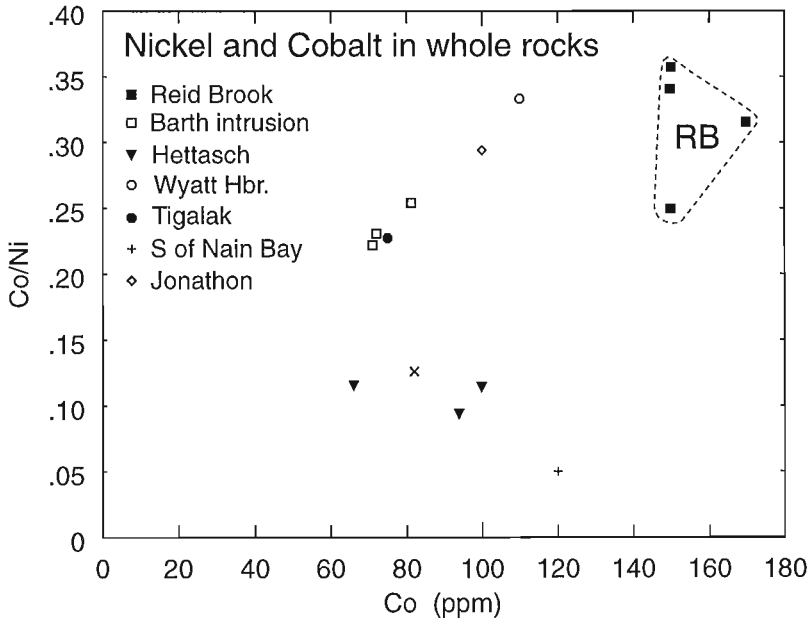

Figure 7.

Co/Ni plotted against Co (ppm) in whole rocks. Several of the more prominent mafic intrusions of the Nain Plutonic Suite are included for comparison.

concentrations. The decrease in Co as Mg# decreases in Nain Plutonic Suite rocks is much less pronounced than Ni. The Reid Brook troctolitic rocks have notably higher cobalt concentrations than any other samples at any Mg# range. This offers support for a Reid Brook-Voisey Bay Ni-Cu-Co deposit association. The ratio Co/Ni is plotted against Co (ppm) in whole rocks in Figure 7, showing that Reid Brook rocks have high Co/Ni coupled with high Co concentrations. The relationship suggests a genetic association with the relatively high-Co Voisey Bay sulphide ores (The Northern Miner, May 8, 1995). Jonathon and Wyatt Harbour samples have high Co/Ni (within the range of Reid Brook samples) but much lower Co concentrations. Several of the more prominent mafic intrusions of the Nain Plutonic Suite are included for comparison.

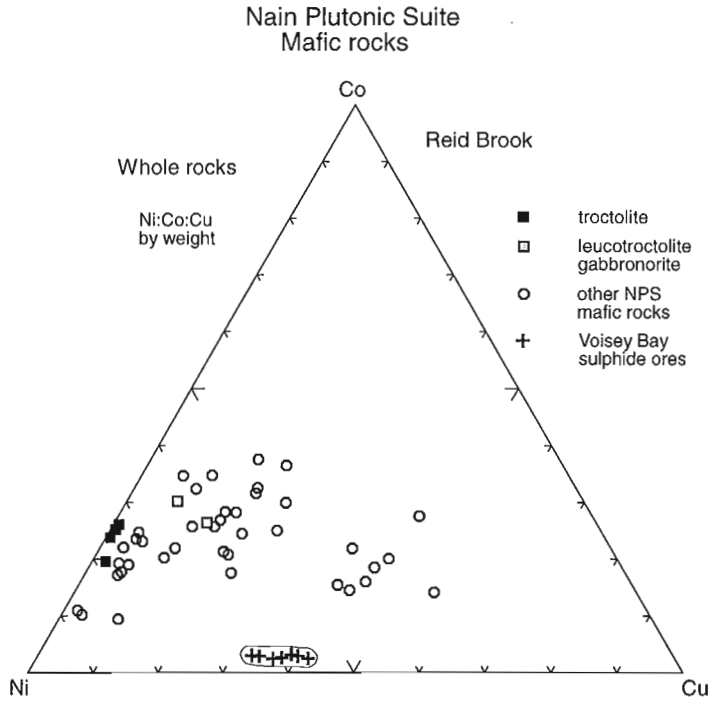

Figure 8.

Relative proportions of Ni:Co:Cu in whole rocks.

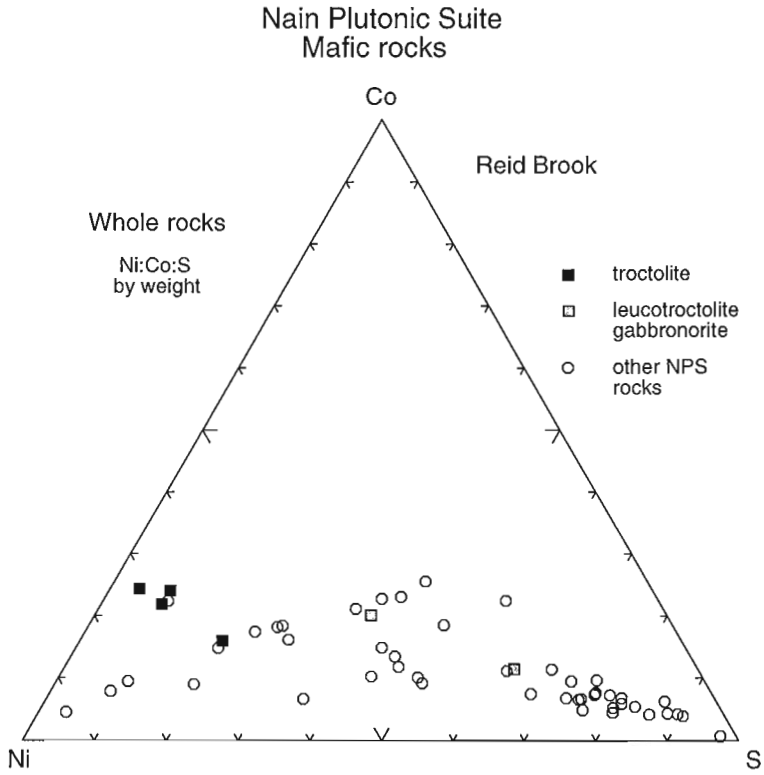

Figure 9.

Relative proportions of Ni:Co:S in whole rocks.

Table 2. Olivine, pyroxene, and plagioclase compositions from the Reid Brook intrusion.

	EC91	EC91	EC91	EC91	EC91	EC91	EC91	EC91	EC91	EC91	EC91	EC91	EC91
	-89	-90	-91	-92	-93	-89	-89A	-89A	-90	-91	-92	-93	-93
wt%	ol	ol	ol	ol	ol	opx	opx	cpx	cpx	cpx	cpx	opx	cpx
SiO2	34.68	35.38	36.24	36.24	33.84	51.39	51.00	50.04	50.06	48.78	49.61	51.09	49.70
TiO2	0.03	0.03	0.05	0.03	0.03	0.45	0.30	0.57	0.92	1.62	1.35	0.07	1.13
Al2O3	0.02	0.04	0.06	0.04	0.02	1.30	0.96	2.04	2.89	3.44	3.08	1.06	2.83
Cr2O3	0.03	0.03	0.02	0.00	0.00	0.03	0.06	0.04	0.19	0.12	0.10	0.03	0.02
FeO	35.04	33.02	28.29	30.24	42.43	20.70	25.40	10.72	7.63	8.48	9.32	24.11	10.95
MnO	0.44	0.44	0.37	0.36	0.58	0.40	0.46	0.23	0.23	0.16	0.19	0.52	0.27
MgO	28.59	29.95	34.46	32.65	22.19	22.85	20.51	13.37	14.64	14.18	14.28	21.13	12.97
NiO	0.11	0.10	0.13	0.11	0.06	0.04	0.06	0.04	0.05	0.02	0.05	0.08	0.02
CaO	0.03	0.04	0.06	0.06	0.06	1.69	1.64	21.88	21.81	21.18	20.41	0.35	20.69
Na2O	...	...	...	...	...	0.03	0.03	0.34	0.32	0.61	0.55	0.01	0.32
K2O	...	...	...	...	...	0.01	0.00	0.01	0.01	0.01	0.02	0.02	0.00
Total	98.97	99.03	99.68	99.73	99.21	98.89	100.42	99.28	98.75	98.60	98.96	98.47	98.90
^{IV}Si	0.978	0.985	0.978	0.986	0.989	1.923	1.916	1.886	1.875	1.834	1.862	1.946	1.885
^{IV}Ti	0.001	0.001	0.001	0.001	0.001	0.013	0.008	0.016	0.026	0.046	0.038	0.002	0.032
^{IV}Al						0.057	0.043	0.091	0.125	0.152	0.136	0.048	0.115
^{VI}Al	0.001	0.001	0.002	0.001	0.001	0.000	0.000	0.000	0.003	0.000	0.000	0.000	0.012
Cr	0.001	0.001	0.000	0.000	0.000	0.001	0.002	0.001	0.006	0.003	0.003	0.001	0.000
Fe3+*	0.000	0.000	0.000	0.000	0.000	0.074	0.109	0.129	0.088	0.130	0.102	0.057	0.061
Fe2+	0.826	0.769	0.639	0.688	1.036	0.574	0.689	0.208	0.151	0.136	0.190	0.711	0.286
Mn	0.010	0.010	0.009	0.008	0.014	0.013	0.015	0.007	0.007	0.005	0.006	0.017	0.009
Mg	1.202	1.243	1.387	1.324	0.966	1.275	1.149	0.751	0.818	0.795	0.799	1.200	0.733
Ni	0.002	0.002	0.002	0.003	0.001	0.001	0.002	0.001	0.002	0.001	0.002	0.002	0.001
Ca	0.001	0.001	0.002	0.002	0.002	0.068	0.066	0.884	0.876	0.853	0.821	0.014	0.841
Na	...	...	...	...	...	0.002	0.002	0.025	0.023	0.044	0.040	0.001	0.024
K	...	...	...	...	...	0.001	0.000	0.001	0.001	0.001	0.001	0.001	0.000
Cations	3.022	3.013	3.020	3.013	3.010	4.002	4.001	4.000	4.001	4.000	4.000	4.000	3.999
O	4.000	4.000	4.000	4.000	4.000	6.000	6.000	6.000	6.000	6.000	6.000	6.000	6.000
Ca	...	...	...	...	...	3.42	3.28	44.83	45.32	44.57	42.94	0.71	43.78
Mg	59.25	61.78	68.47	65.8	48.25	64.04	57.08	38.08	42.32	41.54	41.79	60.54	38.16
Fe	40.75	38.22	31.53	34.2	51.75	32.55	39.64	17.09	12.36	13.90	15.27	38.75	18.06
Coexisting modal plagioclase													
avg.	$An_{52.7}$	$An_{54.7}$	$An_{61.1}$	$An_{57.4}$	$An_{63.5}$	$An_{52.7}$			$An_{54.7}$	$An_{61.1}$	$An_{57.4}$	$An_{63.5}$	$An_{63.5}$
rims							$An_{46.8}$	$An_{46.8}$					
cores							$An_{51.6}$	$An_{51.6}$					
Whole rock CIPW norm (wt%)													
Plag.	37.5	34.8	33.4	26.3	80.6		42.8						
Olivine	47.9	56.1	58.7	59.8	10.0		0.8						
Pyrox.	11.8	6.1	4.0	8.8	6.3		52.7						
Log fO2 @ 1000°C													
	-11.3	-13.4	-12.8	-12.7	-12.1		-13.5						
ΔFMQ @ 1000°C													
	-0.7	-2.7	-0.4	-2.0	-1.4		-2.8						

Notes: Fe3+ was calculated from stoichiometry. Log fO2 and ΔFMQ were calculated using the program QUILF (Anderson et al., 1993).

Ratios of Ni:Co:Cu by weight in mafic whole rocks of the Nain Plutonic Suite are shown in Figure 8. The low Cu content of the Reid Brook troctolitic cumulates is also in accord with their sulphide-poor character. The reported Co:Ni ratio of Voisey Bay massive sulphides is 0.04, significantly higher than the 0.01-0.02 characteristic of many Ni-rich primary magmatic sulphide ores. The much lower Co:Ni ratio in massive sulphides at Voisey Bay than that of the Reid Brook intrusion whole rocks is in agreement with the long known less sulphophile nature of Co relative to Ni.

Ratios of Ni:Co:S by weight in mafic whole rocks of the Nain Plutonic Suite are shown in Figure 9. The high Ni and Co relative to S in Reid Brook troctolitic rocks is in accord with their cumulate character and the concentration of Ni and Co in silicate minerals (primarily olivine). Rocks with higher S contain visible amounts of sulphides.

To summarize, nickel and cobalt in whole rocks of the Reid Brook troctolites exhibit high Co/Ni coupled with high Co concentrations – suggesting a genetic association with the Voisey Bay sulphides which also have relatively high Co:Ni of 0.04. Magmatic sulphides with Co:Ni in the range of 0.03 to 0.06 are most commonly associated with somewhat evolved magmas like those parental to Reid Brook cumulates, whereas Co:Ni ratios of 0.01-0.02 are more typical of Ni-rich sulphide ores associated with less-evolved magmas like picrites or komatiites (e.g. Rankama and Sahama, 1950; Naldrett, 1989). The Reid Brook troctolitic rocks exhibit the highest observed nickel concentrations for their Mg#s of any Nain Plutonic Suite rocks observed. Cobalt contents of whole rock Reid Brook troctolites are notably higher than any other Nain Plutonic Suite rocks for any Mg# range. The low Cu content of Reid Brook troctolite samples is in accord with their cumulate character and their low S contents (i.e., as cumulates, there are reduced amounts of trapped liquid in the rocks and trapped liquids would be expected to contain the bulk of incompatible elements).

A single sample from the Reid Brook intrusion (EC91-91) yielded initial Nd at 1.30 Ga with ε_{Nd} = -3.0 and initial $^{87}Sr/^{86}Sr$ at 1.30 Ga = 0.703429 as reported by Emslie et al. (1994). In terms of Nd and Sr, these values display among the least crustal influence for results so far reported from rocks of the Nain Plutonic Suite. If an upper limit for ε_{Nd} values in mafic magmas of the suite is shown to remain near -3.0 in further work, the controlling source is more likely to reside in the subcontinental lithospheric mantle than in the crust.

Mineral chemistry

Mineral compositions were analyzed on a Cameca SX50 instrument in the Mineralogy Section of the Geological Survey of Canada. Chemical compositions of minerals in the samples are shown in Tables 2, 3, and 4.

Table 3. Ilmenite and magnetite compositions from the Reid Brook intrusion.

	EC91 -89	EC91 -89A	EC91 -90	EC91 -91	EC91 -92	EC91 -93	EC91 -89A	EC91 -90	EC91 -91	EC91 -92
wt%	ilm	ilm	ilm	ilm	ilm	ilm	mt	mt	mt	mt
SiO_2	0.26	0.00	0.02	0.00	0.00	0.26	0.00	0.04	0.32	0.49
TiO_2	49.72	48.11	51.68	50.25	51.76	50.78	0.42	2.10	1.23	6.64
Al_2O_3	0.09	0.06	0.04	0.11	0.06	0.08	0.78	1.59	1.04	2.17
Cr_2O_3	0.09	0.13	0.04	0.06	0.10	0.02	2.08	4.46	0.88	2.54
FeO	46.60	48.59	44.60	45.99	44.73	46.85	90.30	83.95	87.65	75.73
MnO	0.44	0.41	0.61	0.49	0.75	0.58	0.05	0.09	0.09	0.21
MgO	1.53	1.56	1.76	2.37	1.71	1.23	0.13	0.22	0.48	0.76
CaO	0.10	0.01	0.11	0.01	0.01	0.06	0.00	0.03	0.04	0.15
NiO	...	...	...	...	...	...	0.06	0.13	0.09	0.06
Total	98.83	98.87	98.86	99.28	99.12	99.86	93.83	92.60	91.82	88.75
Si	0.006	0.000	0.001	0.000	0.000	0.006	0.000	0.002	0.012	0.020
Ti	0.940	0.908	0.977	0.943	0.977	0.953	0.012	0.061	0.036	0.200
Al	0.003	0.002	0.001	0.003	0.002	0.002	0.035	0.072	0.047	0.103
Cr	0.002	0.003	0.001	0.001	0.002	0.000	0.063	0.136	0.027	0.081
Fe^{3+*}	0.102	0.179	0.042	0.110	0.042	0.078	1.879	1.667	1.829	1.378
Fe^{2+}	0.877	0.841	0.896	0.844	0.897	0.900	1.001	1.042	1.013	1.158
Mn	0.009	0.009	0.013	0.010	0.016	0.012	0.002	0.003	0.003	0.007
Mg	0.057	0.058	0.066	0.088	0.064	0.046	0.008	0.012	0.028	0.046
Ca	0.003	0.000	0.003	0.000	0.000	0.001	0.000	0.001	0.002	0.007
Ni	...	...	...	...	...	...	0.002	0.004	0.003	0.002
Cations	1.999	2.000	2.000	1.999	2.000	1.998	3.002	3.000	3.000	3.002
O	3.000	3.000	3.000	3.000	3.000	3.000	4.000	4.000	4.000	4.000
Hem	5.7	9.6	2.2	6.1	2.3	4.4				
Ilm	94.3	90.4	97.8	93.9	97.7	95.6				
Usp							1.2	6.7	3.6	22.2
Mt							98.8	93.3	96.4	77.8

Gabbronorite EC91-89A has plagioclase with substantial normal zoning, consistent with mesocumulate characteristics. Leucotroctolite EC91-93 has significantly more Fe-rich olivine but also more calcic plagioclase than the melatroctolites, suggesting a separate intrusion or a locally more strongly contaminated part of the same large intrusion.

Table 4. Biotite and hornblende compositions from the Reid Brook intrusion.

	EC91 -89	EC91 -89A	EC91 -90	EC91 -93	EC91 -91	EC91 -92	EC91 -93
wt%	biot	biot	biot	biot	hbl	hbl	hbl
SiO_2	36.78	36.86	37.42	36.84	40.24	41.46	42.53
TiO_2	4.50	5.29	2.80	2.35	3.59	3.54	1.70
Al_2O_3	13.85	13.81	15.57	15.83	11.77	11.87	12.24
Cr_2O_3	0.15	0.16	0.18	0.03	0.02	0.15	0.04
FeO	10.20	13.97	9.47	14.54	10.84	10.70	13.91
MnO	0.08	0.06	0.00	0.05	0.14	0.06	0.10
MgO	18.12	15.59	19.04	16.45	13.43	13.66	12.95
CaO	0.10	0.01	0.04	0.03	11.84	11.95	11.32
Na_2O	0.09	0.03	0.38	0.61	2.47	2.60	1.81
K_2O	10.13	10.01	9.84	8.65	1.51	1.22	1.12
BaO	0.10	0.32	0.34	0.26	...	...	...
H_2O	3.91	3.64	4.12	4.00	1.85	1.91	2.00
F	0.34	0.69	...	0.09	0.26	0.20	0.00
Cl	0.05	0.17	...	0.02	0.05	0.06	0.06
O=F	0.14	0.29	...	0.04	0.11	0.08	0.00
O=Cl	0.01	0.04	...	0.01	0.01	0.01	0.01
Total	98.25	100.28	99.20	99.70	97.89	99.29	99.77
^{IV}Si	5.493	5.486	5.492	5.469	6.090	6.157	6.313
^{IV}Al	2.438	2.423	2.508	2.531	1.910	1.843	1.687
^{IV}Ti	0.069	0.091	0.000	0.000	0.000	0.000	0.000
^{VI}Al	0.000	0.000	0.185	0.239	0.189	0.234	0.455
^{VI}Ti	0.436	0.501	0.309	0.263	0.408	0.395	0.190
Cr	0.017	0.019	0.020	0.003	0.002	0.017	0.005
Fe^{2+}	1.274	1.739	1.162	1.805	1.370	1.328	1.484
Mn	0.010	0.008	0.000	0.006	0.018	0.008	0.013
Mg	4.036	3.459	4.165	3.640	3.030	3.025	2.866
Ba	0.006	0.019	0.019	0.015	...	...	...
Ca	0.016	0.002	0.007	0.004	1.919	1.901	1.800
Na	0.027	0.008	0.107	0.175	0.668	0.749	0.520
K	1.930	1.901	1.843	1.638	0.291	0.231	0.212
Cations	15.752	15.656	15.817	15.788	15.895	15.888	15.545
O	20.000	20.000	20.000	20.000	22.000	22.000	22.000
OH	3.827	3.632	4.000	3.953	1.863	1.891	1.985
F	0.161	0.325	...	0.042	0.124	0.094	0.000
Cl	0.013	0.043	...	0.005	0.013	0.015	0.015
Mg#	76.0	66.5	78.2	66.8	68.8	69.5	65.9

Ilmenites tend to have relatively low hematite concentrations, consistent with the low ΔFMQ values given in Table 2. Magnetites, except for sample EC91-92, have very low TiO_2 contents likely due to subsolidus re-equilibration.

Compositions of the small amounts of biotite and/or hornblende present in most samples are shown in Table 4. Fluorine concentrations exceed chlorine in all biotites and hornblendes contrary to the whole rock analyses which have F:Cl <1, a feature that requires further investigation.

Small amounts of pentlandite, nickel-bearing pyrrhotite, and chalcopyrite are present in sample EC91-91. Cobalt concentrations from 1.30 to 2.55 wt. % were determined in the analyzed pentlandite.

Silicate-oxide equilibria examined using the program QUILF (Anderson et al., 1993) indicate T-fO_2 conditions of -0.4 to -2.8 log fO_2 units below the FMQ buffer at 1000°C (Table 2). Olivine and pyroxene compositions for the Reid Brook samples are displayed in Figure 10 where they may be compared with pyroxene composition fields compiled from Nain Plutonic Suite basic and anorthositic rocks.

Concentrations of Ni in olivine in Nain Plutonic Suite rocks, as determined by microprobe, are plotted in Figure 11. The most magnesian Reid Brook olivine is comparable in Mg and Ni contents to the most Ni-rich olivine reported from the Kiglapait intrusion.

DISCUSSION

Most of the present samples of the Reid Brook intrusion are olivine-plagioclase mesocumulates to adcumulates. Samples EC91-89 and -90, in addition to having low REE levels and prominent positive Eu anomalies, have very low levels of incompatible elements like Rb and Nb and most closely approach adcumulates.

The small sulphide grains present in sample EC91-91 contain pentlandite with up to 2.6 wt.% cobalt. Cobalt-rich pentlandite is also present in the Kiglapait intrusion (Shirey, 1975a, b) and in the Harp Lake complex (Emslie, 1980). The elevated cobalt contents accord with the only moderately magnesian olivine compositions of the host rocks and low nickel content of Voisey Bay massive sulphides and point to

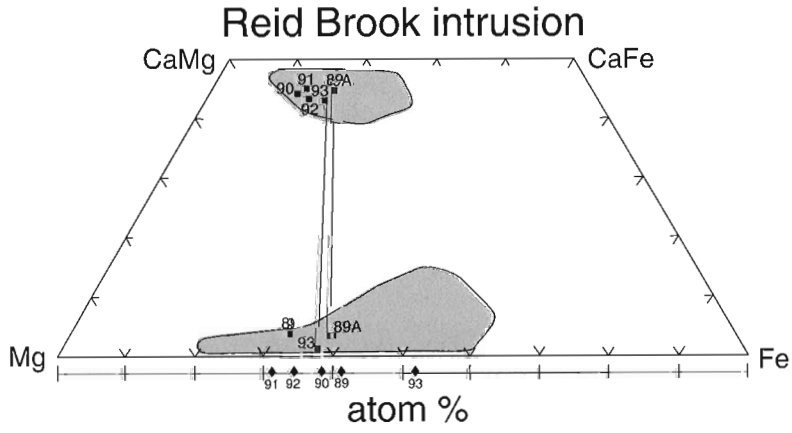

Figure 10.

Compositions of pyroxenes and olivine (below) from samples of the Reid Brook intrusion. Shaded areas indicate compositional fields of pyroxenes compiled from anorthositic and basic rocks of the Nain Plutonic Suite (Emslie et al., 1994).

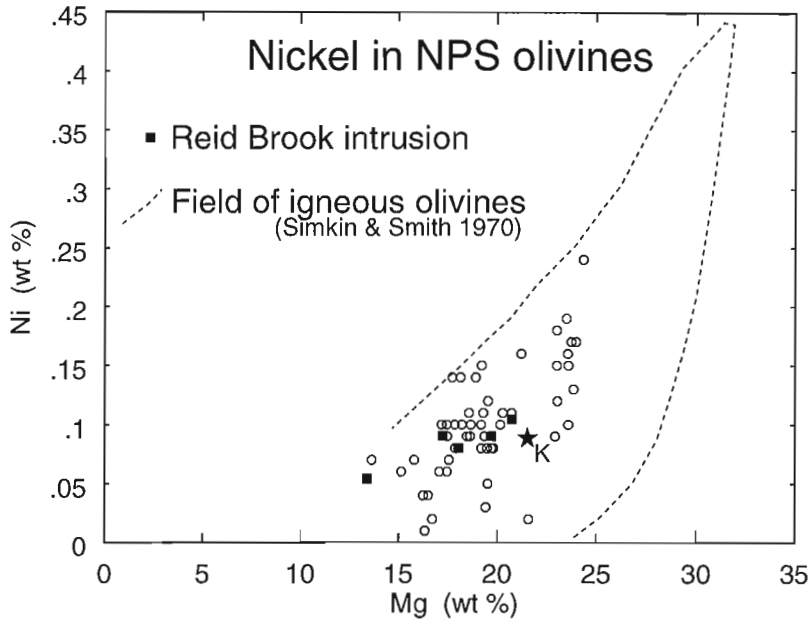

Figure 11.

Nickel in olivine in troctolitic rocks of the Nain Plutonic Suite. Star symbol marked K is the most Ni-rich olivine reported from the Kiglapait intrusion by Morse et al. (1991).

relatively evolved parental magmas. The Voisey Bay sulphide deposit clearly has the earmarks of a magmatic sulphide deposit formed by separation of a Ni-, Cu-, Co-bearing, Fe-monosulphide melt from a mafic, rather than ultramafic, melt.

The Tasiuyak gneiss must be considered as a potential source of sulphur for the Voisey Bay deposit. It is known to contain graphite and sulphide zones and layers (Emslie and Russell, 1988; Hamilton, 1993) and sulphur contents up to 3.5 weight percent have been determined (M.A. Hamilton, pers. comm., October 1995). A recent study of the geochemistry and Nd isotopes in Tasiuyak gneiss (Thériault and Ermanovics, unpub. report, 1995) provides data that can be used to test some hypotheses involving assimilation of Tasiuyak gneiss by magmas like that parental to the Reid Brook intrusion. The study indicates that the average composition (nine samples) is relatively siliceous (65.6% SiO_2), and also that many incompatible elements have up to 50x greater concentration in the gneiss than the most incompatible element-rich Reid Brook samples. Both features are inconsistent with substantial bulk assimilation of the gneiss which would be expected to cause olivine to react out forming orthopyroxene, and thus produce dominantly noritic rocks from the Reid Brook magma. The initial ε_{Nd} of five Tasiuyak gneiss samples at 1.3 Ga are tightly grouped between -8.7 and -9.8 (Thériault and Ermanovics, unpub. report 1995), much more negative than the value of -3.0 for sample EC91-91. In addition, the initial $^{87}Sr/^{86}Sr$ of four samples of Tasiuyak gneiss at 1.3 Ga ranges from 0.7097 to 0.7104 (Hamilton, 1993), very much higher than the 0.7034 for sample EC91-91 cited above, so that Sr and Nd isotopes do not support large scale bulk assimilation of Tasiuyak gneiss by Reid Brook magma. It seems likely that, if the Tasiuyak gneiss acted as a source of sulphur, the sulphur was selectively assimilated.

ACKNOWLEDGMENTS

John Stirling and Gordon Pringle provided essential assistance in obtaining the microprobe data. Figures 1 and 2 were prepared by Deborah Lemkow. Bob Baragar, Mike Hamilton, and Larry Hulbert critically read and provided constructive input to earlier drafts of the manuscript.

REFERENCES

Anderson, D.J., Lindsley, D.H., and Davidson, P.M.
1993: QUILF: A Pascal program to assess equilibria among Fe-Mg-Mn-Ti oxides, pyroxenes, olivine, and quartz; Computers and Geosciences, v. 19, p. 1333-1350.

Berg, J.H.
1980: Snowflake troctolite in the Hettasch intrusion: evidence for magma mixing and supercooling in a plutonic environment; Contributions to Mineralogy and Petrology, v. 72, p. 339-351.

Berg, J.H. and Briegel, J.S.
1983: Geology of the Jonathon intrusion and associated rocks; in The Nain Anorthosite Project, Labrador: Field Report 1981, (ed.) S.A. Morse; Contribution No. 40, Department of Geology and Geography, University of Massachusetts, Amherst, Massachusetts, p. 43-50.

Berg, J.H., Emslie, R.F., Hamilton, M.A., Morse, S.A., Ryan, A.B., and Wiebe, R.A.
1994: Anorthositic, Granitoid and Related Rocks of the Nain Plutonic Suite; Guidebook for Field Excursion to the Nain Area, August 4-10, 1994, International Geological Correlation Program Project 290 and 315, (ed.) R.F. Emslie, 69 p.

Chaussidon, M., Albarède, F., and Sheppard, S.M.F.
1989: Sulphur isotope variations in the mantle from ion microprobe analyses of micro-sulphide inclusions; Earth and Planetary Science Letters, v. 92, p. 144-156.

Connelly, J.N. and Ryan, B.
1994: Late Archean and Proterozoic events in the central Nain Craton; in Eastern Canadian Shield Onshore-Offshore Transect (ECSOOT), (comp.) R.J. Wardle and J. Hall; Transect Meeting (Dec. 10-12, 1993), p. 53-61.

De Paolo, D.J.
1985: Isotopic studies of processes in mafic magma chambers: I. The Kiglapait intrusion, Labrador; Journal of Petrology, v. 26, p. 925-951.

de Waard, D.
1976: Anorthosite-adamellite-troctolite layering in the Barth Island structure of the Nain complex, Labrador; Lithos, v. 9, p. 293-308.
de Waard, D., Mulhern, K., and Merriam, D.F.
1976: Mineral variation in anorthositic, troctolitic, and adamellitic rocks of the Barth Island layered structure in the Nain anorthosite complex, Labrador; Mathematical Geology, v. 8, p. 561-574.
Emslie, R.F.
1980: Geology and Petrology of the Harp Lake complex, central Labrador: an example of Elsonian magmatism; Geological Survey of Canada, Bulletin 293, 136 p.
Emslie, R.F. and Russell, W.J.
1988: Umiakovik Lake batholith and other felsic intrusions, Okak Bay area, Labrador; in Current Research, Part C; Geological Survey of Canada, Paper 88-1C, p. 27-32.
Emslie, R.F., Hamilton, M.A., and Theriault, R.J.
1994: Petrogenesis of a mid-Proterozoic anorthosite-mangerite-charnockite-granite (AMCG) complex: isotopic and chemical evidence from the Nain Plutonic Suite; Journal of Geology, v. 102, p. 539-558.
Hamilton, M.A.
1993: Contamination of massif anorthosite and Precambrian crustal evolution in central Labrador: a combined trace element and Sr, Nd and Pb isotopic study; PhD. thesis, University of Massachusetts, Amherst, Massechusetts, 195 p.
Hamilton, M.A., Emslie, R.F., and Roddick, J.C.
1994: Detailed emplacement chronology of basic magmas of the mid-Proterozoic NainPlutonic Suite, Labrador: insights from U-Pb systematics in zircon and baddeleyite; Eighth International Conference on Geochronology, Cosmochronology, and Isotope Geology [Program Abstracts], United States Geological Survey Circular 1107, p. 124.
Keays, R.R.
1994: The role of komatiitic and picritic magmatism and S-saturation in the formation of ore-deposits; Lithos, v. 34, p. 18.
Morse, S.A.
1969: The Kiglapait Layered Intrusion, Labrador; Geological Society of America Memoir 112, 204 p.
1979: Kiglapait geochemistry II: Petrography; Journal of Petrology, v. 20, p. 591-624.
1981: Kiglapait geochemistry IV: The major elements; Geochimica et Cosmochimica Acta, v. 45, p. 461-479.
Morse, S.A., Rhodes, J.M., and Nolan, K.M.
1991: Redox effect on the partitioning of nickel in olivine; Geochimica et Cosmochimica Acta, v. 55, p. 2373-2378.
Naldrett, A.J.
1989: Magmatic sulfide deposits; Oxford University Press, Oxford, 186 p.
Rankama, K. and Sahama, Th.G.
1950: Geochemistry; University of Chicago Press, Chicago, 912 p.
Ryan, B.
1990: Geological map of the Nain Plutonic Suite and surrounding rocks (Nain-Nutak, NTS 14SW); Newfoundland Department of Mines and Energy, Geological Survey Branch, Map 90-44, scale 1:500 000.
Ryan, B. and Lee, D.
1986: Gneiss-anorthosite-granite relationships in the Anaktalik Brook-Kogaluk River area (NTS 14D/1,8), Labrador; in Current Research, Newfoundland Department of Mines and Energy, Mineral Development Division, Report 86-1, p. 79-88.
Ryan, B., Wardle, R.J., Gower, C.F., and Nunn, G.A.G.
1995: Nickel-copper-sulphide mineralization in Labrador: the Voisey Bay discovery and its exploration implications; Current Research, Newfoundland Department of Natural Resources, Geological Survey, Report 95-1, p. 177-204.
Shirey, S.B.
1975a: Sulfides and sulphur content of the Kiglapait layered intrusion, Labrador; MSc. thesis, University of Massachusetts, Amherst, Massachusetts, 76 p.
1975b: Sulfides and sulfur content of the Kiglapait layered intrusion, Labrador; Geological Society of America, Abstracts with Programs, v. 7, no. 6, p. 858.
Simkin, T. and Smith, J.V.
1970: Minor-element distribution in olivine; Journal of Geology, v. 78, p. 304-325.
Snyder, D., Carmichael, I.S.E., and Wiebe, R.A.
1993: Experimental study of liquid evolution in an Fe-rich, layered mafic intrusion: constraints of Fe-Ti oxide precipitation on the T-fO2 and T-ρ paths of tholeiitic magmas; Contributions to Mineralogy and Petrology, v. 113, p. 73-86.
Weibe, R.A.
1988: Structural and magmatic evolution of a magma chamber: the Newark Island layered intrusion, Nain, Labrador; Journal of Petrology, v. 29, p. 383-411.
Wiebe, R.A. and Snyder, D.
1993: Slow, dense replenishments of a basic magma chamber: the layered series of the Newark Island layered intrusion, Nain, Labrador; Contributions to Mineralogy and Petrology, v. 113, p. 59-72.

Geological Survey of Canada Project 790025

Surficial sediments, permafrost, and geomorphic processes, Kikerk Lake and Coppermine map areas, west Kitikmeot, District of Mackenzie, Northwest Territories[1]

D.E. Kerr, S.A. Wolfe, B.C. Ward, and L.A. Dredge
Terrain Sciences Division, Ottawa

Kerr, D.E., Wolfe, S.A., Ward, B.C., Dredge, L.A., 1996: Surficial sediments, permafrost, and geomorphic processes, Kikerk Lake and Coppermine map areas, west Kitikmeot, District of Mackenzie, Northwest Territories; in Current Research 1996-C; Geological Survey of Canada, p. 197-204.

Abstract: Surficial sediments in the Coppermine (86O, east half) and Kikerk Lake (86P) sheets were mapped at a 1:125 000 scale. Till blankets and veneers, representing a single till sheet, are the most common surficial sediments, with exceptionally long drumlinoid features west of Kikerk Lake. Esker and outwash complexes occur throughout the area, serving as potential aggregate resources. Permafrost features include mudboils and solifluction lobes on till. Coarse grained glaciofluvial and deltaic deposits typically contain large ice-wedge polygons with wide, deeply incised troughs. These features may result from partial or complete meltout of underlying wedge ice, or signify the presence of massive ground ice at depth resulting in widening of troughs through creep deformation of underlying ice. Marine deposits composed primarily of clayey silt cover much of the coastal plain and are typically ice-rich in the upper 1.5 m, with numerous but relatively small retrogressive thaw flowslides.

Résumé : Les feuillets 86O (moitié est, Coppermine) et 86P (lac Kikerk) ont fait l'objet de travaux de cartographie géologique à l'échelle de 1:125 000. Les couvertures et les placages de till, formant une nappe, sont les sédiments superficiels les plus abondants; des formes drumlinoïdes exceptionnellement longues sont signalées à l'ouest du lac Kikerk. Des eskers et des dépôts d'épandage fluvioglaciaire s'observent dans toute la région et servent de sources d'agrégats. Les formes périglaciaires comprennent des ostioles et des lobes de solifluxion. La plupart des sédiments fluvioglaciaires et deltaïques grossiers contiennent des fentes de glace découpées de profonds et larges fossés. Ces formes peuvent résulter de la fonte partielle ou complète du pergélisol avec effondrement local ou signifier la présence de glace massive en profondeur qui entraîne l'élargissement des fossés par reptation de la glace souterraine. Des sédiments marins (principalement des silts argileux) recouvrent la majeure partie de la plaine côtière; ils contiennent généralement beaucoup de glace dans la partie supérieure (1,5 m) et présentent plusieurs petites zones où il y a eu des glissements rétrogressifs par liquéfaction.

[1]Contribution to Slave NATMAP Project

INTRODUCTION

Ongoing geological exploration and development in the central and north Slave geological province have resulted in the need for a wide range of baseline information. In response, Terrain Sciences Division initiated regional surficial mapping through the Slave Province National Mapping (NATMAP) Program to provide fundamental regional data of surficial materials and till geochemistry. Surficial mapping continued during the summer of 1995 in two 1:250 000 map areas north of the previous map sheets (Dredge et al., 1994; Kerr et al., 1995), covering Coppermine (86O, east half) and Kikerk Lake (86P) (Fig. 1). A permafrost and terrain information component was incorporated into the 1995 investigation because of increasing prospects for development, including proposed winter roads and a marine port facility along the Coronation Gulf coast.

METHODS

The area was mapped by helicopter-assisted traversing and interpretation of 1:60 000 airphotos. Approximately 240 till samples of 3 kg were taken for grain size and trace element geochemical analyses (Fig. 2). At each site, 50 pebbles (2 to 6 cm in diameter) were collected for provenance investigations; where bedrock was exposed, striae were measured and the nature of the rock noted. Sediment samples were taken for grain size analysis, moisture content, and basic engineering properties. Till was collected predominantly from pits dug in mudboils at depths of 0.2 to 0.9 m. Major stratigraphic sections along rivers near the coast were logged. Marine shells and organic (twigs, leaves, peat) samples were collected for radiocarbon dating for chronological control of deglaciation and sea level studies. Permafrost features, observations on bedrock weathering, and other geomorphic processes were identified at each sample location in the map area. Approximately 30 samples of surface water, snow, icings, wedge ice, and ice-rich sediments were collected for isotopic and geochemical analysis. A CRREL corer was used to obtain ice samples to a depth of 2 m, and associated sediments were collected for analyses as with other frozen samples. Six air temperature and near surface ground temperature monitoring stations were installed within the map area (Fig. 2) to monitor climatic controls on the active layer and permafrost.

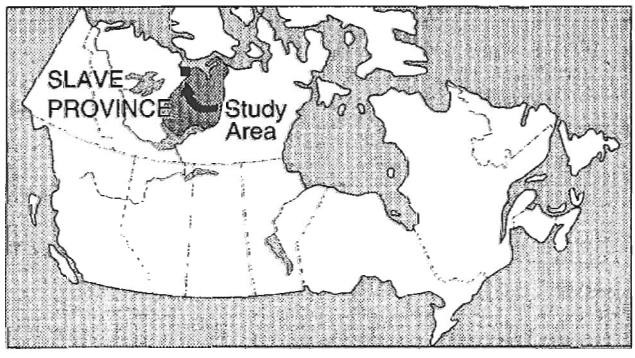

Figure 1. *Location of Slave Province and study area.*

Programmed thermistors recording air temperatures were placed within Gill-type radiation shields at heights of 1.5 m using masts similar to those described by Nixon and Taylor (1994). Thermistors recording near surface temperatures were placed 25 mm below the ground. Two ground temperature profile stations with seven thermistors were installed using the jet-drilling method (Judge et al., 1976) to depths of 30 and 19 m, respectively, within marine sediments near the Coronation Gulf (Fig. 2).

REGIONAL SETTING

The Coppermine-Kikerk Lake region is in the zone of continuous permafrost. Climatic data from a weather station at Coppermine (Atmospheric Environment Service, 1982) indicates that the mean annual air temperature is -11.6°C. The mean daily temperature is -30.1°C for January, and 9.7°C for July with 4 months (June, July, August, September) having a mean daily temperature greater than 0°C. Total annual precipitation averages 202.3 mm per year, with approximately 50% (100 cm) in the form of snow.

The study area was entirely glaciated by Laurentide Ice during the Late Wisconsin. Striae and fluted landforms reflect regional ice flow patterns that record a dominant north-northwestward flow in the southern and central parts of the study area with a gradual shift to northwestward flow in the vicinity of Coronation Gulf. During deglaciation, the coastal regions of the Coppermine-Kikerk Lake map area experienced rapid ice retreat which was simultaneous with the marine incursion across isostatically-depressed terrain. Marine limit, frequently defined by ice-contact deltas, ranges from about 170 m a.s.l. near Coppermine (St-Onge, 1995) to 210 m a.s.l. in the upper Tree River valley (Fig. 2) and was formed from approximately 11 to 10.2 ka BP respectively (Kerr, 1994). Wood from the base of a thermokarstic depression on a marine delta 32 km southwest of Coppermine suggests that vegetation development began by at least 9150 ± 100 BP (Geurts, 1985). This date is comparable to, but slightly younger than, the onset of the early Holocene warm period which initiated extensive mass wasting in the MacKenzie Delta region to the west between 9500 and 10 000 BP (Mackay and Dallimore, 1992). However, the timing and potential terrain impacts of an early Holocene warm period in the Coppermine-Kikerk Lake region are presently unknown.

BEDROCK GEOLOGY AND WEATHERING

The northeast-trending boundary between the Archean Slave Province and the Proterozoic Bear Province crosses the map area (Hoffman and Hall, 1993). Archean rocks outcrop in the southeast corner of the Kikerk Lake map area (Jackson, 1994). These Archean rocks consist of supracrustal rocks of the Yellowknife Supergroup and younger granitoid and gneissic rocks. Proterozoic rocks are divided into two broad groups: (a) argillite and stromatolitic dolomite (Epworth, Recluse and Mellville Groups) that have been pervasively folded and

faulted occupy the central part of the study area; and (b) flow basalts and minor clastic sediments of the Rae Group underlie the northwest region. The study area is crosscut by a variety of diabase dykes of which the north-northwest-trending Mackenzie swarm is most prominent. Thick diabase sheets (Franklin Sills) form spectacular palisades exhibiting columnar jointing near the coast and along the eastern part of Kikerk Lake map area.

Differences in weathering and susceptibility to frost-shattering were noted among rock types. Granitic outcrops show low to moderate evidence of frost shattering or heaving, depending on the joint pattern; most frost shattering was concentrated as haloes around the edges of outcrops. Argillite is typically extensively frost-shattered and heaved, especially near base of slopes. The frost-heaved argillites are most pronounced downslope of ponded water and/or in close proximity to perennial springs (Fig. 3A). Dolomite is somewhat less frost-shattered, breaking into large blocks along joints. These blocks rotate outward on shallow slopes, and steep terrain is susceptible to small rockfalls. Solution weathering is ubiquitous in the dolomite where pits and more resistant, intercalated chert layers and lenses have relief up to 5 cm. Basalt and diabase sills are not extensively shattered or heaved but may exhibit large talus slopes along the edges of palisades, and contain grussified zones which appear to be more common on bedrock once submerged by the postglacial sea.

SURFICIAL SEDIMENTS AND PERMAFROST FEATURES

Tills

Till is the dominant surficial sediment in the map area. It consists of a matrix-supported diamicton, with a clayey silt to fine sand matrix, and exhibits low to high compaction. Clasts range in size from small pebbles to large boulders, although medium to large pebbles predominate. Subangular to subrounded clasts are most common but some exposures, notably those close to bedrock, may be dominated by angular blocks; rounded clasts are quite rare. Till is composed of up to 50% clasts, but most exposures have between 10 and 30%. Striated clasts are frequently found in till. Matrix grain size varies according to bedrock source; till derived from sedimentary and volcanic rocks is silty whereas granitoid rocks produced a more sandy till.

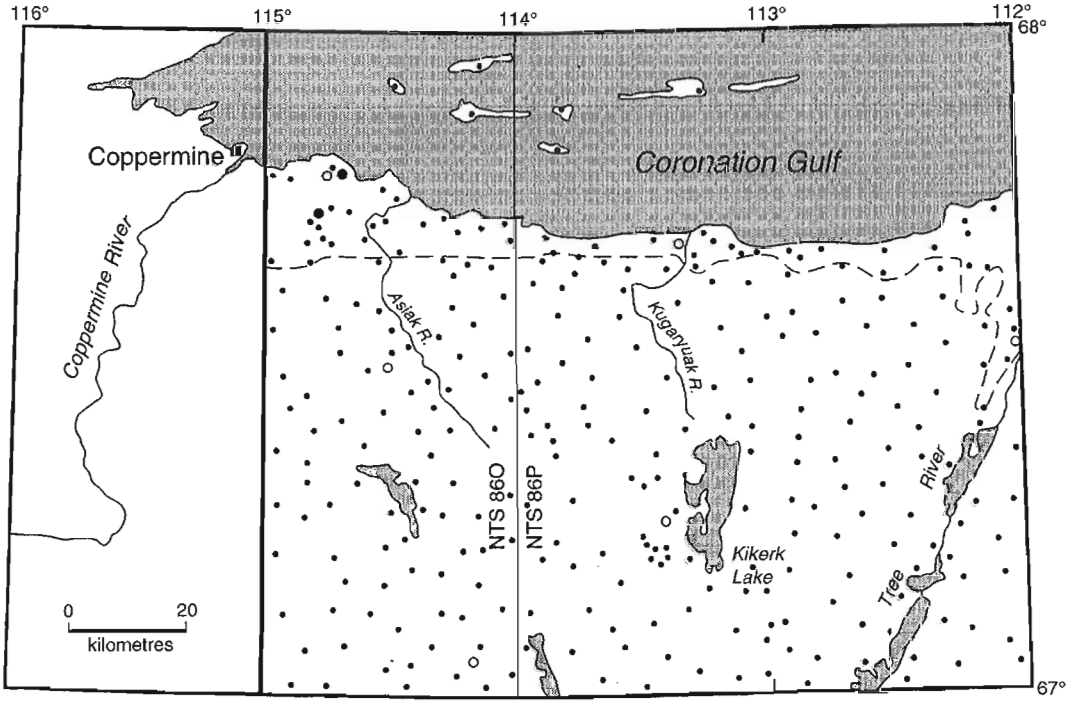

Figure 2. *Location of sediment sample and monitoring stations in the study area. Large black dots represent ground thermal profile stations; large white circles represent air and near surface ground temperature stations. Small dots represent sample/observations sites. Limit of marine submergence represented by dashed line.*

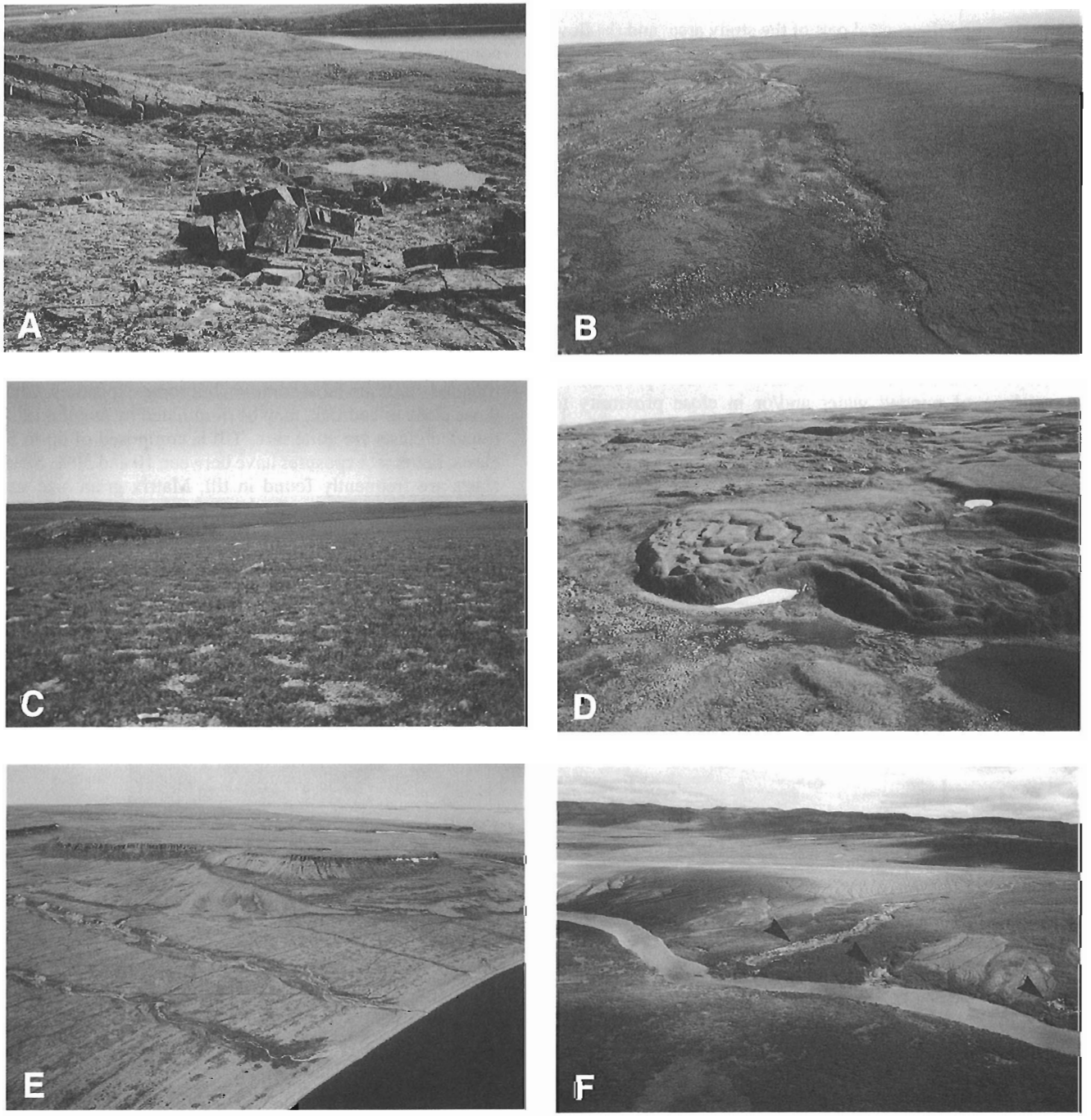

Figure 3.

A) *Frost heaved argillites downslope from small lake (not in picture). Note spring issuing from base of slope and draining into lake in distance. GSC 1995-246B*

B) *Large drumlinoid feature consisting of till blanket (right) with solifluction lobes advancing over washed till veneer (left). GSC 1995-246G*

C) *Gently rolling till plain with unvegetated mudboils on surface and small dolomite outcrop to the left. GSC 1995-246F*

D) *Glaciofluvial outwash complex near the Kugaryuak River. Note deeply incised ice wedge polygons and kettled (hummocky) outwash plain in centre and relatively featureless plain to the right. GSC 1995-246C*

E) *Raised marine beaches 7 km east of the mouth of the Kugaryuak River, Coronation Gulf. Note ice-wedge polygons parallel to and crosscutting beach ridges. GSC 1995-246E*

F) *Silty clay marine sediments in the Tree River valley. Note small thawslides (arrows) and unvegetated, gullied exposures. GSC 1995-246D*

Till veneers, generally less than 2 m thick, cover large areas containing small bedrock outcrops, and conform to underlying bedrock morphology (Fig. 3B). Till veneer is generally loosely compact with high concentrations of cobbles and boulders at the surface; where veneer is thin and discontinuous, structural bedrock features are visible. In certain areas, many of the fine grained sediments in the matrix were removed by meltwater, resulting in isolated lag deposits consisting of pebble- to boulder-sized clasts less than 2 m in diameter. Till blankets are generally greater than 2 m thick and either drape over the underlying bedrock, forming undulating till plains, or are low to moderate-relief drumlinoid and crag-and-tail features. These tills tend to be relatively compact.

Till blankets and veneers are the main surficial sediment south of the limit of marine submergence (Fig. 2). Bouldery veneers were most common and blankets were rare in areas of Archean bedrock. In areas of Proterozoic clastic and carbonate bedrock, till blankets are more abundant and are commonly associated with crag-and-tail and drumlinoid features. Along the western margin of the Kikerk Lake and eastern margin of the Coppermine map areas, there is an extensive area of large, parallel crag-and-tail and drumlinoid features, some of which are up to 35 km long (Fig. 3B), separated by zones consisting of bare bedrock, thin till veneer, and glaciofluvial outwash deposits. To the north of marine limit, till is rare, only occurring at the surface as isolated remnants commonly having been reworked by marine processes or covered with marine sediments.

Frost action within the active layer results in the widespread occurrence of mudboils in all till units. Mudboils are best developed on till blankets (Fig. 3C), frequently occurring as stripes on inclined surfaces. Solifluction lobes are also common and are most pronounced near the base of drumlinoids (Fig. 3B). Ice wedge polygons are rarely visible on tills, probably due to a thick active layer (>1.0 m) resulting from mudboils and solifluction activity on slopes. However, ice wedges rooted in till may occur in depressions, where peat cover is on the order of 0.25 m thick or greater.

Glaciofluvial sediments

Glaciofluvial sediments consist of eskers, kames, and proglacial outwash. Eskers have a sinuous to linear form and generally trend northwest and north. Cobble and boulder lags are associated with the sides of eskers as well as bedrock surfaces between esker segments. Eskers range from small, sinuous ridges a few tens of metres long, to large, more linear features up to 30 km long. Composition ranges from fine sand to cobbles, and may change rapidly over short distances. Throughout much of the map areas, outwash plains scarred by braided channels and kettle lakes are associated with the esker complexes. Some of these sand and gravel outwash plains cover areas of eight square kilometres or more (Fig. 3D). As with eskers, their grain size is variable. Such glaciofluvial deposits are potential resources for large volumes of granular materials.

Glaciofluvial deposits are geographically widespread but limited in extent. Esker-outwash complexes generally parallel the dominant glacial flow direction; however, a large esker near marine limit on the Coppermine map area is approximately perpendicular to the dominant ice flow direction. Some outwash complexes were observed to cut across drumlinoid and crag-and-tail features, while others terminated at marine limit in the form of ice-contact deltas such as along the Asiak and Kugaryuak rivers. Compared to regions immediately to the south mapped in previous years, outwash is much more extensive in the Kikerk Lake and Coppermine map areas.

The presence of permafrost typically results in the formation of ice-wedge polygons in glaciofluvial sediments and mudboils are rarely present in these relatively coarse grained materials. Ice-wedge polygons are exceptionally well developed on most flat-topped outwash deposits despite the thin (<0.2 m) organic cover. Polygons are on the order of 30 to 100 m in diameter with troughs up to 2 m deep and raised rims up to 1 m high are common, and some troughs are over 6 m wide (Fig. 3D). Smaller polygons approximately 10 m in diameter, with troughs on the order of 0.3 m deep also occur on outwash sediments. In some areas, both sets of polygons occur together, which possibly indicates multiple periods of ice wedge growth. Ice wedge polygons are seldom visible on eskers in the map areas, perhaps due to the narrow and steep-sided nature of these features.

Glaciomarine/marine sediments

Raised glaciomarine and fossiliferous marine sediments are extensive along the coastal lowlands of Coronation Gulf and extend up to 40 km inland in the Tree River valley; they provide evidence for marine inundation and subsequent postglacial emergence. These sediments occur below marine limit and consist primarily of four types: (1) undifferentiated, massive to well stratified silt and clay which may be overlain by a thin sand layer forming a blanket more than 2 m and up to 30 m thick; (2) a veneer of similar composition less than 2 m in thickness covering extensive regions below marine limit; (3) coarse sand, pebbles, and cobbles of littoral origin (raised beaches) found at various elevations from marine limit to present sea level (Fig. 3E); and (4) sand to cobbles forming perched glaciomarine and marine deltas which occur predominantly at or near marine limit, as well as at lower elevations along major rivers.

Permafrost has extensively affected the marine sediments and mudboils are widespread on marine silts and clays. In many areas along the coast, particularly within the Tree River valley, the fine grained marine blanket deposits are gullied and bare of vegetation cover (Fig. 3F). Retrogressive thaw flowslides are common along streams in these areas, with active slides typically more than 10 m in diameter and headwalls 1-2 m high (Fig. 3F). As with till, ice wedge polygons are rarely visible on fine grained marine deposits, probably due to mudboil and solifluction activity. Ice-wedge polygons are common on most raised beach and sandy littoral sediments while mudboils are rare. Where littoral sediments form laterally extensive veneers over marine silts or clays, tundra ponds and low centre polygons are common (Fig. 3E). As

with the outwash plains, large ice-wedge polygons in excess of 30 m diameter with deeply incised troughs are found on the coarse glaciomarine/marine deltaic deposits.

Organic sediments

Organic sediments consist of peat formed by the accumulation of fibrous, woody and mossy vegetative matter up to 1 m or more in thickness, locally overlain by a dense grass or shrub cover. They occur predominantly in topographic depressions and valley bottoms with poor drainage, but are most noticeable below marine limit where they overlie fine grained marine sediments. Ice-wedge polygons are common in organic sediments, and are rooted in the underlying till, glaciofluvial, or marine deposits. Frozen ground was encountered at depths as shallow as 0.13 m below the surface in peat in late summer.

Alluvial sediments

Alluvial sediments comprise gravel- to silt-size sediment deposited by modern streams and rivers. They range from massive to well stratified and vary in thickness from 1 to 5 m. Alluvial sediments are associated with meandering and braided environments, as well as floodplains and alluvial fans, in places covered by icings. The coarse grained alluvial sediments often form stripes and sorted circles within perennially active stream beds. In one instance meltout of ground ice, covered by a veneer of alluvial gravels, was observed in a flowing streambed. The ice was approximately 70 cm thick and appeared to have grown in-situ over the winter months. Meltout of the ice and subsequent collapse of overlying gravels resulted in a pattern of sorted circles and stripes, oriented with the flow of water.

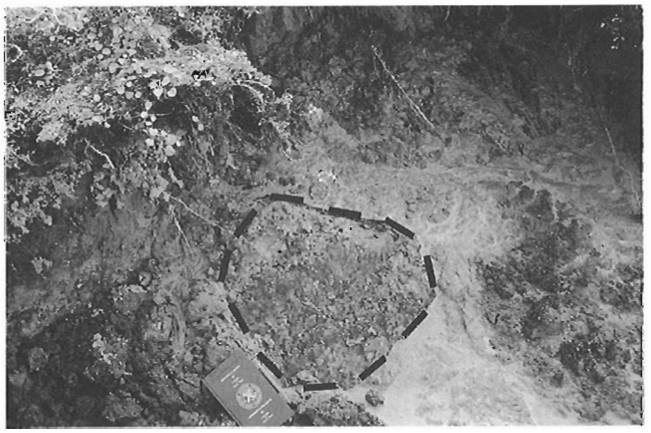

Figure 4. *Ground ice in silty marine sediments. Ice (outlined) contains suspended inclusions of marine sediments and small bubble-rich pockets. GSC 1995-246H*

PERMAFROST CONSTRAINTS AND HAZARDS

Should engineered structures, transportation right of ways, or borrow pits be developed in the region, several permafrost constraints or hazards could exist, stemming from the presence of thaw-sensitive material and active periglacial processes within various terrain units.

The fine grained marine sediments are probably the most sensitive to permafrost degradation. These silty sediments are typically ice-rich in the upper 1.5 m, and lenses of ice up to 1.0 m thick are present (Fig. 4). The presence of ice-rich sediments results in thaw-sensitive slopes, particularly along the Tree River valley and coastal plains (Rampton and Thomas, 1993). The deposits are saline, with salinities of 5 to 20 ppt in the upper 1.5 m and likely continuing at depth. The thickness of these deposits is variable and may exceed 30 m. Ice-rich silty marine sediments also occur beneath veneers of sandy littoral sediments. Removal or disturbance of the overlying littoral sediments would likely induce melting and slumping of the ice-rich sediments.

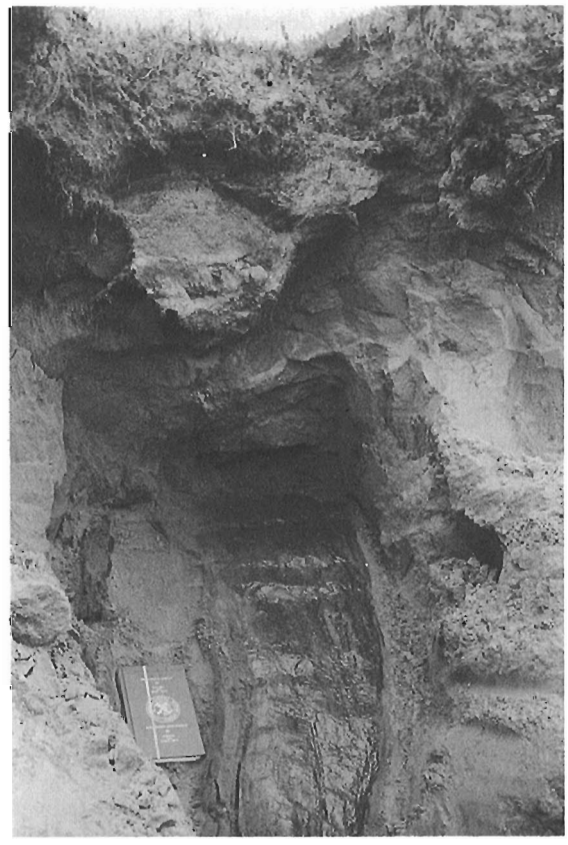

Figure 5. *Cross-section of ice wedge in littoral sediments. GSC 1995-246A*

Ice wedge polygons are present on most flat-topped coarse grained deposits including littoral sediments, marine deltas, alluvial terraces, outwash, kames, and in most areas with an organic mat at least 0.3 m thick (Fig. 5). However, the implications drawn from the presence of ice-wedges on these units must be interpreted with caution. Ice-wedge troughs on many marine deltas, outwash, and kame deposits can be exceedingly large; the largest, greater than 2 m deep and up to 6 m wide (Fig. 3D). The enormity of these features suggests that slumping and infilling has occurred. This may be due to partial or complete meltout of ice. Meltout could well be attributed to an early Holocene warm period, although this constrains the initial ice-wedge growth to a time period no more than 2000 years, and possibly much less, prior to the onset of warming. Alternatively, the large ice-wedge troughs may due to the presence of buried massive ground ice within the glaciofluvial sediments. In this case, creep deformation of the massive ground ice as described by Dallimore et al. (1995) may be responsible for the widening and deepening of the overlying ice-wedge troughs. These over-deepened wedges can also occur in conjunction with a set of smaller ice-wedges. Certainly, granular deposits associated with the features must be investigated for potential ground ice prior to removal of aggregates.

Mudboils and solifluction lobes are common on till and marine blanket deposits. These deposits show considerable sediment translocation, dependent upon slope angle, with lobes 10 to 30 m long protruding over rock or littoral sediment. It is clear that significant sediment translocation has occurred since deglaciation, although the rate of downslope has probably varied.

Fine grained sediments and organic accumulations limit the depth of the active layer. Active layers are shallowest over fine grained marine and till deposits where peat accumulations exceed 0.3 m. In these areas, the active layer is commonly restricted to a depth of 0.2 to 0.4 m. Mudboils and gullying restrict vegetation growth on some marine silts and clays. Preliminary investigations show that active layer thicknesses are typically only 0.6 m or less on these deposits. In comparison, active layer thicknesses on mudboils in sandy tills are on the order of 1.0 m. Esker, outwash, and beach deposits commonly have thick active layers, due to the coarse sediment and poor organic accumulations. Littoral and outwash sands with 0.1 m to 0.15 m of organic cover have active layers on the order of 0.7 m thick while those on unvegetated gravels are in excess of 1.3 m thick. Results from the thermal monitoring stations to be released at a later date will provide seasonal temperatures in permafrost and active layers on a variety of terrains, and assist in determining the susceptibility of the terrain to thermal disturbance.

SUMMARY

This report summarizes preliminary results from the 1995 field season of Terrain Sciences Division's contribution to the Slave NATMAP program. Till blankets and veneers are the most common surficial deposits in the area, and only one till sheet, attributed to the Late Wisconsin Laurentide Ice Sheet, was identified. Glaciofluvial deposits, consisting predominantly of esker and outwash complexes, occur throughout the area. Outwash was more common than in areas mapped to the south in 1993 and 1994. Raised marine sediments are predominantly blankets and veneers of silt and clay but coarser grained beaches and deltas are also present. They extend from the coast to as much as 40 km inland and range from sea level to an elevation of more than 200 m. Samples of shells and organics obtained from marine sediments for radiocarbon dating will help refine the timing of deglaciation and sea level history for the area.

Ice-wedge polygons are frequently found on outwash and littoral deposits comprised of sand or gravel, and beneath most organic deposits. Finer grained deposits such as tills and marine silts and clays commonly contain mudboils and solifluction lobes or stripes, but seldomly include ice-wedges. The marine blanket deposits frequently contain excess ice in the upper 1.5 m, and thawslides are common on slopes in these deposits. These permafrost features and processes have numerous implications with respect to development in the region, stemming from active slope processes and thaw-sensitive materials.

ACKNOWLEDGMENTS

Ray Roberts and Paul Wilson were field assistants on the project. Polar Continental Shelf Project provided helicopter and fixed-wing support, and Craig Nicholson maintained radio contact and expediting services from Yellowknife. The authors would like to thank T. Barry for drafting assistance, and R.A. Klassen for critical review. Quaternary geology mapping was supported by the Slave NATMAP program while geomorphic process studies were supported by through a co-operative research agreement between Indian and Northern Affairs Canada (INAC) and the GSC.

REFERENCES

Atmospheric Environment Service
1982: Canadian climate normals, temperature and precipitation 1951-1980. The North: Yukon Territory and Northwest Territories; Environment Canada, Downsview, 59 p.

Dallimore, S.R., Egginton, P.A., Nixon, F.M., Ladanyi, B., and Foriero, A.
1995: Creep deformation of massive ground ice, Tuktoyaktuk coastlands, N.W.T.; in Proceedings of the 48th Canadian Geotechnical Conference, September 25-27, Vancouver, BC, p. 1015-1022.

Dredge, L.A., Ward, B.C., and Kerr, D.E.
1994: Glacial geology and implications for drift prospecting in the Lac de Gras, Winter Lake and Aylmer Lake map areas, central Slave Province, Northwest Territories; in Current Research 1994-C; Geological Survey of Canada, p. 33-38.

Geurts, M.-A.
1985: Le paysage végétal Holocène dans la région d'Escape Rapids, Territoires du nord-ouest; Géographie physique et Quaternaire, vol. 39, no. 2, p. 215-220.

Hoffman, P. and Hall, L.
1993: Geology, Slave craton and environs, District of Mackenzie, Northwest Territories; Geological Survey of Canada, Open File 2559, scale 1: 1 000 000.

Jackson, V.
1994: Preliminary geological compilation of the Eokuk Uplift, part of NTS area 86P; Indian and Northern Affairs Canada, EGS 1994-16, scale 1:125 000.

Judge, A.S., MacAuley, H.A., and Hunter, J.A.
1976: Thermistor cable installation in permafrost materials with a water jet-drilling method; in Report of Activities, Part C; Geological Survey of Canada, Paper 76-1A p. 27-34.

Kerr, D.E.
1994: Late Quaternary stratigraphy and depositional history of the Parry Peninsula-Perry River area, District of Mackenzie, Northwest Territories; Geological Survey of Canada, Bulletin 465, 34 p.

Kerr, D.E., Dredge, L.A., Ward, B.C., and Gebert, J.S.
1995: Quaternary geology and implications for drift prospecting in the Napaktulik Lake, Point Lake and Contwoyto Lake map areas, northwest Slave Province, Northwest Territories; in Current Research 1995-E; Geological Survey of Canada, p. 201-209.

Mackay, J.R. and Dallimore, S.R.
1992: Massive ice of the Tuktoyaktuk area, western Arctic coast, Canada; Canadian Journal of Earth Sciences, v. 29, no. 6, p. 1235-1249.

Nixon, F.M. and Taylor, A.E.
1994: Active layer monitoring in natural environments, Mackenzie Valley, Northwest Territories; in Current Research 1994-B, Geological Survey of Canada, p. 27-34.

Rampton, V.N. and Thomas, R.D.
1993: Surficial geology, Hepburn Island, District of Mackenzie (76M), Northwest Territories; Geological Survey of Canada, Open File 2662, scale 1:125 000.

St-Onge, D.A.
1995: Surficial geology, Coppermine, District of Mackenzie, Northwest Territories (86O E/2); Geological Survey of Canada, Open File 3076, scale 1:125 000.

Geological Survey of Canada Projects 920072 and 950035-03

AUTHOR INDEX

Bird, R.T. 117
Bleeker, W. 37
Boullier, A.-M. 147
Buchan, K.L. 117
Dionne, J.-C. 177
Dixon, J.M. 93
Dredge, L.A. 197
Dumaresq, C.G. 137
Emslie, R.F. 183
Ernst, R.E. 117
Firdaous, K. 147
Gale, D. 93
Gerabek, P. 169
Hanmer, S. 63. 73
Heather, K.B. 125
Hendry, K.B. 137
Kerr, D.E. 197
Kurfurst, P. 169
Kwong, Y.T.J. 137
Lambert, M.B. 19
LeCheminant, A.N. 1, 11
Lowe, C. 29
Lucas, S.B. 93
Michel, F.A. 137
Miller, A.R. 49
Nadeau, L. 157
Percival, J.A. 157
Percival, J.B. 137
Pilkington, M. 117
Pilon, J. 169
Rainbird, R.H. 1
Robert, F. 147
Roest, W.R. 117
Ryan, J.J. 105
Scaife, J. 169
Scott, D.J. 63, 73, 83
Seemann, D.A. 29
Shore, G.T. 125
Skulski, T. 157
St-Onge, M.R. 63, 73
Timoshenko, E. 169
van Breemen, O. 125
Villeneuve, M.E. 1
Ward, B.C. 197
Williams, P.F. 105
Wolfe, S.A. 197

NOTE TO CONTRIBUTORS

Submissions to the Discussion section of Current Research are welcome from both the staff of the Geological Survey of Canada and from the public. Discussions are limited to 6 double-spaced typewritten pages (about 1500 words) and are subject to review by the Chief Scientific Editor. Discussions are restricted to the scientific content of Geological Survey reports. General discussions concerning sector or government policy will not be accepted. All manuscripts must be computer word-processed on an IBM compatible system and must be submitted with a diskette using WordPerfect. Illustrations will be accepted only if, in the opinion of the editor, they are considered essential. In any case no redrafting will be undertaken and reproducible copy must accompany the original submissions. Discussion is limited to recent reports (not more than 2 years old) and may be in either English or French. Every effort is made to include both Discussion and Reply in the same issue. Current Research is published in January and July. Submissions should be sent to the Chief Scientific Editor, Geological Survey of Canada, 601 Booth Street, Ottawa K1A 0E8 Canada.

AVIS AUX AUTEURS D'ARTICLES

Nous encourageons tant le personnel de la Commission géologique que le grand public à nous faire parvenir des articles destinés à la section discussion de la publication Recherches en cours. Le texte doit comprendre au plus six pages dactylographiées à double interligne (environ 1500 mots), texte qui peut faire l'objet d'un réexamen par le rédacteur scientifique en chef. Les discussions doivent se limiter au contenu scientifique des rapports de la Commission géologique. Les discussions générales sur le Secteur ou les politiques gouvernementales ne seront pas acceptées. Le texte doit être soumis à un traitement de texte informatisé par un système IBM compatible et enregistré sur disquette WordPerfect. Les illustrations ne seront acceptées que dans la mesure où, selon l'opinion du rédacteur, elles seront considérées comme essentielles. Aucune retouche ne sera faite au texte et dans tous les cas, une copie qui puisse être reproduite doit accompagner le texte original. Les discussions en français ou en anglais doivent se limiter aux rapports récents (au plus de 2 ans). On s'efforcera de faire coïncider les articles destinés aux rubriques discussions et réponses dans le même numéro. La publication Recherches en cours paraît en janvier et en juillet. Les articles doivent être envoyés au rédacteur en chef scientifique, Commission géologique du Canada, 601, rue Booth, Ottawa K1A 0E8 Canada.

Geological Survey of Canada Current Research, is released twice a year, in January and July. The four parts published in January 1996 (Current Research 1996-A to D) are listed below and can be purchased separately.

Recherches en cours, une publication de la Commission géologique du Canada, est publiée deux fois par année, en janvier et en juillet. Les quatre parties publiées en janvier 1996 (Recherches en cours 1996-A à D) sont énumérées ci-dessous et sont vendues séparément.

Part A: Cordillera and Pacific Margin
Partie A : Cordillère et marge du Pacifique

Part B: Interior Plains and Arctic Canada
Partie B : Plaines intérieures et région arctique du Canada

Part C: Canadian Shield
Partie C : Bouclier canadien

Part D: Eastern Canada and national and general programs
Partie D : Est du Canada et programmes nationaux et généraux